UC Irvine

UC Irvine Electronic Theses and Dissertations

Title

Synthesis and Study of Amyloidogenic and Antimicrobial Peptides

Permalink

https://escholarship.org/uc/item/4mn9x5jg

ISBN

9798190903577

Author

Zhu, Jason

Publication Date

2026-09-04

Copyright Information

This work is made available under the terms of a Creative Commons Attribution License, available at https://creativecommons.org/licenses/by/4.0/

Peer reviewed|Thesis/dissertation

eScholarship.org Powered by the California Digital Library
University of California

UNIVERSITY OF CALIFORNIA,
IRVINE

Synthesis and Study of Amyloidogenic and Antimicrobial Peptides

DISSERTATION

submitted in partial satisfaction of the requirements
for the degree of

DOCTOR OF PHILOSOPHY

in Chemistry

by

Jason Zhu

Dissertation Committee:
Distinguished Professor James S. Nowick, Chair
Professor Jennifer A. Prescher
Professor Rachel W. Martin

2026

Chapter 1 © 2025 Elsevier
Chapter 2 © 2025 Royal Society of Chemistry
All other materials © 2026 Jason Zhu

DEDICATION

To

my chosen family and friends

for their love and support.

Table of Contents

LIST OF FIGURES iv

LIST OF SCHEMES vi

ACKNOWLEDGEMENTS vii

VITA viii

ABSTRACT OF THE DISSERTATION xi

Chapter 1: Using Solution-phase NMR Spectroscopy to Study the Folding and Supramolecular Assembly of Conformationally Constrained β-Sheet Peptides 1

Chapter 2: A β-Hairpin Peptide Derived from Aβ Forms Different Oligomers in the Crystal State and in Aqueous Solution 38

Chapter 3: Synthesis and Study of the Peptide Antibiotic Hypeptin 71

Appendix A: Additional Data for Chapter 2 97

Appendix B: Additional Data for Chapter 3 197

LIST OF FIGURES

Figure 1.1. Different types of conformational constraints our laboratory has used to promote β-sheet secondary structure 2
Figure 1.2. Representative chemical shifts for the 20 canonical amino acids in aqueous solution 7
Figure 1.3. Overview of generating peak assignments using TOCSY and ROESY NMR..... 23
Figure 1.4. Spectroscopic hallmarks of β-sheet folding 27
Figure 1.5. Spectroscopic hallmarks of supramolecular assembly observed in ^{1}H NMR and DOSY spectra 33
Figure 2.1. Peptide 1 and 2, and X-ray crystallographic structure of peptide 1 42
Figure 2.2. X-ray crystallographic structure of the hexamer formed by peptide 2..... 46
Figure 2.3. SDS-PAGE and CD spectra of peptides 1 and 2 47
Figure 2.4. ^{1}H NMR spectra of peptide 2 at 1.0, 6.0, and 11.0 mM in D_2O 49
Figure 2.5. ^{1}H,^{15}N HSQC and TOCSY spectra illustrating peak assignments of peptide 2 50
Figure 2.6. (A) Chemical shift differences between the peptide 2 Hα protons and random coil (B) Molecular model of the δ-linked ornithine turns unit and magnetic anisotropies of the pro-*R* and pro-*S* protons observed for peptide 2. 52
Figure 2.7. Key intramolecular NOEs for the peptide 2 monomer and oligomer species A and B 53
Figure 2.8. Key Hα-to-Hα intermolecular NOEs in the NOESY spectrum of the peptide 2 oligomer 54
Figure 2.9. Chemical structure of peptide 2D and key intermolecular contacts observed in the ^{15}N-edited NOESY-HSQC spectrum 56
Figure 2.10. NMR-based molecular model of the asymmetric hexamer formed by peptide 2..... 58
Figure 2.11. Three representative dodecamer configurations observed in different MD simulations 63
Figure 3.1. Chemical structures of hypeptin, clovibactin, and teixobactin..... 73
Figure 3.2. Synthetic strategy to hypeptin highlighting key disconnections and β-hydroxy amino acid building blocks. 76
Figure 3.3. First-generation synthesis of hypeptin..... 82
Figure 3.4. Summary of major hypeptin side reactions. 84
Figure 3.5. Second-generation synthesis of hypeptin. Red highlights change from the first-generation synthesis and key amino acid building blocks 87
Figure 3.6. Analytical RP-HPLC traces of natural, synthetic, and a mixture of natural and synthetic hypeptin 88
Figure 3.7. (A) Analytical RP-HPLC trace showing the conversion of hypeptin, A, into decomposition byproducts B and C. (B) Decomposition kinetics of hypeptin illustrating the disappearance of hypeptin over time 90

LIST OF TABLES

Table 1.1. Typical distances and relative NOE strength for β-sheet peptides. 8
Table 1.2. Relative phases of NOE and EXSY crosspeaks in the NOESY and ROESY spectrum. 11
Table 1.3. Typical diffusion coefficient quotients for small oligomers 12
Table 1.4. Summary of key NMR acquisition parameters 14
Table 2.1. Key intermolecular contacts observed for the peptide 2 oligomer 58
Table 2.2. Summary of peptide 2 analogues and their assembly in aqueous solution. 64
Table 3.1. Select chemical shift tabulations of hypeptin in DMSO-d_6 at 298 K 89

LIST OF SCHEMES

Scheme 3.1. Synthesis of protected (2*S*,3*R*)-3-hydroxyasparagine 1 77
Scheme 3.2. Synthesis of protected (2*R*,3*R*)-3-hydroxyasparagine 2..... 78
Scheme 3.3. Synthesis of protected (2*S*,3*R*)-3-hydroxytyrosine 3 79
Scheme 3.4. Synthesis of protected (2*S*,3*R*)-3-hydroxyleucine 4..... 81

ACKNOWLEDGEMENTS

I would like to thank my research advisor, Professor James Nowick for his unwavering belief in me both as a scientist and as a person. I have thoroughly enjoyed our innumerable conversations about NMR spectroscopy over the past five years. Thank you for helping me develop into the scientist, writer, and speaker that I am today. I am eternally grateful.

I would like to thank my committee members, Professor Jennifer Prescher and Professor Rachel Martin for their support, guidance, and feedback throughout my graduate studies. Professor Prescher, I still remember the advice that you gave me at the beginning of my 5th year to prioritize getting the chemistry done. It was exactly what I needed to hear at the time. Professor Martin, I have enjoyed collaborating on projects together and getting to know members of your group.

To all the past Nowick lab alumni and current group members, thank you for being the best group of people I could have asked for to share my PhD woes with! Xingyue, thank you for taking me in as a bright-eyed (and naïve) first year and taking the time out of your schedule to share your NMR expertise. Maj and Gretchen, thank you for all the solicited (and unsolicited) advice in navigating job hunting. Chelsea J., thank you for teaching me how to handle difficult peptide purifications. Sophie, thank you for sharing a bay with me for the last four years and being a friendly (loud) voice in the lab. To Carolina, Harry, and Kat, thank you for hearing out this grumpy 5th year and for sharing the joys (and pains) of graduate school together. I look forward to seeing where the science takes you in graduate school and beyond.

To my two undergraduate mentees, Sabrina and Emily, thank you for teaching me how to be a research mentor. Sabrina, thank you for taking a chance on me as my first undergraduate mentee. Your ability to pick up new skills and make them your own never ceases to amaze me. Emily, thank you for enthusiastically jumping into amino acid syntheses. I will never forget how you ran a picture-perfect column on your first try. I'm certain both of you will succeed in your future endeavors.

To my friends in other labs, thank you for always reminding me to spend time outside of lab. Lucas and Jared, thank you for playing tennis with me on weekends. Jayme, thank you for making so many treats and reminding me to eat and sleep. Jacob, thank you for sharing Pepper and teaching me about game development. Julia, thank you turning me into a cat person. Matthew, thank you for being an awesome friend. I will fondly remember the beach days, games nights, and picnics we shared.

I thank *Elsevier* for permission to publish Chapter 1, which is a reprint of materials originally published in *Methods in Enzymology*. I thank RSC for permission to publish Chapter 2, which was originally published in *Organic and Biomolecular Chemistry*. Financial support for the research described in Chapters 1 and 2 were provided by the National Institute of Health (grant P30 GM124169-01) and National Institute on Aging (grant AG072587).

VITA

Jason Zhu

Synthetic organic chemistry Ph.D. candidate with extensive experience in small molecule and peptide synthesis. Detail-oriented and results-driven collaborative researcher with a passion for applied synthetic organic chemistry and NMR spectroscopy. Looking to apply my synthesis and NMR experience to solving problems in the pharmaceutical industry.

Education

University of California Irvine, Irvine CA 2021 –2026
Doctor of Philosophy: Chemistry
Cumulative GPA: 3.85/4.00

Northwestern University, Evanston IL 2017 –2021
Bachelor of Science: Chemistry
Bachelor of Science: Chemical & Biological Engineering

Experience

University of California, Irvine, *Graduate Student Researcher* 2021 –2026
Advisor: Professor James S. Nowick

- Pioneered two noncanonical amino acid syntheses and the first synthesis of hypeptin, a potent cyclodepsipeptide antibiotic.
- Synthesized, purified, and characterized over 100 peptides to investigate the folding and supramolecular assembly of peptides involved in Alzheimer's disease progression.
- Isolated and characterized ~16 small molecules, drugs, and natural products to teach Organic Spectroscopy to 40 graduate students.
- Co-authored an R21 grant proposal (~$220,000/yr) on hypeptin.
- Serviced and maintained critical laboratory equipment

Northwestern University, *Laboratory Aide* 2019 – 2020
Advisors: Professor Katie G. Gesmundo and Professor Derek W. Nelson

- Started a working inventory of 300+ student lockers and 50+ stockroom reagents.
- Synthesized reference organic products for students to analyze via IR, MS, and NMR.

NeuroLux, *Engineering Intern* 2020

- Prototyped a life-sized silicone model that mimics the mechanical properties of a rat.
- Identified structural defects in an existing implantable sensor design through mechanical testing and proposed design recommendations.

Northwestern University, *Undergraduate Student Researcher* 2018 – 2021
Advisor: Professor John. A. Rogers

- Assembled phone-powered skin hydration devices to help doctors diagnose skin diseases.
- Compiled examples of thermal sensing on human skin for a review article detailing methods for characterizing skin thermal transport and hydration.

Publications

Zhu, J.; Brunicardi, J. H. E.; De Benedetti, S.; Small, J. J.; Ung, H.; Strombeck, C.; Le, E. T.; Schneider, T.; Nowick, J. S. Synthesis and Study of the Peptide Antibiotic Hypeptin. (in preparation).

Zhu, J.; Nowick, J. S. Using solution-phase NMR spectroscopy to study the folding and supramolecular assembly of conformationally constrained β-sheet peptides. *Methods Enzymol.* **2025**, *723*, 477–509.

Sroge, C.; Suk, J.; **Zhu, J.**; Padilla, M. S. T. L.; Baca, C.; Butts, C. T.; Martin, R. W. Mini-αA-crystallin (MAAC) protects a client lens from catastrophic aggregation due to heat stress. *Protein Sci.* **2025**, *34* (7), e70199.

Zhu, J.; Kreutzer, A. G.; Liu, Z.; Li, X.; Richter, S. M.; Pophristic, V.; Nowick, J. S. A β-Hairpin Peptide Derived from Aβ Forms Different Oligomers in the Crystal State and in Aqueous Solution. *Org. Biomol. Chem*. **2025**, *23* (16), 3881–3893.

Ouyang, W.; Lu, W.; Zhang, Y.; Liu, Y.; Kim, J. U.; Shen, H.; Wu, Y.; Luan, H.; Kilner, K.; Lee, S. P.; Lu, Y.; Yang, Y.; Wang, J.; Yu, Y.; Wegener, A. J.; Moreno, J. A.; Xie, Z.; Wu, Y.; Won, S. M.; Kwon, K.; Wu, C.; Bai, W.; Guo, H.; Liu, T.; Bai, H.; Monti, G.; **Zhu, J.**; Madhvapathy, S. R.; Trueb, J.; Stanslaski, M.; Higbee-Dempsey, E. M.; Stepien, I.; Ghoreishi-Haack, N.; Haney, C. R.; Kim, T.; Huang, Y.; Ghaffari, R.; Banks, A. R.; Jhou, T. C.; Good, C. H.; Rogers, J. A. A Wireless and Battery-Less Implant for Multimodal Closed-Loop Neuromodulation in Small Animals. *Nat. Biomed. Eng.* **2023**, *7* (10), 1252–1269.

Madhvapathy, S. R.; Arafa, H. M.; Patel, M.; Winograd, J.; Kong, J.; **Zhu, J.**; Xu, S.; Rogers, J. A. Advanced Thermal Sensing Techniques for Characterizing the Physical Properties of Skin. *Appl. Phys. Rev.* **2022**, *9* (4), 041307.

Madhvapathy, S. R.; Wang, H.; Kong, J.; Zhang, M.; Lee, J. Y.; Park, J. B.; Jang, H.; Xie, Z.; Cao, J.; Avila, R.; Wei, C.; D'Angelo, V.; **Zhu, J.**; Chung, H. U.; Coughlin, S.; Patel, M.; Winograd, J.; Lim, J.; Banks, A.; Xu, S.; Huang, Y.; Rogers, J. A. Reliable, Low-Cost, Fully Integrated Hydration Sensors for Monitoring and Diagnosis of Inflammatory Skin Diseases in Any Environment. *Sci. Adv.* **2020**, *6* (49), eabd7146.

Conferences and Talks

Amgen Day at UCI, *Poster Presentation*	February 2026
American Peptide Symposium, *Poster Presentation*	June 2025
Speaking of Structures, *Oral Presentation*	October 2024
Synthetic and Chemical Biology Club, *Oral Presentation*	November 2023
Peptide Therapeutics Symposium, *Poster Presentation*	October 2023
Experimental Nuclear Magnetic Resonance Conference, *Poster Presentation*	April 2023

Leadership, Mentorship and Outreach

Department of Chemistry, *Mentor* 2023 – 2026

- Mentored two undergraduate students in small molecule and solid-phase peptide synthesis. First mentee is an NSF-GRFP fellow pursuing a Ph.D. at UC Berkeley. Second mentee is synthesizing unnatural amino acid building blocks.

Department of Chemistry, *Safety Officer* 2023 – 2026

- Maintained a working chemical inventory of >2000 chemicals and ensured adherence with standard laboratory safety practices.
- Led safety walkthroughs with all undergraduates and graduate students joining the lab.

UC Irvine Chemistry Outreach Program, *Performer* 2023 – 2026

- Planned 8 chemistry demonstrations that would be accessible for K-12 students.
- Performed a chemistry demonstration to ~50 students at a local elementary school.

Teaching

Teaching Assistant

- Graduate Organic Spectroscopy 2022 – 2023
- Organic Chemistry Lab 2021 – 2026
- General Chemistry Lecture 2022

Honors

Tau Beta Pi 2020
Helen L. Uchitel Scholarship 2019
Simpson-Querrey Center of Bio-Integrated Electronics Fellowship 2018

Affiliations

American Peptide Society
Tau Beta Pi

ABSTRACT OF THE DISSERTATION

Synthesis and Study of Amyloidogenic and Antimicrobial Peptides

by

Jason Zhu

Doctor of Philosophy in Chemistry

University of California, Irvine, 2026

Professor James S. Nowick, Chair

Peptides are strings of amino acids that fold and self-assemble. The folding and supramolecular assembly of these peptides are central their function. Amyloid beta (Aβ) aggregates into soluble oligomers responsible for neurodegeneration. However, the structures formed by these soluble toxic oligomers remains poorly understood because of their heterogeneity and metastability. Chemical model systems can be used to investigate the structures formed by these soluble oligomers. The folding and self-assembly of peptides is also involved in the activity of cyclodepsipeptide antibiotics. To better understand peptide folding and self-assembly, my thesis describes the synthesis and study of amyloidogenic and antimicrobial peptides.

Chapter 1 outlines a systematic approach for studying peptide model systems using solution-phase NMR spectroscopy. The chapter begins with preparing peptide NMR samples starting from lyophilized peptide. Then the chapter describes selecting, running, and processing NMR experiments. Next the chapter describes how to generate sequence specific peak assignments and identify β-sheet folding. The chapter concludes with the five spectroscopic hallmarks of supramolecular assembly. Although they focus on conformationally constrained β-

sheet peptides, these protocols can be generalized to studying peptide folding and supramolecular assembly.

Chapter 2 applies the protocols described in Chapter 1 to studying the folding and supramolecular assembly of a peptide that mimics the $A\beta_{16–36}$ hairpin. This project expands upon a previous $A\beta_{16–36}$ hairpin mimic that assembles into crystallographic hexamers but does not assemble into well-defined oligomers in solution-phase NMR conditions. A strategic phenylalanine to cyclohexylalanine (Cha) mutation at position 19 stabilizes the solution-phase NMR assembly into an asymmetric hexamer. Diffusion order NMR spectroscopy (DOSY) and molecular dynamic simulations provide a model for the asymmetric hexamer and suggest how two asymmetric hexamers can form a dodecamer. Chapter 2 concludes with remarks on which hydrogen bonding interactions are critical for solution-phase supramolecular assembly and how hydrophobic interactions drive solution-phase oligomerization.

Chapter 3 details the first synthesis of hypeptin, a cyclodepsipeptide antibiotic that is active against Gram positive bacteria. The sterochemical configuration of hydroxytyrosine$_6$ was originally reported to be (2*S*,3*S*) and later revised to (2*S*,3*R*) based on the biosynthesis. I synthesized the suitably protected (2*S*,3*R*)-hydroxytyrosine, and (2*S*,3*R*)-hydroxyleucine building blocks. These amino acid building blocks were used in the synthesis of hypeptin. LCMS and NMR comparison of synthetic hypeptin with natural hypeptin confirms the sterochemical configuration of hydroxytyrosine at position 6 to be (2*S*,3*R*). Chapter 3 ends with how this synthesis could be applied to other β-hydroxytyrosine peptide natural products and ideas on how to further develop the hypeptin scaffold as a potential drug candidate.

Chapter 1: Using Solution-phase NMR Spectroscopy to Study the Folding and Supramolecular Assembly of Conformationally Constrained β-Sheet Peptides

Preface to Chapter 1

Chapter 1 details a systemic approach for studying β-sheet interactions and self-assembly by solution phase NMR spectroscopy. As the study of aggregation-prone peptides have moved from organic solvents towards aqueous solution, we have gained insights into how hydrogen bonding and hydrophobic interactions drive solution-phase self-assembly. The procedures described in Chapter 1 form the basis of Chapter 2 in which I apply these protocols to elucidating the solution-phase NMR assembly of a peptide that mimics the $A\beta_{16–36}$ hairpin. We thank Dr. Sergiy Levin, Dr. Omid Khakshoor, Dr. Johnny Pham, Dr. Nick Truex, and Dr. Xingyue Li for developing these procedures over the past two decades.

This chapter is adapted from or taken verbatim from Zhu, J.; Nowick, J. S. Using solution-phase NMR spectroscopy to study the folding and supramolecular assembly of conformationally constrained β-sheet peptides. *Meth*. *Enzymol*. ***2025****, 723, 477–509*.

Introduction

Our laboratory has utilized solution-phase NMR spectroscopy to study the folding and supramolecular assembly of conformationally constrained β-sheet peptides.[1–8] We are especially interested in using these peptides as model systems to mimic Aβ oligomers involved in neurodegeneration in Alzheimer's disease. Aβ oligomers are difficult to characterize because they are metastable and often not conformationally defined. By incorporating conformational constraints into these peptides — such as β-strand templates, linking the *N*-and *C*-termini together with a δ-linked ornithine turn unit ($^{\delta}$Orn), and adding disulfide staples — we reduce oligomer heterogeneity and enable high-resolution studies on Aβ oligomer mimetics. (Figure **1.1**)[9–11]

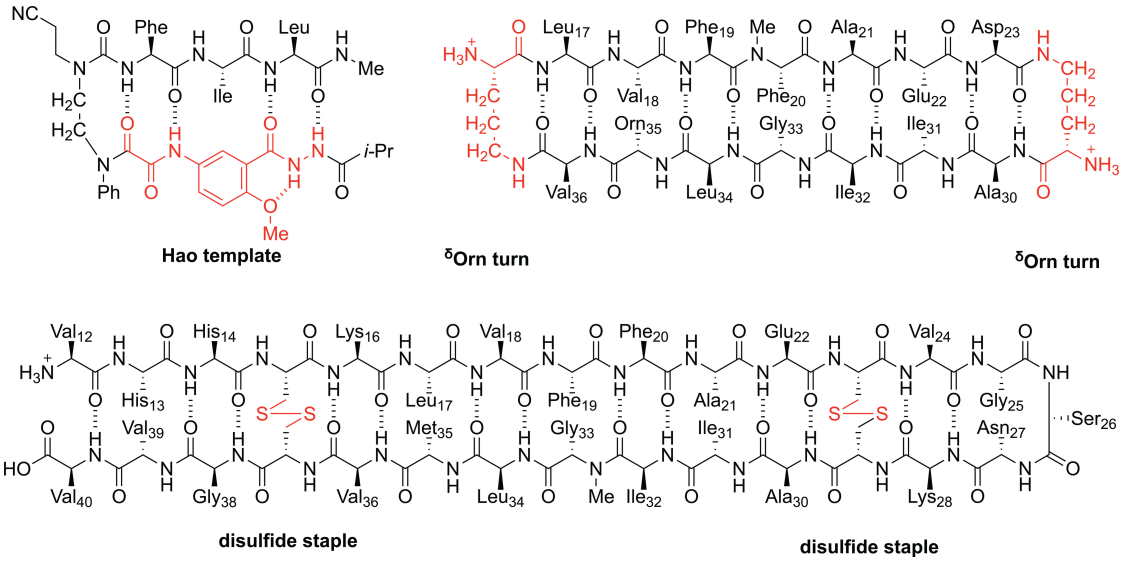

Figure 1.1. Different types of conformational constraints our laboratory has used to promote β-sheet secondary structure.[9,5,11]

Constrained peptides are typically prepared by chemical synthesis, rather than expression, so it is generally not feasible to incorporate full ^{15}N and ^{13}C isotopic labeling. For this reason,

many of the heteronuclear 2D and 3D experiments routinely used in protein NMR are not applicable to the study of constrained peptides. Homonuclear 2D NMR experiments therefore become the primary working tools of peptide NMR spectroscopy.

Here, we describe the study of conformationally constrained β-sheet peptides using solution-phase NMR spectroscopy. We detail how to prepare a sample, run an experiment, and process the NMR data. Based on the acquired data, we describe how to systematically generate peak assignments and utilize those peak assignments to identify spectroscopic hallmarks of β-sheet folding. We then detail the identification and validation of intermolecular contacts using isotopic labeling. Lastly, we conclude by illustrating the spectroscopic hallmarks of β-sheet folding and supramolecular assembly. These methods can be adapted to the study of the folding and supramolecular assembly of other peptides by solution-phase NMR spectroscopy.

Preparing a solution-phase NMR sample

Solution-phase NMR samples are prepared from purified (≥ 95%) lyophilized dry peptide synthesized through Fmoc-based solid-phase peptide synthesis (SPPS) protocols previously published by our laboratory.[12] These peptides are purified in binary acetonitrile-water mixtures with 0.1% trifluoroacetic acid (TFA), which provides trifluoroacetate counterions and improves separation of impurities. The molecular weight of the peptides is calculated as TFA salts, with side chains such as arginine, lysine, and aspartic acid assumed to be protonated. Use either D_2O or 9:1 H_2O/D_2O for NMR studies. Peptide samples run in D_2O provide information about the Hα protons while peptide samples run in 9:1 H_2O/D_2O provide complementary information about the amide NH protons.

Field strength, sample tubes, and solvent selection

Use NMR spectrometers with a field strength of ≥ 500 MHz for greater dispersion of peaks. Wilmad 5 mm Precision NMR tubes (528, 535, 541, 542) are recommended. NMR tubes should be stored in a 60 ºC oven to remove adventitious water when not in use. D_2O should be sourced from freshly opened ampules (≥ 99.9%) to minimize the size of the residual HOD peak. For samples run in 9:1 H_2O/D_2O, use deionized water (≥ 18 MΩ·cm) from a Barnstead GenPure Pro water purification system, or alternatively a Milli-Q water purification system.

Note:

- The oven temperature must remain below 70 ºC to prevent warping of the NMR tubes.

Sample preparation

1. Calculate the target mass of lyophilized peptide required for a 550 µL sample at your desired peptide concentration. A concentration of 1 or 2 mM is good starting point.
2. Weigh out the calculated mass of the lyophilized peptide in a low-binding Eppendorf tube on an analytical balance. Discharge static with a static gun prior to weighing.
3. Dissolve the lyophilized peptide in either D_2O or 9:1 H_2O/D_2O. Adjust the volume of solvent as needed to achieve the desired peptide concentration. (For dilute solutions, dissolve the peptide in 550 µL and assume the effect of the peptide on the total volume of solution is negligible.)
4. Vortex the Eppendorf tube until all lyophilized peptide has dissolved.
5. Transfer the solution to an oven-dried 5 mm NMR tube and cap immediately.

Notes:

- When weighing, err on the side of adding slightly more than the target mass required for a 550 µL sample. Insufficient sample volume can cause undesired distortions to NMR spectra.
- To let the amide NHs exchange out, let the sample stand at room temperature for 24 hr.

Internal standard (optional)

Several NMR standards are commonly used for peptide NMR such as sodium 3-trimethylsilyltetradeuteriopropionate (TSP-d_4), sodium 4,4-dimethyl-4-silapentane-1-sulfonate (DSS), and 4,4-dimethyl-4-silapentane-1-ammonium trifluoroacetate (DSA).[13] These standards can be used to reference chemical shifts. DSS is typically used for anionic peptides, as the negatively charged sulfonate group can interact undesirably with cationic peptides.[14] DSA replaces the negatively charged sulfonate with a positive charged ammonium group, which does not interact with cationic peptides. To add an internal standard, make a concentrated stock of the NMR standard in D_2O and titrate in as needed.

1. Weigh out approximately 10 mg of the NMR standard. Record the exact mass on the analytical balance.
2. Dissolve the standard in D_2O to make a 10 mM stock solution.
3. Add ~1 – 5 μL of the 10 mM stock solution to the NMR sample. The slight (<1%) dilution of the peptide that occurs on adding the stock solution can be ignored.

Selecting, loading, and running NMR experiments

Solution-phase NMR spectroscopy contains numerous experiments that can be used to study the folding and supramolecular assembly of conformationally constrained β-sheet peptides. Below are the experiments that have proven to be the most useful in our studies: ^{1}H NMR, TOCSY, NOESY, ROESY, EXSY, DOSY, ^{1}H,^{15}N HSQC, and ^{15}N-edited NOESY. These NMR experiments collectively provide insight into the folding and supramolecular assembly of peptides. In this section, we describe what information each experiment provides and how our laboratory sets up and processes NMR experiments.

3.a. Selecting an NMR experiment

^{1}H NMR

^{1}H NMR provides an overview of the behavior of the conformationally constrained peptide in aqueous solution. Amide NH, Hα, and aliphatic methyl side chains all have characteristic chemical shifts. Significant deviation from these characteristic chemical shifts can reveal information about the folding and supramolecular assembly.

Total correlation spectroscopy (TOCSY)

Total correlation spectroscopy (Total Correlation Spectroscopy) is useful for identifying intraresidue correlations associated with amino acid side chains. For peptide NMR, TOCSY is superior to the correlation spectroscopy (COSY) because the TOCSY experiment illuminates longer-range correlations between protons within the same spin system that are not observed in the COSY experiment. A key parameter in the TOCSY experiment is the mixing time, with longer mixing times (e.g. 150–200 msec) being needed to achieve full correlation within longer spin systems, such as Lys. The additional longer-range correlations simplify the identification of longer amino acid side chains, such as Leu, Ile, and Lys, which are often difficult to identify by COSY. In the TOCSY spectrum, the 20 canonical amino acids have characteristic chemical shifts and patterns which are illustrated in Figure **1.2**.

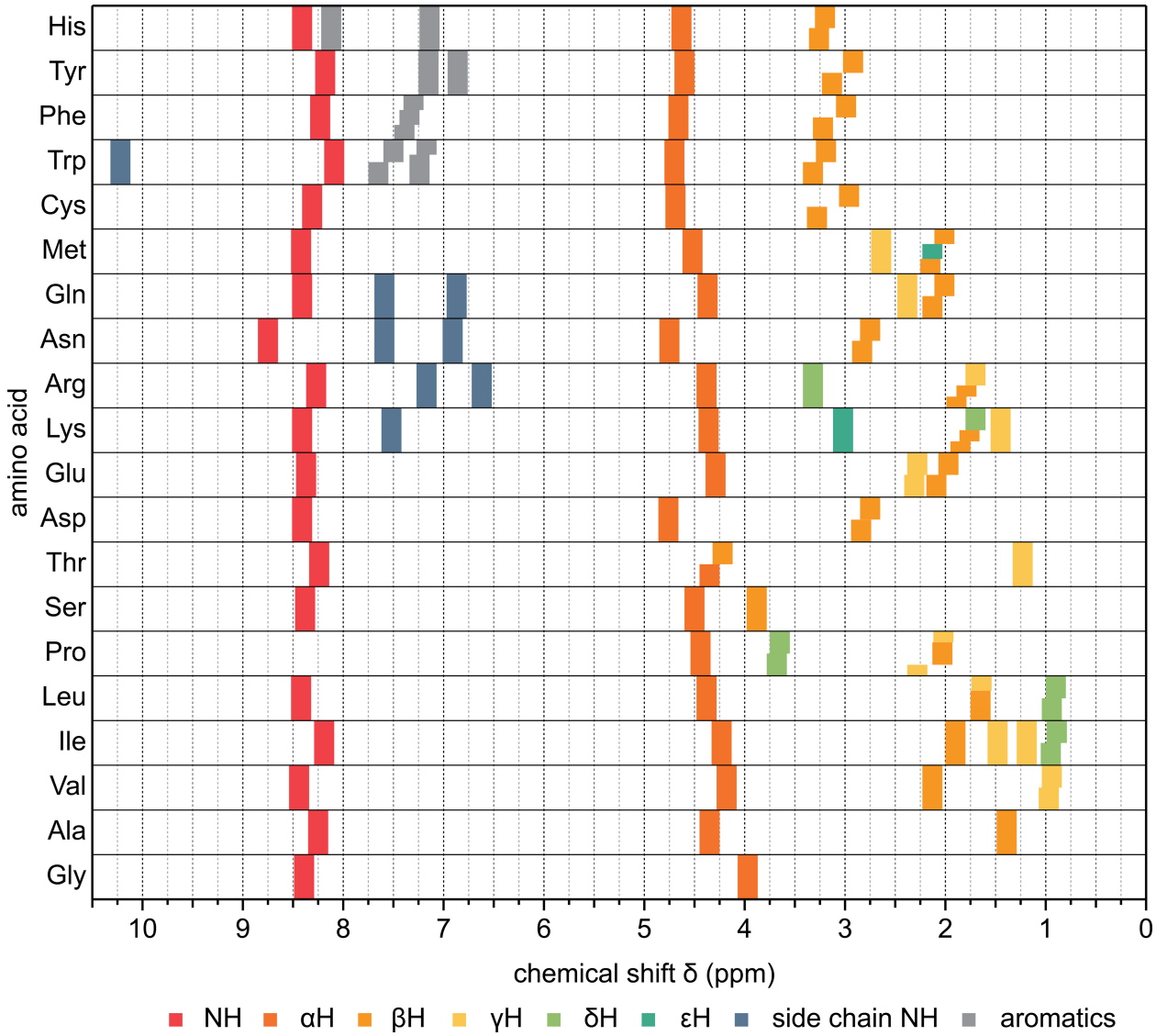

Figure 1.2. Representative chemical shifts for the 20 canonical amino acids in aqueous solution. Chemical shifts based on values reported by Wüthrich.[15]

Nuclear Overhauser effect (NOE) experiments: NOESY and ROESY

Nuclear Overhauser Effect spectroscopy (NOESY) and rotating frame Overhauser effect spectroscopy (ROESY) provide structural information on which protons are close in space based on the enhancement observed through the nuclear Overhauser effect (NOE). The strength of the NOE decays with an r^{-6} relationship, where r is the distance between the two protons. The upper

limit for a detectable H–H NOE is approximately 5 Å. Table **1.1** lists typical distances for β-sheet contacts and their relative NOE strength.

Table 1.1. Typical distances and relative NOE strength for β-sheet peptides.

H – H distance (Å)	Description	Relative NOE strength
1.8	Geminal CH_2	7.2
2.2	Hα to NH (interresidue)	2.2
2.5	Hα to Hα (interstrand)	1
3.0	NH to Hα (intraresidue)	0.3
3.2	NH to Hα (interstrand)	0.2
3.3	NH to NH (interstrand)	0.2
5	Upper limit of detection	0.02

While the NOESY and ROESY experiments both provide distance constraints, the two experiments are not fully interchangeable. NOESY measures the buildup of NOEs in a fixed frame of reference, while ROESY measures the buildup of NOEs in a rotating frame. A practical consequence of this distinction is that the sign and intensity of NOE crosspeaks in the NOESY experiment depend strongly on the rate of molecular tumbling, which correlates with molecular weight (MW). NOE crosspeaks appear positively phased in the NOESY spectrum for small molecules (MW < ca. 1000 Da) and negatively phased for large molecules (MW > ca. 2000 Da). For intermediately sized molecules (ca. 2000 > MW > ca. 1000), NOESY spectra will give weak to no NOE crosspeaks. Therefore, ROESY is recommended for intermediately sized molecules. In the ROESY experiment, NOE crosspeaks always appear positively phased opposite of the diagonal, irrespective of the molecular weight. However, the ROESY experiment is less sensitive than the NOESY experiment for large molecules (MW > ca. 2000).

For supramolecular assemblies of β-sheet peptides, we recommend running both the NOESY and ROESY experiments. The lower sensitivity of the ROESY experiments makes it easier to identify larger NOEs that typically correlate with intramolecular contacts useful for

peak assignments. Once peak assignments are complete, the NOESY spectra can then used to identify intermolecular contacts. For very large molecules or supramolecular assemblies (MW > ca. 5000 Da), which are in the negative NOE regime, the mixing time of NOESY experiments should be decreased to < 200 msec to limit spin diffusion which can convolute the analysis of the NOESY spectra.

Small molecular weight (MW < ca. 1000 Da)

- NOESY is recommended, because NOESY crosspeaks are strong than ROESY crosspeaks in this size regime.

Intermediate molecular weight (ca. 1000 Da < MW < ca. 2000 Da)

- ROESY is recommended, since NOESY crosspeaks are weak or absent in the intermediate molecular weight regime.

Large molecular weight (MW > ca. 2000 Da)

- Both NOESY and ROESY are recommended.
- Use the ROESY to assign peaks and identify intramolecular contacts.
- Use the NOESY to identify intermolecular contacts.

Exchange spectroscopy (EXSY)

Some peptides exhibit multiple sets of peaks because two (or more) conformers are in slow equilibrium or because monomeric and oligomeric species are in a slow equilibrium. These peptides can exhibit EXSY crosspeaks in the NOESY or ROESY spectra

If a peptide adopts multiple conformations that interconvert slowly, EXSY crosspeaks may appear in the NOESY or ROESY spectrum. EXSY crosspeaks can also appear if a peptide monomer is in slow equilibrium with an oligomer. These crosspeaks show correlation between identical protons in the different species. An EXSY experiment identifies protons that are correlated through either chemical or conformational exchange. EXSY experiments utilize the

exact same pulse sequence as that of a NOESY or ROESY experiment. To run an EXSY experiment, run a NOESY or ROESY experiment and look for peaks associated with exchange.

For EXSY crosspeaks to appear, the rate of exchange must occur on the NMR timescale, typically on the order of a hundred milliseconds. If exchange is substantially faster than tens of milliseconds, individual peaks are not seen for the different species. If exchange is substantially slower, than a few seconds, exchange crosspeaks are not observed. Variable-temperature (VT) NMR can be used to modulate the rate of exchange to occur on the order of hundreds of milliseconds.

Depending on the NMR experiment and molecular weight, the NOE crosspeak can either be the same or oppositely phased as that of EXSY crosspeaks (Table **1.2**). In NOESY experiments on small molecules (MW < ca. 1000), EXSY crosspeaks appear opposite in phase to NOE crosspeaks and in the same phase as the diagonal. For large molecules (MW > ca. 2000), the EXSY and NOE crosspeaks and the diagonal all appear in the same phase. In ROESY experiments, the EXSY crosspeaks always appear opposite in phase to the NOE crosspeaks and the diagonal. The phasing of the EXSY crosspeaks relative to the NOE crosspeaks. Because the exchange crosspeaks are always oppositely phased relative to NOE crosspeaks, ROESY is generally preferred for EXSY experiments.

Table 1.2. Relative phases of NOE and EXSY crosspeaks in the NOESY and ROESY spectrum.

	Molecular weight (Da)	Crosspeak	Phase (+/–)
NOESY	MW < ca. 1000 (small)	NOE	+
		EXSY	–
	ca. 2000 > MW > ca. 1000 (intermediate)	NOE	~ 0
		EXSY	~ 0
	MW > ca. 2000 (large)	NOE	–
		EXSY	–
ROESY	MW < ca. 1000 (small)	NOE	+
		EXSY	–
	ca. 2000 > MW > ca. 1000 (intermediate)	NOE	+
		EXSY	–
	MW > ca. 2000 (large)	NOE	+
		EXSY	–

Notes:

- The diagonal of both NOE experiments should be negatively phased.
- TOCSY artifacts appear in the ROESY spectra in the same phase as that of EXSY crosspeaks.

Diffusion ordered spectroscopy (DOSY)

The diffusion ordered spectroscopy experiment (DOSY) provides information about the translational diffusion coefficient of molecules in aqueous solution. DOSY measures the decay of signal from molecular diffusion according to the Stejskal-Tanner equation, where I is the signal intensity, γ is the gyromagnetic ratio, G is the gradient strength (*gpz6*), D is the diffusion coefficient, δ is the gradient duration (*p30*), and Δ is the diffusion time (*d20*).

Stejskal-Tanner Equation:

$$I_G = I_{G=0}{}^{-(\gamma\delta G)^2 D\left(\Delta-\frac{\delta}{3}\right)}$$

DOSY can be used to assess the oligomerization state and size of supramolecular assemblies formed by constrained β-sheet peptides. Assuming that peptides can be approximated as compact (spherical) structures, the diffusion coefficient scales proportionally with inverse cube of the molecular weight, $D \propto MW^{-1/3}$. (The compact-structure assumption applies well to

the cyclic peptides that our laboratory typically studies.) Therefore, the quotient of the diffusion coefficient for an oligomer relative to the diffusion coefficient of monomer provides an estimation of the oligomerization state (Table **1.3**). While distinguishing a dimer from a monomer is simple, distinguishing the oligomerization state for higher-order oligomers (n > 6) can be difficult to discern because of the smaller changes in the diffusion coefficient quotient.

Table 1.3. Typical diffusion coefficient quotients for small oligomers.

Oligomer	Quotient (relative to monomer)
monomer	1
dimer	0.79
trimer	0.69
tetramer	0.63
hexamer	0.55
dodecamer	0.46
hexadecamer	0.44

Loading an NMR Sample

1. Place the NMR tube in the sample spinner and adjust the height of the tube according to the depth gauge. Ensure that the solvent meniscus is above the recommended fill line; if it is slightly below, adjust the NMR tube to split the difference.
2. Load the NMR sample into the magnet using the *ij* command. **Caution: Remove keys, wallet, and other magnetic items from your pockets before approaching the magnet.**
3. Set up a ^{1}H NMR experiment on the computer using the *edcp* command in TopSpin.
4. Check that the sample is set to the correct temperature, typically 298 K, using the *edte* command and that the sample spinning is set to the appropriate position (*ON/OFF*). Spin the NMR sample for 1D experiments and do not spin for 2D experiments. If the sample spinning setting is changed, the sample must be reshimmed.

5. Match and tune the magnet by first typing the *wobb* command. Manually adjust the ^{1}H match and tune pins located underneath the magnet while observing the wobble curve on the computer screen. Adjust the tune pin before adjusting the match pin. Alternate between both pins until the magnet is matched and tuned. Alternatively, use the *atma* command if the spectrometer can match and tune automatically.
6. Lock to the solvent of the NMR sample.
7. Shim the magnet using the *lockdisp* command. Adjust the *[Z^1]* and *[Z^2]* shims to maximize the lock signal.
8. Adjust the *[X, Z^0]* and *[Y, Z^0]* shims to further maximize the lock signal.
9. Repeat steps 6 and 7 until no further increases to the lock signal can be obtained. Then press *[STD BY]*. Alternatively, use the *optshim* command to automatically optimize the shims.

Running NMR experiments

1. Set the receiver gain using the *rga* command and run an 8 scan ^{1}H NMR experiment using the *zg* command. Wait until the experiment completes.
2. Use the *ft* and *apks* commands to process the ^{1}H NMR spectra to verify the shims. Inspect the HOD peaks to check the shims.
3. Set up another experiment using the *iexpno 2* command. For each subsequent experiment, increment the experiment number by 1.
4. Set the receiver gain using the *rga* command and optimize the parameters corresponding to the NMR experiment(s) shown in Table **1.4**.
5. Run the experiment using the *zg* command.

Table 1.4. Summary of key NMR acquisition parameters.

Experiment	Key parameters
^{1}H NMR	ns = 64 scans sw = 12 ppm o1p = 4.79 ppm experiment time = 8 min
TOCSY (gradient)	ns = 4 scans sw = 12 ppm o1p = 4.79 ppm td = 512 increments d9 = 25, 50, or 200 msec experiment time = 1 hour 20 min Note: Use the same receiver gain used for the proton NMR to avoid ADC overflow.
NOESY (gradient)	ns = 4 scans sw = 12 ppm o1p = 4.79 ppm d8 = 1 sec td = 512 increments experiment time = 2 hours
ROESY	ns = 4 scans sw = 12 ppm o1p = 4.79 td = 512 p15 = 200 msec experiment time = 1 hour 30 min
DOSY	sw = 12 ppm o1p = 4.79 ppm gpz6 = 2 or 95 % d1 = 5 sec p1 = variable, typically about 10 μsec d20 = variable, typically 50–100 msec p30 = variable, typically 1200–2500 μsec experiment time = 1 hour
^{1}H,^{15}N HSQC	ns = 4 scans sw = 12 ppm o1p = 4.79 ppm d1 = 1 sec td (f_2, f_1) = 2048, 512 experiment time = 45 min
^{1}H,^{15}N-edited NOESY	ns = 4 scans sw = 12 ppm d8 = 120 msec o1p = 4.79 ppm td (f_3, f_2, f_1) = 2048, 1, 1024 experiment time = 1 hour 30 min

Always double check the acquisition parameters save before running the experiment!

The acquisition parameters listed in Table **1.4** are general recommendations and can be adjusted to maximize spectral resolution and signal-to-noise (S/N) ratio. To maximize spectral resolution and S/N, we recommend the following:

1. Narrow the spectral window (sw, o1p) to maximize resolution of the f_2 dimension.
2. For 2D experiments, increase the number of increments (td) in the f_1 dimension to reduce the distortion of crosspeaks in the f_1 dimension.
3. Select the appropriate mixing time maximizes the observed signal. The mixing time (d8, d9, or p15 depending on the experiment) refers to the time between applying a pulse and observing the resulting FID.

Multiple experiments

To minimize the burden on the NMR facilities, we recommend queueing up experiments overnight.

1. Follow steps 1–5 in the Running NMR experiments section.
2. Use the *iexpno* command to create a new NMR experiment and set up the parameters corresponding to the experiment.
3. Use the *rga* command to set the receiver gain for the experiment.
4. Repeat Steps 2 and 3 as needed for each new experiment.
5. Run the experiments using the *multizg* command. The computer will prompt which experiment number to start on.

Solvent suppression

Water suppression by gradient tailored excitation (WATERGATE) is required for all samples run in 9:1 H_2O/D_2O.

1. Follow steps 1–3 in the Running NMR experiments section.

2. Use the *cop 2* command to create a copy of the ^{1}H NMR experiment.
3. Use the *setsfo1* and *keepsfo1* commands to set and load the observation frequency to the water peak into the solvent suppressed ^{1}H NMR. Make sure to select *h1sup.** experiment prior to closing the experiment window.
4. Set the acquisition, *aq*, to 1.5 and the relaxation delay, *d1*, to 5.
5. Use the *aqcu* command to go to the acquisition window and type *gs*.
6. Adjust the *o1* frequency to minimize the size of the FID. Save the frequency and stop the pulsing.
7. Verify that the spectral width, *sw*, covers the entire spectral window.
8. Use the *rgazg* command to set the receiver gain and start the experiment.
9. For subsequent 2D experiments that require solvent suppression, select the corresponding experiment with the solvent suppression suffix.

Note:

- The WATERGATE solvent suppression also suppresses peaks within ~1 ppm of the HOD peak.

Variable temperature (VT)

1. Follow steps 1–3 in the Running NMR experiments section.
2. Use the *edte* command to open the temperature controller.
3. Change the *Target temp.* to the desired setpoint. Once the *Sample temp.* has reached the desired setpoint, wait five minutes to allow the sample to thermally equilibrate.
4. Use the *iexpno* # command to create a new experiment. Set the desired acquisition parameters and run with *rgazg*.
5. For each additional temperature, the *Target temp.* needs to be reset and equilibrated.

6. Once all variable temperature experiments are complete, change the Target temp back to 298 K and wait until the sample equilibrates.
7. Use the *ej* command to eject the sample.

Notes:

- Do not heat or cool the NMR sample past the boiling and freezing point. Note that D_2O freezes at 3.8 ºC and boils at 101.4 ºC. Always leave a 10 ºC margin of error when setting *Target temp*.
- Because the chemical shift of the HOD peak varies with temperature, VT NMR can be used to walk the water peak to enable analysis of the Hα protons buried underneath the residual HOD peak.
- VT NMR is also useful for studying the exchange rates of EXSY crosspeaks.

DOSY

1. Run an 8-scan ^{1}H NMR to check shims. Verify sample spinning is OFF.
2. Use *iexpno 2* command and change the pulse program from *zg30* to *zg0*. Vary *p0* value to calibrate the pulse time (default: 32 μsec).
3. Type *edcp* to create a new experiment and select the *dosy1D* experiment to calibrate the diffusion time and diffusion gradient length.
4. Set *p1* to equal *p0*/4. Set Δ (*d20*) to 75 ms, δ (*p30*) to 1200 μs, and gradient strength, *gpz6* to 2%. Use the *etde* command to verify that the parameters saved. Run the experiment with *rgazg*.
5. Run the *1D DOSY* experiment and process using the FID using the *efp* command. Phase-correct the ^{1}H NMR spectra as needed.
6. Use *iexpno 4* command to create an identical instance of the *dosy1D* experiment. Set the gradient strength, *gpz6* to 95%. Run the experiment with *zg* (do not use *rgazg* because the receiver gain must remain constant between both 1D DOSY experiments). Phase correct the ^{1}H NMR spectra as needed.

7. Create a stacked plot of both *dosy1D* spectra. The attenuation of signal between both *dosy1D* experiments should be 20x. If the attenuation is not 20, rerun both *dosy1D* experiments while varying *d20* and/or *p30* until the 20x signal attenuation is achieved.
8. Use the *makedosy2d* to set up a pseudo two dimensional DOSY experiment. Use the edte command to check *p1*, *d20*, and *p30* saved.
9. Run the pseudo 2D DOSY experiment using *dosy 2 95 16 l y y*.

Notes:

- Accurate DOSY measurements require calibration of *p1*, Δ, and *δ*. Increasing either Δ or δ leads to greater signal attenuation.
- To minimize the number of scans required for adequate S/N at high gradient strengths (*gpz6* = 95%), the ^{1}H NMR spectra can be processed with increased line broadening, *lb* to increase the S/N. Increase *lb* from 0.3 Hz to 5 Hz for both 1D DOSY experiments.
- **The gradient duty cycle, p30/(d1+aq) ≤ 0.05, must never exceed 5%. Increasing the gradient duty cycle above 5% can damage NMR hardware.**

^{1}H,^{15}N HSQC and ^{15}N-edited NOESY

1. On TopSpin click on the *Acquire* Tab, go to *More*, and open *BioTop*.
2. In Sample Information Tab, enter in the molecular size (kDa), isotopic labeling, solvent, and tube. Select the check box for the *Temperature*, *Lock automatically*, *Tune/Match Automatically*, and *Shim Automatically*.
3. In the *Optimization tab*, select the check box for *Auto opt.* corresponding to the isotopes present in your sample. Press *Start optimization* at the bottom of the Menu. The automated optimization takes around five minutes, and you may encounter an ADC overflow warning as the program is optimizing the solvent suppression parameters.
4. In the *Experiments tab*, select the ^{1}H NMR experiment with WATERGATE solvent suppression (*ZGGPW5*), add the experiment to the queue, and press *Run Experiments*. Once the ^{1}H NMR experiment is complete, process the spectrum to verify the shims.

5. To set up a $^{1}H,^{15}N$ HSQC experiment, select ^{15}N HSQC and adjust the acquisition parameters (see Table **4** for recommended parameters).
6. To set up a ^{15}N-edited NOESY experiment, select the *2D WaterGATE NOESY* experiment and adjust the acquisition parameters (see Table **4** for recommended parameters).
7. Press Run Experiments to run the isotope edited experiments.

Processing NMR experiments

1D Experiments

1. Type *ft* to Fourier Transform the FID and *apks* to phase correct.
2. In the *Processing* menu, select *Adjust Phase* to manually phase correct the ^{1}H NMR spectrum. Iterate between applying zero-order (*p0*) and 1st-order (*p1*) phase corrections until all peaks appear symmetrical. Press the *Return & Saved Spectrum* button.
3. In the *Processing* menu, select the *baseline correction* option. Use the polynomial baseline correction up to the third term (Cx^2). Press the *Return, save regions button*.
4. In the *Processing* Tab, select the *Calib. Axis*. For peptide samples run in D_2O, reference to the solvent residual at 4.79 ppm for samples run at 298 K. For peptide samples run in 9:1 H_2O/D_2O reference to a diagnostic peak such as a methyl singlet for the same peptide run at the same concentration and temperature in D_2O.
5. In the *Analysis* tab, integrate all observed protons and pick peaks.

Notes:

- As a rule of thumb, the integrations for peptide NMR should be within 5 – 10% for a properly phased and baseline corrected ^{1}H NMR spectrum.
- Normalize integrals to a proton of known integration such as an aromatic resonance, Hα proton, or distinct methyl group.
- The integration of the residual HOD peak should be smaller than 100 mM for D_2O samples. Estimate this by comparing the integration of the HOD peak at 4.79 ppm for samples run at 298 K to the integration of peptide proton or known NMR standard.

2D Homonuclear experiments

1. Type *xfb* to Fourier Transform and *abs2* to phase correct.
2. In the Processing menu, select Adjust Phase and pick three points along the diagonal to phase correct. Phase correct the Rows by iterating between applying zero-order (*p0*) and 1st-order (*p1*) phase corrections until all peaks appear symmetric. Press the *Return & Save phased spectrum*. Then, phase correct on the columns. Press the *Return* button.
3. In the *Processing* menu, calibrate the 2D homonuclear experiment to either a solvent residual or to the same peak used to calibrate the reference ^{1}H NMR spectrum.
4. Click on f_2 projection above the 2D homonuclear spectrum and right click to open a dropdown menu. Select *External Projection* and specify the *External Projection* to point to the processed ^{1}H NMR spectrum. Repeat the same process to set an *External Projection* in the f_1 axis.

2D Heteronuclear experiments

^{1}H,^{15}N HSQC

1. Type *xfb* to Fourier Transform and *abs2* to phase correct.
2. In the Processing menu, select *Adjust Phase* and pick three points along the diagonal to phase correct. Phase-correct the *rows* by iterating between applying 0 order (*p0*) and 1st order (*p1*) phase corrections until all peaks appear symmetric. Press the *Return & Save phased spectrum*. Repeat the Phase correction on the *columns*. Then press the *Return* button.
3. Use the *xiref* command to reference the peaks.

4. Click on the f_2 and f_1 projection around the 2D heteronuclear spectra reference the ^{1}H,^{15}N HSQC to the corresponding NMR spectra for the unlabeled peptide at the same concentration and temperature.

^{15}N-edited NOESY

1. Type *xfb* to Fourier Transform and specify a new experiment number to save the 2D data. Then type *abs2* to phase correct the 2D spectrum.
2. In the *Processing* menu, select *Adjust Phase* and pick three amide NHs along the diagonal to phase correct. Phase-correct the rows by iterating between applying zero-order (*p0*) and 1st-order (*p1*) phase corrections until all peaks appear symmetric. Press *Return & Save phased spectrum*. Repeat the phase-correction on the columns. Then press the *Save for nD Spectrum* button.
3. Use the *xiref* command to reference the peaks.
4. Click on f_2 projection above the 2D homonuclear spectrum and right click to open a dropdown menu. Select *External Projection* and specify the *External Projection* to point to the processed ^{1}H NMR spectrum. Repeat the same process to set an external projection in the f_1 axis. We recommend referencing the ^{15}N-edited NOESY to the unlabeled peptide in 9:1 H_2O/D_2O for the f_2 axis and the unlabeled peptide in either D_2O or 9:1 H_2O/D_2O for the f_1 axis.

DOSY

1. Type *rser* to phase correct *FID# 1* and name it *EXPNO 999*. Press *Okay*.
2. Process the ^{1}H NMR spectrum using the *efp* command.
3. In the *Process Tab*, select adjust phase and manually phase correct the ^{1}H NMR spectrum. Press the *Save for nD spectrum* button, then press *Return*.

4. Return to the 2D DOSY experiment. Type *xf2* and *abs2* to Fourier Transform and baseline correct.
5. Type *setdiffparm* to prepare the DOSY parameters for processing.
6. Type *eddosy* to view the processing parameters with DOSY. We recommend windowing the *DISPmin* and *DISPmax* parameters between -12 and -8, respectively.
7. Type *dosy2d* to process the 2D DOSY experiment.
8. Calibrate the diffusion coefficient of the residual HOD peak (4.79, -8.7212).[16]
9. To calculate the translational diffusion coefficient, identify a horizontal track in the DOSY track and record the f_1 coordinates. For example, a track at -9.008 in the f_1 axis would correspond to a diffusion coefficient of $10^{-9.008} = 9.81 \times 10^{-10}$ m^2/s.

Generating peak assignments

Peak assignments are essential for studying the folding and assembly of β-sheet peptides. Here, we describe a systematic approach for generating peak assignments (Figure **1.3**). We recommend first identifying residue-specific tracks in the TOCSY spectra. Once these residue-specific tracks are identified, analyze the ROESY spectra to identify adjacent residues. Finally, generate sequence specific assignments by analyzing the TOCSY in conjunction with the ROESY data.

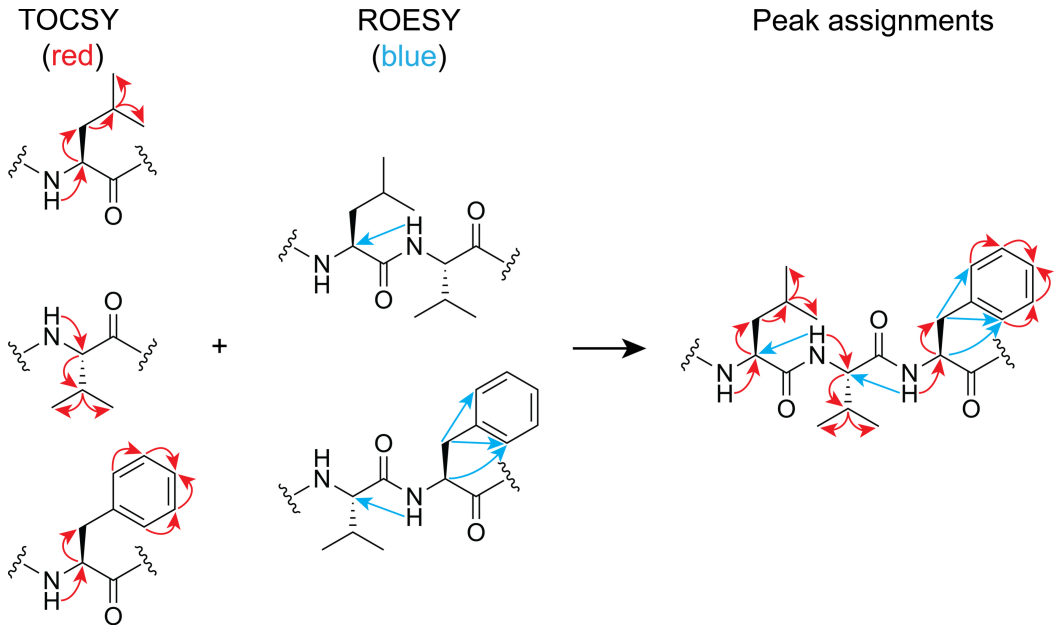

Figure 1.3. Overview of generating peak assignments using TOCSY and ROESY NMR.

TOCSY

1. Analyze the TOCSY spectra of your peptide in 9:1 H_2O/D_2O with WATERGATE solvent suppression between 10 – 7 ppm in the f_2 dimension and 10 – 7 ppm in the f_1 dimension.
2. Draw a vertical line corresponding to each amide NH observed in the NMR spectra and verify that the number of tracks corresponds with the number of residues in the peptide sequence.
3. Inspect each vertical TOCSY track and compare the observed crosspeaks to the typical chemical shifts for the 20 canonical amino acid (Figure **1.2**).
4. For each vertical TOCSY track, make tentative assignments based on the peptide sequence and observed crosspeaks. It is often helpful to group and assign residues by asking a series of diagnostic questions. Ambiguous residues can be left unassigned at this stage and revisited later.
    a. Does this residue lack side chain protons (Gly) or an amide NH (Pro)?
    b. Does this residue contain an aliphatic methyl group (Ala, Val, Leu, Ile)?

i. How many methyl groups does this aliphatic residue contain?

ii. What is the splitting for the aliphatic residues?

c. Does this residue contain aromatic side chains (Phe, Tyr, Trp, His)?

i. What is the integration and splitting for the aromatic side chains?

d. Does this residue contain a side chain NH (Trp, Gln, Asn, Arg, Lys)?

i. How many methylenes does the side chain contain and how many are observed?

e. Does this residue contain an aliphatic alcohol (Ser, Thr)?

f. Based on process of elimination, can this residue be one of the remaining amino acids (Met, Glu, Asp, Cys)?

i. How many methylene protons are observed?

5. Once all the TOCSY tracks have been analyzed, proceed onwards with analyzing the ROESY spectra.

Notes:

- The chemical shifts for the 20 canonical amino acids shown in Figure **2** should be taken as a guideline because the shifts can be affected by secondary structure and supramolecular assembly. The resulting changes in chemical shift can affect the chemical shifts of resonances by up to 1 ppm, or more in some cases.
- It is particularly challenging to assign residues when multiple resonances overlap (≤ 0.02 ppm). Make sure to consider different possibilities for the amino acids that are involved, as it is easy to make mistakes.
- If you are unsure about an assignment, record all possible residues assignments and revisit later.

ROESY

1. Analyze the ROESY spectra of your peptide in 9:1 H_2O/D_2O with WATERGATE solvent suppression between 10 – 7 ppm in the f_2 dimension and 6 – 4 ppm in the f_1 dimension.
2. Draw a vertical line corresponding to each amide NH observed in the ROESY spectra.

3. For each ROESY track, analyze the NH to Hα crosspeaks based on your tentative peak assignments. Within a β-strand, the strongest NOE should correspond to an interresidue NH to Hα contact between adjacent residues.
4. For residues containing aromatic side chains, analyze the ROESY spectra for intraresidue NOE crosspeaks between the aromatic protons (~7 – 8 ppm) to the adjacent methylene (~3 ppm) or Hα proton (~4 – 6 ppm).
5. Once all the ROESY tracks have been analyzed, revisit the TOCSY tracks corresponding to unassigned residues. Iterate between analyzing the peptide sequence, TOCSY, and ROESY spectra until all the residues have been assigned.

Note:

- Additional weaker intraresidue NOE crosspeaks associated with the NH-Hα protons may be observed as well as NOEs associated with intermolecular contacts (discussed in a subsequent section).

Peak assignments

1. Inspect the peptide sequence to identify entry points to generate sequence specific assignments. An entry point can be any residue that can be unambiguously assigned. Useful entry points often include *N*-methylated amino acids, glycine, and any residue that appears once in the peptide sequence.
2. For each entry point, use the ROESY spectra to identify adjacent residues and build peptide fragments. The TOCSY provides intraresidue NH to Hα correlations while the ROESY provides interresidue NH to Hα correlations for building out peptide fragments.
3. TOCSY and ROESY spectra can be chained to perform an NH to Hα walk. We recommend performing an NH to Hα walk starting from the *N*-terminal residue to the *C*-terminal residue to check the sequence specific peak assignments. For cyclic peptides, systematically walk around the peptide using both the TOCSY and ROESY spectra.

Note:

- Accurate peak assignments are the foundation of all peptide NMR studies. We strongly recommend using a variety of different methods to validate peak assignments including isotope-edited experiments (partial deuteration, ^{15}N-labeling), considering pairwise swaps of residues with similar chemical shifts (e.g., Cys and Met), and carefully analyzing the peak assignments in areas of heavy spectral overlap.

Identifying spectroscopic hallmarks of β-sheet folding

The chemical shifts of the Hα protons, interstrand NOEs, and magnetic anisotropy of the $^{\delta}$Orn turn units are three spectroscopic signs of folding in aqueous solution (Figure **1.4**). Pioneering work by Wishart identified that the chemical shifts of Hα protons correlate with the secondary structure in peptides and proteins.[17] Upfield shifts of the Hα resonances suggest α-helical secondary structure while downfield shifts of Hα resonances suggest β-sheet secondary structure. Specifically, downfield shifts of ≥ 0.2 ppm relative to random coil values is characteristic of β-sheet secondary structure. Even greater downfield shift often occurs if there is further supramolecular assembly through β-sheet interactions. The NOESY spectra reveal networks of interstrand contacts when cyclic peptides fold in aqueous solution. These interstrand contacts typically occur between NH-NH, NH-Hα, and Hα-Hα protons. Previous spectroscopic studies established that the magnetic anisotropy of the diasterotopic δ-linked ornithine ($^{\delta}$Orn) δ-protons is a spectroscopic probe for folding.[10] For β-sheet peptides, a magnetic anisotropy of 0.6–0.7 ppm indicates complete folding, while a magnetic anisotropy of ≤ 0.1 indicates little or no folding. Intermediate values reflect partial folding.

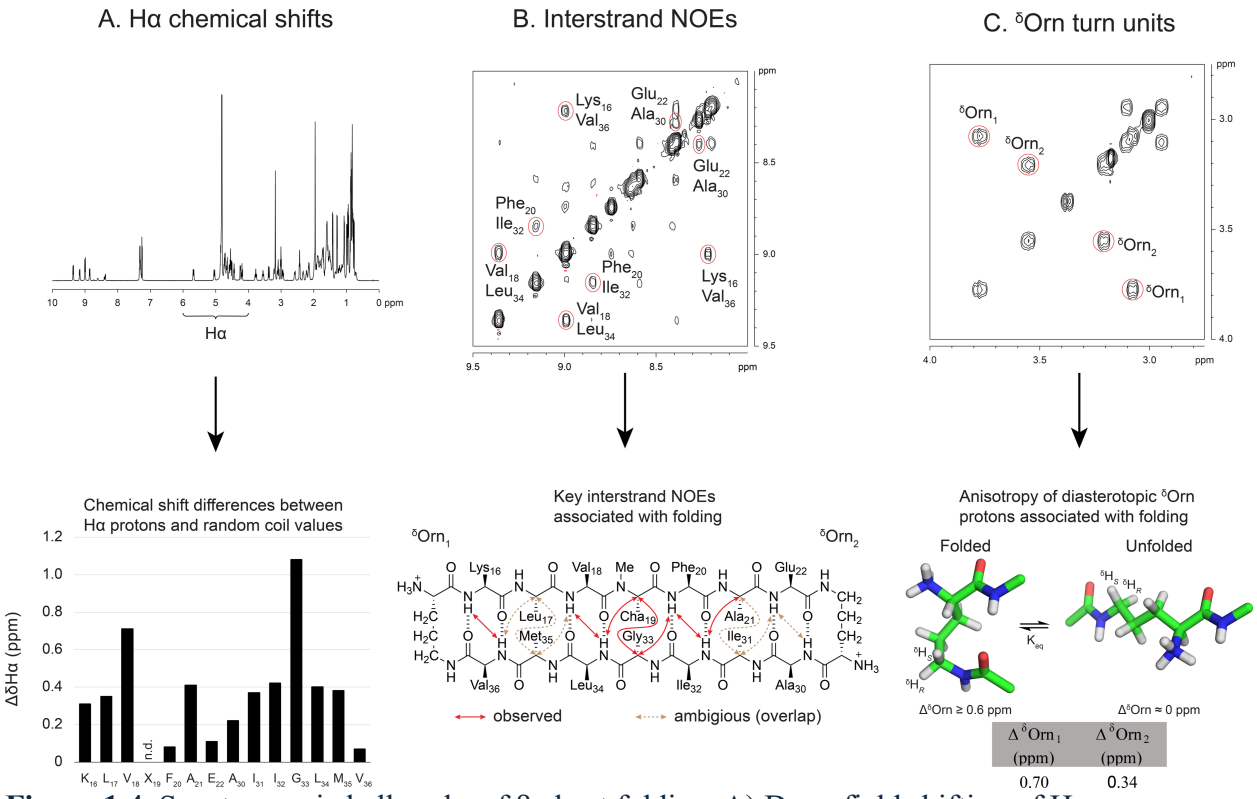

Figure 1.4. Spectroscopic hallmarks of β-sheet folding. A) Downfield shifting of Hα resonances relative to random coil values. B) Interstrand NOEs associated with folding. C) Magnetic anisotropy of the diastereotopic $^{\delta}$Orn protons.

Chemical shifts of Hα protons

1. Tabulate the chemical shifts of all the assigned Hα proton.
2. Calculate the difference between the observed Hα chemicals and random coil values. We recommend the chemical shifts reported by Wishardt, Sykes, and Richards.[18,19]
3. Plot the chemical shifts differences between the observed and random coil values to visualize the secondary structure.

Interstrand NOEs

1. Analyze in the NOESY spectra of your peptide in D_2O between 6 – 4 ppm in the f_2 dimension and 6 – 4 ppm in the f_1 dimension. Using the sequence-specific peak assignments, identify Hα–Hα NOE crosspeaks consistent with β-sheet folding.

2. Analyze the NOESY spectra of your peptide in 9:1 H_2O/D_2O with WATERGATE solvent suppression between 10 – 7 ppm in the f_2 dimension and 10 – 7 ppm in the f_1 dimension. Based on the sequence specific peak assignments, identify NH-NH NOE crosspeaks consistent with β-sheet folding.
3. Analyze the NOESY spectra of your peptide in 9:1 H_2O/D_2O with WATERGATE solvent suppression between 10 – 7 ppm in the f_2 dimension and 6 – 4 ppm in the f_1 dimension. Identify NH-Hα NOE crosspeaks consistent with folding.

δ-Linked ornithine turn unit

1. Inspect the ^{1}H NMR spectra in D_2O between 4 – 2.75 ppm to identify the *pro-S* $^{\delta}$Orn proton(s).
2. Analyze in the NOESY spectra of your peptide in D_2O between 4 – 2.75 ppm in the f_2 dimension and 4 – 2.75 ppm in the f_1 dimension. Identify the strong crosspeak between the diasterotopic *pro-S* and *pro-R* $^{\delta}$Orn protons.
3. Calculate the magnetic anisotropy based on the difference in chemical shift between the f_2 and f_1 dimensions to assess the extent of β-sheet folding.

Identifying intermolecular contacts

The appearance of intermolecular NOEs is a hallmark of the supramolecular assembly of constrained β-sheet peptides. The following workflow outlines a systematic approach for identifying intermolecular NOEs in the homonuclear 2D NOESY spectra and utilizing those NOE crosspeaks to elucidate the close contacts between molecules.

1. Generate sequence-specific peak assignments using the TOCSY and ROESY spectra.
2. Analyze the homonuclear 2D NOESY spectra for NH-NH, NH-Hα, and Hα-Hα contacts. Annotate all observed crosspeaks.

3. Identify all intramolecular contacts associated with residue specific peak assignments and folding. Additionally, note any crosspeaks arising from chemical exchange. Mark off all NOE crosspeaks that correspond to intramolecular contacts.
4. Analyze the remaining NOE crosspeaks to identify the intermolecular contacts. Outer-facing amide NH and Hα protons form intermolecular contacts. Inner-facing amide NH and Hα protons form interstrand intramolecular contacts.
5. Categorize the intermolecular contacts based on crosspeak strength and look for patterns. For each intermolecular contact, examine adjacent NH or Hα protons for additional intermolecular NOEs. Typically, a minimum of three intermolecular contacts is used to confirm the formation of a stable intermolecular interface.

Notes:

- Contacts between identical protons at the same chemical shift cannot be identified by NOESY or ROESY experiments.
- NOEs that can either be intermolecular or intramolecular cannot be used to unambiguously identify intermolecular contacts.

Confirming intermolecular contacts with isotopic labeling

While homonuclear 2D NMR experiments are the primary tools for studying constrained β-sheet peptides by solution phase NMR spectroscopy, heteronuclear 2D NMR experiments can also be useful to study the supramolecular assembly of peptides. The incorporation of an isotope aids in the confirmation of intermolecular contacts. We have found ^{15}N labeling of selected amino acids to be a powerful tool for identifying key contacts in constrained β-sheet peptides. Deuterium labeling can also be useful. Isotope edited experiments should be performed to address specific ambiguous crosspeaks after 2D homonuclear NMR experiments have been fully analyzed. We have found isotopic labeling to be useful in dealing with mixtures of monomer and complex oligomers in which the NMR spectra is heavily overlapped. Here, we describe how to

design an isotope labeling scheme, preparing the suitably protected amino acid, and analyzing the resulting heteronuclear 2D NMR experiment.

Isotope labeling design

1. Analyze intermolecular interfaces identified in determining the intermolecular NOE crosspeaks and list two protons involved in each intermolecular contact.
2. For intermolecular contacts involving amide NHs, consider using a ^{15}N-labeled amino acid. For intermolecular contacts involving Hα protons, consider using specifically or fully deuterated amino acids.
3. Identify key intermolecular contacts along each interface and design suitable isotopic labeling scheme(s) by selecting one of the protons involved in an intermolecular contact to isotopically label. At minimum, label the strongest contact along teach interface.

Note:

- The pricing and availability of isotopically labeled amino acids may influence the design of the isotope labeling scheme.

Fmoc-protection of isotopically labeled amino acids

1. Purchase the corresponding isotopically labeled amino acid from a commercial vendor, such as Cambridge Isotope Laboratories. ^{15}N-Labeled amino acids without functional groups in the side chains (Gly, Ala, Phe, Leu, and to a lesser extent Met and Ile) are relatively economical and are good choices for isotopic labeling. Some deuterated amino acids are also available albeit at higher cost.
2. Weigh out the isotopically labeled amino acid in a round bottom flask. Add a stir bar. Then add 0.95 equivalents of Fmoc-OSu to a round bottom flask.
3. Add 1:1 acetonitrile/H_2O to the round bottom flask. We recommend adding 5 mL of solvent per 100 mg of amino acid.

4. Dissolve the solids in 1:1 acetonitrile/H_2O. Add 5 mL of solvent per 100 mg of amino acid. The solids won't dissolve right away.
5. Then add 1 equivalent of neat Et_3N and let the reaction stir for 15 minutes.
6. Add additional Et_3N slowly, dropwise via syringe, as needed until the solution becomes homogeneous. Do not add a gross excess of Et_3N because Fmoc is base-labile. Check and record the pH of the solution.
7. Let the reaction stir for 1 hr at room temperature.
8. Precipitate the Fmoc-protected amino acid by the solution to 1 M HCl while stirring vigorously. We recommend 25 mL of 1 M HCl per 100 mg of amino acid.
9. Filter the Fmoc-protected amino acid using filter paper and a Büchner funnel.
10. Assess the purity of Fmoc-protected amino acid by NMR and mass spectrometry. Pay special attention to $^1J_{NH}$ splitting for ^{15}N amino acids and the isotopic pattern in the mass spec for deuterated amino acids.
11. Typical yields of the Fmoc-protected amino acid are ≥85%.

Note:

- We recommend purchasing the unprotected amino acid and doing the Fmoc protection in-house, because the reaction is high yielding and does not require purification by column chromatography prior to use. Fmoc-protected isotopically labeled amino acids are significantly more expensive than their unprotected counterparts.

Deuteration

Deuterated peptides can be analyzed by running the standard homonuclear 2D NMR experiment. If a proton involved in an intermolecular contact is deuterated, the corresponding NOE disappears from the NOESY spectra. Additionally. the ^1H NMR spectra of a deuterated peptide can also be used to cross-check peak assignments.

^{1}H,^{15}N HSQC

Heteronuclear HSQC experiments can be analyzed comparing the chemical shifts and number of crosspeaks to the peak assignments for the unlabeled peptide. The ^{1}H, ^{15}N HSQC experiment can be useful for quickly discerning the number of distinct oligomer species present when constrained peptides self-assemble because each peak corresponds to a single species.

^{15}N-edited NOESY

The ^{15}N-edited NOESY can be an essential experiment for verifying key intermolecular contacts and resolving heavy overlap in the amide NH region. The extra dispersion afforded by access to an orthogonal dimension (^{15}N) greatly simplifies the NOESY spectra by greatly reducing the observed number of crosspeaks. A limitation of the ^{15}N-edited NOESY experiment is that it cannot resolve overlapping resonances in the f_1 dimension. Distinguishing ambiguous crosspeaks from spectral overlap in the f_1 dimension requires chemical intuition and knowledge of sequence-specific peak assignments.

Elucidating spectroscopic hallmarks of supramolecular assembly

The supramolecular assembly of constrained β-sheet peptides is characterized by several spectroscopic hallmarks of assembly in solution-phase NMR spectroscopy (Figure **1.5**). These characteristics include peak broadening, further downfield shifting of oligomer Hα resonances, upfield shifting of some aromatic and aliphatic methyl protons, new peaks associated with oligomer, and a specific reduction in the diffusion coefficient. Here, we describe how to identify the spectroscopic hallmarks of supramolecular assembly.

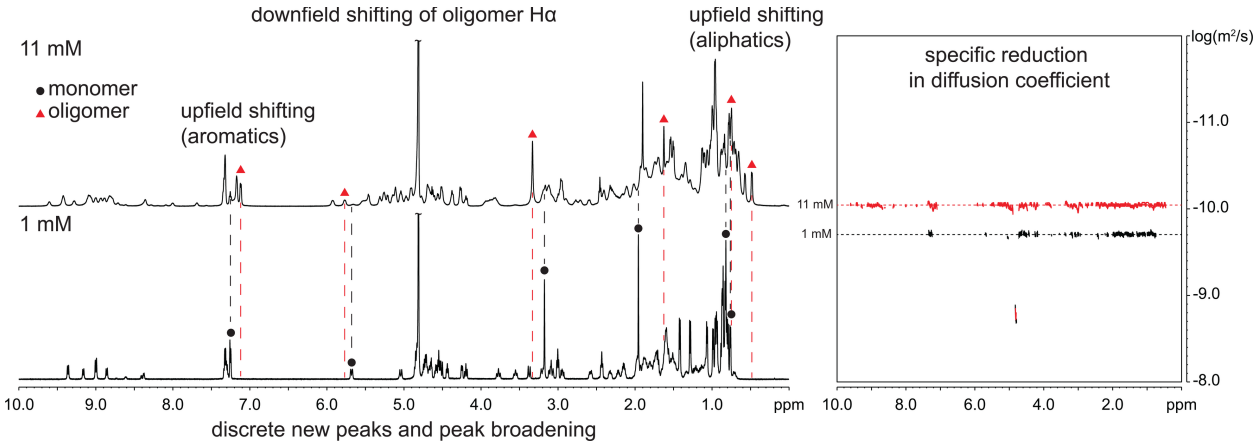

Figure 1.5. Spectroscopic hallmarks of supramolecular assembly observed in ^{1}H NMR and DOSY spectra. These hallmarks are discrete new peaks associated with oligomer, downfield shifting of oligomer Hα protons, upfield shifting of some aromatic and aliphatic resonances, peak broadening, and a specific reduction in diffusion coefficient.

Discrete new peaks associated with oligomer

1. Inspect the ^{1}H NMR stacked plot and look for the appearance of new peaks associated with oligomer. These new peaks should be clearly distinct in chemical shift from the monomer resonances
2. Analyze the homonuclear NOESY and ^{15}N-edited NOESY to identify intermolecular contacts.

Notes:

- If a peptide oligomerizes through transient, nonspecific interactions, the ^{1}H NMR spectrum at high concentration may look virtually identical to the ^{1}H NMR spectrum at low concentrations but significantly broadened.
- At intermediate concentrations, multiple sets of peaks may appear, corresponding to both monomer and oligomer species.

Downfield shifting of Hα resonances associated with oligomer

1. Look at the stacked plot of your constrained β-sheet peptide, paying special attention to the Hα region around 4 – 6 ppm.

2. Look for downfield shifting of the Hα oligomer resonances with increasing peptide concentration. As a rule of thumb, Hα chemical shifts downfield of 5 ppm are significant.
3. Compare the Hα chemical shifts of the monomer relative to the oligomer. The supramolecular assembly of constrained peptides into well-defined oligomers often reinforces β-sheet secondary structure, which is reflected as further downfield shifting of Hα resonances for the oligomer relative to the monomer. This can further be corroborated with the magnetic anisotropy of the diasterotopic $^{\delta}$Orn protons.

Upfield shifting of some aromatic and aliphatic resonances

1. Examine the stacked ^{1}H NMR plot, focusing on the the aromatic region around 7 – 8 ppm and the aliphatic region around 0 – 2 ppm.
2. Look in the stacked plot and look for upfield shifting of aromatic resonances and appearance of methyl groups upfield of 0.5 ppm.
3. Corroborate the upfield shifting of the upfield shifted resonances with NOE crosspeaks in the NOESY spectra. The presence of these NOE crosspeaks often indicates hydrophobic packing associated with the formation of a well-defined oligomer.

Peak broadening

1. Generate a stacked plot of your constrained β-sheet peptide at a variety of different peptide concentrations. We recommend 1 – 10 mM in D_2O as a starting point.
2. Identify distinct peaks in the ^{1}H NMR spectrum at your lowest concentration. Some examples would include isolated methyl singlets, Hα protons, and the *pro-S* $^{\delta}$Orn proton.

3. Inspect the appearance of the peaks in the NMR spectra with increasing peptide concentration. Look for the disappearance of splitting associated with Hα protons and aliphatic methyl groups, indicative of peak broadening.

Note:

- The slower rate of tumbling for larger species, such as oligomer, leads to more rapid T_2 relaxation and peak broadening in the ^1H NMR spectra. Part of the inherent challenge with studying supramolecular assembly by solution-phase NMR spectroscopy is in designing constrained β-sheet peptides to oligomerize without uncontrollably aggregating into large NMR-invisible aggregates.

Specific reduction in the diffusion coefficient

1. Run DOSY NMR of your constrained peptide β-sheet peptide at several different peptide concentrations in D_2O. Make sure to calibrate the DOSY spectra to the residual HOD peak before calculating the diffusion coefficient.
2. Look for a specific reduction in diffusion coefficient corresponding to the formation of a well-defined oligomer. Calculate the quotient of the oligomer diffusion coefficient relative to monomer to estimate the oligomer size.

Notes:

- You may observe the appearance of multiple tracks at intermediate concentrations in between that of the monomer and oligomer. This reflects exchange between monomer and oligomer occurring on the NMR timescale of the DOSY experiment.
- If the diffusion coefficient continuously decreases with increasing peptide concentration, it may suggest that the peptide is oligomerizing through transient non-specific interactions rather than forming a well-defined oligomer.

Summary

In this chapter, we have detailed how to use solution-phase NMR spectroscopy to study the folding and supramolecular assembly of constrained β-sheet peptides. These constrained β-sheet peptides are designed to assemble into well-defined soluble oligomers through the incorporation of $^{\delta}$Orn turn linkers that double as a spectroscopic probe for folding and a single *N*-methylated amino acid to prevent fibril formation. We describe how to prepare an NMR sample, run a variety of NMR experiments (^{1}H NMR, TOCSY, NOESY, ROESY, DOSY), and process NMR spectra. We then detail how to systematically process the NMR data to generate sequence specific peak assignment that further serve as the foundation for identifying intermolecular contacts. These intermolecular contacts can be further verified through isotope-edited experiments discussed in this protocol. Lastly, we conclude with spectroscopic hallmarks of supramolecular assembly that can be observed in aqueous solution. We anticipate that the protocols described herein can be adapted to studying the folding and supramolecular assembly of other peptides by solution-phase NMR spectroscopy.

References

(1) Cheng, P.-N.; Liu, C.; Zhao, M.; Eisenberg, D.; Nowick, J. S. Amyloid β-Sheet Mimics That Antagonize Protein Aggregation and Reduce Amyloid Toxicity. *Nat. Chem.* **2012**, *4* (11), 927–933. https://doi.org/10.1038/nchem.1433.

(2) Khakshoor, O.; Demeler, B.; Nowick, J. S. Macrocyclic β-Sheet Peptides That Mimic Protein Quaternary Structure through Intermolecular β-Sheet Interactions. *J. Am. Chem. Soc.* **2007**, *129* (17), 5558–5569. https://doi.org/10.1021/ja068511u.

(3) Li, X.; Rios, S. E.; Nowick, J. S. Enantiomeric β-Sheet Peptides from Aβ Form Homochiral Pleated β-Sheets Rather than Heterochiral Rippled β-Sheets. *Chem. Sci.* **2022**, *13* (26), 7739–7746. https://doi.org/10.1039/D2SC02080G.

(4) Pham, J. D.; Demeler, B.; Nowick, J. S. Polymorphism of Oligomers of a Peptide from β-Amyloid. *J. Am. Chem. Soc.* **2014**, *136* (14), 5432–5442. https://doi.org/10.1021/ja500996d.

(5) Truex, N. L.; Wang, Y.; Nowick, J. S. Assembly of Peptides Derived from β-Sheet Regions of β-Amyloid. *J. Am. Chem. Soc.* **2016**, *138* (42), 13882–13890. https://doi.org/10.1021/jacs.6b06000.

(6) Truex, N. L.; Nowick, J. S. Coassembly of Peptides Derived from β-Sheet Regions of β-Amyloid. *J. Am. Chem. Soc.* **2016**, *138* (42), 13891–13900. https://doi.org/10.1021/jacs.6b06001.
(7) Woods, R. J.; Brower, J. O.; Castellanos, E.; Hashemzadeh, M.; Khakshoor, O.; Russu, W. A.; Nowick, J. S. Cyclic Modular β-Sheets. *J. Am. Chem. Soc.* **2007**, *129* (9), 2548–2558. https://doi.org/10.1021/ja0667965.
(8) Zhu, J.; Kreutzer, A. G.; Liu, Z.; Li, X.; Richter, S. M.; Pophristic, V.; Nowick, J. S. A β-Hairpin Peptide Derived from Aβ Forms Different Oligomers in the Crystal State and in Aqueous Solution. *Org. Biomol. Chem.* **2025**, *23* (16), 3881–3893. https://doi.org/10.1039/D5OB00296F.
(9) Nowick, J. S.; Lam, K. S.; Khasanova, T. V.; Kemnitzer, W. E.; Maitra, S.; Mee, H. T.; Liu, R. An Unnatural Amino Acid That Induces β-Sheet Folding and Interaction in Peptides. *J. Am. Chem. Soc.* **2002**, *124* (18), 4972–4973. https://doi.org/10.1021/ja025699i.
(10) Nowick, J. S.; Brower, J. O. A New Turn Structure for the Formation of β-Hairpins in Peptides. *J. Am. Chem. Soc.* **2003**, *125* (4), 876–877. https://doi.org/10.1021/ja028938a.
(11) Samdin, T. D.; Jones, C. R.; Guaglianone, G.; Kreutzer, A. G.; Freites, J. A.; Wierzbicki, M.; Nowick, J. S. A β-Barrel-like Tetramer Formed by a β-Hairpin Derived from Aβ. *Chem. Sci.* **2023**, *15* (1), 285–297. https://doi.org/10.1039/D3SC05185D.
(12) Guaglianone, G.; Kreutzer, A. G.; Nowick, J. S. Chapter Five - Synthesis and Study of Macrocyclic β-Hairpin Peptides for Investigating Amyloid Oligomers. In *Methods in Enzymology*; Petersson, E. J., Ed.; Synthetic and Enzymatic Modifications of the Peptide Backbone; Academic Press, 2021; Vol. 656, pp 123–168. https://doi.org/10.1016/bs.mie.2021.04.023.
(13) Nowick, J. S.; Khakshoor, O.; Hashemzadeh, M.; Brower, J. O. DSA: A New Internal Standard for NMR Studies in Aqueous Solution. *Org. Lett.* **2003**, *5* (19), 3511–3513. https://doi.org/10.1021/ol035347w.
(14) Shimizu, A.; Ikeguchi, M.; Sugai, S. Appropriateness of DSS and TSP as Internal References for ^{1}H NMR Studies of Molten Globule Proteins in Aqueous Media. *J. Biomol. NMR* **1994**, *4* (6), 859–862. https://doi.org/10.1007/BF00398414.
(15) Wüthrich, K. *NMR of Proteins and Nucleic Acids*; John Wiley & Sons, 1991.
(16) Longsworth, L. G. The Mutual Diffusion of Light and Heavy Water. *J. Phys. Chem.* **1960**, *64* (12), 1914–1917. https://doi.org/10.1021/j100841a027.
(17) Wishart, D. S.; Sykes, B. D. Chemical Shifts as a Tool for Structure Determination. In *Methods in Enzymology*; Nuclear Magnetic Resonance, Part C; Academic Press, 1994; Vol. 239, pp 363–392. https://doi.org/10.1016/S0076-6879(94)39014-2.
(18) Wishart, D. S.; Sykes, B. D.; Richards, F. M. Relationship between Nuclear Magnetic Resonance Chemical Shift and Protein Secondary Structure. *J. Mol. Biol.* **1991**, *222* (2), 311–333. https://doi.org/10.1016/0022-2836(91)90214-Q.
(19) Wishart, D. S.; Sykes, B. D.; Richards, F. M. The Chemical Shift Index: A Fast and Simple Method for the Assignment of Protein Secondary Structure through NMR Spectroscopy. *Biochemistry* **1992**, *31* (6), 1647–1651. https://doi.org/10.1021/bi00121a010.

Chapter 2: A β-Hairpin Peptide Derived from Aβ Forms Different Oligomers in the Crystal State and in Aqueous Solution

Preface to Chapter 2

Chapter 2 aims to better understand the solution-phase NMR assembly of the *N*-methylated macrocyclic peptides that mimic Aβ β-hairpins. This project was motivated by the observation that many macrocyclic β-sheet peptides readily crystallize into oligomers but do not assemble into well-defined oligomers in aqueous solution that can be characterized by solution-phase NMR spectroscopy. Prior to this work, our laboratory only had success stabilizing solution-phase NMR assembly with the use of a tripeptide mimetic called Hao, named after its three constituent components: hydrazine, 5-amino-2-methoxybenzoic acid, and oxalic acid.

This chapter is adapted from or taken verbatim from Zhu, J.; Kreutzer, A. G.; Liu, Z.; Li, X.; Richter, S. M.; Vojislava, P.; Nowick, J. S. A β-Hairpin Peptide Derived from Aβ Forms Different Oligomers in the Crystal State and in Aqueous Solution. *Org. Biomol. Chem.* ***2025***, *23, 3881-3893*. I performed all experiments described in this chapter except for the SPPS of peptides 3a and 3b which were synthesized by Sabrina Richter, a summer REU student whom I mentored.

Introduction

Supramolecular assembly of amyloid-β (Aβ) peptide into soluble toxic oligomers and insoluble fibrils is central to Alzheimer's disease (AD) pathogenesis.[1–3] While advances in cryogenic electron microscopy and solid-state NMR spectroscopy have provided structural insights into different Aβ fibril polymorphs, the structures of soluble Aβ oligomers remain largely unknown.[4–9] The metastability and heterogeneity of soluble oligomers have hampered structural elucidation by high-resolution techniques such as X-ray crystallography and solution-phase NMR spectroscopy.

β-Hairpins have emerged as building blocks of many soluble Aβ oligomers. The β-hairpin conformation was originally postulated by Pollard and coworkers in 1994 and supported by subsequent *in silico* models.[10–12] In 2008, Härd and coworkers reported the first high-resolution NMR structure of $A\beta_{1–40}$ in a β-hairpin conformation and postulated that the β-hairpin conformation is involved in the formation of oligomers.[13] In a subsequent study, Härd and coworkers constrained $A\beta_{1–40}$ and $A\beta_{1–42}$ into β-hairpin conformations through intramolecular disulfide linkages and found that disulfide-stabilized Aβ β-hairpins exhibited greater propensity to oligomerize than the unconstrained Aβ peptides.[14] Yu and coworkers have also demonstrated that $A\beta_{1–42}$ can assemble to form soluble oligomers composed of Aβ β-hairpins.[15] Additional work by Okumara and coworkers clarified the role of Arg_5 in the formation of β-hairpins for $A\beta_{1–40}$ and $A\beta_{1–42}$.[16] The multiple possible β-hairpin registrations reflects the polymorphic nature of soluble Aβ oligomers. It is still unclear which β-hairpin registration is the predominant assembly formed by full-length Aβ oligomers. Collectively, these early *in silico* and experimental studies support the importance of the β-hairpin conformation in soluble Aβ oligomers.

More recently, seminal work by Carulla and coworkers elucidated the first high-resolution solution-phase NMR structure of a soluble Aβ oligomer.[17] This $A\beta_{1–42}$ tetramer contains a six stranded β-sheet formed by two β-hairpins and two antiparallel β-strands. Size exclusion chromatography and native ion mobility mass spectrometry support the formation of an octamer at higher peptide concentrations consisting of a β-sheet sandwich of two tetramers. Molecular dynamics (MD) simulations suggest how the tetramers and octamers may form pores in cell membranes, leading to cell toxicity. This work underscores how high-resolution structural studies of Aβ oligomers shed light on potential mechanisms of soluble Aβ oligomers toxicity.

Our laboratory has reported the X-ray crystallographic structures of several Aβ oligomer models formed by macrocyclic β-hairpin peptides designed to mimic native Aβ β-hairpins.[18,19] In these β-hairpin peptides, we constrain amyloidogenic fragments from the central and *C*-terminal regions of Aβ into a macrocycle using two δ-linked ornithine turn units.[20] To prevent uncontrolled aggregation, we incorporate an *N*-methyl amino acid that disrupts intermolecular hydrogen bonding. In studying different Aβ β-hairpin peptides, we have observed twisted dimers, triangular trimers, barrel-like tetramers, compact hexamers, ball-shaped dodecamers, and annular pore structures, illustrating the numerous assemblies that Aβ β-hairpin peptides can form.[18,19] Several of the Aβ β-hairpin peptides that assemble crystallographically have also been demonstrated to exhibit neurotoxicity and/or have been recognized by A11, an antibody that recognizes Aβ oligomers.[18,21,22]

While X-ray crystallography provides insights into the structures of oligomers formed by β-hairpin peptides in the crystal lattice, this technique only provides a static snapshot of the oligomer structure. Crystal lattice formation typically favors a single, homogenous low-energy structure, that may not reflect the variety of oligomer structures present in solution. Solution-

phase NMR spectroscopy thus complements X-ray crystallography with insights into the structures and dynamics of oligomers in aqueous solution.

Here, we set out to characterize the assembly of Aβ β-hairpin peptide **1** using solution-phase NMR spectroscopy.[18] Peptide **1** contains $A\beta_{16–22}$ and $A\beta_{30–36}$ constrained into a macrocycle by two δ-linked ornithine turn units ($^{\delta}$Orn) and an *N*-methyl group on Phe_{19} (Figure 2.1A). This particular alignment between the $A\beta_{16–22}$ and $A\beta_{30–36}$ fragments has been proposed Tycko and co-workers based on cryogenic electron microscopy and solid-state NMR spectroscopy data of brain-derived $A\beta_{40}$ fibrils.[6] We previously reported that peptide **1** assembles in the crystal lattice to form a symmetric hexamer composed of two identical triangular trimers (Figure 2.1B).[18] In the current study, we found that peptide **1** does not assemble in solution to form a well-defined oligomer that can be fully characterized by solution NMR spectroscopy.

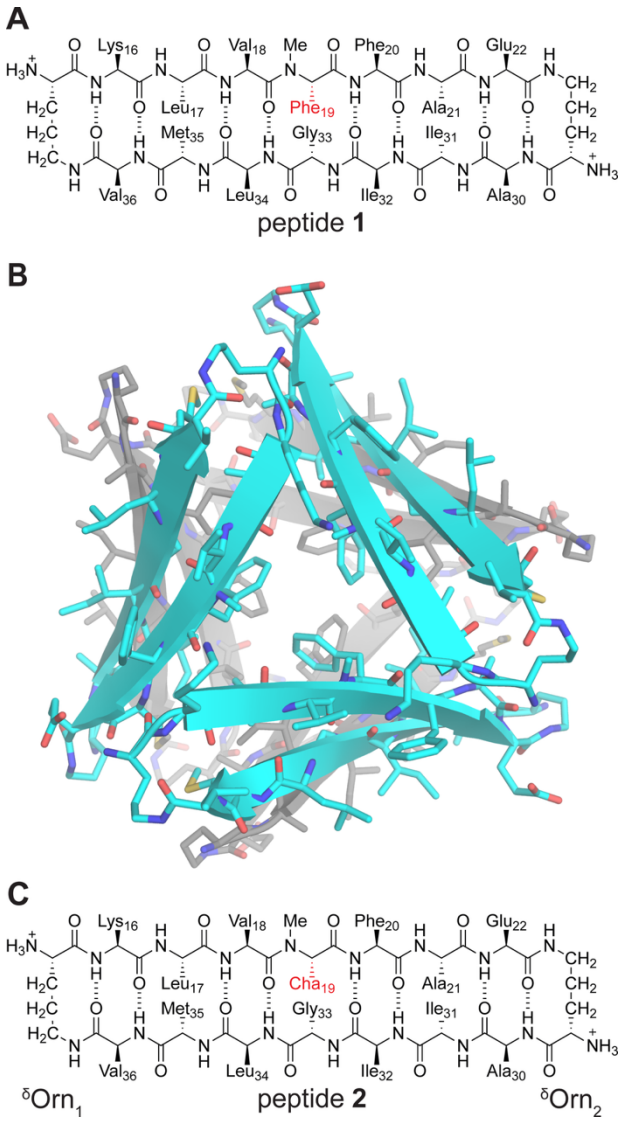

Figure 2.1. Peptide **1** and **2**, and X-ray crystallographic structure of peptide **1** (PDB 5W4H).[18] Red side chains highlight the Phe-to-Cha mutation. The two triangular trimer subunits of the crystallographic hexamer are colored in cyan and grey.

To promote the solution phase assembly of peptide **1** into a well-defined oligomer, we varied the side chain of Phe_{19} to cyclohexylalanine (Cha) to better pack the hydrophobic core of the crystallographic hexamer. The resulting peptide **2** is shown in Figure 2.1C. We hypothesized that solution-phase assembly is driven by hydrophobic core formation, and that Phe-to-Cha mutation would enhance hydrophobic core formation and thus lead to the assembly of a well-defined oligomer. X-ray crystallography shows that peptide **2** assembles to form a symmetric

hexamer in the crystal lattice identical to that of peptide **1**, whereby two triangular trimers assemble in a sandwich-like fashion. Solution-phase NMR spectroscopy reveals that peptide **2** assembles into a well-defined asymmetric hexamer in solution that differs in structure from the symmetric hexamer in the crystal lattice. ^{1}H NMR, TOCSY, and ^{1}H,^{15}N HSQC experiments establish that the asymmetric hexamer is composed of two species, **A** and **B**. ^{15}N-edited NOESY reveals that species **A** is a cylindrin-like trimer and species **B** is a triangular trimer, akin to the trimer observed crystallographically. Species **A** and **B** come together to form a well-defined asymmetric hexamer. Diffusion ordered spectroscopy (DOSY), and MD simulations suggest that two asymmetric hexamers further assemble to form a dodecamer and that the dodecamer is the predominant assembly in solution.

Results and Discussion

Peptide 1 does not assemble to form well-defined oligomers in aqueous solution

In studying the solution-phase assembly of a related class of macrocyclic peptides, our laboratory has established spectroscopic hallmarks indicative of well-defined peptide oligomer assembly in solution.[23,24] These hallmarks include: new resonances appearing as the peptide concentration increases that correspond to an increasing oligomer fraction, downfield shifting of Hα resonances associated with β-sheet structure, upfield shifting of some of the aromatic and methyl side chain resonances associated with hydrophobic packing, a specific reduction in diffusion coefficient associated with the formation of an oligomer of a specific size, and the appearance of new NOE crosspeaks that correspond to intermolecular contacts associated with oligomer formation.

The ^{1}H NMR spectra of peptide **1** lack many hallmarks of oligomer assembly, indicating that peptide 1 does not assemble to form well-defined oligomers (Figure S2.1). At 1.0 mM, the

proton resonances of peptide **1** are sharp. At 8.0 and 16.0 mM, the ^{1}H NMR spectra broaden significantly without the appearance of distinct new resonances associated with the formation of a well-defined oligomer. The ^{1}H NMR spectra do not show significant downfield shifting of Hα proton resonances. Although some aromatic and methyl side chain resonances shift upfield slightly, these resonances are broad and not well-defined. The peak broadening in the ^{1}H NMR spectra may reflect exchange between monomer and one or more oligomeric species at an intermediate rate on the NMR timescale.

DOSY is a valuable tool for comparing the relative sizes of oligomers and monomers. When well-defined oligomers assemble in aqueous solution, the diffusion coefficient as measured by DOSY decreases with increasing peptide concentration. The decrease in diffusion coefficient reflects the change in equilibrium from monomer to oligomer. At low peptide concentrations, a single track appears in the DOSY spectrum corresponding to the monomer. At intermediate concentrations, multiple DOSY tracks appear that reflect a change in equilibrium from monomer to oligomer. At high peptide concentrations, a new track appears in the DOSY spectrum corresponding to the oligomer, and the diffusion coefficient of the oligomer remains invariant with further increasing peptide concentration.

DOSY NMR studies reveal that peptide **1** does not form well-defined oligomers of a specific size. At 1.0 mM peptide 1, the DOSY spectrum shows a monomer with a diffusion coefficient of 1.99 x 10^{-10} m^2/s. At 8.0 mM and 16.0 mM, the DOSY spectra show a single track with a diffusion coefficient of 1.42 x 10^{-10} m^2/s and 0.86 x 10^{-10} m^2/s, respectively. The continuous decrease in the diffusion coefficient with increasing peptide concentration suggests that peptide **1** is in equilibrium with a variety of species of increasing size and the oligomers formed by peptide **1** are not discrete and well-defined.

Peptide **2** assembles to form a hexamer in the crystal state and in SDS-PAGE

The X-ray crystallographic structure of peptide **1** demonstrated that the formation of a hydrophobic core is a key driver of hexamer formation. We hypothesized that mutating Phe_{19}, which contributes to the hydrophobic core of the peptide **1** hexamer, to cyclohexylalanine (Cha) would stabilize the hydrophobic interior of the hexamer and promote the formation of a well-defined oligomer in aqueous solution (Figure S2.2). Studies by Nilsson and coworkers showed how strategic Phe-to-Cha mutations can stabilize fibril formation of $A\beta_{16–22}$ fragments.[25] Our laboratory has also used a Phe-to-Cha mutation to promote the crystallographic assembly of a related macrocyclic peptide.[26] To investigate the effect of the Phe-to-Cha mutation, we compared peptide **2** (the Cha_{19} mutant) to peptide **1** using X-ray crystallography, SDS-PAGE, and circular dichroism (CD) spectroscopy.

Peptide 2 afforded crystals suitable for X-ray diffraction in aqueous HEPES buffer with sodium citrate and isopropanol, nearly identical to the crystallization conditions for peptide **1** (Table S2.1). Elucidation of the X-ray crystallographic structure of peptide **2** reveals that it forms a symmetrical hexamer identical to that of peptide **1**, whereby two triangular trimers pack together in a sandwich-like fashion (Figure S2.3). The amide backbones of the two hexamers overlay with a 0.36 Å RMSD.

The interior of the peptide **2** hexamer is packed with the hydrophobic side chains of Leu_{17}, Cha_{19}, Ala_{21}, Ile_{31}, Gly_{33}, and Met_{35}, while the exterior of the hexamer is decorated by the side chains of Lys_{16}, Val_{18}, Phe_{20}, Glu_{22}, Ala_{30}, Ile_{32}, Leu_{34}, and Val_{36}. A network of 30 intermolecular hydrogen bonds between the six monomer subunits stabilize the crystallographic hexamer (Figure 2.2). At the vertices of the triangular trimers, three intermolecular hydrogen bonds stabilize the assembly of the triangular trimers, accounting for 18 hydrogen bonds. At the

interface of the two trimers, four intermolecular hydrogen bonds form between adjacent monomers, creating an antiparallel β-sheet, accounting for 12 hydrogen bonds.

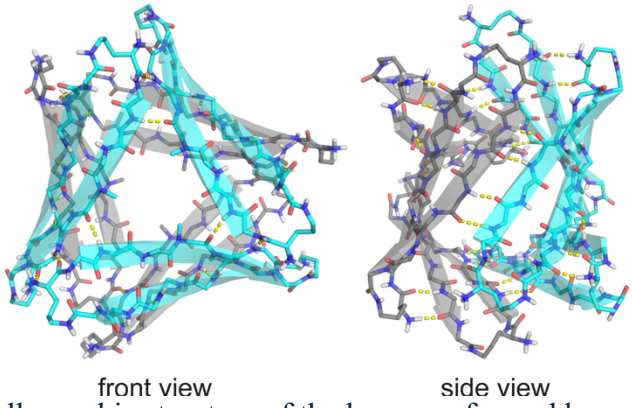

Figure 2.2. X-ray crystallographic structure of the hexamer formed by peptide **2** (PDB 9EEC). The two triangular trimer subunits of the crystallographic hexamer are colored in cyan and grey. Intermolecular hydrogen bonds are shown in yellow.

To preliminarily evaluate the effect of the Cha mutation on assembly, we used SDS-PAGE, where we ran three different loadings per lane of peptides **1** and **2** (Figure 2.3). Peptide **1** migrates as a comet-shaped band near the 10-kDa standard, consistent with the molecular weight of a hexamer (10.6 kDa). The upper bounds of the peptide **1** bands decrease with decreasing peptide concentration. The concentration dependence and downward streaking of the peptide **1** bands suggest that the hexamer is in equilibrium with lower molecular weight species. Peptide **2** also migrates as hexamers in SDS-PAGE, running as tighter bands that streak less than those of peptide **1**. As the loading of peptide **2** decreases, the upper bounds of the peptide **2** bands decrease less than those of peptide **1**, suggesting the hexamer formed by peptide **2** is more stable than that formed by peptide **1**.

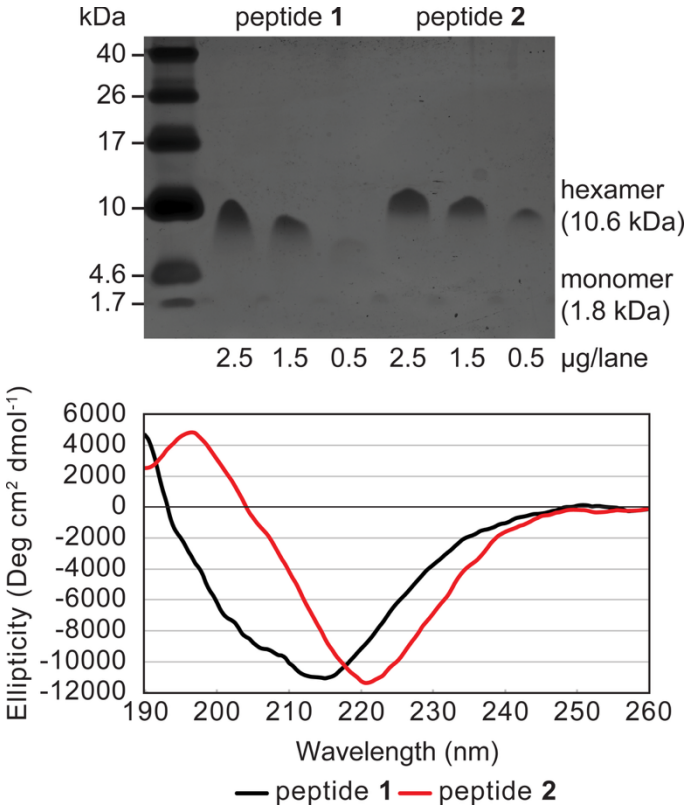

Figure 2.3. SDS-PAGE and CD spectra of peptides **1** and **2**. SDS-PAGE was performed in Tris buffer (pH 6.8) with 2% (w/v) SDS on a 16% polyacrylamide gel with 2.5, 1.5, and 0.5 µg of peptide per lane and visualized by silver staining. CD spectra were run with 100 µM peptide in 10 mM phosphate buffer at pH 7.4. The contrast of the image of the SDS-PAGE was uniformly adjusted for clarity (Figure S2.4).

We evaluated the secondary structure of peptides **1** and **2** by CD spectroscopy. Peptide **1** shows a strong negative band at ca. 214 nm and a positive band at ca. 190 nm. Peptide **2** displays a strong negative band at ca. 221 nm and a positive band at ca. 196 nm. Although the CD spectra of both peptides show β-sheet structure, peptide **2** appears to reflect a higher degree of folding, as evidenced by the narrower negative band ca. 221 nm and positive band at ca. 196 nm.

X-ray crystallography, SDS-PAGE, and CD spectroscopy studies show that peptide **2** assembles into hexamers in the solid state and in SDS-PAGE, and that it exhibits enhanced β-sheet folding in aqueous solution. Collectively, these studies demonstrate that mutation of Phe_{19} to Cha_{19} does not impact the ability of peptide **2** to form hexamers, and may better stabilize hexamer formation.

Peptide 2 assembles into well-defined oligomers in aqueous solution

The ^{1}H NMR spectra of peptide **2** exhibit many of the hallmarks of well-defined oligomer assembly, such as the appearance of new resonances at higher peptide concentrations associated with oligomer and disappearance of the resonances associated with monomer (Figure S2.5). At 1.0 mM, the ^{1}H NMR spectrum of the peptide **2** monomer is sharp, with notable features including the Cha_{19} Hα proton at 5.68 ppm, aromatic resonances from Phe_{20} at 7.22–7.36 ppm, and methyl resonances from Leu, Ile, and Val at 0.74–1.08 ppm (Figure 2.4). At 6.0 mM, oligomeric resonances appear that are roughly equal in intensity to those of the monomer. At 11.0 mM, the oligomeric resonances predominate (Figure 2.4).

NH and Hα peak assignments generated through TOCSY and ROESY experiments (further discussed in the subsequent section) reveal that the oligomer appears as two sets of resonances of equal integration, which we term species **A** and **B**. For example, the Cha_{19} Hα proton shows two oligomer peaks at 5.77 and 5.92 ppm increasing in intensity with increasing peptide concentration as the Cha_{19} Hα monomer peak at 5.68 ppm decreases in size and broadens. The peak broadening of the monomer may reflect chemical exchange with the oligomer.[27] Numerous downfield shifted Hα resonances appear for both oligomer species, between 4.91 and 5.92 ppm. Phe_{20} shows one ortho proton resonance for the monomer at 7.25 ppm and two resonances for the oligomer at 7.12 and 7.17 ppm. At 11.0 mM, one of the Leu_{34} methyl resonance appears upfield, at 0.48 ppm, suggesting packing against the Phe_{20} aromatic ring in the oligomer. Thus, the ^{1}H NMR spectra of peptide **2** show many hallmarks associated with the formation of a well-defined oligomer.

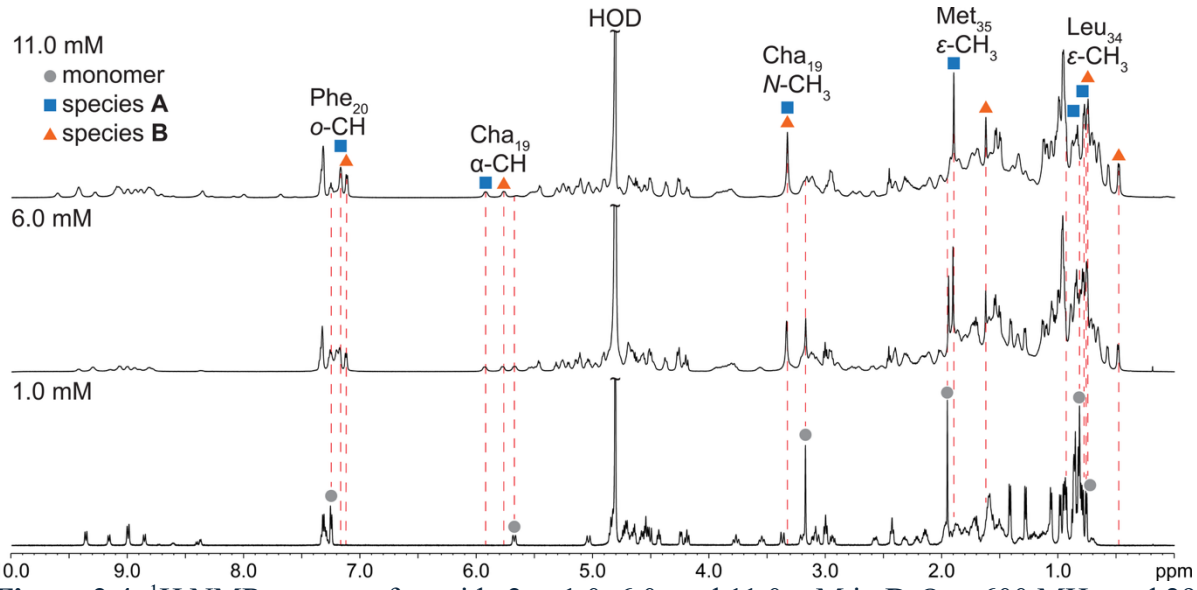

Figure 2.4. ^{1}H NMR spectra of peptide **2** at 1.0, 6.0, and 11.0 mM in D_2O at 600 MHz and 298 K. Dashed lines highlight key resonances associated with monomer (grey circles), oligomer species **A** (blue squares), and oligomer species **B** (orange triangles). Peaks at 7.5–10 ppm are amide NH resonances that have not fully exchanged with D_2O.

^{1}H,^{15}N HSQC, TOCSY, and ROESY NMR verify the presence of two species, **A** and **B**

To corroborate that the oligomer is composed of two distinct species, we introduced an ^{15}N label at Gly_{33} and examined the ^{1}H,^{15}N HSQC spectra of the resulting peptide **2a**. The greater dispersion afforded by the ^{15}N dimension distinguishes each species as a unique crosspeak. At 1.0 mM, the ^{1}H,^{15}N HSQC spectrum of peptide **2a** shows a single crosspeak associated with the monomer at 8.62 ppm in the ^{1}H dimension and 111.4 ppm in the ^{15}N dimension (Figure 2.5A). At 11.0 mM, the ^{1}H,^{15}N HSQC spectrum of peptide **2a** shows two crosspeaks at 9.60 and 8.84 ppm in the ^{1}H dimension and 109.9 and 104.7 ppm in the ^{15}N dimension corresponding to species **A** and **B** (Figure 2.5B and Table S2.2). The ^{1}H,^{15}N HSQC experiments confirm the peptide **2** oligomer is composed of two spectroscopically distinct species **A** and **B**.

To assign the NH and Hα resonances of the monomer, species **A**, and species **B**, we analyzed the TOCSY and ROESY spectra of peptide **2**. At 1.0 mM, peptide **2** exhibits a single set of resonances associated with the NH and Hα of the monomer in the TOCSY spectrum (Figure

2.5C). At 11.0 mM, peptide **2** exhibits two sets of resonances associated with the NH and Hα of species **A** and **B** in the TOCSY spectrum (Figure 2.5D). The sequential peak assignments are shown in Figures S2.6 and S2.7 and are further described in the Materials and Methods section of the Supporting Information.

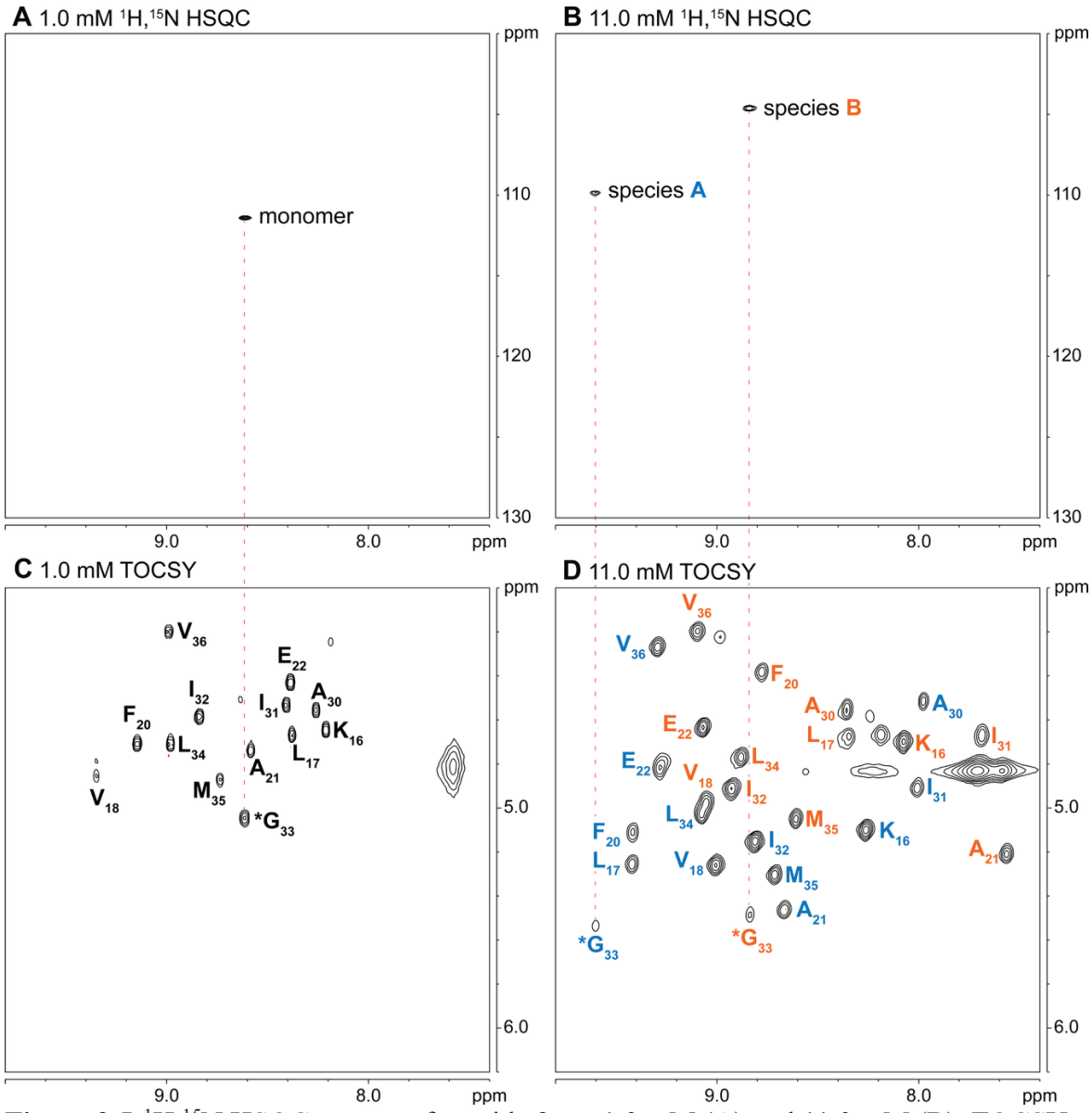

Figure 2.5. $^{1}H,^{15}N$ HSQC spectra of peptide **2a** at 1.0 mM (A) and 11.0 mM (B). TOCSY spectra of peptide **2** at 1.0 mM (C) and 11.0 mM (D). Glycine crosspeaks, indicated by an asterisk (*), refer to the pro-*R* Hα. Dashed lines are shown to correlate the glycine crosspeaks of the $^{1}H,^{15}N$ HSQC and TOCSY spectra. $^{1}H,^{15}N$ HSQC spectra were recorded at 800 MHz. TOCSY spectra were recorded at 600 MHz. All spectra were recorded in 9:1 H_2O/D_2O at 298 K.

Peptide 2 folds into a β-hairpin conformation in aqueous solution

To investigate the secondary structure and folding of peptide **2** in aqueous solution, we analyzed the chemical shifts of Hα protons, magnetic anisotropy of the diasterotopic $^{\delta}$Orn protons, and intramolecular NOEs associated with β-hairpin formation. The resonances of the peptide **2** Hα protons of the monomer, species **A**, and species **B** are downfield of those that would occur for amino acids in a random coil conformation (Figure 2.6A and Table S2.3). This downfield shifting of Hα protons is characteristic of β-sheet secondary structure. The Hα protons of the peptide **2** monomer show an average downfield shift of 0.38 ppm. By comparison, species **A** Hα protons show an average downfield shift of 0.78 ppm and species **B** Hα protons show an average downfield shift of 0.50 ppm. The greater downfield shifting of the oligomer compared to that of the monomer may reflect cooperativity between folding into a β-sheet and oligomerization.

Previous studies have demonstrated that the magnetic anisotropy of the diastereotopic $^{\delta}$Orn protons reflects the extent of folding of the $^{\delta}$Orn turn unit.[20,23,24] In a completely folded macrocyclic β-hairpin peptide, the *pro-S* $^{\delta}$Orn protons appear 0.6–0.7 ppm downfield of the *pro-R* $^{\delta}$Orn protons. In the peptide **2** monomer, $^{\delta}Orn_1$ is well folded, while $^{\delta}Orn_2$ is partially folded (Figure 2.6B). In the peptide **2** oligomer, both $^{\delta}$Orn turn units are well folded. The better folding of the turn units further reflects cooperativity between folding into a β-hairpin and oligomerization.

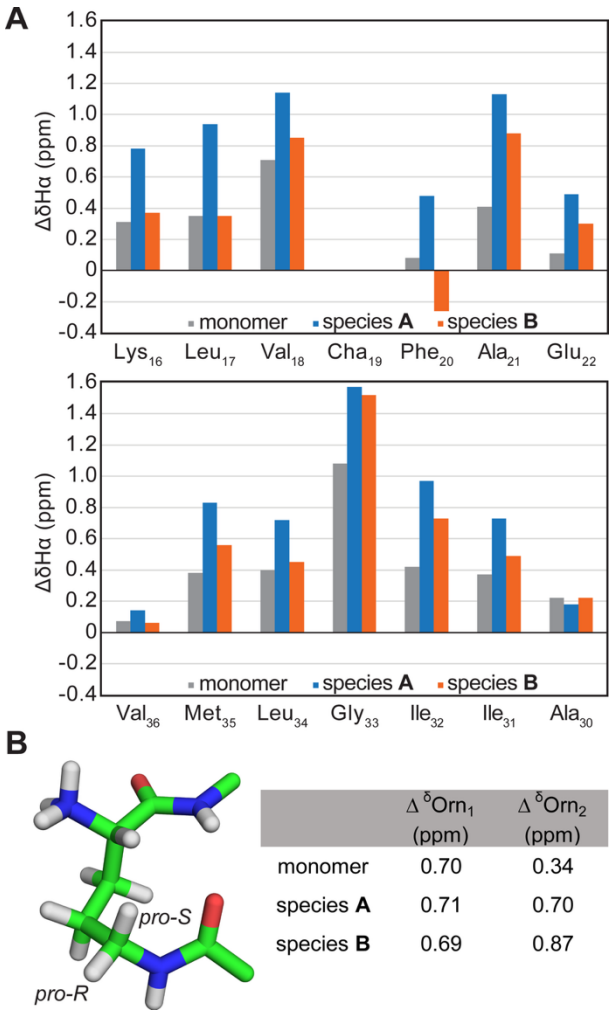

	$\Delta^{\delta}Orn_1$ (ppm)	$\Delta^{\delta}Orn_2$ (ppm)
monomer	0.70	0.34
species **A**	0.71	0.70
species **B**	0.69	0.87

Figure 2.6. (A) Chemical shift differences between the peptide **2** Hα protons and random coil values reported by Wishart and Sykes.[28] Cha_{19} was excluded from chemical shift differences analysis because it is a noncanonical amino acid. The chemical shifts of the monomer were recorded at 1.0 mM, and the chemical shifts of the oligomer were recorded at 11.0 mM. (B) Molecular model of the δ-linked ornithine turns unit and magnetic anisotropies of the pro-*R* and pro-*S* protons observed for peptide **2**.

Networks of intramolecular NOEs involving the NH and Hα protons are a spectroscopic hallmark of well-folded β-hairpins. The peptide **2** monomer shows a network of NOEs consistent with β-hairpin folding (Figure 2.7 and S2.8). When peptide **2** is predominantly oligomeric (11.0 mM), the ^{1}H NMR spectrum is complex, because resonances corresponding to species **A** and **B** are broadened and many are overlapping. Despite the overlap, the NOESY spectra show a network of strong NOEs consistent with well-folded β-hairpins for both species **A** and **B** (Figure

S2.9). The NOESY spectra shows interstrand NOEs consistent with all 26 of the expected interstrand contacts associated with folding for both species **A** and **B**. Ten of the 26 NOEs are ambiguous because of heavy spectral overlap.

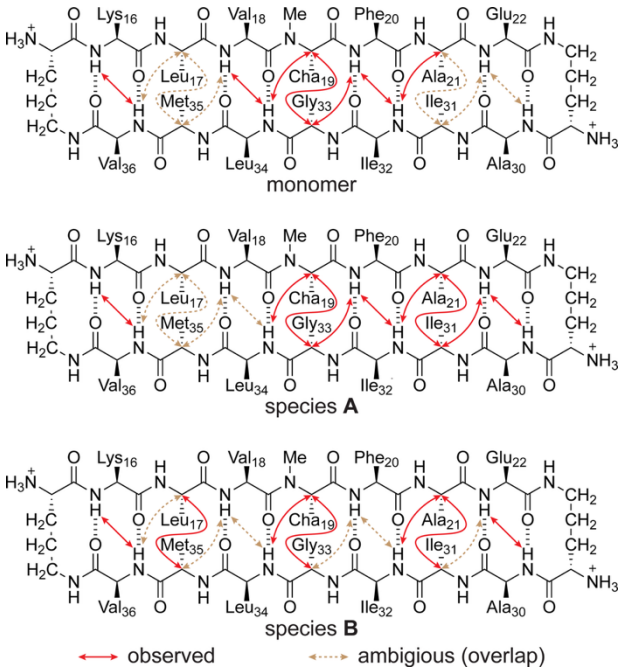

Figure 2.7. Key intramolecular NOEs for the peptide **2** monomer and oligomer species **A** and **B**. Ambiguous NOEs are indicated by dashed lines. NOEs were identified in the NOESY spectra at 1.0 and 11.0 mM in D_2O and 9:1 H_2O/D_2O at 600 MHz and 298 K.

^{2}H and ^{15}N labeling distinguishes key intermolecular contacts from intramolecular contacts

The NOESY spectra for the peptide **2** oligomer contain many additional NOEs consistent with intermolecular contracts and inconsistent with intramolecular contacts (Figure S2.10). However, many of these intermolecular NOEs are ambiguous due to heavy overlap. To corroborate the assignments of key intermolecular NOEs involving amide NH and Hα protons, we prepared isotopologues **2b–d** that contain selectively incorporated ^{2}H and ^{15}N labels.

To corroborate the assignments of key Hα-to-Hα intermolecular NOEs, we prepared isotopologue **2b**, in which Phe_{20} is deuterated, and isotopologue **2c**, in which both Phe_{20} and

Ala_{30} are deuterated. In the NOESY spectrum for the peptide **2** oligomer, we observe strong NOEs between Lys_{16} Hα (species **A**) and Leu_{34} Hα (species **A**), Ala_{30} Hα (species **A**) and Ile_{32} Hα (species **B**), Ala_{30} Hα (species **B**) and Phe_{20} Hα (species **A**), Lys_{16} Hα (species **B**) and Phe_{20} Hα (species **B**) (Figure 2.8). When the Hα protons involved in intermolecular contacts are replaced with deuterium, the corresponding NOEs should disappear, and this is what is observed in the NOESY spectra of peptides **2b** and **2c** (Figure S2.11). The disappearance of the NOEs involving the Phe_{20} and Ala_{30} Hα protons supports the assignments of these heavily overlapped NOE crosspeaks.

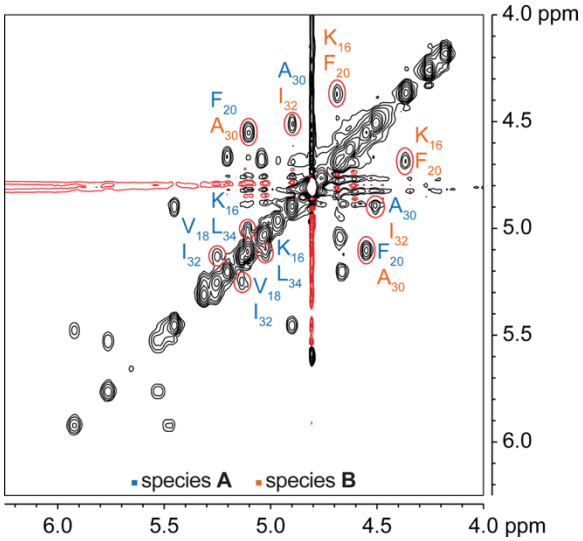

Figure 2.8. Key Hα-to-Hα intermolecular NOEs in the NOESY spectrum of the peptide **2** oligomer. The spectrum was recorded at 11.0 mM peptide in D_2O at 600 MHz and 298 K.

To corroborate the assignments of key amide NH intermolecular NOEs, we prepared isotopologue **2d**, with ^{15}N labels in the outer facing amide NHs of Leu_{17}, Ala_{21}, Ile_{31}, and Met_{35} (Figure 2.9A). ^{1}H,^{15}N NOESY-HSQC spectrum of peptide **2d** was acquired with one increment in the ^{15}N dimension (f_2) and the typical NOESY parameters in the ^{1}H dimensions (f_1 and f_3). The resulting ^{15}N-edited NOESY-HSQC spectrum only shows NOEs involving the ^{15}NH protons. The spectrum exhibits eight distinct vertical tracks, four of which correspond to species **A** and

four of which correspond to species **B** (Figure 2.9B and 2.9C). We assigned the intermolecular NOEs by first assigning the expected intramolecular NOEs and then identifying the remaining intermolecular NOEs — seven ^{15}NH to NH, seven ^{15}NH to Hα, and three ^{15}NH to *N*-Me NOEs. These NOEs support the assignments of the key amide NH intermolecular contacts. A copy of the fully annotated ^{15}N-edited NOESY spectra is shown in Figure S2.12.

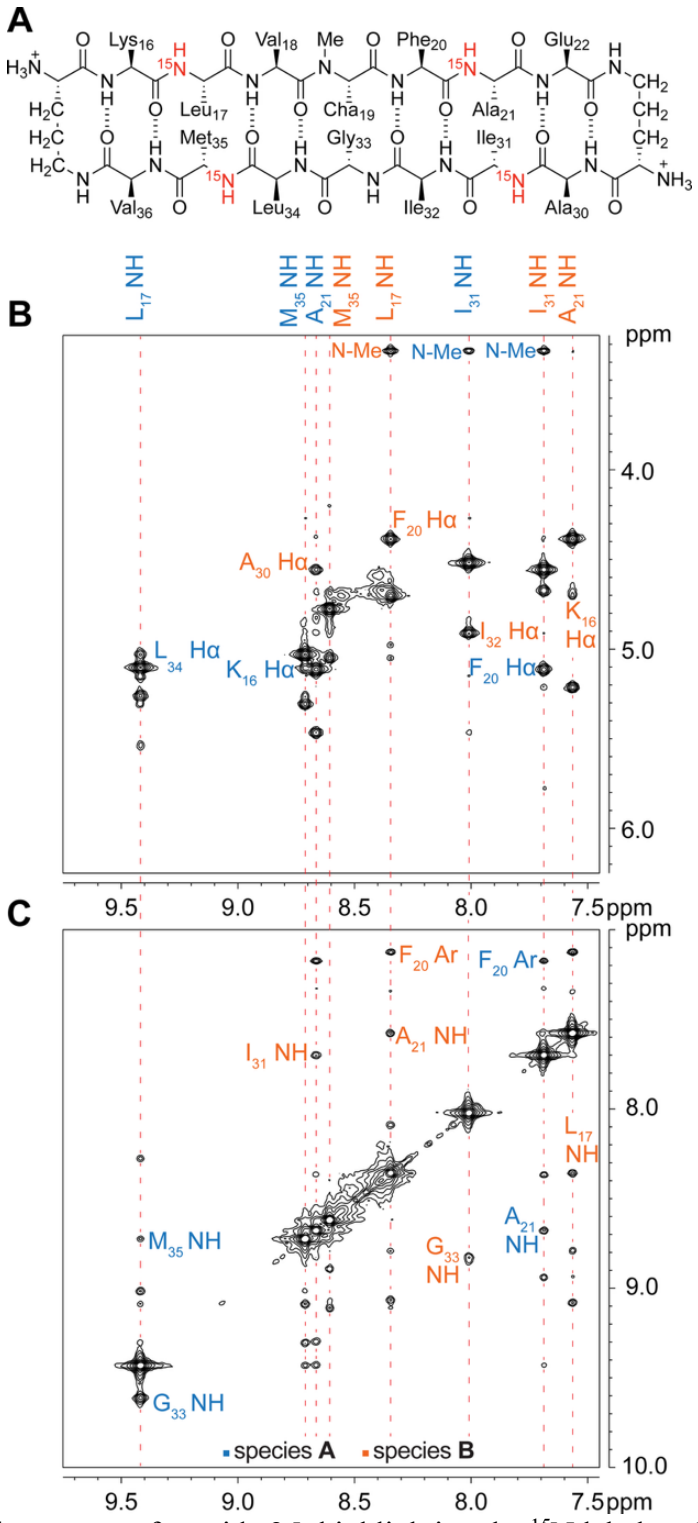

Figure 2.9. Chemical structure of peptide **2d**, highlighting the ^{15}N labels at Leu_{17}, Ala_{21}, Ile_{31}, and Met_{35} in red (A). ^{15}N-edited NOESY-HSQC spectrum of peptide **2d** showing key intermolecular NOEs to either Hα or *N*-Me (B) and NH protons (C). The spectrum was recorded at 11.0 mM in 9:1 H_2O/D_2O at 800 MHz and 298 K.

Molecular model of the solution-phase asymmetric hexamer

We used PyMOL and MacroModel to construct a constrained NMR-based molecular model consistent with the observed intermolecular contacts and symmetry requirements for the **A** and **B** species (Figure 2.10). The A-B intermolecular contacts in conjugation with the A-A and B-B intermolecular contacts indicate one asymmetric oligomer composed of species **A** and **B**, rather than two oligomer species corresponding to species **A** and **B** (Table 2.1). The equal integration of the resonances associated with species **A** and **B** suggest that the oligomer contains both species in a 1:1 ratio. The observation of two distinct species in the NMR spectrum rule out the possibility of a symmetric oligomer, such as that observed crystallographically. As we will describe in detail below, the oligomer that best fulfills these requirements and best explains key intermolecular NOEs is an asymmetric hexamer composed of a cylindrin-like trimer (species **A**) and a triangular trimer (species **B**).[29] Additional models that proved inconsistent with the NMR data are further described in Figure S2.13.

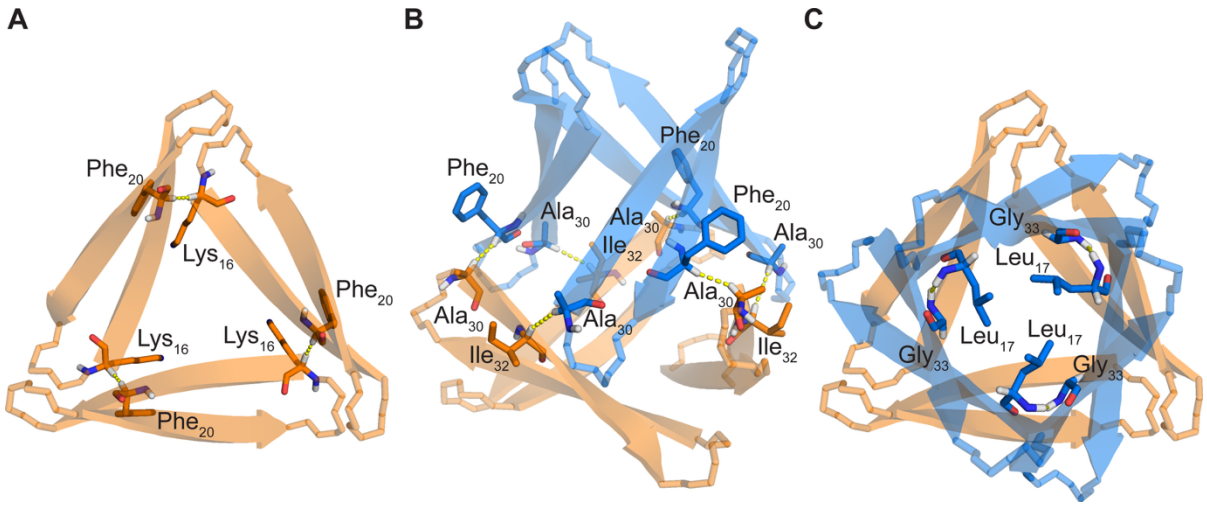

Figure 2.10. NMR-based molecular model of the asymmetric hexamer formed by peptide **2**. Species **A** is shown in blue and species **B** is shown in orange. (A) Top view of triangular trimer subunit formed by species **B** illustrating contacts between Lys_{16} and Phe_{20} within species **B**. (B) Side view of the hexamer illustrating contacts between Phe_{20} of species **A** and Ala_{30} of species **B** and between Ala_{30} of species A and Ile_{32} of species **B**. (C) Top view of the hexamer illustrating contacts between Leu_{17} and Gly_{33} within species **A**. The subunit formed by species **A** (blue) constitutes a cylindrin-like trimer.

Table 2.1. Key intermolecular contacts observed for the peptide **2** oligomer.[a,b]

Interface			
A to **A**	**B** to **B**	**A** to **B (1)**[b]	**A** to **B (2)** [b]
Lys_{16} Hα to Leu_{34} Hα (m)[a]	Lys_{16} Hα to Phe_{20} Hα (s)[a]	Cha_{19} *N*-Me to Ile_{31} NH (m)[a]	Ile_{31} NH to Ile_{32} Hα (m)[a]
Lys_{16} Hα to Met_{35} NH (m)[a]	Lys_{16} Hα to Ala_{21} NH (m)[a]	Cha_{19} *N*-Me to Ile_{32} Hα (w)[a]	Ile_{31} NH to Gly_{33} NH (m)[a]
Leu_{17} NH to Gly_{33} NH (s)[a]	Leu_{17} NH to Cha_{19} *N*-Me (m)[a]	Phe_{20} Hα to Ala_{30} Hα (s)[a]	Ala_{30} Hα to Ile_{32} Hα (s)[a]
Leu_{17} NH to Leu_{34} Hα (w)[a]	Leu_{17} NH to Phe_{20} Hα (s)[a]	Phe_{20} Hα to Ile_{31} NH (m)[a]	Ala_{30} Hα to Gly_{33} NH (w)[a]
Leu_{17} NH to Met_{35} NH (w)[a]	Leu_{17} NH to Phe_{20} *Ar* (m)[a]	Phe_{20} *Ar* to Ile_{31} NH (m)[a]	
Val_{18} Hα to Ile_{32} Hα (m)[a]	Leu_{17} NH to Ala_{21} NH (m)[a]	Ala_{21} NH to Ala_{30} Hα (w)[a]	
Val_{18} Hα to Gly_{33} NH (m)[a]		Ala_{21} NH to Ile_{31} NH (m)[a]	
Cha_{19} *N*-Me to Ile_{31} NH (w)[a]			
Cha_{19} *N*-Me to Ile_{32} Hα (m)[a]			

[a]Letters in parentheses indicates the strength of the NOE as strong (s), medium (m), or weak (w).
[b]Number in parentheses indicates the two **A**-**B** interfaces.

Species **B** exhibits six intermolecular B-B NOE contacts that are consistent with the intermolecular contacts at the interior vertices of the triangular trimers that comprise the peptide 2 crystallographic hexamer. Table 2.1 summarizes these six intermolecular contacts centered around the strong NOE between Lys_{16} Hα and Phe_{20} Hα shown in Figure 10A. We excluded the possibility of the observed B-B NOEs arising from an antiparallel β-sheet dimer, in which Lys_{16} and Phe_{20} form a hydrogen-bonded pair, because the *N*-methyl group on Cha_{19} would disrupt hydrogen bonding at the dimer interface.

Species **A** and **B** exhibit eleven intermolecular A-B NOE contacts that reveal how species **A** interfaces with the species **B** triangular trimer. These NOEs reflect two distinct interfaces between the **A** and **B** species. Seven of the NOEs involve a locus of contacts centered around the strong NOE between Ala_{30} Hα (species **B**) and Phe_{20} Hα (species **A**). Four of the NOEs reflect a locus of contacts centered around the strong NOE between Ile_{32} Hα (species **B**) and Ala_{30} Hα (species **A**). The observed pattern of A-B intermolecular contacts indicates that one molecule of species **A** forms intermolecular contacts with two adjacent molecules of species **B** as shown in Figure **10B**. The 1:1 integration between species **A** and **B** in conjunction with the two observed A-B interfaces suggest that species **A** assembles into a cylindrin-like trimer.

Species **A** exhibits a network of nine intermolecular NOEs consistent with the expected A-A intermolecular contacts within the cylindrin-like trimer (Table **2.1**). In the cylindrin, the KLVFFAE β-strand of each molecule forms an antiparallel interface with the AIIGLMV β-strand of the adjacent molecule. The nine intermolecular NOEs involving outer facing NH, Hα, and *N*-methyl protons of these two strands are consistent with orientation of the strands shown in Figure 10B. Especially notable is a strong NOE between Leu_{17} NH and Gly_{33} NH, which is consistent with the contact between Leu_{17} and Gly_{33} shown in Figure **2.10C**. Collectively, these contacts

between the KLVFFAE and AIIGLMV strands are consistent with the cylindrin-like trimer structure and are distinct from those that would be expected from a triangular trimer, such as that observed in the crystallographic hexamer.

DOSY NMR suggests two asymmetric hexamers further assemble to form a dodecamer We used DOSY NMR to further assess the oligomerization state of the asymmetric hexamer and found — to our surprise — that peptide **2** assembles into a well-defined oligomer that is larger than a hexamer (Figure S2.14). At 1.0 mM, the DOSY spectrum of peptide **2** shows one track associated with the diffusion coefficient of the monomer (1.98×10^{-10} m^2/s). At 6.0 mM, the DOSY spectrum shows multiple tracks corresponding to slow exchange on the NMR timescale between monomer and oligomer. At 11.0 mM, the DOSY spectrum shows one track associated with the diffusion coefficient of a well-defined oligomer (0.90×10^{-10} m^2/s).[30]

Our laboratory has previously characterized a variety of well-defined peptide tetramers using DOSY NMR and has consistently observed that the ratio of the diffusion coefficients of the oligomer and monomer reflects the oligomerization state in solution.[23,24,31–33] For compact structures, the diffusion coefficient scales as the negative cube root of the molecular weight. We have thus observed that the diffusion coefficients of tetramers are about 0.6 that of the monomers. For a hexamer, a ratio of 0.55 would be expected, and for a dodecamer, the ratio should be about 0.44. For peptide **2**, we observe a ratio of 0.46, which is too low to be consistent with a hexamer but is more consistent with that expected for a dodecamer. Other oligomers ranging from an octamer to a tetradecamer should have diffusion coefficients ratios ranging from 0.50 to 0.42, and thus cannot be rigorously distinguished by DOSY alone. The observed 1:1 integration ratio of NH and Hα proton resonances associated with species **A** and **B** in the ^1H NMR spectra rules out all odd-numbered oligomers. Additionally, our laboratory has observed

multiple crystallographic assemblies of dodecamers formed by similar macrocyclic β-hairpin peptides.[22,34] Thus, the DOSY spectra, integration of both oligomer species, and crystallographic precedence collectively suggest that peptide **2** assembles into a dodecamer composed of two hexamers, rather than a single hexamer.

The solution-phase asymmetric hexamer shown in Figure 2.10 has multiple exposed hydrophobic surfaces, which could promote further assembly through hydrophobic interactions. The hydrophobic contacts between a pair of hexamers must be sufficiently rapid on the NMR timescale to allow the three **A** molecules of each hexamer to remain chemically equivalent to each other and the three **B** molecules of each hexamer to remain chemically equivalent to each other. The observation of a single track in the DOSY spectrum of peptide **2** at 11.0 mM supports that the exchange between the two hexamers is rapid on the NMR timescale.

Molecular dynamics simulations on a pair of hexamers

To better understand the structure of the putative dodecamer suggested by the DOSY NMR studies, we performed a series of MD simulations on pairs of hexamers using Amber22 with the ff19SB force field. The initial coordinates of the hexamers were generated from the constrained NMR-based molecular model. The MD simulations were performed without constraints within the hexamers for 500 ns in an NVT ensemble using a periodic box of explicit water. The MD simulations suggest that the asymmetric hexamers are stable and retain the same overall topology shown in Figure 2.10. The asymmetric hexamers observed in the MD simulations are looser than the constrained NMR-based molecular model by about 3 Å backbone RMSD, reflecting the release of the constraints in the MD simulations (Figure S2.15). Intermolecular distances observed during MD simulations associated with key intermolecular

NOEs are largely consistent with the NMR-based molecular model of the asymmetric hexamer (Figure S2.16).

The MD simulations reveal that the interactions between two asymmetric hexamers are dynamic. In three of the MD simulations the two hexamers remain in contact as a loose dodecamer, while in the other two MD simulations the loose dodecamer either comes apart to give two asymmetric hexamers or only stays as a dodecamer with imposed distance constraints (Figure S2.17). This dynamic behavior between two asymmetric hexamers is consistent with absence of specific NOE contacts associated with the dodecamer and variety of contacts between the hexamer subunits. (Figure 2.11). The five MD simulations are further described in the Materials and Methods section of the Supporting Information.

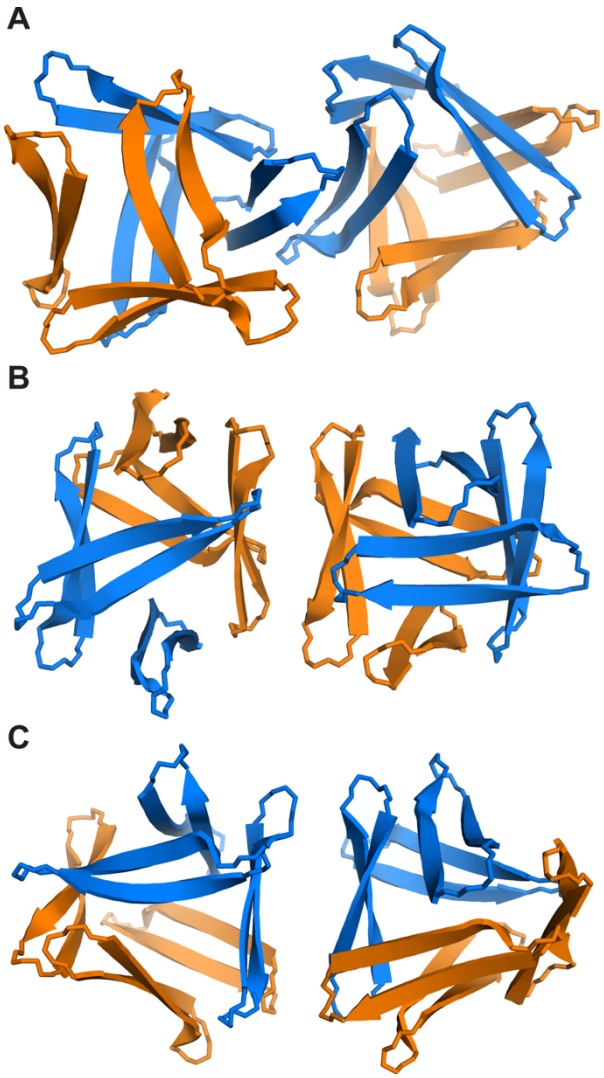

Figure 2.11. Three representative dodecamer configurations observed in different MD simulations. Species **A** is shown in blue and species **B** is shown in orange.

Effect of varying *N*-methylation on assembly in aqueous solution

To better understand which hydrogen bonds are crucial for the assembly of the asymmetric hexamer, we prepared homologues **3a–c** in which the position of *N*-methylation varies from that of peptide **2** (Table 2.2). We started by shifting the position of *N*-methylation from Cha_{19} to Gly_{33} on peptide **3a**.[34] ^{1}H NMR spectroscopy indicates that peptide **3a** does not assemble to form well-defined oligomers at concentration up to 8.0 mM. The absence of

assembly of peptide **3a** suggests that hydrogen bonding at Gly_{33} is important for the assembly of the asymmetric hexamer.

Table 2.2. Summary of peptide **2** analogues and their assembly in aqueous solution.

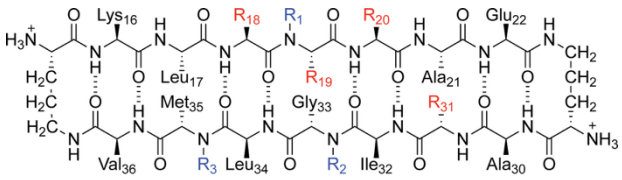

Peptide	R_1	R_2	R_3	R_{18}	R_{19}	R_{20}	R_{31}	Well-defined oligomer?
2	Me	H	H	Val	Cha	Phe	Ile	Yes
3a	H	Me	H	Val	Cha	Phe	Ile	No
3b	Me	Me	H	Val	Cha	Phe	Ile	No
3c	Me	H	Me	Val	Cha	Phe	Ile	Yes
4a	Me	H	H	Val	Cha	Phe	Chg	No
4b	Me	H	H	Val	Cha	Tyr	Ile	Yes
5	Me	H	H	Thr	Phe	Tyr	Ile	No

We prepared doubly methylated homologue **3b**, with methyl groups at Cha_{19} and Gly_{33}, to further probe the role of intermolecular hydrogen bonding between Leu_{17} and Gly_{33} within the cylindrin-like trimer formed by species **A**. Although peptide **3b** shows some propensity to oligomerize in the DOSY spectrum, we do not observe the formation of two discrete species in the ^{1}H NMR spectrum. The absence of two species suggests that intermolecular hydrogen bonds involving the Gly_{33} NH are critical to the formation of species **A** and **B**.

We also prepared doubly methylated homologue **3c**, with methyl groups at Cha_{19} and Met_{35}. The amide NH group of Met_{35} does not participate in hydrogen bonding in model of the asymmetric hexamer. We thus anticipated that *N*-methylation at Met_{35} should be tolerated. In solution, peptide **3c** assembles into a well-defined oligomer analogous to that of peptide **2**. The ^{1}H NMR spectrum of peptide **3c** at 1.0 mM is similar to that of peptide **2** at 1.0 mM, showing one set of resonances associated with monomer. The ^{1}H NMR spectrum of peptide **3c** at 11.0

mM is similar to that of peptide **2** at 11.0 mM, showing two sets of resonances associated with an oligomer.

Effect of hydrophilic and hydrophobic mutations on assembly in aqueous solution

To further probe the structures of the hexamer subunits of the dodecamer, we prepared homologues of peptide **2**, **4a** and **4b**, in which the amphiphilicity is augmented. Peptide **4a** increases the hydrophobicity of peptide **2** by mutating the interior residue Ile_{31} to cyclohexylglycine (Chg). The DOSY spectra show that peptide **4a** self-associates at lower peptide concentrations than peptide **2**. At 1.0 mM, the ^{1}H NMR spectrum is sharp and is similar to that of peptide **2**. At 6.0 mM, the ^{1}H NMR spectrum is broad, without distinct peaks for individual α-protons. The greater propensity of peptide **4a** to self-associate and the absence of a well-defined oligomer suggest that the steric bulk provided by both Cha_{19} and Chg_{31} is too great to permit the formation of a well-packed hydrophobic core of the hexamer subunit.

In peptide **4b**, we decreased the hydrophobicity of the exterior residue Phe_{20} by mutation to Tyr, with the hypothesis that the increased hydrophilicity would diminish uncontrolled aggregation and promote oligomerization. In solution, the propensity of peptide **4b** to form well-defined oligomers is comparable to that of peptide **2**. We also prepared peptide **5**, a homologue of peptide **1** with Phe_{20}-to-Tyr and Val_{18}-to-Thr mutations to explore whether increasing the hydrophilicity of exterior residues can promote oligomerization. Like peptide **1**, peptide **5** shows little propensity to oligomerize at concentrations up to 8.0 mM. Collectively, peptides **4b** and **5** demonstrate that hydrophilic mutations on exterior surfaces are tolerated but do not promote oligomer formation.

Conclusions

Aβ exhibits a remarkable propensity for supramolecular assembly. In the case of full-length Aβ, this assembly typically takes the form of aggregation into fibrils consisting of parallel β-sheets or oligomers with unknown structure. Fragments from the central and *C*-terminal regions of Aβ also have a propensity to aggregate. Macrocyclization and *N*-methylation permit these fragments to be tamed and crystallized into a well-defined oligomer. Strategic Phe-to-Cha mutation promotes assembly of a discrete well-defined oligomer, an asymmetric hexamer that differs in structure from that of the symmetric crystallographic hexamer.

Previously, our laboratory has only observed well-defined oligomer assembly by solution-phase NMR spectroscopy in a related class of macrocyclic β-hairpin peptides that contain Hao, a tripeptide mimic designed to template β-sheet formation. The planar character of Hao template biases the formation of sandwich tetramers in aqueous solution. Peptide **2** provides a more native-like model of Aβ β-hairpins in aqueous solution by reincorporating more of the native Aβ sequence. Solution-phase NMR spectroscopy shows that peptide **2** is the first *N*-methylated macrocyclic β-hairpin peptide to assemble to form a well-defined oligomer that can be characterized by solution-phase NMR spectroscopy. When compared to the Hao-containing peptides, peptide **2** adopts a much more twisted β-hairpin conformation, suggesting that the extent of hairpin twisting may influence the resulting oligomer that forms.

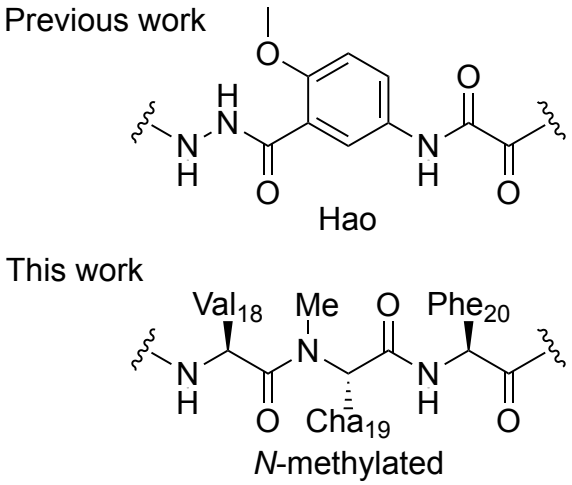

In aqueous solution, peptide **2** assembles into an asymmetric hexamer composed of a cylindrin-like trimer and a triangular trimer. Selective isotope incorporation (^{2}H and ^{15}N) proved essential both in enumerating the number of distinct species and identifying key intermolecular contacts, which were used to construct a molecular model of the asymmetric hexamer. DOSY NMR and MD simulations illustrate how the asymmetric hexamer can further assemble to form a loosely packed dodecamer composed of two hexamers. The presence of two distinct subunits and further supramolecular assembly is reminiscent of the oligomer observed by Carulla and coworkers in their tetramer and octamer model of $A\beta_{1-42}$.[17,35]

The supramolecular assembly of Aβ oligomers into soluble oligomers continues to be of fundamental interest in understanding the molecular basis of Alzheimer's disease, yet the observation of soluble Aβ oligomers by solution-phase NMR spectroscopy has largely eluded researchers thus far. The solution-phase NMR studies of peptide **2** and its analogues contribute to the understanding of how amyloidogenic fragments from the central and *C*-terminal regions of Aβ can assemble to form well-defined oligomers in aqueous solution. The observation that peptide **2** forms a well-defined oligomer but peptide **1** does not suggests that these macrocyclic β-hairpin peptides teeter on the border of assembling into well-defined oligomers in aqueous

solution. Studies on peptide **2** analogues demonstrate how solution-phase assembly depends on a delicate balance of intermolecular hydrogen bonding, hydrophobic interactions, and steric considerations. The characterization of well-defined oligomers of Aβ at atomic resolution continues to be an important and formidable challenge. We envision that *N*-methylation and hydrophobic Phe-to-Cha mutations may also be also useful in stabilizing other soluble Aβ oligomers and facilitating their observation by solution-phase NMR spectroscopy.

References and Notes

(1) Benilova, I.; Karran, E.; De Strooper, B. The Toxic Aβ Oligomer and Alzheimer's Disease: An Emperor in Need of Clothes. *Nat. Neurosci.* **2012**, *15* (3), 349–357. https://doi.org/10.1038/nn.3028.

(2) Cline, E. N.; Bicca, M. A.; Viola, K. L.; Klein, W. L. The Amyloid-β Oligomer Hypothesis: Beginning of the Third Decade. *J. Alzheimers Dis. 64* (Suppl 1), S567–S610. https://doi.org/10.3233/JAD-179941.

(3) Shankar, G. M.; Li, S.; Mehta, T. H.; Garcia-Munoz, A.; Shepardson, N. E.; Smith, I.; Brett, F. M.; Farrell, M. A.; Rowan, M. J.; Lemere, C. A.; Regan, C. M.; Walsh, D. M.; Sabatini, B. L.; Selkoe, D. J. Amyloid-β Protein Dimers Isolated Directly from Alzheimer's Brains Impair Synaptic Plasticity and Memory. *Nat. Med.* **2008**, *14* (8), 837–842. https://doi.org/10.1038/nm1782.

(4) Gremer, L.; Schölzel, D.; Schenk, C.; Reinartz, E.; Labahn, J.; Ravelli, R. B. G.; Tusche, M.; Lopez-Iglesias, C.; Hoyer, W.; Heise, H.; Willbold, D.; Schröder, G. F. Fibril Structure of Amyloid-β(1–42) by Cryo–Electron Microscopy. *Science* **2017**, *358* (6359), 116–119. https://doi.org/10.1126/science.aao2825.

(5) Kollmer, M.; Close, W.; Funk, L.; Rasmussen, J.; Bsoul, A.; Schierhorn, A.; Schmidt, M.; Sigurdson, C. J.; Jucker, M.; Fändrich, M. Cryo-EM Structure and Polymorphism of Aβ Amyloid Fibrils Purified from Alzheimer's Brain Tissue. *Nat. Commun.* **2019**, *10* (1), 4760. https://doi.org/10.1038/s41467-019-12683-8.

(6) Ghosh, U.; Thurber, K. R.; Yau, W.-M.; Tycko, R. Molecular Structure of a Prevalent Amyloid-β Fibril Polymorph from Alzheimer's Disease Brain Tissue. *Proc. Natl. Acad. Sci.* **2021**, *118* (4), e2023089118. https://doi.org/10.1073/pnas.2023089118.

(7) Yang, Y.; Arseni, D.; Zhang, W.; Huang, M.; Lövestam, S.; Schweighauser, M.; Kotecha, A.; Murzin, A. G.; Peak-Chew, S. Y.; Macdonald, J.; Lavenir, I.; Garringer, H. J.; Gelpi, E.; Newell, K. L.; Kovacs, G. G.; Vidal, R.; Ghetti, B.; Ryskeldi-Falcon, B.; Scheres, S. H. W.; Goedert, M. Cryo-EM Structures of Amyloid-β 42 Filaments from Human Brains. *Science* **2022**, *375* (6577), 167–172. https://doi.org/10.1126/science.abm7285.

(8) Frieg, B.; Han, M.; Giller, K.; Dienemann, C.; Riedel, D.; Becker, S.; Andreas, L. B.; Griesinger, C.; Schröder, G. F. Cryo-EM Structures of Lipidic Fibrils of Amyloid-β (1-40). *Nat. Commun.* **2024**, *15* (1), 1297. https://doi.org/10.1038/s41467-023-43822-x.

(9) Tycko, R. Solid State NMR Studies of Amyloid Fibril Structure. *Annu. Rev. Phys. Chem.* **2011**, *62*, 279–299. https://doi.org/10.1146/annurev-physchem-032210-103539.

(10) Durell, S. R.; Guy, H. R.; Arispe, N.; Rojas, E.; Pollard, H. B. Theoretical Models of the Ion Channel Structure of Amyloid Beta-Protein. *Biophys. J.* **1994**, *67* (6), 2137–2145. https://doi.org/10.1016/S0006-3495(94)80717-9.
(11) George, A. R.; Howlett, D. R. Computationally Derived Structural Models of the β-Amyloid Found in Alzheimer's Disease Plaques and the Interaction with Possible Aggregation Inhibitors. *Biopolymers* **1999**, *50* (7), 733–741. https://doi.org/10.1002/(SICI)1097-0282(199912)50:7<733::AID-BIP6>3.0.CO;2-7.
(12) Li, L.; Darden, T. A.; Bartolotti, L.; Kominos, D.; Pedersen, L. G. An Atomic Model for the Pleated *β*-Sheet Structure of A*β* Amyloid Protofilaments. *Biophys. J.* **1999**, *76* (6), 2871–2878. https://doi.org/10.1016/S0006-3495(99)77442-4.
(13) Hoyer, W.; Grönwall, C.; Jonsson, A.; Ståhl, S.; Härd, T. Stabilization of a β-Hairpin in Monomeric Alzheimer's Amyloid-β Peptide Inhibits Amyloid Formation. *Proc. Natl. Acad. Sci.* **2008**, *105* (13), 5099–5104. https://doi.org/10.1073/pnas.0711731105.
(14) Sandberg, A.; Luheshi, L. M.; Söllvander, S.; Pereira de Barros, T.; Macao, B.; Knowles, T. P. J.; Biverstål, H.; Lendel, C.; Ekholm-Petterson, F.; Dubnovitsky, A.; Lannfelt, L.; Dobson, C. M.; Härd, T. Stabilization of Neurotoxic Alzheimer Amyloid-β Oligomers by Protein Engineering. *Proc. Natl. Acad. Sci.* **2010**, *107* (35), 15595–15600. https://doi.org/10.1073/pnas.1001740107.
(15) Yu, L.; Edalji, R.; Harlan, J. E.; Holzman, T. F.; Lopez, A. P.; Labkovsky, B.; Hillen, H.; Barghorn, S.; Ebert, U.; Richardson, P. L.; Miesbauer, L.; Solomon, L.; Bartley, D.; Walter, K.; Johnson, R. W.; Hajduk, P. J.; Olejniczak, E. T. Structural Characterization of a Soluble Amyloid β-Peptide Oligomer. *Biochemistry* **2009**, *48* (9), 1870–1877. https://doi.org/10.1021/bi802046n.
(16) Itoh, S. G.; Yagi-Utsumi, M.; Kato, K.; Okumura, H. Key Residue for Aggregation of Amyloid-β Peptides. *ACS Chem. Neurosci.* **2022**, *13* (22), 3139–3151. https://doi.org/10.1021/acschemneuro.2c00358.
(17) Ciudad, S.; Puig, E.; Botzanowski, T.; Meigooni, M.; Arango, A. S.; Do, J.; Mayzel, M.; Bayoumi, M.; Chaignepain, S.; Maglia, G.; Cianferani, S.; Orekhov, V.; Tajkhorshid, E.; Bardiaux, B.; Carulla, N. Aβ(1-42) Tetramer and Octamer Structures Reveal Edge Conductivity Pores as a Mechanism for Membrane Damage. *Nat. Commun.* **2020**, *11* (1), 3014. https://doi.org/10.1038/s41467-020-16566-1.
(18) Kreutzer, A. G.; Spencer, R. K.; McKnelly, K. J.; Yoo, S.; Hamza, I. L.; Salveson, P. J.; Nowick, J. S. A Hexamer of a Peptide Derived from Aβ16–36. *Biochemistry* **2017**, *56* (45), 6061–6071. https://doi.org/10.1021/acs.biochem.7b00831.
(19) Kreutzer, A. G.; Hamza, I. L.; Spencer, R. K.; Nowick, J. S. X-Ray Crystallographic Structures of a Trimer, Dodecamer, and Annular Pore Formed by an $A\beta_{17–36}$ β-Hairpin. *J. Am. Chem. Soc.* **2016**, *138* (13), 4634–4642. https://doi.org/10.1021/jacs.6b01332.
(20) Nowick, J. S.; Brower, J. O. A New Turn Structure for the Formation of β-Hairpins in Peptides. *J. Am. Chem. Soc.* **2003**, *125* (4), 876–877. https://doi.org/10.1021/ja028938a.
(21) McKnelly, K. J.; Kreutzer, A. G.; Howitz, W. J.; Haduong, K.; Yoo, S.; Hart, C.; Nowick, J. S. Effects of Familial Alzheimer's Disease Mutations on the Assembly of a β-Hairpin Peptide Derived from Aβ16–36. *Biochemistry* **2022**, *61* (6), 446–454. https://doi.org/10.1021/acs.biochem.1c00664.
(22) Kreutzer, A. G.; Yoo, S.; Spencer, R. K.; Nowick, J. S. Stabilization, Assembly, and Toxicity of Trimers Derived from Aβ. *J. Am. Chem. Soc.* **2017**, *139* (2), 966–975. https://doi.org/10.1021/jacs.6b11748.

(23) Truex, N. L.; Wang, Y.; Nowick, J. S. Assembly of Peptides Derived from β-Sheet Regions of β-Amyloid. *J. Am. Chem. Soc.* **2016**, *138* (42), 13882–13890. https://doi.org/10.1021/jacs.6b06000.
(24) Pham, J. D.; Demeler, B.; Nowick, J. S. Polymorphism of Oligomers of a Peptide from β-Amyloid. *J. Am. Chem. Soc.* **2014**, *136* (14), 5432–5442. https://doi.org/10.1021/ja500996d.
(25) Senguen, F. T.; Lee, N. R.; Gu, X.; Ryan, D. M.; Doran, T. M.; Anderson, E. A.; Nilsson, B. L. Probing Aromatic, Hydrophobic, and Steric Effects on the Self-Assembly of an Amyloid-β Fragment Peptide. *Mol. Biosyst.* **2011**, *7* (2), 486–496. https://doi.org/10.1039/C0MB00080A.
(26) Haerianardakani, S.; Kreutzer, A. G.; Salveson, P. J.; Samdin, T. D.; Guaglianone, G. E.; Nowick, J. S. Phenylalanine Mutation to Cyclohexylalanine Facilitates Triangular Trimer Formation by β-Hairpins Derived from Aβ. *J. Am. Chem. Soc.* **2020**, *142* (49), 20708–20716. https://doi.org/10.1021/jacs.0c09281.
(27) We diluted an 11 mM solution of peptide 2 to 1 mM and observed that the sample re-equilibrated to the monomer on the order of hours. This experiment indicated that the equilibrium between monomer and oligomer is reversible and that the rate of exchange occurs slowly on the NMR timescale.
(28) Wishart, D. S.; Sykes, B. D. Chemical Shifts as a Tool for Structure Determination. In *Methods in Enzymology*; Nuclear Magnetic Resonance, Part C; Academic Press, 1994; Vol. 239, pp 363–392. https://doi.org/10.1016/S0076-6879(94)39014-2.
(29) Laganowsky, A.; Liu, C.; Sawaya, M. R.; Whitelegge, J. P.; Park, J.; Zhao, M.; Pensalfini, A.; Soriaga, A. B.; Landau, M.; Teng, P. K.; Cascio, D.; Glabe, C.; Eisenberg, D. Atomic View of a Toxic Amyloid Small Oligomer. *Science* **2012**, *335* (6073), 1228–1231. https://doi.org/10.1126/science.1213151.
(30) Peptide 2 is not fully soluble at 16.0 mM. However, the nominal 16.0 mM DOSY spectrum gave a nearly identical diffusion coefficient (0.90×10^{-10} m^2/s), which suggests the soluble oligomer is well-defined.
(31) Li, X.; Rios, S. E.; Nowick, J. S. Enantiomeric β-Sheet Peptides from Aβ Form Homochiral Pleated β-Sheets Rather than Heterochiral Rippled β-Sheets. *Chem. Sci.* **2022**, *13* (26), 7739–7746. https://doi.org/10.1039/D2SC02080G.
(32) Khakshoor, O.; Demeler, B.; Nowick, J. S. Macrocyclic β-Sheet Peptides That Mimic Protein Quaternary Structure through Intermolecular β-Sheet Interactions. *J. Am. Chem. Soc.* **2007**, *129* (17), 5558–5569. https://doi.org/10.1021/ja068511u.
(33) Pham, J. D.; Spencer, R. K.; Chen, K. H.; Nowick, J. S. A Fibril-Like Assembly of Oligomers of a Peptide Derived from β-Amyloid. *J. Am. Chem. Soc.* **2014**, *136* (36), 12682–12690. https://doi.org/10.1021/ja505713y.
(34) Salveson, P. J.; Spencer, R. K.; Kreutzer, A. G.; Nowick, J. S. X-Ray Crystallographic Structure of a Compact Dodecamer from a Peptide Derived from Aβ16-36. *Org. Lett.* **2017**, *19* (13), 3462–3465. https://doi.org/10.1021/acs.orglett.7b01445.
(35) The Carulla tetramer and octamer model may differ from the asymmetric hexamer model because of the different β-hairpin registrations. The offset in hairpin registration by one residue alters the pattern of hydrogen bonding, pairing of amino acid side chains, and the resulting oligomer that forms.

Chapter 3: Synthesis and Study of the Peptide Antibiotic Hypeptin

Preface to Chapter 3

Chapter 3 aims to build on previous work done studying two structurally related cyclodepsipeptide antibiotics, texiobactin and clovbactin. In establishing the stereochemical configuration of Novo29 (clovibactin), Dr. Maj Krumberger and Dr. Xingyue Li pioneered the syntheses of the hydroxyasparagines that Jackson Brundicardi further optimized in his structure-activity-relationship on clovibactin. I set out to synthesize the two remaining β-hydroxylated amino acids and to complete the first synthesis of hypeptin.

Sections of this chapter are adapted from a publication in progress. Jackson Brunicardi, Jeramiah Small, and Cheyenne Strombeck synthesized the suitably protected (2*S*,3*R*)-hydroxyasparagine and (2*R*,3*R*)-hydroxyasparagine amino acid building blocks. Jackson Brunicardi and Adam Kreutzer identified the nitrile byproduct that forms during coupling of the two hydroxyasparagines. Stefania De Benedetti, a post-doctorate researcher in Professor Tanja Scheider's research group graciously expressed natural hypeptin. I performed all other experiments described in this chapter.

Introduction

New antibiotics are desperately needed to combat the ongoing antibiotic resistance crisis. In 2023, the World Health Organization estimated that 17.2% of all laboratories confirmed bacterial infections were caused by antimicrobial resistant bacteria.[1] Antibiotic-resistant infections are projected to reduce average global life expectancy by 1.8 years over the next decade without the development of new antibiotics.[2] This crisis is compounded by the greatly diminished number of antibiotics currently in development.

Hypeptin is an unexplored cyclodepsipeptide antibiotic that is active against Gram-positive MRSA at 0.25 μg/mL, VRE at 2 μg/mL, and *M. bovis* (bovine tubercuolosis) at 0.25 μg/mL.[3] Serial passaging of hypeptin against *S.* aureus failed to induce antibiotic resistance. It was originally isolated from *Pseudomonas sp*. PB-6269 by Yoshida and coworkers in 1989 and later reisolated from *Lysobacter sp*. K5869 by Schneider and coworkers in 2021.[4,3] Hypeptin targets the pyrophosphate group of lipid II and related bacterial cell wall precursors.[3] Binding to pyrophosphate inhibits peptidoglycan and wall teichoic acid biosynthesis, prevents Gram-positive bacteria from forming a cell wall, and leads to bacterial cell lysis. Gram-positive bacteria cannot readily develop antibiotic resistance because the pyrophosphate moiety is extracellular and conserved in multiple essential biosynthetic pathways.

As a cyclodepsipeptide antibiotic, hypeptin shares structural similarities with both clovibactin and teixobactin (Figure 3.1).[5,6] All three antibiotics share a 13-membered macrolactone ring with a linear tail. Clovibactin and hypeptin conserve (2*R*,3*R*)-hydroxyAsn at residue 5 to link the ring to the tail.[7] The unique combinations of alternating L- and D-stereochemistry along the tail promote supramolecular assembly of these cyclodepsipeptide antibiotics. In teixobactin, for example, the alternating pattern of L- and D-residues result in the

assembly to form novel amphiphilic β-sheets that bind lipid II and ultimately result in bacterial cell lysis.[6,8]

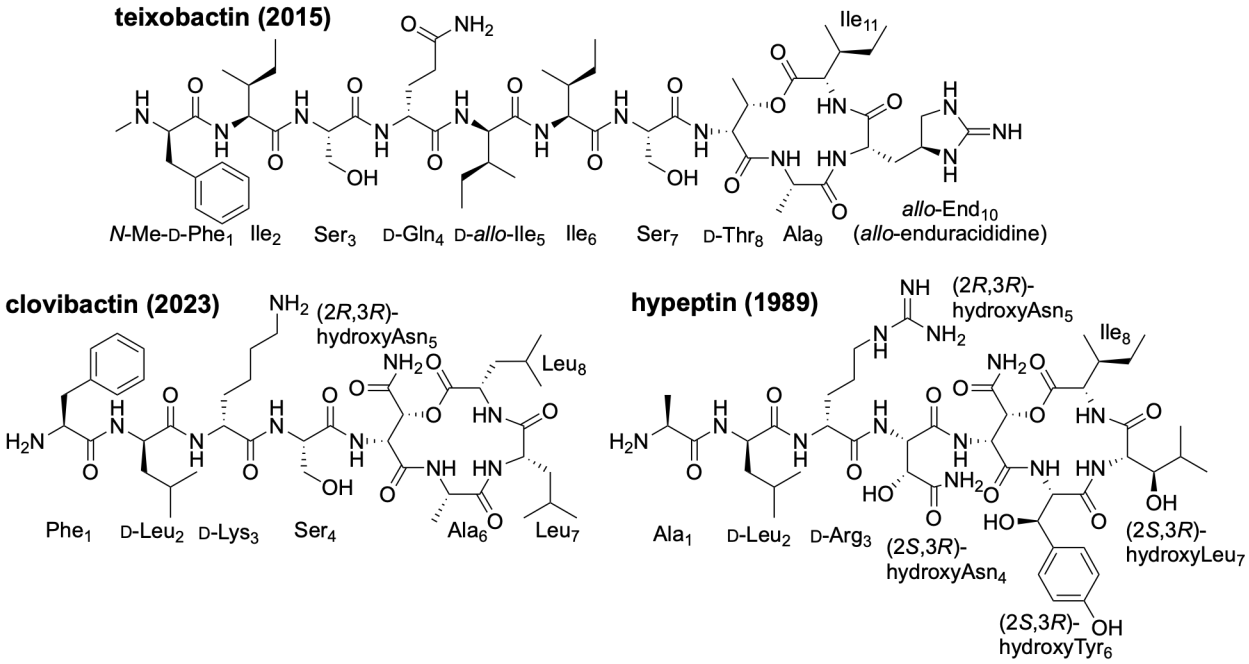

Figure 3.1. Chemical structures of hypeptin, clovibactin, and teixobactin.

The macrolactone ring of each of these cyclodepsipeptide antibiotics recognizes the pyrophosphate group of lipid II and related cell-wall precursors. In texiobactin, the cationic *allo*-enduracididine residue forms electrostatic contacts with the anionic pyrophosphate and additional contacts with the MurNAc sugar of lipid II, which result in especially strong binding.[6] In clovibactin, the amide NH groups within the ring and Lys_3 side-chain amine bind to pyrophosphate.[5] Hypeptin is thought to complex with pyrophosphate in an analogous fashion, although the exact contacts and conformation are unknown. Among this family of three cyclodepsipeptide antibiotics, hypeptin is the most enigmatic because six of its eight residues are non-proteinogenic, and four of its non-proteinogenic residues contain unusual hydroxylation. While several syntheses of texiobactin and clovibactin were reported within a few years of their discovery, no synthesis of hypeptin has been reported even though its structure was first reported 37 years ago.[7,9–12]

The absolute configuration of hypeptin was first assigned by acid hydrolysis of the peptide followed by analysis of the constituent amino acids by chiral chromatography.[4,13] Analysis of the retention times revealed that hypeptin contains L-Ala$_1$, D-Leu$_2$, D-Arg$_3$, (2*S*,3*R*)-hydroxyAsn$_4$, (2*R*,3*R*)-hydroxyAsn$_5$, (2*S*,3*R*)-hydroxyLeu$_7$, and L-Ile$_8$. The configuration hydroxyTyr$_6$ was not determined because it decomposed during acid hydrolysis.[4] It was postulated to be (2*S*,3*S*), however, on the basis of NMR data that were never published.

Subsequent work by Schneider et al. elucidated the biosynthesis of hypeptin and identified the two hydroxylases—HynC and HynE—responsible for the four non-proteogenic β-hydroxylated amino acids from which hypeptin derives its name.[3] HynC is a non-heme diiron monooxygenase that hydroxylates L-Tyr$_6$ in a *syn*-configuration. This strongly suggests that hypeptin contains (2*S*,3*R*)-hydroxyTyr$_6$, rather than (2*S*,3*S*)-hydroxyTyr$_6$. Although NMR spectroscopy also suggests the (2*S*,3*R*) stereochemistry, the stereochemical configuration at hydroxyTyr$_6$ has not been confirmed by chemical synthesis.

More than ten other peptide natural products contain β-hydroxytyrosine, including ralstonins A and B, burkholidine-1097, and balticidins A−D (Figure S3.1 and Table S3.1).[14–18] Although chemical syntheses of all four β-hydroxtyrosine stereoisomers have been reported, there are no published syntheses of any β-hydroxytyrosine-containing peptide natural products.[19] The lack of published syntheses stands in contrast to the published syntheses of β-hydroxyleucine- and β-hydroxyasparagine-containing peptide natural products.[20–25,7] There is only one report of the synthesis of a β-hydroxytyrosine-containing peptide—a simplified analogue of burkholidine-1097 in which the other noncanonical hydroxylated amino acids were replaced with synthetically more accessible amino acids.[26] In this synthesis, the authors found it necessary to use anhydrous TFA to remove side-chain protecting groups without dehydration or

reduction of β-hydroxytyrosine residue. The absence of water reduces the decomposition of the β-hydroxytyrosine residue by a resonance stabilized carbocation or quinone methide intermediate. The lability of the β-hydroxytyrosine residue thus makes hypeptin and other β-hydroxytyrosine-containing peptide natural products challenging synthetic targets.

Herein, we report the first synthesis of hypeptin and confirm that the stereochemical configuration of hydroxytyrosine at position 6 to be 2*S*,3*R*. We detail the syntheses of the four suitably protected β-hydroxylated amino acid building blocks that enable a solid-peptide synthesis of an acyclic octapeptide precursor, which we cyclize in solution to generate protected hypeptin. Our initial efforts to deprotect hypeptin failed, because the TBS protecting groups could not be removed with tetrabutylammonium fluoride (TBAF) and the β-hydroxytyrosine residue proved too acid-labile for deprotection with TFA. This failure prompted us to develop a second-generation synthesis of hypeptin that circumvented these problems by changing the protecting groups and deprotection conditions. In the second-generation synthesis, we replaced the Boc and *t*-Bu protecting groups with Cbz and Bn groups, switched to hydrogenolytic deprotection conditions, and used HF-pyridine in palce of TBAF.

Through LC-MS and NMR spectroscopy, we confirmed that natural and synthetic hypeptin are identical. We envision that this synthesis of hypeptin will lay the foundation of future structure-activity studies and will also enable the synthesis of other β-hydroxytyrosine-containing peptide natural products.

Results and Discussion

Synthetic Strategy to Hypeptin

We initially envisioned an Fmoc-based solid-phase peptide synthesis (SPPS) approach to hypeptin that involved on-resin Steglich esterification, solution-phase macrolactamization, fluoride-mediated silyl deprotection, and anhydrous TFA global deprotection (Figure 3.2).

Previously, we published a similar on-resin esterification and solution-phase macrolactamization approach to synthesize clovibactin and texiobactin analogues.[7,27] Hypeptin presented an additional layer of complexity with five hydroxy groups that must be differentiated during Steglich esterification. To regioselectively esterify at (2*R*,3*R*)-hydroxyAsn$_5$, we *tert*-butyldimethylsilyl (TBS) protected β-hydroxy groups of (2*S*,3*R*)-hydroxyAsn$_4$, (2*S*,3*R*)-hydroxyTyr$_6$, and (2*S*,3*R*)-hydroxyLeu$_7$ and *tert*-butyl (*t*-Bu) protected the (2*S*,3*R*)-hydroxyTyr$_6$ phenol. Two independent on-resin syntheses of clovibactin unequivocably demonstrates that the primary side-chain amide groups of hydroxyasparagine tolerate solid-phase peptide synthesis (SPPS) and Steglich esterification without protection.[7,9] To enable an on-resin synthesis of hypeptin, we first prepared four β-hydroxylated amino acid building blocks: protected (2*S*,3*R*)-3-hydroxyasparagine **1**, protected (2*R*,3*R*)-3-hydroxyasparagine **2**, protected (2*S*,3*R*)-3-hydroxytyrosine **3**, and protected (2*S*,3*R*)-3-hydroxyleucine **4** (Figure 3.2).

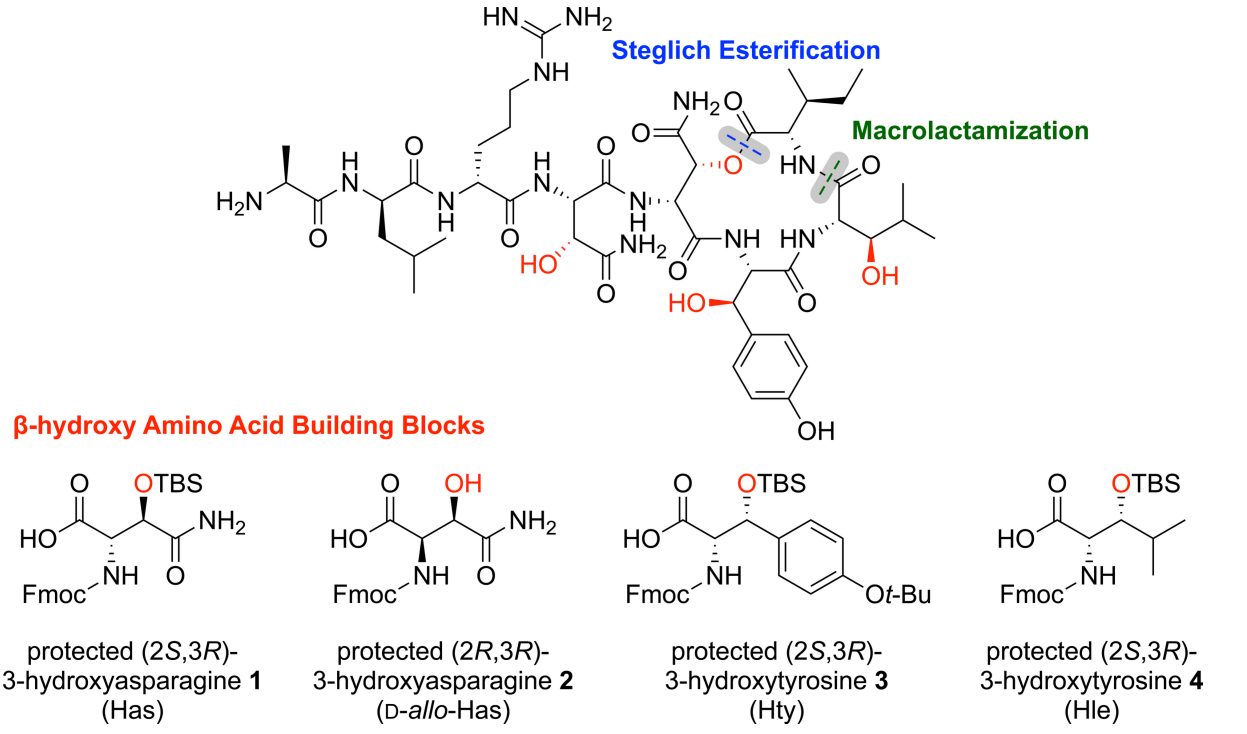

Figure 3.2. Synthetic strategy to hypeptin highlighting key disconnections and β-hydroxy amino acid building blocks.

Synthesis of four β-hydroxy amino acids

To synthesize protected (2*S*,3*R*)-3-hydroxyasparagine **1**, we adapted our published synthesis of the (2*R*,3*S*)-3-hydroxyasparagine enantiomer previously used to verify the stereochemical configuration of clovibactin (Scheme 3.1).[7] This route desymmetrized commercially available (2*R*,3*R*)-(+)-diethyl L-tartrate **5** via formation of a cyclic sulfite followed by S_N2 azide opening to afford the desired (2*S*,3*R*) anti-configuration of azido alcohol **6**. Reduction of the α-azido group, hydrolysis of both ethyl ester groups revealed a diacid, and regioselective Fisher esterification afforded amino alcohol **7** as an HCl salt. The greater electron withdrawing character of the α-ammonium group compared to the β-hydroxy group enabled kinetic differentiation of the two carboxylic acid groups. Subsequent ammonolysis of the methyl ester group, Fmoc protection of the α-amino group, and TBS protection of the β-hydroxy group furnished the protected (2*S*,3*R*)-hydroxyaspargine **1** in 8 steps with 16% overall yield.

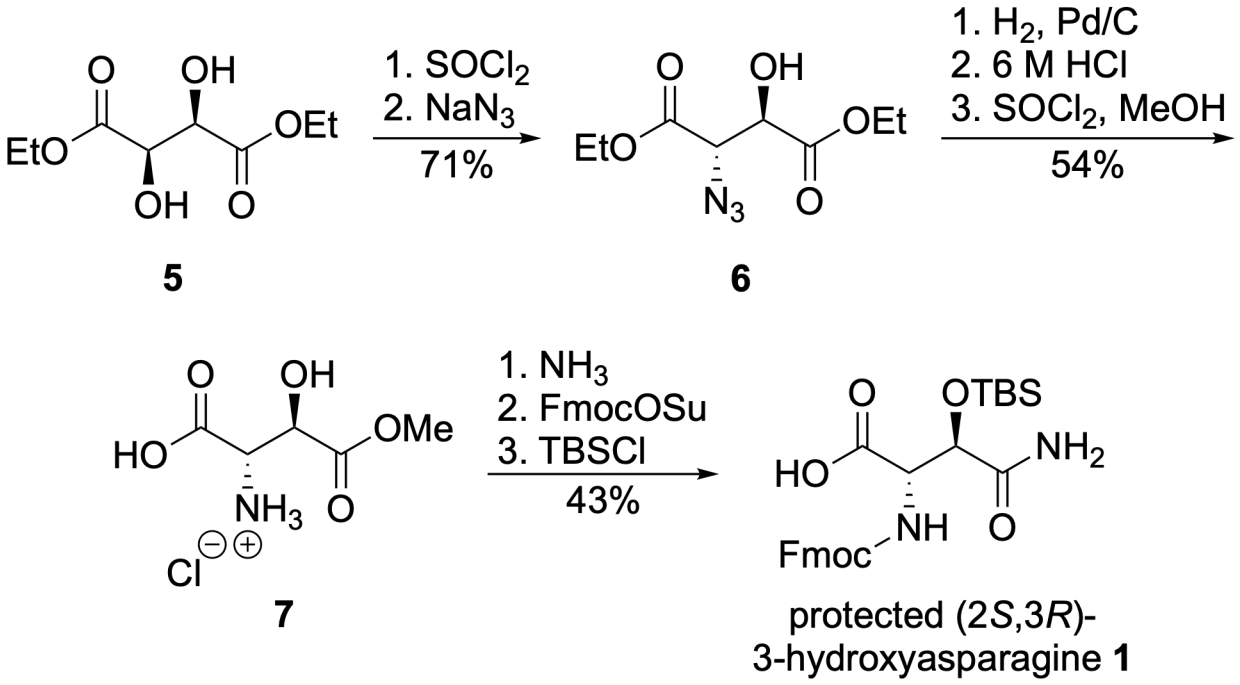

Scheme 3.1. Synthesis of protected (2*S*,3*R*)-3-hydroxyasparagine **1**

To synthetize protected (2*R*,3*R*)-3-hydroxyasparagine **2**, we applied our optimized synthesis that previously enabled an alanine scan on clovibactin (Scheme 3.2).[28] This optimized route reduced the (2*R*,3*R*)-3-hydroxyasparagine synthesis from 13 steps to 7 steps by directly setting the stereochemical configuration via an oxazoline intermediate and removing extraneous Boc and benzyl protection and deprotection steps. D-Aspartic acid **8** was Fischer esterified and benzoylated using modified Schotten–Baumann conditions to afford benzamide **9**. Formation of a lithium-chelated enolate dianion directs iodination with 3*S* stereochemistry that subsequently undergoes an intramolecular S_N2 displacement to afford oxazoline with 3*R* stereochemistry. Hydrolysis of the oxazoline group reveals diacid **10** as an HCl salt. Subsequent kinetic differentiation of the two carboxylic acid groups and Fmoc protection of the α-amino group afforded protected (2*R*,3*R*)-3-hydroxyasparagine **2** in 7 steps with 18% overall yield.

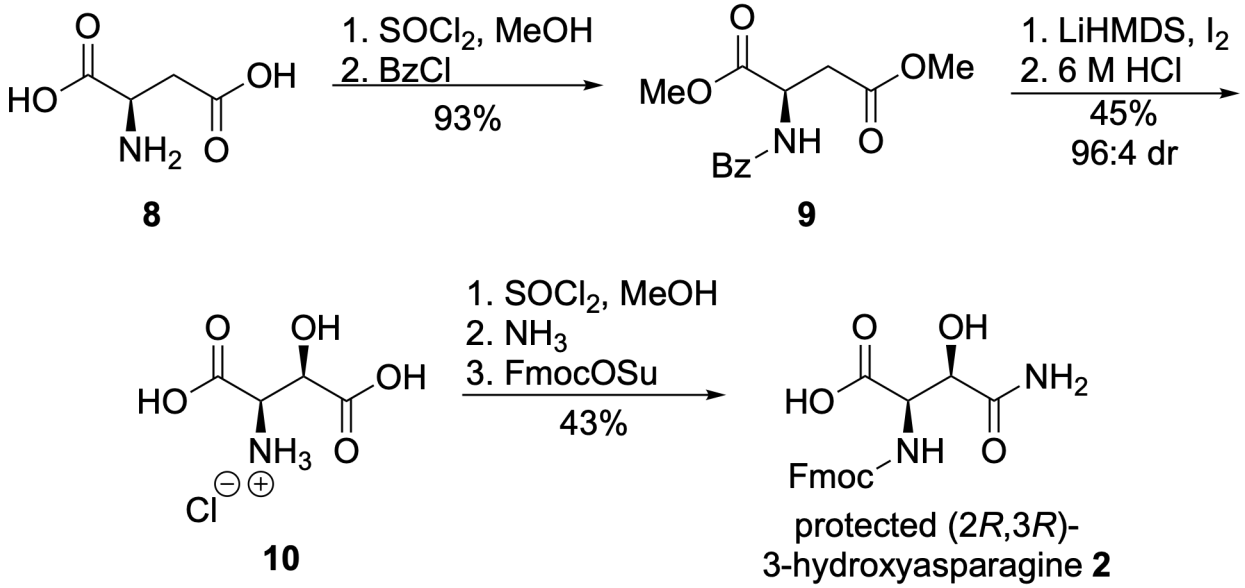

Scheme 3.2. Synthesis of protected (2*R*,3*R*)-3-hydroxyasparagine **2**

To synthesize protected (2*S*,3*R*)-3-hydroxytyrosine **3**, we pioneered an enantioselective synthesis that applied an α-azido enolate to simultaneously set both (2*S*,3*R*) stereocenters through an asymmetric aldol reaction (Scheme 3.3).[29] (*S*)-Thiazolidinethione **11** was prepared via

a T3P amide coupling to conjugate on α-azido acetic acid onto a commercially available chiral thiazolidine.[30] Formation of the syn aldol product proceeds through a titanium-chelated Zimmerman-Traxler transition state with high diastereoselectivity (> 98:2 dr) where the thiocarbonyl group of the auxiliary is not coordinated to titanium (Figure S2). While we originally envisioned an exocyclic cleavage of the auxiliary with lithium hydroperoxide to directly access azidoacid **13**, we discovered that exocyclic cleavage of the thiazolidine auxiliary proved low-yielding from competing undesired endocyclic cleavage, peroxide mediated side-reactions, and retro-aldol reaction.[31] For these reasons, we elected to subject the aldol product to methanolysis and LiOH saponification to afford azidoacid **13** in two steps. TBS protection of the β-hydroxy group, reduction of the azide group with catalytic hydrogenolysis, and Fmoc protection of the α-amino group afforded protected (2*S*,3*R*)-3-hydroxytyrosine **3** in 7 steps with 27% overall yield.

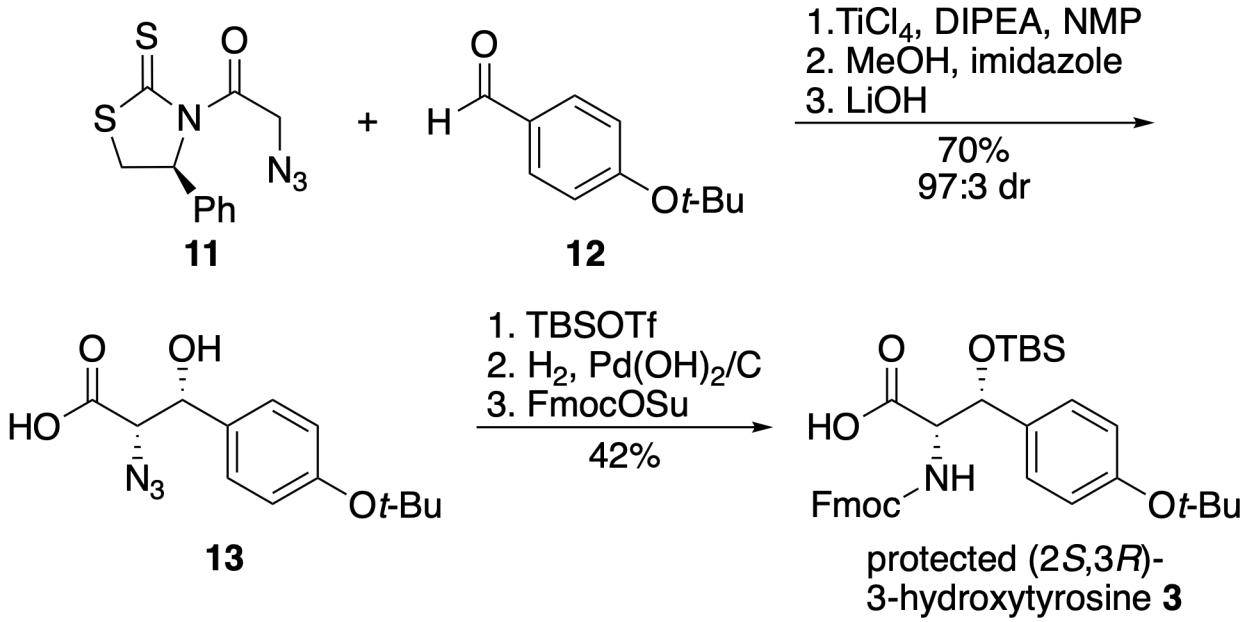

Scheme 3.3. Synthesis of protected (2*S*,3*R*)-3-hydroxytyrosine **3**

To synthesize protected (2*S*,3*R*)-3-hydroxyleucine **4**, we adapted a published synthesis of the (2*R*,3*R*)-3-hydroxyleucine diastereomer (Scheme 3.4).[32] Hale and coworkers previously set

the (2*R*,3*R*) stereocenters via a single S_N2 displacement of the α-stereocenter on a syn diol prepared by Sharpless asymmetric dihydroxylation. We envisioned that a strategic double displacement of the α-stereocenter via a regioselective bromoacylation reaction followed by an S_N2 azide displacement would afford the (2*S*,3*R*) configuration. This regioselective bromoacylation reaction was established by Fleming and Sharpless in their studies on analogous diol esters.[33] Diol **14** can readily be prepared on gram scale with a Wittig olefination and Sharpless asymmetric dihydroxylation. Treatment of diol **14** with HBr/AcOH forms a cyclic acetoxonium ion that regioselectively ring opens with bromide at the α-position because of the inductive effect of the adjacent ester (Figure S3). Subsequent deacetylation in acidic ethanol reveals bromoalcohol **15**. Our efforts to directly S_N2 azide displace bromoalcohol **15** led to 11% epimerization of the α-stereocenter that could not be separated during column chromatography of the later intermediates. TBS protection of the β-hydroxy group prior to azide displacement enabled separation of the undesired diastereomer with 96:4 diasteroselectivity. Removal of the TBS group and saponification of the ethyl ester group furnished azidoalcohol **17**. Lastly, Fmoc protection of the α-amino group and TBS protection of the β-hydroxy group afforded protected (2*S*,3*R*)-3-hydroxyleucine **4** in 9 steps with 2% overall yield. Although the overall yield is low, this synthesis provided enough protected hydroxyleucine to proceed with the synthesis of hypeptin because less protected amino acid is used during resin loading compared to that of amide coupling.

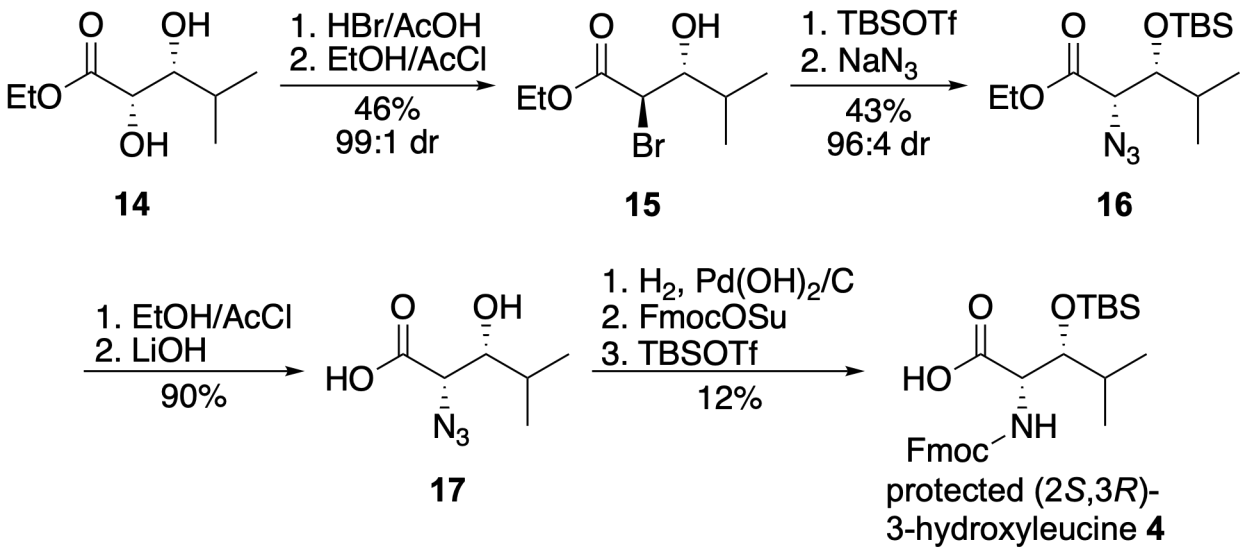

Scheme 3.4. Synthesis of protected (2*S*,3*R*)-3-hydroxyleucine **4**

First-generation synthesis of hypeptin

The four protected β-hydroxy amino acids enabled us to attempt the solid-phase peptide synthesis of hypeptin (Figure 3.3). This Fmoc-based SPPS proceeded by loading at Hle_7 onto 2-chlorotrityl resin and coupling residues 6 to 1. The coupling of the hydroxyasparagine amino acids (Has_4 and D-*allo*-Has_5) proved challenging. Activation with HCTU resulted in substantial conversion of the side-chain primary amide group into a nitrile group, with about a 2:1 ratio of nitrile to primary amide incorporated into the growing peptide chain at each position.[34,35] To mitigate this problem, we modified the coupling conditions. Use of HBTU coupling agent and HOAt additive suppressed nitrile formation to acceptable levels of nitrile formation (5–15%). After completion of the linear chain, Ile_8 was incorporated by Steglich esterification, with DIC and DMAP. Although this reaction resulted in the formation of approximately 25% of the D-*allo*-Ile diastereomer at position 8, our prior related syntheses of clovibactin and teixobactin analogues demonstrated that separation of the diastereomeric product during reverse-phase HPLC purification is not difficult.[36,37] Subsequent Fmoc deprotection and cleavage with 20%

hexafluoroisopropanol (HFIP) afforded the protected peptide with a free carboxylic acid group on Hle_7 and free α-amino group on Ile_8 (Appendix 3.1). Solution-phase cyclization with HATU and HOAt closed the macrolactam linkage between Hle_7 and Ile_8.

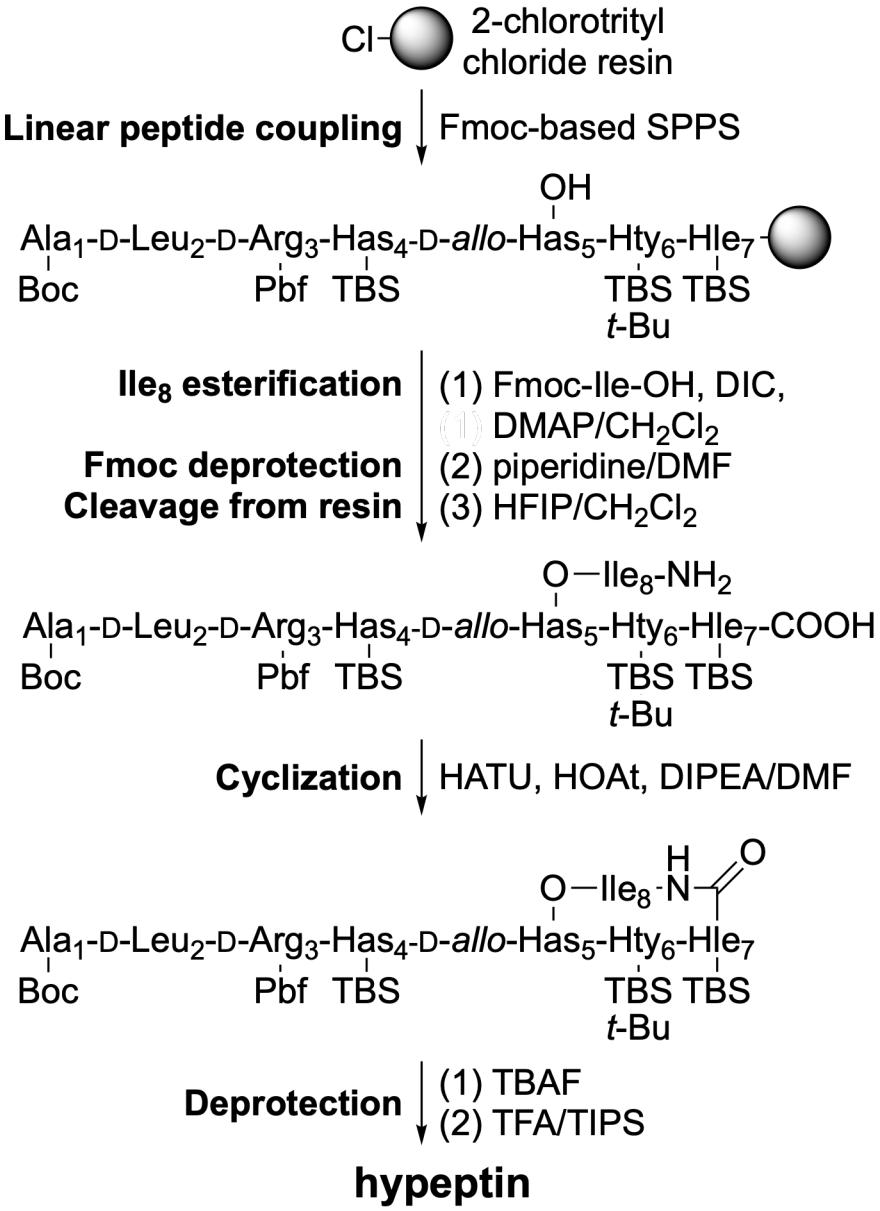

Figure 3.3. First-generation synthesis of hypeptin.

The global deprotection strategy using tetrabutylammonium fluoride (TBAF) followed by anhydrous TFA was the Achilles heel of the first-generation synthesis. Removal of the TBS groups using TBAF proved challenging. When treated the unpurified protected peptide with TBAF, we

observed the formation of a complex mixture of products by HPLC and LC-MS analysis. The lactone linkage to the (2*R*,3*R*)-hydroxyAsn$_5$ residue has the potential to be labile under the TBAF deprotection conditions, and we were concerned that base-promoted hydrolysis might contribute to the observed decomposition (Figure 3.4). To mitigate base-promoted decomposition, we attempted the silyl deprotection with additional batches of peptide under neutral or slightly acidic conditions. Although base-catalyzed decomposition was not observed, only partial and limited cleavage of the TBS protecting groups occurred overnight. Further attempts to drive the reaction to completion using additional TBAF and longer reaction times failed to drive the silyl deprotection reaction to completion.

Furthermore, the deprotection conditions that allowed the successful synthesis of a β-hydroxytyrosine containing simplified burkholidine analogue—anhydrous TFA at 0 °C—led to decomposition of the β-hydroxytyrosine group in hypeptin.[26] Anhydrous conditions are required because water accelerates the formation of a resonance stabilized carbocation or quinone methide intermediate. In the absence of TIPS, treatment of crude partially silyl deprotected hypeptin with anhydrous TFA led to dehydration of the β-hydroxytyrosine group. In the presence of TIPS, treatment of crude partially silyl deprotected hypeptin led to reduction of the β-hydroxytyrosine residue to tyrosine. The absence of water and lower temperature also slowed the removal of the other acid-labile protecting groups (Pbf, Boc, *t*Bu). We ultimately had to abandon the use these acid-labile protecting groups, because there was no way to completely remove them without decomposition of the acid-labile β-hydroxytyrosine group.

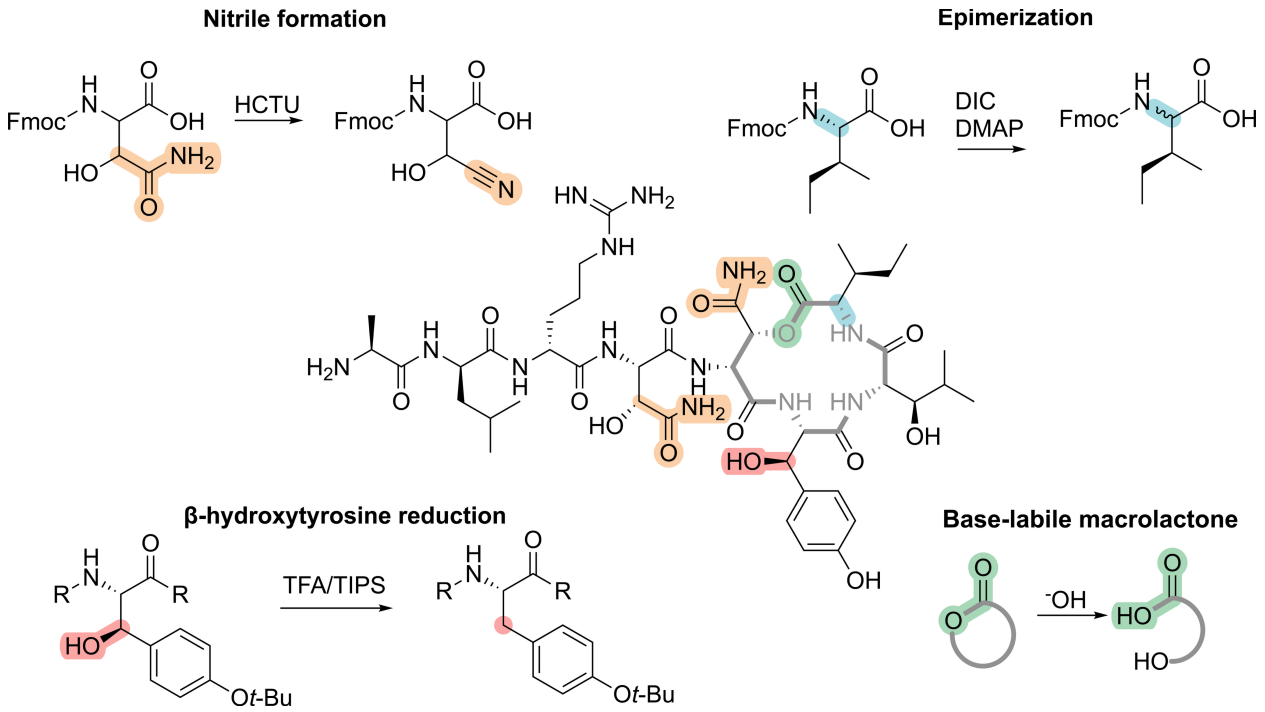

Figure 3.4. Summary of major hypeptin side reactions.

To gain further insight into the failure of the global deprotection strategy and lack of published syntheses of β-hydroxytyrosine-containing peptide natural products, we looked at natural products containing related amino acids, such as β-hydroxyphenylalanine and β-methoxytyrosine (Figure S4 and Table S2).[38–44,23,24,45–58,25] Our search revealed ten natural products, seven of which have been synthesized. Of the seven syntheses, five used TFA to remove the acid-labile side-chain protecting groups. The difference in number of published syntheses underscores the acid instability of β-hydroxytyrosine.

We designed the second-generation synthesis of hypeptin to avoid global deprotection using TFA altogether. Several of the published syntheses of natural products containing related β-hydroxy amino acids (papuamide B, lysobactin, cyclomarins, ecumicin, and callipeltins) rely on palladium-catalyzed deprotection reactions of Cbz and Bn groups. The synthesis of a simplified burkholidine analogue demonstrated that β-hydroxtyrosine tolerates hydrogenation conditions without reduction of the benzylic alcohol. The synthesis of callipeltin E demonstrated that

arginine can be protected as the *bis*-Cbz derivative, and that the Cbz protecting groups could subsequently be removed by hydrogenation. These two syntheses suggested a second-generation synthesis that relies upon hydrogenolytic global deprotection instead of TFA-based global deprotection.

Second-generation synthesis of hypeptin

To enable a TFA-free synthesis of hypeptin, we prepared two additional suitably protected amino acids: Fmoc-D-Arg(Z)$_2$-OH (**18**) and Fmoc-Hty(TBS/Bn)-OH (**19**) (Figure S3.5). Although a four-step synthesis of Fmoc-D-Arg(Z)$_2$-OH starting from D-Arg-OH has been published, we found it more expedient to purchase Boc-D-Arg(Z)$_2$-OH and then perform a one-pot Boc deprotection and Fmoc protection. The synthesis of Fmoc-Hty(TBS/Bn)-OH largely followed the preceding synthesis of Fmoc-Hty(TBS/*t*Bu)-OH with a key chemoselective reduction of an azide group in the presence of a benzyl protected phenol. To prevent premature benzyl deprotection, we pre-treated the Pd/C with ethylene diamine to generate Pd/C (en) that successfully reduced in the azide with a 55% yield.[59]

The second-generation synthesis of hypeptin largely mirrors the first-generation synthesis of hypeptin, with protected Cbz-Ala-OH, Fmoc-D-Arg(Z)$_2$-OH, and Fmoc-Hty(TBS/Bn)-OH used in place of Fmoc-Ala-OH, Fmoc-D-Arg(Boc)$_2$-OH, and Fmoc-Hty(TBS/*t*Bu)-OH (Figure 3.5). In developing this second-generation synthesis, we identified that coupling following Fmoc-D-Arg(Z)$_2$-OH with HCTU led to D-Leu deletion because of the two bulky Cbz protecting groups. Use of HATU and HOAt coupling successfully incorporated D-Leu into the growing peptide chain.

After cleaving the acyclic peptide from the resin and cyclization, we removed coupling agents and byproducts by medium-pressure reverse-phase chromatography using a Biotage

Isolera system. To address the sluggish silyl deprotection encountered in the first-generation synthesis, a more aggressive fluoride source, HF-py, was used to fully remove the three TBS protecting groups. The Cbz and Bn groups were removed by hydrogenolysis using $Pd(OH)_2/C$ in MeOH spiked with 0.5% acetic acid to afford fully deprotected hypeptin. A 0.045 mmol scale synthesis afforded 0.4 mg (0.7% yield) of synthetic hypeptin as a trifluoroacetate salt after RP-HPLC purification.

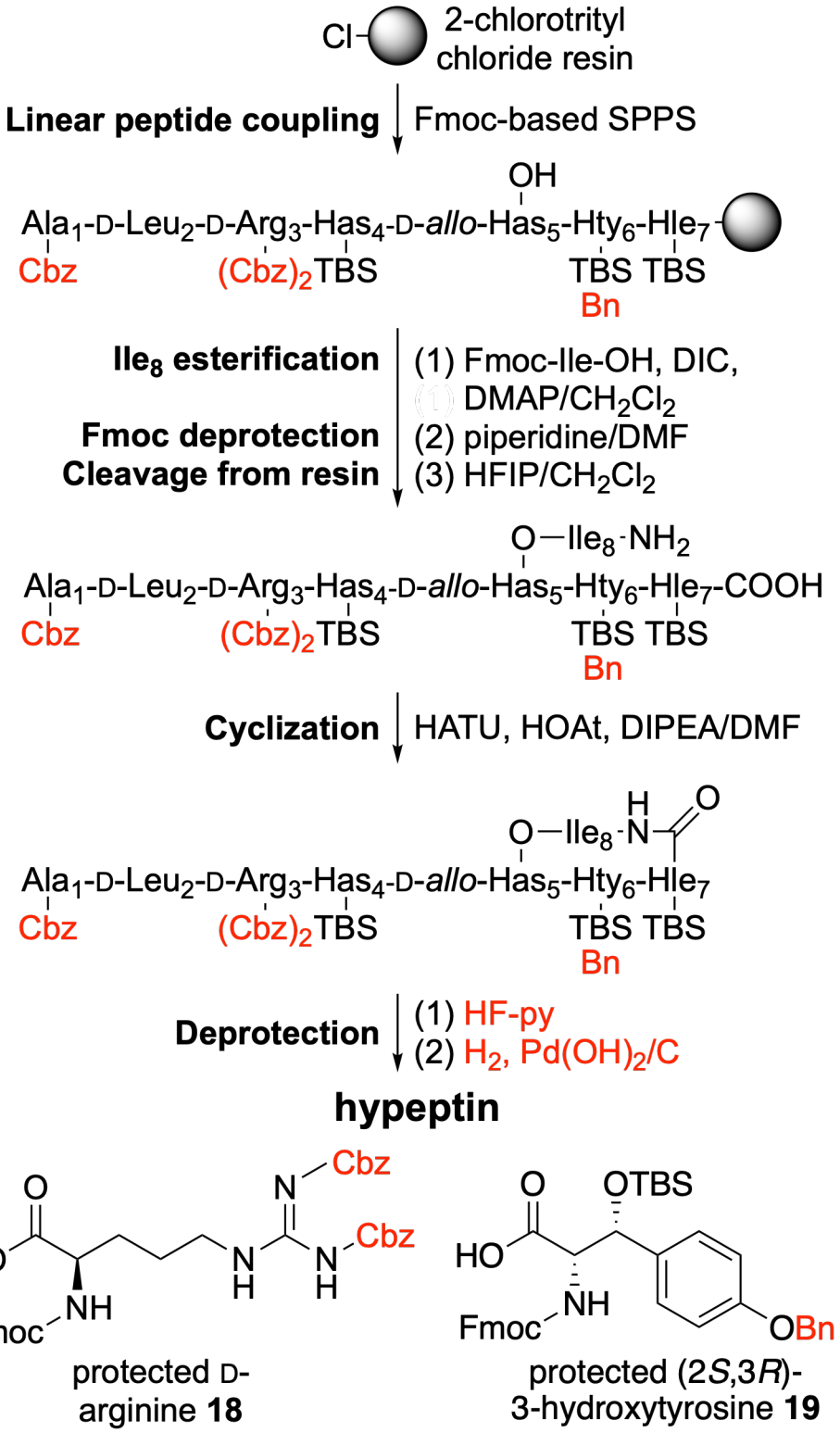

Figure 3.5. Second-generation synthesis of hypeptin. Red highlights change from the first-generation synthesis and key amino acid building blocks

Comparison of natural and synthetic hypeptin

The synthetic hypeptin provide identical to a sample of natural hypeptin through comparison by analytical HPLC and mass spectrometry. The separate and co-injection of natural and synthetic hypeptin on an analytical HPLC shows a single peak at 8.06 min (Figure 3.6). Complementary mass spectrometric analysis confirmed that natural and synthetic hypeptin are identical, both ionizing as the $[M+H]^+$ and $[M+2H]^{2+}$ adducts at 511.8 and 1022.5 m/z respectively (Figure S3.6).

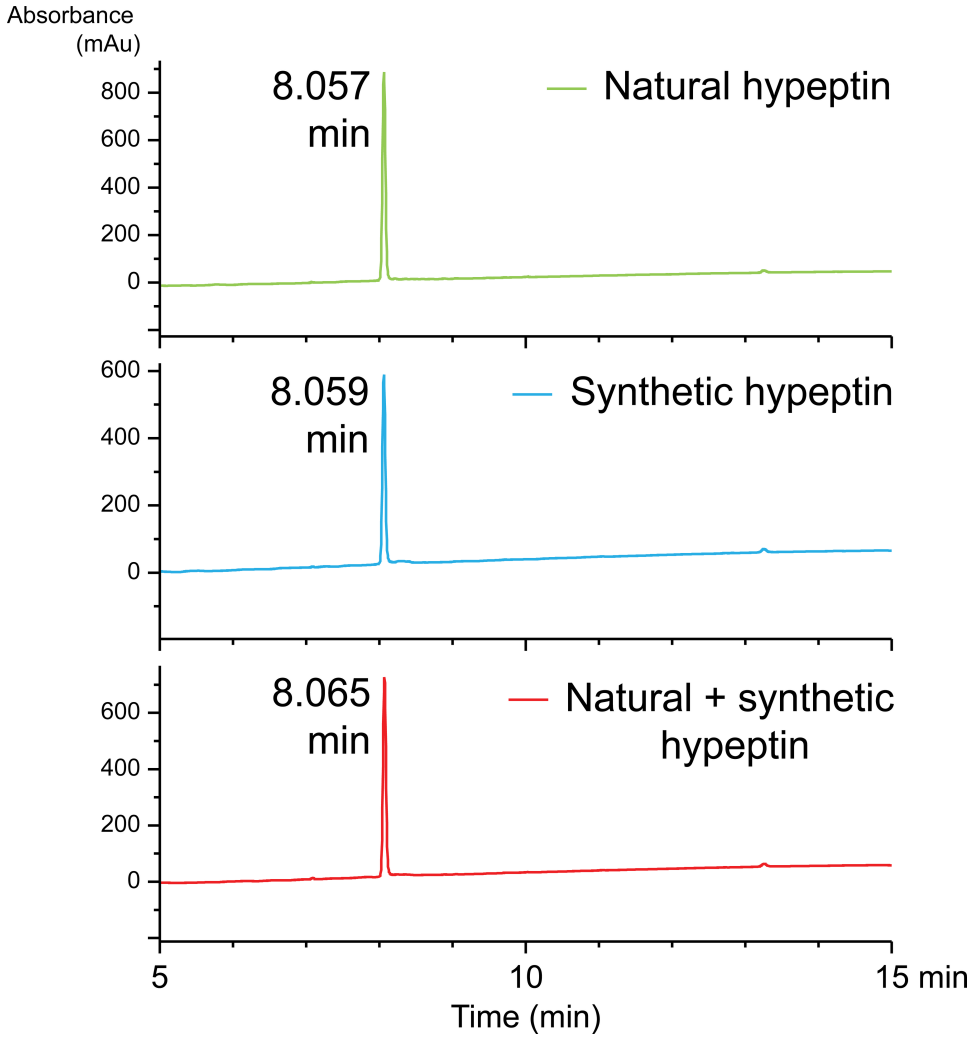

Figure 3.6. Analytical RP-HPLC traces of natural, synthetic, and a mixture of natural and synthetic hypeptin. HPLC was run on a C18 column with a gradient of 5–100% acetonitrile over 20 min, with monitoring of absorbance at 214 nm.

The NMR spectra of natural and synthetic hypeptin match, confirming that Schneider's stereochemical revision of hydroxyTyr$_6$ to (2*S*,3*R*) based on the biosynthesis from the (2*S*,3*S*) configuration originally proposed by Shoji was correct. Surprisingly, the ^{1}H NMR spectrum of natural and synthetic hypeptin showed two sets of peaks that exhibit chemical exchange (EXSY) in the ROESY spectra (Figure S3.7). This second minor set of peaks reflects slow chemical exchange relative to the NMR timescale perhaps reflecting a conformer or oligomer. Chemical shift comparison of major hypeptin peaks around the four β-hydroxylated amino acids show that natural and synthetic hypeptin are identical (Table 3.1). A complete set of proton chemical shift comparisons between natural and synthetic hypeptin are shown in Table S3.3. The largest chemical shift difference among all proton resonances was 0.02 ppm with an average difference of less than 0.004 ppm.

Table 3.1. Select chemical shift tabulations of natural and synthetic hypeptin in DMSO-d$_6$ at 298 K.

Residue	Proton	Natural (ppm)	Synthetic (ppm)	Difference (Δ ppm)
(2*S*,3*R*) Has$_4$	NH	8.10	8.10	0.00
	Hα	4.70	4.70	0.00
	Hβ	4.02	4.02	0.00
(2*R*,3*R*) D-*allo*-Has$_5$	NH	8.25	8.26	-0.01
	Hα	4.96	4.96	0.00
	Hβ	5.19	5.19	0.00
(2*S*,3*R*) Hty$_6$	NH	8.14	8.14	0.00
	Hα	4.22	4.21	0.01
	Hβ	4.79	4.79	0.00
(2*S*,3*R*) Hle$_7$	NH	7.93	7.93	0.00
	Hα	4.41	4.41	0.00
	Hβ	3.43	3.43	0.00

Hypeptin is unstable under physiologically relevant conditions

The lactone linkage to the (2*R*,3*R*)-hydroxyasparagine residue renders hypeptin unstable in aqueous solution under physiological conditions. When we incubated hypeptin in pH 7.4 HEPES buffer at 37 °C, we observed degradation with first-order kinetics and a half-life of 2.6 hrs

(Figure 3.7). The complete degradation pathway of hypeptin is complex but predominantly follows an A → B → C pathway, where A is hypeptin and B/C are the major decomposition byproducts. A stacked plot with additional timepoints is shown in Figure S3.8.

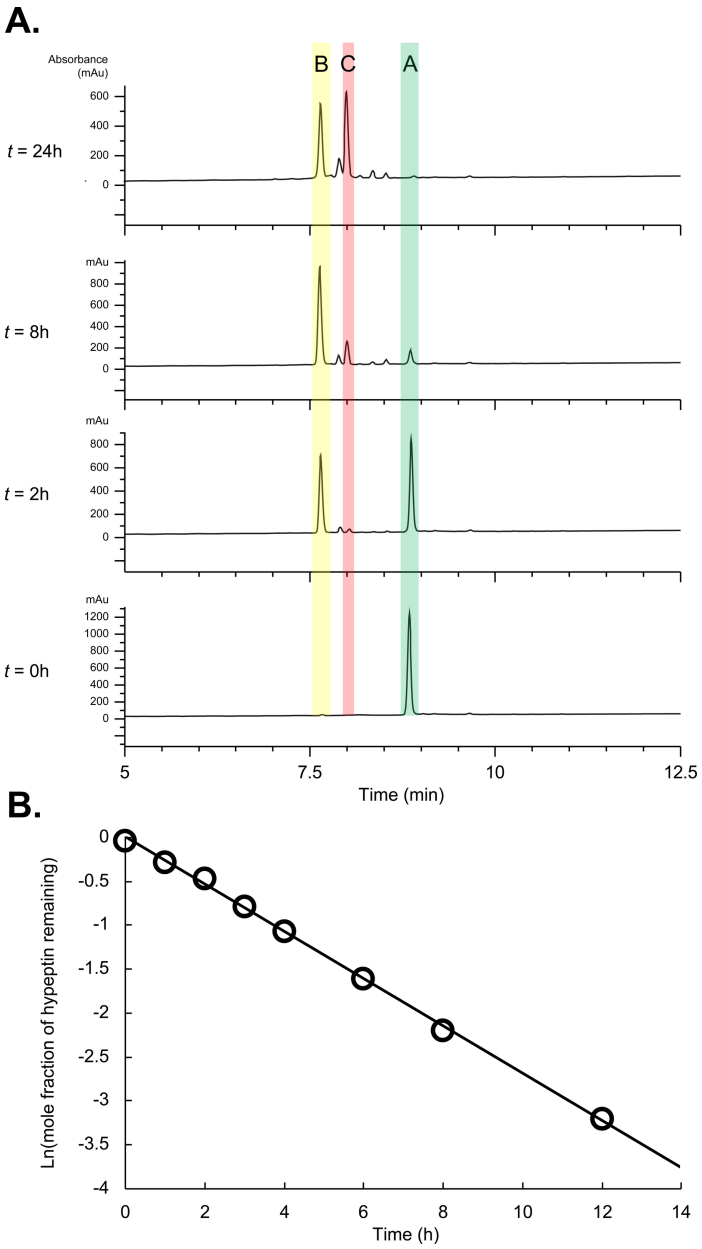

Figure 3.7. (A) Analytical RP-HPLC trace showing the conversion of hypeptin, A, into decomposition byproducts B and C. HPLC was run on a C18 column with a gradient of 5–67% acetonitrile over 15 min, with monitoring of absorbance at 214 nm. (B) Decomposition kinetics of hypeptin illustrating the disappearance of hypeptin over time. All reactions were run at pH 7.4 and 37 °C with 0.5 mg/mL peptide in 25 mM HEPES buffer.

Conclusions

In summary, we completed the first synthesis of hypeptin and verified that hypeptin contains the (2*S*,3*R*) hydroxytyrosine and position 6. To enable a solid-phase peptide synthesis of hypeptin, we prepared four β-hydroxylated amino acid building blocks for the (2*S*,3*R*)-3-hydroxyasparagine, (2*R*,3*R*)-3-hydroxyasparagine, (2*S*,3*R*)-3-hydroxytyrosine, and (2*S*,3*R*)-3-hydroxyleucine. Our initial synthesis proceeded by coupling the acyclic peptide using SPPS, Steglich esterifying on resin, followed by a solution-phase macrolactamization to afford fully protected hypeptin. The selection of mild deprotection conditions proved crucial to the synthesis of hypeptin, which is both acid and base labile. Under anhydrous TFA/TIPS deprotection conditions, β-hydroxytyrosine reduces to tyrosine. Under standard basic TBAF conditions, the (2*R*,3*R*)-3-hydroxyasparagine ester linkage readily degrades. To address the challenges associated with our initial global deprotection strategy, we rerouted our synthesis to use a more aggressive fluoride source, HF-py, and catalytic hydrogenolysis to successfully deprotect hypeptin. Correlation of natural and synthetic hypeptin by LC-MS and NMR spectroscopy confirms Schneider's proposed stereochemical revision of hypeptin.[3] To our knowledge, this is the first completed β-hydroxytyrosine containing peptide natural product synthesis. The work described here lays the foundation for further structure-activity-relationship studies on the hypeptin scaffold and the syntheses of other β-hydroxytyrosine containing peptide natural products.

References

(1) Global Antibiotic Resistance Surveillance Report 2025: Summary. https://www.who.int/publications/i/item/B09585.
(2) Towards Specific Commitments and Action in Response to Antimicrobial Resistance. https://www.amrleaders.org/about-us/what-we-do/glg-report.

(3) Wirtz, D. A.; Ludwig, K. C.; Arts, M.; Marx, C. E.; Krannich, S.; Barac, P.; Kehraus, S.; Josten, M.; Henrichfreise, B.; Müller, A.; König, G. M.; Peoples, A. J.; Nitti, A.; Spoering, A. L.; Ling, L. L.; Lewis, K.; Crüsemann, M.; Schneider, T. Biosynthesis and Mechanism of Action of the Cell Wall Targeting Antibiotic Hypeptin. *Angew. Chem. Int. Ed.* **2021**, *60* (24), 13579–13586. https://doi.org/10.1002/anie.202102224.
(4) Shoji, J.; Hinoo, H.; Hattori, T.; Hirooka, K.; Kimura, Y.; Yoshida, T. Isolation and Characterization of Hypeptin from Pseudomonas Sp. *J. Antibiot. (Tokyo)* **1989**, *42* (10), 1460–1464. https://doi.org/10.7164/antibiotics.42.1460.
(5) Shukla, R.; Peoples, A. J.; Ludwig, K. C.; Maity, S.; Derks, M. G. N.; De Benedetti, S.; Krueger, A. M.; Vermeulen, B. J. A.; Harbig, T.; Lavore, F.; Kumar, R.; Honorato, R. V.; Grein, F.; Nieselt, K.; Liu, Y.; Bonvin, A. M. J. J.; Baldus, M.; Kubitscheck, U.; Breukink, E.; Achorn, C.; Nitti, A.; Schwalen, C. J.; Spoering, A. L.; Ling, L. L.; Hughes, D.; Lelli, M.; Roos, W. H.; Lewis, K.; Schneider, T.; Weingarth, M. An Antibiotic from an Uncultured Bacterium Binds to an Immutable Target. *Cell* **2023**, *186* (19), 4059-4073.e27. https://doi.org/10.1016/j.cell.2023.07.038.
(6) Shukla, R.; Lavore, F.; Maity, S.; Derks, M. G. N.; Jones, C. R.; Vermeulen, B. J. A.; Melcrová, A.; Morris, M. A.; Becker, L. M.; Wang, X.; Kumar, R.; Medeiros-Silva, J.; van Beekveld, R. A. M.; Bonvin, A. M. J. J.; Lorent, J. H.; Lelli, M.; Nowick, J. S.; MacGillavry, H. D.; Peoples, A. J.; Spoering, A. L.; Ling, L. L.; Hughes, D. E.; Roos, W. H.; Breukink, E.; Lewis, K.; Weingarth, M. Teixobactin Kills Bacteria by a Two-Pronged Attack on the Cell Envelope. *Nature* **2022**, *608* (7922), 390–396. https://doi.org/10.1038/s41586-022-05019-y.
(7) Krumberger, M.; Li, X.; Kreutzer, A. G.; Peoples, A. J.; Nitti, A. G.; Cunningham, V. A.; Jones, C. R.; Achorn, C.; Ling, L. L.; Hughes, D. E.; Nowick, J. S. Synthesis and Stereochemical Determination of the Peptide Antibiotic Novo29. *J. Org. Chem.* **2023**, *88* (4), 2214–2220. https://doi.org/10.1021/acs.joc.2c02648.
(8) Yang, H.; Wierzbicki, M.; Du Bois, D. R.; Nowick, J. S. X-ray Crystallographic Structure of a Teixobactin Derivative Reveals Amyloid-like Assembly. *J. Am. Chem. Soc.* **2018**, *140* (43), 14028–14032. https://doi.org/10.1021/jacs.8b07709.
(9) He, C.; Jing, X.; Liu, B.; Liu, F.; Jin, K. Efficient Synthesis of Clovibactin and Its Analogues: Promoting the Discovery of More Potent Antibiotics via Multiple Screenings. *ACS Infect. Dis.* **2025**, *11* (9), 2568–2576. https://doi.org/10.1021/acsinfecdis.5c00458.
(10) Giltrap, A. M.; Dowman, L. J.; Nagalingam, G.; Ochoa, J. L.; Linington, R. G.; Britton, W. J.; Payne, R. J. Total Synthesis of Teixobactin. *Org. Lett.* **2016**, *18* (11), 2788–2791. https://doi.org/10.1021/acs.orglett.6b01324.
(11) Jin, K.; Sam, I. H.; Po, K. H. L.; Lin, D.; Ghazvini Zadeh, E. H.; Chen, S.; Yuan, Y.; Li, X. Total Synthesis of Teixobactin. *Nat. Commun.* **2016**, *7* (1), 12394. https://doi.org/10.1038/ncomms12394.
(12) Zong, Y.; Fang, F.; Meyer, K. J.; Wang, L.; Ni, Z.; Gao, H.; Lewis, K.; Zhang, J.; Rao, Y. Gram-Scale Total Synthesis of Teixobactin Promoting Binding Mode Study and Discovery of More Potent Antibiotics. *Nat. Commun.* **2019**, *10*, 3268. https://doi.org/10.1038/s41467-019-11211-y.
(13) Kiniwa, H.; Baba, Y.; Ishida, T.; Katoh, H. General Evaluation and Application to Trace Analysis of a Chiral Column for Ligand-Exchange Chromatography. *J. Chromatogr. A* **1989**, *461*, 397–405. https://doi.org/10.1016/S0021-9673(00)94306-1.

(14) Murai, Y.; Mori, S.; Konno, H.; Hikichi, Y.; Kai, K. Ralstonins A and B, Lipopeptides with Chlamydospore-Inducing and Phytotoxic Activities from the Plant Pathogen Ralstonia Solanacearum. *Org. Lett.* **2017**, *19* (16), 4175–4178. https://doi.org/10.1021/acs.orglett.7b01685.
(15) Komatsu, S.; Tsumori, C.; Ohnishi, K.; Kai, K. Genome- and Mass Spectrometry-Guided Discovery of Ralstoamides A and B from Ralstonia Solanacearum Species Complex. *ACS Chem. Biol.* **2020**, *15* (11), 2860–2865. https://doi.org/10.1021/acschembio.0c00605.
(16) Tawfik, K. A.; Jeffs, P.; Bray, B.; Dubay, G.; Falkinham, J. O. I.; Mesbah, M.; Youssef, D.; Khalifa, S.; Schmidt, E. W. Burkholdines 1097 and 1229, Potent Antifungal Peptides from Burkholderia Ambifaria 2.2N. *Org. Lett.* **2010**, *12* (4), 664–666. https://doi.org/10.1021/ol9029269.
(17) Bui, T.-H.; Wray, V.; Nimtz, M.; Fossen, T.; Preisitsch, M.; Schröder, G.; Wende, K.; Heiden, S. E.; Mundt, S. Balticidins A–D, Antifungal Hassallidin-Like Lipopeptides from the Baltic Sea Cyanobacterium Anabaena Cylindrica Bio33. *J. Nat. Prod.* **2014**, *77* (6), 1287–1296. https://doi.org/10.1021/np401020a.
(18) Lim, Y.; Suh, J.-W.; Kim, S.; Hyun, B.; Kim, C.; Lee, C. Cepacidine A, A Novel Antifungal Antibiotic Produced by Pseudomonas Cepacia II. Physico-Chemical Properties and Structure Elucidation. *J. Antibiot. (Tokyo)* **1994**, *47* (12), 1406–1416. https://doi.org/10.7164/antibiotics.47.1406.
(19) Konno, H.; Sasaki, Y.; Sato, R.; Zhu, X.; Otsuki, Y.; Ikoma, M. Synthesis of β-Hydroxytyrosine, A Component of Burkholdineshydro. *Nat. Prod. Commun.* **2016**, *11* (2), 1934578X1601100221. https://doi.org/10.1177/1934578X1601100221.
(20) Boyaud, F.; Mahiout, Z.; Lenoir, C.; Tang, S.; Wdzieczak-Bakala, J.; Witczak, A.; Bonnard, I.; Banaigs, B.; Ye, T.; Inguimbert, N. First Total Synthesis and Stereochemical Revision of Laxaphycin B and Its Extension to Lyngbyacyclamide A. *Org. Lett.* **2013**, *15* (15), 3898–3901. https://doi.org/10.1021/ol401645m.
(21) Darcel, L.; Djibo, M.; Gaillard, M.; Raviglione, D.; Bonnard, I.; Banaigs, B.; Inguimbert, N. Trichormamide C Structural Confirmation through Total Synthesis and Extension to Analogs. *Org. Lett.* **2019**, *22* (1), 145–149. https://doi.org/10.1021/acs.orglett.9b04064.
(22) Wang, H.-Y.; Yang, H.; Holm, M.; Tom, H.; Oltion, K.; Al-Khdhairawi, A. A. Q.; Weber, J.-F. F.; Blanchard, S. C.; Ruggero, D.; Taunton, J. Synthesis and Single-Molecule Imaging Reveal Stereospecific Enhancement of Binding Kinetics by the Antitumour eEF1A Antagonist SR-A3. *Nat. Chem.* **2022**, *14* (12), 1443–1450. https://doi.org/10.1038/s41557-022-01039-3.
(23) Guzman-Martinez, A.; Lamer, R.; VanNieuwenhze, M. S. Total Synthesis of Lysobactin. *J. Am. Chem. Soc.* **2007**, *129* (18), 6017–6021. https://doi.org/10.1021/ja067648h.
(24) von Nussbaum, F.; Anlauf, S.; Benet-Buchholz, J.; Häbich, D.; Köbberling, J.; Musza, L.; Telser, J.; Rübsamen-Waigmann, H.; Brunner, N. A. Structure and Total Synthesis of Lysobactin (Katanosin B). *Angew. Chem. Int. Ed.* **2007**, *46* (12), 2039–2042. https://doi.org/10.1002/anie.200604232.
(25) Martín, M. J.; Rodríguez-Acebes, R.; García-Ramos, Y.; Martínez, V.; Murcia, C.; Digón, I.; Marco, I.; Pelay-Gimeno, M.; Fernández, R.; Reyes, F.; Francesch, A. M.; Munt, S.; Tulla-Puche, J.; Albericio, F.; Cuevas, C. Stellatolides, a New Cyclodepsipeptide Family from the Sponge Ecionemia Acervus: Isolation, Solid-Phase Total Synthesis, and Full Structural Assignment of Stellatolide A. *J. Am. Chem. Soc.* **2014**, *136* (18), 6754–6762. https://doi.org/10.1021/ja502744a.

(26) Kato, S.; Sasaki ,Mio; Yano ,Shigekazu; and Konno, H. Synthesis of a Burkholdine Analogue Containing β-Hydroxytyrosine. *Biosci. Biotechnol. Biochem.* **2019**, *83* (7), 1216–1219. https://doi.org/10.1080/09168451.2019.1594678.
(27) Yang, H.; Pishenko, A. V.; Li, X.; Nowick, J. S. Design, Synthesis, and Study of Lactam and Ring-Expanded Analogues of Teixobactin. *J. Org. Chem.* **2020**, *85* (3), 1331–1339. https://doi.org/10.1021/acs.joc.9b02631.
(28) Brunicardi, J. E. H.; Griffin, J. H.; Ferracane, M. J.; Kreutzer, A. G.; Small, J.; Mendoza, A.-T.; Ziller, J. W.; Nowick, J. S. Structure–Activity Relationship Studies of the Peptide Antibiotic Clovibactin. *J. Org. Chem.* **2024**, *89* (17), 12479–12484. https://doi.org/10.1021/acs.joc.4c01414.
(29) Patel, J.; Clavé, G.; Pierre-Yves Renard; Franck, X. Straightforward Access to Protected Syn α-Amino-β-Hydroxy Acid Derivatives. *Angew. Chem. Int. Ed.* **2008**, *47* (22), 4224–4227. https://doi.org/10.1002/anie.200800860.
(30) Dunetz, J. R.; Xiang, Y.; Baldwin, A.; Ringling, J. General and Scalable Amide Bond Formation with Epimerization-Prone Substrates Using T3P and Pyridine. *Org. Lett.* **2011**, *13* (19), 5048–5051. https://doi.org/10.1021/ol201875q.
(31) Evans, D. A.; Britton, T. C.; Ellman, J. A. Contrasteric Carboximide Hydrolysis with Lithium Hydroperoxide. *Tetrahedron Lett.* **1987**, *28* (49), 6141–6144. https://doi.org/10.1016/S0040-4039(00)61830-0.
(32) J. Hale, K.; Manaviazar, S.; M. Delisser, V. A Practical New Asymmetric Synthesis of (*2S*,*3S*)- and (*2R*,*3R*)-3-Hydroxyleucine. *Tetrahedron* **1994**, *50* (30), 9181–9188. https://doi.org/10.1016/S0040-4020(01)85384-9.
(33) Fleming, P. R.; Sharpless, K. B. Selective Transformations of Threo-2,3-Dihydroxy Esters. *J. Org. Chem.* **1991**, *56* (8), 2869–2875. https://doi.org/10.1021/jo00008a051.
(34) Gausepohl, H.; Kraft, M.; Frank, R. w. Asparagine Coupling in Fmoc Solid Phase Peptide Synthesis. *Int. J. Pept. Protein Res.* **1989**, *34* (4), 287–294. https://doi.org/10.1111/j.1399-3011.1989.tb01576.x.
(35) We synthesized a model tetrapeptide (H_2N-Lys-Phe-Has-Leu-COOH) and identified the nitrile formation using NMR spectroscopy.
(36) Neises, B.; Steglich, W. Simple Method for the Esterification of Carboxylic Acids. *Angew. Chem. Int. Ed. Engl.* **1978**, *17* (7), 522–524. https://doi.org/10.1002/anie.197805221.
(37) Steglitch esterification is known to epimerize amino acids. Xevo analysis of the crude linear peptide showed an 7:3 ratio of hypeptin and the epimeric D-*allo*-Ile_8 hypeptin. The epimer was fully separated during downstream RP-HPLC purification.
(38) Kim, C.-K.; Wang, D.; Bokesch, H. R.; Fuller, R. W.; Smith, E.; Henrich, C. J.; Durrant, D. E.; Morrison, D. K.; Bewley, C. A.; Gustafson, K. R. Swinhopeptolides A and B: Cyclic Depsipeptides from the Sponge Theonella Swinhoei That Inhibit Ras/Raf Interaction. *J. Nat. Prod.* **2020**, *83* (4), 1288–1294. https://doi.org/10.1021/acs.jnatprod.0c00136.
(39) Oku, N.; Gustafson, K. R.; Cartner, L. K.; Wilson, J. A.; Shigematsu, N.; Hess, S.; Pannell, L. K.; Boyd, M. R.; McMahon, J. B. Neamphamide A, a New HIV-Inhibitory Depsipeptide from the Papua New Guinea Marine Sponge Neamphius Huxleyi. *J. Nat. Prod.* **2004**, *67* (8), 1407–1411. https://doi.org/10.1021/np040003f.
(40) Tran, T. D.; Pham, N. B.; Fechner, G.; Zencak, D.; Vu, H. T.; Hooper, J. N. A.; Quinn, R. J. Cytotoxic Cyclic Depsipeptides from the Australian Marine Sponge Neamphius Huxleyi. *J. Nat. Prod.* **2012**, *75* (12), 2200–2208. https://doi.org/10.1021/np3006474.

(41) Plaza, A.; Gustchina, E.; Baker, H. L.; Kelly, M.; Bewley, C. A. Mirabamides A–D, Depsipeptides from the Sponge Siliquariaspongia Mirabilis That Inhibit HIV-1 Fusion. *J. Nat. Prod.* **2007**, *70* (11), 1753–1760. https://doi.org/10.1021/np070306k.
(42) Lu, Z.; Van Wagoner, R. M.; Harper, M. K.; Baker, H. L.; Hooper, J. N. A.; Bewley, C. A.; Ireland, C. M. Mirabamides E−H, HIV-Inhibitory Depsipeptides from the Sponge Stelletta Clavosa. *J. Nat. Prod.* **2011**, *74* (2), 185–193. https://doi.org/10.1021/np100613p.
(43) Bonner, D. P.; O'sullivan, J.; Tanaka, S. K.; Clark, J. M.; Whitney, R. R. Lysobactin, A Novel Antibacterial Agent Produced by Lysobacter Sp. II. Biological Properties. *J. Antibiot. (Tokyo)* **1988**, *41* (12), 1745–1751. https://doi.org/10.7164/antibiotics.41.1745.
(44) Shoji, J.; Hinoo, H.; Matsumoto, K.; Hattori, T.; Yoshida, T.; Matsuura, S.; Kondo, E. Isolation and Characterization of Katanosins A and B. *J. Antibiot. (Tokyo)* **1988**, *41* (6), 713–718. https://doi.org/10.7164/antibiotics.41.713.
(45) Gao, W.; Kim, J.-Y.; Chen, S.-N.; Cho, S.-H.; Choi, J.; Jaki, B. U.; Jin, Y.-Y.; Lankin, D. C.; Lee, J.-E.; Lee, S.-Y.; McAlpine, J. B.; Napolitano, J. G.; Franzblau, S. G.; Suh, J.-W.; Pauli, G. F. Discovery and Characterization of the Tuberculosis Drug Lead Ecumicin. *Org. Lett.* **2014**, *16* (23), 6044–6047. https://doi.org/10.1021/ol5026603.
(46) Hawkins, P. M. E.; Giltrap, A. M.; Nagalingam, G.; Britton, W. J.; Payne, R. J. Total Synthesis of Ecumicin. *Org. Lett.* **2018**, *20* (4), 1019–1022. https://doi.org/10.1021/acs.orglett.7b03967.
(47) Um, S.; Choi, T. J.; Kim, H.; Kim, B. Y.; Kim, S.-H.; Lee, S. K.; Oh, K.-B.; Shin, J.; Oh, D.-C. Ohmyungsamycins A and B: Cytotoxic and Antimicrobial Cyclic Peptides Produced by Streptomyces Sp. from a Volcanic Island. *J. Org. Chem.* **2013**, *78* (24), 12321–12329. https://doi.org/10.1021/jo401974g.
(48) Hur, J.; Jang, J.; Sim, J.; Son, W. S.; Ahn, H.-C.; Kim, T. S.; Shin, Y.-H.; Lim, C.; Lee, S.; An, H.; Kim, S.-H.; Oh, D.-C.; Jo, E.-K.; Jang, J.; Lee, J.; Suh, Y.-G. Conformation-Enabled Total Syntheses of Ohmyungsamycins A and B and Structural Revision of Ohmyungsamycin B. *Angew. Chem. Int. Ed.* **2018**, *57* (12), 3069–3073. https://doi.org/10.1002/anie.201711286.
(49) Li, L.; MacIntyre, L. W.; Ali, T.; Russo, R.; Koirala, B.; Hernandez, Y.; Brady, S. F. Biosynthetic Interrogation of Soil Metagenomes Reveals Metamarin, an Uncommon Cyclomarin Congener with Activity against Mycobacterium Tuberculosis. *J. Nat. Prod.* **2021**, *84* (4), 1056–1066. https://doi.org/10.1021/acs.jnatprod.0c01104.
(50) Fei, F.; Lun, S.; Saxena, A.; Raghavan, M.; DeRisi, J. L.; Bishai, W. R.; Sello, J. K. Total Syntheses of Cyclomarin and Metamarin Natural Products. *Org. Lett.* **2024**, *26* (45), 9698–9703. https://doi.org/10.1021/acs.orglett.4c03473.
(51) Renner, M. K.; Shen, Y.-C.; Cheng, X.-C.; Jensen, P. R.; Frankmoelle, W.; Kauffman, C. A.; Fenical, W.; Lobkovsky, E.; Clardy, J. Cyclomarins A−C, New Antiinflammatory Cyclic Peptides Produced by a Marine Bacterium (Streptomyces Sp.). *J. Am. Chem. Soc.* **1999**, *121* (49), 11273–11276. https://doi.org/10.1021/ja992482o.
(52) Zampella, A.; D'Auria, M. V.; Paloma, L. G.; Casapullo, A.; Minale, L.; Debitus, C.; Henin, Y. Callipeltin A, an Anti-HIV Cyclic Depsipeptide from the New Caledonian Lithistida Sponge Callipelta Sp. *J. Am. Chem. Soc.* **1996**, *118* (26), 6202–6209. https://doi.org/10.1021/ja954287p.
(53) Valeria D'Auria, M.; Zampella, A.; Paloma, L. G.; Minale, L.; Debitus, C.; Roussakis, C.; Le Bert, V. Callipeltins B and C; Bioactive Peptides from a Marine Lithistida Sponge

Callipelta Sp. *Tetrahedron* **1996**, *52* (28), 9589–9596. https://doi.org/10.1016/0040-4020(96)00496-6.
(54) Zampella, A.; Randazzo, A.; Borbone, N.; Luciani, S.; Trevisi, L.; Debitus, C.; D'Auria, M. V. Isolation of Callipeltins A–C and of Two New Open-Chain Derivatives of Callipeltin A from the Marine Sponge *Latrunculia* Sp. A Revision of the Stereostructure of Callipeltins. *Tetrahedron Lett.* **2002**, *43* (35), 6163–6166. https://doi.org/10.1016/S0040-4039(02)01334-5.
(55) Çalimsiz, S.; Morales Ramos, Á. I.; Lipton, M. A. Solid-Phase Synthesis and Configurational Reassigment of Callipeltin E. Implications for the Structures of Callipeltins A and B. *J. Org. Chem.* **2006**, *71* (17), 6351–6356. https://doi.org/10.1021/jo060351h.
(56) Krishnamoorthy, R.; Vazquez-Serrano, L. D.; Turk, J. A.; Kowalski, J. A.; Benson, A. G.; Breaux, N. T.; Lipton, M. A. Solid-Phase Total Synthesis and Structure Proof of Callipeltin B. *J. Am. Chem. Soc.* **2006**, *128* (48), 15392–15393. https://doi.org/10.1021/ja0666250.
(57) Ford, P. W.; Gustafson, K. R.; McKee, T. C.; Shigematsu, N.; Maurizi, L. K.; Pannell, L. K.; Williams, D. E.; Dilip de Silva, E.; Lassota, P.; Allen, T. M.; Van Soest, R.; Andersen, R. J.; Boyd, M. R. Papuamides A−D, HIV-Inhibitory and Cytotoxic Depsipeptides from the Sponges Theonella Mirabilis and Theonella Swinhoei Collected in Papua New Guinea. *J. Am. Chem. Soc.* **1999**, *121* (25), 5899–5909. https://doi.org/10.1021/ja990582o.
(58) Xie, W.; Ding, D.; Zi, W.; Li, G.; Ma, D. Total Synthesis and Structure Assignment of Papuamide B, A Potent Marine Cyclodepsipeptide with Anti-HIV Properties. *Angew. Chem. Int. Ed.* **2008**, *47* (15), 2844–2848. https://doi.org/10.1002/anie.200705557.
(59) Sajiki, H.; Hattori, K.; Hirota, K. The Formation of a Novel Pd/C−Ethylenediamine Complex Catalyst: Chemoselective Hydrogenation without Deprotection of the O-Benzyl and N-Cbz Groups. *J. Org. Chem.* **1998**, *63* (22), 7990–7992. https://doi.org/10.1021/jo9814694.

Appendix A: Additional Data for Chapter 2

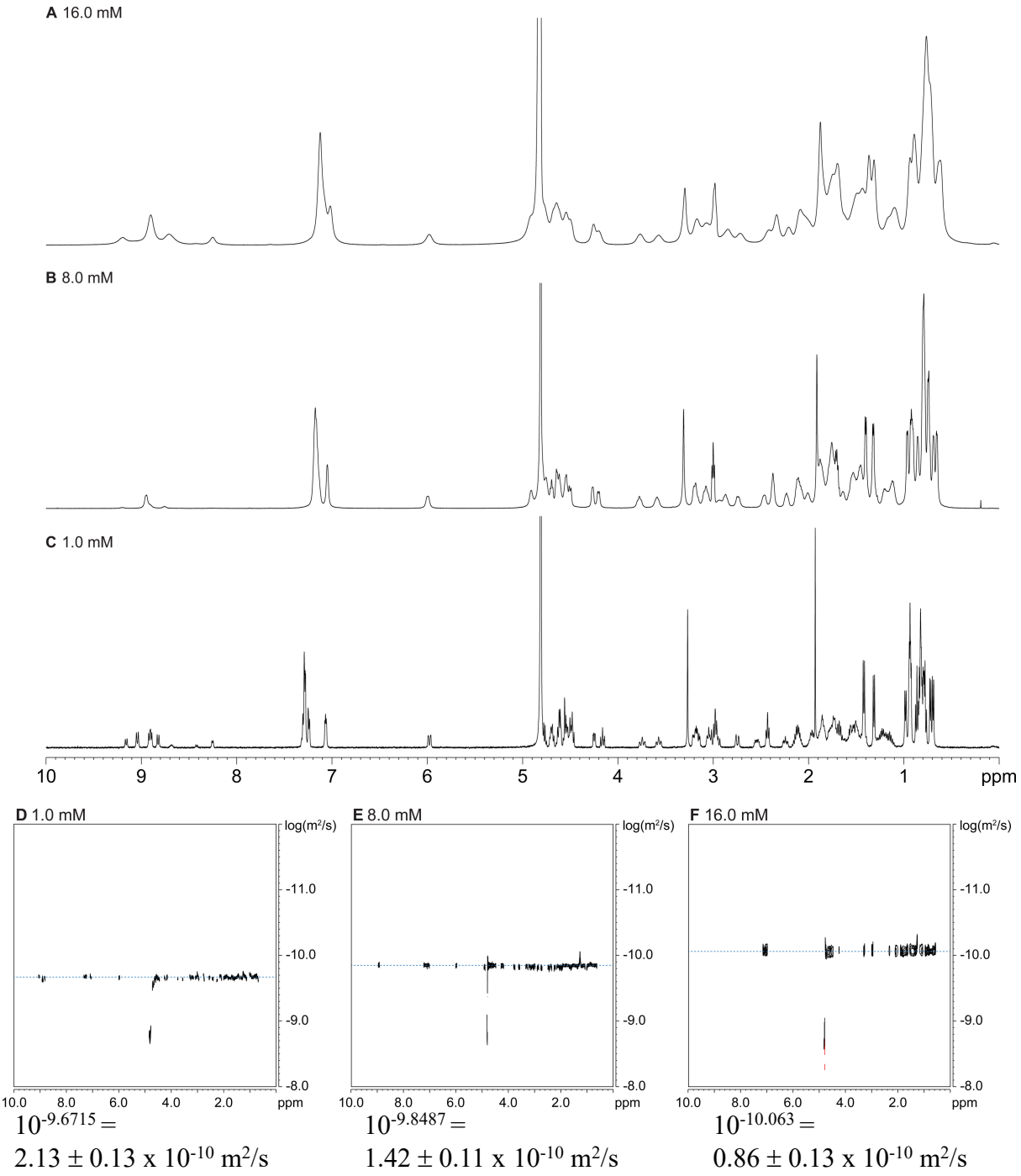

Figure S2.1. ^{1}H NMR and DOSY spectra of peptide **1** at 1.0, 8.0, and 16.0 mM in D_2O at 500 or 600 MHz at 298 K. The unlabeled peaks between 7.5 – 10 ppm correspond to incomplete NH exchange with D_2O. The HOD peak is calibrated to 19.0 x 10^{-10} m^2/s.[1]

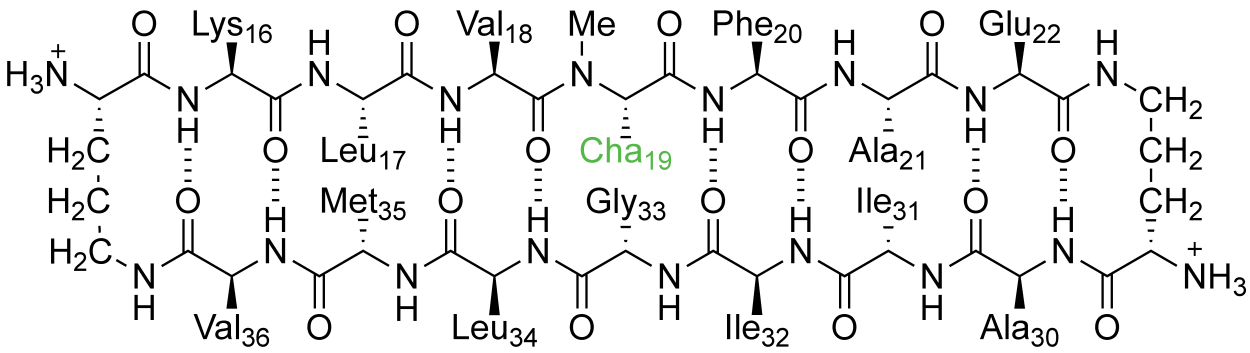

peptide **2**

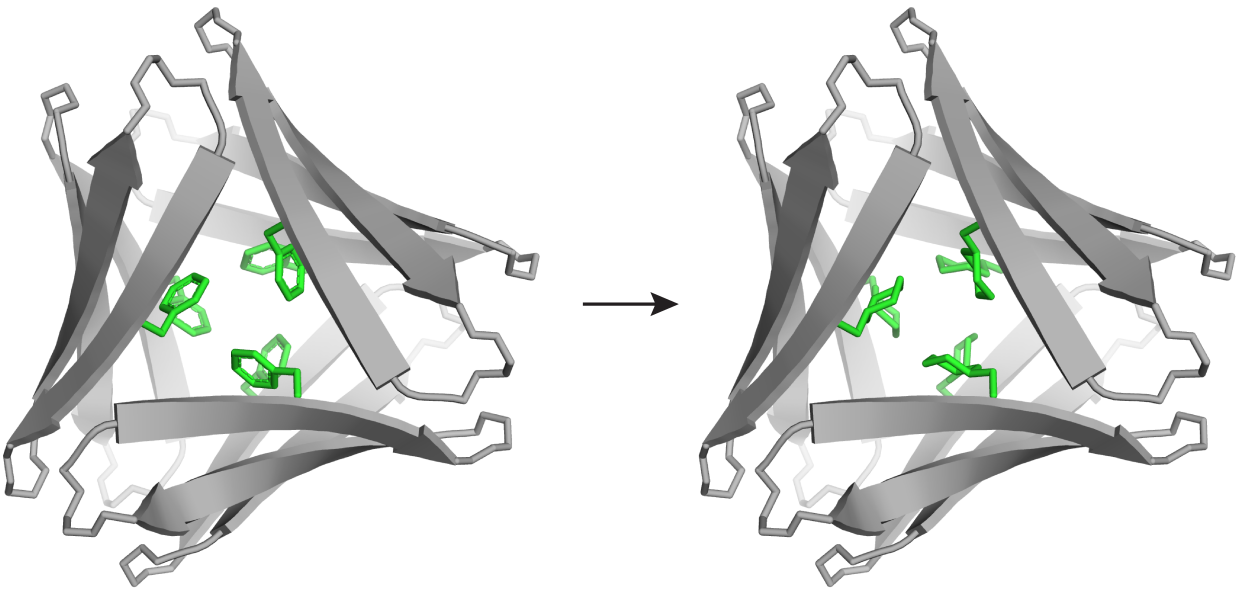

Figure S2.2. Molecular models illustrating the Phe_{19} to Cha_{19} mutation shown in green. Models based on the peptide **1** crystallographic hexamer (PDB 5W4H).

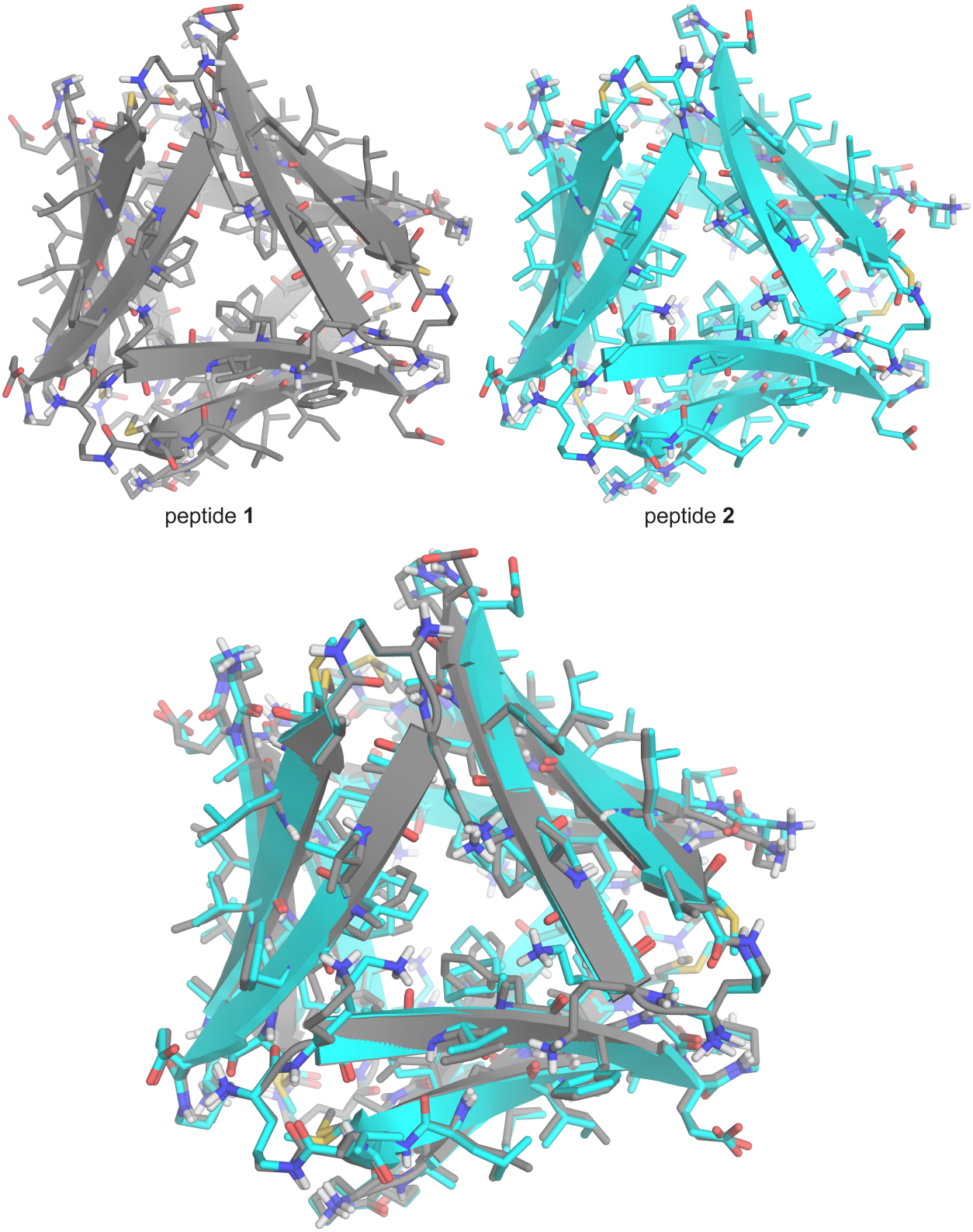

Figure S2.3. Peptide **1** and peptide **2** crystallographic hexamer side-by-side and overlay. Crystallographic coordinates taken from PDB 5W4H and 9EEC.

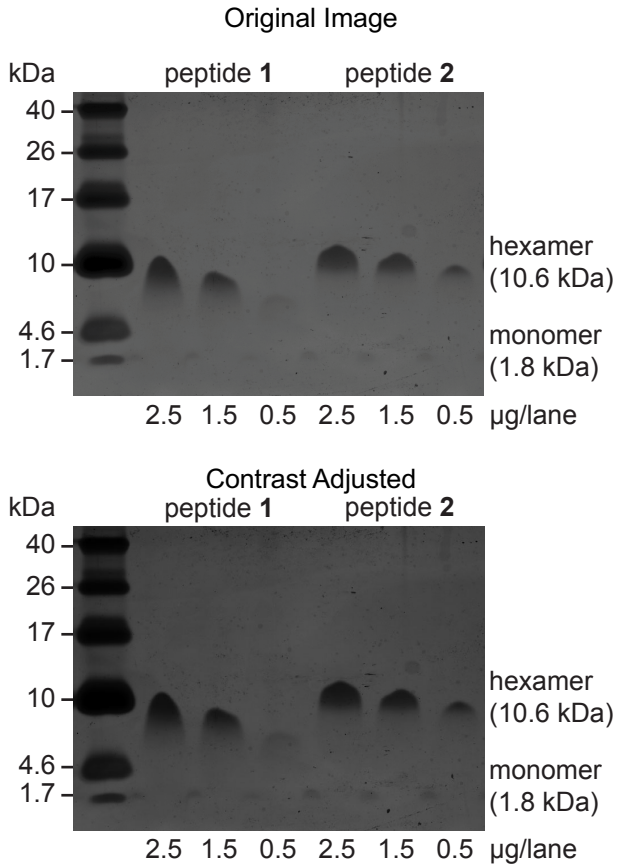

Figure S2.4. Two images of the silver-stained SDS-PAGE gel from Figure 2.3. In the top image the contrast has not been adjusted; in the bottom image the contrast has been uniformly adjusted.

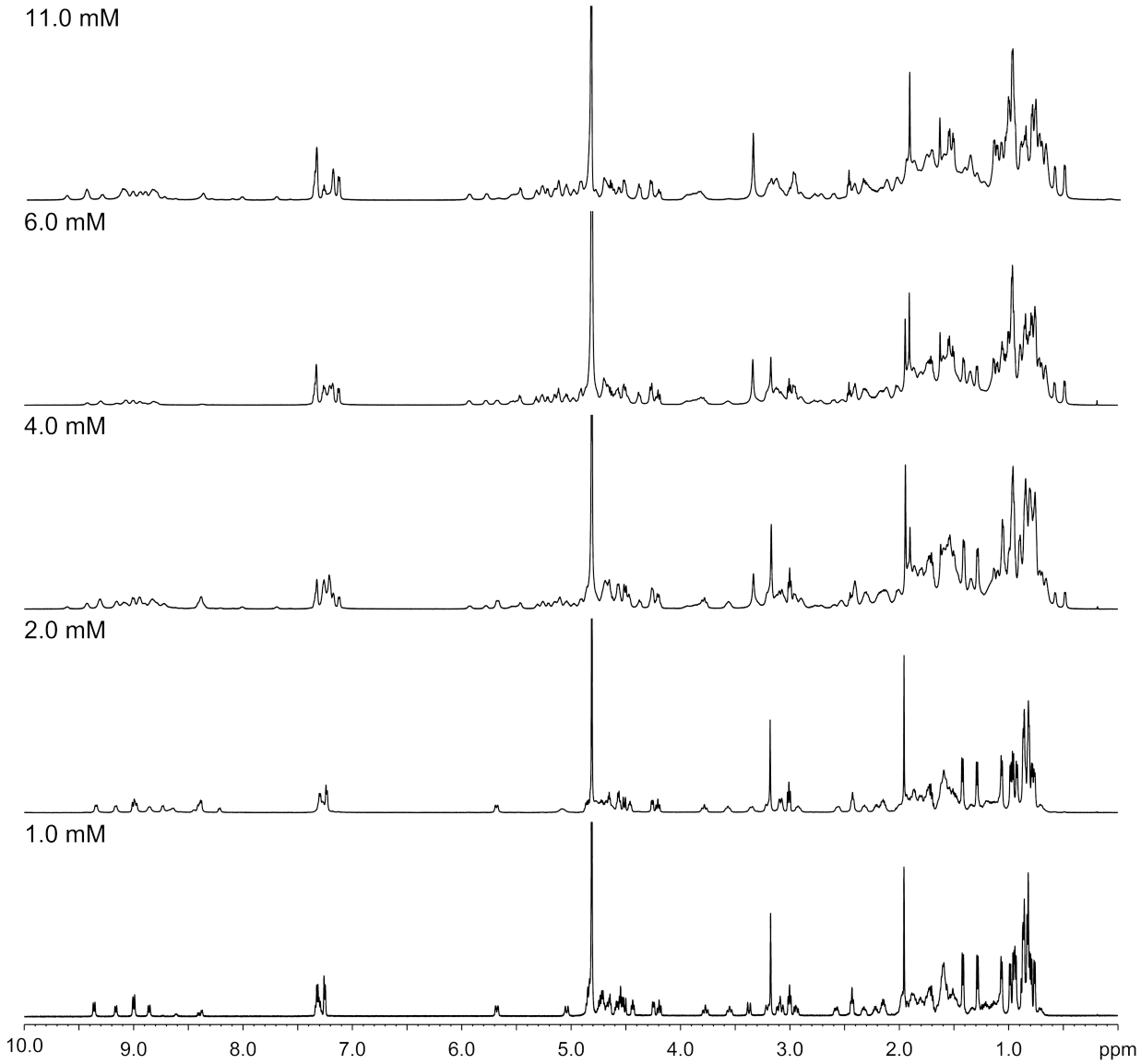

Figure S2.5. ^{1}H NMR stacked plot of peptide **2** between 1.0 and 11.0 mM in D_2O at 600 MHz and 298 K.

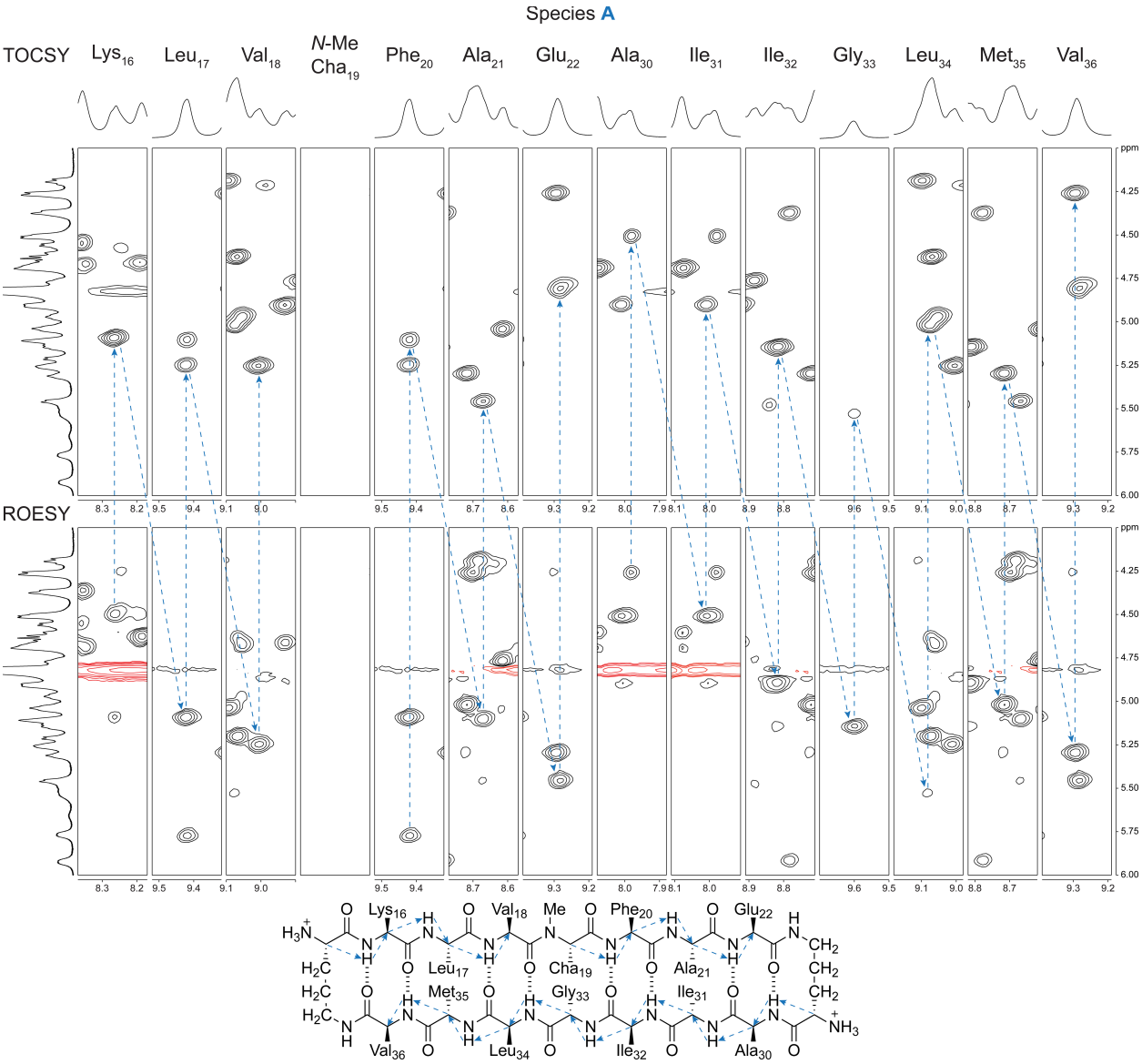

Figure S2.6. Strips from TOCSY and ROESY spectra showing peak assignments from species **A**. Spectra were recorded at 11.0 mM peptide **2** in 9:1 H_2O/D_2O or D_2O at 600 MHz and 298 K.

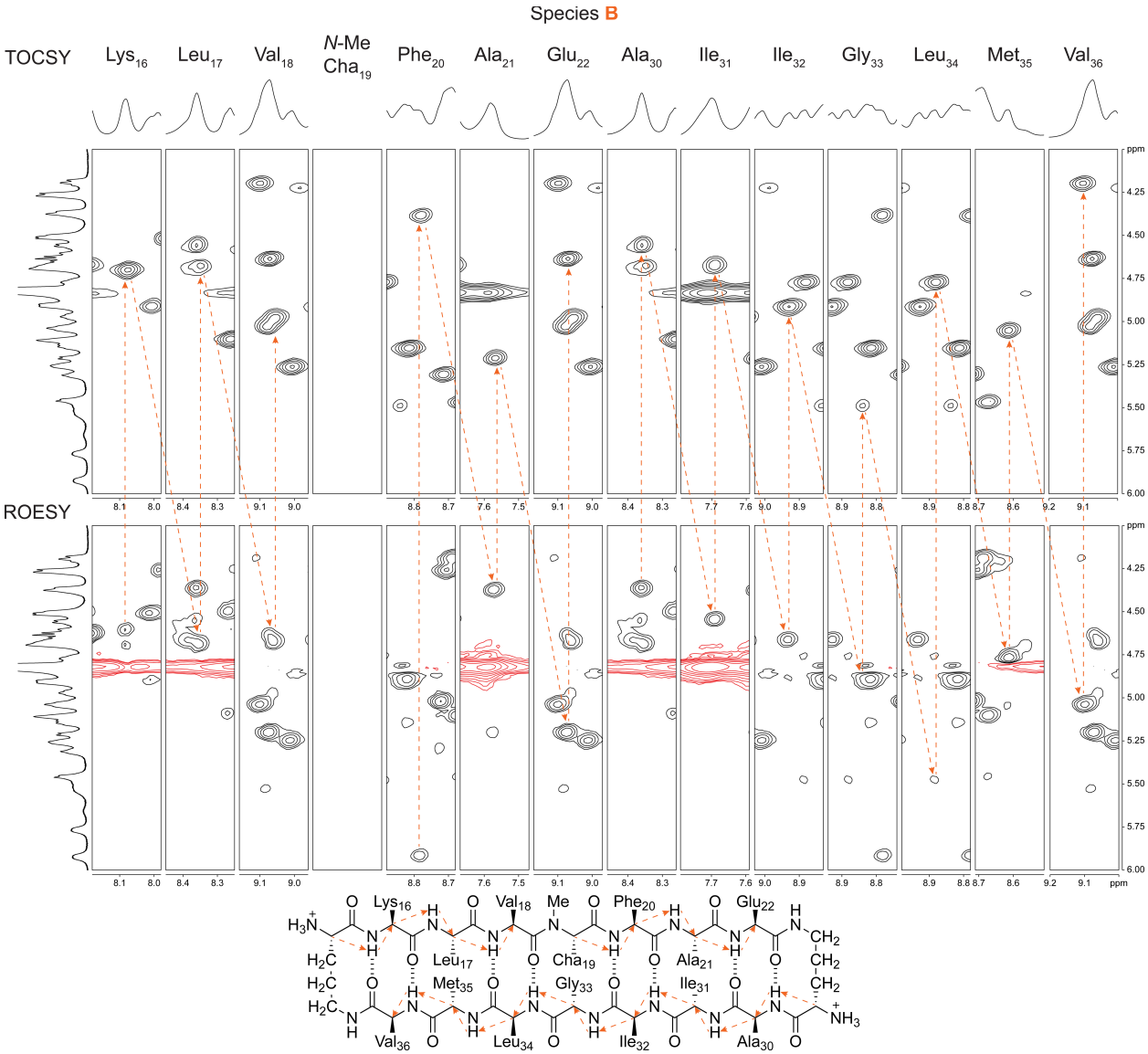

Figure S2.7. Strips from TOCSY and ROESY spectra showing peak assignments from species **B**. Spectra were recorded at 11.0 mM peptide **2** in 9:1 H_2O/D_2O or D_2O at 600 MHz and 298 K.

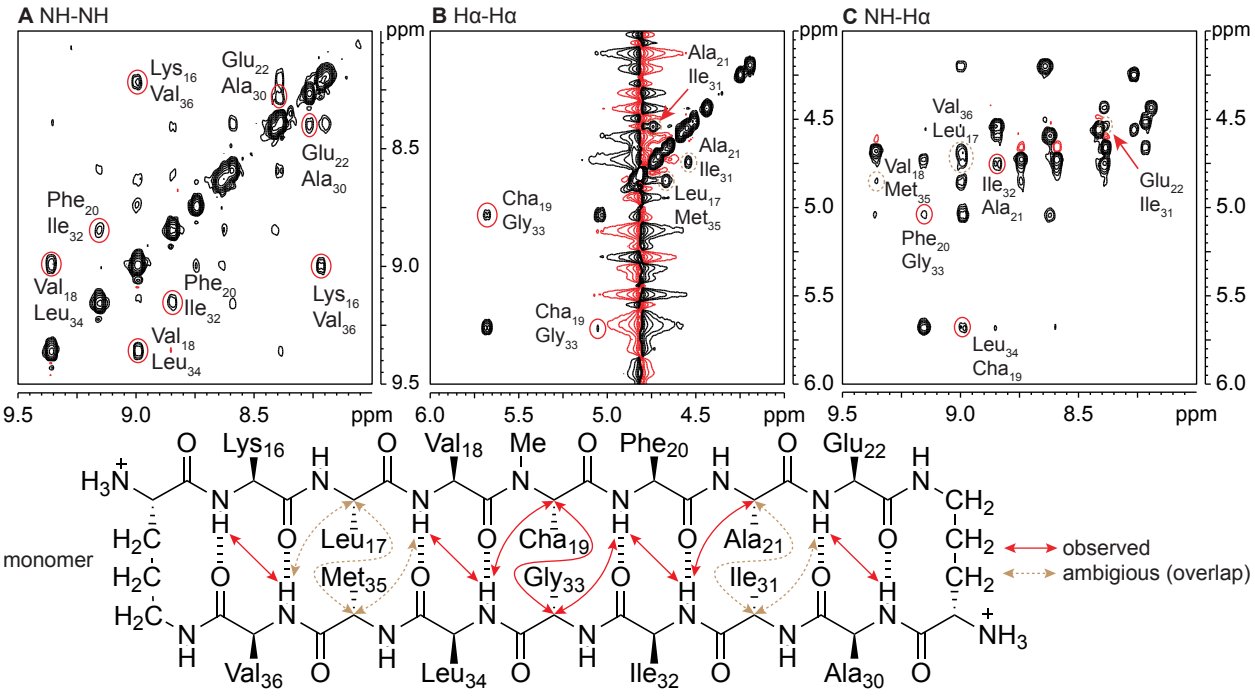

Figure S2.8. NOESY spectrum of peptide **2** showing key intramolecular NOEs associated with β-sheet folding for monomer. Spectra were recorded at 1.0 mM in 9:1 H_2O/D_2O or D_2O at 600 MHz and 298 K.

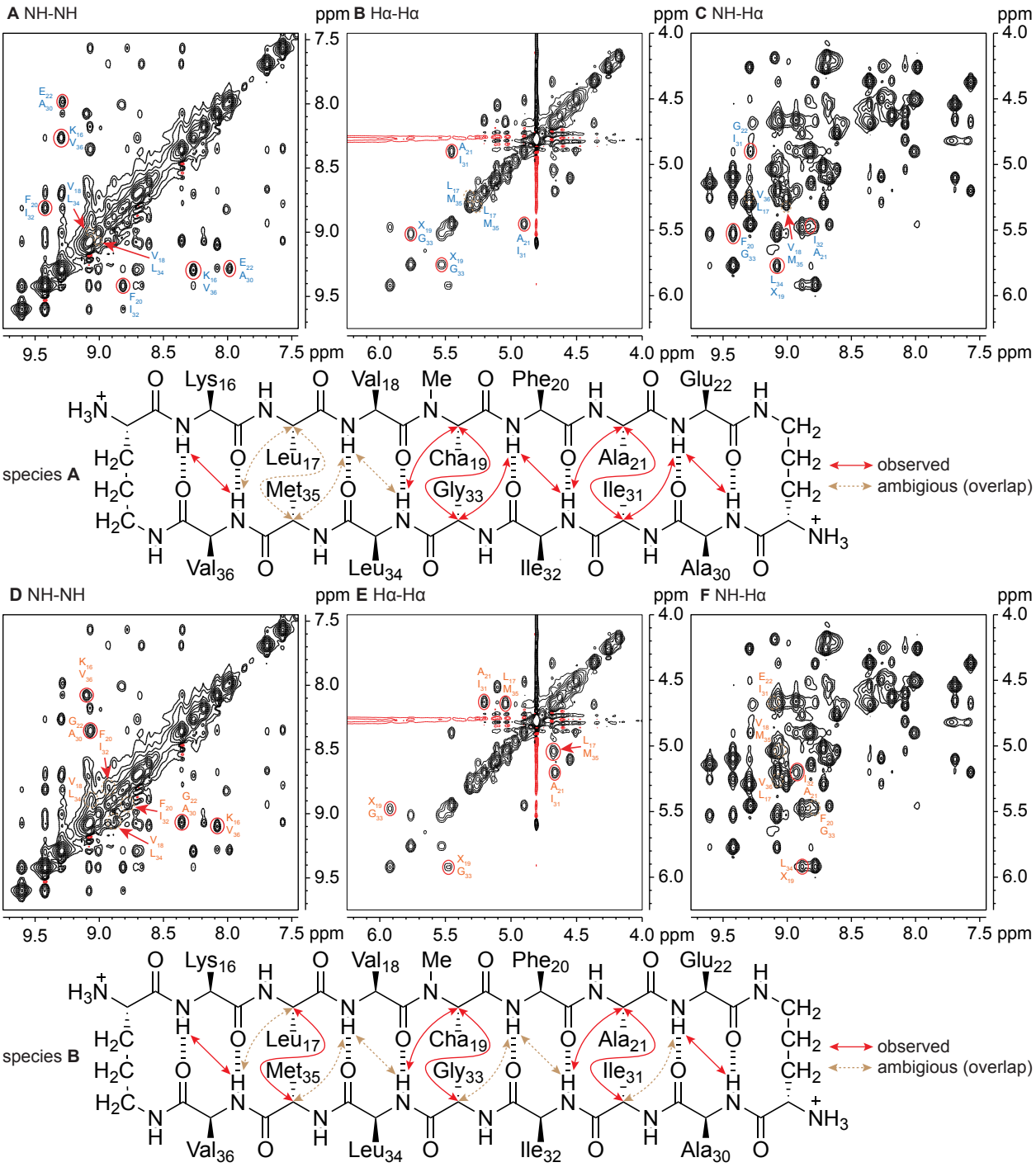

Figure S2.9. NOESY spectrum of peptide **2** showing key intramolecular NOEs associated with β-sheet folding for species **A** and **B**. Spectra were recorded at 11.0 mM in 9:1 H_2O/D_2O or D_2O at 600 MHz and 298 K. X_{19} refers to Cha_{19}.

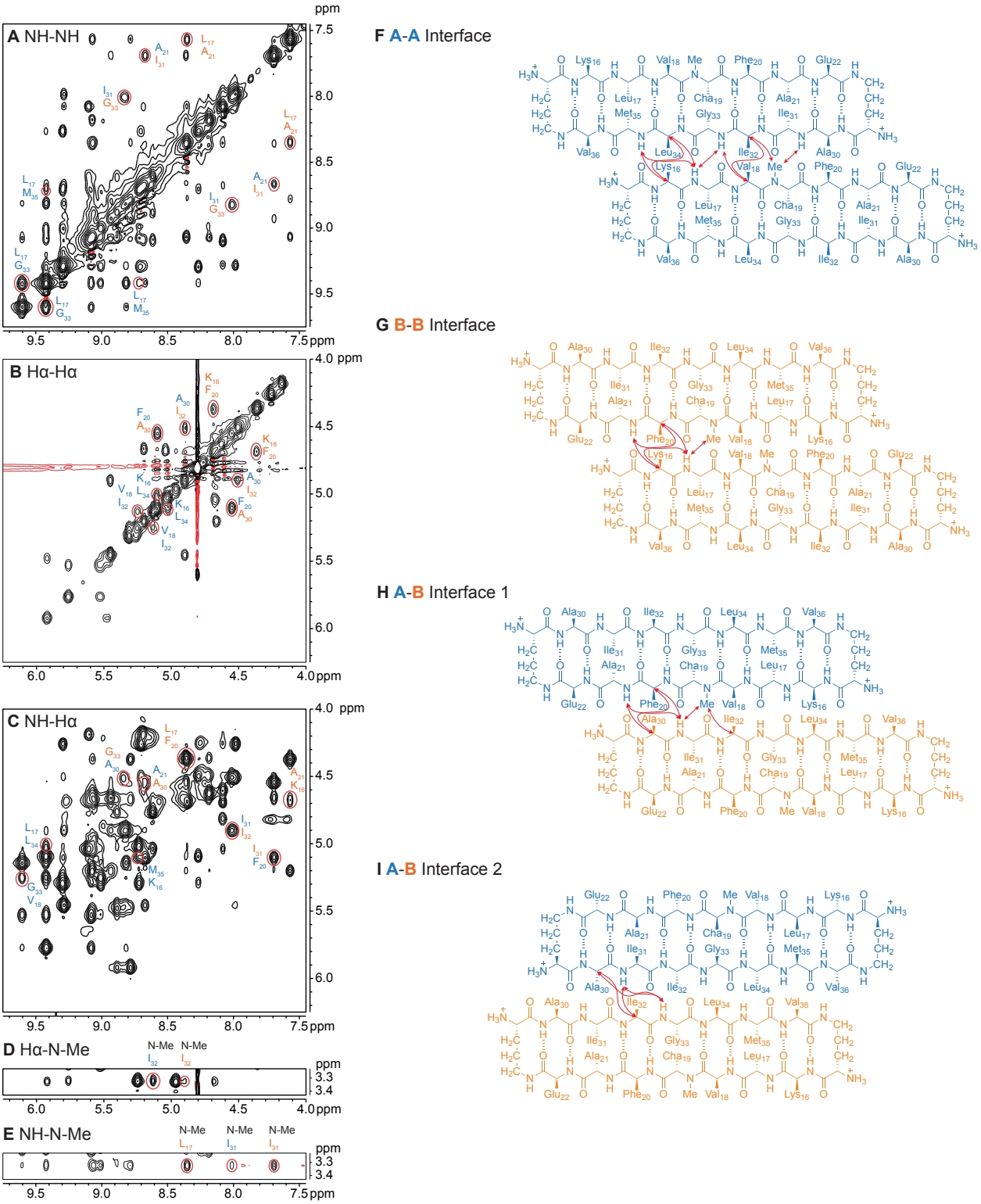

Figure S2.10. Summary of key peptide **2** intermolecular NOEs. NOESY spectra were recorded at 11.0 mM in 9:1 H_2O/D_2O or D_2O at 600 MHz and 298 K. Simplified ChemDraw illustrations of the intermolecular contacts are shown as dimers for visualization purposes only.

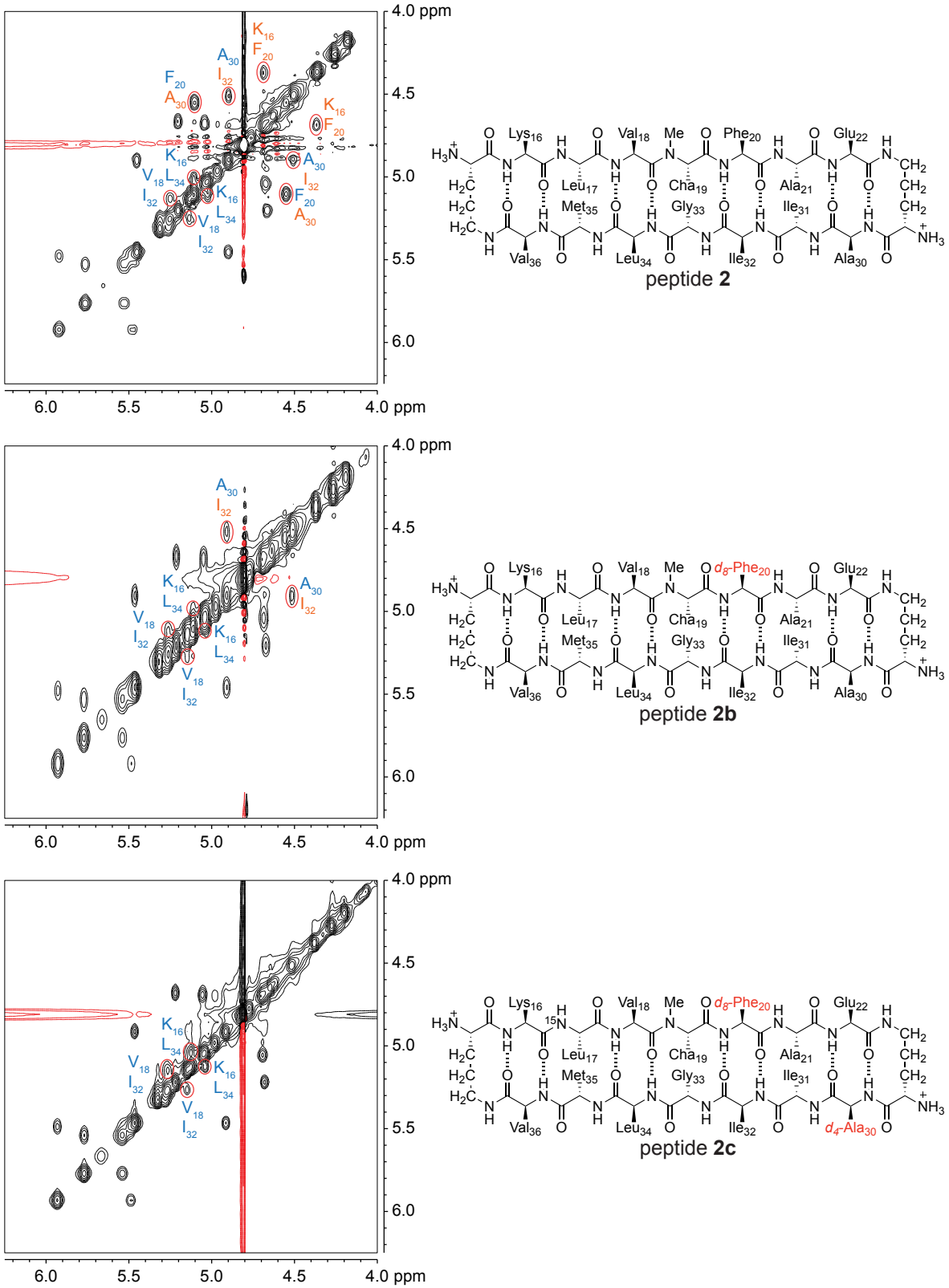

Figure S2.11. NOESY spectra of peptide **2**, **2b**, and **2c** showing key intermolecular Hα-to-Hα NOEs that disappear with deuteration. Peptide **2** was recorded at 600 MHz. Peptides **2b** and **2c** was recorded at 800 MHz. All spectra were recorded at 11.0 mM in D_2O at 298 K.

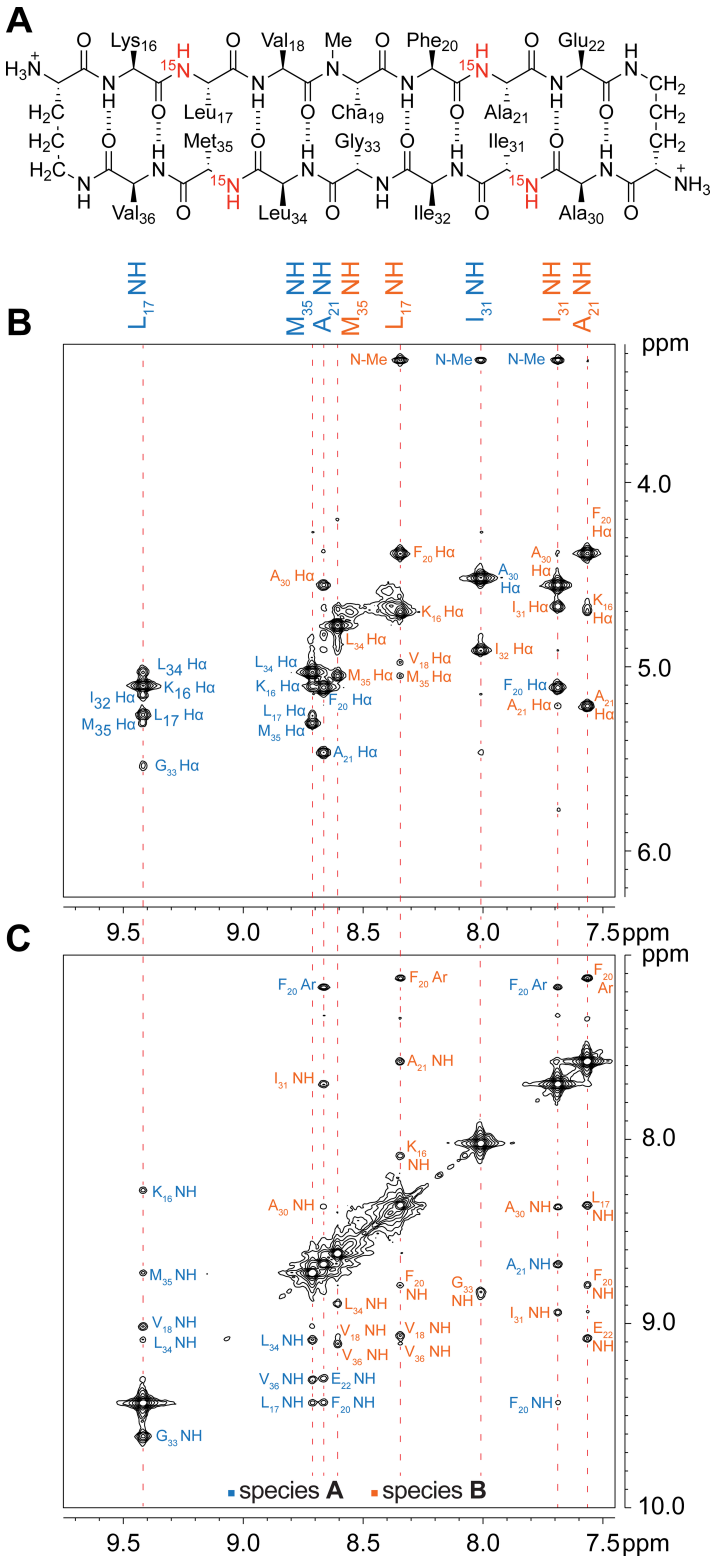

Figure S2.12. Fully annotated ^{15}N-edited NOESY HSQC spectrum of peptide **2d**. Chemical structure of peptide **2d**, highlighting the ^{15}N labels at Leu$_{17}$, Ala$_{21}$, Ile$_{31}$, and Met$_{35}$ in red (A). ^{15}N-edited NOESY-HSQC spectrum of peptide **2d** showing all NOEs to either Hα or *N*-Me (B) and NH protons (C). The spectrum was recorded at 11.0 mM in 9:1 H_2O/D_2O at 800 MHz and 298 K.

In building the model of the asymmetric hexamer, we considered numerous other models that proved to be inconsistent with the NMR data. These oligomer models that are inconsistent with the data can be categorized both by the oligomer state and by key underlying assumptions made. We excluded all odd numbered oligomers because of the 1:1 integration of resonances associated with associated with species **A** and **B**. Additionally, the presence of multiple A-B intermolecular contacts indicates there is one oligomer species composed of species **A** and **B**.

The quotient of diffusion coefficients of peptide **2** shown in Figure **S14** provides a rough estimate that peptide **2** is between a decamer and a tetradecamer. We considered all cases between a tetramer and hexadecamer to account for the possibility that the oligomer may be anisotropic (not perfectly spherical).

Tetramer: Species **B** forms a strong locus of intermolecular contacts between Lys_{16} Hα and Phe_{20} Hα. Assuming a tetramer, species **B** must make a dimer which is forbidden because of the two *N*-methyl groups on Cha_{19} would disrupt hydrogen bonding along the dimer interface.

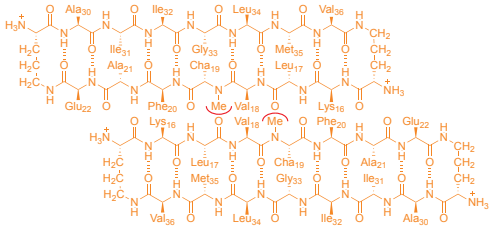

Hexamer: Based on molecularity, there are three molecules of species **A** and **B**. The only way to satisfy the Lys_{16} Hα and Phe_{20} Hα for species **B** is to make triangular trimers analogous to that observed in the crystal structure (shown below on the left). We ruled out the crystallographic hexamer because we do not observe any NOE between Ala_{30} Hα and Leu_{34} Hα for either **A**-**A**, **A**-**B**, or **B**-**B** (shown below on the right) that would be expected based on the crystallographic hexamer. We could not conceptualize any other hexameric oligomer models outside of the proposed asymmetric hexamer.

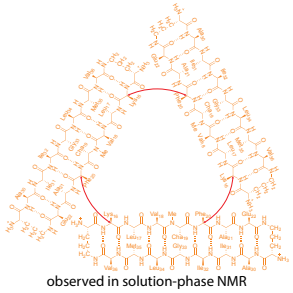

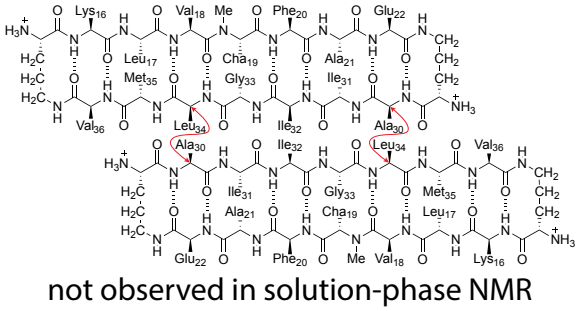

Octamer: Based on molecularity, there are four molecules of species **A** and four molecules of species **B**. We can exclude the possibility that species **B** makes two sets of dimers because the N-methyl groups on Cha_{19} would disrupt hydrogen bonding same as for the tetrameric models (shown above) of the oligomer. This leaves the possibility that species **B** makes a square tetramer where

the Lys_{16} Hα and Phe_{20} Hα is located on the interior vertices of a square. There are two possible arrangements of the remaining four molecules of **A**: all four molecules of **A** above the plane of the square or two molecules of **A** below and two molecules of **B** above. In the first case, the model contains a solvent exposed cavity that is unlikely to assemble in aqueous solution. In the second case, there is no way to satisfy the observed **A-A** intermolecular contacts with an arrangement of dimers either above or below the plane of the square tetramer formed by species **B**.

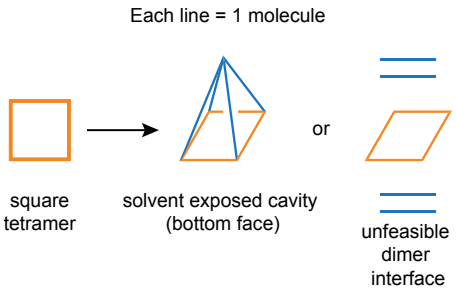

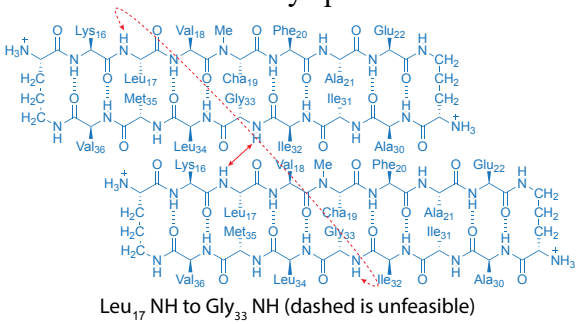

Decamer and Tetradecamer: By analogy described for the octamer oligomer model, we can make a pentamer or heptamer for species **B** using the Lys_{16} Hα and Phe_{20} Hα NOE. However, we run into the same issues encountered in the octamer oligomer model. The odd number of molecules of species **A** means that all five molecules of species **A** would have to pack on one face of the pentamer or heptamer. The resulting model runs into the same issues as the octamer with a solvent exposed cavity on one face.

Dodecamer: There are two main possibilities with a dodecamer model, species **B** can either make two triangular trimers as described in the asymmetric hexamer model or a hexamer based on the Lys_{16} Hα and Phe_{20} Hα NOEs. In the case where species **B** makes two triangular trimers, species A would have to hexameric structure that is sandwiched between the two species **B** triangular trimers (shown as B-A-B). We did not find a reasonable conformation for the species **A** monomer that simultaneously satisfied the **A-A** intermolecular NOEs (Leu_{17} NH to Gly_{33} NH) and two unique **A-B** intermolecular NOEs (Ala_{30} Hα to Ile_{32} Hα **B-A** and Ile_{32} Hα to Phe_{20} Hα **B-A**) within 5 Å. In the case where species **B** makes a hexamer, we considered placement of six molecules of species **A** on one face as well as a symmetrical placement of three molecules of **A** on both faces. The placement of six molecules of species **A** on the same face contains an exposed cavity. We did not find a reasonable arrangement of the three molecules of **A** on both faces of a hexamer formed by species **B** that simultaneously satisfied the **A-A** and two **A-B** intermolecular interfaces.

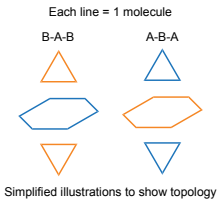

Hexadecamer: Given that species **B** cannot make dimers as described in the tetramer model, we considered whether species **B** can make two sets of square tetramers or one set of octamers. The hexadecamer models run into the same issues described in the tetramer and octamer model.

Figure S2.13. Consideration and elimination of alternative models of the asymmetric hexamer.

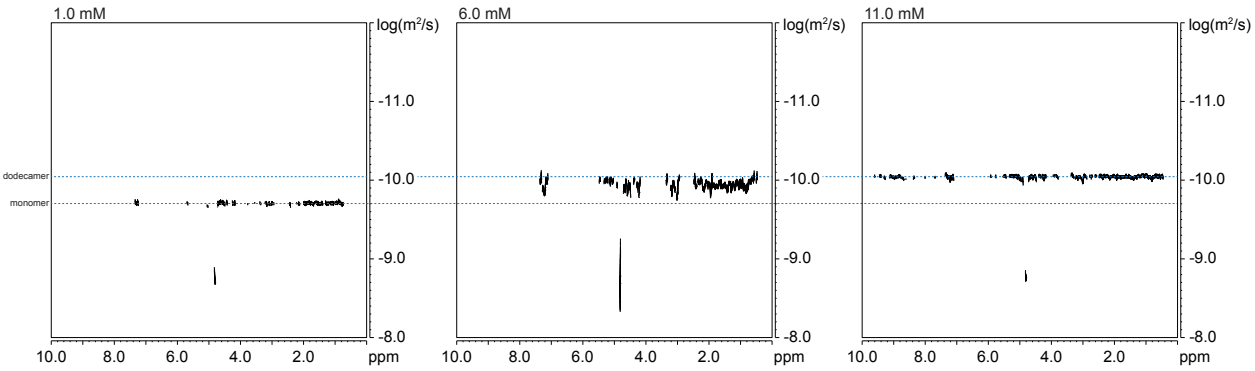

Calculations for monomer and dodecamer

For monomer at 1.0 mM, log $D_{monomer}$ = -9.703, $D_{monomer} = 10^{-9.703} = 1.98 \times 10^{-10}$ m^2/s.

For dodecamer at 11.0 mM, log $D_{dodecamer}$ = -10.044, $D_{dodecamer} = 10^{-10.044} = 0.904 \times 10^{-10}$ m^2/s.

To assess oligomer state,

Oligomer	Ratio
dimer	0.794
trimer	0.693
hexamer	0.550
decamer	0.464
undecamer	0.450
dodecamer	0.437
tridecamer	0.425
tetradecamer	0.415

Figure S2.14. DOSY NMR spectra of 1.0, 6.0, and 11.0 mM peptide **2** in D_2O at 600 MHz and 298 K. The 11.0 mM spectrum shows one track with a diffusion coefficient of 0.904 ± 0.08 x 10^{-10} m^2/s. The 1.0 mM spectrum shows one track with a diffusion coefficient of 1.98 ± 0.11 x 10^{-10} m^2/s. The HOD peak is calibrated to 19.0 x 10^{-10} m^2/s.[1]

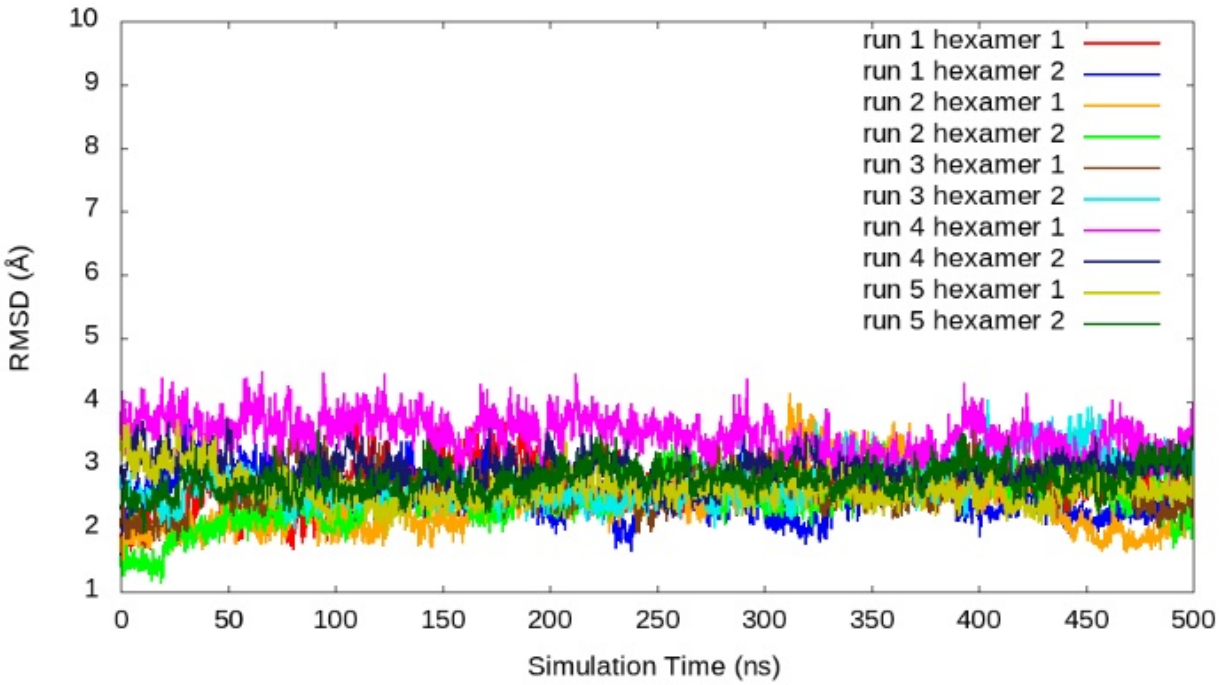

Figure S2.15. Root mean square displacement (RMSD) of hexamers backbone atoms with respect to the NMR-based molecular model.

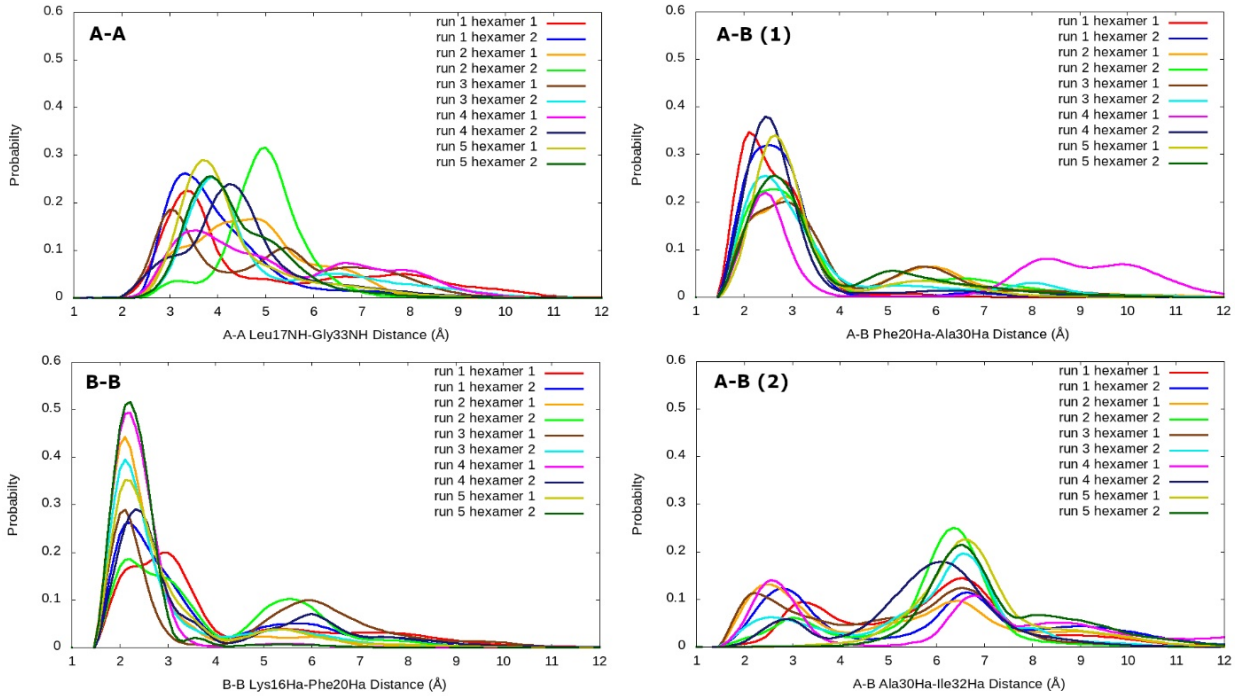

Figure S2.16. Probability distributions of key NOE distances observed during MD simulations. Each histogram is calculated from three equivalent pairs of proton-proton distances in one hexamer and among 50,000 frames (500 ns) per pair.

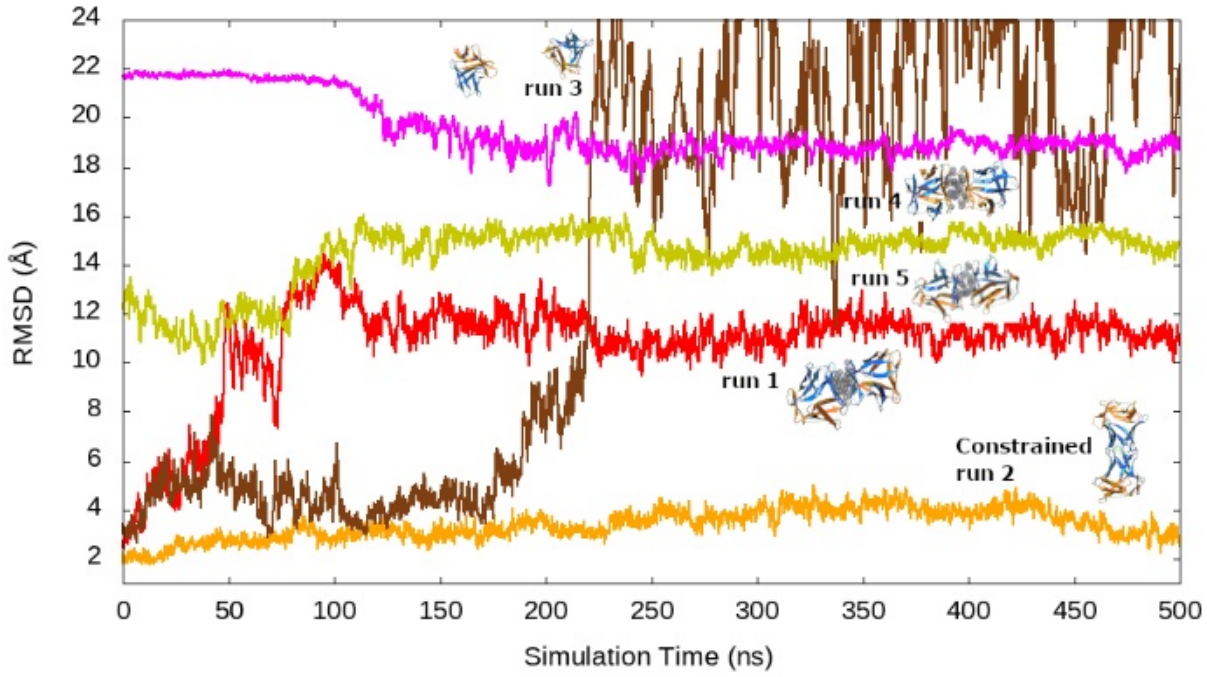

Figure S2.17. RMSD of dodecamer backbone atoms with respect to initial structure of run 1.

Table S2.1. Crystallographic properties, crystallization conditions, and data collection and model refinement statistics for peptide **2**.

PDB ID	9EEC
space group	*P*432
a, *b*, *c* (Å)	67.511 67.511 67.511
α, β, λ (°)	90, 90, 90
molecules per asymmetric unit	3
wavelength (Å)	1.0
resolution (Å)	38.98–1.58 (1.64–1.58)
total reflections	744201 (3145)
unique reflections	13661 (287)
multiplicity	62.6 (11.0)
completeness (%)	99.95 (99.09)
mean I/σ(I)	33.09 (0.06)
Wilson B factor	32.25
R_{merge}	0.05796 (15.74)
$R_{measure}$	0.05846 (16.44)
$CC_{1/2}$	1 (0.0818)
CC^{*}	1 (0.389)
R_{work}	0.2110 (0.3321)
R_{free}	0.2250 (0.3454)
number of non-hydrogen atoms	390
RMS_{bonds}	0.012
RMS_{angles}	1.41
Ramachandran favored (%)	100
Ramachandran allowed (%)	0
Ramachandran outliers (%)	0
rotamer outliers (%)	0
clashscore	13.29
average B-factor	40.47
number of TLS groups	3
ligands/ions	0
water molecules	15
crystallization conditions	0.1 M HEPES at pH 7.0, 0.25 M $MgCl_2$, 30% isopropanol

Table S2.2. Chemical shift tabulations for ^{15}N-labeled isotopologues **2a** and **2d**. Data taken from ^{1}H,^{15}N HSQC recorded at 1.0 mM or 11.0 mM peptide in 9:1 H_2O/D_2O at 800 MHz and 298 K.

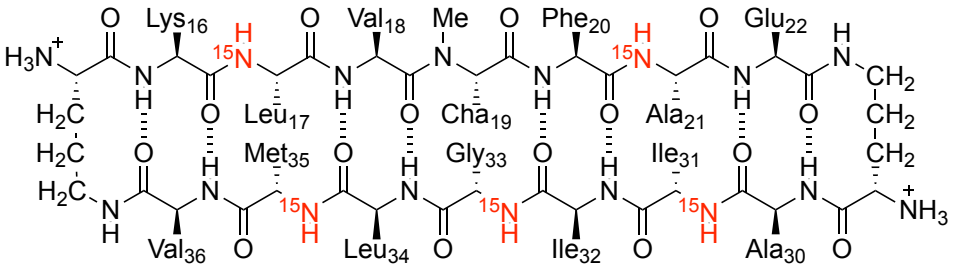

Residue	^{15}N Chemical Shift (ppm)		
	monomer	species **A**	species **B**
Leu_{17}	123.3	125.2	123.3
Ala_{21}	127.0	121.8	125.8
Ile_{31}	121.8	121.7	120.5
Gly_{33}	111.4	109.9	104.7
Met_{35}	123.9	123.8	121.7

Table S2.3. Chemical shifts of NH and Hα protons of peptide **2** monomer, species **A**, and species **B** in D_2O or 9:1 H_2O/D_2O at 600 MHz and 298 K.

Residue	Chemical Shift (ppm)					
	monomer		species **A**		species **B**	
	NH	Hα	NH	Hα	NH	Hα
Lys_{16}	8.21	4.64	8.27	5.11	8.09	4.70
Leu_{17}	8.38	4.67	9.43	5.26	8.36	4.67
Val_{18}	9.35	4.83	9.01	5.26	9.06	4.97
N-Me Cha_{19}	-	5.68	-	5.77	-	5.92
Phe_{20}	9.15	4.71	9.42	5.11	8.79	4.37
Ala_{21}	8.59	4.74	8.67	5.46	7.57	5.21
Glu_{22}	8.39	4.44	9.29	4.82	9.08	4.63
Ala_{30}	8.26	4.55	7.99	4.51	8.37	4.55
Ile_{31}	8.41	4.54	8.02	4.90	7.70	4.66
Ile_{32}	8.84	4.59	8.82	5.14	8.94	4.90
Gly_{33}	8.62	5.04	9.61	5.53	8.85	5.48
Leu_{34}	8.98	4.72	9.08	5.04	8.89	4.77
Met_{35}	8.74	4.86	8.72	5.31	8.62	5.04
Val_{36}	8.99	4.19	9.30	4.26	9.10	4.18

Materials and Methods[2]

General information

Chemicals and Supplies All chemicals were used as received unless otherwise noted. Dry methylene chloride (CH_2Cl_2), *N,N*-dimethylformamide (DMF), and diethyl ether were obtained by passing through alumina under argon prior to use. The DMF was additionally passed through an amine scavenger resin column under argon. Amine-free *N,N*-dimethylformamide (DMF) and piperidine were purchased from Alfa Aesar. 2,4,6-collidine and diisopropylethylamine (DIPEA) was purchased from Thermo Scientific. 1,1,1,3,3,3-Hexafluoro-2-propanol (HFIP) and trifluoroacetic acid (TFA) were purchased from Oakwood Chemicals. Deionized water (18 MΩ) was obtained from a Barnstead NANOpure Diamond water purification system. HPLC grade acetonitrile and deionized water (18 MΩ), each spiked with 0.1% (v/v) trifluoroacetic acid (TFA), were used for analytical and preparative reverse-phase HPLC. Isotopically labeled alanine (^{15}N, 98% isotopic purity), glycine (^{15}N, 98% isotopic purity), isoleucine (^{15}N, 98% isotopic purity), leucine (^{15}N, 98% isotopic purity), methionine (^{15}N, 96-98% isotopic purity), alanine (d_4-Phe, 98% isotopic purity), and phenylalanine (d_8-Phe, 98% isotopic purity) were purchased from Cambridge *N*-(9-flurenylmethoxycarbonyloxy)succinimide (Fmoc-Osu) was purchased from GL Biochem. Isotope Laboratories. Deuterium oxide (D, 99.9%) was purchased from Sigma Aldrich.

Instrumentation All peptides were first purified on a Biotage® Isolera™ One system equipped with a Biotage® Sfr Bio C18 Duo 300 Å 20 µm column prior to purification on the Shimazu instrument equipped with an Agilent Zorbax 7 µm 300SB-C18 column (21.2 x 250 mm). Analytical reverse-phase HPLC was performed on an Agilent 1260 Infinity II instrument with a Phenomonex bioZen PEPTIDE 2.6 µm XB-C18 column. Yields refer to isolated purified

compounds confirmed chromatographically. UV absorption was measured using the Thermo Scientific™ Varioskan™ LUX. Matrix-assisted desorption ionization time-of-flight (MALDI-TOF) mass spectrometry was performed on the AB SCIEX TOF/TOF 5800 system in linear reflector mode with α-cyano-4-hydroxycinnamic acid (CHCA) used as the matrix. All peptides were assumed to have one trifluoroacetate ion per ammonium group present in each peptide.

Synthesis and purification of peptides

Peptide synthesis procedure Macrocyclic peptides **1**, **2**, and subsequent homologues were synthesized by manual solid-phase peptide synthesis on 2-chlorotrityl resin, followed by HFIP cleavage, solution-phase cyclization, global deprotection, and reverse phase HPLC purification. A step-by-step procedure is detailed below.

Resin loading 2-chlorotrityl resin (300 mg, 1.07 mmol/g) and Boc-Orn(Fmoc)-OH (100 mg) was added to a 10-mL Bio-Rad Poly-Prep chromatography column. The resin was loaded overnight (8-12 h) in a solution of 6 mL DCM and 0.3 mL 2,4,6-collidine under gentle agitation. The loading solution was drained and the resin was washed three times with DCM. After washing, the resin was capped using a solution of DCM/MeOH/DIPEA (17:2:1, 8 mL) for 1 h under gentle agitation. The solution was drained and the resin was washed three times with DCM. The resin was dried under a flow of nitrogen. Once dry, loading was checked on the Varioskan through UV analysis (290 nm) of the Fmoc cleavage product. Nominal loading values range from 0.12 – 0.15 mmol.

Solid-phase peptide coupling The loaded was re-suspended in amine-free DMF, allowed to swell for 30 min, and transferred to a clean 25 mL coupling vessel. The linear peptide was synthesized

from the *C*-terminus to the *N*-terminus using standard coupling cycles unless otherwise noted. A standard coupling cycle consists of the following: (1) Fmoc deprotection with 20% (v/v) piperidine in DMF (5 mL) for 10 min, (2) resin washing with DMF (5X), (3) coupling of the amino acid (4 equiv) with HCTU (4 equiv) in 20% (v/v) collidine in DMF for 30 min, and (4) resin washing with DMF (5X). For the amino acid after the *N*-methylated amino acid, the resin was double coupled for 1 h each using 4 equiv of HATU/HOAt. Once the linear synthesis was complete, the resin was transferred to a 10-mL Bio-Rad Poly-Prep chromatography column and washed with DCM (3X).

Cleavage of the linear peptide from resin The linear peptide was cleaved from using a cleavage solution of 20% (v/v) HFIP in DCM (7.5 mL) under gentle agitation. The filtrate was collected in a 1-L round-bottom flask. Another 7.5 mL of cleavage solution was added to the resin under gentle agitation for 30 min and combined with the original filtrate. The combined filtrates were concentrated under reduced pressure to afford a translucent film.

Cyclization of the linear peptide (125 mL) was added to dissolve the clear oil. HATU (6 equiv) and HOAt (6 equiv) were added to the solution. The solution was stirred before DIPEA (300 μL) was added dropwise. The flask was flushed three times with nitrogen and allowed to cyclize at room temperature for 2 d. The reaction was concentrated under reduced pressure (65 °C) to afford a beige solid. The round bottom was placed under vacuum to remove residual DMF.

Global deprotection of the cyclic peptide The protected peptide was dissolved in a mixture of TFA/TIPS/H_2O (90:5:5, 10 mL) with NH_4I (250 mg) and Me_2S (ca. 1 mL). The mixture was stirred for 1 h and transferred into two 50-mL conical tubes each containing 35 mL of chilled diethyl

ether. Both conical tubes were centrifuged (600xg, 4 ℃) to pellet the precipitate. The supernatant was decanted into a 125-mL Erlenmeyer flask. This process was repeated twice more by adding additional ether, shaking to break up the pellet, and centrifuging. The pellet was dried under reduced pressure.

Biotage Reverse-phase HPLC purification The dried peptide was dissolved in 20% (v/v) ACN in H_2O and purified on the Biotage® Isolera™ One system equipped with a Biotage® Sfr Bio C18 Duo 300 Å 20 µm column using an ACN/H_2O gradient (20 – 60%) over 8 column volumes. Fractions were analyzed by MALDI-TOF and analytical HPLC. Fractions containing predominantly desired peptide were combined and concentrated under reduced pressure to afford an off-white solid.

Shimadzu Reverse-phase HPLC purification The peptide was dissolved in 20% (v/v) ACN in H_2O and filtered through a 0.2 µm PVDF syringe filter to remove insoluble aggregates and purified by RP-HPLC using an ACN/H_2O gradient (25–45%, 15 mL/min) over 90 min. Fractions were analyzed by MALDI-TOF and analytical HPLC. Pure fractions were and lyophilized to afford peptide as white trifluoroacetate (TFA) salts.

Isotopologues **2a-d** were synthesized the same as peptides **1** and **2**. Fmoc-protected ^{15}N glycine replaced Gly_{33} in the preparation of **2a**. Fmoc-protected d_8 phenylalanine replaced Phe_{20} in preparation of **2b**. Fmoc-protected d_8 phenylalanine and d_4 alanine replaced Phe_{20} and Ala_{30} in preparation of **2c**. Fmoc-protected ^{15}N alanine, ^{15}N isoleucine, ^{15}N leucine, and ^{15}N methionine replaced Ala_{21}, Ile_{31}, Leu_{17}, and Met_{35} in preparation of **2d**.

X-ray crystallography of peptide 2

*Crystallization procedure of peptide **2*** Crystal screening trays for peptide **2** were prepared based on previously reported crystallization conditions for peptide 1 in a 4x6 matrix Hamptom VDX 24-well plate. Two optimization trays conditions were tested. In both trays, the HEPES buffer pH was varied in each row in increments of 0.5 pH units (6.5, 7.0, 7.5, and 8.0) and the isopropanol concentration in each column in increments of 2% (28%, 30%, 32%, 34%, 36%, 38%). The first well of the first tray was prepared by combining 100 µL of 1 M HEPES at pH 6.5, 250 µL of 1 M $MgCl_2$, 280 µL of isopropanol, and 370 µL of (18 MΩ water). The other wells were prepared in analogous fashion, by combining 100 µL of HEPES buffer of varying pH, isopropanol in varying amounts, $MgCl_2$, and 18 MΩ water for a total volume of 1 mL per well. The first well of the second tray was prepared by combining 100 µL of 1 M HEPES at pH 6.5, 200 µL of 1 M sodium citrate, 280 µL of isopropanol, and 420 µL of (18 MΩ water). The other wells for the second tray were prepared in analogous fashion.

Three hanging-drops were prepared per borosilicate glass slide by combining of peptide 2 (10 mg/mL in 18 MΩ water) and well solution in the following amounts: 1 µL: 1 µL, 2 µL: 1 µL, 1 µL: 2 µL of peptide solution to well solution. Slides were inverted and sealed by pressing firmly against the silicone grease surrounding each well.

Crystals of peptide **2** suitable for X-ray diffraction grew in ~3-5d. Crystals were harvested with a nylon loop attached to a copper or steel pin, cryoprotected using MPD and flash frozen in liquid nitrogen prior to data collection.

*X-ray crystallographic data collection, data processing, and structure determination of peptide **2***

Diffraction data for peptide **2** were collected on the Advanced Light Source Synchrotron at the Berkeley Center for Structural Biology on beamline 5.0.2. at 1.0 Å wavelength with 0.5° oscillation. Diffraction data were collected using b4. Diffraction data were integrated, scaled, and merged using XDS and pointless and aimless. The resolution was limited to the $CC_{1/2}$ resolution of 1.58 Å. The electron density map for peptide **2** was generated by molecular replacement with the coordinates from the X-ray crystallographic structure of peptide **1** (PDB 5W4H) as a search model using Phaser in the Phenix software suite 1.10.1. Molecular manipulations of the model were performed with Coot. Coordinates were refined in the *P*432 space group with phenix.refine. The optimal number and composition of the TLS groups were chosen automatically by phenix.refine.

Silver-stained SDS-PAGE

Pouring gels The reagents for Tricine SDS-PAGE were prepared according to recipes and procedures detailed in Schägger, N. *Nat. Protoc.* 2006, *1*, 16-22.[3] Fresh resolving separation gel (16%) were prepared by mixing the following: Acrylamide bis-acrylamide (AB-3) (5 mL), Gel Buffer (5 mL), H_2O, and 10% (w/v) ammonium persulfate solution (100 µL) and tetramethylethylenediamine TEMED (10 µL). The solution was poured into a cast and allowed to polymerize over 30 min. The resolving gel was topped with isopropanol (IPA) during the polymerization process. Once the resolving gel has set, the isopropanol was discarded and the resolving gel was rinsed with water. The stacking gel (4%) was prepared in an analogous fashion and poured on top of the resolving gel. The comb was inserted, and the gel was allowed to set for 15 min.

Loading and running Concentrated SDS-loading dye (6X) was mixed with peptide to give the working concentrations listed and loaded onto the gel lanes (12 μL per lane). The migration of peptides was compared with molecular weight protein ladder (Spectra^{TM} Multicolor Low Range Protein Ladder, ThermoFisher Scientific, catalog #: 26628). The gels were run at a constant 90 V at room temperature.

Silver-staining The reagents for silver staining were prepared according to procedures detailed in Simpson, R. J. *CHS Protoc*. **2007**.[4] [For best results, we prepared the sodium thiosulfate, silver nitrate, and developing solution fresh each time. The silver nitrate solution was chilled at 4 °C prior to use. Pure sodium carbonate (≥ 99.5 %) was used to prepare the developing solution.] The gel was rocked in 20 mL of fixing solution (MeOH/AcOH/H_2O, 50:5:45). Next, the fixing solution was discarded and 20 mL of fresh solution (MeOH/H_2O, 1:1) was added to the gel and rocked for 10 min before being discarded. After that, the gel was rocked in RO water for 10 min. The gel was submerged in 0.02 % (w/v) aqueous sodium thiosulfate solution and rinsed for 1 min with RO water three times. Freshly made chilled 0.1 % (w/v) aqueous silver nitrate solution (20 mL) was added to the gel and rocked for 20 min. The solution was discarded and the gel was rinsed again with RO water for 1 min three times. The gel was developed using 2% (w/v) sodium carbonate solution with 0.04% (w/v) formaldehyde. The gel then was submerged in 5% (v/v) aqueous acetic acid. The silver-stained gels were visualized with a ChemiDocTM MP Imaging System using the "Optimal Auto-exposure" exposure under the "Silver Stain Gel" application of the Image Lab Touch Software.

Circular dichroism (CD) spectroscopy

A 100 μM solution of each peptide was prepared by dissolving weighed portion of peptide in the appropriate volume of 10 mM sodium phosphate buffer at pH 7.4. Each solution was transferred to a 1 mM quartz cuvette for data acquisition. Circular dichroism spectra were acquired on a Jasco-810 circular dichroism spectropolarimeter at ambient temperature. Data was collected with a 0.5 nm pitch, 1 nm bandwidth, from 260 nm to 190 nm averaged over 5 accumulations with 11-point smoothing.

Fmoc-Protection of Isotopically Labeled Amino Acids

Fmoc-protected d_4-Ala-OH and Fmoc-protected d_8-Phe-OH were prepared as previously reported.[2]

Fmoc-Protection of ^{15}N-Labeled Amino Acids

Fmoc [^{15}N] Ala-OH: A 100-mL one-neck round-bottom flask equipped with a magnetic stirring bar was charged with ^{15}N-labeled alanine (0.5 g, 5.6 mmol), and Fmoc-OSu (1.80 g, 5.3 mmol). A solution of 1:1 CH_3CN/H_2O (25 mL) and Et_3N (782 μL, 5.6 mmol)) were added then the reaction mixture was stirred for 15 min. Additional Et_3N was added until a clear solution formed (pH 7.2). The solution was stirred for an additional 1 h. The solution was poured into a solution of 1.0 M HCl (125 mL) in a 250 mL beaker while stirring vigorously. The Fmoc-[^{15}N]Ala-OH precipitated from the solution and the solid was isolated by filtering the mixture through a 7 cm Büchner funnel equipped with a piece of filter paper. The solid was dried by aspirating air through the funnel, suspended in EtOAc (ca. 100 mL) to form a clear solution, dried over Na_2SO_4, filtered, and then concentrated by rotary evaporation. The isolated solid was dried overnight under vacuum and ground up to give ca. 1.64 g (94%) of white powder.

^{1}H NMR (600 MHz, DMSO-d_6): δ 12.53 (br s, 1H), 7.89 (d, J = 7.5 Hz, 2H), 7.72 (d, J = 6.7 Hz, 2H), 7.66 (dd, $^{1}J_{HN}$ = 93.1, 7.2 Hz, 1H), 7.42 (t, J = 7.4 Hz, 2H), 7.33 (appar t, J = 7.4 Hz, 2H), 4.32 – 4.26 (m, 2H), 4.22 (t, J = 7.0 Hz, 1H), 4.00 (quint, J = 7.2 Hz, 1H), 1.28 (dd, J = 7.4, 1.5 Hz, 3H) ppm.

^{13}C NMR (150.9 MHz, DMSO-d_6): δ 174.4, 155.8 (d, $^{1}J_{CN}$ = 26.2 Hz), 143.86, 143.82, 140.73, 140.72, 127.6, 127.1, 125.3, 120.12, 120.11, 65.6, 49.2 (d, $^{1}J_{CN}$ = 12.4 Hz), 46.6, 17.1 ppm. [The following pairs of peaks correspond to the diastereotopic carbons of the Fmoc protecting group: 143.86 and 143.82; 140.73 and 140.72; 120.12 and 120.11. There are 2 coincident carbons at 127.6, 127.1, and 125.3 ppm that could not be resolved.]

Fmoc-[^{15}N] Ile-OH: A 50-mL one-neck round-bottom flask equipped with a magnetic stirring bar was charged with ^{15}N-labeled isoleucine (0.25 g, 1.9 mmol), and Fmoc-OSu (0.61 g, 1.8 mmol). A solution of 1:1 CH_3CN/H_2O (12.5 mL) and Et_3N (264 L, 1.9 mmol) were added then the reaction mixture was stirred for 15 min. Additional Et_3N was added until a clear solution formed (pH 7.5). The solution was stirred for an additional 1 h. The solution was poured into a solution of 1.0 M HCl (62.5 mL) in a 100 mL beaker while stirring vigorously. The Fmoc-[^{15}N]Ile-OH precipitated from the solution and the solid was isolated by filtering the mixture through a 7 cm Büchner funnel equipped with a piece of filter paper. The solid was dried by aspirating air through the funnel, suspended in EtOAc (ca. 50 mL) to form a homogenous solution, dried over Na_2SO_4, filtered, concentrated by rotary evaporation, and then stripped twice with DCM. The isolated solid was dried overnight under vacuum and ground up to give ca. 0.64 g (95%) of white powder.

^{1}H NMR (600 MHz, DMSO-d_6): δ 12.58 (br s, 1H), 7.89 (d, J = 7.9 Hz, 2H), 7.75 (dd, J = 7.4, 2.6 Hz, 2H), 7.61 (dd, $^{1}J_{HN}$ = 92.9, 8.6 Hz, 1H), 7.42 (t, J = 7.4 Hz, 2H), 7.36 – 7.28 (m, 2H), 4.36 –

4.16 (m, 3H), 3.92 (ddd, J = 8.3, 6.6, 1.5 Hz, 1H), 1.87 – 1.75 (m, 1H), 1.49 – 1.38 (m, 1H), 1.29 – 1.19 (m, 1H), 0.88 (d, J = 6.9 Hz, 3H), 0.85 (t, J = 7.4 Hz, 3H) ppm.

^{13}C NMR (150.9 MHz, DMSO-d_6): 173.3, 156.3 (d, $^{1}J_{CN}$ = 26.5 Hz), 143.9, 143.8, 140.71, 140.69, 127.65, 127.64, 127.07, 127.05, 125.38, 125.37, 120.11, 120.10, 65.7, 58.5 (d, $^{1}J_{CN}$ = 12.3 Hz), 46.6, 36.0, 24.7, 15.6, 11.2 ppm. [The following pairs of peaks correspond to the diastereotopic carbons of the Fmoc protecting group: 143.9 and 143.8; 140.71 and 140.69; 127.65 and 127.64; 127.07 and 127.05; 125.38 and 125.37; 120.11 and 120.10.]

Fmoc-[^{15}N] Leu-OH: A 100-mL one-neck round-bottom flask equipped with a magnetic stirring bar was charged with ^{15}N-labeled leucine (1.0 g, 7.6 mmol), and Fmoc-OSu (2.44 g, 7.2 mmol). A solution of 1:1 CH_3CN/H_2O (50 mL) and Et_3N (1.062 mL, 7.6 mmol)) were added then the reaction mixture was stirred for 15 min. Additional Et_3N was added until a clear solution formed (pH 7.3). The solution was stirred for an additional 1 h. The solution was poured into a solution of 1.0 M HCl (250 mL) in a 400 mL beaker while stirring vigorously. The Fmoc-[^{15}N]Leu-OH precipitated from the solution and the solid was isolated by filtering the mixture through a 7 cm Büchner funnel equipped with a piece of filter paper. The solid was dried by aspirating air through the funnel, suspended in EtOAc (ca. 200 mL) to form a slightly turbid solution, dried over Na_2SO_4, filtered, concentrated by rotary evaporation, and then stripped twice with DCM. The isolated solid was dried overnight under vacuum and ground up to give ca. 2.54 g (94%) of white powder.

^{1}H NMR (600 MHz, DMSO-d_6): δ 12.53 (br s, 1H), 7.89 (d, J = 7.6 Hz, 2H), 7.72 (d, J = 7.5 Hz, 2H), 7.63 (dd, $^{1}J_{HN}$ = 92.7, 8.3 Hz, 1H), 7.42 (t, J = 7.4 Hz, 2H), 7.32 (ddd, J = 7.4, 3.5, 1.0 Hz, 2H), 4.37 – 4.25 (m, 2H), 4.22 (t, J = 7.1 Hz, 1H), 4.02 – 3.94 (m, 1H), 1.72 – 1.61 (m, 1H), 1.61 – 1.52 (m, 1H), 1.52 – 1.42 (m, 1H), 0.90 (d, J = 6.6 Hz, 3H), 0.85 (d, J = 6.5 Hz, 3H) ppm.

^{13}C NMR (150.9 MHz, DMSO-d_6): δ 174.4, 156.1 (d, $^{1}J_{CN}$ = 26.4 Hz), 143.9, 143.8, 140.73, 140.71, 127.64, 127.62, 127.06, 127.04, 125.29, 125.26, 120.12, 120.10, 65.5, 52.1 (d, $^{1}J_{CN}$ = 12.3 Hz), 46.7, 24.3, 22.9, 21.1 ppm. [The following pairs of peaks correspond to the diastereotopic carbons of the Fmoc protecting group: 143.9 and 143.8; 140.73 and 140.71; 127.64 and 127.62; 127.06 and 127.04; 125.29 and 125.26; 120.12 and 120.10.]

Fmoc-[^{15}N] Met-OH: A 100-mL one-neck round-bottom flask equipped with a magnetic stirring bar was charged with ^{15}N-labeled methionine (0.5 g, 3.4 mmol), and Fmoc-OSu (1.07 g, 3.2 mmol). A solution of 1:1 CH_3CN/H_2O (25 mL) and Et_3N (466 L, 3.4 mmol) were added then the reaction mixture was stirred for 15 min. Additional Et_3N was added until a clear solution formed (pH 7.4). The solution was stirred for an additional 1 h. The solution was poured into a solution of 1.0 M HCl (125 mL) in a 250 mL beaker while stirring vigorously. The Fmoc-[^{15}N]Met-OH precipitated from the solution and the solid was isolated by filtering the mixture through a 7 cm Büchner funnel equipped with a piece of filter paper. The solid was dried by aspirating air through the funnel, suspended in EtOAc (ca. 100 mL) to form a clear solution, dried over Na_2SO_4, filtered, concentrated by rotary evaporation, and then stripped twice with DCM. The isolated solid was dried overnight under vacuum and ground up to give ca. 1.18 g (95%) of white powder.

^{1}H NMR (600 MHz, DMSO-d_6): δ 12.66 (br s, 1H), 7.89 (d, J = 7.6 Hz, 2H), 7.72 (dd, J = 7.6, 2.7 Hz, 2H), 7.68 (dd, $^{1}J_{HN}$ = 92.6, 8.2 Hz, 1H), 7.42 (t, J = 7.4 Hz, 2H), 7.33 (t, J = 7.1 Hz, 2H), 4.37 – 4.26 (m, 2H), 4.23 (t, J = 7.1 Hz, 1H), 4.10 (appar ddd, J = 8.6, 8.5 4.2 Hz, 1H), 2.57 – 2.45 (m, 2H), 2.04 (s, 3H), 2.00 – 1.92 (m, 1H), 1.92 – 1.83 (m, 1H) ppm.

^{13}C NMR (150.9 MHz, DMSO-d_6): δ 173.7, 156.2 (d, $^{1}J_{CN}$ = 26.3 Hz), 143.84, 143.77, 140.73, 140.72, 127.6, 127.1, 125.3, 125.2, 120.13, 120.12, 65.6, 52.6 (d, $^{1}J_{CN}$ = 12.4 Hz), 46.7, 30.3, 29.8,

14.5 ppm. [The following pairs of peaks correspond to the diastereotopic carbons of the Fmoc protecting group: 143.84 and 143.77; 140.73 and 140.72; 125.3 and 125.2; 120.13 and 120.12. There are 2 coincident carbons at 127.6 and 127.1 ppm that could not be resolved.]

Sample Preparation NMR spectroscopic studies of peptides were performed in D_2O or 9:1 H_2O/D_2O. NANOpure water was used in all 9:1 H_2O/D_2O samples. The solutions were prepared gravimetrically by dissolving a weighed portion of peptide in the appropriate volume of solvent. The peptides were dissolved by vortexing and sonicating the sample the sample until the sample appeared homogenous. The molecular weight of peptides was calculated as TFA salts with all amino groups assumed to be protonated. [For peptide **2**, the samples needed to be sonicated and vortexed for at least 30 minutes before the peptide fully dissolved. Furthermore, peptide **2** is prone to precipitation out upon exposure to dissolved ions (e.g. Na^+, Cl^-, etc.) particularly at the peptide higher concentrations (> 6 mM).]

NMR Spectroscopy of Unlabeled Peptides

Data acquisition NMR spectra were of unlabeled peptides were generally recorded on a Bruker 600 MHz spectrometer with a Bruker CBBFO helium-cooled cryoprobe or TBI probe. Presaturation water suppression was applied as needed. TOCSY spectra were recorded with 2048 points in the f_2 dimension and 256 increments in the f_1 dimension with NS = 8 or 16 and a spinlock mixing time between 60 and 200 ms. NOESY spectra were recorded with 2048 points in the f_2 and 256 increments in the f_1 with NS = 8 or 16 and a mixing time of 1 s. A 200-ms mixing time was used for samples containing higher peptide concentrations to limit spin diffusion. ROESY (EXSY)

spectra were recorded with 2048 points in the f_2 and 256 increments in the f_1 with NS = 8 and a mixing time of 150-ms.

Data processing NMR spectra were processed with the Bruker TopSpin software. Manual baseline correction was applied to both dimensions after manually phasing the spectra. For TOCSY, NOESY, and ROESY spectra run in D_2O, the spectra were referenced to the solvent residual (δ = 4.81). Solvent suppressed NMR spectra were referenced to diagnostic peaks in the D_2O spectra.

Diffusion-Ordered Spectroscopy (DOSY) Experiments DOSY experiments[5] (@dosy1D.c with the ledbpgp2s1d pulse program) were performed on a Bruker 600 MHz spectrometer equipped with a Bruker CBBFO helium-cooled cryoprobe, with a diffusion delay (Δ) of 75-ms. Variable diffusion gradient lengths (δ) were selected to achieve the appropriate signal attenuation (ca. 20 x) between the 5% – 95% gradient strength. Sixteen sets of FIDs were Fourier transformed in Bruker's Topspin software to give a pseudo-2D spectra. After phasing and baseline correction, each pseudo-2D spectra was calibrated using the residual HOD peak (1.9 x 10^{-9} m^2/s at 298 K). The diffusion coefficients were read as logarithmic values and converted to linear values.

NMR Spectroscopy of ^{15}N-Labeled Peptides

^{1}H,^{15}N HSQC and ^{1}H,^{15}N NOESY-HSQC (^{15}N-edited NOESY) Data Acquisition NMR spectra for isotopically labeled peptides were recorded on the Avance 800 MHz NMR spectrometer equipped with a TXI probe. BioTop was used to optimize parameters for all isotopically labeled experiments run on the 800 MHz spectrometer. ^{1}H,^{15}N HSQC spectra were generally recorded with 2048 points in the f_2 dimension and 282 increments in the f_1 dimension NS = 16. ^{1}H,^{15}N NOESY-HSQC were

generally recorded with 2048 points in the f_3 dimension (^{1}H), 1 increment in the f_2 dimension (^{15}N), and 1024 increments in the f_1 dimension (^{1}H) with NS = 16 and a 120-ms mixing time.

^{1}H,^{15}N HSQC and ^{1}H,^{15}N NOESY-HSQC (^{15}N-edited NOESY) Data Processing NMR spectra were Fourier transformed in Bruker TopSpin software with forward linear prediction and a Qsine weighting function. Manual baseline correction was applied to both dimensions after manually phasing the spectra. The ^{1}H,^{15}N HSQC spectra were processed to a final matrix size of 2048 x 256 real points and with GB = 0.1 in the f_1 dimension. The ^{1}H,^{15}N NOESY-HSQC spectra were processed to a final matrix size of 2048 x 256 real points with GB = 0.1 in the f_2 dimension, using the Qsine weighting function and forward linear prediction in the f_1 dimension. The ^{1}H,^{15}N-HSQC and ^{15}N-edited NOESY were referenced using the xiref command in TopSpin.

Peak Assignments Residue specific peak assignments were determined by performing an NH to Hα walk. Within each residue, the NH proton gives a strong cross peak to the Hα proton in the TOCSY spectra. Between two adjacent residues the Hα (*i*) gives a strong cross peak to the NH proton (*i+1*) on the adjacent residue in the ROESY spectra. The TOCSY and ROESY enables sequential peak assignments of each strand in macrocyclic peptide for both monomer and species **A** and **B**. For the top-strand bearing the *N*-methyl amino acid, the ROESY spectra provides a strong crosspeak between the *N*-methyl group and Hα of Val_{18}. Intramolecular NOEs in the NOESY spectra were used to corroborate the peak assignments of the top and bottom strands. In cases of heavy overlap in either the NH or Hα region (particularly for the peptide **2** oligomer), all possible cases were considered and invalid cases that were inconsistent with the NMR data were ruled out. The peak assignments for species **A** and **B** were cross-checked with the ^{1}H,^{15}N HSQC spectra of

^{15}N labeled analogues (peptides **2a** and **2d**) and with the ^{1}H NMR spectra of the deuterated analogs (peptides **2b** and **2c**).

Molecular Modeling of the Asymmetric Hexamer

We used PyMOL in conjugation with MacroModel to build energy minimized models (local minima) with constraints that are consistent with the observed intermolecular contacts and symmetry requirements. We started with one copy of the monomer from the crystallographic hexamer for species **B**. Then, we used the sculpt function in PyMOL to alter the conformation of the monomer to better match the observed **A**-**B** intermolecular contacts on the exterior of the triangular trimer while also preserving the network of interstrand intramolecular hydrogen bonds (ca. 1.8 – 2.2 Å). Three copies of the species **B** monomer were initially aligned to the crystallographic triangular trimers. Then, we manually adjusted the position of the three molecules to better accommodate the observed **A**-**B** intermolecular contacts while preserving approximate C_3 symmetry. From there, we used the crystallographic coordinates of a more-twisted hairpin (PDB 1HS0) to model our initial conformation for species **A**. We grafted on our sequence onto the 1HS0 structure and locally minimized the conformation using the clean function in PyMOL.[5] The additional twisting of the hairpin for species **A** better accommodated the top-to-bottom strand **A**-**A** intermolecular contacts. Three molecules of **A** were positioned manually in PyMOL onto the triangular trimers while simultaneously satisfying the **A**-**A** intermolecular contacts, **A**-**B** intermolecular contacts, and approximate C_3 symmetry.

We minimized (local minima) our rough model of the hexamer in MacroModel using the MMFFs force field with GB/SA water solvation and two to three distance constraints along each of the

observed **A**-**A**, **A**-**B** (1), **A**-**B** (2), and **B**-**B** interfaces. Force constants were 100 kJ/mol-Å^2 for all interatomic distance with a ± 1 Å tolerance. We used a 2 Å distance for strong NOEs, 3 Å distance for moderate NOEs, and 4 Å distance for weaker NOEs. The PRCG method was used with a maximum of 9000 iterations and a 0.05 kJ/Å-mol convergence threshold on the gradient. The coordinates were exposed in .pdb file format and imported into PyMOL. The initial coordinates of the solution phase dodecamer were generated by duplicating the hexamer structure and manually positioning the relative orientation of the two hexamers.

Molecular Dynamic Simulations on a pair of hexamers

Molecular dynamics simulation was performed using the Amber22 software package,[6] with the FF19SB force field for protein.[7] The non-standard residues CHA and ORN are generated utilizing the same RESP charge fitting protocol[3] as the amino acid residues in Amber22. The system was solvated with explicit OPC water molecules[9] in a periodic box of ~100Å in each dimension, and just the necessary number of counterions (Na^+ or Cl^-) to neutralize the overall charge of the system. Equilibration of the system followed a consistent protocol which began with short minimization runs to fix possible bad contacts in initial structure, proceeded to gradually heating the system to 300 K, then constant pressure (NPT) simulation at 1 atm and 300 K to equilibrate the simulation box size to be consistent with experimental density of an aqueous solution. In the case of run 4 and 5, a 50 ns run with distance constraints to optimize the hydrophobic contacts between the desired surfaces is carried out for each system. Finally, a production run (no constraints except for run 2) was performed in the NVT ensemble at 300 K for 500 ns, with a timestep of 1 fs. The trajectories were then analyzed, focusing on the structural features and conformational changes, with the cpptraj program in the Amber22 package.

We initially hypothesized that the exposed hydrophobic ends of the cylindrin-like trimer might form a contact. We thus started with a pair of simulations in which two hexamers are arranged with the ends of the cylindrin-like trimer facing each other and stabilized by a network of intermolecular hydrogen bonds between the two cylindrins' Orn_{1} and Met_{35} residues. Simulation 1 was run without distance constraints, while simulation 2 was run with additional distance constraints along the hypothesized interface. The constrained dimer of hexamers was stable for the duration of simulation 2. However, in simulation 1 the hypothesized interface broke apart, and the two hexamers rearranged to come together on the sides of two cylindrin-like trimer, stabilized by hydrophobic contacts involving the side chains of residues Val_{18}, Phe_{20}, Ala_{30}, Ile_{32}, Leu_{34}, and Val_{36}. Simulation 3, starting with a frame from simulation 2 and then removing the constraints along the interface, also resulted in the interface between the two hexamers breaking apart. Collectively, simulations 1–3 show that the hypothesized configuration of the dodecamer is not stable, but that there are other possible stable arrangements of two hexamers.

To further investigate possible stable arrangements of two hexamers, we ran two additional simulations that varied the relative orientation of the two hexamers. Simulation 4 started with the solvent exposed ends of the triangular trimer subunits of each hexamer stacked on top of each other while simulation 5 started with the cylindrin-like trimer subunits of each hexamer arranged in a side-to-side manner. In both simulations 4 and 5, similar to that of simulation 1, the two hexamers stayed together with stabilizing hydrophobic contacts between the side chains of residues Val_{18}, Phe_{20}, Ala_{30}, Ile_{32}, Leu_{34}, and Val_{36} in between the two asymmetric hexamers.

References and Notes

1. Longsworth, L. G. The Mutual Diffusion of Light and Heavy Water. *J. Phys. Chem.* **1960**, *64*, 1914–1917.

2. The general information and procedures in this section follow closely to those our laboratory has previously published. The procedures in this section are adapted and, in some cases, taken verbatim from:

   Kreutzer, A. G.; Spencer, R. K.; McKnelly, K. J.; Yoo, S.; Hamza, I. L.; Salveson, P. J.; Nowick, J. S. A Hexamer of a Peptide Derived from Aβ16–36. *Biochemistry* **2017**, *56* (45), 6061–6071. https://doi.org/10.1021/acs.biochem.7b00831.

   Samdin, T. D.; Jones, C. R.; Guaglianone, G.; Kreutzer, A. G.; Freites, J. A.; Wierzbicki, M.; Nowick, J. S. A β-Barrel-Like Tetramer Formed by a β-Hairpin Derived from Aβ. *Chem. Sci.* **2024**, *15*, 285-297. https://doi.org/10.1039/D3SC05185D.

   Truex, N. L.; Wang, Y.; Nowick, J. S. Assembly of Peptides Derived from β-Sheet Regions of β-Amyloid *J. Am. Chem. Soc.* **2016**, *138*, 13882-13890. https://doi.org/10.1021/jacs.6b06000.

   Li, X.; Rios, S. E.; Nowick, J. S. Enantiomeric β-Sheet Peptides from Aβ Form Homochiral Pleated β-Sheets Rather than Heterochiral Rippled β-Sheets. *Chem. Sci.* **2022**, *13* (26), 7739–7746. https://doi.org/10.1039/D2SC02080G.

3. Schägger, H. Tricine-SDS-PAGE. *Nat. Protoc.* **2006**, *1*, 16–22. https://doi.org/10.1038/nprot.2006.4

4. Simpson, R. J. Staining proteins in gels with silver nitrate. *CSH Protoc.* **2007**. doi:10.1101/pdb.prot4727.

5. Wu, D. H.; Chen, A. D.; Johnson, C. S. An Improved Diffusion-Ordered Spectroscopy Experiment Incorporating Bipolar-Gradient Pulses. *J. Magn. Reson. A* **1995**, *115* (2), 260–264. https://doi.org/10.1006/jmra.1995.1176.

6. Cochran, A. G.; Skelton, N. J.; Starovasnik. Tryptophan zippers: Stable, monomeric β-hairpins. *Proc. Natl. Acad. Sci. U. S. A.* **2001**, *98* (10), 5578-5583. https://doi.org/10.1073/pnas.091100898.

7. Case, D. A.; Aktulga, H. M.; Belfon, K.; Ben-Shalom, I. Y.; Berryman, J. T.; Brozell, S. R.; Cerutti, D. S.; Cheatham, T. E. I.; Cisneros, G. A.; Cruzeiro, V. W. D.; et al. AMBER 2022. University of California San Francisco: San Francisco, 2022.

8. Tian, C.; Kasavajhala, K.; Belfon, K. A. A.; Raguette, L.; Huang, H.; Migues, A. N.; Bickel, J.; Wang, Y.; Pincay, J.; Wu, Q.; et al. ff19SB: Amino-Acid-Specific Protein Backbone Parameters Trained against Quantum Mechanics Energy Surfaces in Solution.

J Chem Theory Comput **2020**, *16* (1), 528-552. DOI: 10.1021/acs.jctc.9b00591 From NLM Medline.

9. Cieplak, P.; Cornell, W. D.; Bayly, C.; Kollman, P. A. Application of the multimolecule and multiconformational RESP methodology to biopolymers: Charge derivation for DNA, RNA, and proteins. *Journal of Computational Chemistry* **1995**, *16* (11), 1357-1377. DOI: https://doi.org/10.1002/jcc.540161106.

10. Izadi, S.; Anandakrishnan, R.; Onufriev, A. V. Building Water Models: A Different Approach. *J Phys Chem Lett* **2014**, *5* (21), 3863-3871. DOI: 10.1021/jz501780a From NLM Publisher.

NMR Characterization Data

^{1}H NMR, and ^{13}C NMR spectra of Fmoc-^{15}N-Ala-OH in CD_3SOCD_3 at 600 MHz and 298 K.

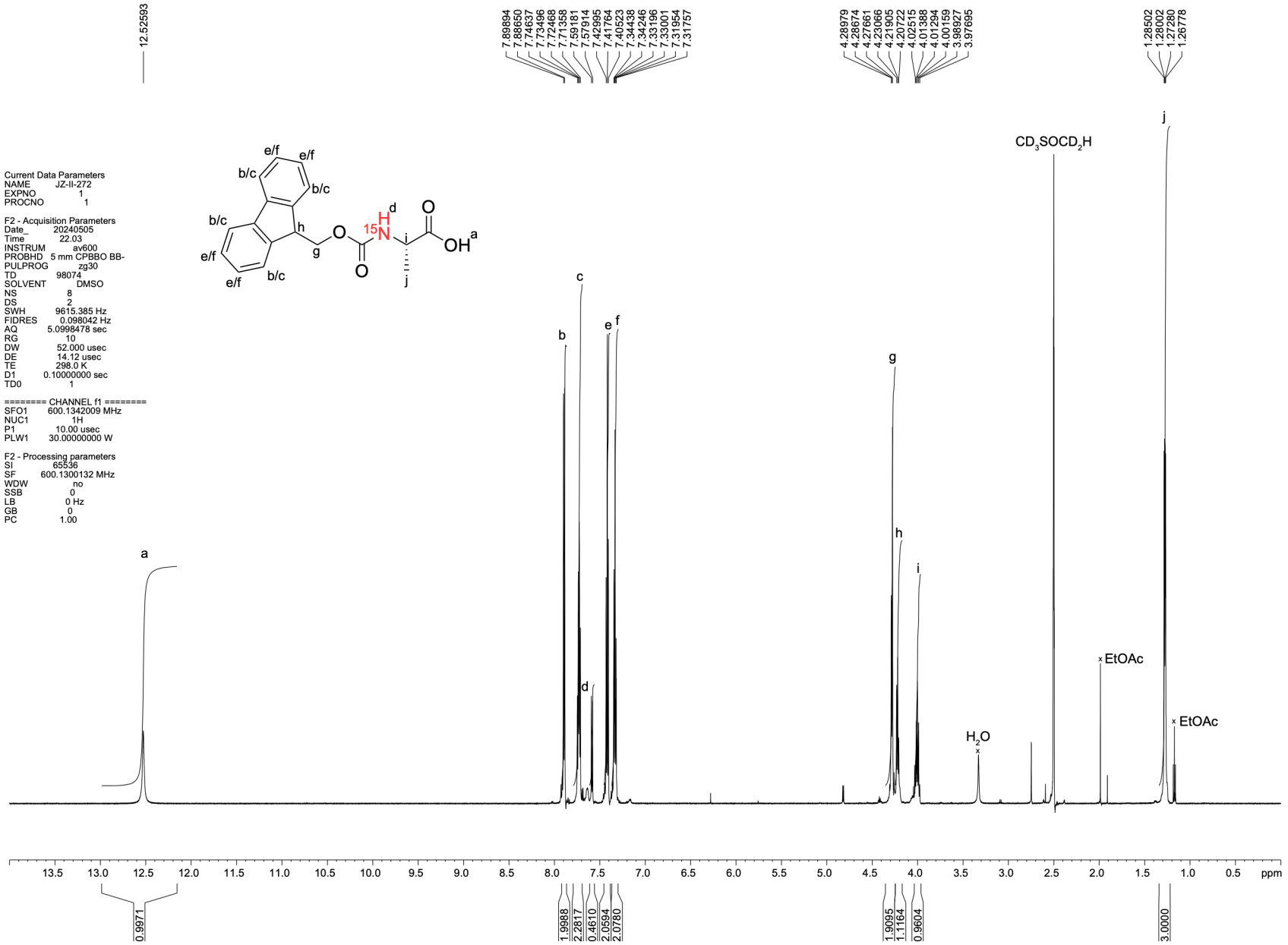

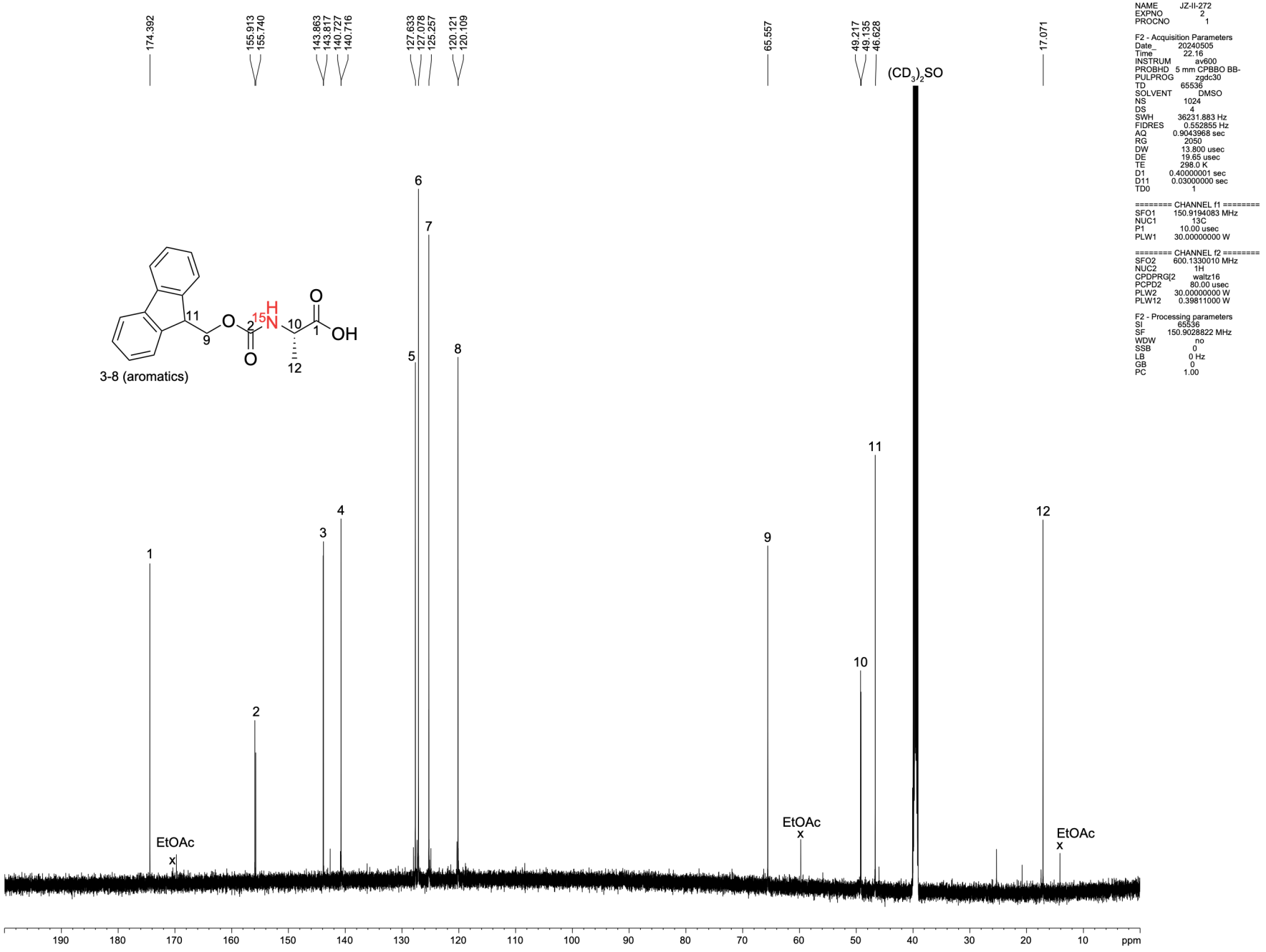

NAME JZ-II-272
EXPNO 2
PROCNO 1

F2 - Acquisition Parameters
Date_ 20240505
Time 22.16
INSTRUM av600
PROBHD 5 mm CPBBO BB-
PULPROG zgdc30
TD 65536
SOLVENT DMSO
NS 1024
DS 4
SWH 36231.883 Hz
FIDRES 0.552855 Hz
AQ 0.9043968 sec
RG 2050
DW 13.800 usec
DE 19.65 usec
TE 298.0 K
D1 0.40000001 sec
D11 0.03000000 sec
TD0 1

======== CHANNEL f1 ========
SFO1 150.9194083 MHz
NUC1 13C
P1 10.00 usec
PLW1 30.00000000 W

======== CHANNEL f2 ========
SFO2 600.1330010 MHz
NUC2 1H
CPDPRG[2 waltz16
PCPD2 80.00 usec
PLW2 30.00000000 W
PLW12 0.39811000 W

F2 - Processing parameters
SI 65536
SF 150.9028822 MHz
WDW no
SSB 0
LB 0 Hz
GB 0
PC 1.00

^{1}H NMR, and ^{13}C NMR spectra of Fmoc-^{15}N-Ile-OH in CD_3SOCD_3 at 600 MHz and 298 K.

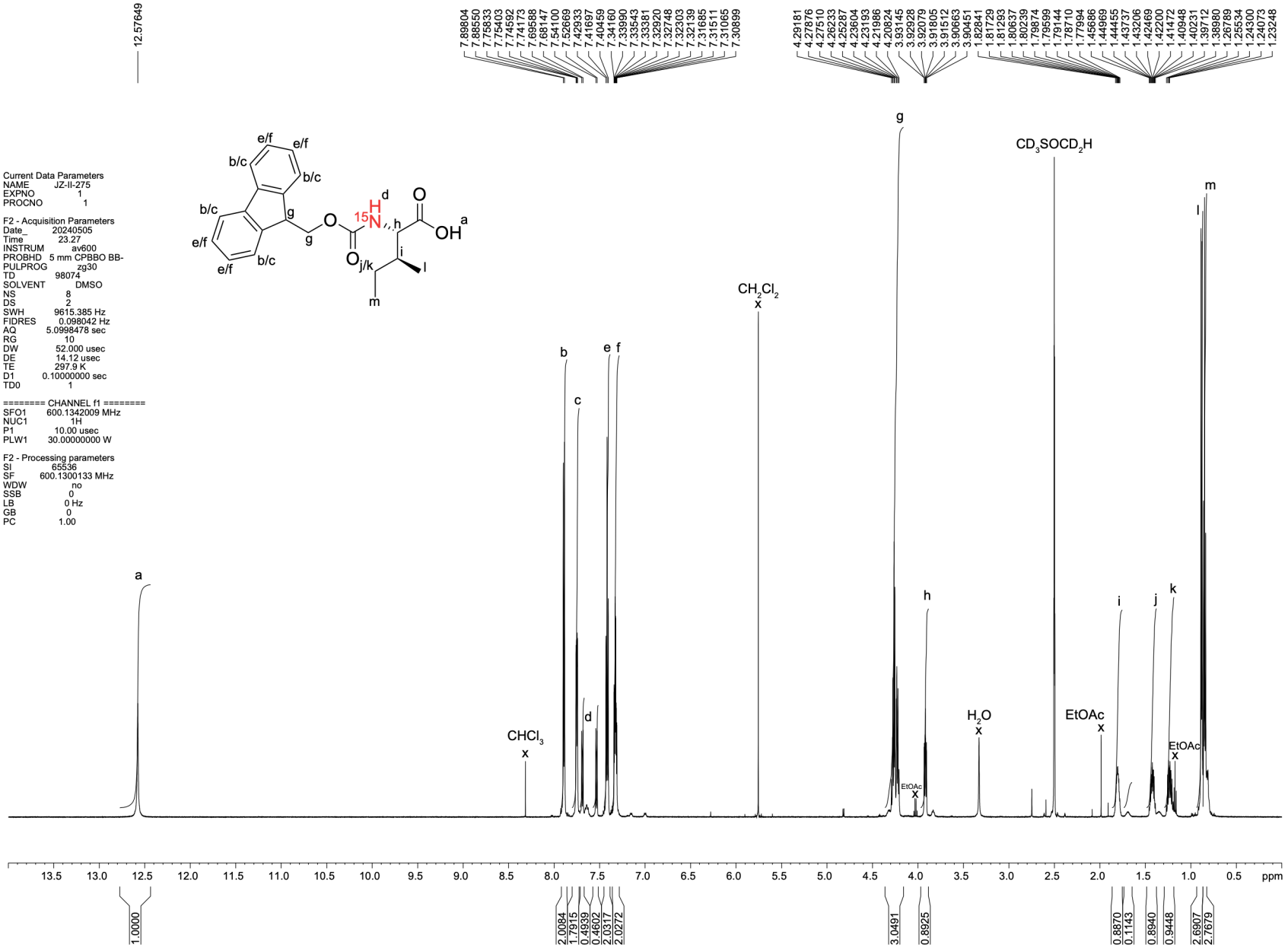

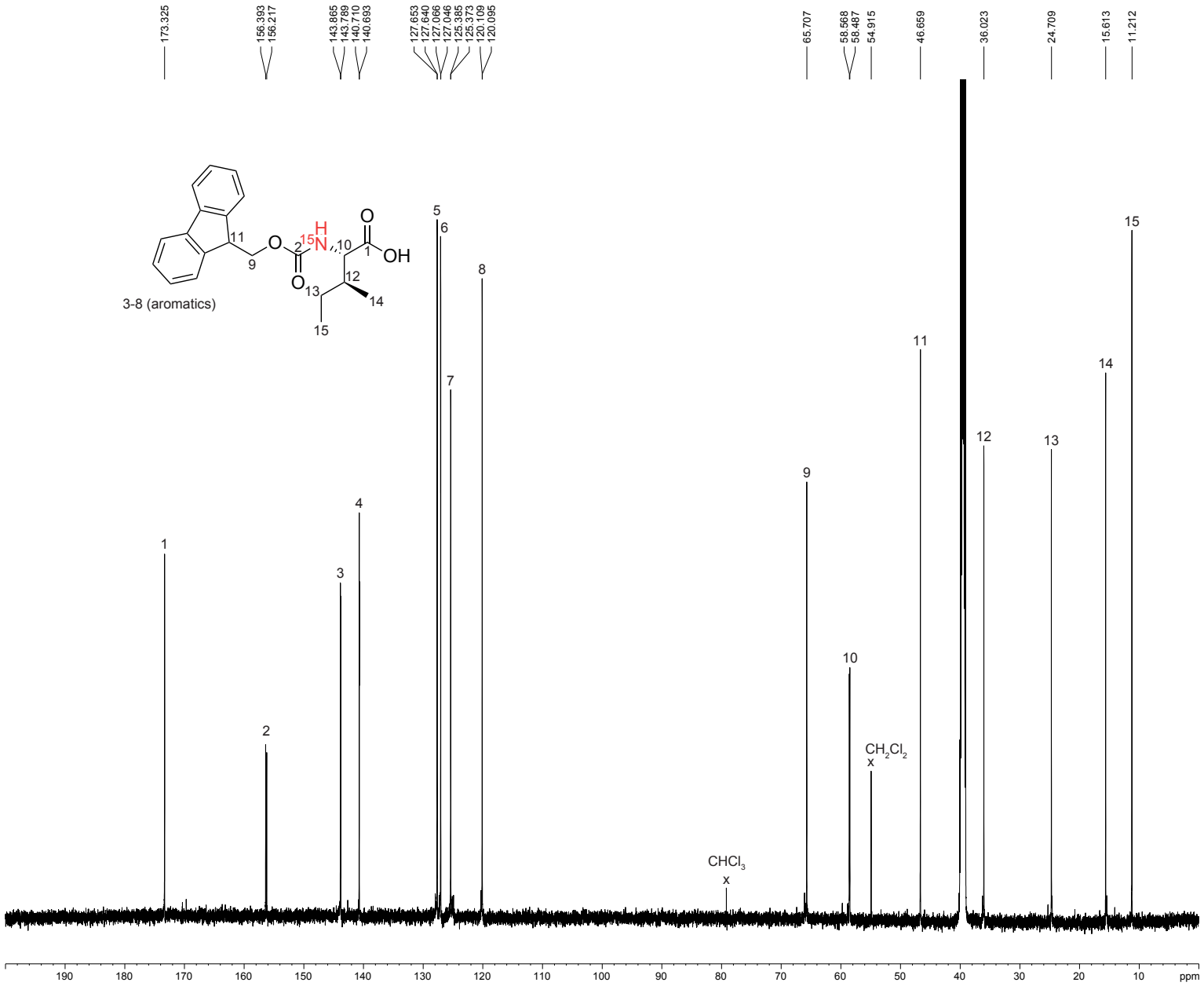

Current Data Parameters
NAME JZ-II-275
EXPNO 2
PROCNO 1

F2 - Acquisition Parameters
Date_ 20240505
Time 23.31
INSTRUM av600
PROBHD 5 mm CPBBO BB-
PULPROG zgdc30
TD 65536
SOLVENT DMSO
NS 1024
DS 4
SWH 36231.883 Hz
FIDRES 0.552855 Hz
AQ 0.9043968 sec
RG 2050
DW 13.800 usec
DE 19.65 usec
TE 298.0 K
D1 0.40000001 sec
D11 0.03000000 sec
TD0 1

======== CHANNEL f1 ========
SFO1 150.9194083 MHz
NUC1 13C
P1 10.00 usec
PLW1 30.00000000 W

======== CHANNEL f2 ========
SFO2 600.1330010 MHz
NUC2 1H
CPDPRG[2 waltz16
PCPD2 80.00 usec
PLW2 30.00000000 W
PLW12 0.39811000 W

F2 - Processing parameters
SI 65536
SF 150.9028822 MHz
WDW EM
SSB 0
LB 1.00 Hz
GB 0
PC 1.00

^{1}H NMR, and ^{13}C NMR spectra of Fmoc-^{15}N-Leu-OH in CD_3SOCD_3 at 600 MHz and 298 K.

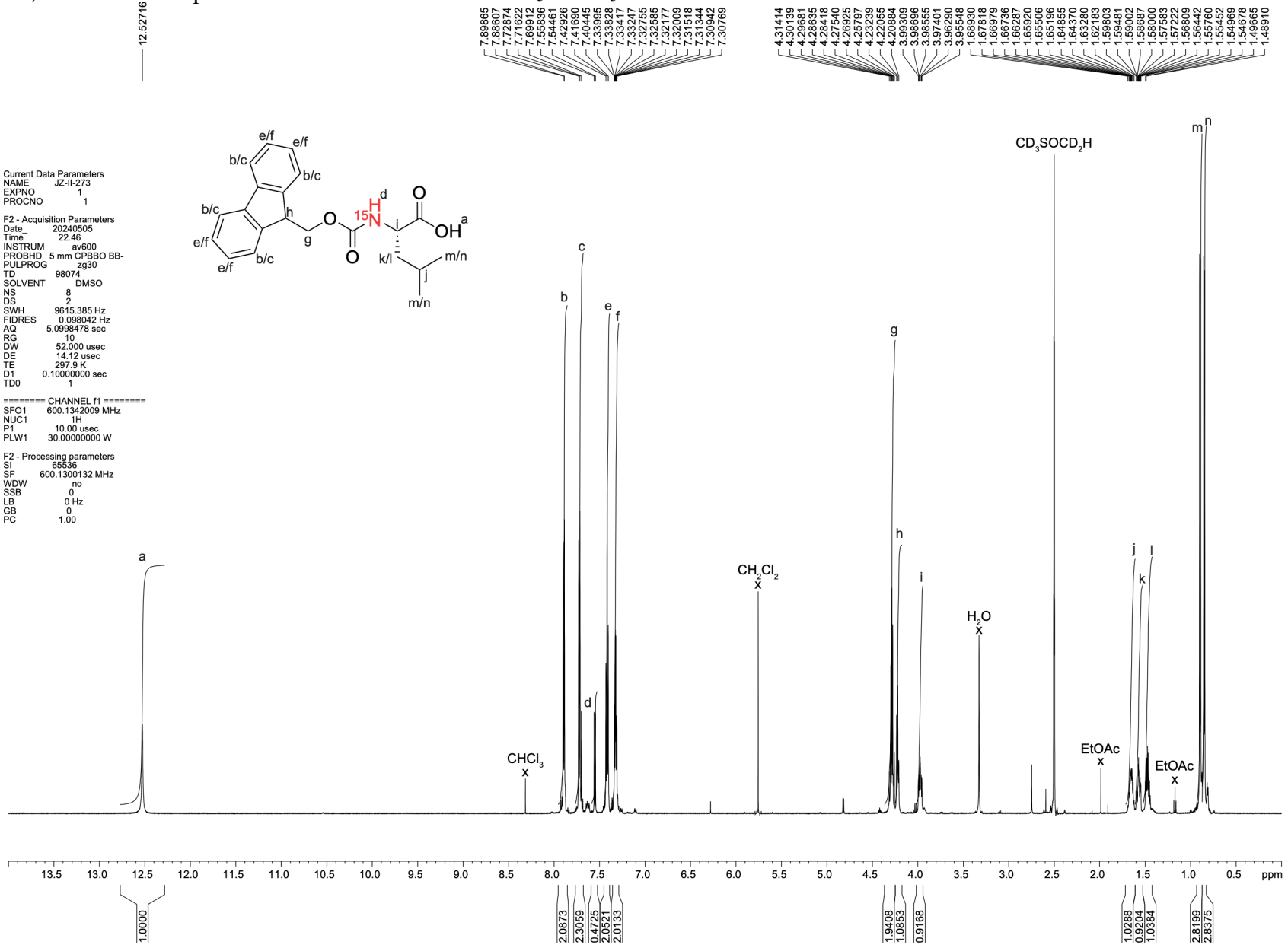

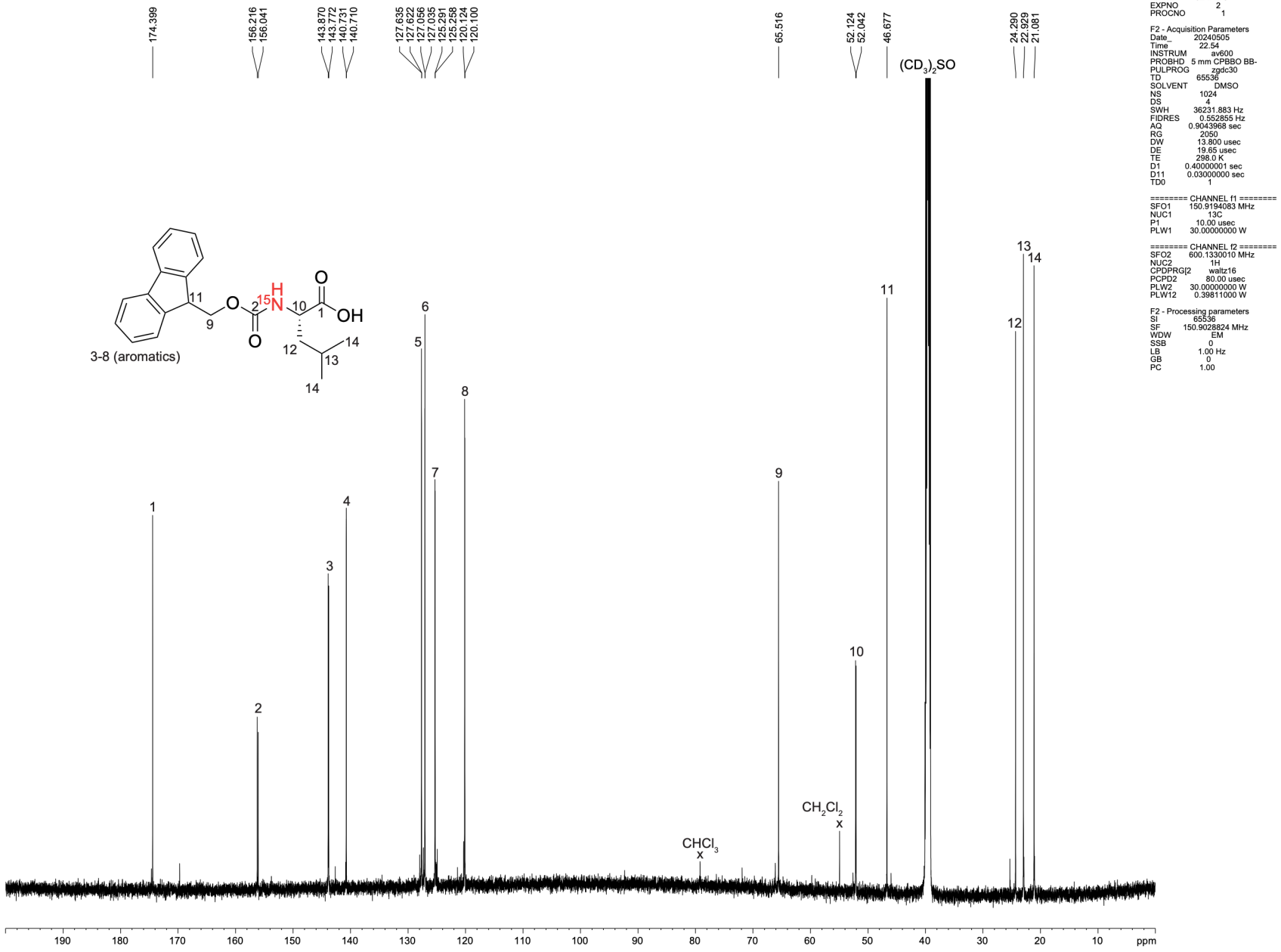

Current Data Parameters
NAME JZ-II-273
EXPNO 2
PROCNO 1

F2 - Acquisition Parameters
Date_ 20240505
Time 22.54
INSTRUM av600
PROBHD 5 mm CPBBO BB-
PULPROG zgdc30
TD 65536
SOLVENT DMSO
NS 1024
DS 4
SWH 36231.883 Hz
FIDRES 0.552855 Hz
AQ 0.9043968 sec
RG 2050
DW 13.800 usec
DE 19.65 usec
TE 298.0 K
D1 0.40000001 sec
D11 0.03000000 sec
TD0 1

======== CHANNEL f1 ========
SFO1 150.9194083 MHz
NUC1 13C
P1 10.00 usec
PLW1 30.00000000 W

======== CHANNEL f2 ========
SFO2 600.1330010 MHz
NUC2 1H
CPDPRG[2 waltz16
PCPD2 80.00 usec
PLW2 30.00000000 W
PLW12 0.39811000 W

F2 - Processing parameters
SI 65536
SF 150.9028824 MHz
WDW EM
SSB 0
LB 1.00 Hz
GB 0
PC 1.00

^{1}H NMR, and ^{13}C NMR spectra of Fmoc-^{15}N-Met-OH in CD_3SOCD_3 at 600 MHz and 298 K.

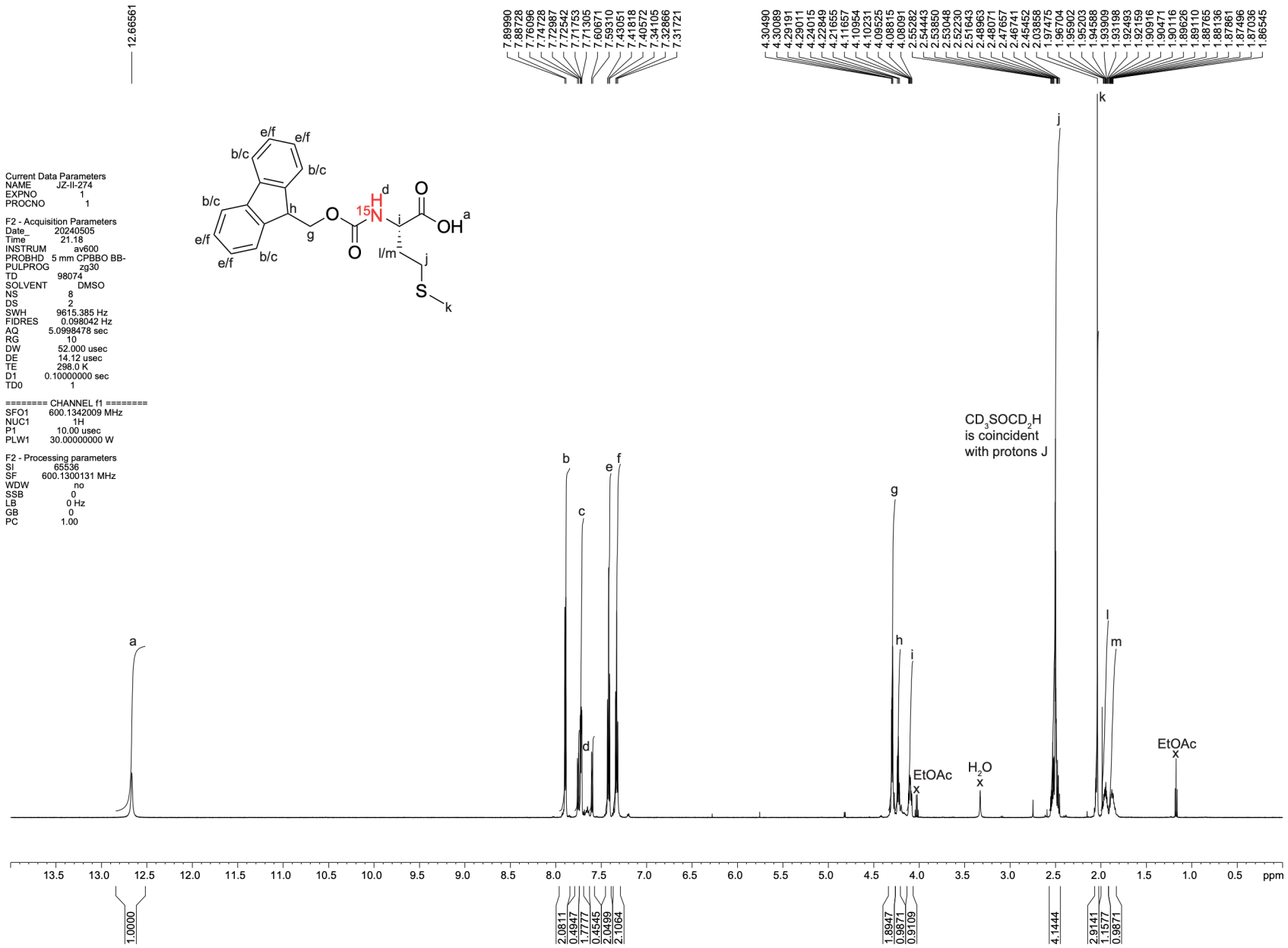

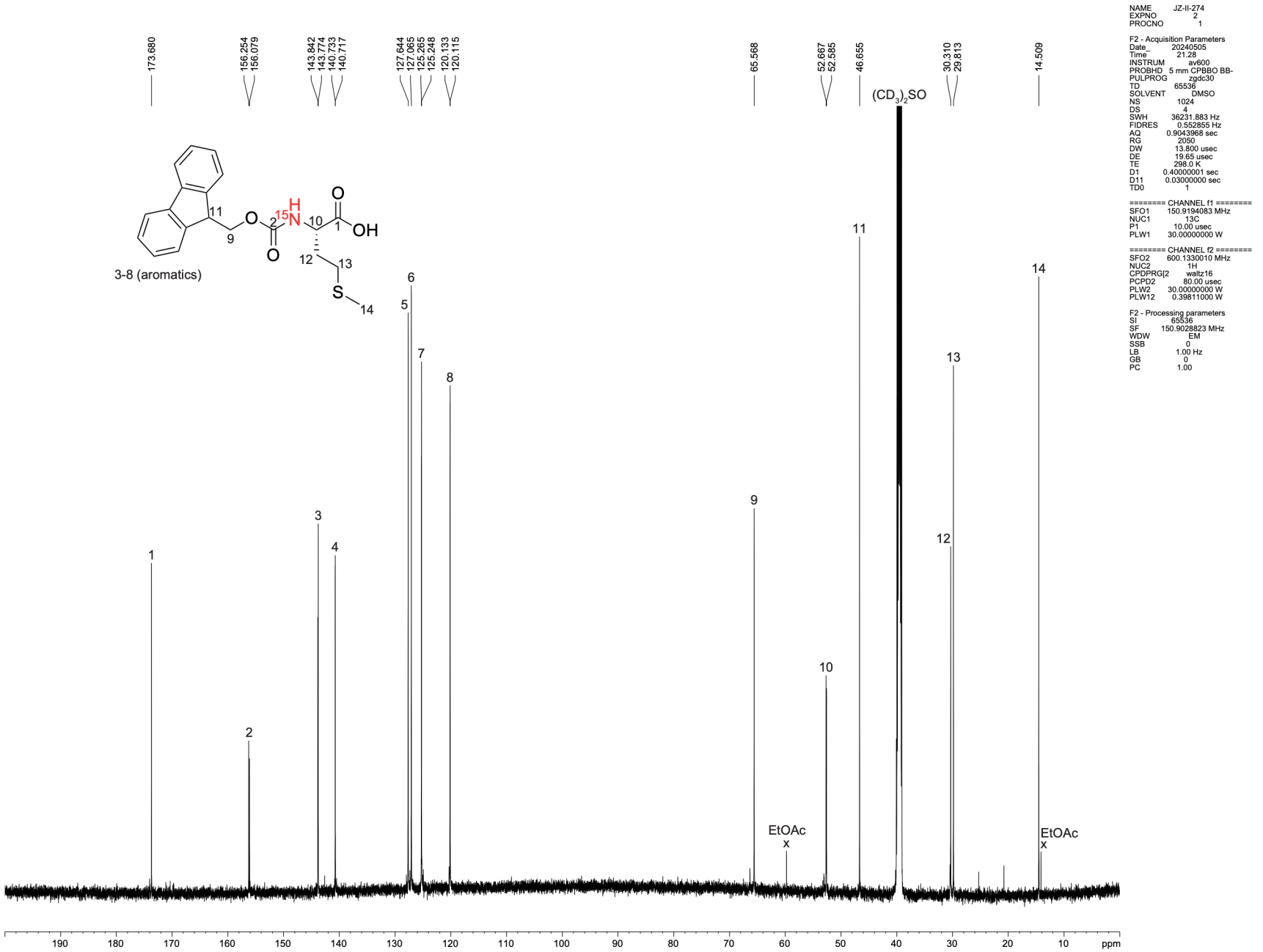


```
NAME        JZ-II-274
EXPNO               2
PROCNO              1

F2 - Acquisition Parameters
Date_        20240505
Time           21.28
INSTRUM          av600
PROBHD  5 mm CPBBO BB-
PULPROG       zgdc30
TD             65536
SOLVENT         DMSO
NS              1024
DS                 4
SWH        36231.883 Hz
FIDRES      0.552855 Hz
AQ          0.9043968 sec
RG              2050
DW          13.800 usec
DE          19.65 usec
TE             298.0 K
D1          0.40000001 sec
D11         0.03000000 sec
TD0                1

======== CHANNEL f1 ========
SFO1       150.9194083 MHz
NUC1              13C
P1            10.00 usec
PLW1       30.00000000 W

======== CHANNEL f2 ========
SFO2       600.1330010 MHz
NUC2              1H
CPDPRG[2       waltz16
PCPD2         80.00 usec
PLW2       30.00000000 W
PLW12       0.39811000 W

F2 - Processing parameters
SI              65536
SF       150.9028823 MHz
WDW               EM
SSB                0
LB              1.00 Hz
GB                 0
PC              1.00
```

^{1}H NMR spectrum of 1.0 mM peptide **1** in D_2O at 600 MHz and 298 K

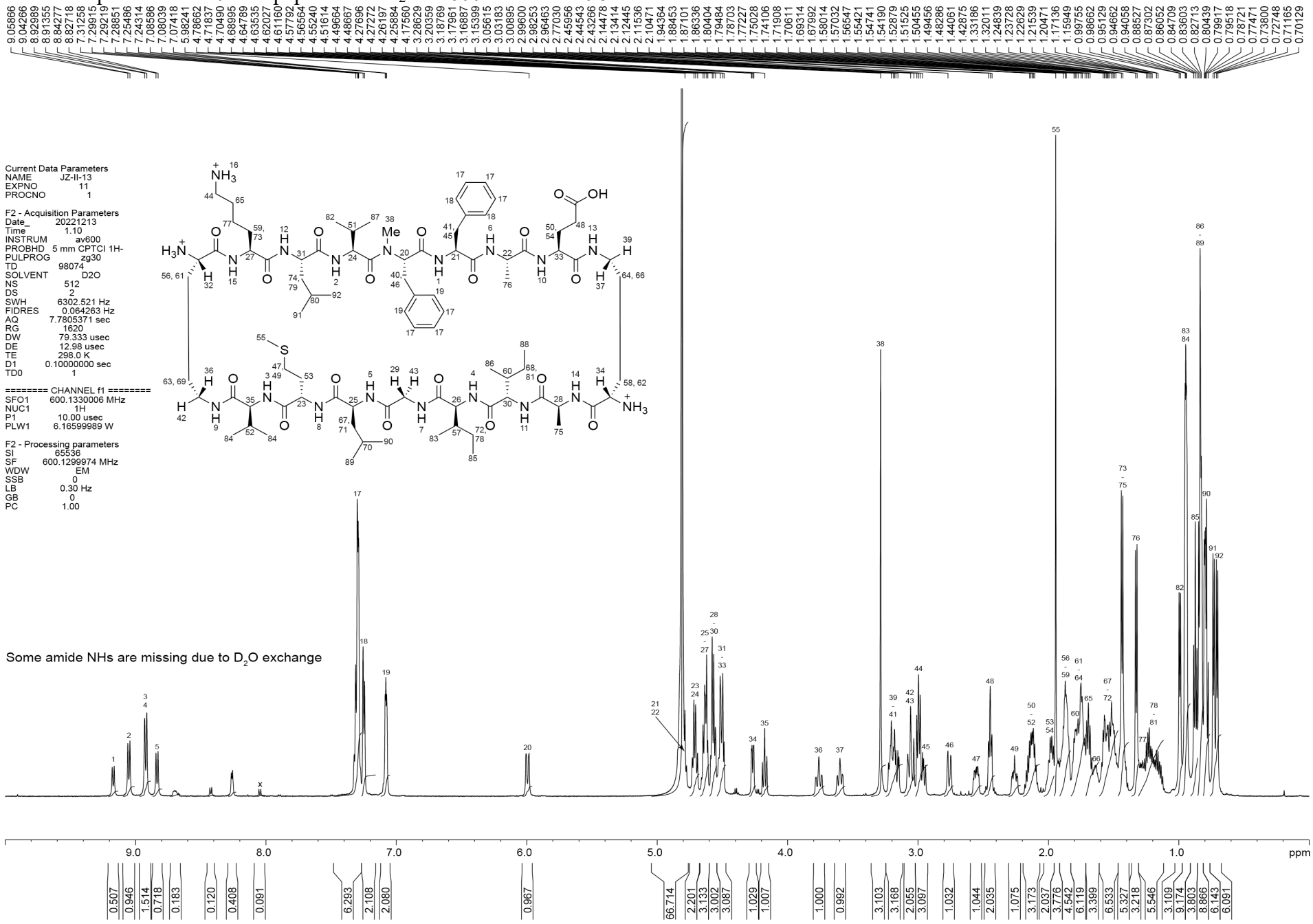

^{1}H NMR spectrum of 1.0 mM peptide **1** in 9:1 H_2O/D_2O at 600 MHz and 298 K with WATERGATE suppression of the HOD peak.

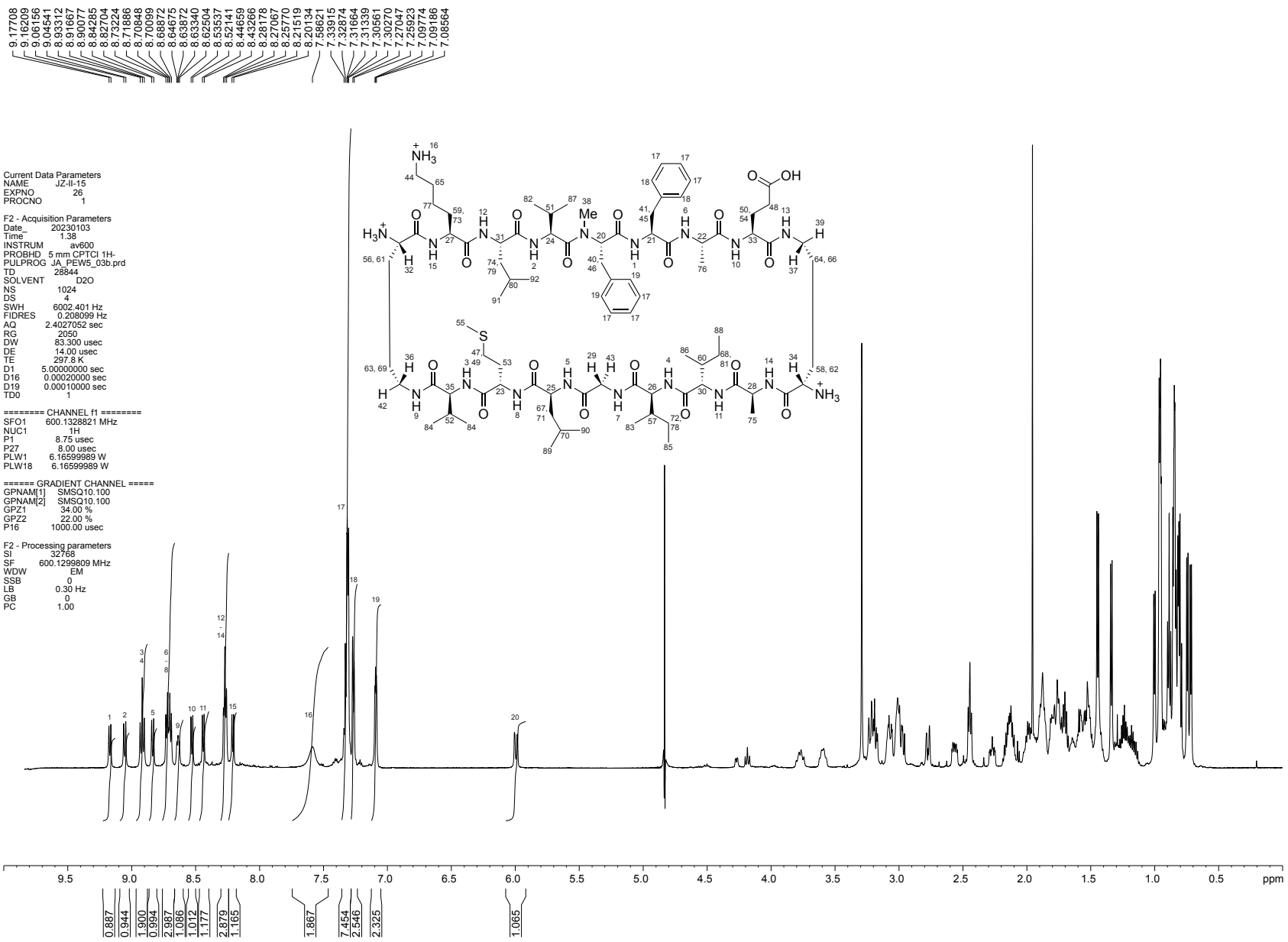

^{1}H NMR 2D TOCSY spectrum of 1.0 mM peptide **1** in D_2O at 600 MHz and 298 K with 200-ms spin-lock mixing time

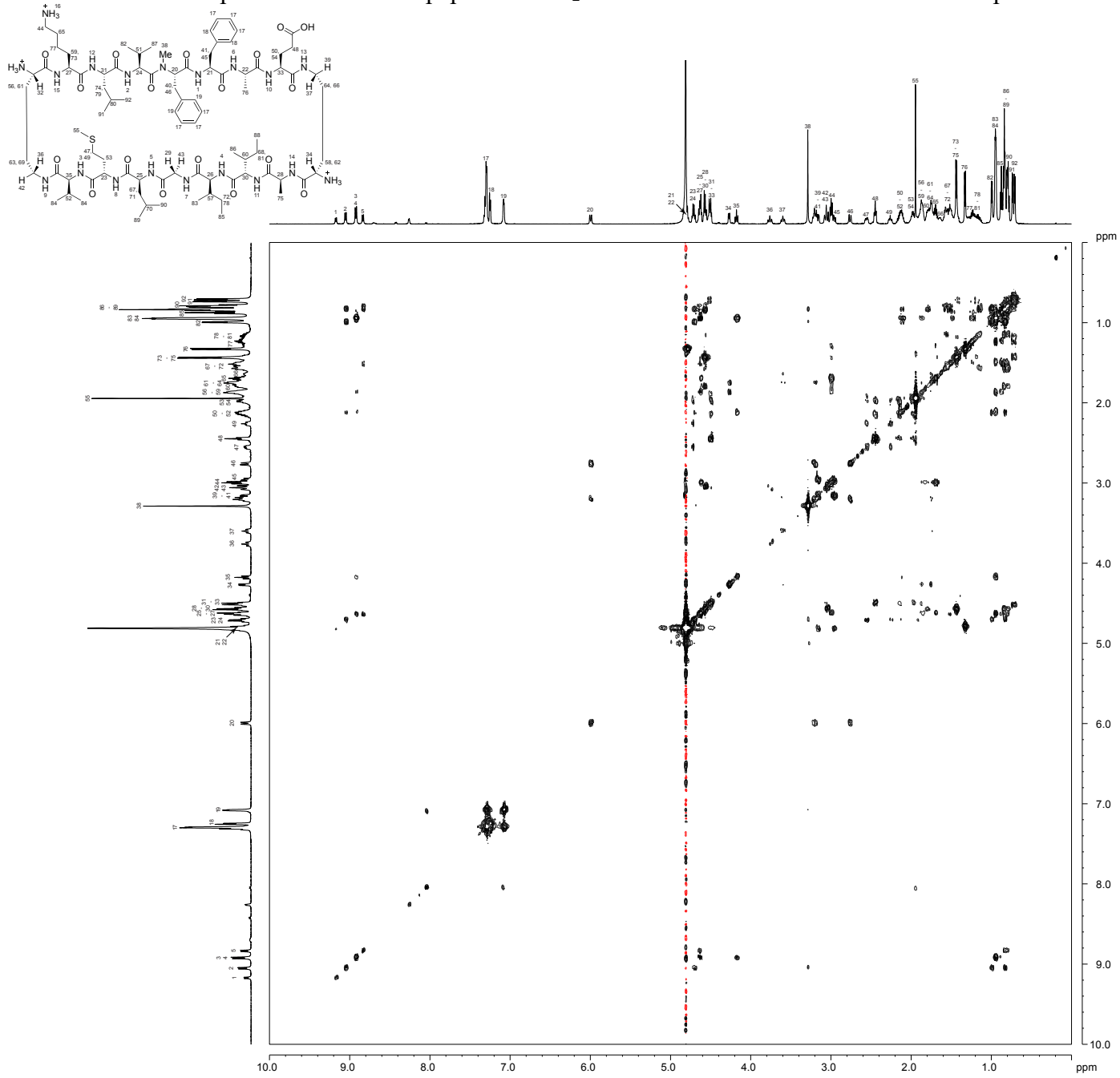


```
Current Data Parameters
NAME          JZ-II-13
EXPNO             12
PROCNO             1

F2 - Acquisition Parameters
Date_         20221213
Time              1.11
INSTRUM           av600
PROBHD    5 mm CPTCI 1H-
PULPROG   mlevgp_mo.prd
TD                2048
SOLVENT           D2O
NS                   8
DS                  16
SWH          6313.131 Hz
FIDRES          3.082584 Hz
AQ           0.1622016 sec
RG                1620
DW              79.200 usec
DE              10.00 usec
TE              298.0 K
D0           0.00000300 sec
D1           2.00000000 sec
D9           0.20000000 sec
D12          0.00002000 sec
D16          0.00020000 sec
IN0          0.00015840 sec
L1                 126

======== CHANNEL f1 ========
SFO1       600.1330006 MHz
NUC1               1H
P1              10.00 usec
P5              16.67 usec
P6              25.00 usec
P7              50.00 usec
P17           2500.00 usec
PLW1        6.16599989 W
PLW10       0.63095999 W

====== GRADIENT CHANNEL =====
GPNAM[1]     SMSQ10.100
GPNAM[2]     SMSQ10.100
GPZ1            10.00 %
GPZ2            10.00 %
P16           1000.00 usec

F1 - Acquisition parameters
TD                 256
SFO1         600.133 MHz
FIDRES        49.321339 Hz
SW            10.520 ppm
FnMODE             QF

F2 - Processing parameters
SI                1024
SF         600.1299988 MHz
WDW               SINE
SSB                  0
LB                0 Hz
GB                   0
PC                1.40

F1 - Processing parameters
SI                1024
MC2                QF
SF         600.1299987 MHz
WDW               SINE
SSB                  0
LB                0 Hz
GB                   0
```

^{1}H NMR 2D TOCSY spectrum of 1.0 mM peptide **1** in 9:1 H_2O/D_2O at 600 MHz and 298 K with WATERGATE suppression of the HOD peak and 60-ms spin-lock mixing time

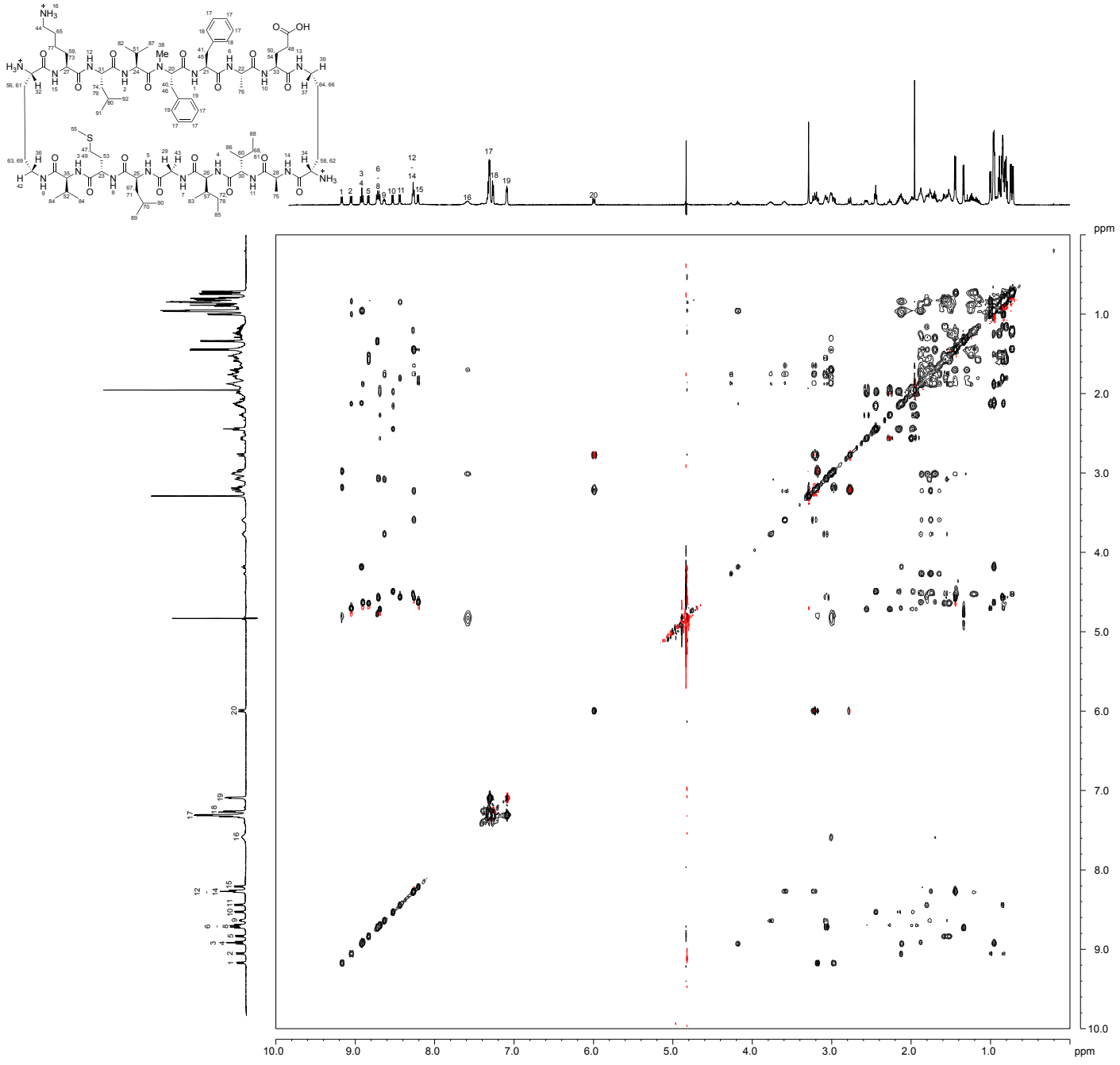


```
Current Data Parameters
NAME          JZ-II-15
EXPNO               27
PROCNO               1

F2 - Acquisition Parameters
Date_         20230103
Time              1.39
INSTRUM          av600
PROBHD   5 mm CPTCI 1H-
PULPROG      mlevgpphw5
TD                2048
SOLVENT            D2O
NS                   8
DS                  16
SWH          6602.113 Hz
FIDRES       3.223688 Hz
AQ           0.1551019 sec
RG                2050
DW            75.733 usec
DE            10.00 usec
TE             297.8 K
D0           0.00006661 sec
D1           2.00000000 sec
D9           0.06000000 sec
D12          0.00002000 sec
D16          0.00020000 sec
D19          0.00010000 sec
IN0          0.00015140 sec
L1                  36
P2            16.00 usec

======== CHANNEL f1 ========
SFO1       600.1328825 MHz
NUC1               1H
P1            8.00 usec
P5           16.67 usec
P6           25.00 usec
P7           50.00 usec
P17        2500.00 usec
P27           8.00 usec
PLW1       6.16599989 W
PLW10      0.63095999 W
PLW18      6.16599989 W

====== GRADIENT CHANNEL =====
GPNAM[1]    SMSQ10.100
GPNAM[2]    SMSQ10.100
GPZ1          34.00 %
GPZ2          22.00 %
P16         1000.00 usec

F1 - Acquisition parameters
TD                 256
SFO1         600.1329 MHz
FIDRES      51.601719 Hz
SW           11.006 ppm
FnMODE      States-TPPI

F2 - Processing parameters
SI                1024
SF         600.1299799 MHz
WDW             QSINE
SSB                2
LB              0 Hz
GB                 0
PC              1.00

F1 - Processing parameters
SI                1024
MC2         States-TPPI
SF         600.1299805 MHz
WDW             QSINE
SSB                2
LB              0 Hz
GB                 0
```

^{1}H NMR 2D NOESY spectrum of 1.0 mM peptide **1** in D_2O at 600 MHz and 298 K with 1-s mixing time

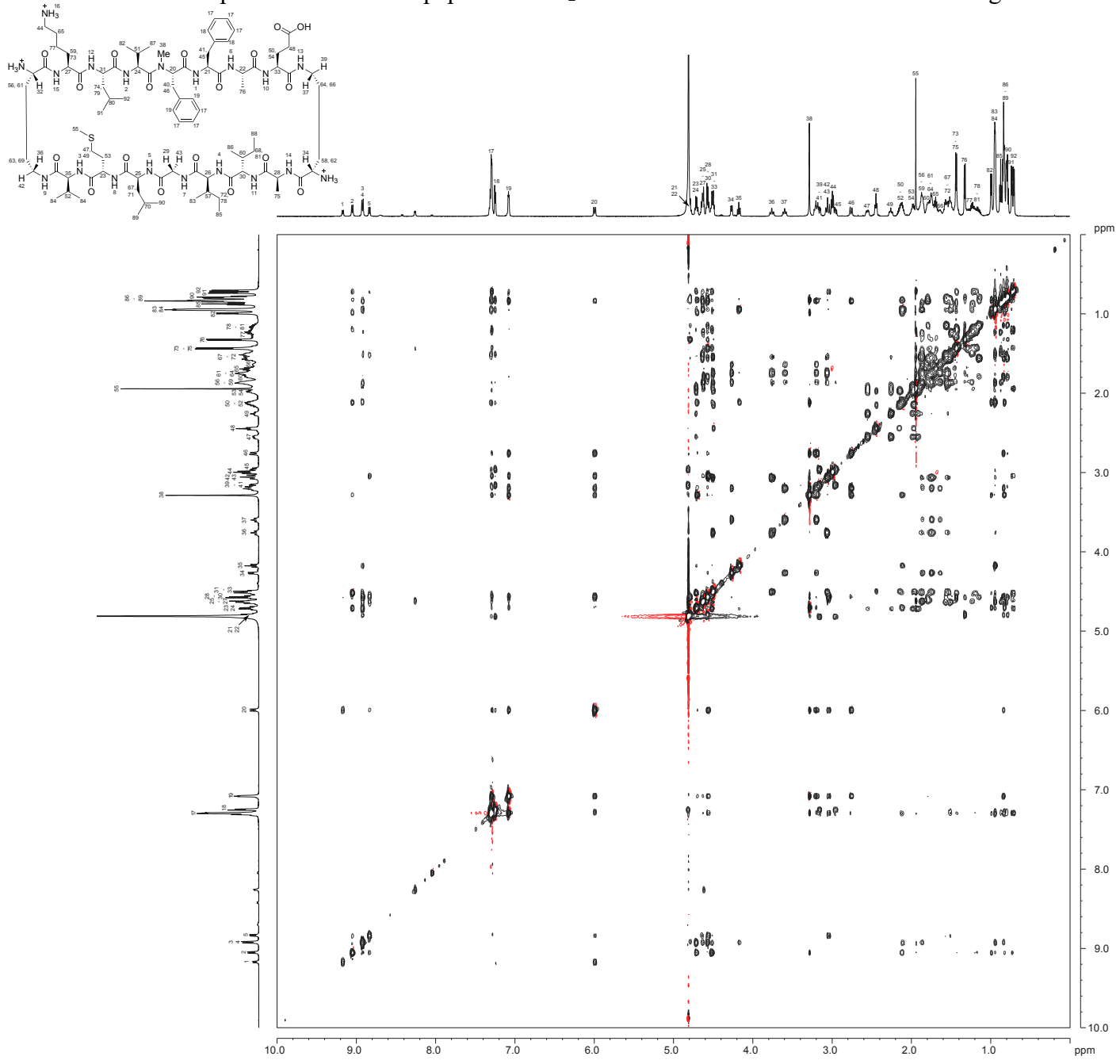


```
Current Data Parameters
NAME          JZ-II-13
EXPNO             13
PROCNO             1

F2 - Acquisition Parameters
Date_         20221213
Time              2.34
INSTRUM          av600
PROBHD   5 mm CPTCI 1H-
PULPROG       noesygpph
TD                2048
SOLVENT             D2O
NS                  16
DS                  16
SWH          6302.521 Hz
FIDRES          3.077403 Hz
AQ           0.1624747 sec
RG                2050
DW              79.333 usec
DE              18.63 usec
TE              297.9 K
D0           0.00006657 sec
D1           2.00000000 sec
D8           1.00000000 sec
D16          0.00020000 sec
IN0          0.00015860 sec

======== CHANNEL f1 ========
SFO1       600.1330006 MHz
NUC1               1H
P1               10.00 usec
P2               20.00 usec
PLW1          6.16599989 W

====== GRADIENT CHANNEL =====
GPNAM[1]     SMSQ10.100
GPZ1             40.00 %
P16            1000.00 usec

F1 - Acquisition parameters
TD                 256
SFO1         600.133 MHz
FIDRES       49.259144 Hz
SW           10.506 ppm
FnMODE       States-TPPI

F2 - Processing parameters
SI                1024
SF           600.1299945 MHz
WDW               QSINE
SSB                2
LB               0 Hz
GB                 0
PC               1.40

F1 - Processing parameters
SI                1024
MC2          States-TPPI
SF           600.1299942 MHz
WDW               QSINE
SSB                2
LB               0 Hz
GB                 0
```

^{1}H NMR 2D NOESY spectrum of 1.0 mM peptide **1** in 9:1 H_2O/D_2O at 600 MHz and 298 K with WATERGATE suppression of the HOD peak and 1-s mixing time

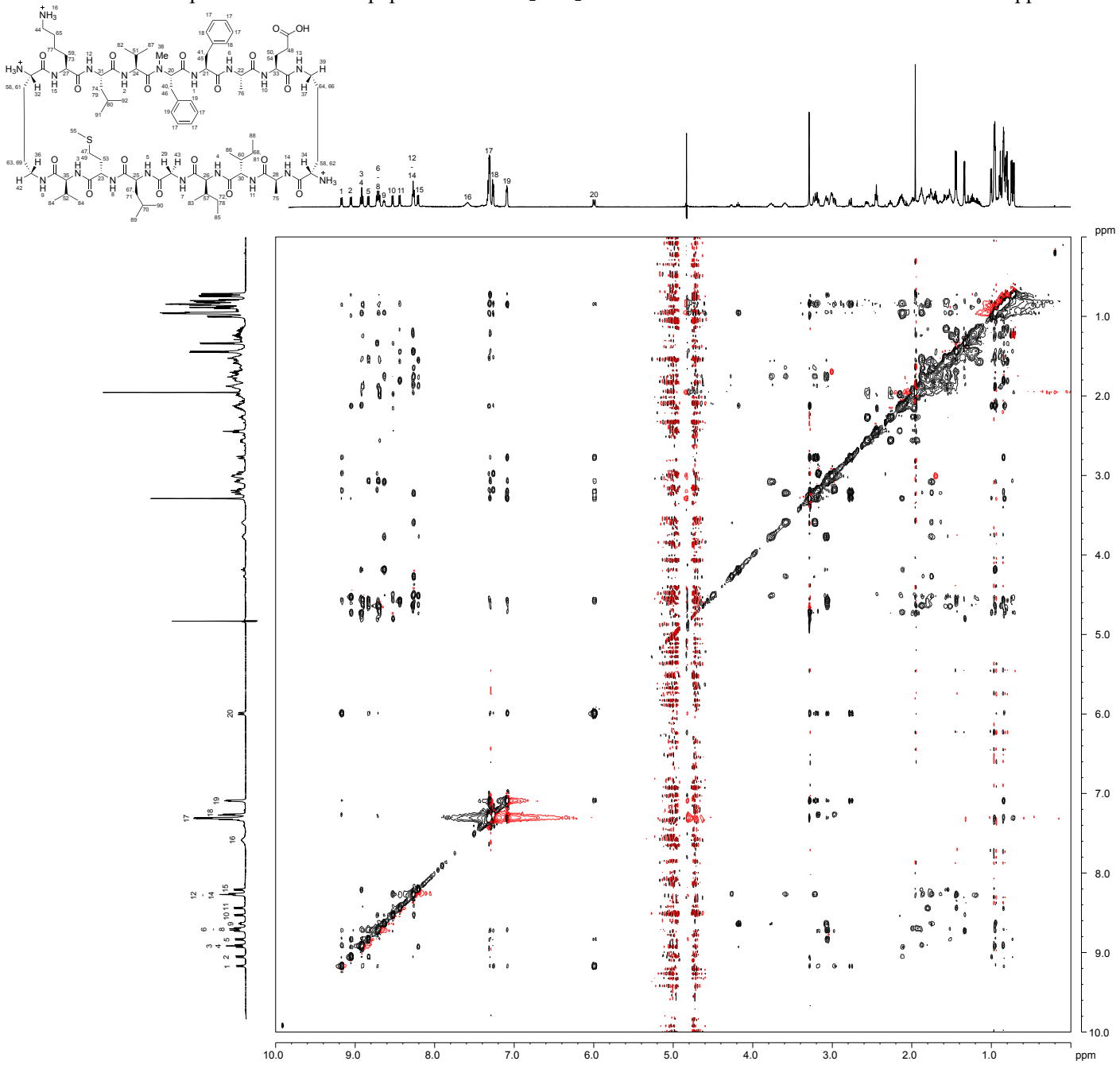

Current Data Parameters
NAME JZ-II-15
EXPNO 28
PROCNO 1

F2 - Acquisition Parameters
Date_ 20230103
Time 2.57
INSTRUM av600
PROBHD 5 mm CPTCI 1H-
PULPROG noesygpphw5
TD 2048
SOLVENT D2O
NS 16
DS 16
SWH 6602.113 Hz
FIDRES 3.223688 Hz
AQ 0.1551019 sec
RG 2050
DW 75.733 usec
DE 10.00 usec
TE 297.7 K
D0 0.00006551 sec
D1 2.00000000 sec
D8 1.00000000 sec
D11 0.03000000 sec
D12 0.00002000 sec
D13 0.00000400 sec
D16 0.00020000 sec
D19 0.00010000 sec
IN0 0.00015140 sec

======== CHANNEL f1 ========
SFO1 600.1328968 MHz
NUC1 1H
P1 8.00 usec
P27 8.00 usec
PLW1 6.16599989 W
PLW18 6.16599989 W
PLW32 0.00000063 W

====== GRADIENT CHANNEL =====
GPNAM[1] SMSQ10.100
GPNAM[2] SMSQ10.100
GPZ1 34.00 %
GPZ2 22.00 %
P16 1000.00 usec

F1 - Acquisition parameters
TD 256
SFO1 600.1329 MHz
FIDRES 51.601719 Hz
SW 11.006 ppm
FnMODE States-TPPI

F2 - Processing parameters
SI 1024
SF 600.1299831 MHz
WDW QSINE
SSB 2
LB 0 Hz
GB 0
PC 1.00

F1 - Processing parameters
SI 1024
MC2 States-TPPI
SF 600.1299804 MHz
WDW QSINE
SSB 2
LB 0 Hz
GB 0

^{1}H NMR spectrum of 8.0 mM peptide **1** in D_2O at 600 MHz and 298 K

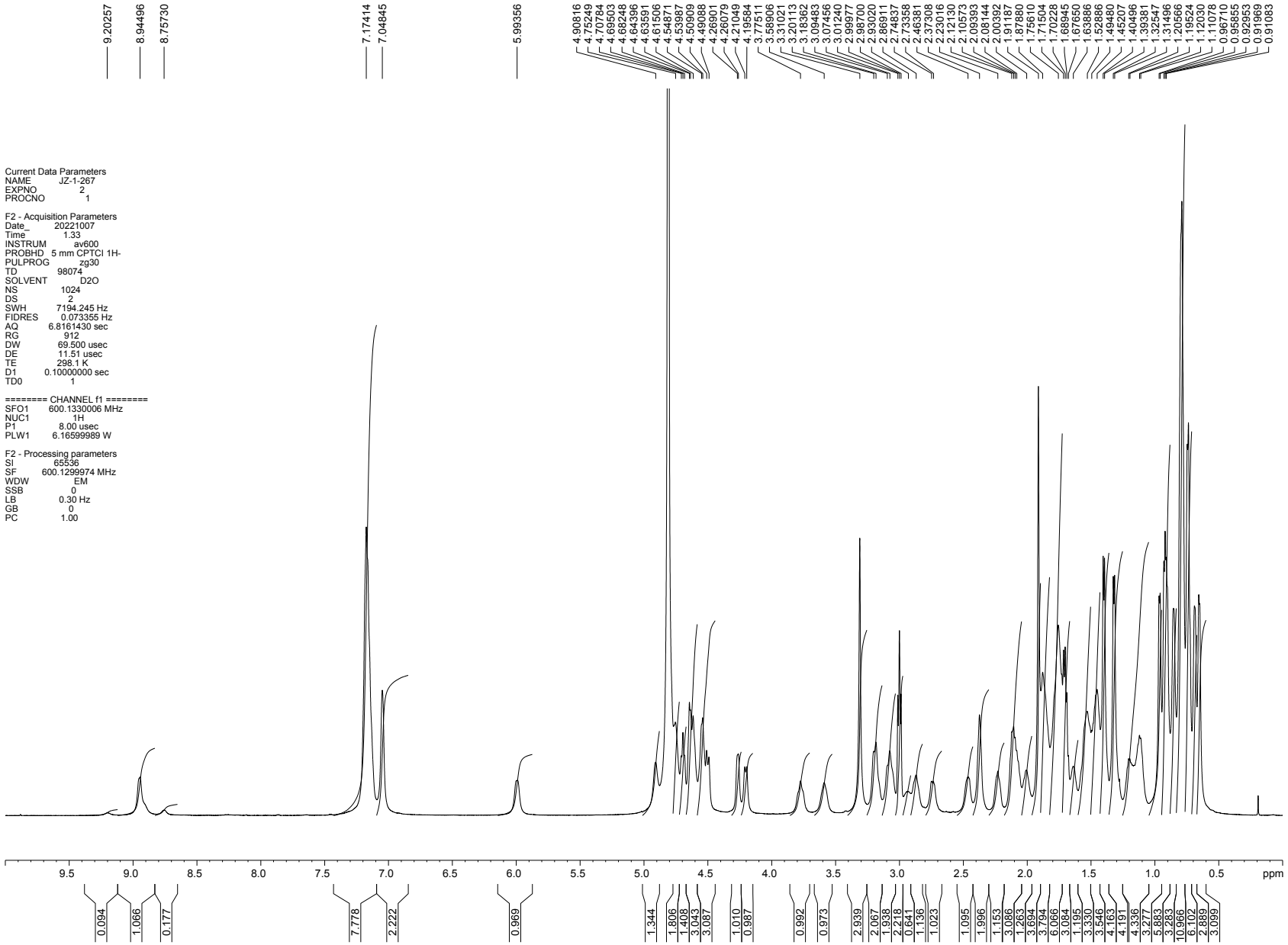

^{1}H NMR spectrum of 16.0 mM peptide **1** in D_2O at 500 MHz and 298 K

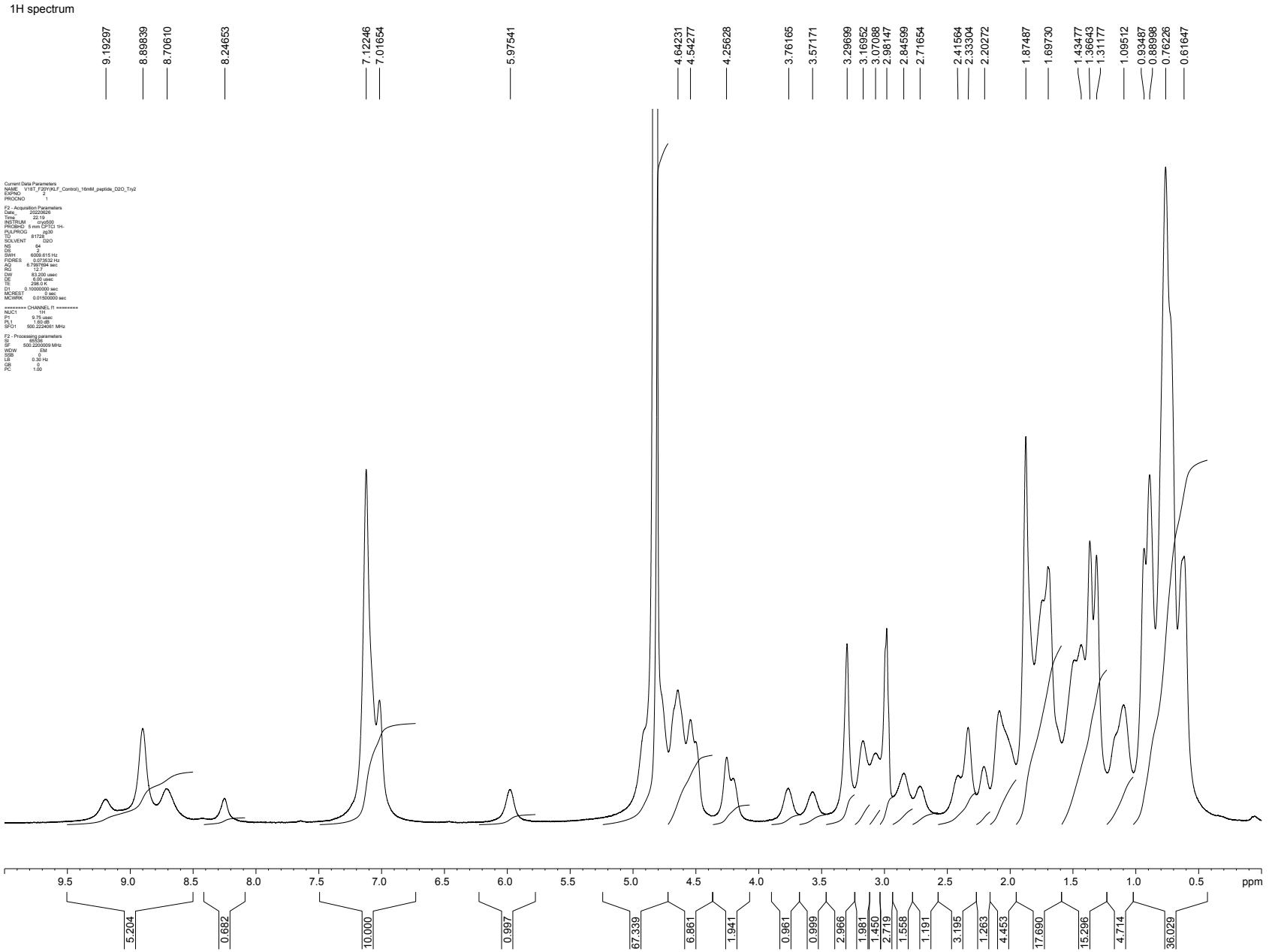

^{1}H NMR spectrum of 1.0 mM peptide **2** in D_2O at 600 MHz and 298 K

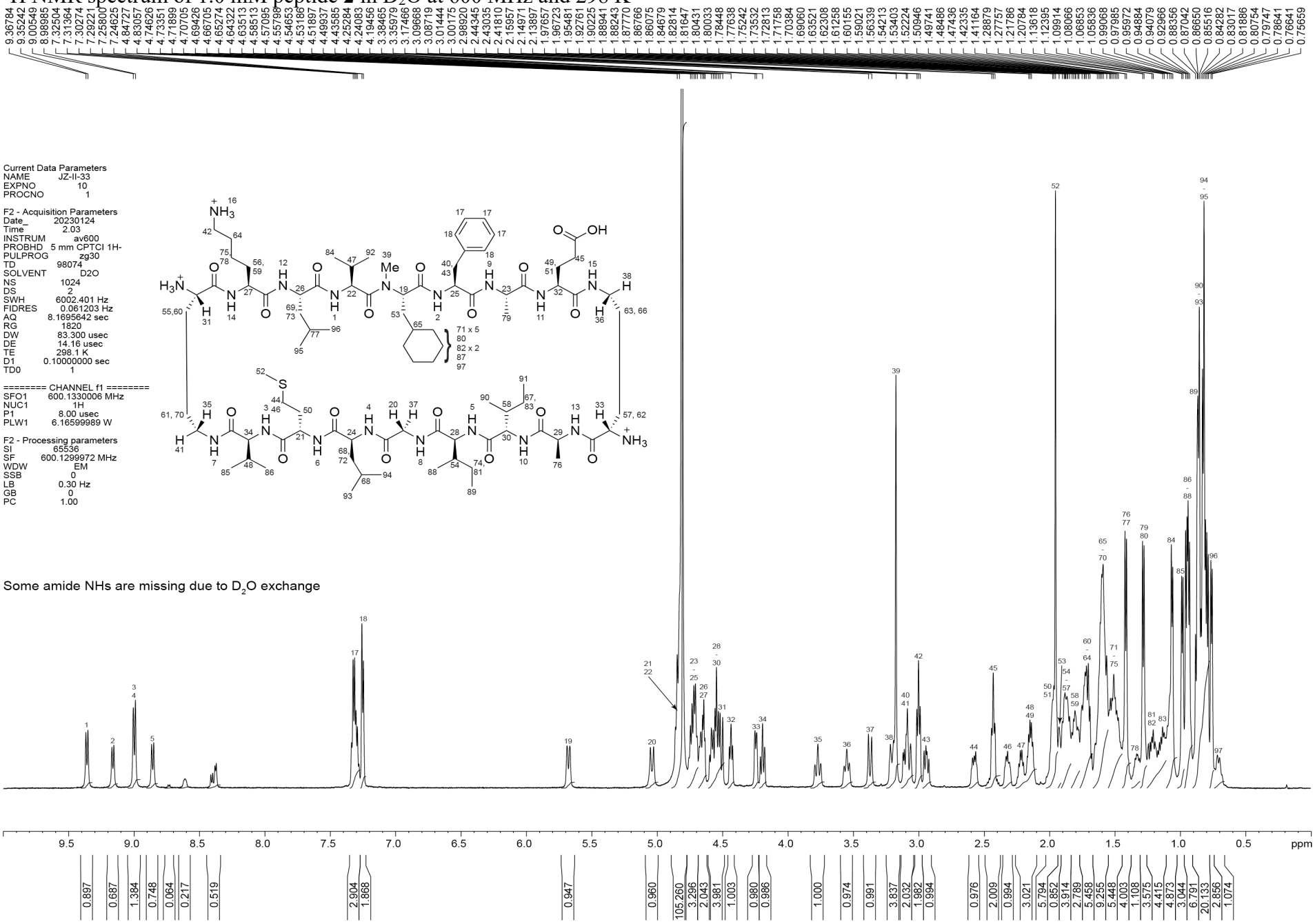

^{1}H NMR spectrum of 1.0 mM peptide **2** in 9:1 H_2O/D_2O at 600 MHz and 298 K with WATERGATE suppression of the HOD peak

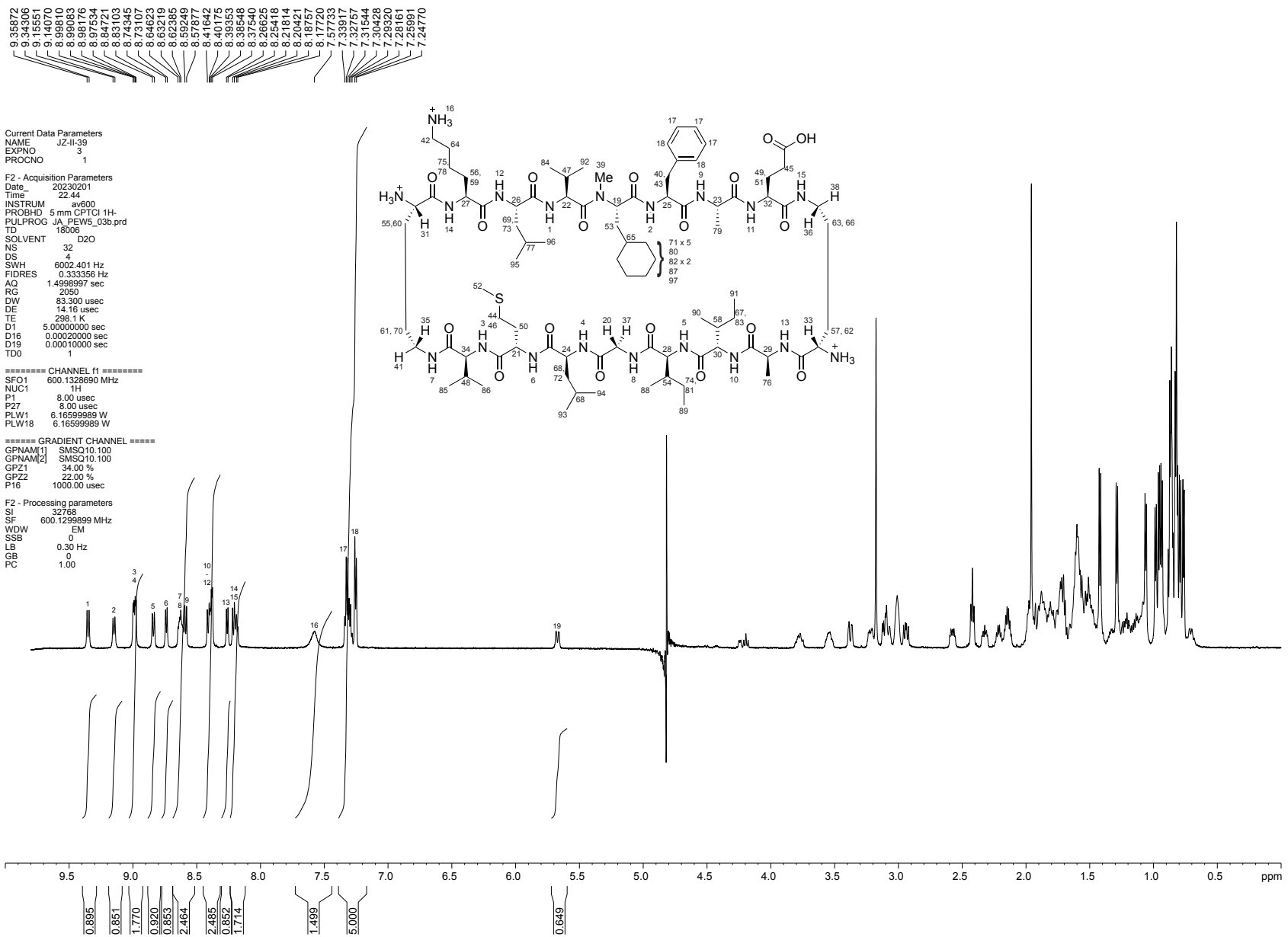

^{1}H NMR 2D TOCSY spectrum of 1.0 mM peptide **2** in D_2O at 600 MHz and 298 K with 100-ms spin-lock mixing time

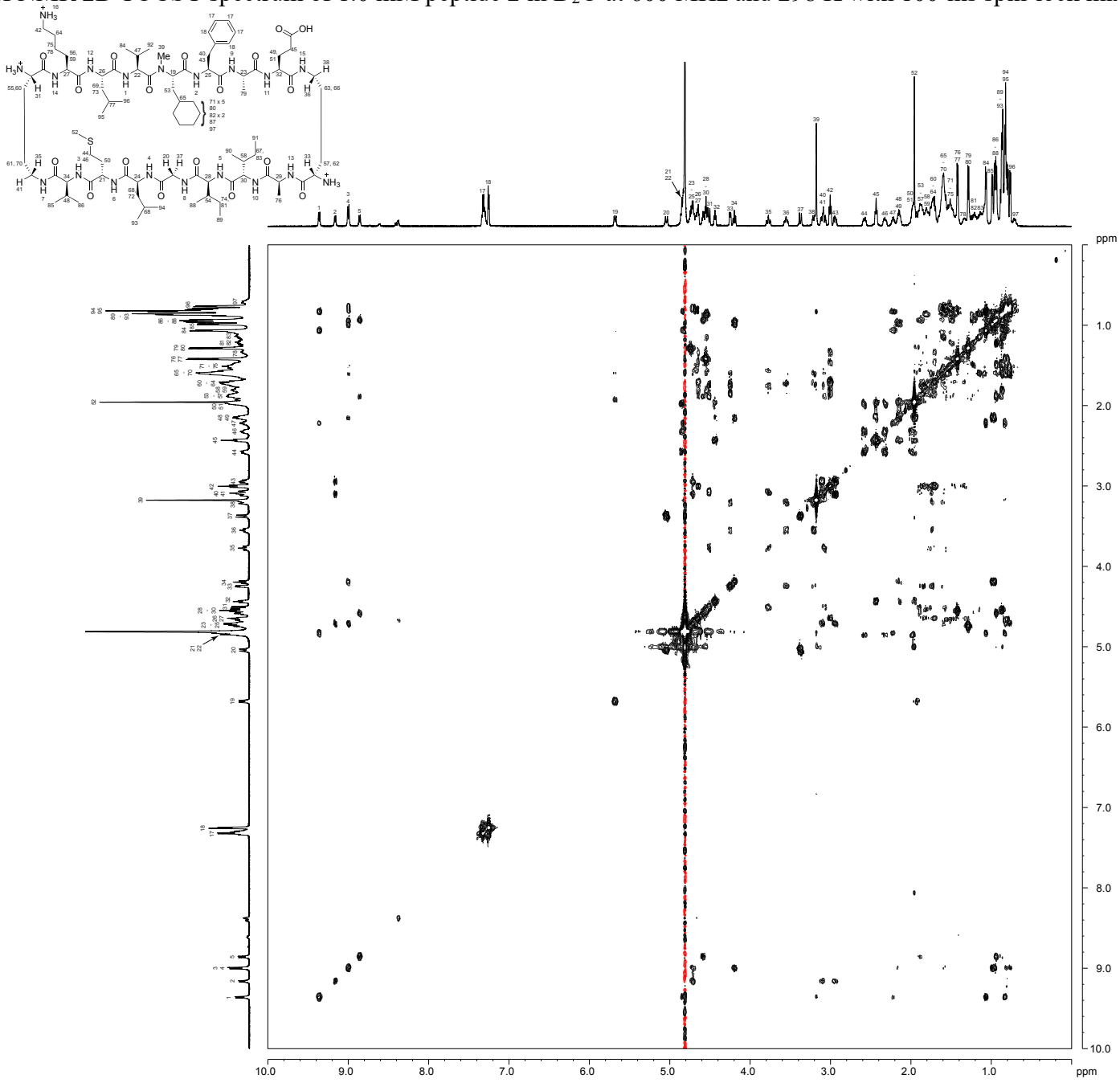


```
Current Data Parameters
NAME          JZ-II-33
EXPNO             11
PROCNO             1

F2 - Acquisition Parameters
Date_         20230124
Time              2.04
INSTRUM          av600
PROBHD   5 mm CPTCI 1H-
PULPROG   mlevgp_mo.prd
TD                2048
SOLVENT            D2O
NS                  16
DS                  16
SWH          6009.615 Hz
FIDRES       2.934382 Hz
AQ           0.1703936 sec
RG                1820
DW            83.200 usec
DE            10.00 usec
TE              298.1 K
D0          0.00000300 sec
D1          2.00000000 sec
D9          0.10000000 sec
D12         0.00002000 sec
D16         0.00020000 sec
IN0         0.00016640 sec
L1                  60

======== CHANNEL f1 ========
SFO1        600.1330006 MHz
NUC1               1H
P1              8.00 usec
P5             16.67 usec
P6             25.00 usec
P7             50.00 usec
P17          2500.00 usec
PLW1        6.16599989 W
PLW10       0.63095999 W

====== GRADIENT CHANNEL =====
GPNAM[1]    SMSQ10.100
GPNAM[2]    SMSQ10.100
GPZ1           10.00 %
GPZ2           10.00 %
P16          1000.00 usec

F1 - Acquisition parameters
TD                 256
SFO1        600.133 MHz
FIDRES      46.950119 Hz
SW          10.014 ppm
FnMODE             QF

F2 - Processing parameters
SI                1024
SF          600.1299967 MHz
WDW              SINE
SSB                 0
LB              0 Hz
GB                  0
PC              1.40

F1 - Processing parameters
SI                1024
MC2                QF
SF          600.1299968 MHz
WDW              SINE
SSB                 0
LB              0 Hz
GB                  0
```

^{1}H NMR 2D TOCSY spectrum of 1.0 mM peptide **2** in 9:1 H_2O/D_2O at 600 MHz and 298 K with WATERGATE suppression of the HOD peak and 200-ms spin-lock mixing time

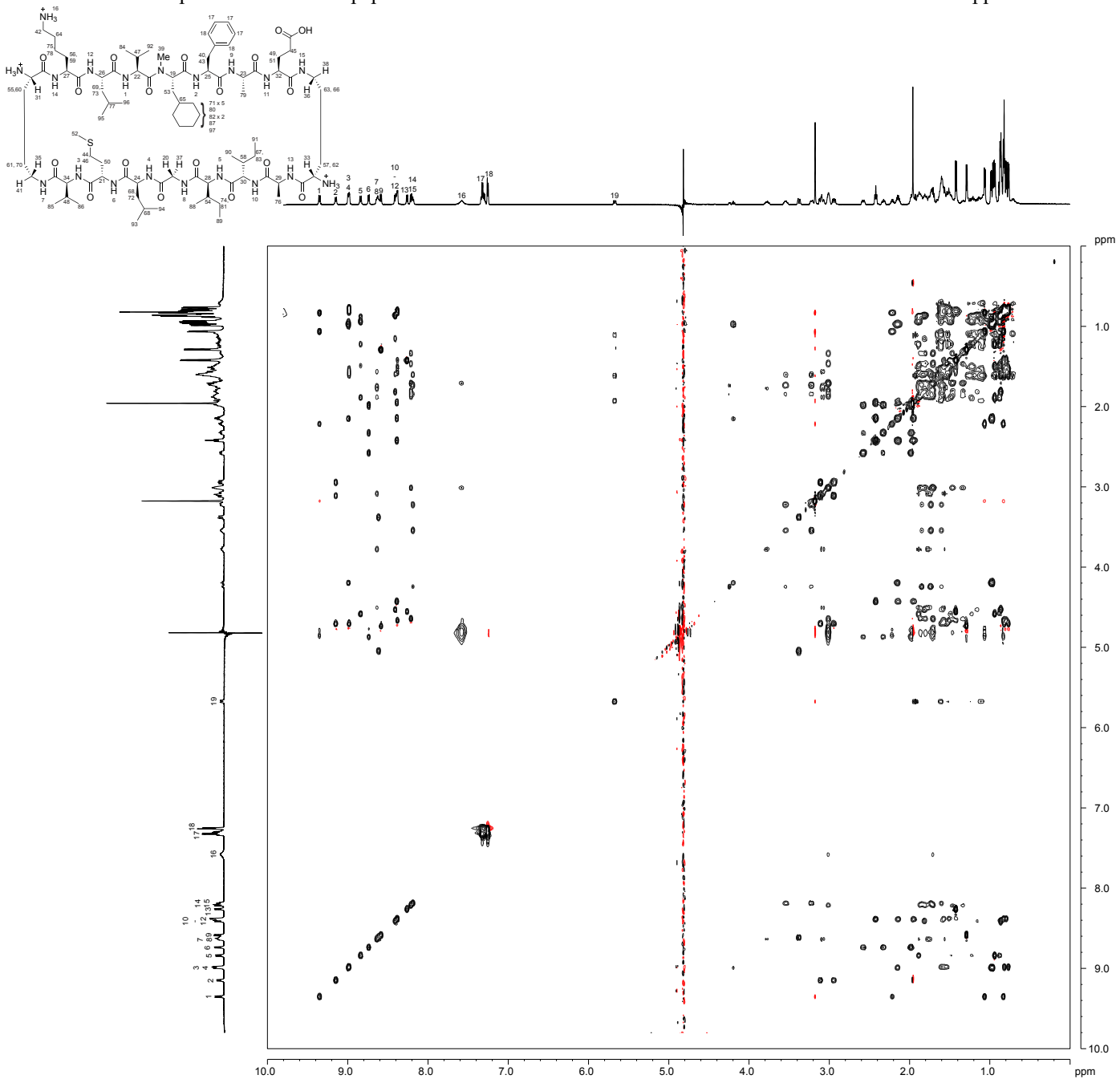


```
Current Data Parameters
NAME          JZ-II-39
EXPNO             5
PROCNO            1

F2 - Acquisition Parameters
Date_         20230202
Time              0.47
INSTRUM           av600
PROBHD    5 mm CPTCI 1H-
PULPROG       mlevgpphw5
TD                2048
SOLVENT           D2O
NS                16
DS                16
SWH           6009.615 Hz
FIDRES        2.934382 Hz
AQ            0.1703936 sec
RG                2050
DW            83.200 usec
DE            10.00 usec
TE            298.1 K
D0            0.00007411 sec
D1            2.00000000 sec
D9            0.20000000 sec
D12           0.00002000 sec
D16           0.00020000 sec
D19           0.00010000 sec
IN0           0.00016640 sec
L1                120
P2            16.00 usec

======== CHANNEL f1 ========
SFO1          600.1328692 MHz
NUC1              1H
P1            8.00 usec
P5            16.67 usec
P6            25.00 usec
P7            50.00 usec
P17           2500.00 usec
P27           8.00 usec
PLW1          6.16599989 W
PLW10         0.63095999 W
PLW18         6.16599989 W

====== GRADIENT CHANNEL =====
GPNAM[1]      SMSQ10.100
GPNAM[2]      SMSQ10.100
GPZ1          34.00 %
GPZ2          22.00 %
P16           1000.00 usec

F1 - Acquisition parameters
TD                256
SFO1          600.1329 MHz
FIDRES        46.950119 Hz
SW            10.014 ppm
FnMODE        States-TPPI

F2 - Processing parameters
SI                1024
SF            600.1299901 MHz
WDW               QSINE
SSB               2
LB            0 Hz
GB                0
PC            1.00

F1 - Processing parameters
SI                1024
MC2           States-TPPI
SF            600.1299893 MHz
WDW               QSINE
SSB               2
LB            0 Hz
GB                0
```

^{1}H NMR 2D NOESY spectrum of 1.0 mM peptide **2** in D_2O at 600 MHz and 298 K with 1-s mixing time

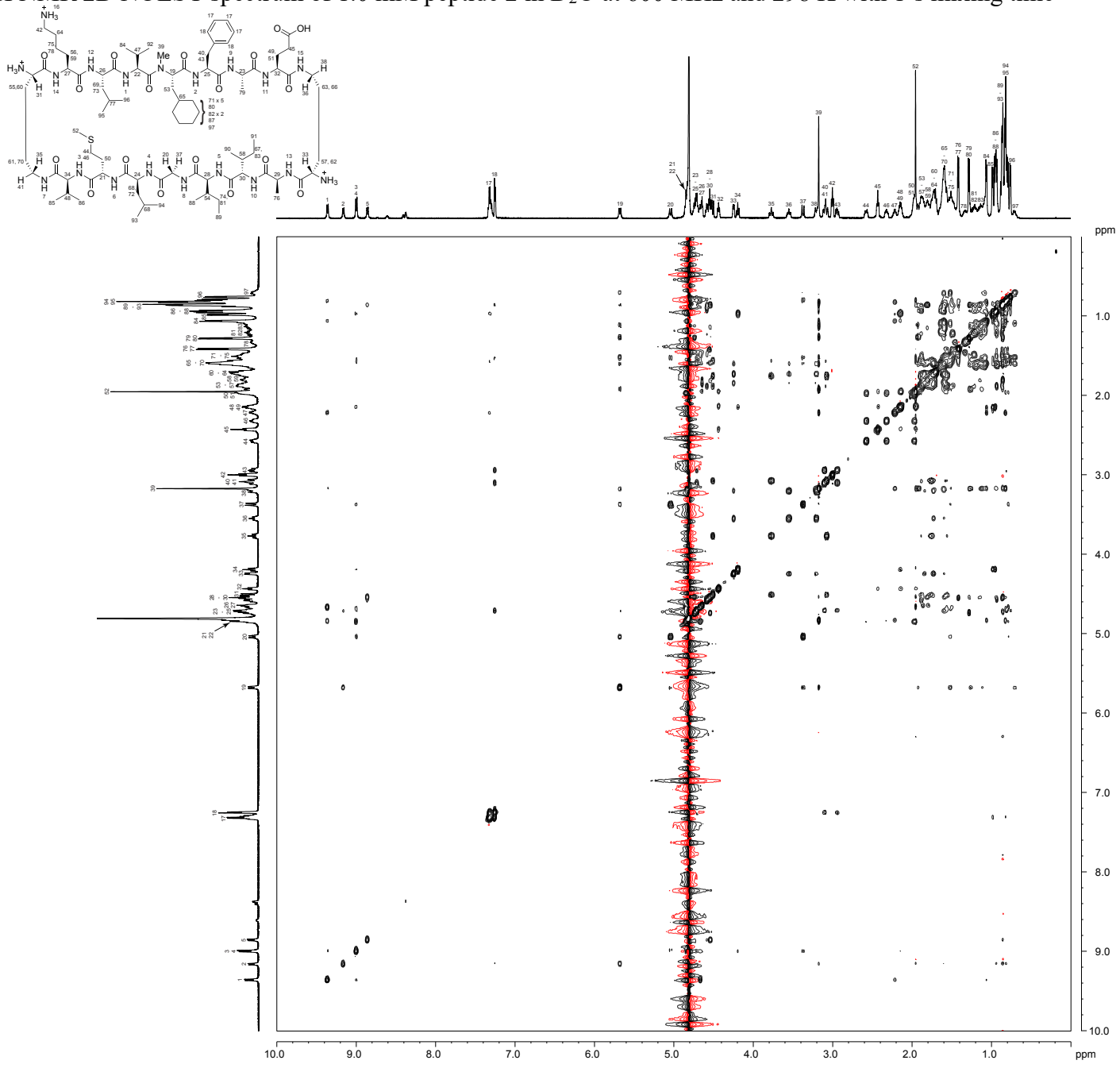


```
Current Data Parameters
NAME          JZ-II-33
EXPNO             12
PROCNO             1

F2 - Acquisition Parameters
Date_       20230124
Time            4.43
INSTRUM         av600
PROBHD   5 mm CPTCI 1H-
PULPROG       noesyphrv
TD              2048
SOLVENT           D2O
NS                16
DS                16
SWH         6002.401 Hz
FIDRES      2.930860 Hz
AQ          0.1705984 sec
RG              812
DW           83.300 usec
DE           10.74 usec
TE            298.1 K
D0          0.00007311 sec
D1          2.00000000 sec
D8          1.00000000 sec
IN0         0.00016660 sec

======== CHANNEL f1 ========
SFO1        600.1330006 MHz
NUC1               1H
P1              8.00 usec
PLW1        6.16599989 W

F1 - Acquisition parameters
TD                256
SFO1        600.133 MHz
FIDRES      46.893757 Hz
SW          10.002 ppm
FnMODE      States-TPPI

F2 - Processing parameters
SI                1024
SF          600.1299968 MHz
WDW               QSINE
SSB               2
LB              0 Hz
GB              0
PC              1.40

F1 - Processing parameters
SI                1024
MC2         States-TPPI
SF          600.1299977 MHz
WDW               QSINE
SSB               2
LB              0 Hz
GB              0
```

^{1}H NMR 2D NOESY spectrum of 1.0 mM peptide **2** in 9:1 H_2O/D_2O at 600 MHz and 298 K with WATERGATE suppression of the HOD peak and 1-s mixing time

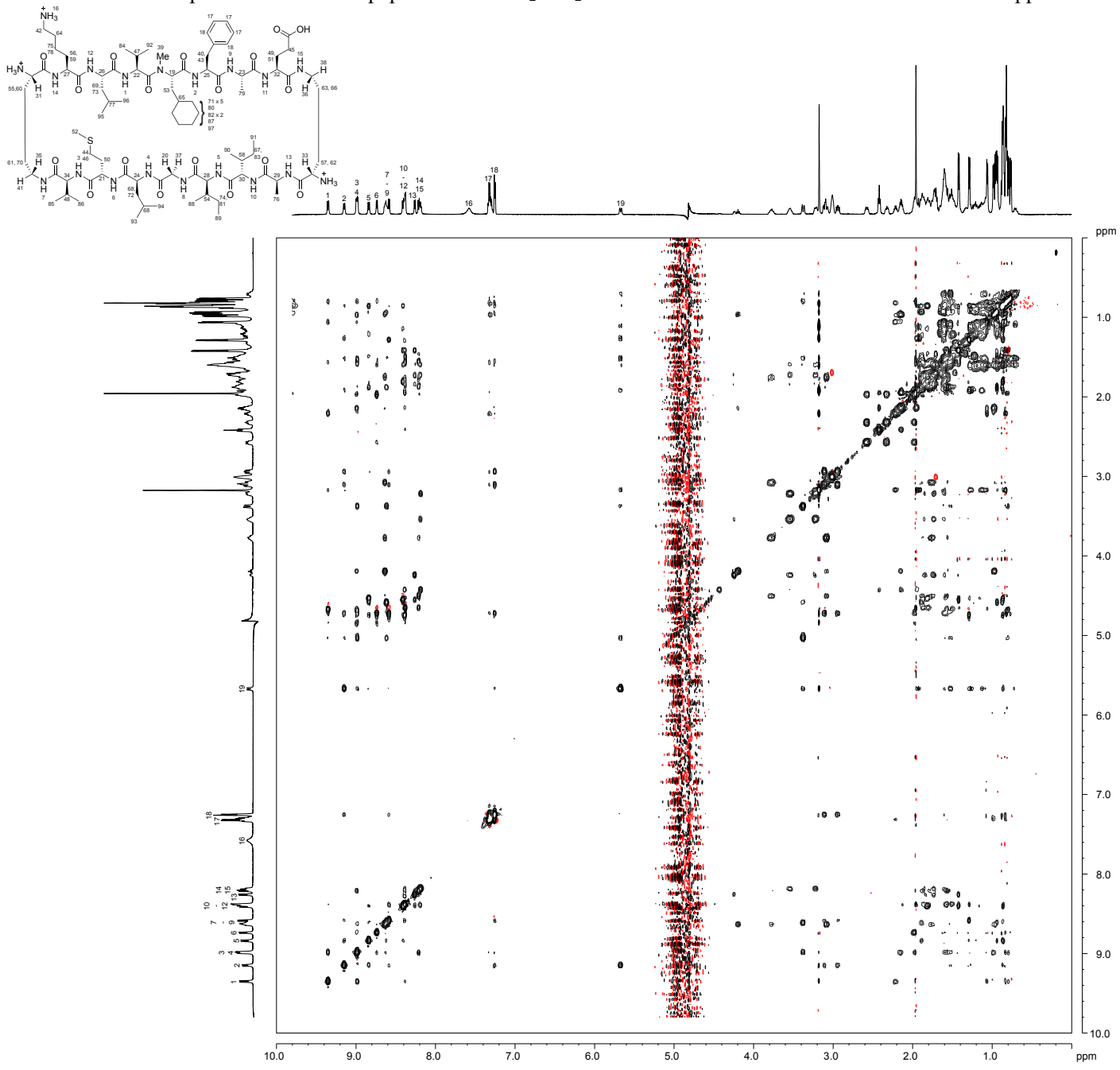


```
Current Data Parameters
NAME          JZ-II-39
EXPNO                6
PROCNO               1

F2 - Acquisition Parameters
Date_         20230202
Time              3.31
INSTRUM           av600
PROBHD   5 mm CPTCI 1H-
PULPROG     noesygpphw5
TD                2048
SOLVENT            D2O
NS                  16
DS                  16
SWH          6009.615 Hz
FIDRES       2.934382 Hz
AQ           0.1703936 sec
RG                2050
DW           83.200 usec
DE            10.00 usec
TE            298.1 K
D0           0.00007301 sec
D1           2.00000000 sec
D8           1.00000000 sec
D11          0.03000000 sec
D12          0.00002000 sec
D13          0.00000400 sec
D16          0.00020000 sec
D19          0.00010000 sec
IN0          0.00016640 sec

======== CHANNEL f1 ========
SFO1         600.1328692 MHz
NUC1               1H
P1             8.00 usec
P27            8.00 usec
PLW1        6.16599989 W
PLW18       6.16599989 W
PLW32       0.00000063 W

====== GRADIENT CHANNEL =====
GPNAM[1]     SMSQ10.100
GPNAM[2]     SMSQ10.100
GPZ1           34.00 %
GPZ2           22.00 %
P16          1000.00 usec

F1 - Acquisition parameters
TD                 256
SFO1         600.1329 MHz
FIDRES       46.950119 Hz
SW           10.014 ppm
FnMODE       States-TPPI

F2 - Processing parameters
SI                1024
SF           600.1299892 MHz
WDW               QSINE
SSB                2
LB              0 Hz
GB                 0
PC              1.00

F1 - Processing parameters
SI                1024
MC2          States-TPPI
SF           600.1299908 MHz
WDW               QSINE
SSB                2
LB              0 Hz
GB                 0
```

^{1}H NMR spectrum of 11.0 mM peptide **2** in D_2O at 600 MHz and 298 K

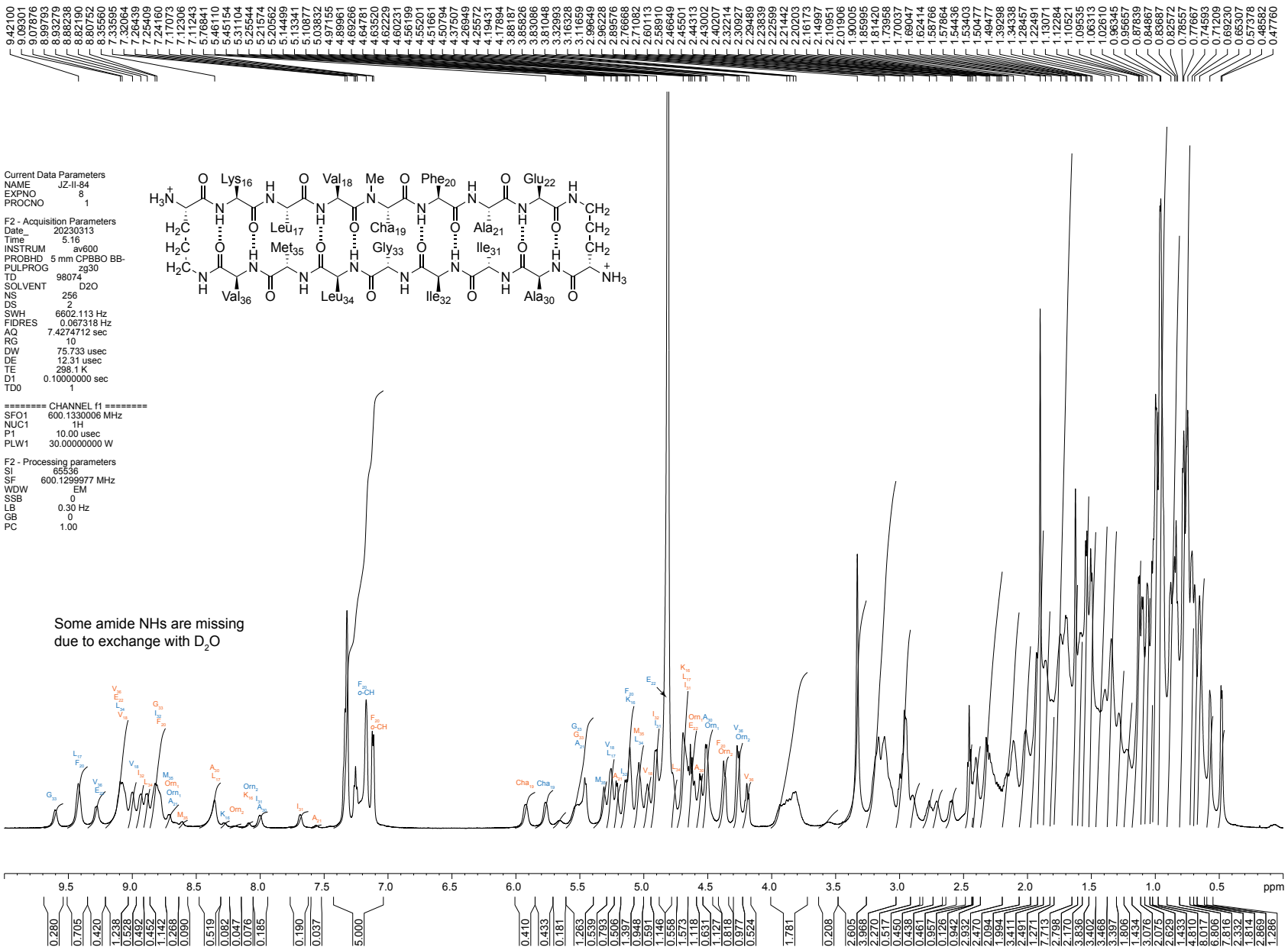

^{1}H NMR spectrum of 11.0 mM peptide **2** in 9:1 H_2O/D_2O at 600 MHz and 298 K with WATERGATE suppression of the HOD peak

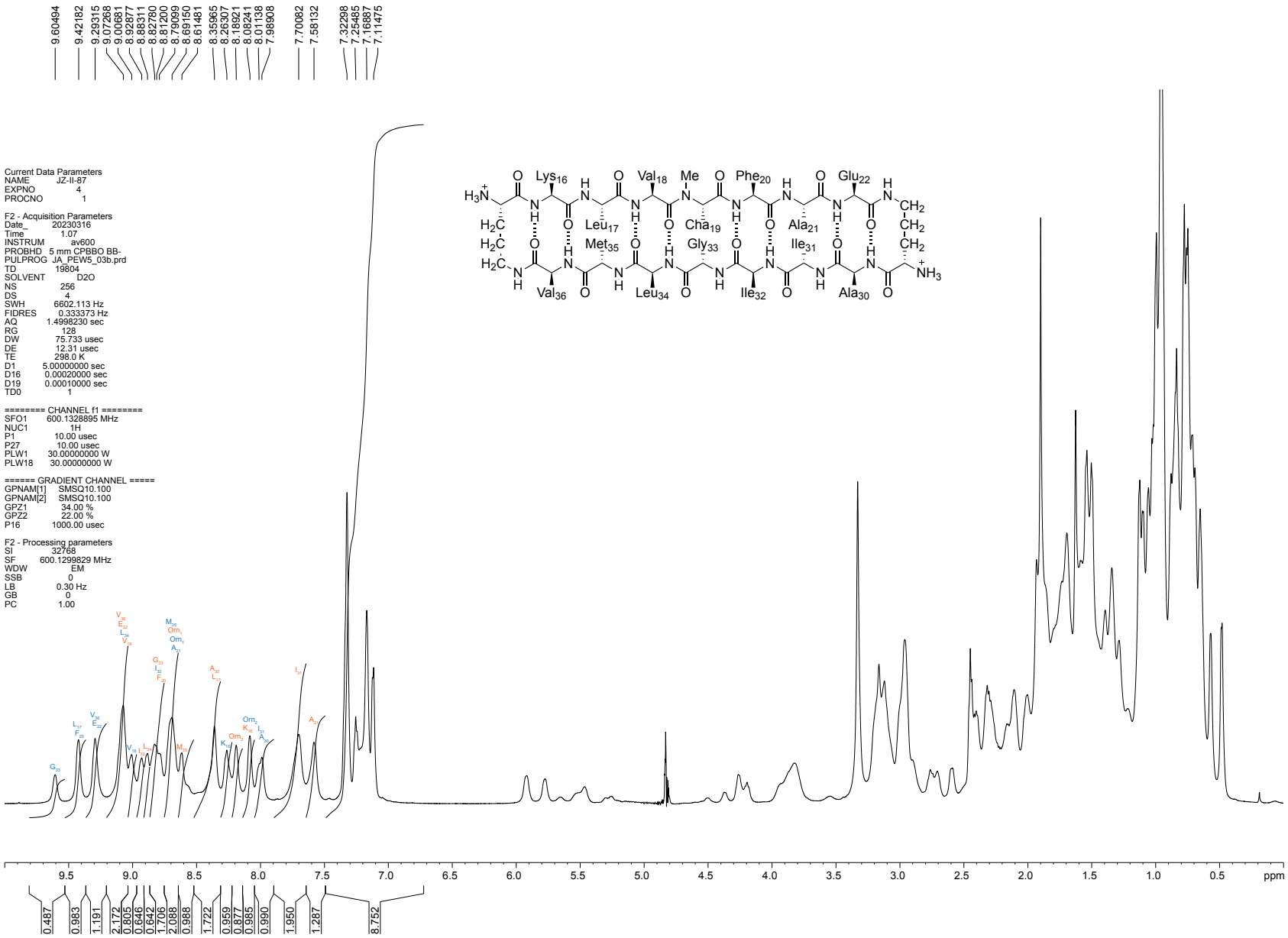

^{1}H NMR 2D TOCSY spectrum of 11.0 mM peptide **2** in D_2O at 600 MHz and 298 K with 50-ms spin-lock mixing time

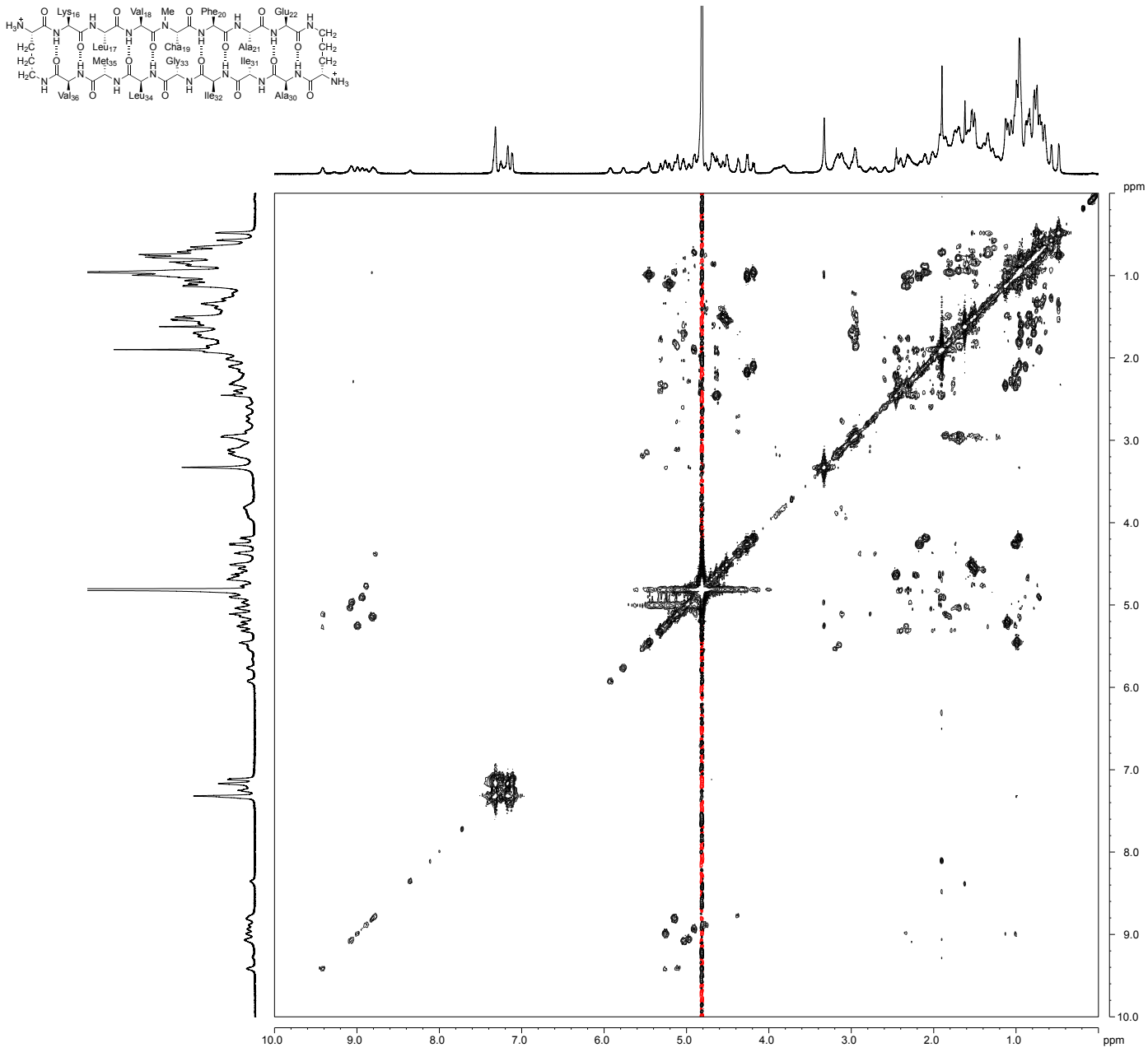


```
Current Data Parameters
NAME          JZ-II-84
EXPNO             15
PROCNO             1

F2 - Acquisition Parameters
Date_         20230321
Time              3.02
INSTRUM          av600
PROBHD  5 mm CPBBO BB-
PULPROG   mlevgp_mo.prd
TD                2048
SOLVENT            D2O
NS                   8
DS                  16
SWH           6602.113 Hz
FIDRES        3.223688 Hz
AQ            0.1551019 sec
RG                  10
DW             75.733 usec
DE             10.00 usec
TE               298.0 K
D0           0.00000300 sec
D1           2.00000000 sec
D9           0.05000000 sec
D12          0.00002000 sec
D16          0.00020000 sec
IN0          0.00015140 sec
L1                  30

======== CHANNEL f1 ========
SFO1       600.1330006 MHz
NUC1               1H
P1              10.00 usec
P5              16.67 usec
P6              25.00 usec
P7              50.00 usec
P17           2500.00 usec
PLW1       30.00000000 W
PLW10       5.15000010 W

====== GRADIENT CHANNEL =====
GPNAM[1]    SMSQ10.100
GPNAM[2]    SMSQ10.100
GPZ1           10.00 %
GPZ2           10.00 %
P16          1000.00 usec

F1 - Acquisition parameters
TD                 256
SFO1       600.133 MHz
FIDRES     51.601719 Hz
SW         11.006 ppm
FnMODE             QF

F2 - Processing parameters
SI                1024
SF         600.1299980 MHz
WDW              SINE
SSB                 0
LB              0 Hz
GB                  0
PC              1.40

F1 - Processing parameters
SI                1024
MC2                QF
SF         600.1299978 MHz
WDW              SINE
SSB                 0
LB              0 Hz
GB                  0
```

^{1}H NMR 2D TOCSY spectrum of 11.0 mM peptide **2** in 9:1 H_2O/D_2O at 600 MHz and 298 K with WATERGATE suppression of the HOD peak and 60-ms spin-lock mixing time

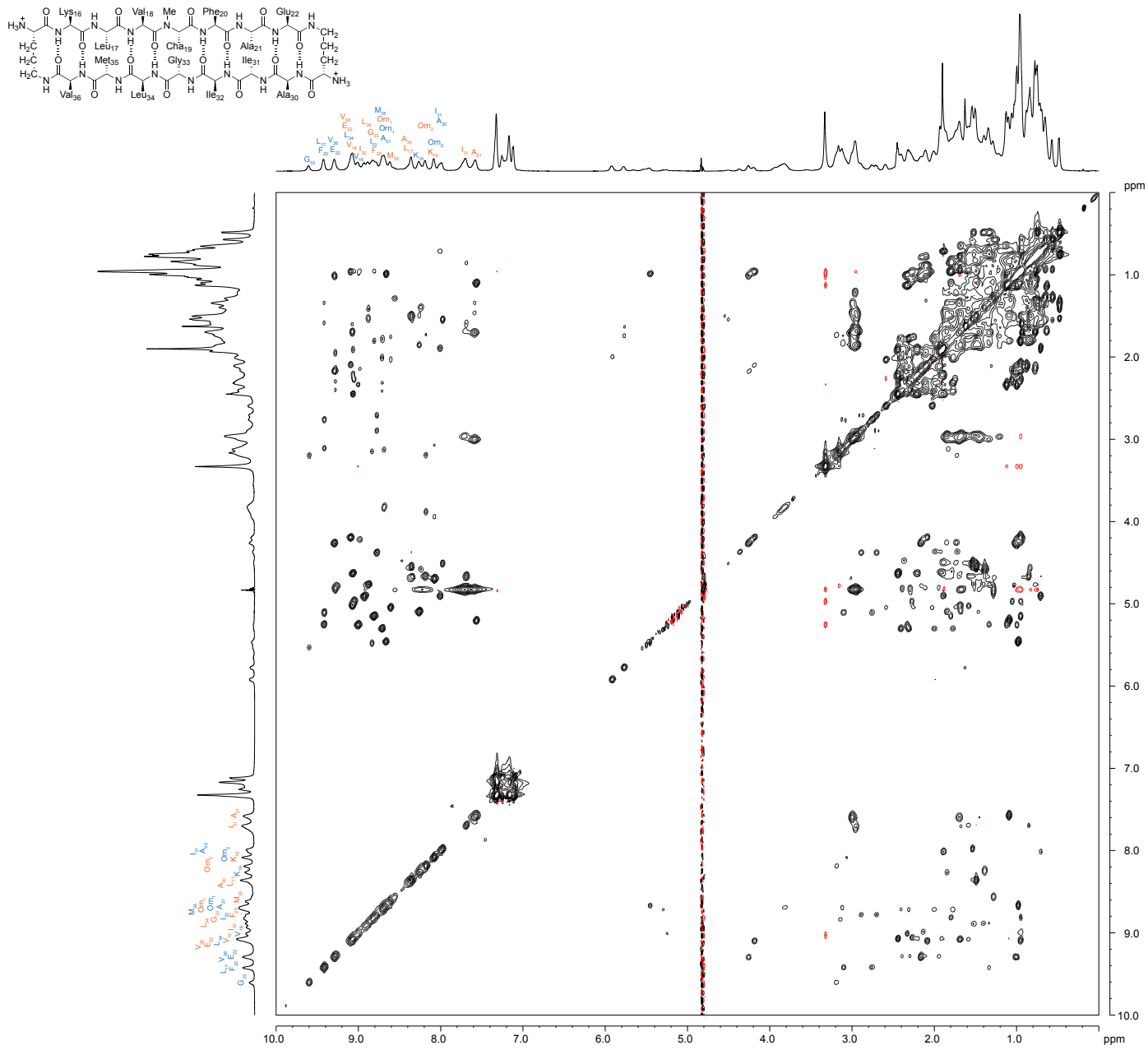


```
Current Data Parameters
NAME          JZ-II-87
EXPNO             5
PROCNO            1

F2 - Acquisition Parameters
Date_         20230316
Time              1.08
INSTRUM           av600
PROBHD    5 mm CPBBO BB-
PULPROG       mlevgpphw5
TD                2048
SOLVENT           D2O
NS                8
DS                16
SWH           6602.113 Hz
FIDRES        3.223688 Hz
AQ            0.1551019 sec
RG                128
DW            75.733 usec
DE            10.00 usec
TE            298.0 K
D0            0.00006533 sec
D1            2.00000000 sec
D9            0.06000000 sec
D12           0.00002000 sec
D16           0.00020000 sec
D19           0.00010000 sec
IN0           0.00015140 sec
L1                36
P2            20.00 usec

======== CHANNEL f1 ========
SFO1          600.1328896 MHz
NUC1              1H
P1            10.00 usec
P5            16.67 usec
P6            25.00 usec
P7            50.00 usec
P17           2500.00 usec
P27           10.00 usec
PLW1          30.00000000 W
PLW10         5.15000010 W
PLW18         30.00000000 W

====== GRADIENT CHANNEL =====
GPNAM[1]      SMSQ10.100
GPNAM[2]      SMSQ10.100
GPZ1          34.00 %
GPZ2          22.00 %
P16           1000.00 usec

F1 - Acquisition parameters
TD                256
SFO1          600.1329 MHz
FIDRES        51.601719 Hz
SW            11.006 ppm
FnMODE        States-TPPI

F2 - Processing parameters
SI                1024
SF            600.1299867 MHz
WDW               QSINE
SSB               2
LB                0 Hz
GB                0
PC                1.40

F1 - Processing parameters
SI                1024
MC2           States-TPPI
SF            600.1299818 MHz
WDW               QSINE
SSB               2
LB                0 Hz
GB                0
```

[1]H NMR 2D ROESY spectrum of 11.0 mM peptide **2** in 9:1 H_2O/D_2O at 600 MHz and 298 K with WATERGATE suppression of the HOD peak and 150-ms spin-lock mixing time

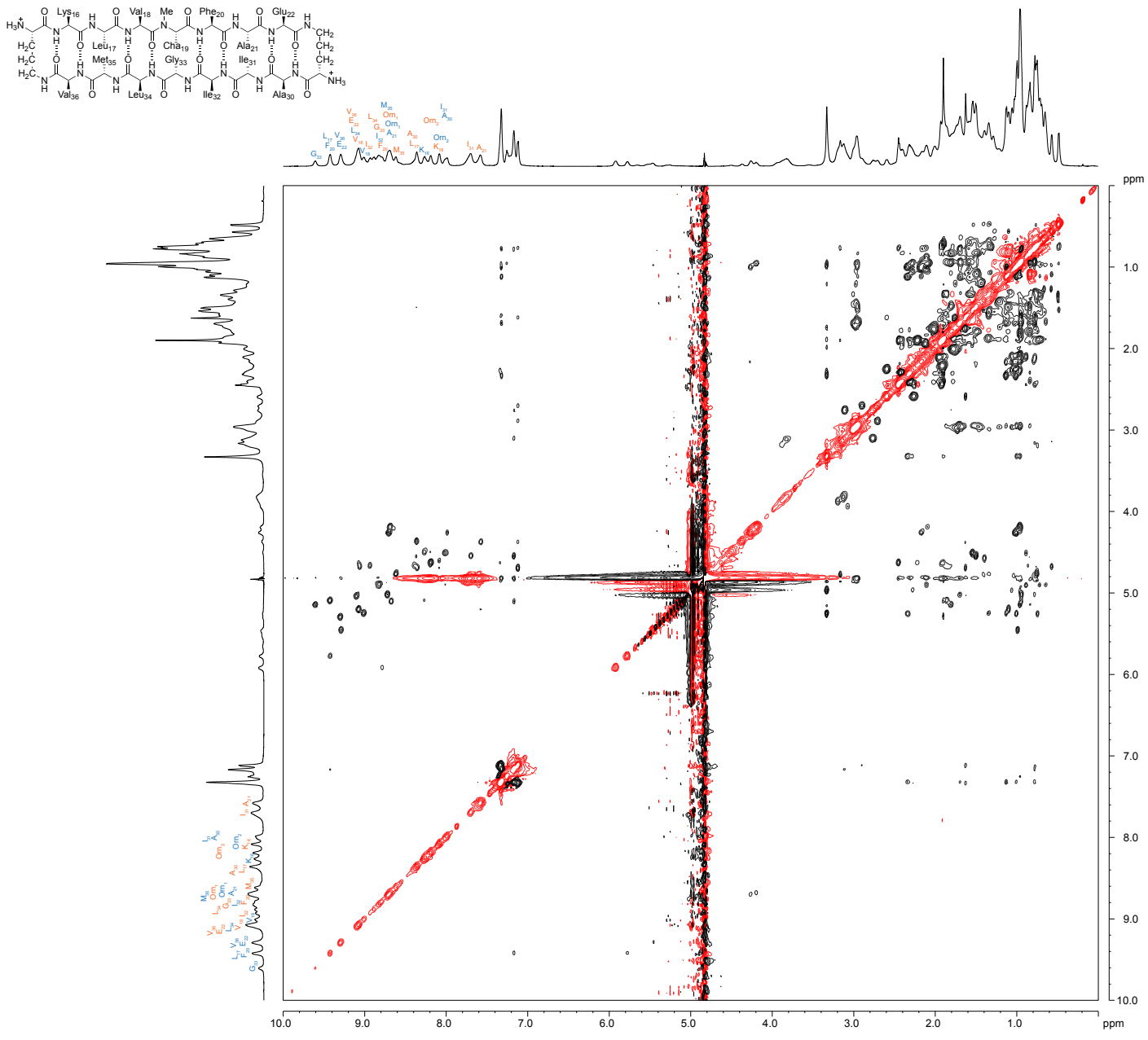


```
Current Data Parameters
NAME          JZ-II-87
EXPNO             8
PROCNO            1

F2 - Acquisition Parameters
Date_         20230316
Time          5.38
INSTRUM       av600
PROBHD   5 mm CPBBO BB-
PULPROG  roesygpph19.2.prd
TD            2048
SOLVENT       D2O
NS            8
DS            16
SWH           6602.113 Hz
FIDRES        3.223688 Hz
AQ            0.1551019 sec
RG            645
DW            75.733 usec
DE            10.00 usec
TE            298.0 K
D0            0.00006533 sec
D1            2.00000000 sec
D8            0.15000001 sec
D12           0.00002000 sec
D16           0.00200000 sec
D19           0.00010000 sec
IN0           0.00015140 sec
L4            417
P15           150000.00 usec

======== CHANNEL f1 ========
SFO1          600.1328896 MHz
NUC1          1H
P0            10.00 usec
P1            10.00 usec
P25           180.00 usec
P27           10.00 usec
PLW1          30.00000000 W
PLW18         30.00000000 W
PLW27         0.31623000 W

====== GRADIENT CHANNEL =====
GPNAM[1]      SMSQ10.100
GPNAM[2]      SMSQ10.100
GPZ1          30.00 %
GPZ2          30.00 %
P16           1000.00 usec

F1 - Acquisition parameters
TD            256
SFO1          600.1329 MHz
FIDRES        51.601719 Hz
SW            11.006 ppm
FnMODE        States-TPPI

F2 - Processing parameters
SI            1024
SF            600.1299845 MHz
WDW           QSINE
SSB           2
LB            0 Hz
GB            0
PC            1.40

F1 - Processing parameters
SI            1024
MC2           States-TPPI
SF            600.1299844 MHz
WDW           QSINE
SSB           2
LB            0 Hz
GB            0
```

[1]H NMR 2D NOESY spectrum of 11.0 mM peptide **2** in D_2O at 600 MHz and 298 K with 200-msec mixing time

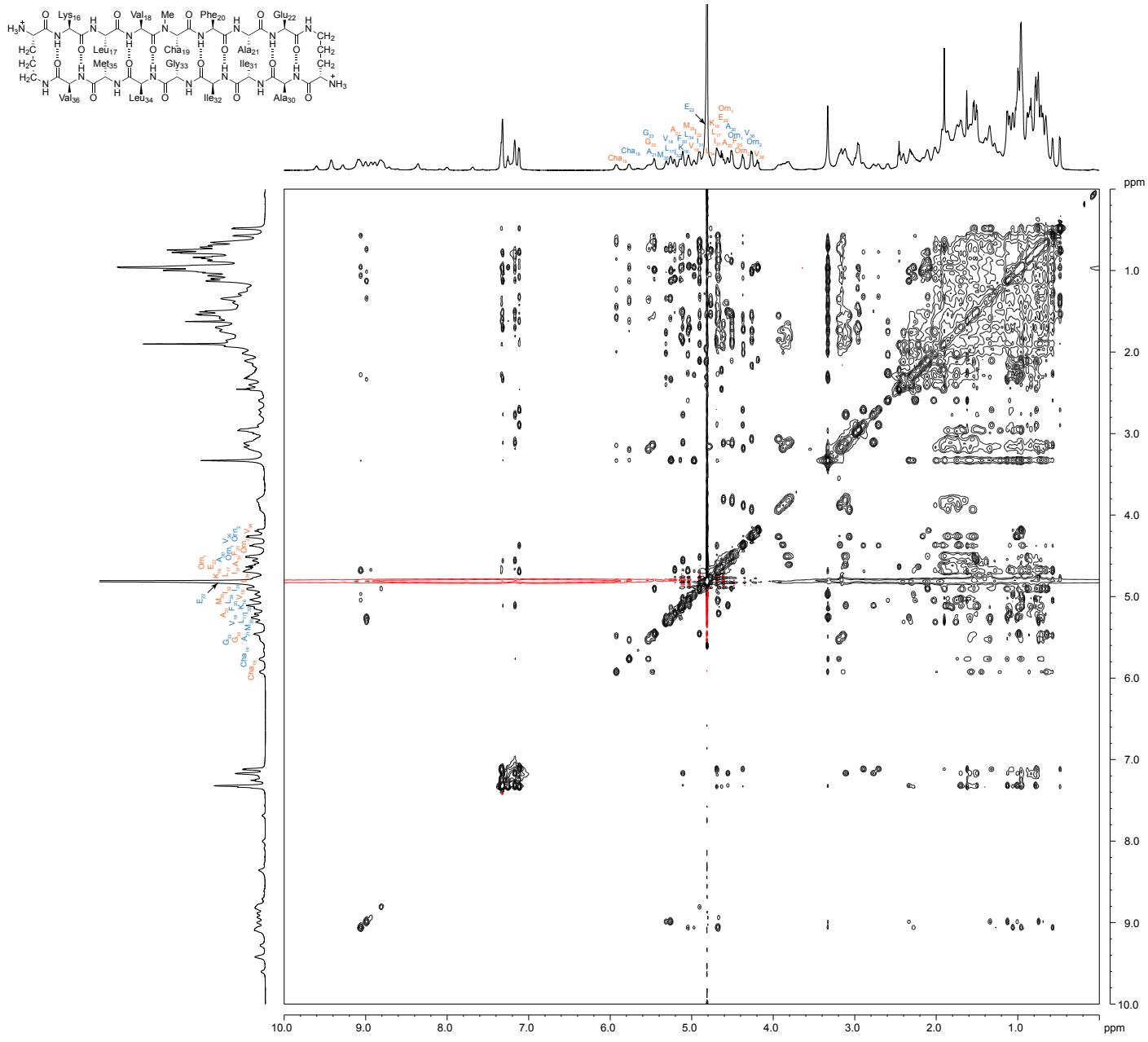


```
Current Data Parameters
NAME        JZ-II-101
EXPNO           2
PROCNO          1

F2 - Acquisition Parameters
Date_       20230505
Time        19.00
INSTRUM     av600
PROBHD   5 mm CPBBO BB-
PULPROG     noesygpph
TD          2048
SOLVENT     D2O
NS          8
DS          16
SWH         6602.113 Hz
FIDRES      3.223688 Hz
AQ          0.1551019 sec
RG          36
DW          75.733 usec
DE          17.51 usec
TE          297.9 K
D0          0.00006297 sec
D1          2.00000000 sec
D8          0.20000000 sec
D16         0.00020000 sec
IN0         0.00015140 sec

======== CHANNEL f1 ========
SFO1        600.1330006 MHz
NUC1        1H
P1          10.00 usec
P2          20.00 usec
PLW1        30.00000000 W

====== GRADIENT CHANNEL =====
GPNAM[1]    SMSQ10.100
GPZ1        40.00 %
P16         1000.00 usec

F1 - Acquisition parameters
TD          256
SFO1        600.133 MHz
FIDRES      51.601719 Hz
SW          11.006 ppm
FnMODE      States-TPPI

F2 - Processing parameters
SI          1024
SF          600.1299980 MHz
WDW         QSINE
SSB         2
LB          0 Hz
GB          0
PC          1.40

F1 - Processing parameters
SI          1024
MC2         States-TPPI
SF          600.1299979 MHz
WDW         QSINE
SSB         2
LB          0 Hz
GB          0
```

^{1}H NMR 2D NOESY spectrum of 11.0 mM peptide **2** in 9:1 H_2O/D_2O at 600 MHz and 298 K with WATERGATE suppression of the HOD peak and 200-msec mixing time

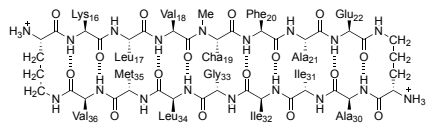

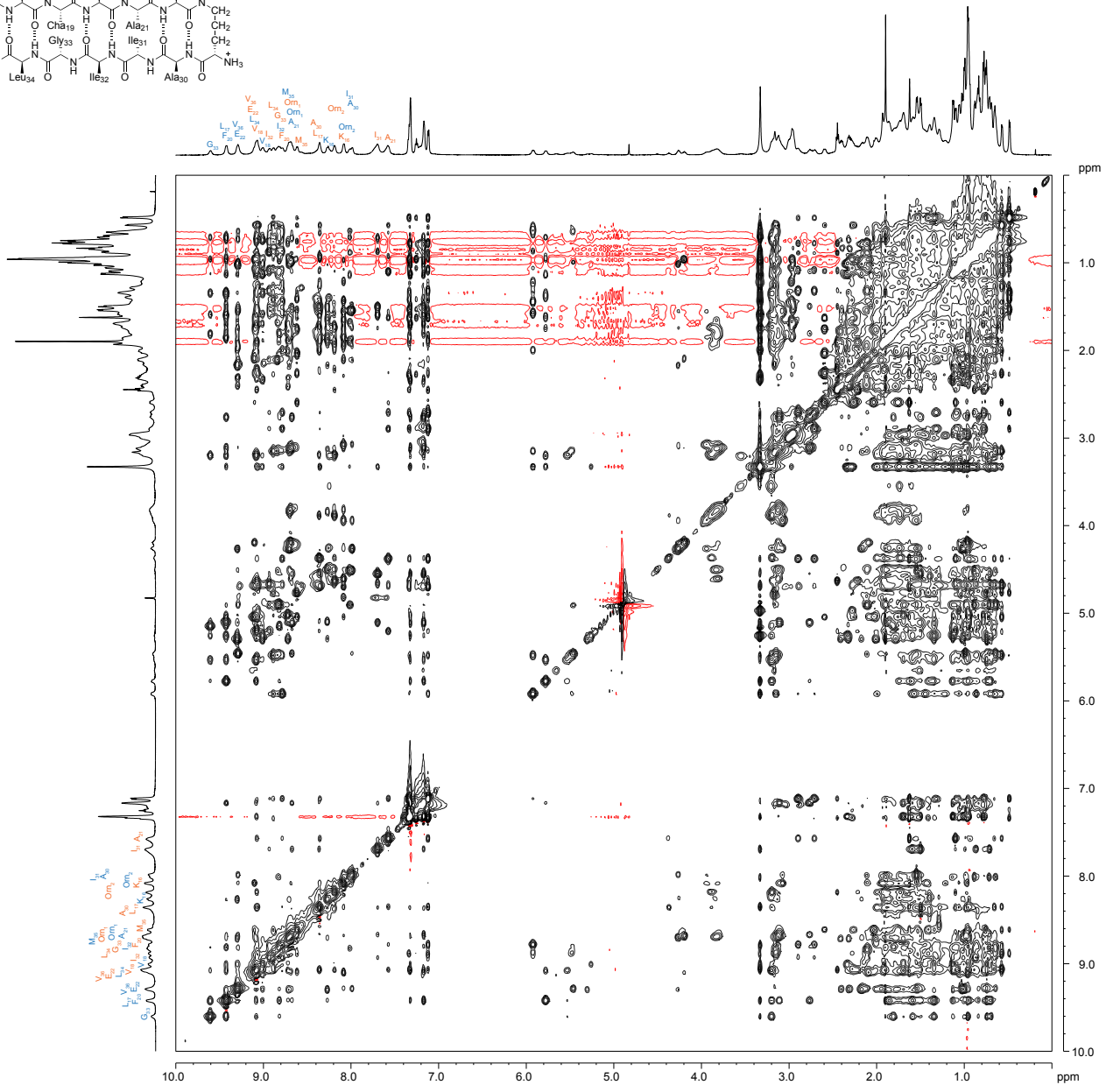


```
Current Data Parameters
NAME          JZ-II-101
EXPNO             12
PROCNO             1

F2 - Acquisition Parameters
Date_         20230514
Time          11.52
INSTRUM       av600
PROBHD   5 mm CPBBO BB-
PULPROG    noesygpphw5
TD            2048
SOLVENT       D2O
NS            8
DS            16
SWH           6602.113 Hz
FIDRES        3.223688 Hz
AQ            0.1551019 sec
RG            456
DW            75.733 usec
DE            10.00 usec
TE            298.0 K
D0            0.00006297 sec
D1            2.00000000 sec
D8            0.20000000 sec
D11           0.03000000 sec
D12           0.00002000 sec
D13           0.00000400 sec
D16           0.00020000 sec
D19           0.00010000 sec
IN0           0.00015140 sec

======== CHANNEL f1 ========
SFO1          600.1328842 MHz
NUC1          1H
P1            10.00 usec
P27           10.00 usec
PLW1          30.00000000 W
PLW18         30.00000000 W
PLW32         0.00000461 W

====== GRADIENT CHANNEL =====
GPNAM[1]      SMSQ10.100
GPNAM[2]      SMSQ10.100
GPZ1          34.00 %
GPZ2          22.00 %
P16           1000.00 usec

F1 - Acquisition parameters
TD            256
SFO1          600.1329 MHz
FIDRES        51.601719 Hz
SW            11.006 ppm
FnMODE        States-TPPI

F2 - Processing parameters
SI            1024
SF            600.1299848 MHz
WDW           QSINE
SSB           2
LB            0 Hz
GB            0
PC            1.40

F1 - Processing parameters
SI            1024
MC2           States-TPPI
SF            600.1299846 MHz
WDW           QSINE
SSB           2
LB            0 Hz
GB            0
```

^{1}H NMR spectrum of nominal 16.0 mM peptide **2** in D_2O at 600 MHz and 298 K

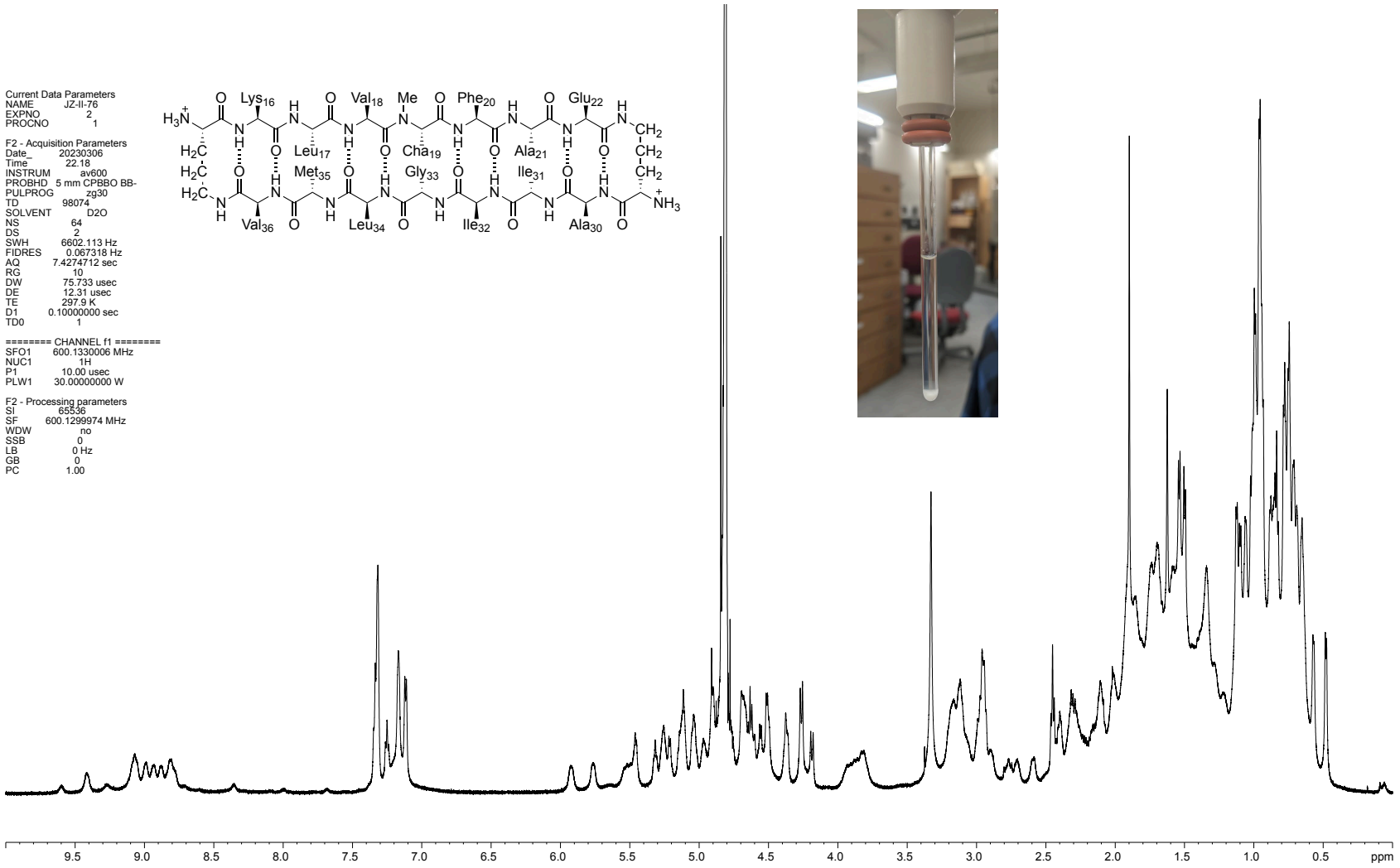

Note: The concentration is nominal because peptide **2** is not fully soluble at 16.0 mM.

^{1}H NMR DOSY spectrum of nominal 16.0 mM peptide **2** in D_2O at 600 MHz and 298 K

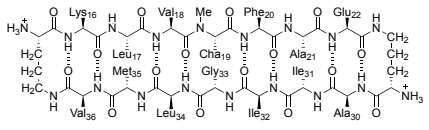

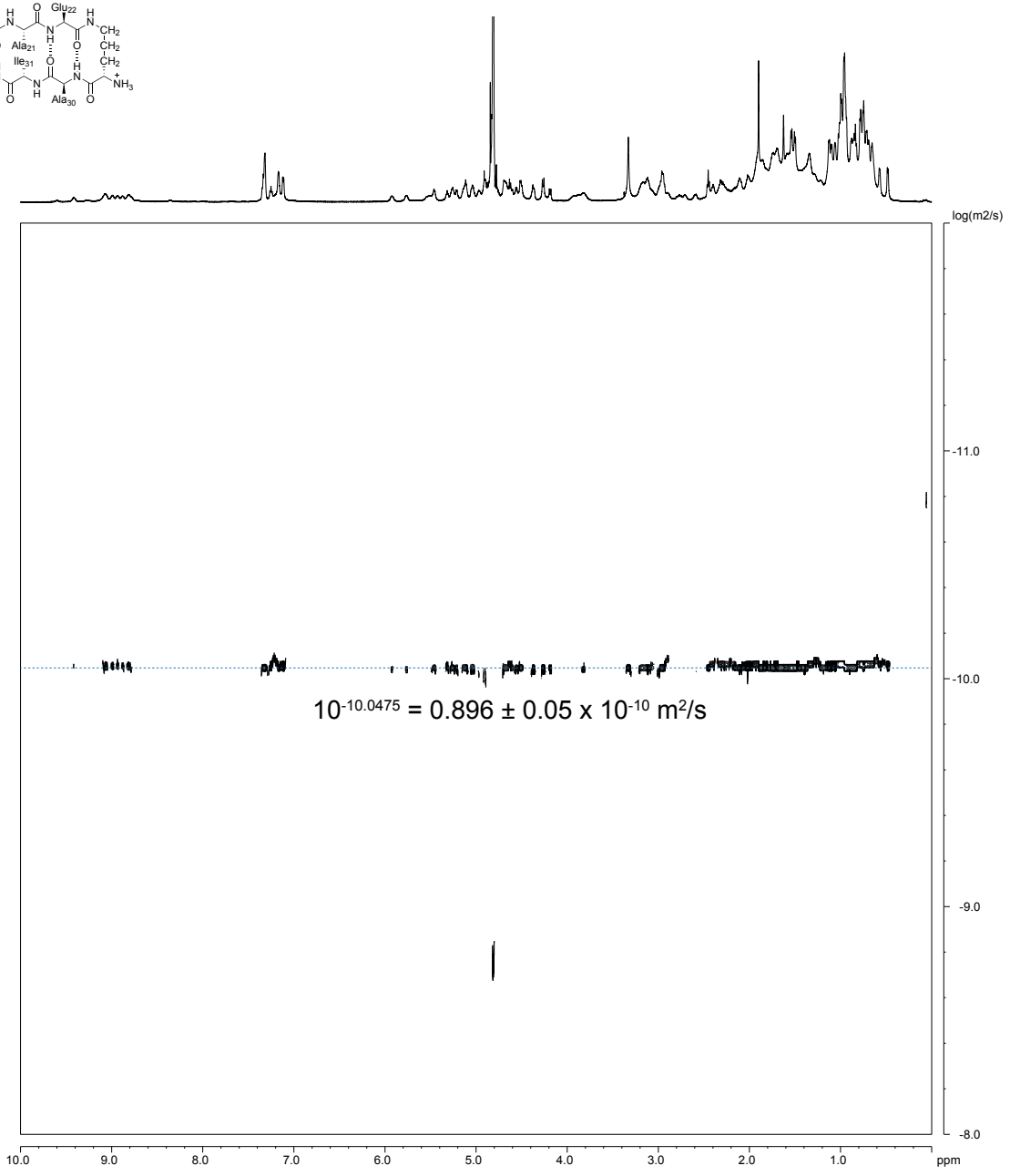

Current Data Parameters
NAME JZ-II-76
EXPNO 6
PROCNO 1

F2 - Acquisition Parameters
Date_ 20230306
Time 23.09
INSTRUM av600
PROBHD 5 mm CPBBO BB-
PULPROG ledbpgp2s
TD 98074
SOLVENT D2O
NS 8
DS 4
SWH 9615.385 Hz
FIDRES 0.098042 Hz
AQ 5.0998478 sec
RG 32
DW 52.000 usec
DE 16.36 usec
TE 297.9 K
D1 5.00000000 sec
D16 0.00020000 sec
D20 0.07500000 sec
D21 0.00500000 sec

======== CHANNEL f1 ========
SFO1 600.1330006 MHz
NUC1 1H
P1 10.00 usec
P2 20.00 usec
PLW1 30.00000000 W

====== GRADIENT CHANNEL =====
GPNAM[6] SMSQ10.100
GPNAM[7] SMSQ10.100
GPNAM[8] SMSQ10.100
GPZ6 100.00 %
GPZ7 -17.13 %
GPZ8 -13.17 %
P19 600.00 usec
P30 2150.00 usec

F1 - Acquisition parameters
TD 16
SFO1 600.1328 MHz
FIDRES 751.201904 Hz
SW 10.014 ppm
FnMODE QF

F2 - Processing parameters
SI 65536
SF 600.1299974 MHz
WDW EM
SSB 0
LB 1.00 Hz
GB 0
PC 1.00

F1 - Processing parameters
SI 256
MC2 QF
SF 600.1375728 MHz
WDW no
SSB 0
LB 0 Hz
GB 0

^{15}N-edited NOESY spectrum of 11.0 mM peptide **2a** in 9:1 H_2O/D_2O at 800 MHz and 298 K with WATERGATE suppression of the HOD peak and 120-msec mixing time

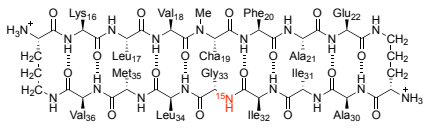

Virtual Projection taken from
11 mM peptide **2** in 9:1 H_2O/D_2O

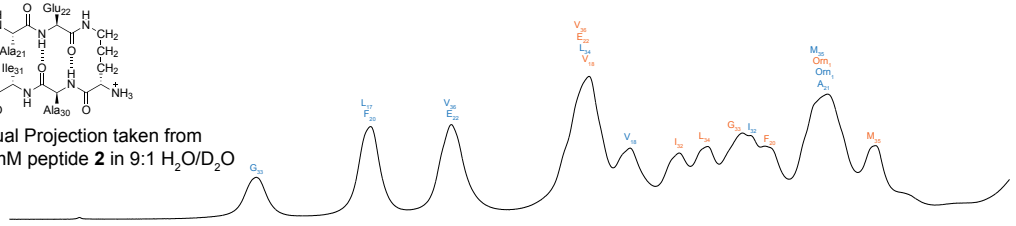

Virtual Projection taken from
11 mM peptide **2** in 9:1 H_2O/D_2O

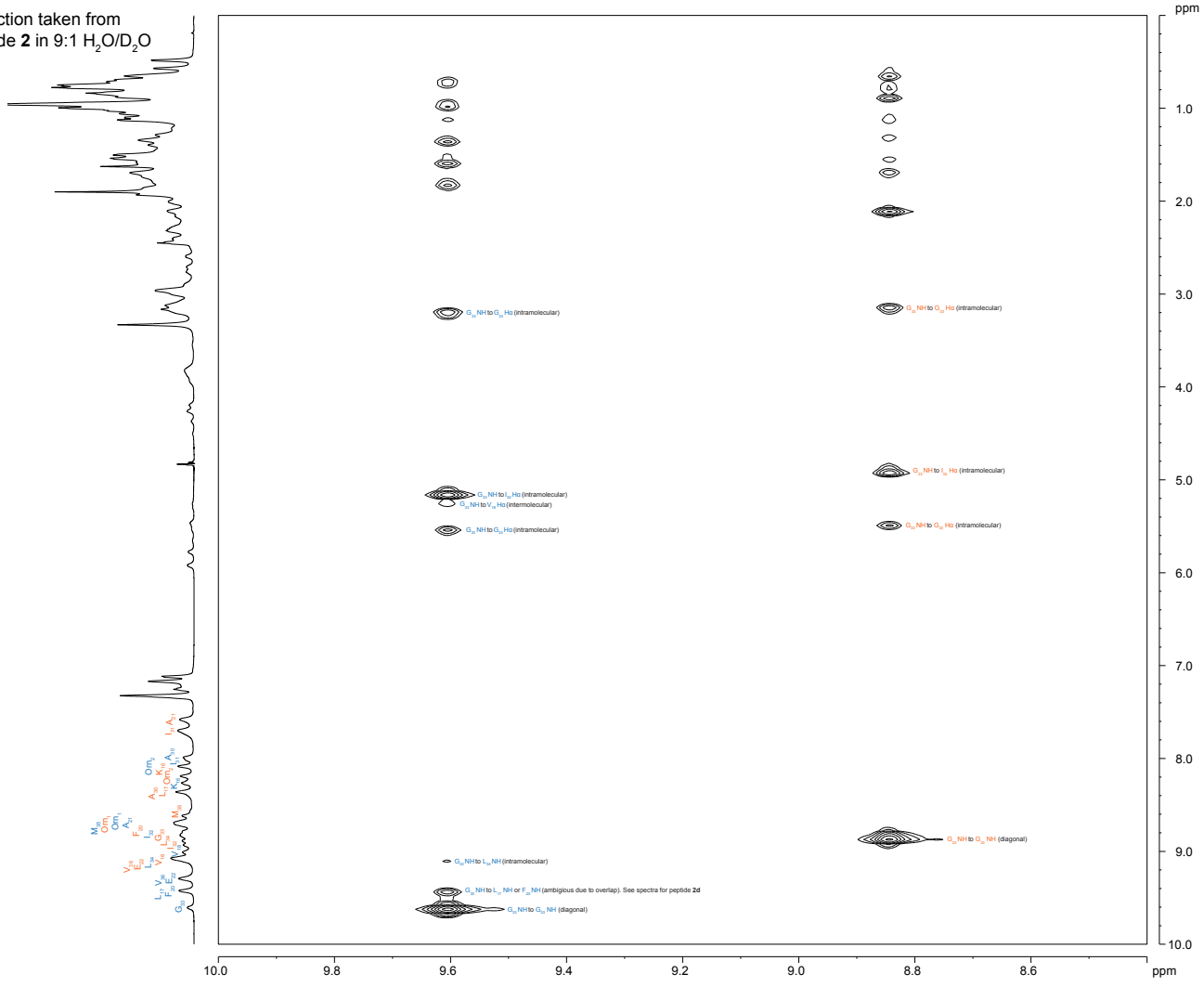


```
Current Data Parameters
NAME          JZ-II-299
EXPNO             14
PROCNO            15

F2 - Acquisition Parameters
Date_         20240704
Time              7.54 h
INSTRUM           Avance
PROBHD    Z8435_0053 (PH
PULPROG   noesyhsqcf3gpwg3d
TD                2048
SOLVENT           H2O+D2O
NS                16
DS                32
SWH           9615.385 Hz
FIDRES        9.390024 Hz
AQ            0.1064960 sec
RG                101
DW            52.000 usec
DE            6.50 usec
TE            298.0 K
CNST4         90.0000000
D0            0.00000300 sec
D1            1.00000000 sec
D8            0.12000000 sec
D10           0.00000300 sec
D11           0.03000000 sec
D16           0.00020000 sec
D26           0.00277778 sec
IN0           0.00005210 sec
IN10          0.00017626 sec
TDav              1
ZGOPTNS
SFO1          799.7537563 MHz
NUC1              1H
P1            8.38 usec
P2            16.76 usec
P11           1000.00 usec
P29           4000.00 usec
PLW1          27.04899025 W
SPNAM[1]      Sinc1.1000
SPOAL1            0.500
SPOFFS1           0 Hz
SPW1          0.00548277 W
SPNAM[11      Sinc1.1000
SPOAL11           0.500
SPOFFS11          0 Hz
SPW11         0.00034232 W
SFO3          81.0474452 MHz
NUC3              15N
CPDPRG[3          garp
P21           32.79 usec
P22           65.58 usec
PCPD3         220.00 usec
PLW3          430.00000000 W
PLW16         9.55510044 W
GPNAM[3]      SMSQ10.100
GPX3              0 %
GPY3              0 %
GPZ3              -50.00 %
GPNAM[4]      SMSQ10.100
GPX4              0 %
GPY4              0 %
GPZ4              40.00 %
GPNAM[5]      SMSQ10.100
GPX5              0 %
GPY5              0 %
GPZ5              50.00 %
GPNAM[6]      SMSQ10.100
GPX6              0 %
GPY6              0 %
GPZ6              30.00 %
GPNAM[7]      SMSQ10.100
GPX7              0 %
GPY7              0 %
GPZ7              31.00 %
P16           1000.00 usec
P30           3000.00 usec
P31           5000.00 usec

======== F2 INDIRECT DIMENSION ========
td2    1
sw_F2    35.000000

======== F1 INDIRECT DIMENSION ========
td1    1024
sw_F1    12.000000

F1 - Acquisition parameters
TD                1
SFO1          81.04745 MHz
FIDRES        5673.321289 Hz
SW                35.000 ppm
FnMODE            States-TPPI

F3 - Acquisition parameters
SW                12.000 ppm
SFO1          799.7538 MHz
HZpPT         1.171514 Hz
TD                1024

F2 - Processing parameters
SI                2048
SF            799.7498992 MHz
WDW               QSINE
SSB               2
LB                0 Hz
GB                0
PC                4.00

F1 - Processing parameters
SI                256
MC2               States-TPPI
SF            799.7498984 MHz
WDW               QSINE
SSB               2
LB                0 Hz
GB                0
```

^{1}H NMR stacked plot of 11.0 mM peptide **2** and **2b** showing key Hα resonances that disappear with deuteration in D_2O at 298 K. Peptide **2** taken at 600 MHz and peptide **2b** taken at 800 MHz.

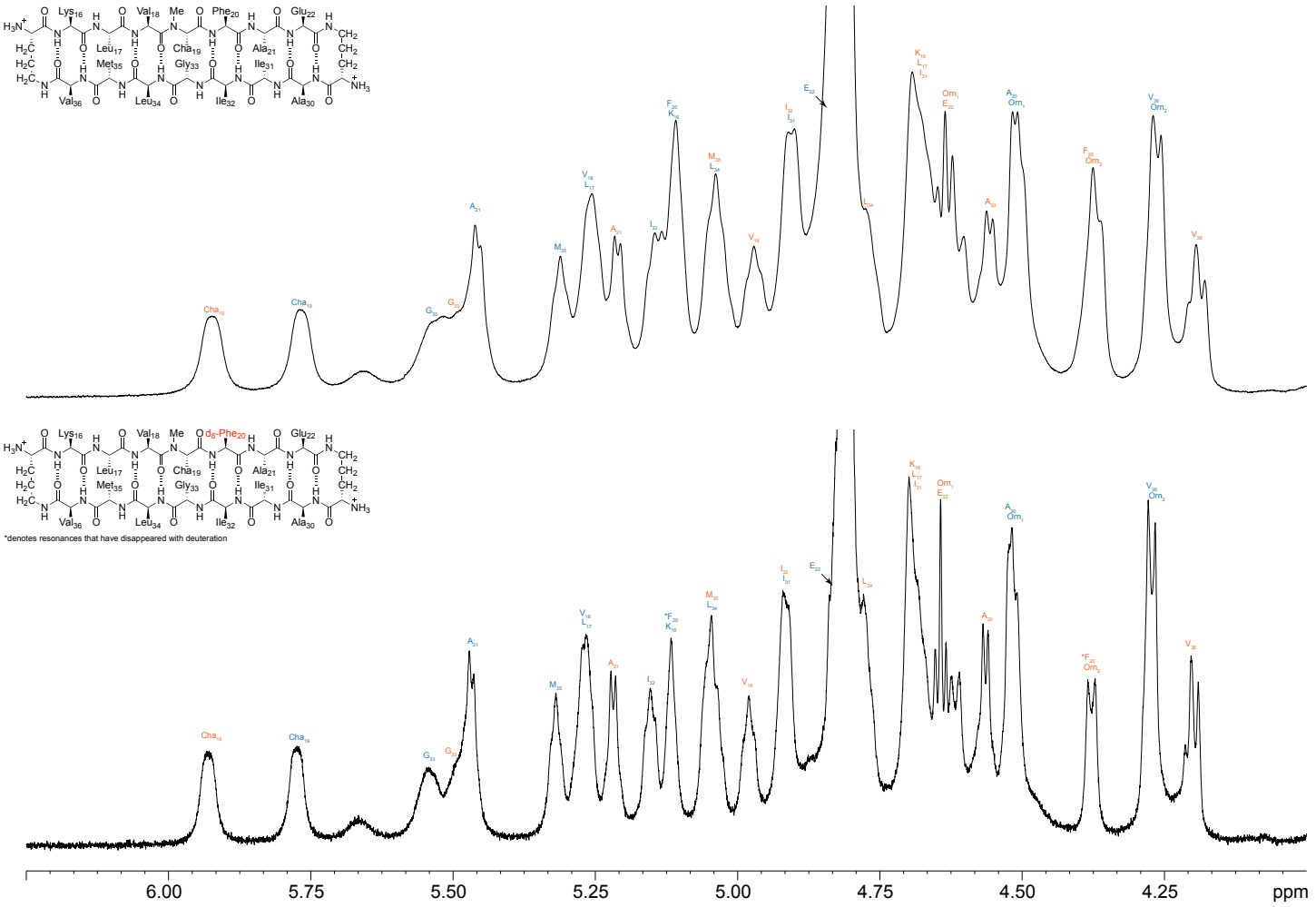

Current Data Parameters
NAME JZ-II-300
EXPNO 11
PROCNO 1

F2 - Acquisition Parameters
Date_ 20240705
Time 0.06 h
INSTRUM Avance
PROBHD Z8435_0053 (PH
PULPROG zg30
TD 65536
SOLVENT D2O
NS 16
DS 2
SWH 16129.032 Hz
FIDRES 0.492219 Hz
AQ 2.0316160 sec
RG 101
DW 31.000 usec
DE 10.26 usec
TE 298.0 K
D1 1.00000000 sec
TD0 1
SFO1 799.7549385 MHz
NUC1 1H
P0 2.67 usec
P1 8.00 usec
PLW1 27.04899979 W

F2 - Processing parameters
SI 65536
SF 799.7499130 MHz
WDW no
SSB 0
LB 0 Hz
GB 0
PC 1.00

^{1}H NMR stacked plot of 11.0 mM peptide **2** and **2c** showing key Hα resonances that disappear with deuteration in D_2O at 298 K. Peptide **2** taken at 600 MHz and peptide **2c** taken at 800 MHz

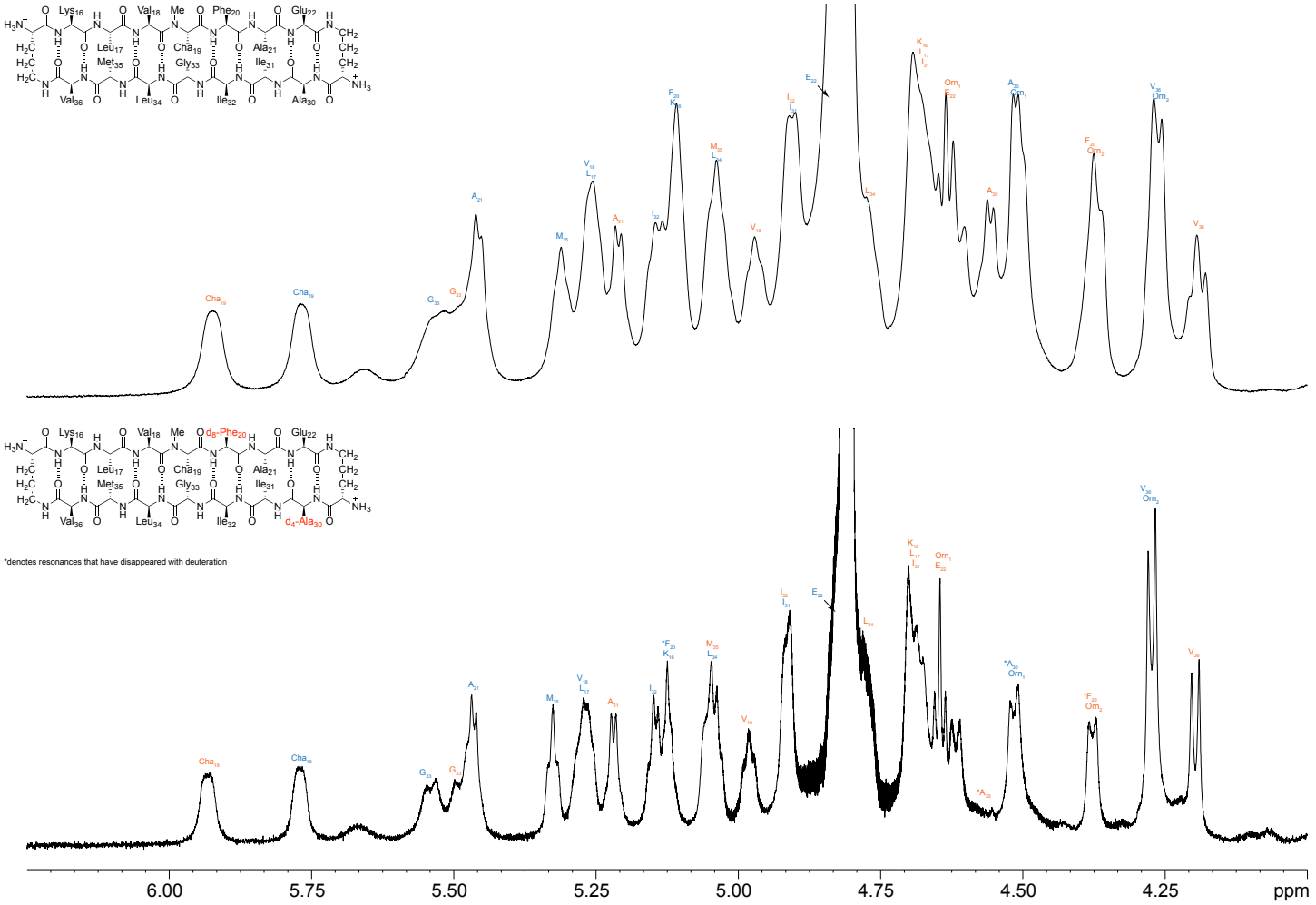

Current Data Parameters
NAME JZ-II-301
EXPNO 1
PROCNO 1

F2 - Acquisition Parameters
Date_ 20240709
Time 8.56 h
INSTRUM Avance
PROBHD Z8435_0053 (PH
PULPROG zg30
TD 65536
SOLVENT D2O
NS 16
DS 2
SWH 16129.032 Hz
FIDRES 0.492219 Hz
AQ 2.0316160 sec
RG 32
DW 31.000 usec
DE 10.26 usec
TE 298.0 K
D1 1.00000000 sec
TD0 1
SFO1 799.7549385 MHz
NUC1 1H
P0 2.67 usec
P1 8.00 usec
PLW1 27.04899979 W

F2 - Processing parameters
SI 65536
SF 799.7499133 MHz
WDW no
SSB 0
LB 0 Hz
GB 0
PC 1.00

$^{1}H,^{15}N$ HSQC spectrum of 1.0 mM peptide **2d** in 9:1 H_2O/D_2O at 800 MHz and 298 K with WATERGATE suppression of the HOD peak

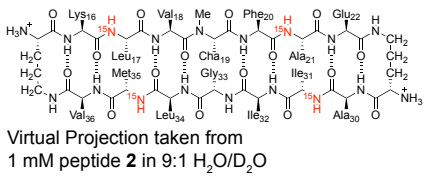

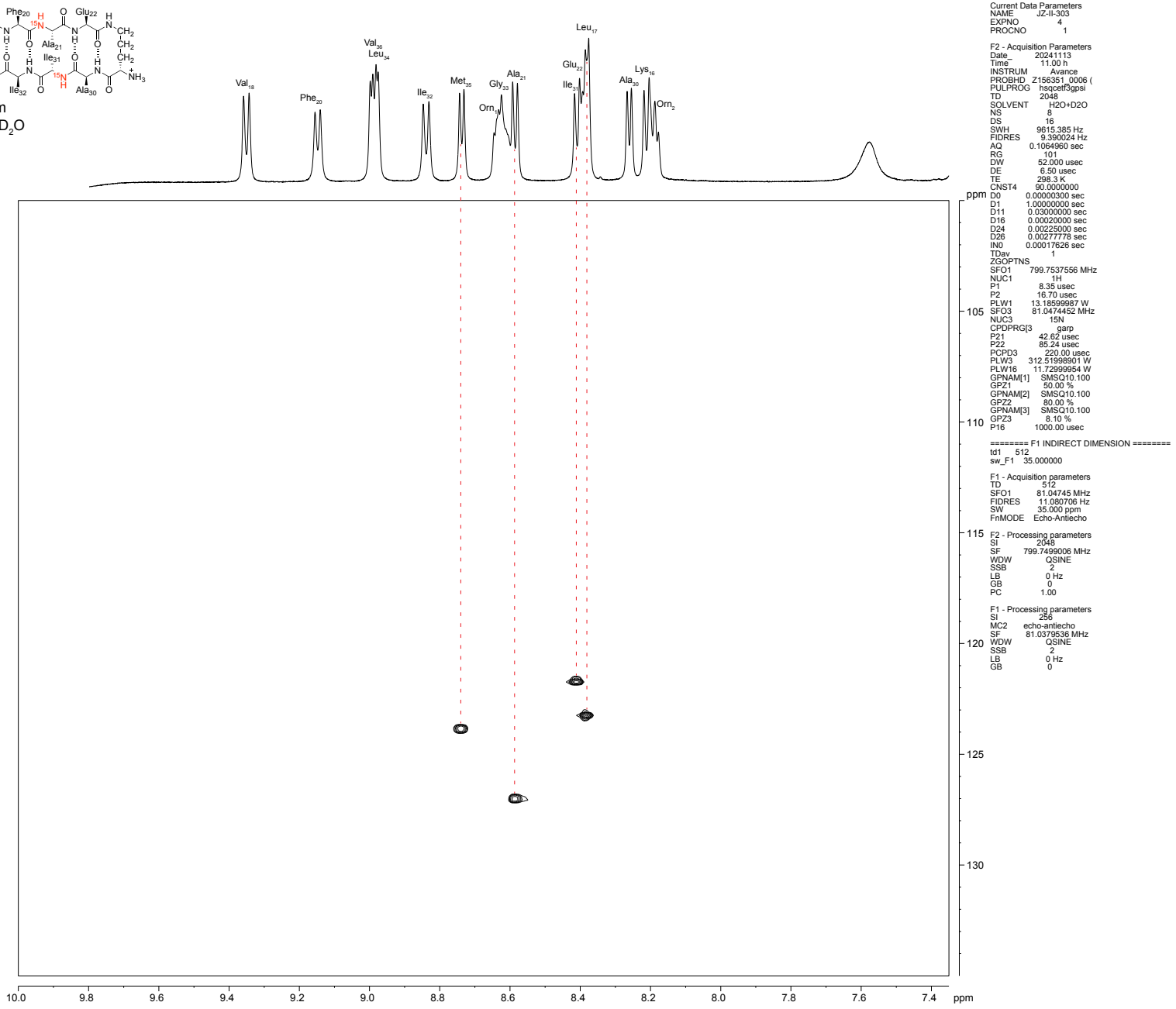

Current Data Parameters
NAME JZ-II-303
EXPNO 4
PROCNO 1

F2 - Acquisition Parameters
Date_ 20241113
Time 11.00 h
INSTRUM Avance
PROBHD Z156351_0006 (
PULPROG hsqcetf3gpsi
TD 2048
SOLVENT H2O+D2O
NS 8
DS 16
SWH 9615.385 Hz
FIDRES 9.390024 Hz
AQ 0.1064960 sec
RG 101
DW 52.000 usec
DE 6.50 usec
TE 298.3 K
CNST4 90.0000000
D0 0.00000300 sec
D1 1.00000000 sec
D11 0.03000000 sec
D16 0.00020000 sec
D24 0.00225000 sec
D26 0.00277778 sec
IN0 0.00017626 sec
TDav 1
ZGOPTNS
SFO1 799.7537556 MHz
NUC1 1H
P1 8.35 usec
P2 16.70 usec
PLW1 13.18599987 W
SFO3 81.0474452 MHz
NUC3 15N
CPDPRG[3 garp
P21 42.62 usec
P22 85.24 usec
PCPD3 220.00 usec
PLW3 312.51998901 W
PLW16 11.72999954 W
GPNAM[1] SMSQ10.100
GPZ1 50.00 %
GPNAM[2] SMSQ10.100
GPZ2 80.00 %
GPNAM[3] SMSQ10.100
GPZ3 8.10 %
P16 1000.00 usec

======== F1 INDIRECT DIMENSION ========
td1 512
sw_F1 35.000000

F1 - Acquisition parameters
TD 512
SFO1 81.04745 MHz
FIDRES 11.080706 Hz
SW 35.000 ppm
FnMODE Echo-Antiecho

F2 - Processing parameters
SI 2048
SF 799.7499006 MHz
WDW QSINE
SSB 2
LB 0 Hz
GB 0
PC 1.00

F1 - Processing parameters
SI 256
MC2 echo-antiecho
SF 81.0379536 MHz
WDW QSINE
SSB 2
LB 0 Hz
GB 0

$^{1}H,^{15}N$ HSQC spectrum of 11.0 mM peptide **2d** in 9:1 H_2O/D_2O at 800 MHz and 298 K with WATERGATE suppression of the HOD peak

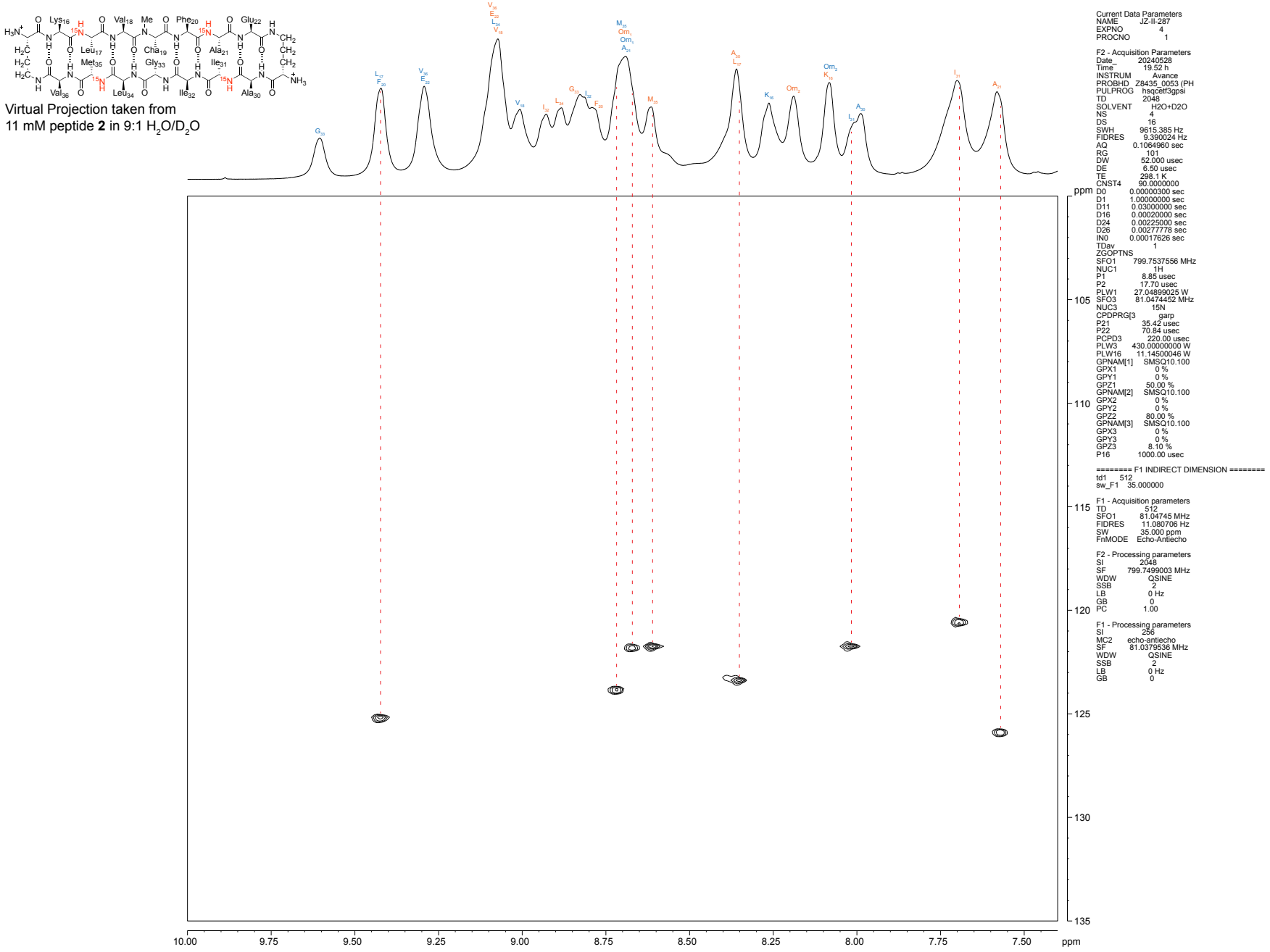

^{1}H NMR DOSY spectrum of 1.0 mM peptide **3a** in D_2O at 600 MHz and 298 K

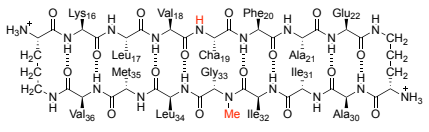

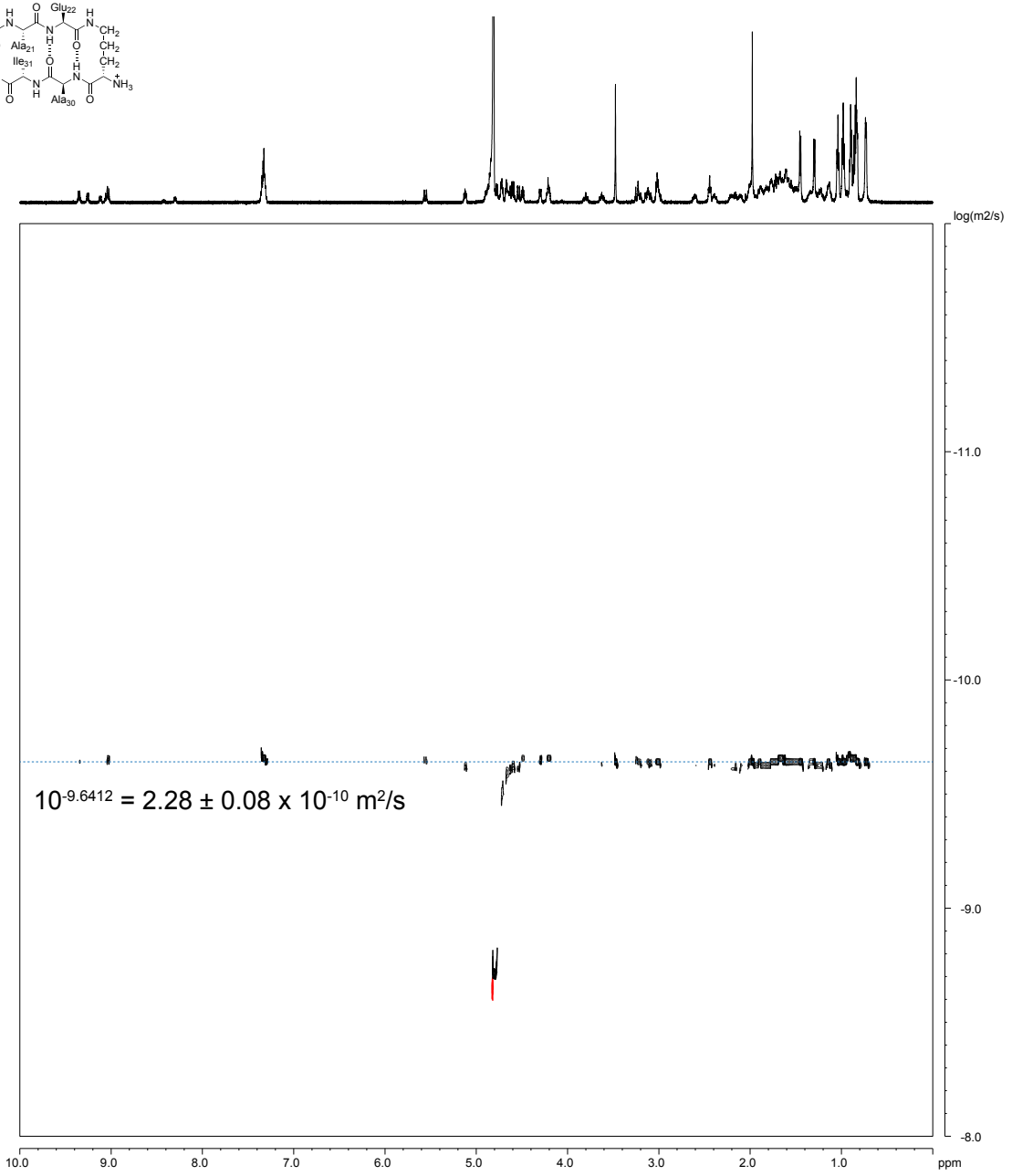

Current Data Parameters
NAME JZ-II-137
EXPNO 17
PROCNO 1

F2 - Acquisition Parameters
Date_ 20230721
Time 0.09
INSTRUM av600
PROBHD 5 mm CPBBO BB-
PULPROG ledbpgp2s
TD 98074
SOLVENT D2O
NS 8
DS 4
SWH 6602.113 Hz
FIDRES 0.067318 Hz
AQ 7.4274712 sec
RG 57
DW 75.733 usec
DE 17.67 usec
TE 298.0 K
D1 5.00000000 sec
D16 0.00020000 sec
D20 0.07500000 sec
D21 0.00500000 sec

======== CHANNEL f1 ========
SFO1 600.1330006 MHz
NUC1 1H
P1 9.75 usec
P2 19.50 usec
PLW1 30.00000000 W

====== GRADIENT CHANNEL =====
GPNAM[6] SMSQ10.100
GPNAM[7] SMSQ10.100
GPNAM[8] SMSQ10.100
GPZ6 100.00 %
GPZ7 -17.13 %
GPZ8 -13.17 %
P19 600.00 usec
P30 1400.00 usec

F1 - Acquisition parameters
TD 16
SFO1 600.1328 MHz
FIDRES 751.201904 Hz
SW 10.014 ppm
FnMODE QF

F2 - Processing parameters
SI 65536
SF 600.1300054 MHz
WDW EM
SSB 0
LB 5.00 Hz
GB 0
PC 1.00

F1 - Processing parameters
SI 256
MC2 QF
SF 600.1376011 MHz
WDW no
SSB 0
LB 0 Hz
GB 0

^{1}H NMR DOSY spectrum of 8.0 mM peptide **3a** in D_2O at 600 MHz and 298 K

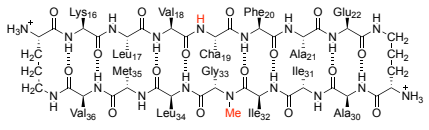

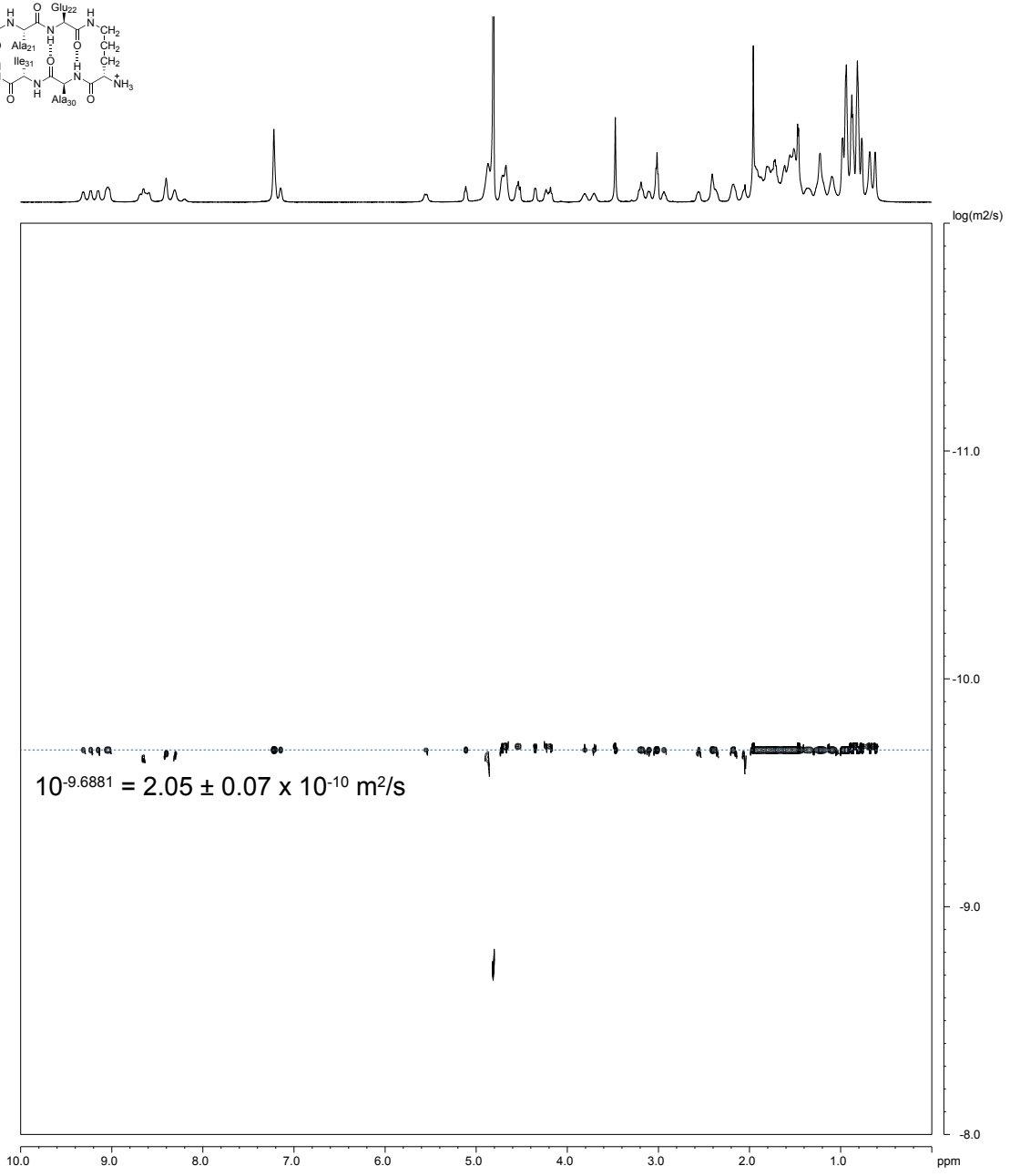

Current Data Parameters
NAME JZ-II-137
EXPNO 7
PROCNO 1

F2 - Acquisition Parameters
Date_ 20230720
Time 22.53
INSTRUM av600
PROBHD 5 mm CPBBO BB-
PULPROG ledbpgp2s
TD 98074
SOLVENT D2O
NS 8
DS 4
SWH 6602.113 Hz
FIDRES 0.067318 Hz
AQ 7.4274712 sec
RG 32
DW 75.733 usec
DE 16.87 usec
TE 298.0 K
D1 5.00000000 sec
D16 0.00020000 sec
D20 0.07500000 sec
D21 0.00500000 sec

======== CHANNEL f1 ========
SFO1 600.1330006 MHz
NUC1 1H
P1 11.00 usec
P2 22.00 usec
PLW1 30.00000000 W

====== GRADIENT CHANNEL =====
GPNAM[6] SMSQ10.100
GPNAM[7] SMSQ10.100
GPNAM[8] SMSQ10.100
GPZ6 100.00 %
GPZ7 -17.13 %
GPZ8 -13.17 %
P19 600.00 usec
P30 1400.00 usec

F1 - Acquisition parameters
TD 16
SFO1 600.1328 MHz
FIDRES 751.201904 Hz
SW 10.014 ppm
FnMODE QF

F2 - Processing parameters
SI 65536
SF 600.1299971 MHz
WDW EM
SSB 0
LB 2.00 Hz
GB 0
PC 1.00

F1 - Processing parameters
SI 256
MC2 QF
SF 600.1376103 MHz
WDW no
SSB 0
LB 0 Hz
GB 0

^{1}H NMR DOSY spectrum of 1.0 mM peptide **3b** in D_2O at 600 MHz and 298 K

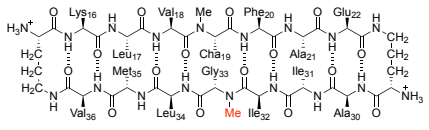

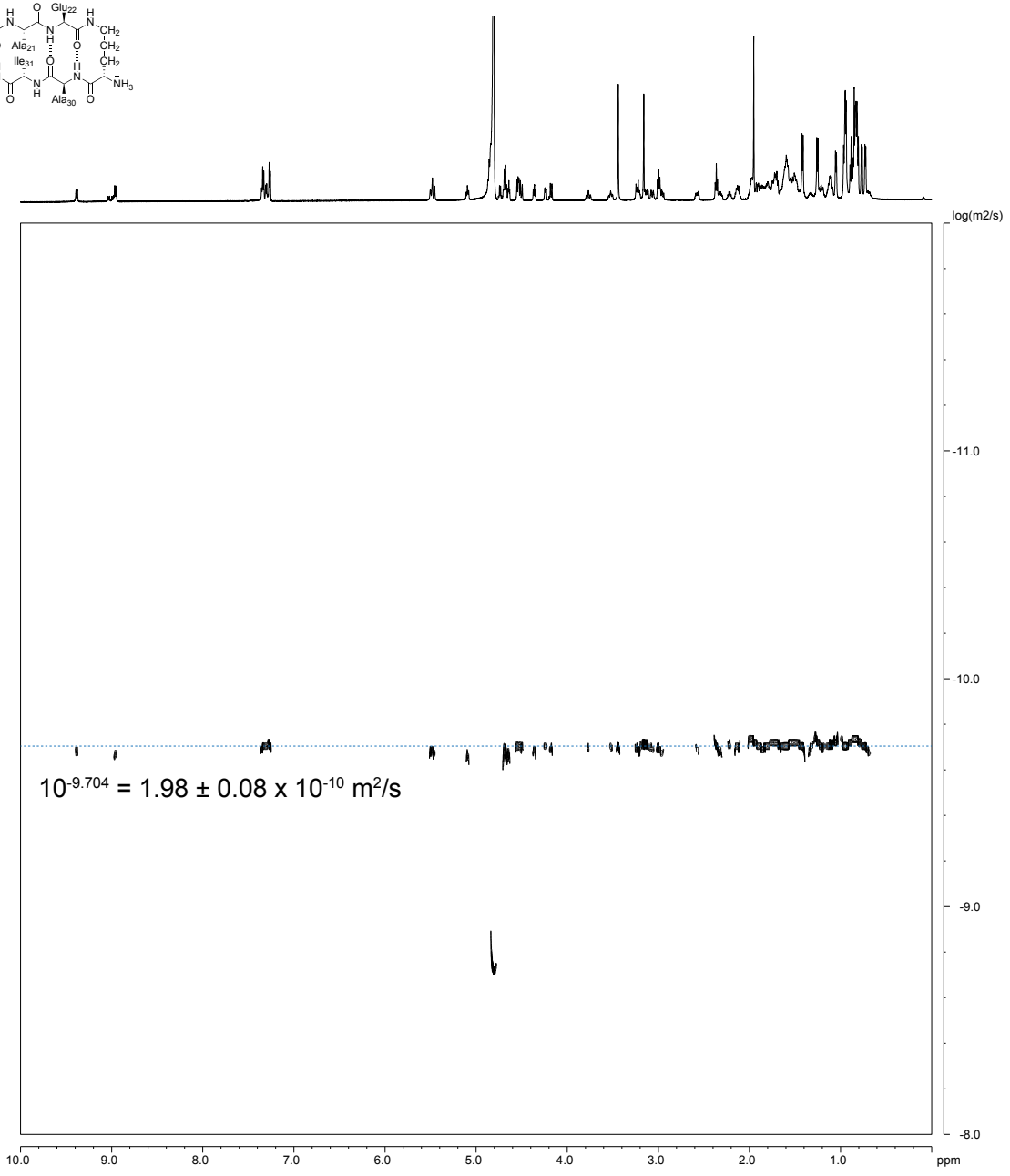


```
Current Data Parameters
NAME          JZ-II-302
EXPNO             65
PROCNO             1

F2 - Acquisition Parameters
Date_         20240819
Time          23.54
INSTRUM       av600
PROBHD   5 mm CPBBO BB-
PULPROG       ledbpgp2s
TD            98074
SOLVENT       D2O
NS                8
DS                4
SWH           9615.385 Hz
FIDRES        0.098042 Hz
AQ            5.0998478 sec
RG            28.5
DW            52.000 usec
DE            17.63 usec
TE            297.9 K
D1            5.00000000 sec
D16           0.00020000 sec
D20           0.07500000 sec
D21           0.00500000 sec

======== CHANNEL f1 ========
SFO1          600.1342009 MHz
NUC1              1H
P1            8.00 usec
P2            16.00 usec
PLW1          30.00000000 W

====== GRADIENT CHANNEL =====
GPNAM[6]      SMSQ10.100
GPNAM[7]      SMSQ10.100
GPNAM[8]      SMSQ10.100
GPZ6          100.00 %
GPZ7          -17.13 %
GPZ8          -13.17 %
P19           600.00 usec
P30           1600.00 usec

F1 - Acquisition parameters
TD                16
SFO1          600.1328 MHz
FIDRES        751.201904 Hz
SW            10.014 ppm
FnMODE            QF

F2 - Processing parameters
SI            65536
SF            600.1299973 MHz
WDW               EM
SSB               0
LB            5.00 Hz
GB                0
PC            1.00

F1 - Processing parameters
SI                256
MC2               QF
SF            600.1375822 MHz
WDW               no
SSB               0
LB            0 Hz
GB                0
```

^{1}H NMR DOSY spectrum of 4.0 mM peptide **3b** in D_2O at 600 MHz and 298 K

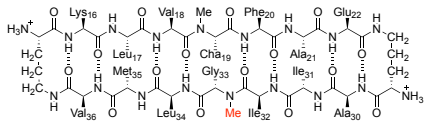

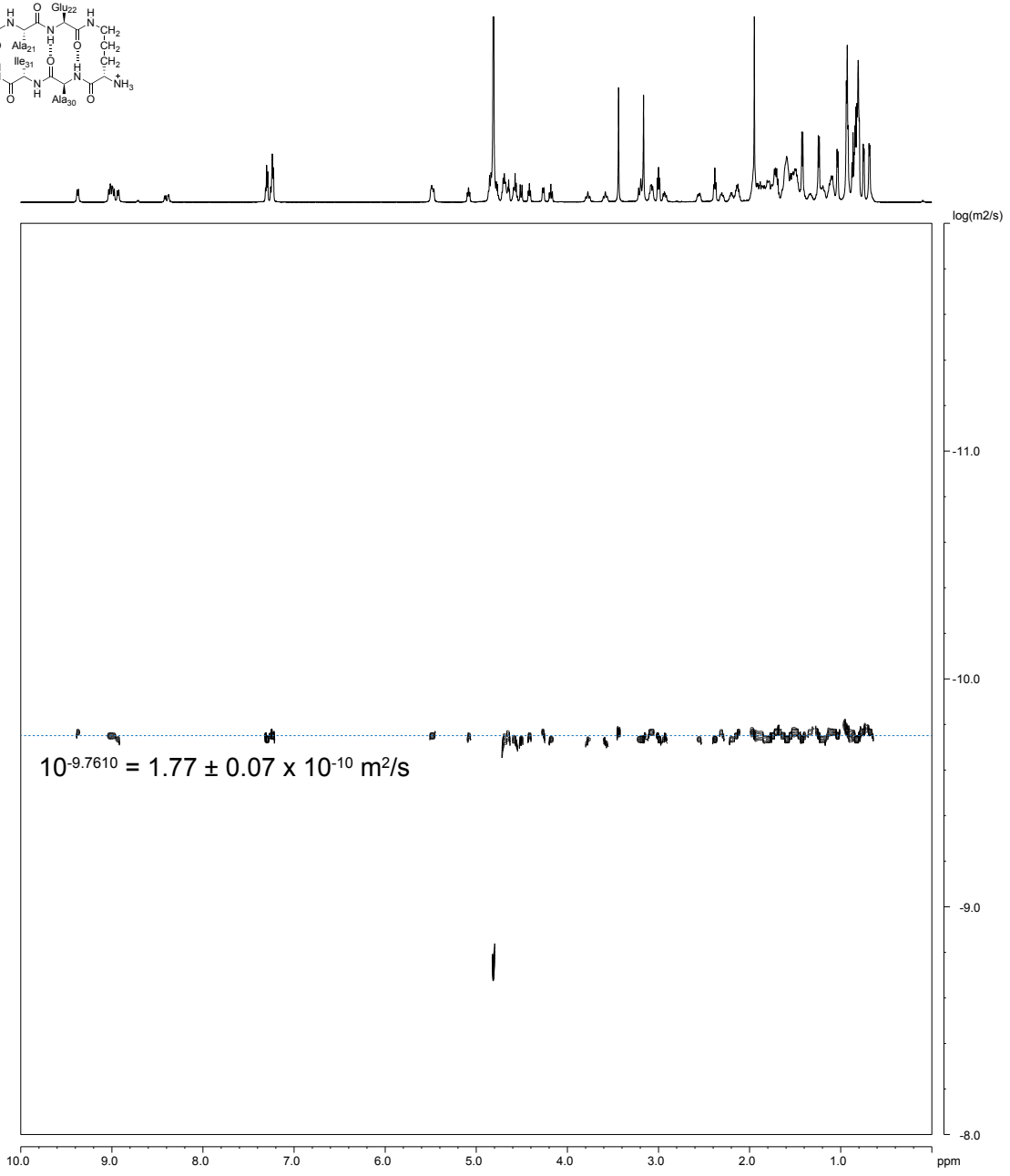


```
Current Data Parameters
NAME          JZ-II-302
EXPNO              55
PROCNO              1

F2 - Acquisition Parameters
Date_         20240819
Time          22.45
INSTRUM       av600
PROBHD   5 mm CPBBO BB-
PULPROG       ledbpgp2s
TD            98074
SOLVENT          D2O
NS                8
DS                4
SWH          9615.385 Hz
FIDRES       0.098042 Hz
AQ           5.0998478 sec
RG               32
DW           52.000 usec
DE           17.63 usec
TE           298.0 K
D1           5.00000000 sec
D16          0.00020000 sec
D20          0.07500000 sec
D21          0.00500000 sec

======== CHANNEL f1 ========
SFO1         600.1342009 MHz
NUC1              1H
P1           8.00 usec
P2           16.00 usec
PLW1         30.00000000 W

====== GRADIENT CHANNEL =====
GPNAM[6]     SMSQ10.100
GPNAM[7]     SMSQ10.100
GPNAM[8]     SMSQ10.100
GPZ6         100.00 %
GPZ7         -17.13 %
GPZ8         -13.17 %
P19          600.00 usec
P30          1900.00 usec

F1 - Acquisition parameters
TD                16
SFO1         600.1328 MHz
FIDRES       751.201904 Hz
SW           10.014 ppm
FnMODE            QF

F2 - Processing parameters
SI            65536
SF           600.1299972 MHz
WDW               EM
SSB               0
LB           5.00 Hz
GB                0
PC           1.00

F1 - Processing parameters
SI               256
MC2               QF
SF           600.1375634 MHz
WDW               no
SSB               0
LB           0 Hz
GB                0
```

^{1}H NMR DOSY spectrum of 1.0 mM peptide **3c** in D_2O at 600 MHz and 298 K

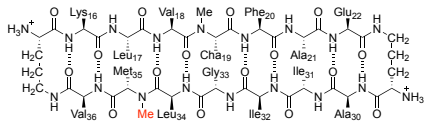

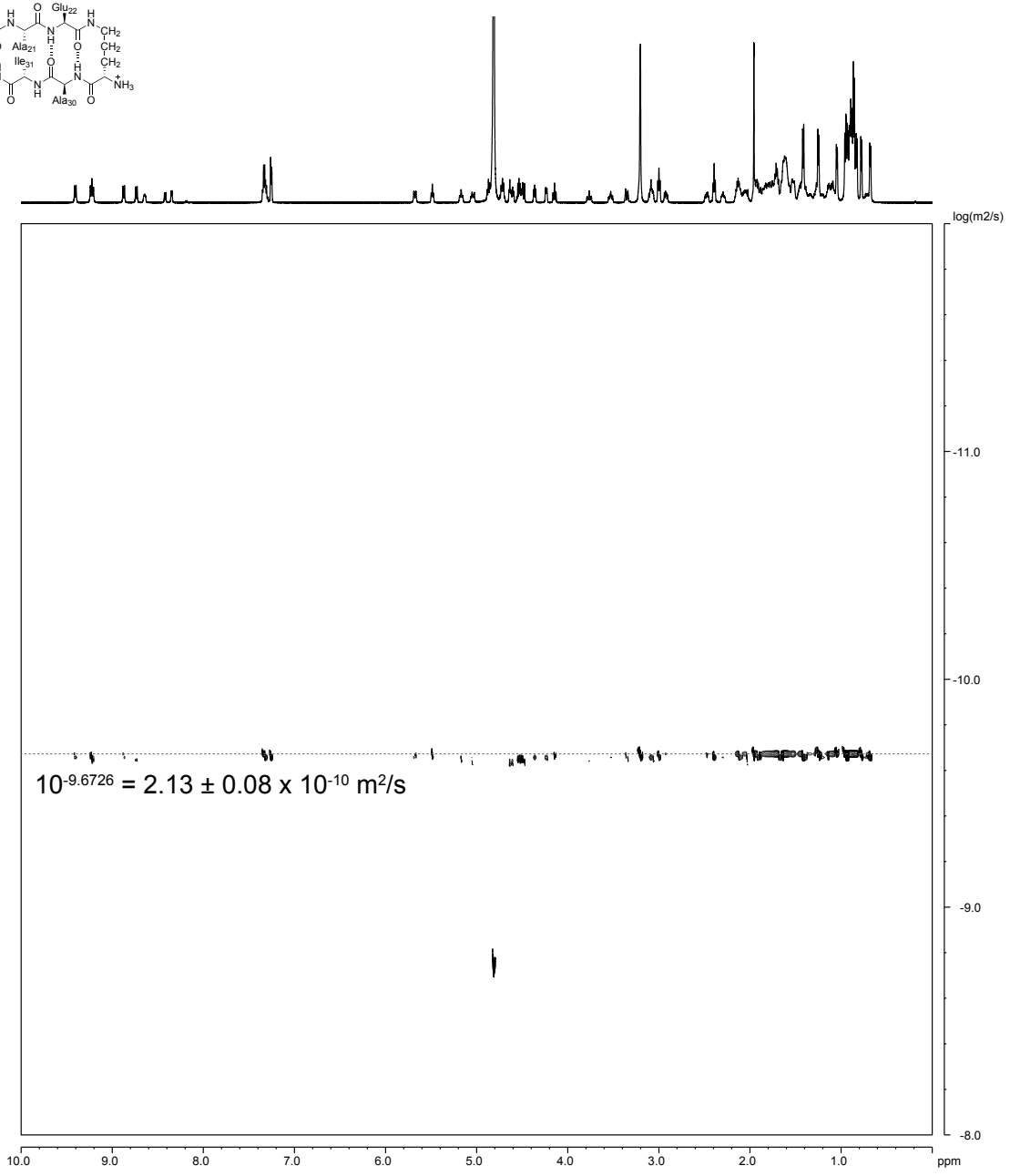


```
Current Data Parameters
NAME          JZ-II-286
EXPNO              15
PROCNO              1

F2 - Acquisition Parameters
Date_         20241020
Time              16.12
INSTRUM           av600
PROBHD   5 mm CPBBO BB-
PULPROG       ledbpgp2s
TD                98074
SOLVENT             D2O
NS                    8
DS                    4
SWH           7194.245 Hz
FIDRES        0.073355 Hz
AQ            6.8161430 sec
RG                 50.8
DW                69.500 usec
DE                16.15 usec
TE                298.0 K
D1            5.00000000 sec
D16           0.00020000 sec
D20           0.07500000 sec
D21           0.00500000 sec

======== CHANNEL f1 ========
SFO1        600.1328866 MHz
NUC1                   1H
P1                 9.00 usec
P2                18.00 usec
PLW1        30.00000000 W

====== GRADIENT CHANNEL =====
GPNAM[6]      SMSQ10.100
GPNAM[7]      SMSQ10.100
GPNAM[8]      SMSQ10.100
GPZ6             100.00 %
GPZ7             -17.13 %
GPZ8             -13.17 %
P19              600.00 usec
P30              1550.00 usec

F1 - Acquisition parameters
TD                    16
SFO1          600.1328 MHz
FIDRES        751.201904 Hz
SW             10.014 ppm
FnMODE                QF

F2 - Processing parameters
SI                 65536
SF            600.1299974 MHz
WDW                   EM
SSB                    0
LB                  5.00 Hz
GB                     0
PC                  1.00

F1 - Processing parameters
SI                   256
MC2                   QF
SF            600.1375821 MHz
WDW                   no
SSB                    0
LB                  0 Hz
GB                     0
```

^{1}H NMR DOSY spectrum of 11.0 mM peptide **3c** in D_2O at 600 MHz and 298 K

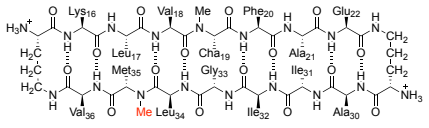

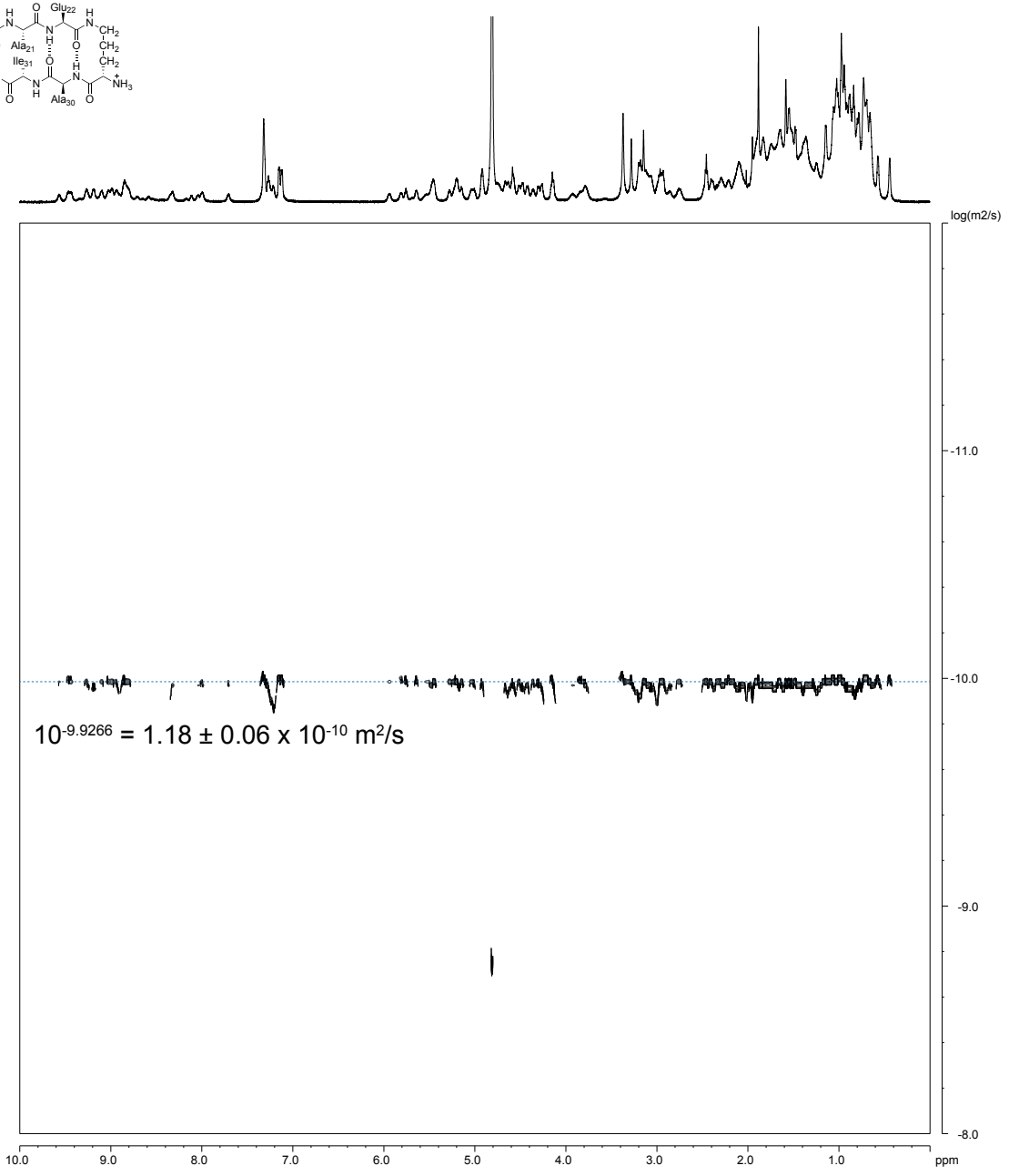

Current Data Parameters
NAME JZ-II-286
EXPNO 5
PROCNO 1

F2 - Acquisition Parameters
Date_ 20240528
Time 12.31
INSTRUM av600
PROBHD 5 mm CPBBO BB-
PULPROG ledbpgp2s
TD 98074
SOLVENT D2O
NS 8
DS 4
SWH 9615.385 Hz
FIDRES 0.098042 Hz
AQ 5.0998478 sec
RG 50.8
DW 52.000 usec
DE 16.36 usec
TE 297.9 K
D1 5.00000000 sec
D16 0.00020000 sec
D20 0.07500000 sec
D21 0.00500000 sec

======== CHANNEL f1 ========
SFO1 600.1330006 MHz
NUC1 1H
P1 10.00 usec
P2 20.00 usec
PLW1 30.00000000 W

====== GRADIENT CHANNEL =====
GPNAM[6] SMSQ10.100
GPNAM[7] SMSQ10.100
GPNAM[8] SMSQ10.100
GPZ6 100.00 %
GPZ7 -17.13 %
GPZ8 -13.17 %
P19 600.00 usec
P30 2300.00 usec

F1 - Acquisition parameters
TD 16
SFO1 600.1328 MHz
FIDRES 751.201904 Hz
SW 10.014 ppm
FnMODE QF

F2 - Processing parameters
SI 65536
SF 600.1299976 MHz
WDW EM
SSB 0
LB 2.00 Hz
GB 0
PC 1.00

F1 - Processing parameters
SI 256
MC2 QF
SF 600.1375728 MHz
WDW no
SSB 0
LB 0 Hz
GB 0

^{1}H NMR DOSY spectrum of 1.0 mM peptide **4a** in D_2O at 600 MHz and 298 K

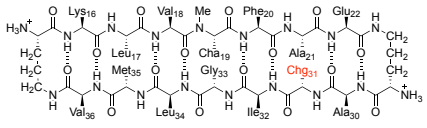

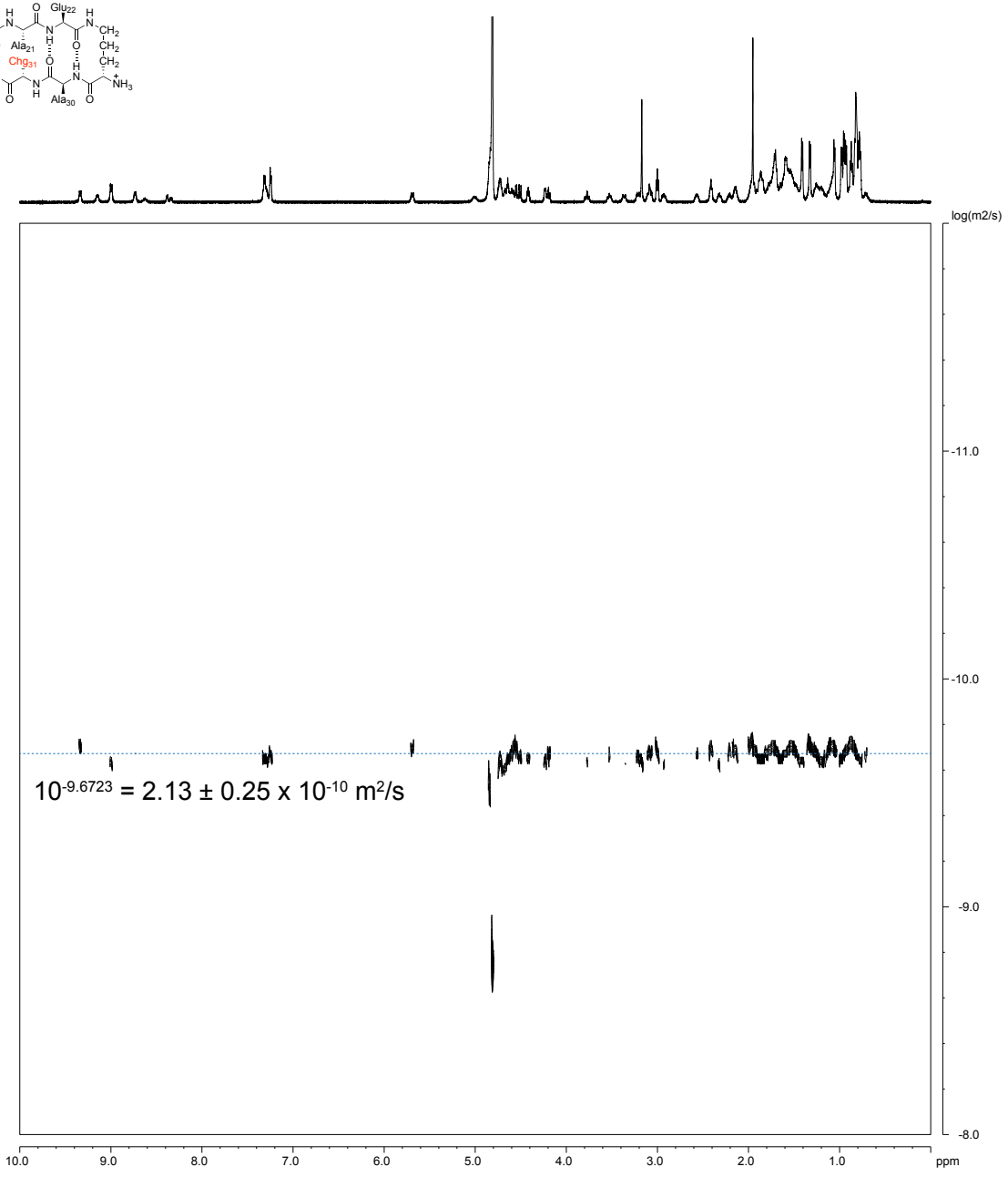

Current Data Parameters
NAME JZ-II-122
EXPNO 8
PROCNO 1

F2 - Acquisition Parameters
Date_ 20230627
Time 23.54
INSTRUM av600
PROBHD 5 mm CPBBO BB-
PULPROG ledbpgp2s
TD 98074
SOLVENT D2O
NS 8
DS 4
SWH 6602.113 Hz
FIDRES 0.067318 Hz
AQ 7.4274712 sec
RG 71.8
DW 75.733 usec
DE 18.78 usec
TE 298.2 K
D1 5.00000000 sec
D16 0.00020000 sec
D20 0.07500000 sec
D21 0.00500000 sec

======== CHANNEL f1 ========
SFO1 600.1330006 MHz
NUC1 1H
P1 8.00 usec
P2 16.00 usec
PLW1 30.00000000 W

====== GRADIENT CHANNEL =====
GPNAM[6] SMSQ10.100
GPNAM[7] SMSQ10.100
GPNAM[8] SMSQ10.100
GPZ6 100.00 %
GPZ7 -17.13 %
GPZ8 -13.17 %
P19 600.00 usec
P30 1700.00 usec

F1 - Acquisition parameters
TD 16
SFO1 600.1328 MHz
FIDRES 751.201904 Hz
SW 10.014 ppm
FnMODE QF

F2 - Processing parameters
SI 65536
SF 600.1299677 MHz
WDW EM
SSB 0
LB 2.00 Hz
GB 0
PC 1.00

F1 - Processing parameters
SI 256
MC2 QF
SF 600.1375450 MHz
WDW no
SSB 0
LB 0 Hz
GB 0

^{1}H NMR DOSY spectrum of 6.0 mM peptide **4a** in D_2O at 600 MHz and 298 K

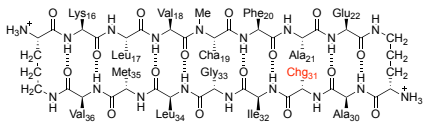

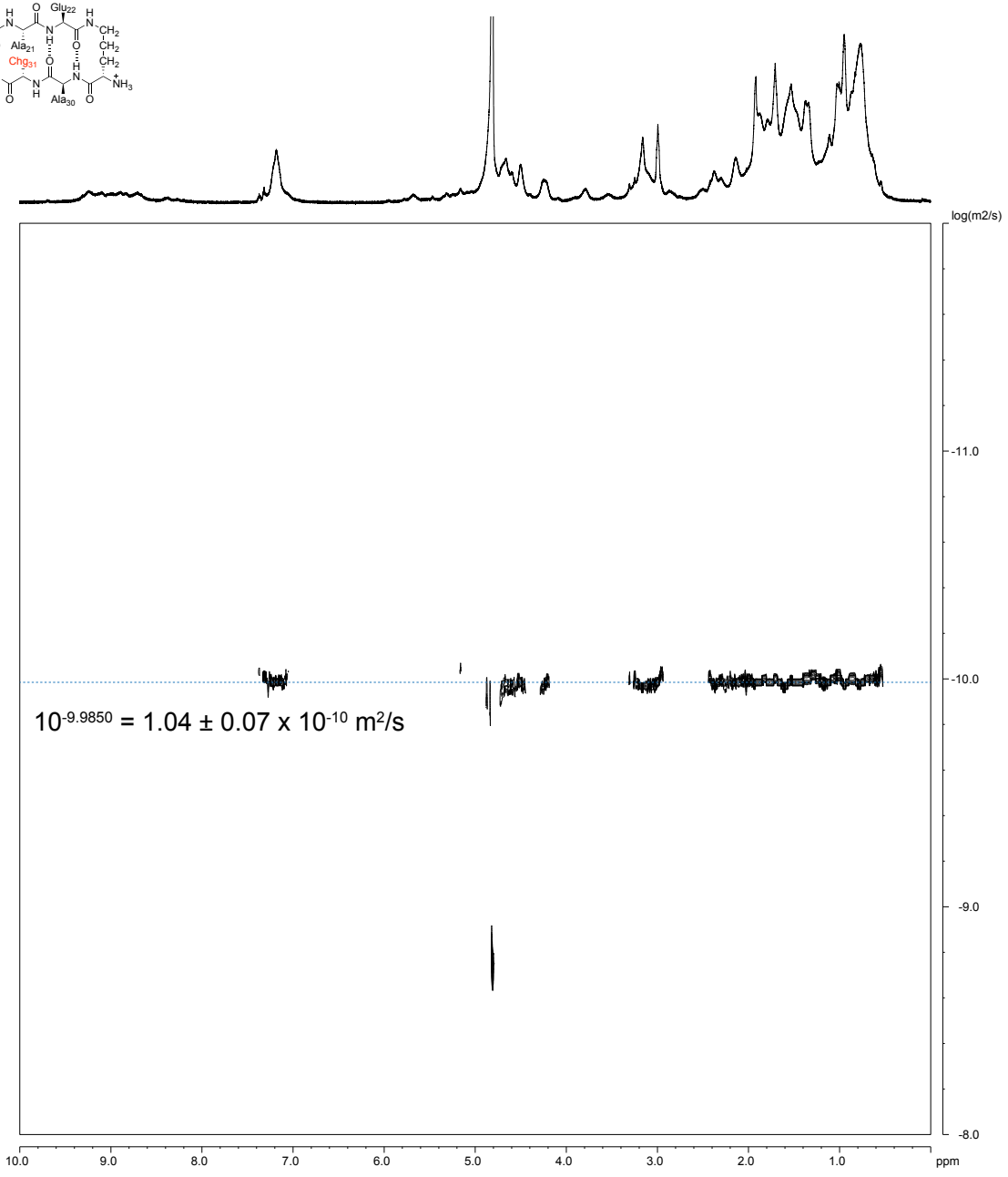

Current Data Parameters
NAME JZ-II-122
EXPNO 14
PROCNO 1

F2 - Acquisition Parameters
Date_ 20230628
Time 1.18
INSTRUM av600
PROBHD 5 mm CPBBO BB-
PULPROG ledbpgp2s
TD 98074
SOLVENT D2O
NS 8
DS 4
SWH 9615.385 Hz
FIDRES 0.098042 Hz
AQ 5.0998478 sec
RG 57
DW 52.000 usec
DE 17.63 usec
TE 298.2 K
D1 5.00000000 sec
D16 0.00020000 sec
D20 0.07500000 sec
D21 0.00500000 sec

======== CHANNEL f1 ========
SFO1 600.1330006 MHz
NUC1 1H
P1 8.00 usec
P2 16.00 usec
PLW1 30.00000000 W

====== GRADIENT CHANNEL =====
GPNAM[6] SMSQ10.100
GPNAM[7] SMSQ10.100
GPNAM[8] SMSQ10.100
GPZ6 100.00 %
GPZ7 -17.13 %
GPZ8 -13.17 %
P19 600.00 usec
P30 2400.00 usec

F1 - Acquisition parameters
TD 16
SFO1 600.1328 MHz
FIDRES 751.201904 Hz
SW 10.014 ppm
FnMODE QF

F2 - Processing parameters
SI 65536
SF 600.1299974 MHz
WDW EM
SSB 0
LB 2.00 Hz
GB 0
PC 1.00

F1 - Processing parameters
SI 256
MC2 QF
SF 600.1375542 MHz
WDW no
SSB 0
LB 0 Hz
GB 0

[1]H NMR DOSY spectrum of 1.0 mM peptide **4b** in D_2O at 600 MHz and 298 K

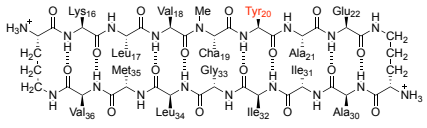

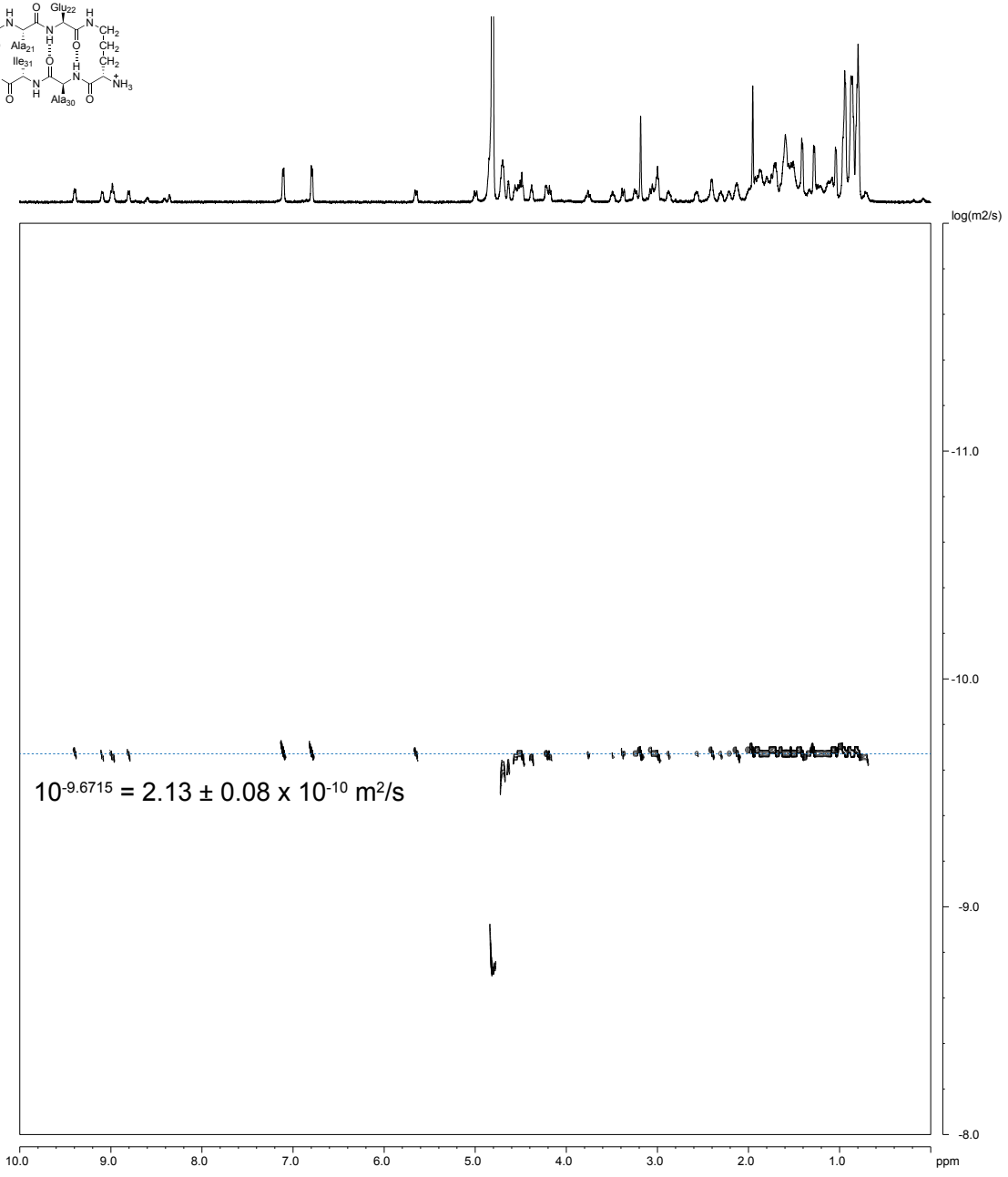

Current Data Parameters
NAME JZ-II-175
EXPNO 4
PROCNO 1

F2 - Acquisition Parameters
Date_ 20231011
Time 12.34
INSTRUM av600
PROBHD 5 mm CPBBO BB-
PULPROG ledbpgp2s
TD 98074
SOLVENT D2O
NS 8
DS 4
SWH 9615.385 Hz
FIDRES 0.098042 Hz
AQ 5.0998478 sec
RG 50.8
DW 52.000 usec
DE 16.36 usec
TE 297.9 K
D1 5.00000000 sec
D16 0.00020000 sec
D20 0.07500000 sec
D21 0.00500000 sec

======== CHANNEL f1 ========
SFO1 600.1330006 MHz
NUC1 1H
P1 10.00 usec
P2 20.00 usec
PLW1 30.00000000 W

====== GRADIENT CHANNEL =====
GPNAM[6] SMSQ10.100
GPNAM[7] SMSQ10.100
GPNAM[8] SMSQ10.100
GPZ6 100.00 %
GPZ7 -17.13 %
GPZ8 -13.17 %
P19 600.00 usec
P30 1550.00 usec

F1 - Acquisition parameters
TD 16
SFO1 600.1328 MHz
FIDRES 751.201904 Hz
SW 10.014 ppm
FnMODE QF

F2 - Processing parameters
SI 65536
SF 600.1299678 MHz
WDW EM
SSB 0
LB 10.00 Hz
GB 0
PC 1.00

F1 - Processing parameters
SI 256
MC2 QF
SF 600.1375820 MHz
WDW no
SSB 0
LB 0 Hz
GB 0

[1]H NMR DOSY spectrum of 11.0 mM peptide **4b** in D_2O at 600 MHz and 298 K

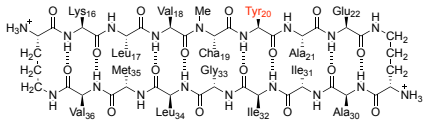

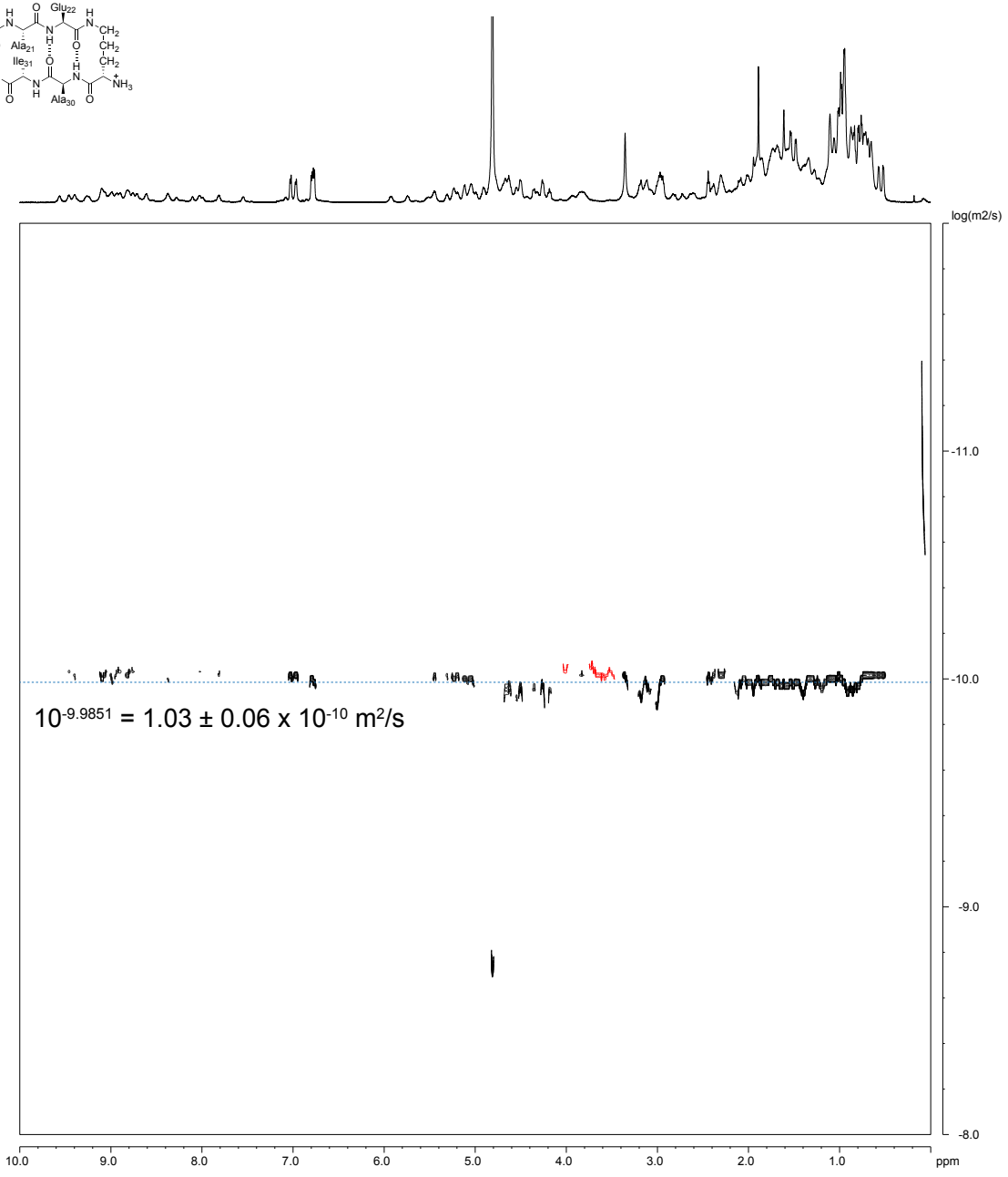


```
Current Data Parameters
NAME        JZ-II-172
EXPNO           12
PROCNO           1

F2 - Acquisition Parameters
Date_       20231006
Time        23.19
INSTRUM         av600
PROBHD   5 mm CPBBO BB-
PULPROG     ledbpgp2s
TD              98074
SOLVENT           D2O
NS                 8
DS                 4
SWH         9615.385 Hz
FIDRES      0.098042 Hz
AQ          5.0998478 sec
RG               128
DW          52.000 usec
DE          16.36 usec
TE          298.0 K
D1          5.00000000 sec
D16         0.00020000 sec
D20         0.07500000 sec
D21         0.00500000 sec

======== CHANNEL f1 ========
SFO1        600.1330006 MHz
NUC1              1H
P1          10.00 usec
P2          20.00 usec
PLW1        30.00000000 W

====== GRADIENT CHANNEL =====
GPNAM[6]    SMSQ10.100
GPNAM[7]    SMSQ10.100
GPNAM[8]    SMSQ10.100
GPZ6        100.00 %
GPZ7        -17.13 %
GPZ8        -13.17 %
P19         600.00 usec
P30         2200.00 usec

F1 - Acquisition parameters
TD                16
SFO1        600.1328 MHz
FIDRES      751.201904 Hz
SW          10.014 ppm
FnMODE            QF

F2 - Processing parameters
SI              65536
SF          600.1299977 MHz
WDW               EM
SSB               0
LB             5.00 Hz
GB                0
PC             1.00

F1 - Processing parameters
SI                256
MC2               QF
SF          600.1375728 MHz
WDW               no
SSB               0
LB             0 Hz
GB                0
```

[1]H NMR DOSY spectrum of 1.0 mM peptide **5** in D_2O at 600 MHz and 298 K

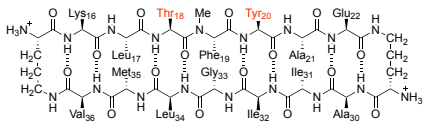

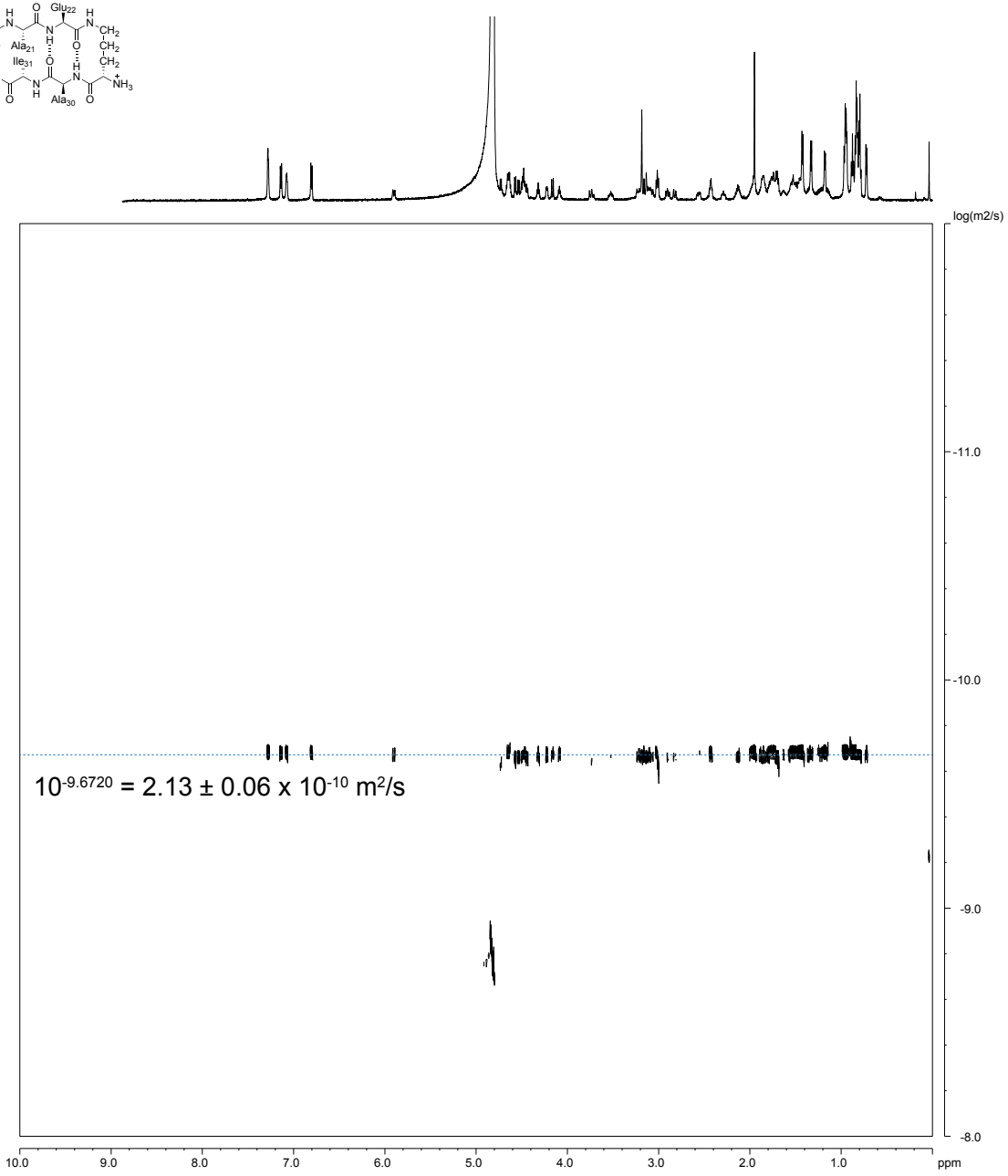


```
Current Data Parameters
NAME      V18T_F20Y(KLF)_1.0mM_peptide_D2O
EXPNO              5
PROCNO             1

F2 - Acquisition Parameters
Date_          20220412
Time              22.50
INSTRUM           av600
PROBHD   5 mm CPBBO BB-
PULPROG       ledbpgp2s
TD               98074
SOLVENT            D2O
NS                   8
DS                   4
SWH           5482.456 Hz
FIDRES        0.055901 Hz
AQ            8.9443483 sec
RG                 181
DW              91.200 usec
DE              21.95 usec
TE              298.0 K
D1           5.00000000 sec
D16          0.00020000 sec
D20          0.07500000 sec
D21          0.00500000 sec

======== CHANNEL f1 ========
SFO1        600.1324563 MHz
NUC1                    1H
P1                10.25 usec
P2                20.50 usec
PLW1       30.00000000 W

====== GRADIENT CHANNEL =====
GPNAM[6]     SMSQ10.100
GPNAM[7]     SMSQ10.100
GPNAM[8]     SMSQ10.100
GPZ6           100.00 %
GPZ7           -17.13 %
GPZ8           -13.17 %
P19           600.00 usec
P30          1350.00 usec

F1 - Acquisition parameters
TD                  16
SFO1         600.1328 MHz
FIDRES       751.201904 Hz
SW           10.014 ppm
FnMODE              QF

F2 - Processing parameters
SI                65536
SF          600.1299973 MHz
WDW                 EM
SSB                  0
LB              0.30 Hz
GB                   0
PC              1.00

F1 - Processing parameters
SI                  256
MC2                  QF
SF          600.1372381 MHz
WDW                  no
SSB                  0
LB               0 Hz
GB                   0
```

^{1}H NMR DOSY spectrum of 8.0 mM peptide **5** in D_2O at 600 MHz and 298 K

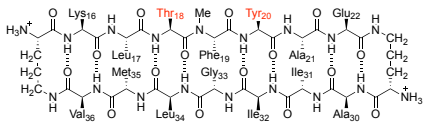

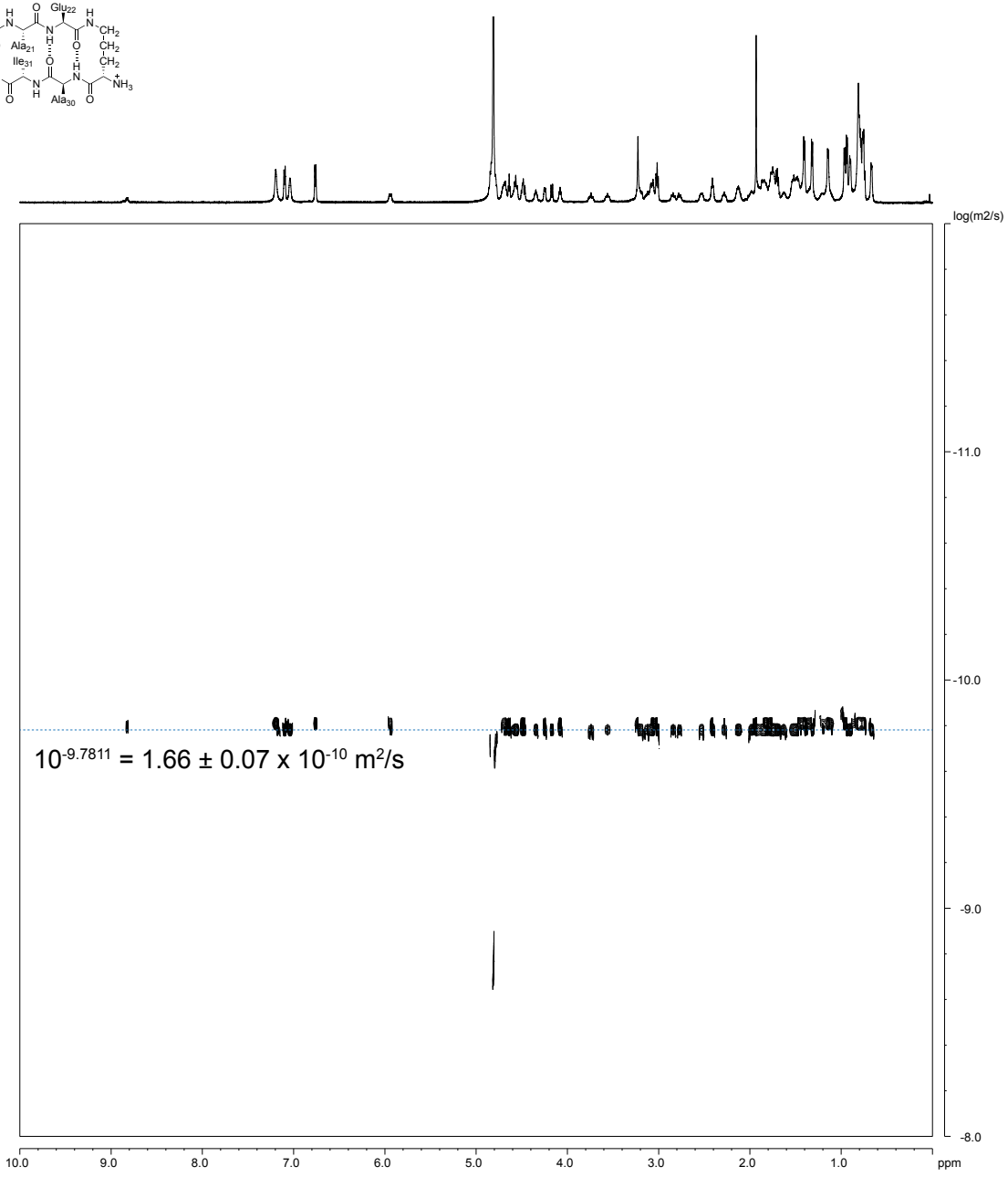

Current Data Parameters
NAME XL_VI_35_engineering project_Mut2A_D2
EXPNO 7
PROCNO 1

F2 - Acquisition Parameters
Date_ 20220202
Time 22.23
INSTRUM av600
PROBHD 5 mm CPBBO BB-
PULPROG ledbpgp2s
TD 98074
SOLVENT D2O
NS 8
DS 4
SWH 6361.323 Hz
FIDRES 0.064862 Hz
AQ 7.7086163 sec
RG 114
DW 78.600 usec
DE 18.70 usec
TE 298.0 K
D1 5.00000000 sec
D16 0.00020000 sec
D20 0.07500000 sec
D21 0.00500000 sec

======== CHANNEL f1 ========
SFO1 600.1328206 MHz
NUC1 1H
P1 9.50 usec
P2 19.00 usec
PLW1 30.00000000 W

====== GRADIENT CHANNEL =====
GPNAM[6] SMSQ10.100
GPNAM[7] SMSQ10.100
GPNAM[8] SMSQ10.100
GPZ6 100.00 %
GPZ7 -17.13 %
GPZ8 -13.17 %
P19 600.00 usec
P30 1800.00 usec

F1 - Acquisition parameters
TD 16
SFO1 600.1328 MHz
FIDRES 751.201904 Hz
SW 10.014 ppm
FnMODE QF

F2 - Processing parameters
SI 65536
SF 600.1299977 MHz
WDW EM
SSB 0
LB 0.30 Hz
GB 0
PC 1.00

F1 - Processing parameters
SI 256
MC2 QF
SF 600.1371767 MHz
WDW no
SSB 0
LB 0 Hz
GB 0

Peptide Characterization Data

Summary of purified peptides yields. Percent yields were calculated based on the resin loading.

Peptide	Yield (mg)	% Yield	Calculated MW as a TFA salt
1	42	11	2117.3 (•3 TFA)
2	37	16	2123.4 (•3 TFA)
2a	59	13	2124.4 (•3 TFA)
2b	55	21	2131.4 (•3 TFA)
2c	61	20	2135.5 (•3 TFA)
2d	41	16	2127.3 (•3 TFA)
3a	73	26	2123.4 (•3 TFA)
3b	7	8	2137.4 (•3 TFA)
3c	45	16	2137.4 (•3 TFA)
4a	73	24	2149.4 (•3 TFA)
4b	29	10	2149.4 (•3 TFA)
5	38	12	2149.4 (•3 TFA)

Characterization of peptide **1**

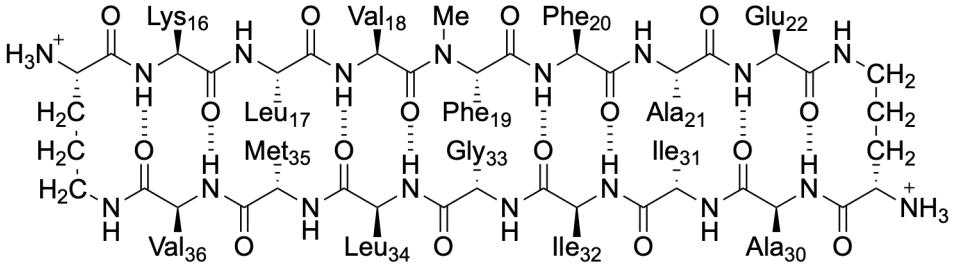

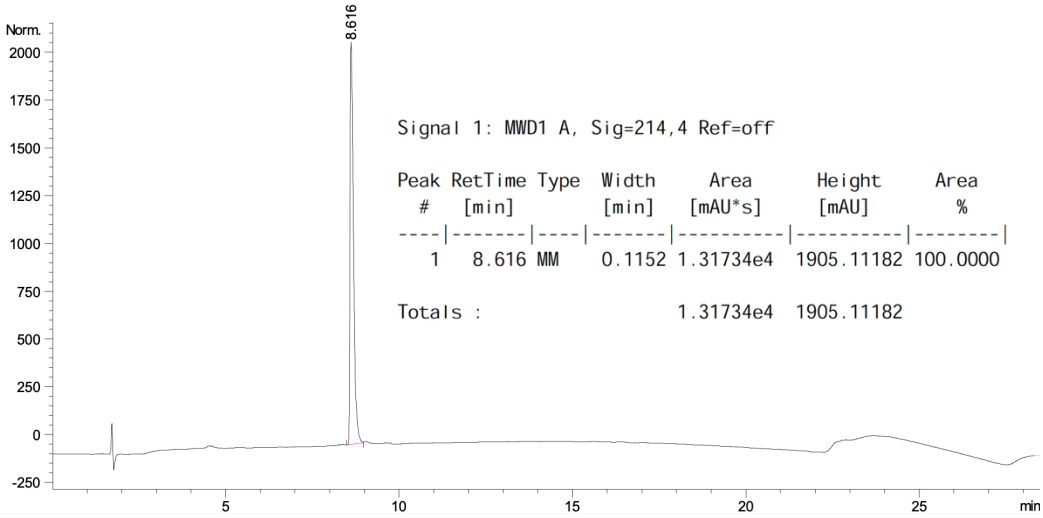

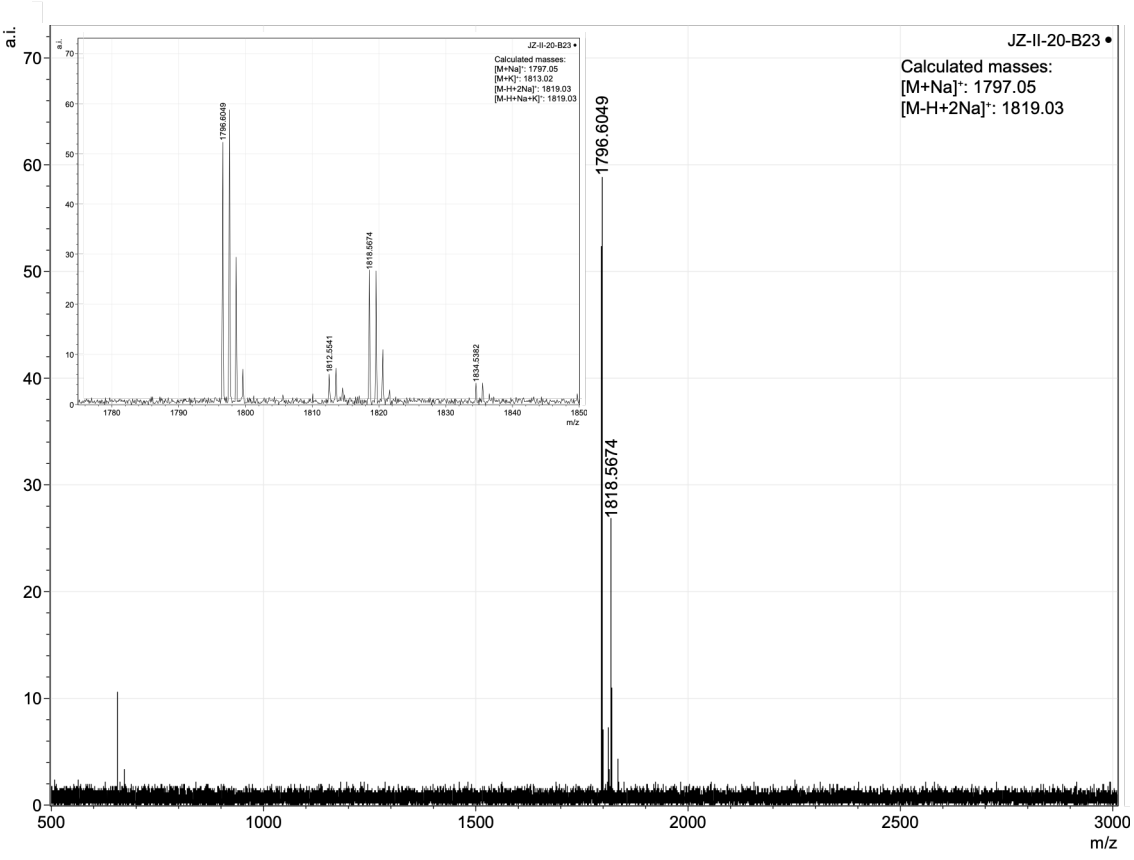

Characterization of peptide **2**

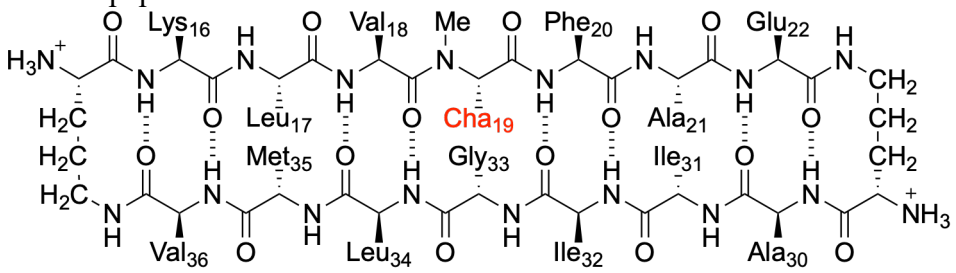

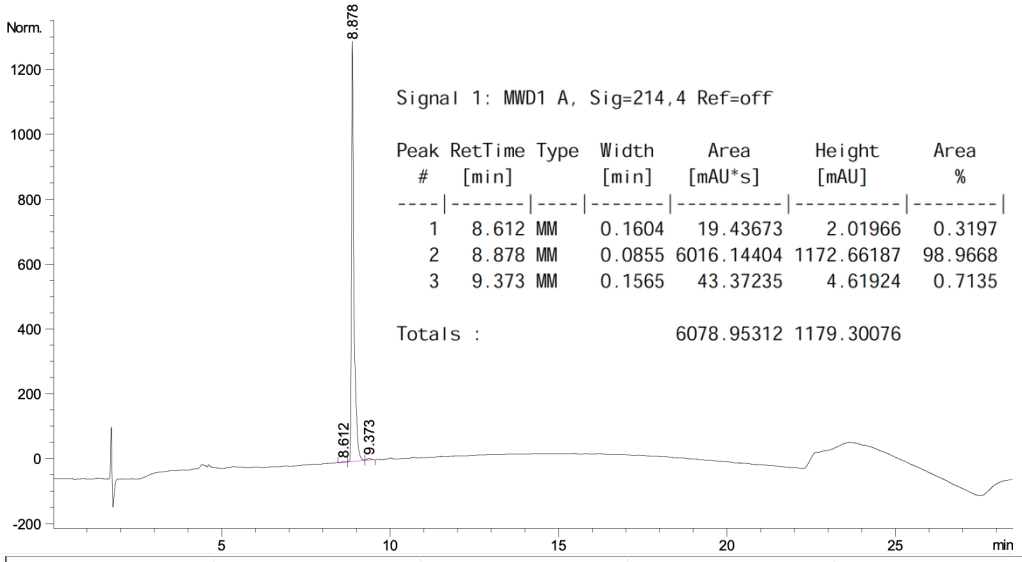

Signal 1: MWD1 A, Sig=214,4 Ref=off

Peak #	RetTime [min]	Type	Width [min]	Area [mAU*s]	Height [mAU]	Area %
1	8.612	MM	0.1604	19.43673	2.01966	0.3197
2	8.878	MM	0.0855	6016.14404	1172.66187	98.9668
3	9.373	MM	0.1565	43.37235	4.61924	0.7135
Totals :				6078.95312	1179.30076	

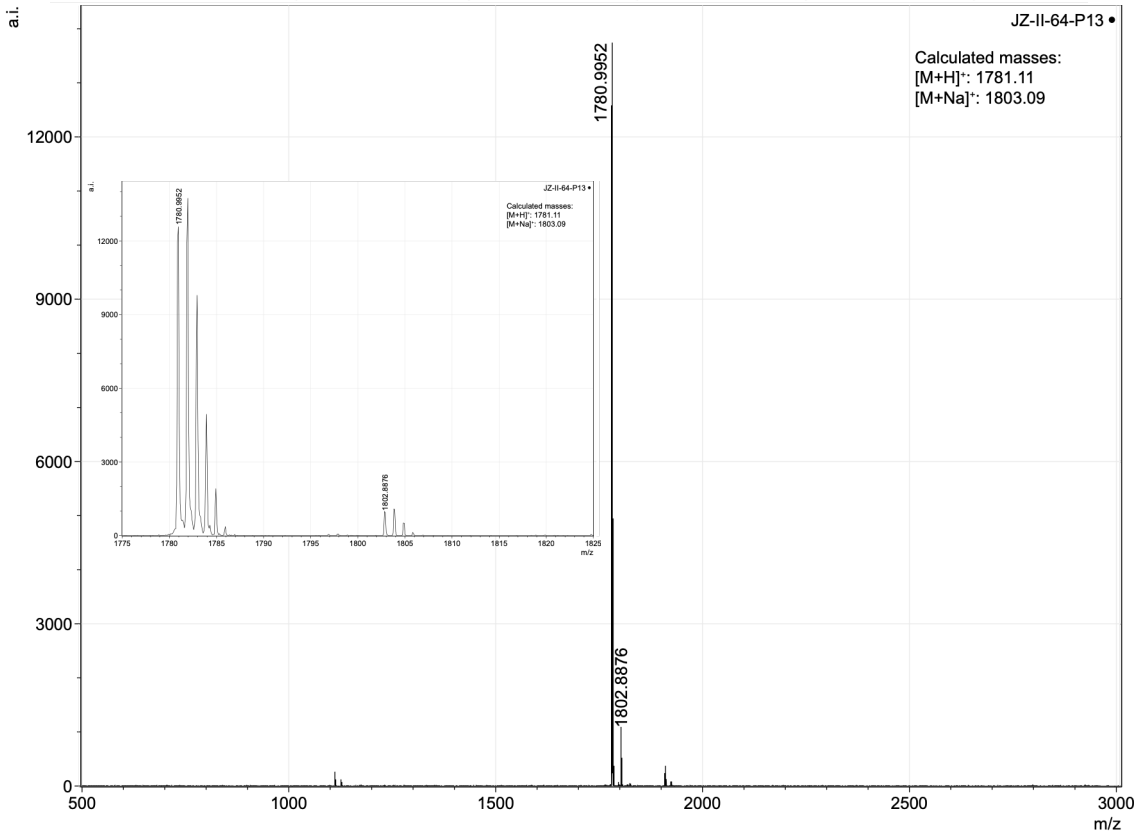

Characterization of peptide **2a**

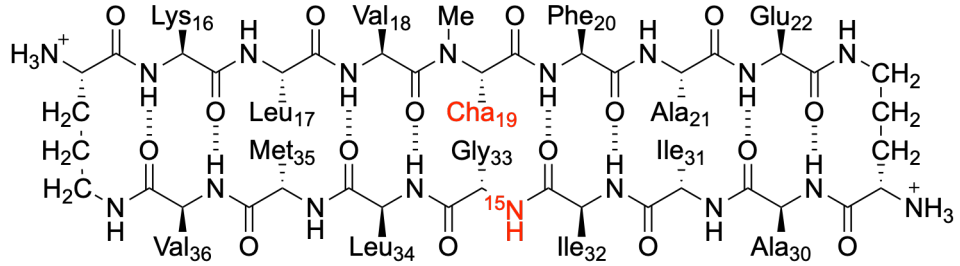

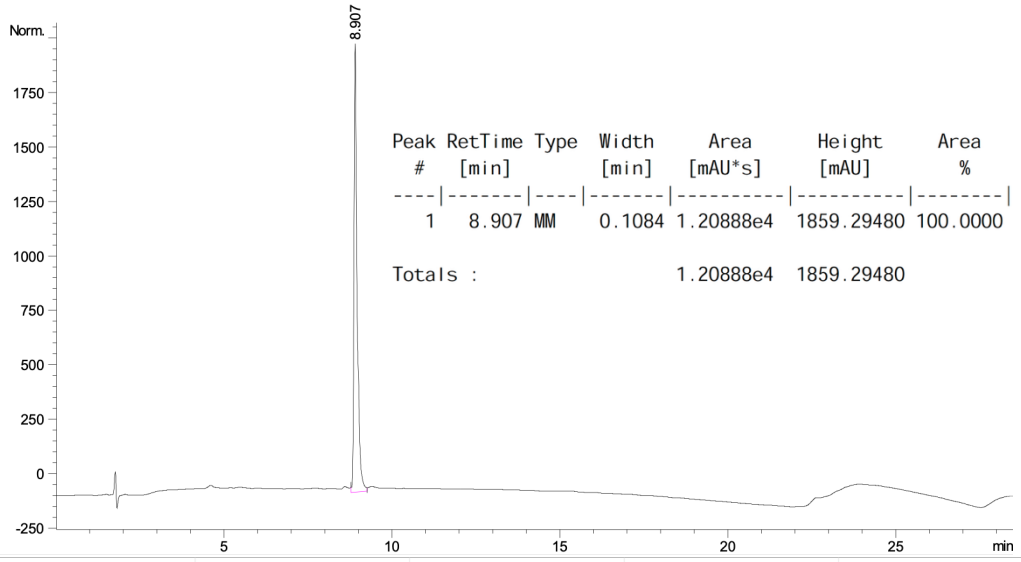

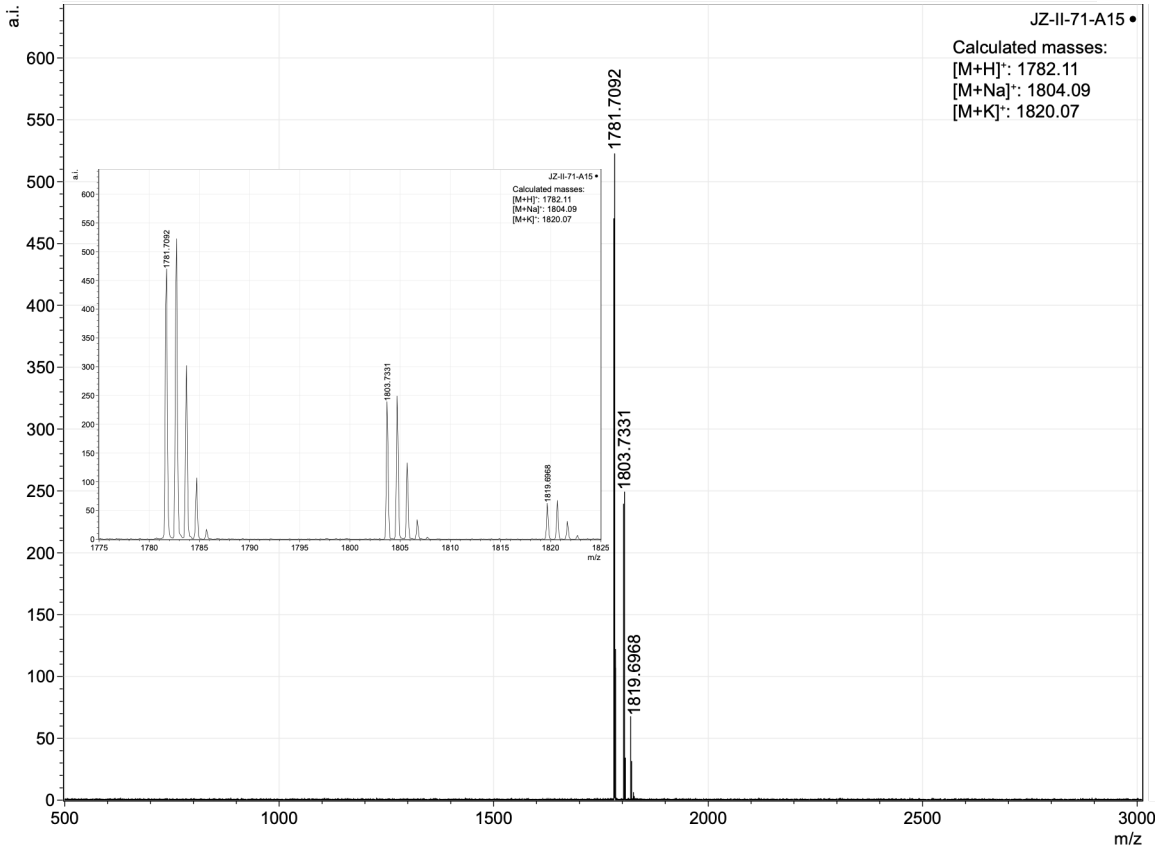

Characterization of peptide **2b**

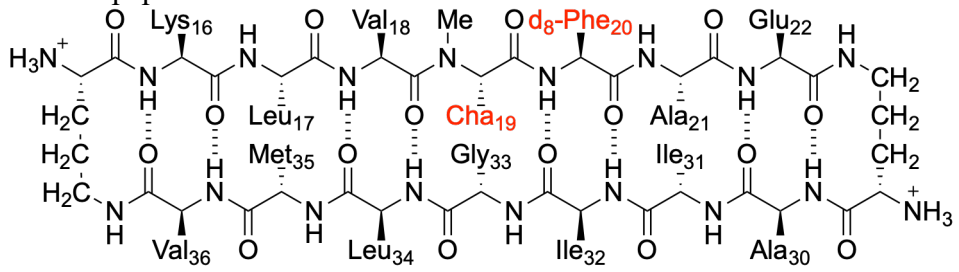

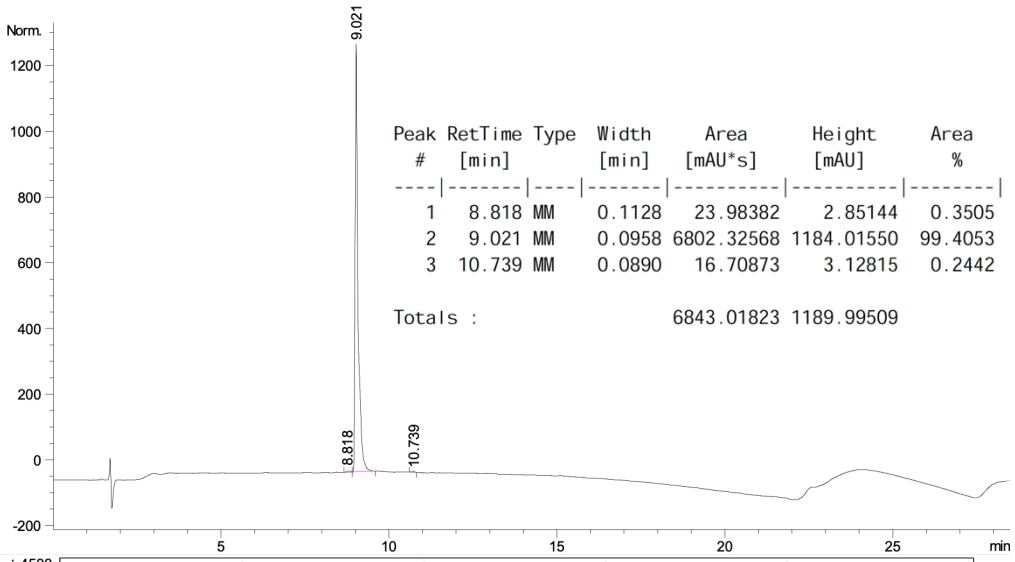

Peak #	RetTime [min]	Type	Width [min]	Area [mAU*s]	Height [mAU]	Area %
1	8.818	MM	0.1128	23.98382	2.85144	0.3505
2	9.021	MM	0.0958	6802.32568	1184.01550	99.4053
3	10.739	MM	0.0890	16.70873	3.12815	0.2442
Totals :				6843.01823	1189.99509	

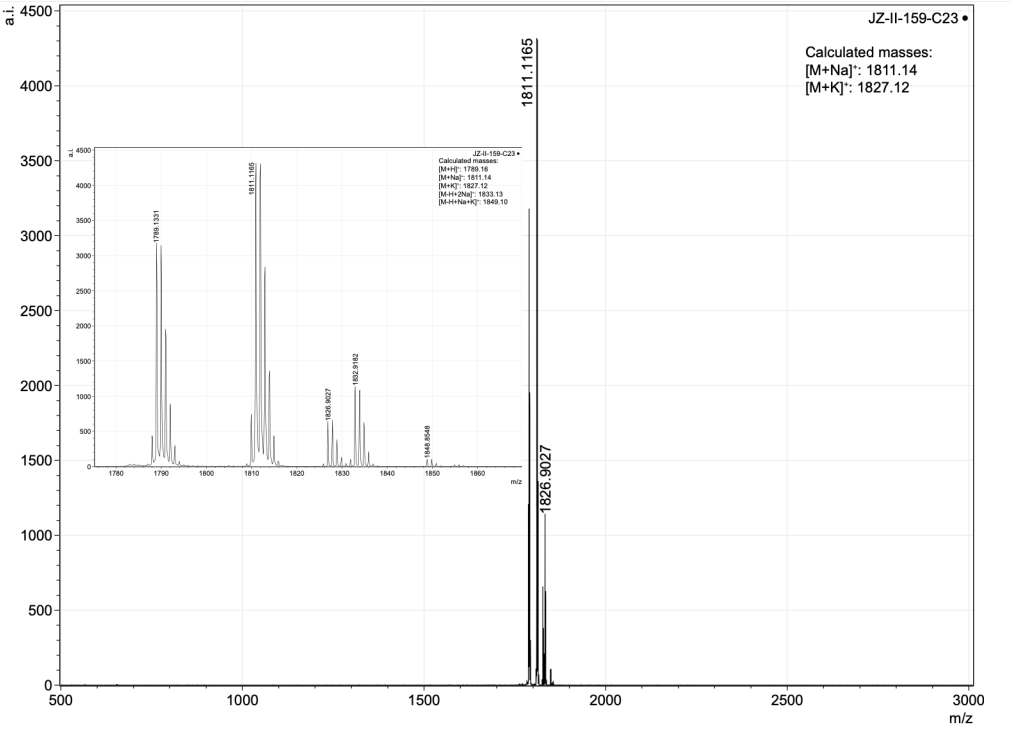

Note: The commercially available d_8-Phe_{20} (98%) contains incomplete deuteration at Hα as reported by Li, X.; *et. al.*[2] This is reflected in the MALDI-TOF characterization data.

Characterization of peptide **2c**

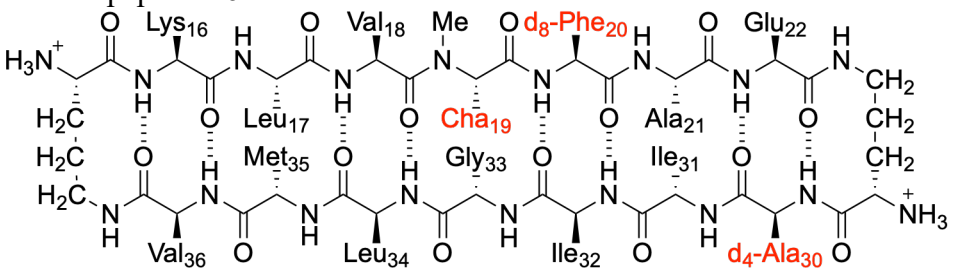

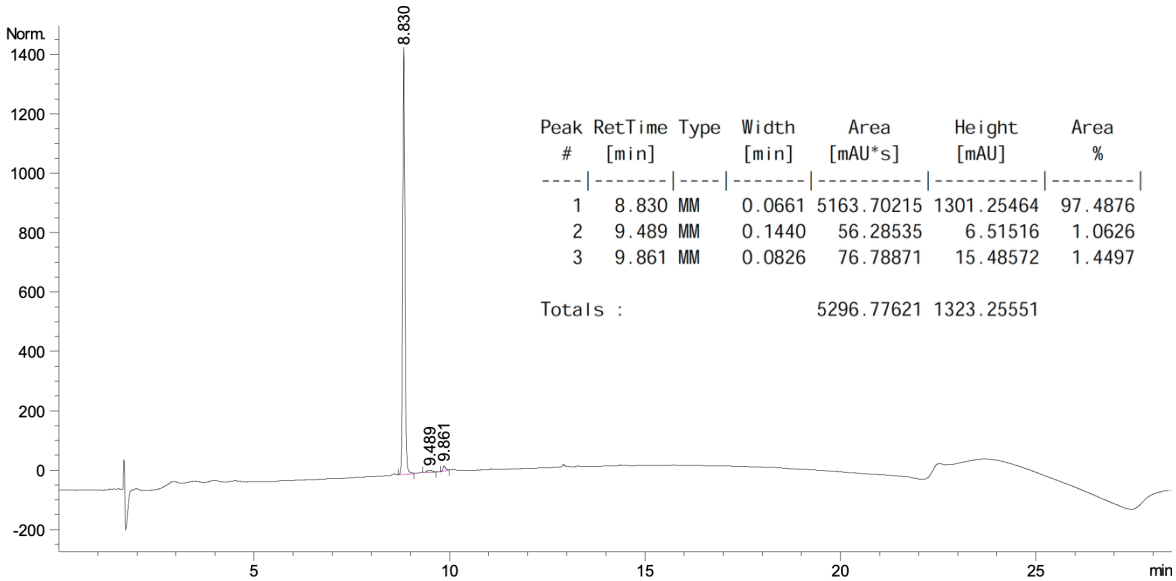

Peak #	RetTime [min]	Type	Width [min]	Area [mAU*s]	Height [mAU]	Area %
1	8.830	MM	0.0661	5163.70215	1301.25464	97.4876
2	9.489	MM	0.1440	56.28535	6.51516	1.0626
3	9.861	MM	0.0826	76.78871	15.48572	1.4497
Totals :				5296.77621	1323.25551	

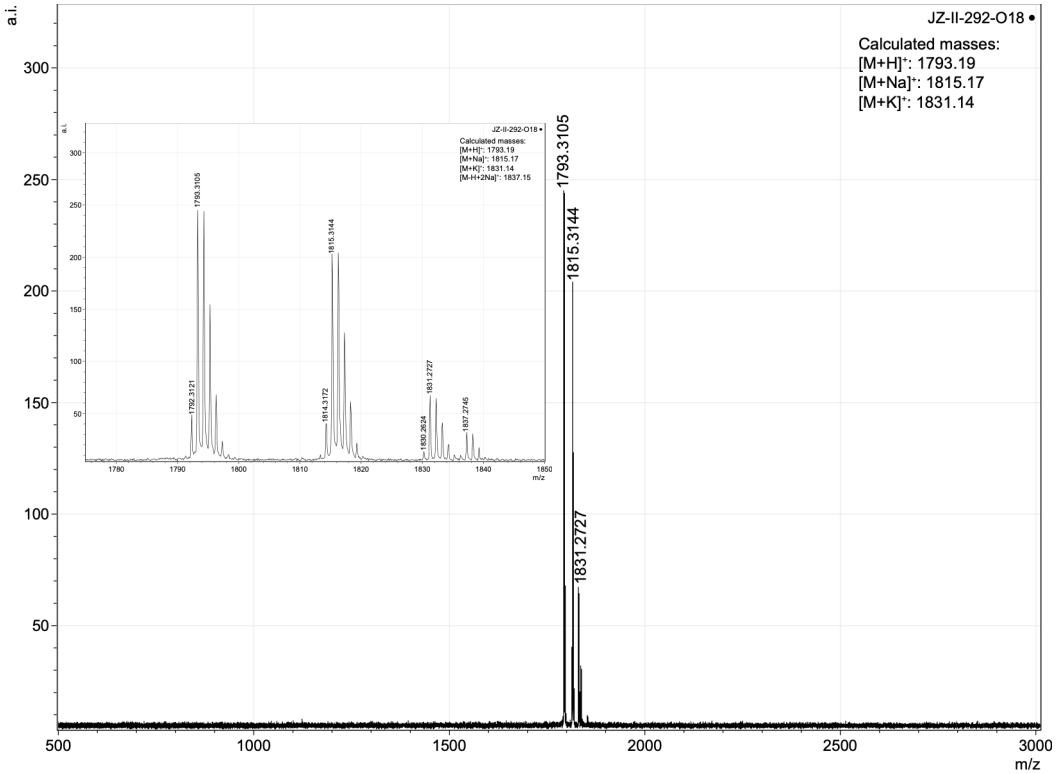

Note: The commercially available d_8-Phe$_{20}$ (98%) contains incomplete deuteration at Hα as reported by Li, X.; *et. al.*[2] This is reflected in the MALDI-TOF characterization data.

Characterization of peptide **2d**

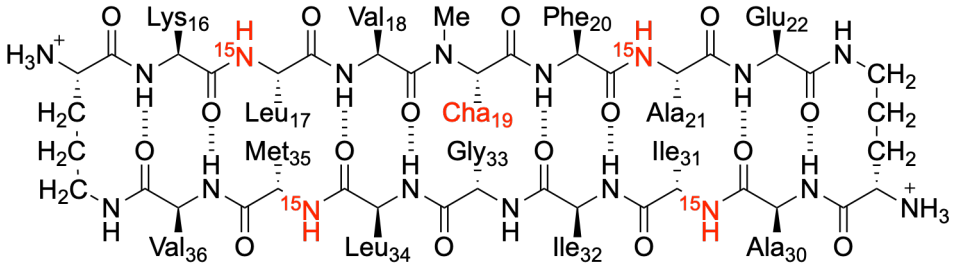

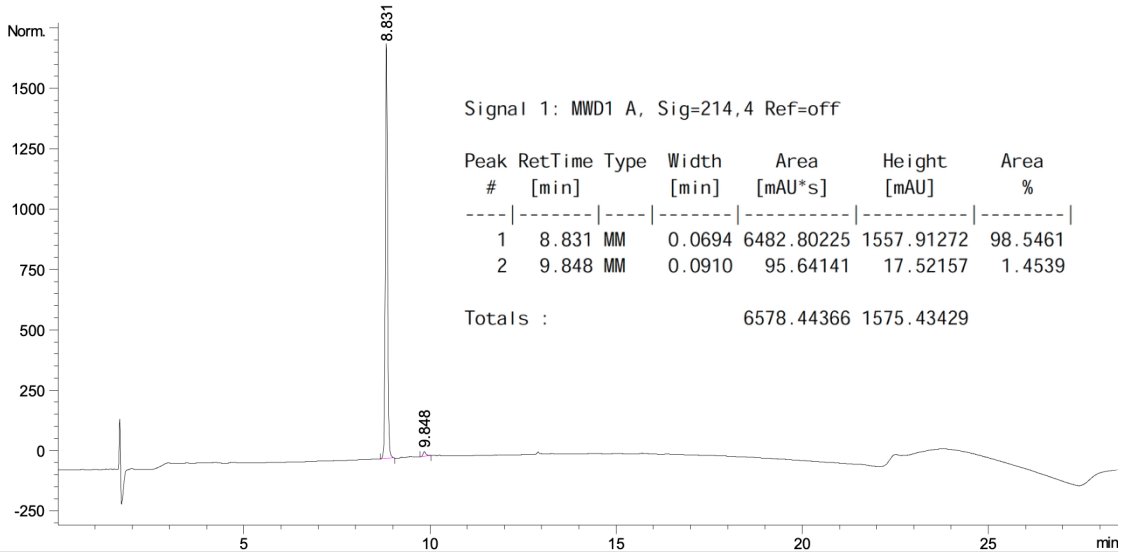

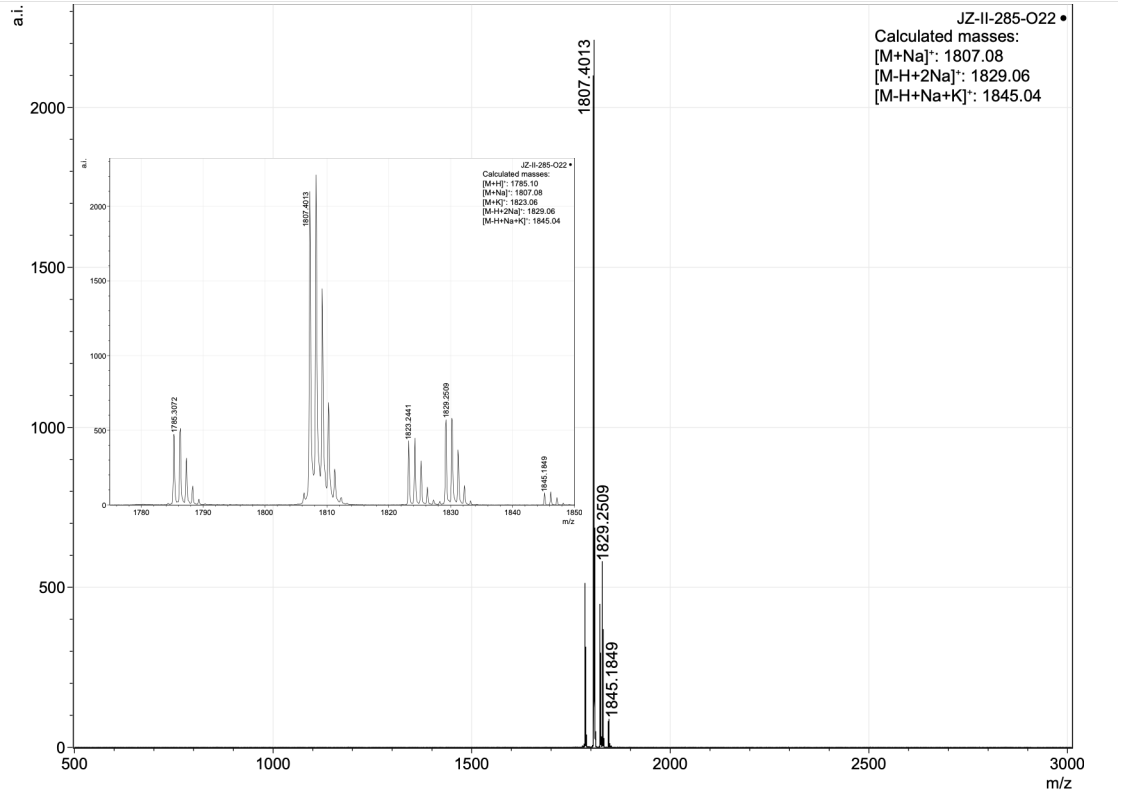

Characterization of peptide **3a**

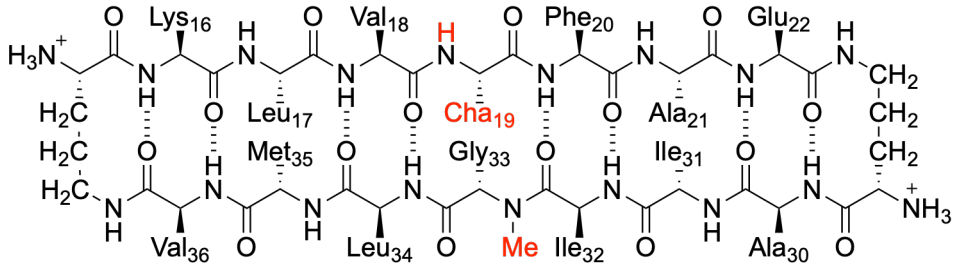

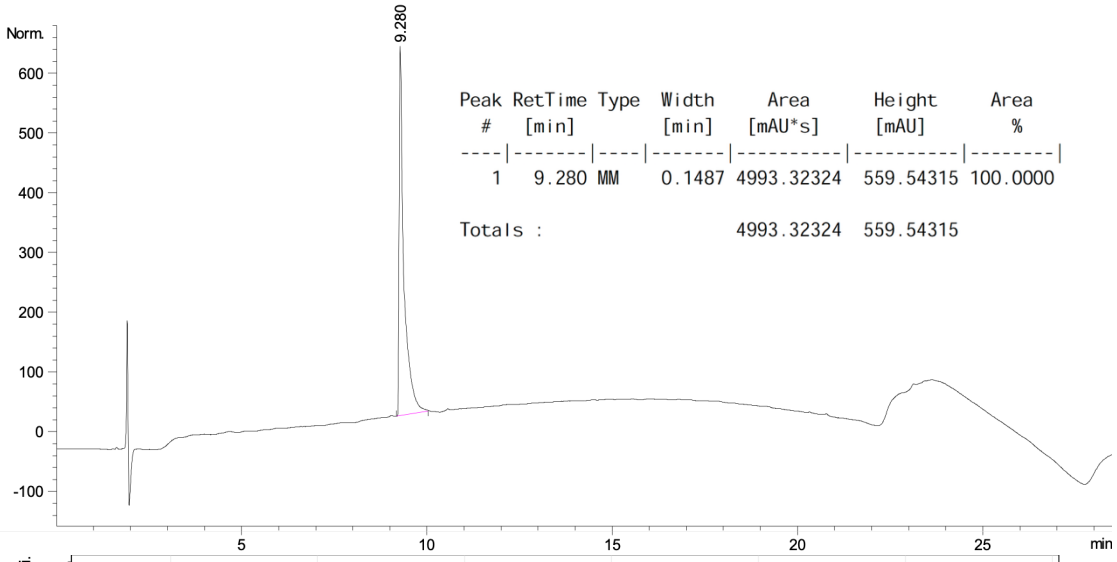

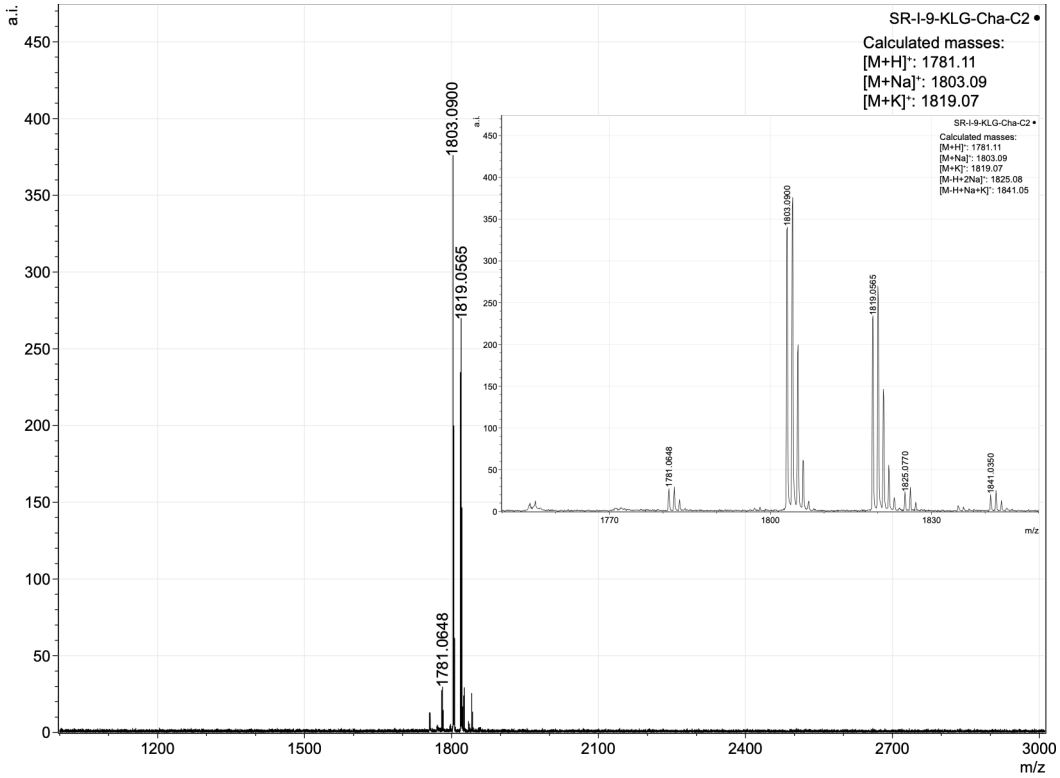

Characterization of peptide **3b**

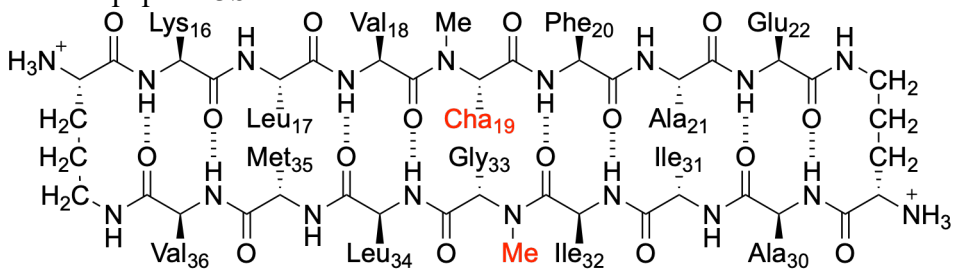

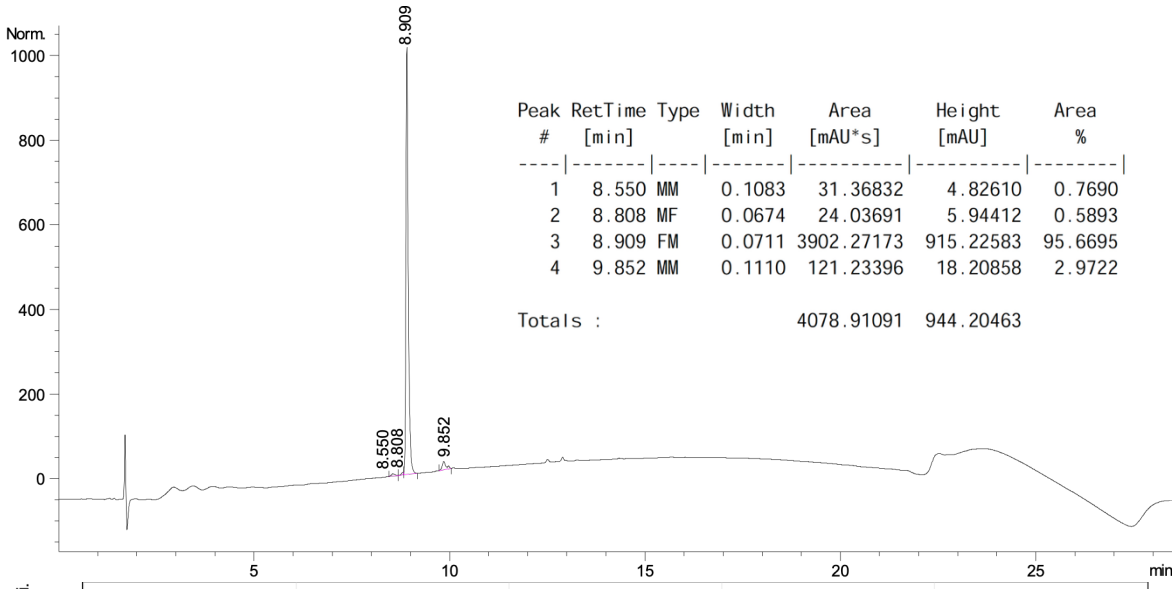

Peak #	RetTime [min]	Type	Width [min]	Area [mAU*s]	Height [mAU]	Area %
1	8.550	MM	0.1083	31.36832	4.82610	0.7690
2	8.808	MF	0.0674	24.03691	5.94412	0.5893
3	8.909	FM	0.0711	3902.27173	915.22583	95.6695
4	9.852	MM	0.1110	121.23396	18.20858	2.9722
Totals :				4078.91091	944.20463	

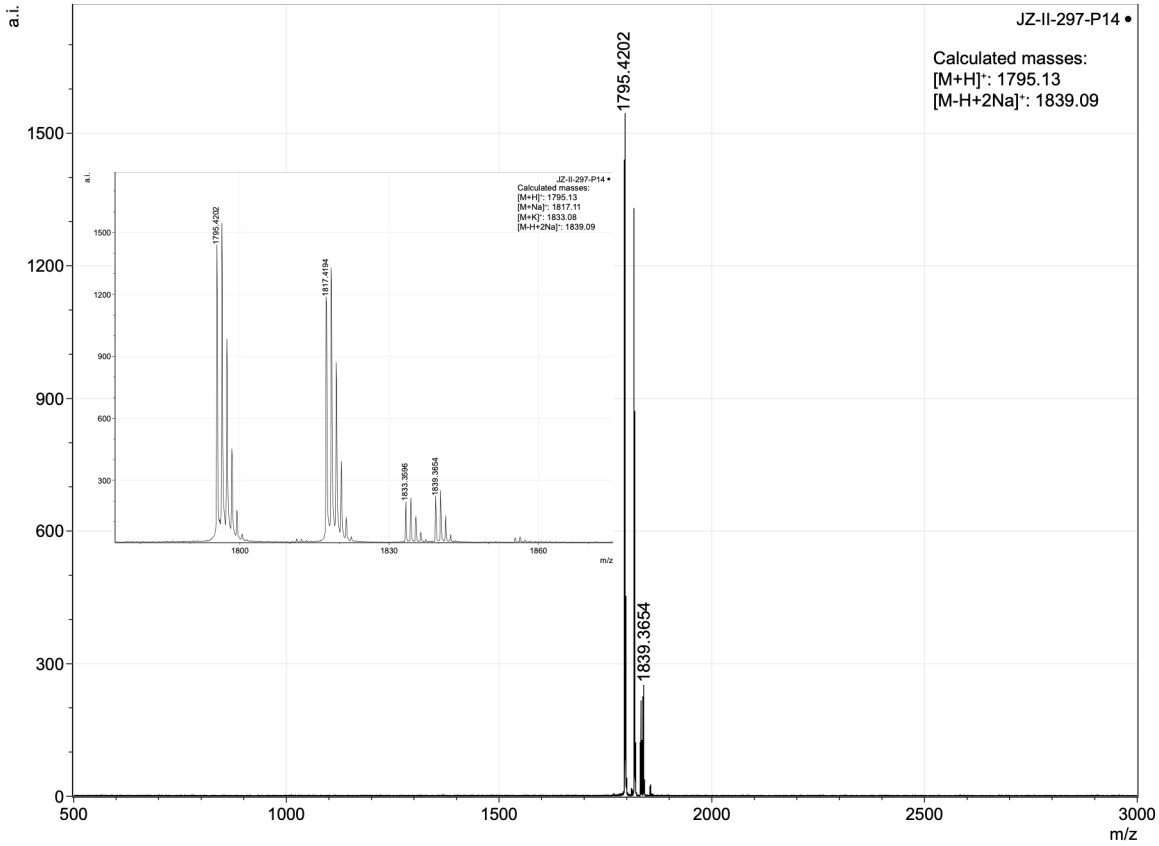

Characterization of peptide **3c**

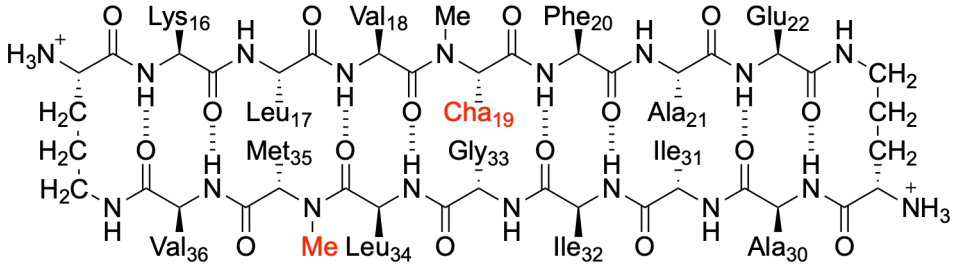

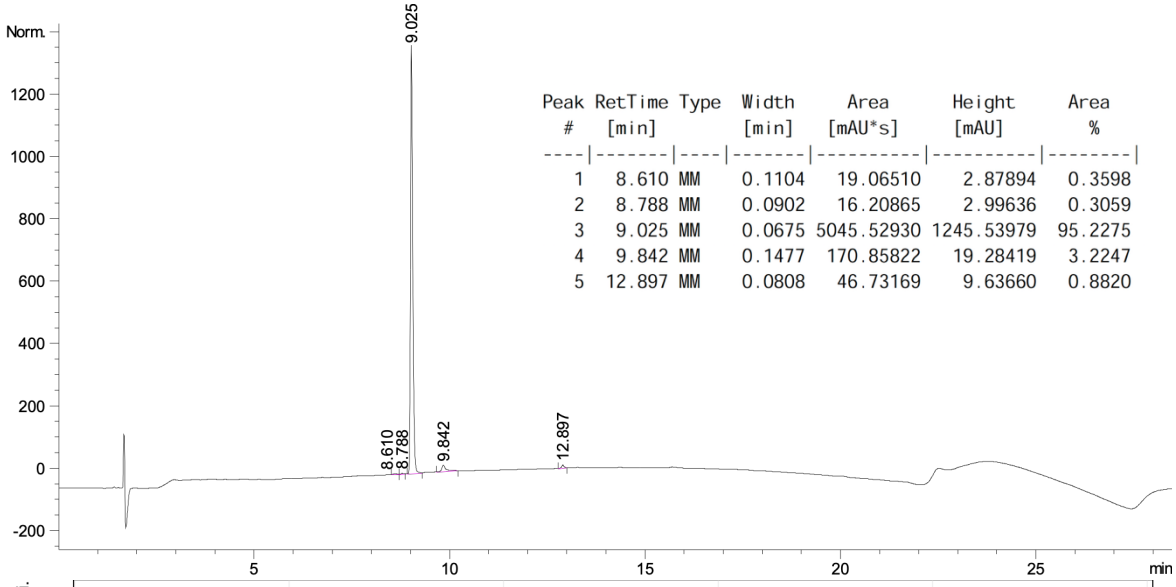

Peak #	RetTime [min]	Type	Width [min]	Area [mAU*s]	Height [mAU]	Area %
1	8.610	MM	0.1104	19.06510	2.87894	0.3598
2	8.788	MM	0.0902	16.20865	2.99636	0.3059
3	9.025	MM	0.0675	5045.52930	1245.53979	95.2275
4	9.842	MM	0.1477	170.85822	19.28419	3.2247
5	12.897	MM	0.0808	46.73169	9.63660	0.8820

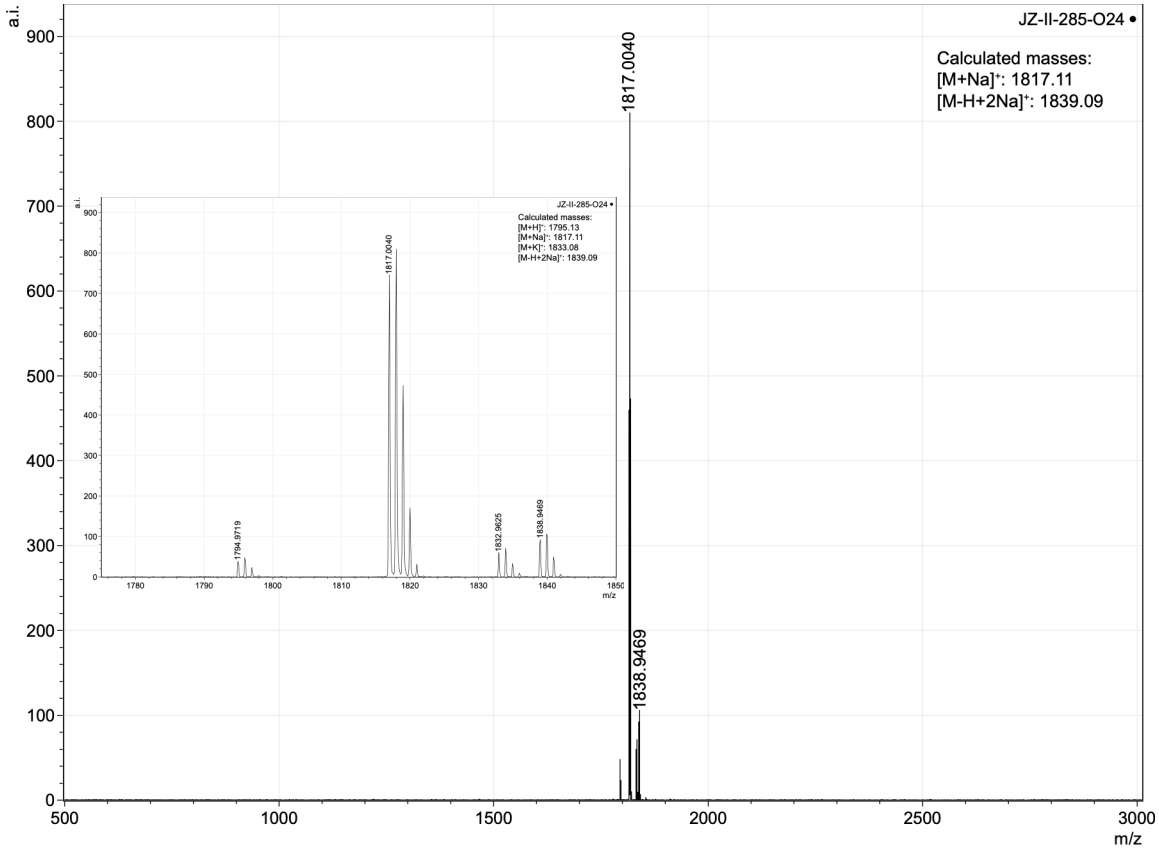

Characterization of peptide **4a**

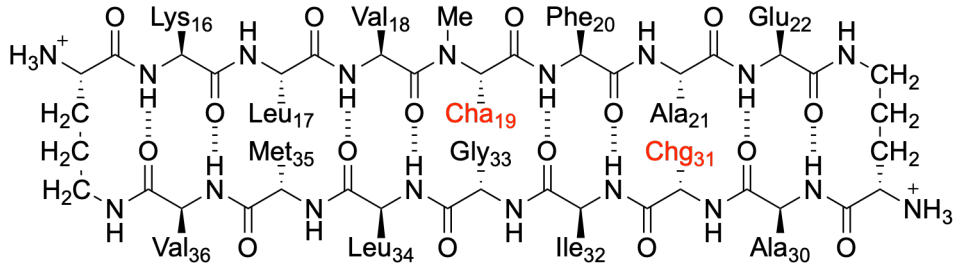

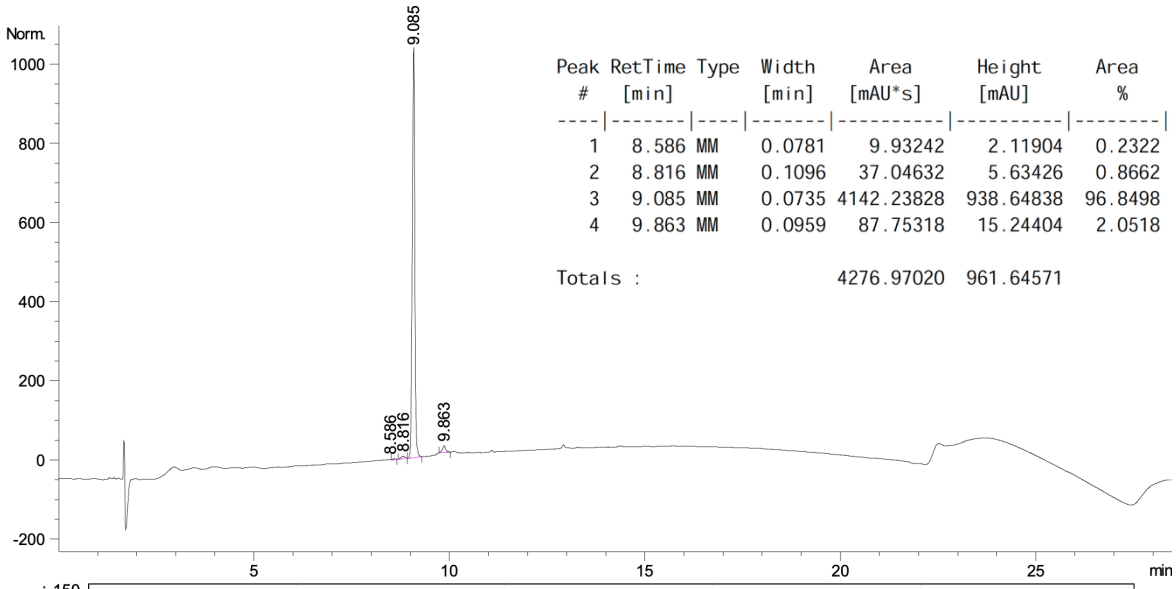

Peak #	RetTime [min]	Type	Width [min]	Area [mAU*s]	Height [mAU]	Area %
1	8.586	MM	0.0781	9.93242	2.11904	0.2322
2	8.816	MM	0.1096	37.04632	5.63426	0.8662
3	9.085	MM	0.0735	4142.23828	938.64838	96.8498
4	9.863	MM	0.0959	87.75318	15.24404	2.0518
Totals :				4276.97020	961.64571	

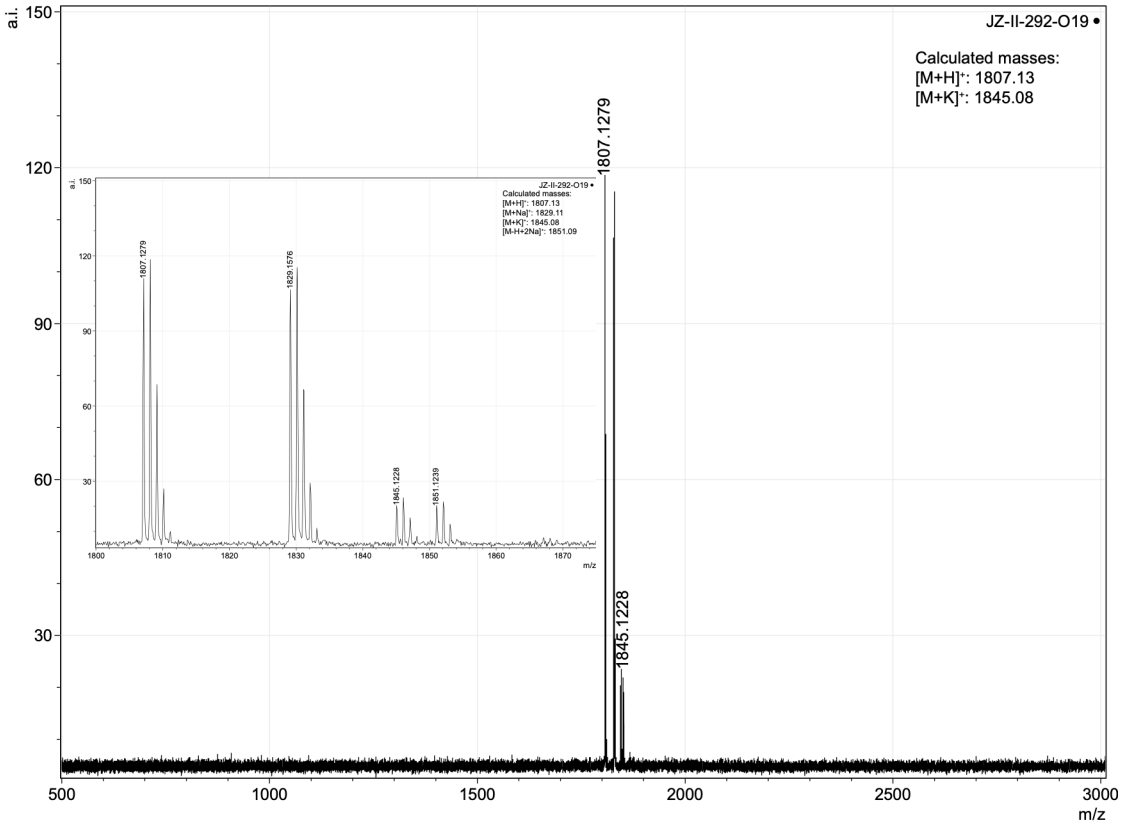

Characterization of peptide **4b**

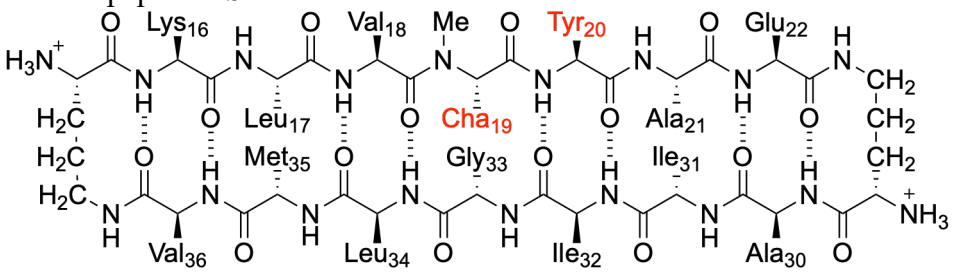

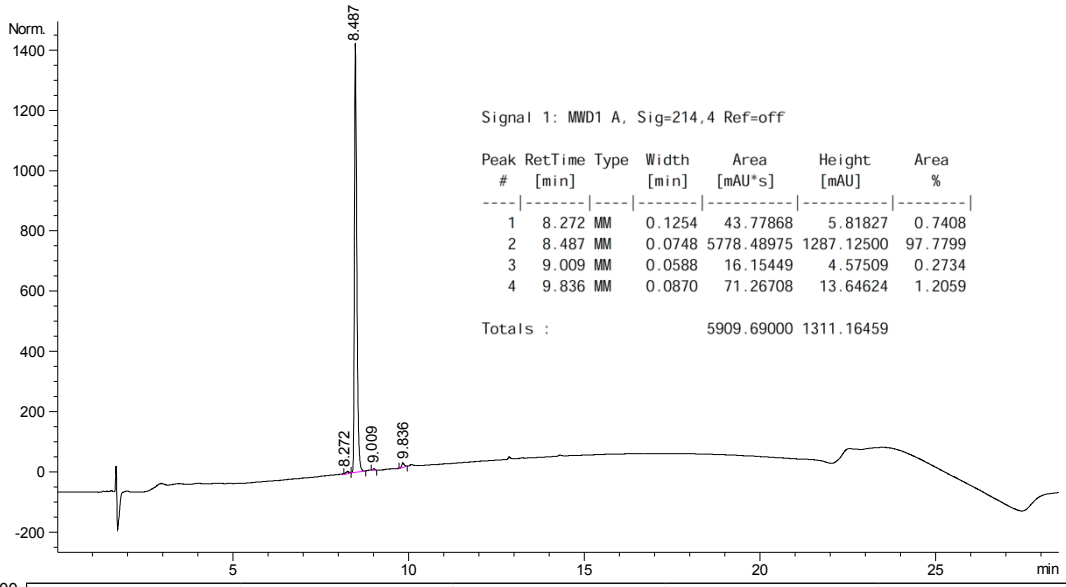

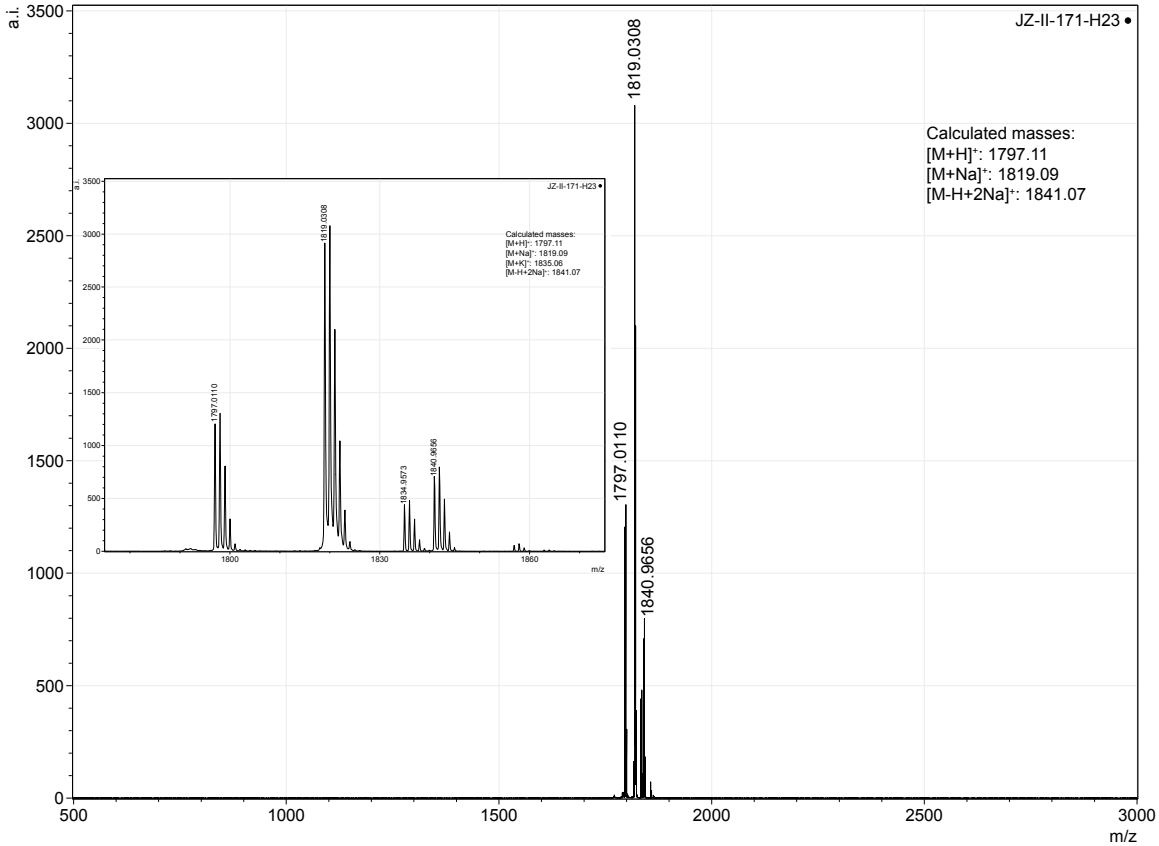

Characterization of peptide **5**

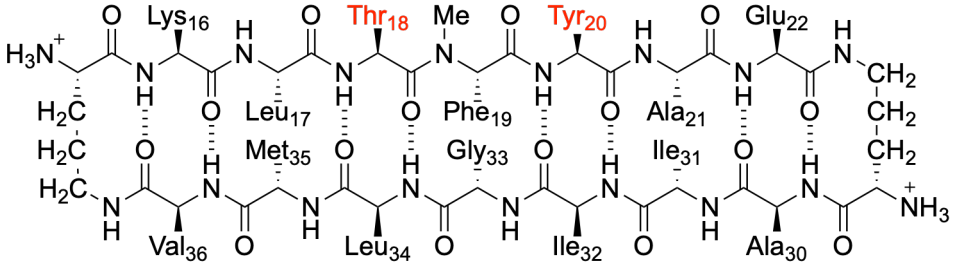

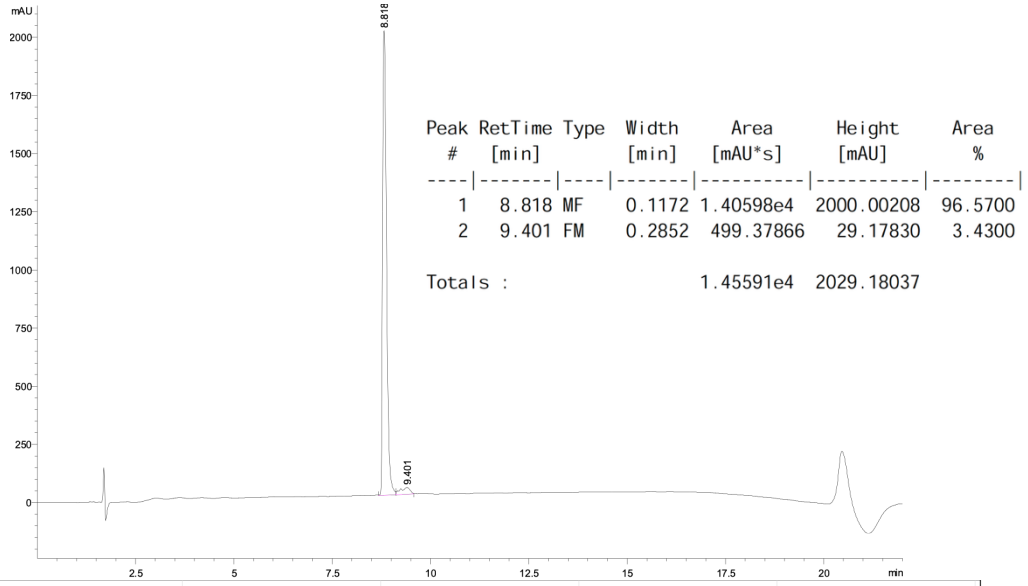

Peak #	RetTime [min]	Type	Width [min]	Area [mAU*s]	Height [mAU]	Area %
1	8.818	MF	0.1172	1.40598e4	2000.00208	96.5700
2	9.401	FM	0.2852	499.37866	29.17830	3.4300
Totals :				1.45591e4	2029.18037	

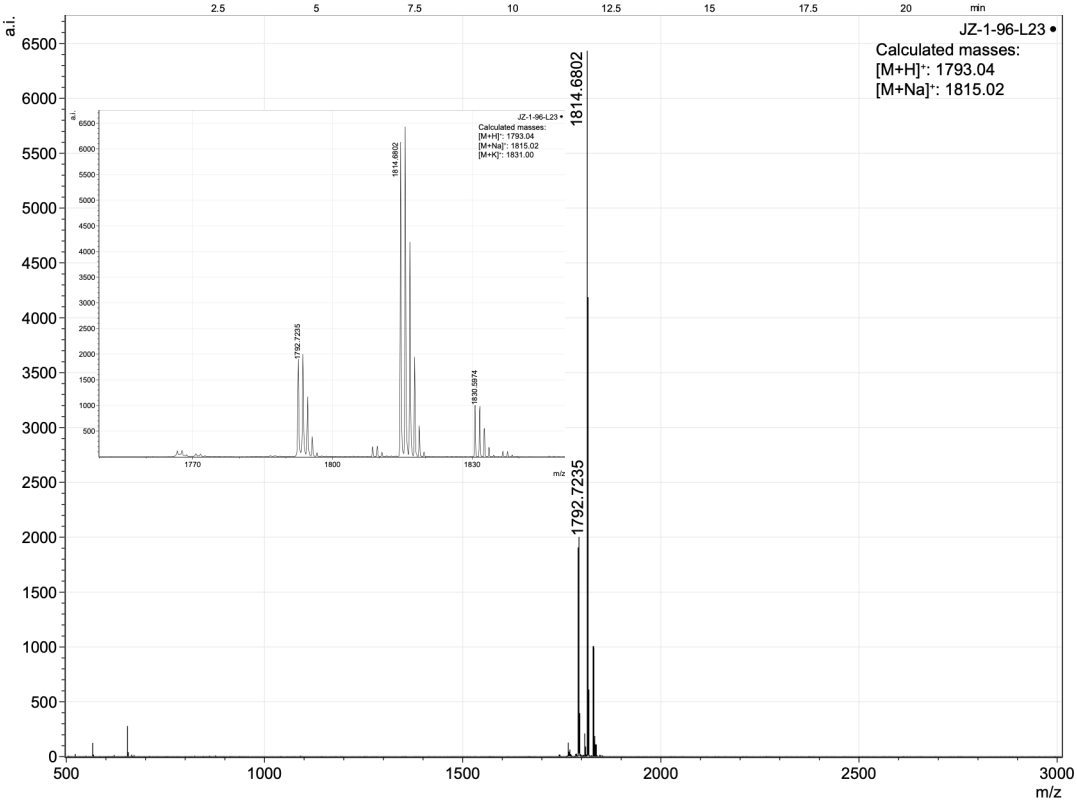

Appendix B: Additional Data for Chapter 3

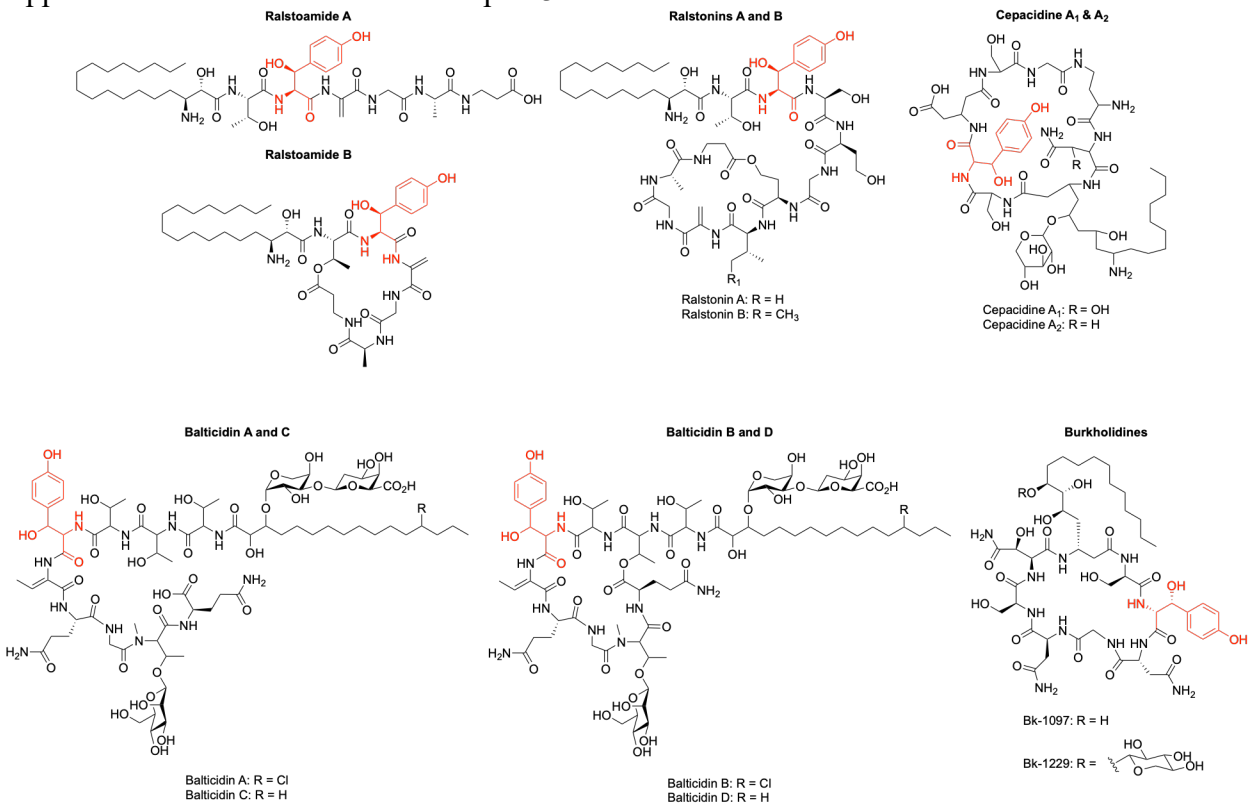

Figure S3.1. Chemical structures of β-hydroxytyrosine containing peptide natural products.

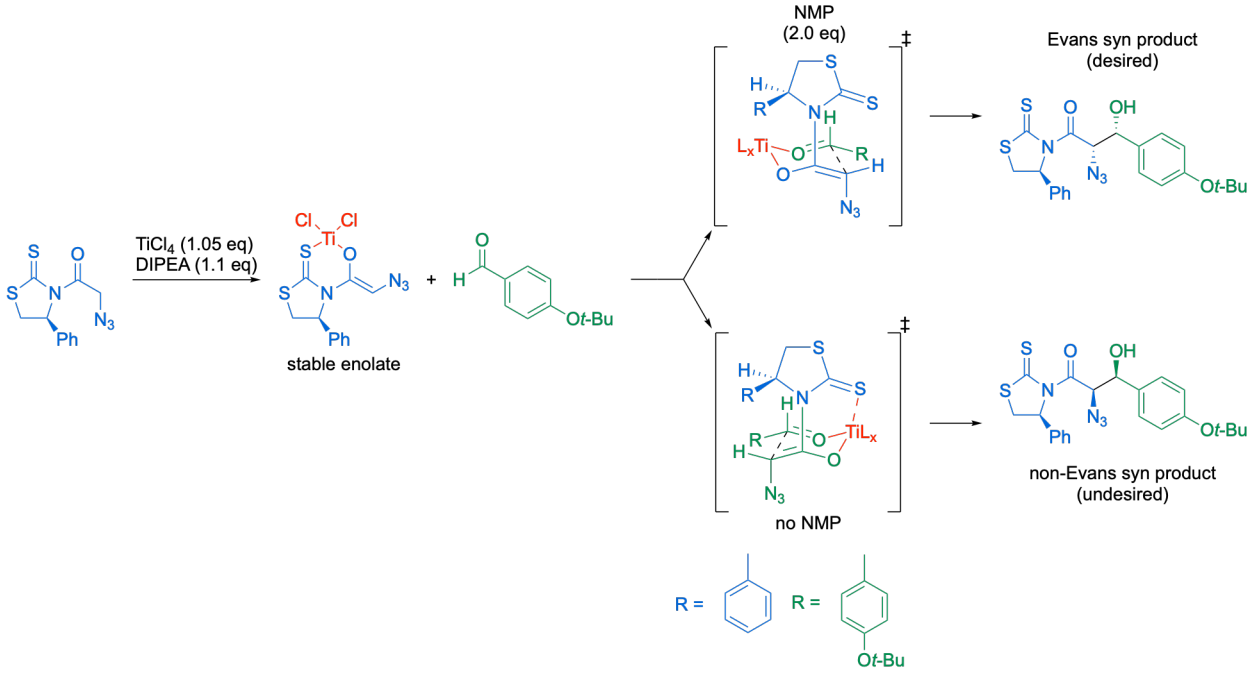

Figure S3.2. Zimmerman-Traxler model illustrating the stereoselectivity of the Crimmins aldol reaction. $TiCl_4$ chelation and soft enolization leads to formation of a stable enolate. *N*-Methyl-2-pyrrolidone (NMP) prevents coordination of the thiazolidine to Ti which leads to the formation of the desired Evans syn product with >98:2 diastereoselectivity.

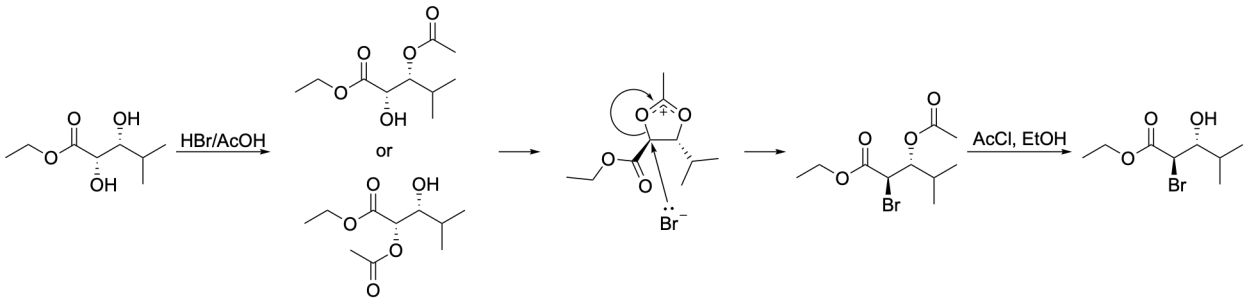

Figure S3.3. Reaction mechanism illustrating the stereoselectivity of the bromination reaction. Acetylation of either alcohol leads to formation of a cyclic acetoxonium ion with retention of stereochemistry. Regioselective bromide displacement with inversion of stereochemistry exclusively favors the α-position because of the inductive effect of the proximal ester. Subsequent acid-catalyzed deacetylation reveals bromoalcohol with 99:1 diastereoselectivity.

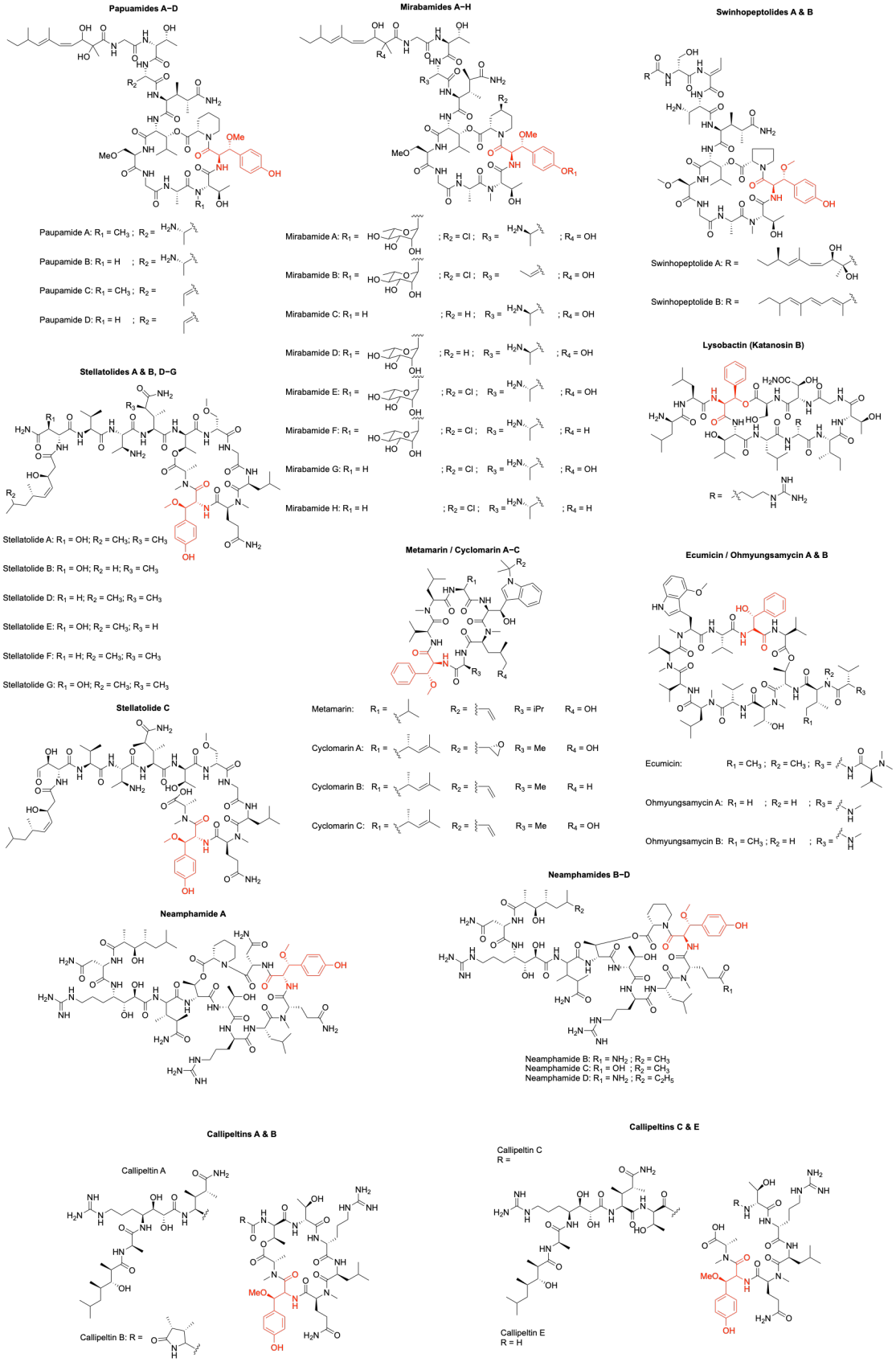

Figure S3.4. Chemical structures of structurally analogous peptide natural products.

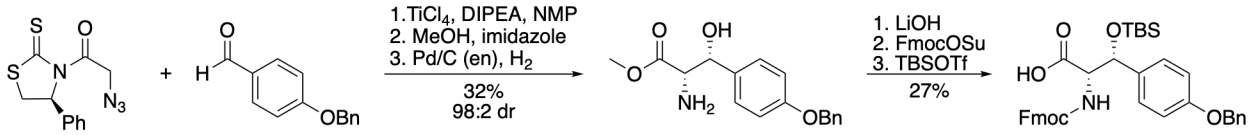

Figure S3.5. Synthesis of Fmoc-Hty(TBS/Bn)-OH.

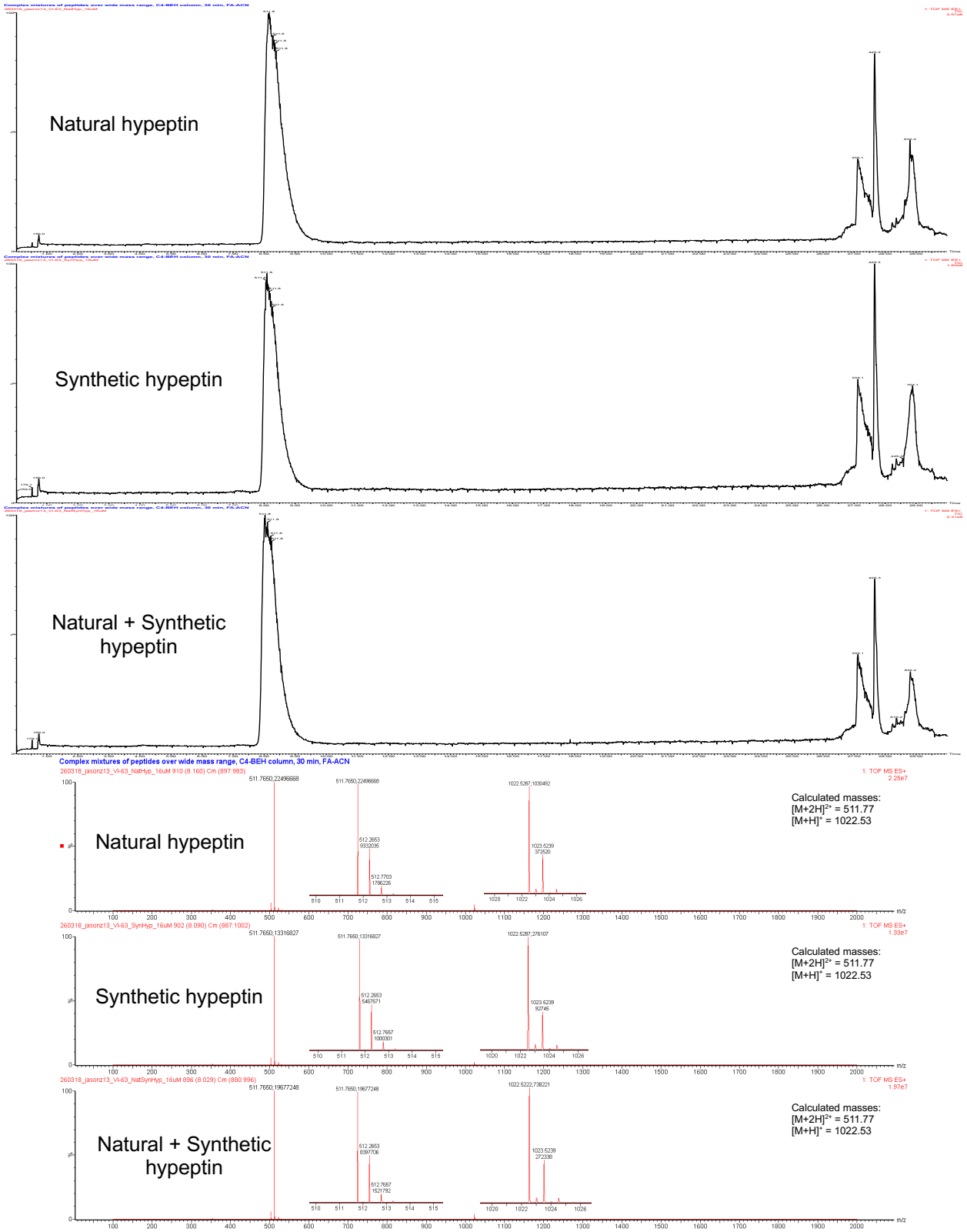

Figure S3.6. Xevo LC-MS comparison of natural and synthetic hypeptin. HPLC was run on a C4 column with a gradient of 3 – 40% acetonitrile over 20 min followed by an acetonitrile flush. MS was run with a Xevo Z-spray source operated in positive MS resolution mode, 100 – 2000 m/z.

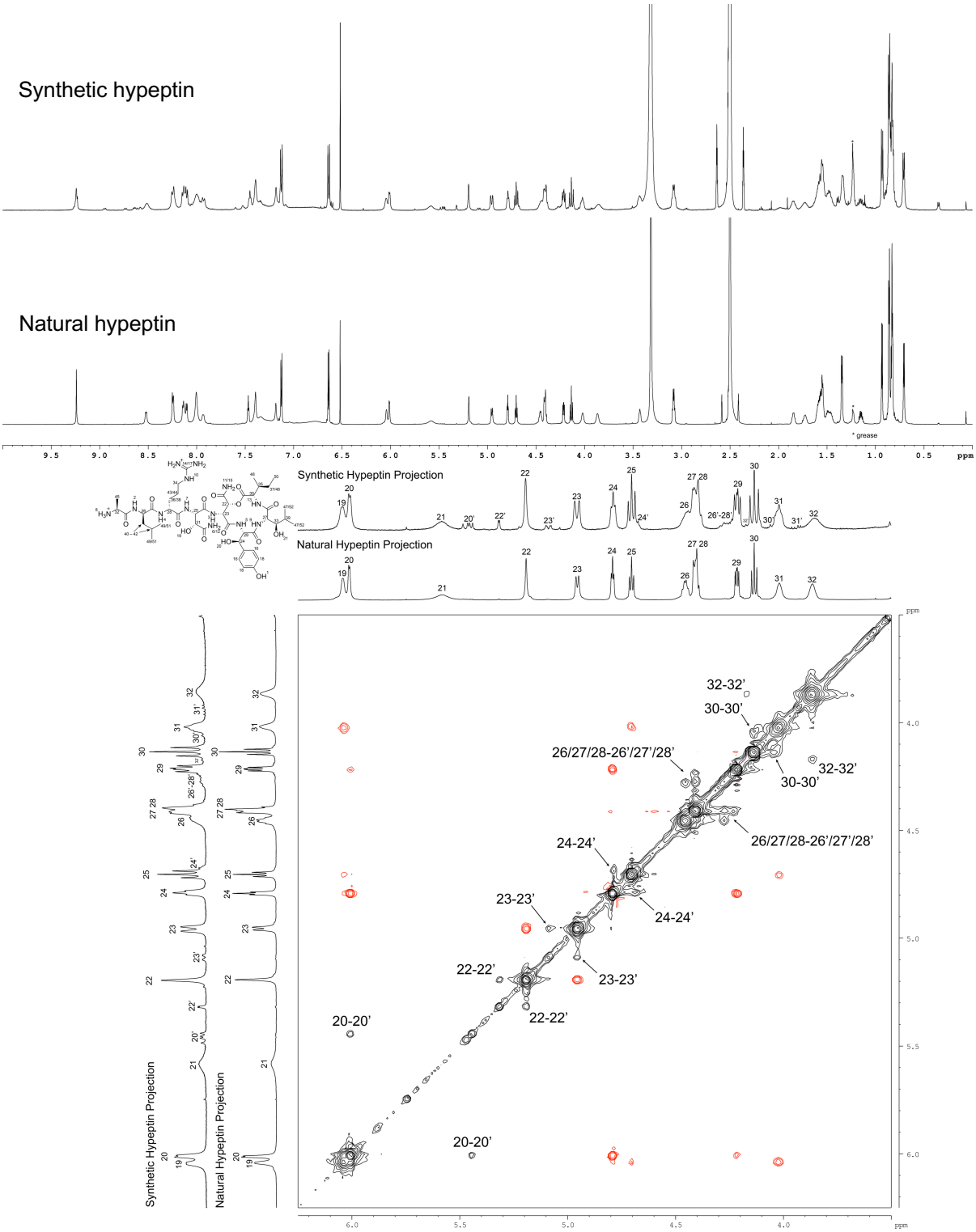

Figure S3.7. ^{1}H NMR comparison of natural and synthetic hypeptin in DMSO-d_6 at 298 K. Natural and synthetic spectra were recorded at 800 and 500 MHz respectively. The ^{1}H NMR spectra of natural and synthetic hypeptin contain two sets of peaks that exhibit exchange crosspeaks (EXSY) as shown in the ROESY spectra of natural hypeptin. ROE crosspeaks are shown in red while EXSY crosspeaks are shown in black.

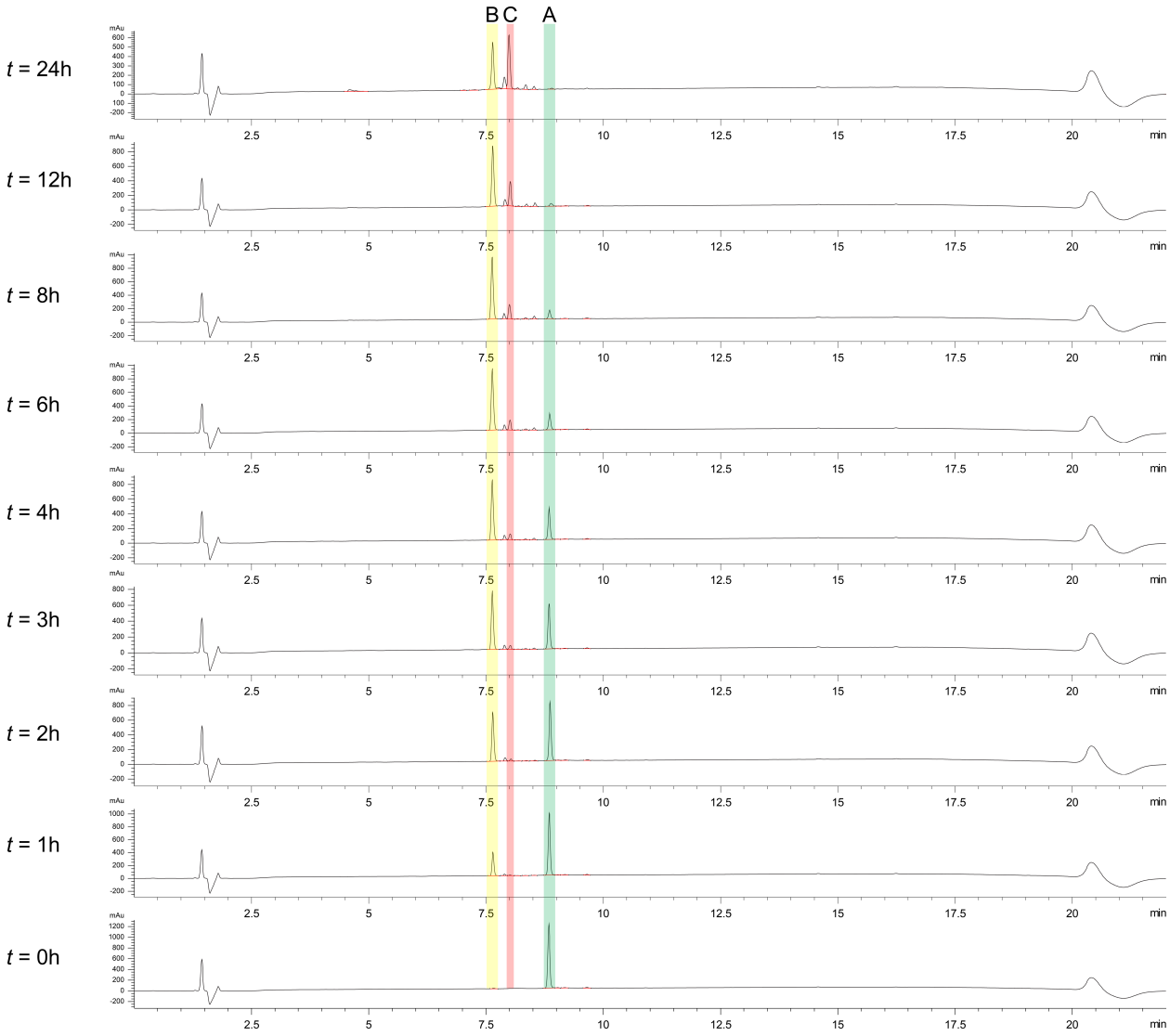

Figure S3.8. Analytical RP-HPLC trace showing the conversion of hypeptin, A, into decomposition byproducts B and C. HPLC was run on a C18 column with a gradient of 5–67% acetonitrile over 15 min, with monitoring of absorbance at 214 nm.

Table S3.1. Summary table of β-hydroxytyrosine containing peptide natural products. Chemical structures are shown in Figure S3.1.

Natural Product	Significance	Key Residue	Reported Stereochemistry	Total synthesis	References
Hypeptin	Antibiotic	β-hydroxytyrosine	(2*S*,3*R*)	No	Isolation[1]
Ralstoamide A & B	Plant pathogen	β-hydroxytyrosine	(2*S*,3*S*)	No	Isolation[2]
Ralstonins A & B	Plant pathogen	β-hydroxytyrosine	(2*S*,3*S*)	No	Isolation[3]
Burkholidines (Bk-1097 & Bk-1229)	Antifungal	β-hydroxytyrosine	(2*R*,3*R*)[4]	No	Isolation[5]
Balticidins A−D	Antifungal	β-hydroxytyrosine	unknown	No	Isolation[6]
Cepacidine A_1 & A_2	Antibiotic	β-hydroxytyrosine	unknown	No	Isolation[7]

Table S3.2. Summary table of structurally analogous peptide natural products. Chemical structures of these natural products are shown in Figures S3.4.

Natural Product	Significance	Key Residue	Reported Stereochemistry	Total synthesis	References
Swinhopeptolides A & B	Ras/Raf inhibitor	β-methoxytyrosine	(2*R*,3*R*)	No	Isolation[8]
Neamphamide A−D	Anti-HIV	β-methoxytyrosine	varies	No	Isolation[9,10]
Mirabamide A−H	Antifungal	β-methoxytyrosine	(2*R*,3*R*)	No	Isolation[11,12]
Lysobactin (Katanosin B)	Antibiotic	β-hydroxyphenylalanine	(2*S*,3*R*)	Yes	Isolation[13,14] Synthesis[15,16]
Ecumicin	Anti-TB	β-hydroxyphenylalanine	(2*S*,3*R*)	Yes	Isolation[17] Synthesis[18]
Ohmyungsamycin A & B	Anti-TB	β-hydroxyphenylalanine	(2*S*,3*R*)	Yes	Isolation[19] Synthesis[20]
Metamarin	Anti-TB	β-methoxyphenylalanine	(2*S*,3*R*)	Yes	Isolation[21] Synthesis[22]
Cyclomarins A−C	Antiinflammatory	β-methoxyphenylalanine	(2*S*,3*R*)	Yes	Isolation[23] Synthesis[22]
Callipeltin A−C, E	Anti-HIV	β-methoxytyrosine	(2*R*,3*R*)	Yes	Isolation[24–26] Synthesis[27,28]
Papuamides A−D	Anti-HIV	β-methoxytyrosine	(2*R*,3*R*)	Yes	Isolation[29] Synthesis[30]
Stellatolides A−G	Anticancer	β-methoxytyrosine	(2*R*,3*R*)	Yes	Isolation[31] Synthesis[31]

Table S3.3. Chemical shift tabulations of natural and synthetic hypeptin in DMSO-d_6 at 298 K. The tabulations correspond to the major set of peaks and were determined through a combination of ^{1}H NMR, HSQC, TOCSY, NOESY, and ROESY.

		Natural Hypeptin	Synthetic Hypeptin	Chemical Shift Difference
Residue	Proton	δ_H	δ_H	$\Delta\delta_H$
Ala_1	NH_2	8.00	8.01	-0.01
	α-CH	3.87	3.86	0.01
	β-CH_3	1.35	1.34	0.01
	NH	8.52	8.51	0.01
D-Leu_2	α-CH	4.45	4.45	0.00
	β-CH_2	1.55	1.55	0.00
	γ-CH	1.55	1.55	0.00
	δ-CH_3	0.86	0.86	0.00
		0.83	0.82	0.01
D-Arg_3	NH	8.24	8.24	0.00
	α-CH	4.41	4.40	0.01
	β-CH_2	1.72	1.73	-0.01
		1.58	1.58	0.00
	γ-CH_2	1.49	1.48	0.01
		1.46	1.48	-0.02
	δ-CH_2	3.08	3.08	0.00
	NH (guandidine)	7.47	7.45	0.02
		7.27	7.26	0.01
		6.78	6.78	0.00
Has_4	NH	8.10	8.10	0.00
	α-CH	4.70	4.70	0.00
	β-CH	4.02	4.02	0.00
	β-OH	6.04	6.04	0.00
	NH_2	7.39	7.38	0.01
		7.18	7.18	0.00
D-*allo*-Has_5	NH	8.25	8.26	-0.01
	α-CH	4.96	4.96	0.00
	β-CH	5.19	5.19	0.00
	NH_2	8.12	8.12	0.00
		7.39	7.39	0.00
Hty_6	NH	8.14	8.14	0.00
	α-CH	4.22	4.21	0.01
	β-CH	4.79	4.79	0.00
	β-OH	6.01	6.01	0.00
	aromatics	7.13	7.13	0.00
		6.64	6.64	0.00
	phenol	9.24	9.24	0.00
	NH	7.93	7.93	0.00
	α-CH	4.41	4.41	0.00
	β-CH	3.43	3.43	0.00

Appendix 3.1. Sequential linear checks in the first-generation synthesis of hypeptin.

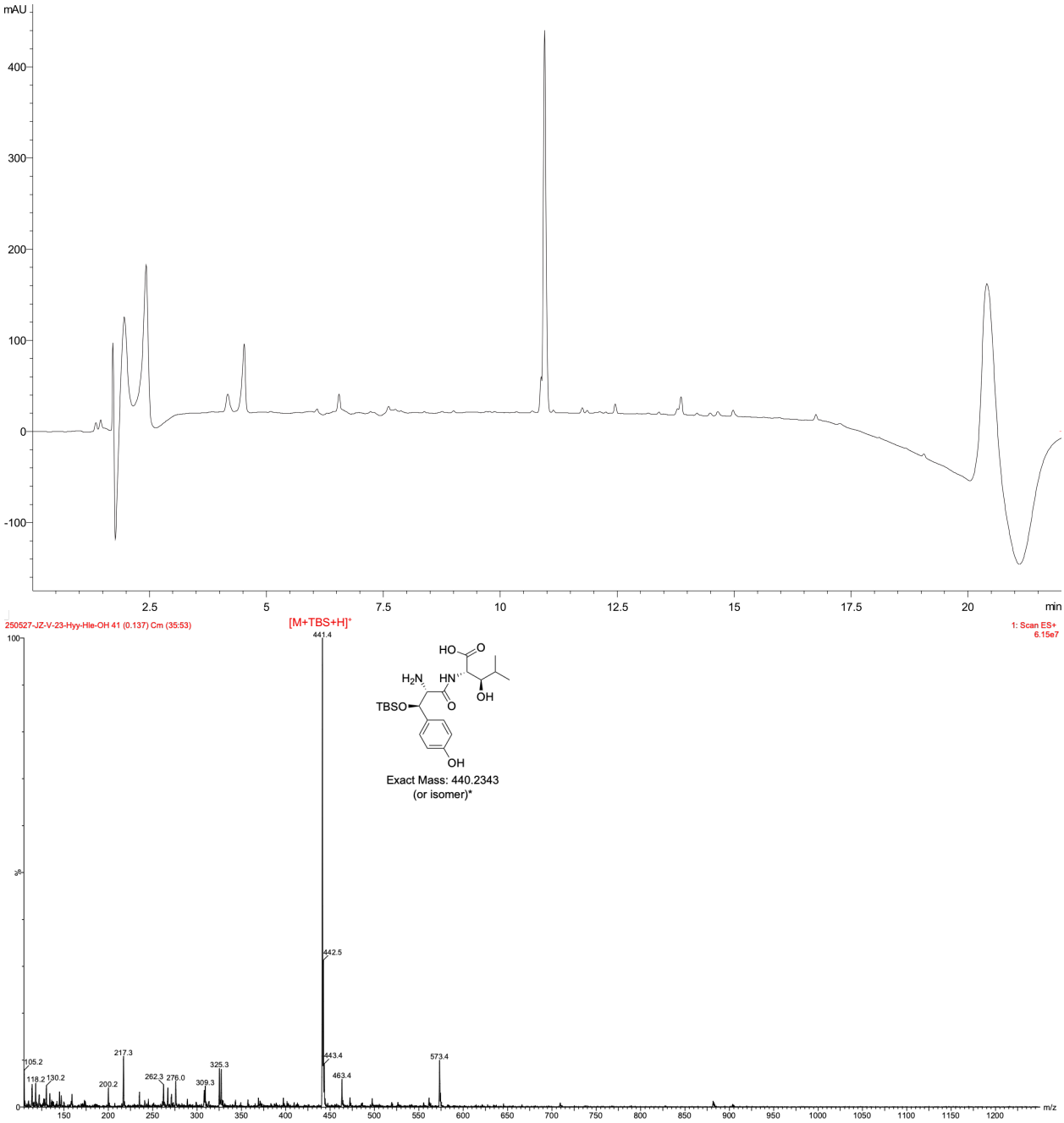

Analytical HPLC trace and MS of crude linear peptide following Fmoc deprotection of Hty_6. Linear check monitored by analytical HPLC analysis on a C18 column with a gradient of 5–67% CH_3CN over 15 min. MS was run with a CH_3CN direct inject onto a QDa in positive ES mode, 100 – 1250 m/z.

*The placement of the TBS protecting group on Hty_6 is arbitrary. Alternatively, the TBS protecting group could be placed on Hle_7.

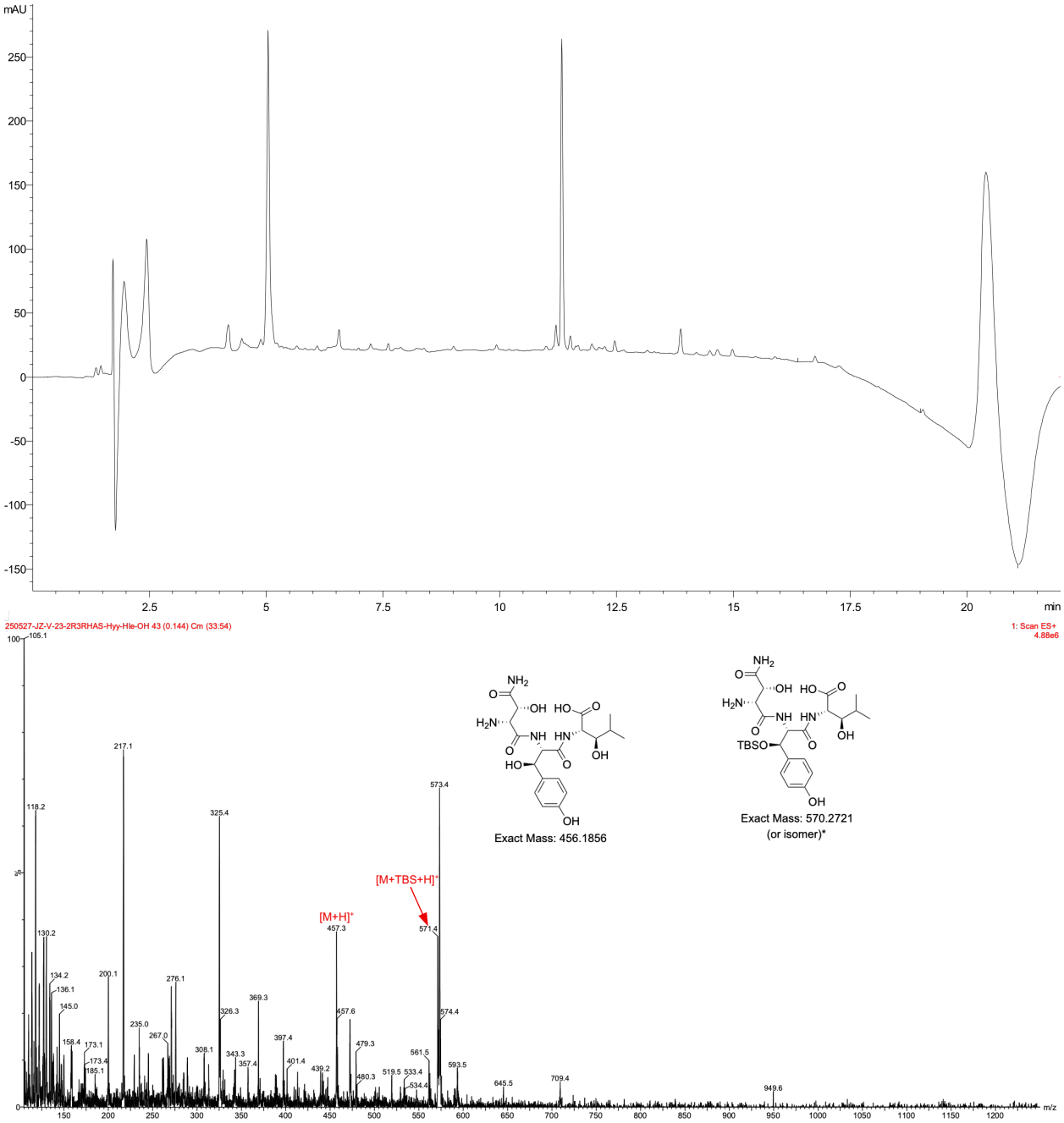

Analytical HPLC trace and MS of crude linear peptide following Fmoc deprotection of Has_5, which was coupled using HBTU/HOAt. Linear check monitored by analytical HPLC analysis on a C18 column with a gradient of 5–67% CH_3CN over 15 min. MS was run with a CH_3CN direct inject onto a QDa in positive ES mode, 100 – 1250 m/z.

*The placement of the TBS protecting group on Hty_6 is arbitrary. Alternatively, the TBS protecting group could be placed on Hle_7.

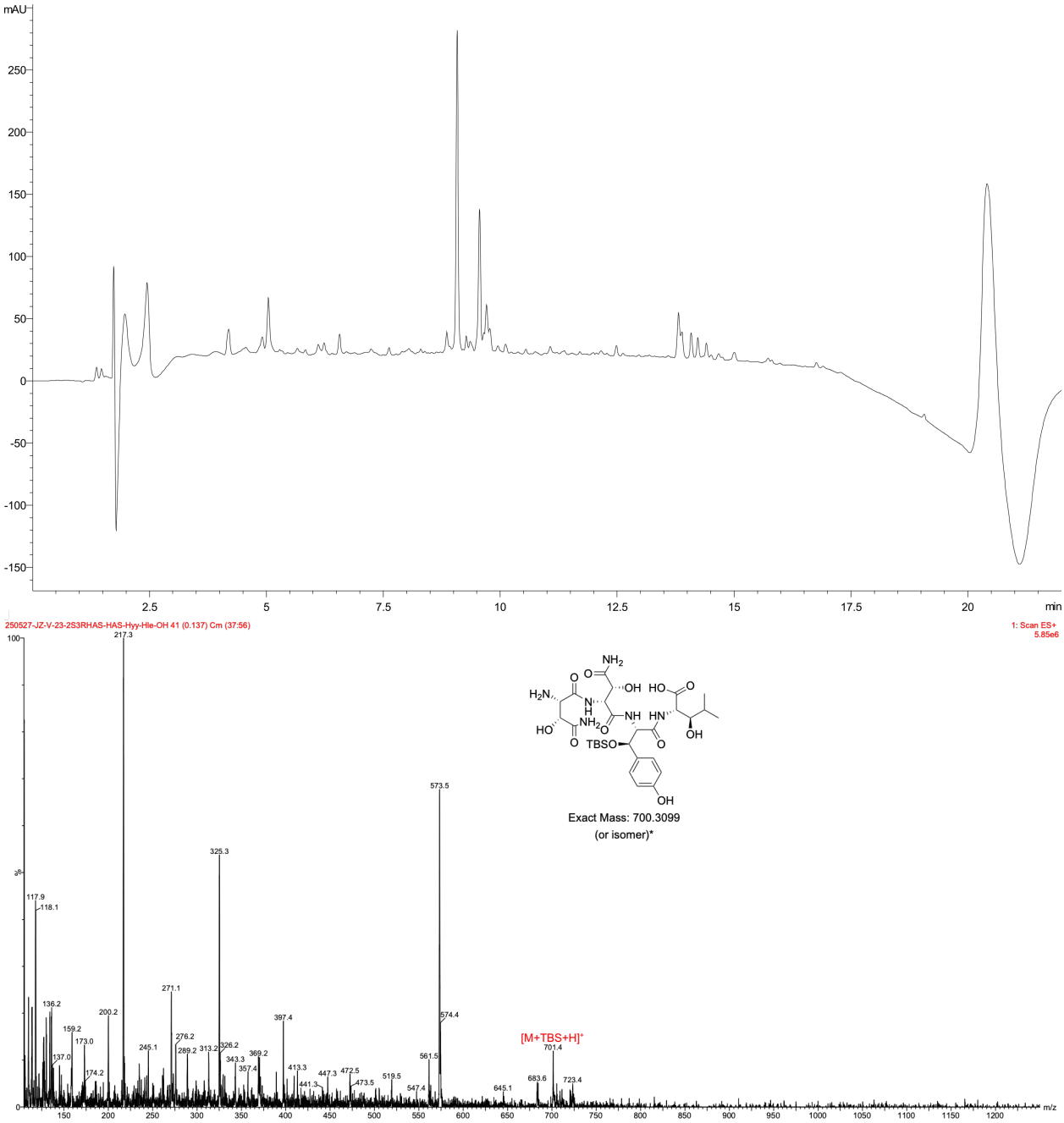

Analytical HPLC trace and MS of crude linear peptide following Fmoc deprotection of Has_4, which was coupled using HBTU/HOAt. Linear check monitored by analytical HPLC analysis on a C18 column with a gradient of 5–67% CH_3CN over 15 min. MS was run with a CH_3CN direct inject onto a QDa in positive ES mode, 100 – 1250 m/z.

*The placement of the TBS protecting group on Hty_6 is arbitrary. Alternatively, the TBS protecting group could be placed on Has_4 or Hle_7.

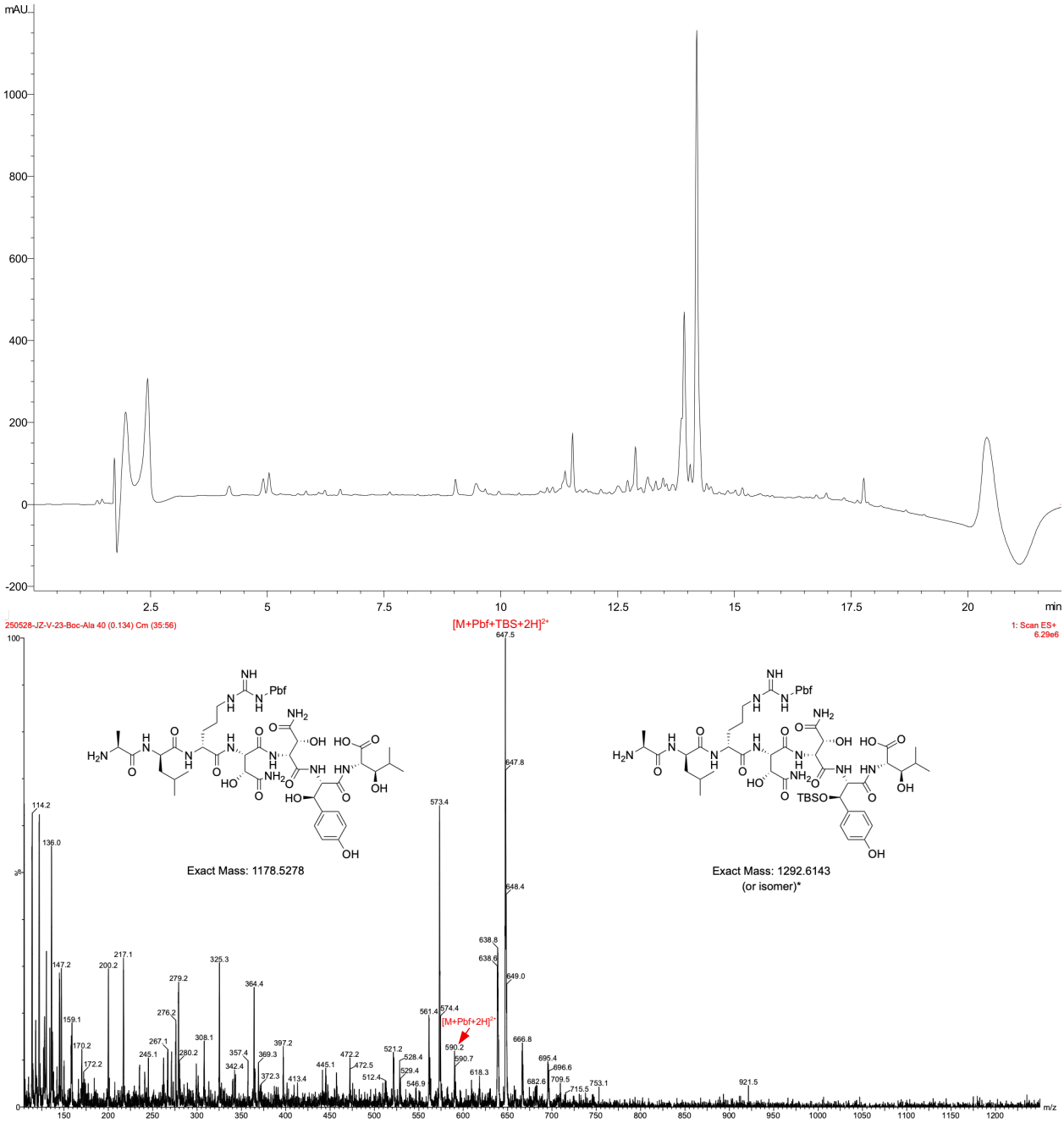

Analytical HPLC trace and MS of crude linear peptide following coupling of Boc-Ala$_1$. Linear check monitored by analytical HPLC analysis on a C18 column with a gradient of 5–67% CH_3CN over 15 min. MS was run with a CH_3CN direct inject onto a QDa in positive ES mode, 100 – 1250 m/z.

*The placement of the TBS protecting group on Hty$_6$ is arbitrary. Alternatively, the TBS protecting group could be placed on Has$_4$ or Hle$_7$.

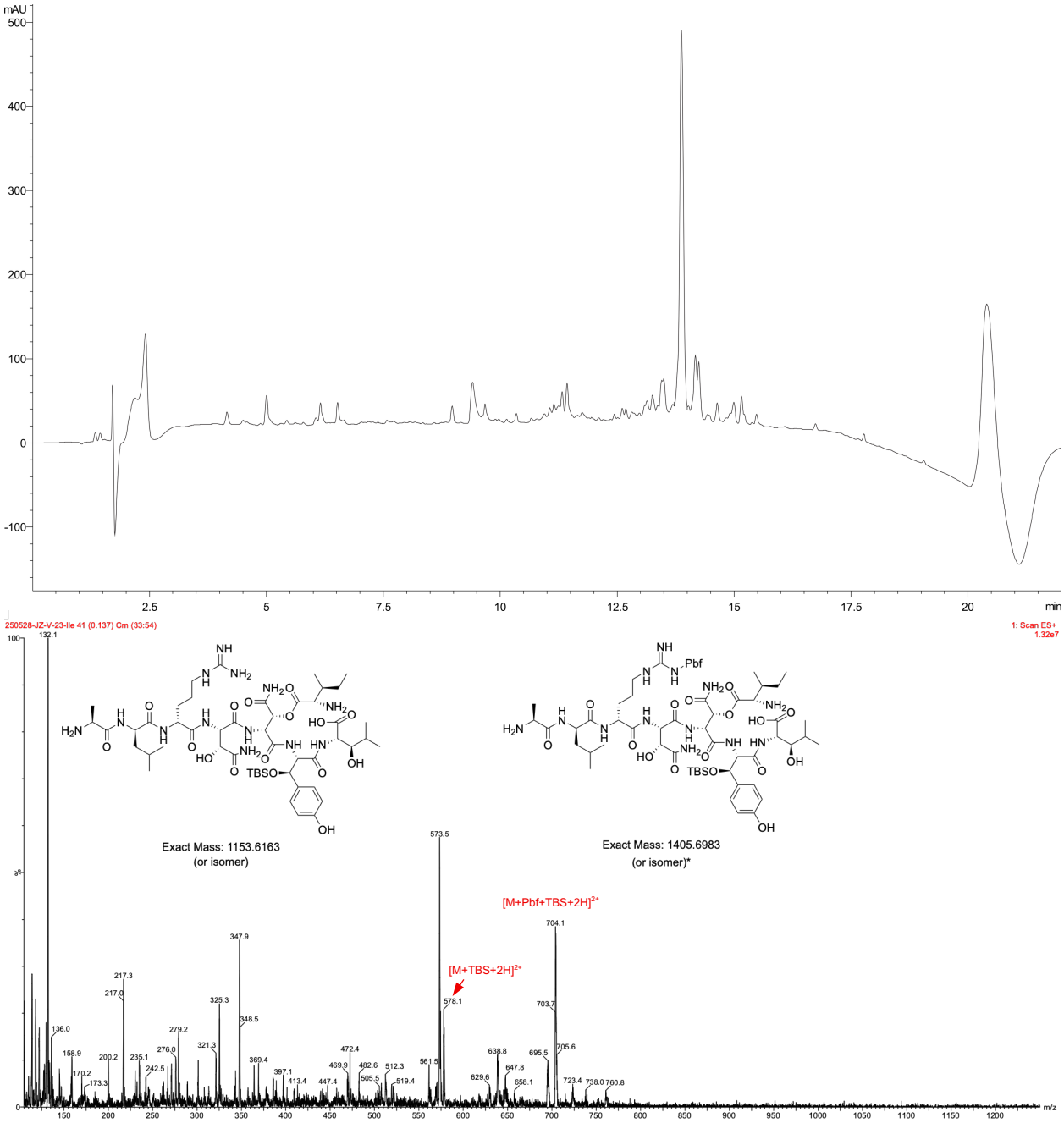

Analytical HPLC trace and MS of crude linear peptide following Steglich esterification and Fmoc-deprotection of Ile_8. Linear check monitored by analytical HPLC analysis on a C18 column with a gradient of 5–67% CH_3CN over 15 min. MS was run with a CH_3CN direct inject onto a QDa in positive ES mode, 100 – 1250 m/z.

*The placement of the TBS protecting group on Hty_6 is arbitrary. Alternatively, the TBS protecting group could be placed on Has_4 or Hle_7.

Materials and Methods

General Information

Chemicals and Supplies All chemicals were used as received unless otherwise noted. Dry methylene chloride (CH_2Cl_2), *N,N*-dimethylformamide (DMF), and diethyl ether were obtained by passing through alumina under argon prior to use. The DMF was additionally passed through an amine scavenger resin column under argon. Amine-free *N,N*-dimethylformamide (DMF) and piperidine were purchased from Alfa Aesar. 2,4,6-collidine and diisopropylethylamine (DIPEA) was purchased from Thermo Scientific. 1,1,1,3,3,3-Hexafluoro-2-propanol (HFIP) and trifluoroacetic acid (TFA) were purchased from Oakwood Chemicals. Deionized water (18 MΩ) was obtained from a Barnstead NANOpure Diamond water purification system. HPLC grade acetonitrile and deionized water (18 MΩ), each spiked with 0.1% (v/v) trifluoroacetic acid (TFA), were used for analytical and preparative reverse-phase HPLC. Deuterated methanol (CD_3OD, 99.8%) and dimethyl sulfoxide (DMSO-d_6, 99.9%) ampules were purchased from Cambridge Isotopes. Key reagents for the four β-hydroxy amino syntheses are summarized below.

Instrumentation All peptides were first purified on a Biotage® Isolera™ One system equipped with a Biotage® Sfr Bio C18 Duo 300 Å 20 µm column prior to purification on the Shimazu instrument equipped with an Agilent Zorbax 7 µm 300SB-C18 column (21.2 x 250 mm). Analytical reverse-phase HPLC was performed on an Agilent 1260 Infinity II instrument with a Phenomonex bioZen PEPTIDE 2.6 µm XB-C18 column. Yields refer to isolated purified compounds confirmed chromatographically. UV absorption was measured using the Thermo Scientific™ Varioskan™ LUX. All peptides were assumed to have one trifluoroacetate ion per ammonium group present in each peptide.

The suitably protected (2*S*,3*R*)-3-hydroxyasparagine-OH **1** was synthesized in the same fashion as its enantiomer, Fmoc-(2*R*,3*S*)-3-hydroxyasparagine-OH.[32]

The suitably protected (2*R*,3*R*)-hydroxyasparagine-OH **2** was synthesized according to previously reported procedures.[33]

Synthesis of protected (2*S*,3*R*)-3-hydroxytyrosine-OH **3**

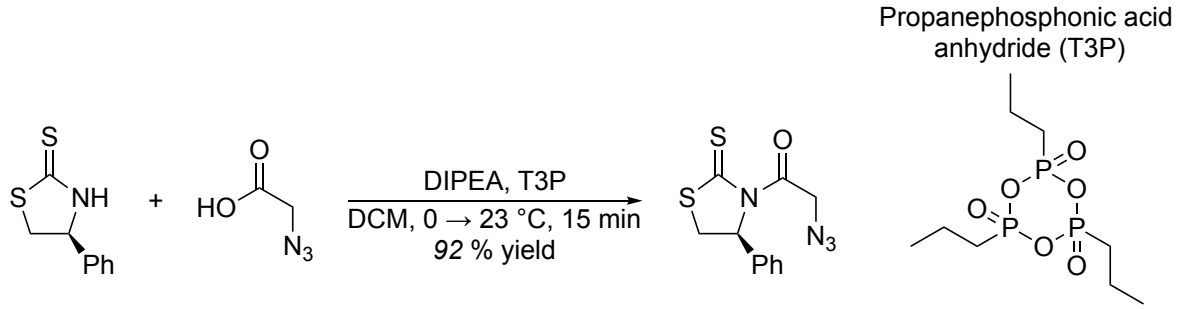

(*S*)-2-azido-1-(4-phenyl-2-thioxothiazolidin-3-yl)ethan-1-one. The following procedure was adapted from Ringling, Franck, and coworkers.[34,35] An oven-dry 250-mL one-neck round-bottom flask equipped with a dry stir bar was charged with (*S*)-4-phenylthiazolidine-2-thione (5.79 g, 29.6 mmol, 1.0 equiv), anhydrous DCM (30 mL), and azidoacetic acid (4.43 mL, 2.0 equiv). The solution was cooled to 0 °C. DIPEA (20.6 mL, 4.0 equiv) was added dropwise via syringe over 3 min. T3P (50 wt % in EtOAc, 22.9 mL, 2.6 equiv) was added dropwise via syringe over 5 min. The solution was allowed to warm to room temperature and stirred for an additional 15 min. The reaction mixture was poured over vigorously stirred 1 M HCl (92 mL) and extracted with DCM (3 x 50 mL). The combined organic layers were dried over Na_2SO_4 and concentrated under reduced pressure (30 °C) to yield a dark brown solid that was purified by column chromatography (250 mL SiO_2, wet-load minimal 70:30 DCM-hexanes with rapid elution, R_f = 0.49, UV active) to afford 7.59 grams of yellow solid (92% yield). The spectra were consistent with that reported in the literature.[35,36]

ATR-FTIR (diamond anvil, solid) 3062 (sp^2 C-H stretch, aromatic), 3033 (sp^2 C-H stretch, aromatic), 2994 (sp^3 C-H stretch), 2907 (sp^3 C-H stretch), 2888 (sp^3 C-H stretch), 2106 (N=N=N, azide), 1693 (C=O stretch), 1684 (C=O stretch) cm^{-1}.

^{1}H NMR (600 MHz, $CDCl_3$) δ 7.48 – 7.30 (m, 5H), 6.26 (dd, *J* = 8.2, 0.9 Hz, 1H), 4.94 (d, *J* = 18.3 Hz, 1H), 4.77 (d, *J* = 18.3 Hz, 1H), 4.05 (dd, *J* = 11.3, 8.3 Hz, 1H), 3.18 (dd, *J* = 11.3, 1.4 Hz, 1H).

^{13}C NMR (150.9 MHz, $CDCl_3$) δ 202.3, 169.0, 138.7, 129.4, 129.1, 125.7, 69.8, 55.6, 37.8.

HRMS (ESI+) m/z: $[M+Na]^+$ calculated 301.0194, observed 301.0183

$[\alpha]_D^{21}$ + 313 (*c* 1.0, $CHCl_3$)

Notes:

- Decreasing the azidoacetic acid equivalents below ~1.5 significantly reduces yields.
- Product hydrolyzes on silica into unreacted starting material and appears as 2 spots on the TLC plate.

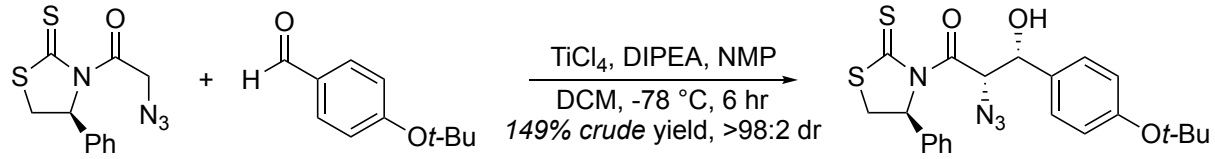

(2*S*,3*R*)-2-azido-3-(4-(*tert*-butoxy)phenyl)-3-hydroxy-1-((*S*)-4-phenyl-2-thioxothiazolidin-3-yl)propan-1-one. The following procedure was adapted from Franck and coworkers.[35] An oven dry 100-mL one-necked round bottom flask with a stir bar was charged with (*S*)-2-azido-1-(4-phenyl-2-thioxothiazolidin-3-yl)ethan-1-one (1.39 g, 5 mmol, 1.0 equiv), and anhydrous CH_2Cl_2 (50 mL). The solution was cooled to -78°C in a dry ice/isopropanol bath. $TiCl_4$ (575 µL, 1.05 equiv) was added dropwise via syringe over 3 min. The solution was stirred for 15 min before DIPEA (960 µL, 1.1 equiv) was added dropwise via syringe over 3 min. The solution was stirred for 1 hr before NMP (965 µL, 2 equiv) was added dropwise via syringe over 3 min. The solution was stirred for 15 min before 4-*tert*-butxoybenzaldehyde (1.31 mL, 1.5 equiv) was added dropwise via syringe over 3 min. The solution was stirred at -78°C for ~6 hr and monitored by TLC for the consumption of starting material (70:30 hexanes-EtOAc, $R_{f\ (pdt)}$ = 0.36, $R_{f\ (sm)}$ = 0.51, both UV active). The reaction was quenched with half-sat NH_4Cl (50 mL) and extracted with DCM (2 x 50 mL). The combined organic layers were dried over Na_2SO_4, passed through a short silica plug (~5 mL silica) to remove TiO_2, and concentrated under reduced pressure (20 °C) to yield 3.40 grams of amber oil that was used in the next step without further purification. A crude NMR confirmed the formation of a single diastereomer.

Notes:

- We have observed that adventitious HCl in the $TiCl_4$ can significantly reduce yields and recommend Sure-Seal $TiCl_4$ bottles.
- The equivalents of the $TiCl_4$, DIPEA, and NMP must be precisely added to ensure the formation of the desired diastereomer and quantitative consumption of starting material.
- Upon addition of the $TiCl_4$, the solution changes color from yellow to orange.
- Upon addition of DIPEA, the solution instantly changes color from orange to black/dark red.
- To monitor by TLC, quench a ~100 µL aliquot in saturated NH_4Cl prior to spotting.

To fully characterize this intermediate, a ca. 50 mg aliquot of crude was further purified by column chromatography (5 mL silica, 70:30 hex:EtOAc) to afford a yellow solid.

ATR-FTIR (diamond anvil, solid) 3358 (OH stretch, alcohol), 3059 (sp^2 C-H stretch, aromatic), 3023 (sp^2 C-H stretch, aromatic), 2977 (sp^3 C-H stretch, alkyl), 2943 (sp^3 C-H stretch, alkyl), 2896 (sp^3 C-H stretch, alkyl), 2111 (N=N=N, azide), 1716 (C=O stretch, amide) cm^{-1}.

^{1}H NMR (500 MHz, $CDCl_3$) δ 7.40 – 7.30 (m, 5H), 7.24 (d, *J* = 6.9 Hz, 2H), 7.04 (d, *J* = 8.5 Hz, 2H), 6.23 (d, *J* = 6.5 Hz, 1H), 5.59 (d, *J* = 7.4 Hz, 1H), 5.08 (d, *J* = 6.5 Hz, 1H), 3.36 (dd, *J* = 11.1, 7.7 Hz, 1H), 2.95 (dd, *J* = 11.1, 1.2 Hz, 1H), 2.74 (br s, 1H) 1.36 (s, 9H).

^{13}C NMR (125.8 MHz, $CDCl_3$) δ 203.0, 170.0, 156.3, 138.0, 133.2, 129.2, 128.8, 127.5, 125.3, 124.2, 79.2, 75.6, 70.4, 67.0, 37.9, 29.0.

HRMS: m/z: $[M+Na]^+$ calculated 479.1187, observed 479.1170

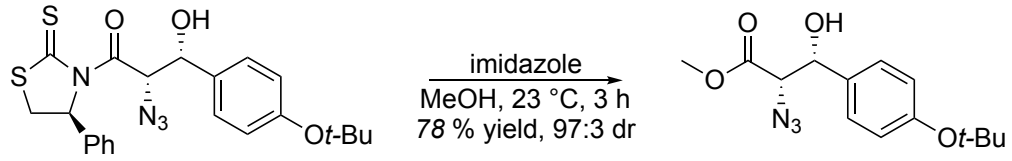

Methyl (2*S*,3*R*)-2-azido-3-(4-(*tert*-butoxy)phenyl)-3-hydroxypropanoate. The following procedure was adapted from Franck and coworkers.[35] A 100 mL one-necked round bottom flask containing crude (2*S*,3*R*)-2-azido-3-(4-(*tert*-butoxy)phenyl)-3-hydroxy-1-((*S*)-4-phenyl-2-thioxothiazolidin-3-yl)propan-1-one (5 mmol, assuming quantitative conversion from the previous step) was charged with a stir bar and MeOH (50 mL). Then imidazole (3.40 g, 10.0 eq) was added in one portion, and the reaction mixture was stirred for 3 hr. Next the reaction was diluted with H_2O (50 mL) and extracted with DCM (3 x 50 mL). The combined DCM layers were washed with half-saturated bicarbonate (2 x 50 mL), brine (1 x 50 mL), dried over Na_2SO_4, and concentrated down under reduced pressure to afford a dark amber oil. The crude oil was purified by column chromatography (150 mL silica, 90:10 DCM-hexanes for 2 CV then a 98:2 ($R_{f\,(pdt)}$ = 0.44) to 95:5 DCM-MeOH gradient over 3 CV, CAM stain, blue spots) to afford a yellow semi-pure oil. The semi-pure oil was repurified by column chromatography (100 mL silica, 70:30 hexanes-EtOAc, R_f = 0.30, CAM stain, blue spots) to afford 1.14 grams of light-yellow solid.

ATR-FTIR (diamond anvil, neat) 3420 (OH stretch, alcohol), 2977 (sp^3 C-H stretch), 2955 (sp^3 C-H stretch), 2933 (sp^3 C-H stretch), 2111 (N=N=N, azide), 1742 (C=O stretch, ester), 1607 (sp^2 C=C stretch, aromatic) cm^{-1}.

^{1}H NMR (500 MHz, $CDCl_3$) 7.29 (d, *J* = 8.5 Hz, 2H), 7.00 (d, *J* = 8.5 Hz, 2H), 5.17 (t, *J* = 4.5 Hz, 1H), 4.03 (d, *J* = 4.7 Hz, 1H), 3.74 (s, 3H), 2.56 (d, *J* = 4.7 Hz, 1H).

^{13}C NMR (125.8 MHz, $CDCl_3$) 169.1, 155.9, 133.8, 127.0, 124.3, 78.9, 74.4, 67.9, 52.9, 29.0.

HRMS: m/z: $[M+Na]^+$ calculated 316.1273, observed 316.1276

Notes:

- The second column was used to separate out NMP from the semi-pure oil.

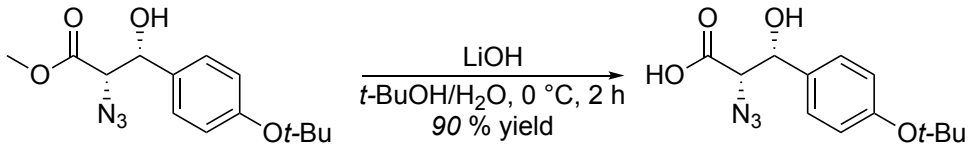

(2*S*,3*R*)-2-azido-3-(4-(*tert*-butoxy)phenyl)-3-hydroxypropanoic acid. A 250 mL one-necked round bottom flask equipped with a stir bar was charged with methyl (2*S*,3*R*)-2-azido-3-(4-(*tert*-butoxy)phenyl)-3-hydroxypropanoate (1.13 g, 3.86 mmol, 1 eq) and 1:1 *t*-BuOH:H_2O (30 mL). The reaction was cooled to 0 °C in an ice bath before LiOH solution (323.6 mg LiOH*H_2O dissolved in 8 mL 1:1 *t*-BuOH-H_2O) was added dropwise over 3 min. The reaction was stirred for 2 hr then acidified with 1M HCl to pH 3. The reaction mixture was extracted with EtOAc (3 x 30 mL). The combined organic layers were dried over Na_2SO_4 and concentrated down. The crude was purified by column chromatography (50 mL silica, 97:3 DCM-MeOH for 2 CV then flushed with MeOH (CAM stain, blue spots) to afford 970 mg of off-white foam.

ATR-FTIR (diamond anvil, solid) 3352 (OH stretch, alcohol), 2977 (sp^3 C-H stretch), 2933 (sp^3 C-H stretch), 2113 (N=N=N, azide), 1607 (C=O stretch, carboxylate) cm^{-1}.

^{1}H NMR (500 MHz, $(CD_3)_2SO$) δ 7.29 (d, *J* = 8.4 Hz, 2H), 6.90 (d, *J* = 8.5 Hz, 2H), 5.08 (br s, 1H), 3.63 (br s, 1H), 1.27 (s, 9H).

^{13}C NMR (125.8 MHz, $(CD_3)_2SO$) δ 171.1, 153.9, 137.5, 127.0, 123.0, 77.7, 73.3, 67.5, 28.6.

HRMS: m/z: $[M+Na]^+$ calculated 302.1117, observed 302.1115

Note:

- Both methines appear as slightly broadened singlets which reflects the chemical exchange of the OH and carboxylic acids.
- The carbon of the carboxylic acid is significantly broadened out due to chemical exchange with the carboxylate.

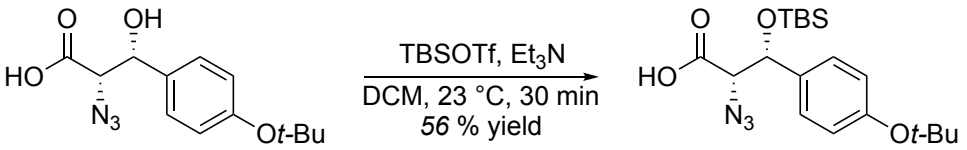

(2*S*,3*R*)-2-azido-3-(4-(*tert*-butoxy)phenyl)-3-((*tert*-butyldimethylsilyl)oxy)propanoic acid. A dry 250-mL one-necked round bottom flask that contained (2*S*,3*R*)-2-azido-3-(4-(*tert*-butoxy)phenyl)-3-hydroxypropanoic acid (970 mg, 3.5 mmol) was charged with an oven dry stir bar and anhydrous DCM (35 mL). Then Et_3N (2.11 mL, 6 eq) was added via syringe. TBSOTf (2.39 mL, 3 equiv) was then added dropwise via syringe over 3 min. The reaction was stirred at rt for 30 min. The reaction was quenched with water and acidified with 1M HCl to pH ~3. The aqueous layer was extracted with DCM (3 x 30 mL), dried with Na_2SO_4, and concentrated under reduced pressure. The crude oil was purified by column chromatography (100 mL silica, 99:1 DCM-MeOH for 2 CV, then 90:10 DCM-MeOH (R_f = 0.39), CAM stain) to afford a semi-pure oil. The semi-pure material was redissolved in DCM (50 mL), washed with 5% LiCl solution (10 x 20 mL), brine (1 x 20 mL), dried with Na_2SO_4, concentrated under reduced pressure and repurified with a DCM plug (20 mL silica, DCM for 5 CV, then flush with MeOH) to afford 770 mg of off-white foam.

ATR-FTIR (diamond anvil, solid) 2976 (sp^3 C-H stretch), 2955 (sp^3 C-H stretch), 2930 (sp^3 C-H stretch), 2986 (sp^3 C-H stretch), 2858 (sp^3 C-H stretch), 2112 (N=N=N, azide), 1723 (C=O stretch, carboxylic acid) cm^{-1}.

^1H NMR (500 MHz, $CDCl_3$) 7.30 (d, *J* = 8.5 Hz, 2H), 6.99 (d, *J* = 8.5 Hz, 2H), 5.29 (d, *J* = 2.5 Hz, 1H), 3.71 (d, *J* = 2.8 Hz, 1H), 1.36 (s, 9H), 0.87 (s, 9H), 0.04 (s, 3H), -0.17 (s, 3H).

^{13}C NMR (125.8 MHz, $CDCl_3$) 173.8, 155.5, 135.0 124.1, 78.9, 76.6, 68.4, 29.0, 25.7, 18.2, -4.6, -5.3.

HRMS: m/z: $[M+Na]^+$ calculated 416.1982, observed 416.1966

Note:

- The carboxylic acid is broadened in the carbon NMR due to chemical exchange.

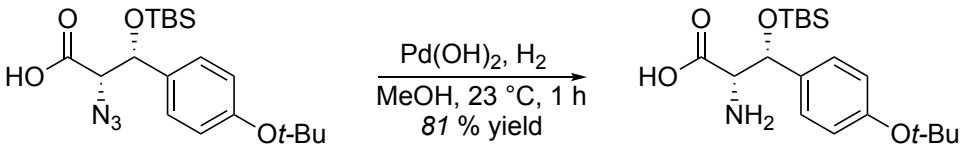

(2*S*,3*R*)-2-amino-3-(4-(*tert*-butoxy)phenyl)-3-((*tert*-butyldimethylsilyl)oxy)propanoic acid. A 250-mL one-necked round bottom flask that contained (2*S*,3*R*)-2-azido-3-(4-(*tert*-butoxy)phenyl)-3-((*tert*-butyldimethylsilyl)oxy)propanoic acid (770 mg, 1.96 mmol, 1 eq) was charged with a stir bar, $Pd(OH)_2$ (231 mg, 30% by wt. relative to azide, 20% loading), and MeOH (20 mL). The flask was backfilled with Argon before hydrogen gas (balloon) was added. The reaction was stirred for 1 hr and then filtered through a PVDF membrane. The crude material concentrated down and purified by column chromatography (75 mL silica, 90:10 DCM-MeOH for 2 CV then flush with MeOH (R_f = 0.83), CAM stain, blue spots) to afford 580 mg of white solid.

ATR-FTIR (diamond anvil, solid) 2975 (sp^3 C-H stretch), 2950 (sp^3 C-H stretch), 2929 (sp^3 C-H stretch), 2885 (sp^3 C-H stretch), 2856 (sp^3 C-H stretch), 1635 (C=O stretch, carboxylate), 1608 (C=C stretch, aromatic) cm^{-1}.

^1H NMR (500 MHz, CD_3OD) 7.39 (d, *J* = 8.5 Hz, 2H), 7.04 (d, *J* = 8.6 Hz, 2H), 5.52 (s, 1H), 3.56 (s, 1H), 1.35 (s, 9H), 0.91 (s, 9H), 0.09 (s, 3H), -0.03 (s, 3H).

^{13}C NMR (125.8 MHz, CD_3OD) 156.6, 137.1, 127.7, 125.3, 79.8, 74.1, 62.8, 29.2, 26.4, 19.2, -4.7, -4.9.

HRMS: m/z: $[M+Na]^+$ calculated 368.2257, observed 368.2255

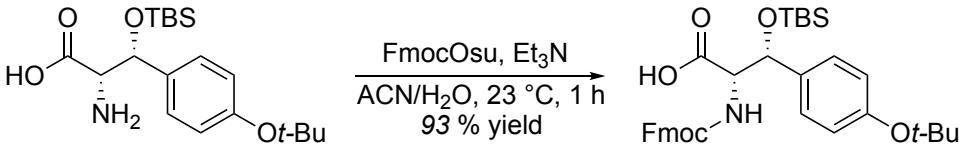

(2*S*,3*R*)-2-((((9*H*-fluoren-9-yl)methoxy)carbonyl)amino)-3-(4-(*tert*-butoxy)phenyl)-3-((*tert*-butyldimethylsilyl)oxy)propanoic acid. A 250-mL one-necked round bottom flask that contained (2*S*,3*R*)-2-amino-3-(4-(*tert*-butoxy)phenyl)-3-((*tert*-butyldimethylsilyl)oxy)propanoic acid (510 mg, 1.39 mmol, 1 eq) was charged with a stir bar, FmocOsu (445 mg, 1.32 mmol, 0.95 eq), and 1:1 ACN:H_2O (14 mL). Then Et_3N (193 μL, 1.39 mmol, 1 eq) was added and the reaction was stirred for 15 min. Additional Et_3N was added dropwise until the solution was pH ca. 7-8. The reaction was stirred for 1 hr, stripped of ACN under reduced pressure, and acidified with 1M HCl to pH ca. 2-3. The aqueous layer was extracted with EtOAc (3 x 15 mL) and the combined organic layers were dried with Na_2SO_4 and concentrated down. The crude product was purified by column chromatography (DCM for 2 CV then 90:10 DCM-MeOH, R_f = 0.71, UV active) to afford 720 mgs of white foam.

ATR-FTIR (diamond anvil, solid) 3065 (sp^2 C-H stretch), 2953 (sp^3 C-H stretch), 2929 (sp^3 C-H stretch), 2897 (sp^3 C-H stretch), 2856 (sp^3 C-H stretch), 1732 (C=O stretch), 1716 (C=O stretch) cm^{-1}.

^{1}H NMR (500 MHz, $(CD_3)_2SO$) 12.90 (s, 1H), 7.88 (d, *J* = 7.6 Hz, 2H), 7.69 (dd, *J* = 10.3, 7.7 Hz, 2H), 7.41 (t, *J* = 7.4 Hz, 2H), 7.36 – 7.22 (m, 5H), 6.79 (d, *J* = 8.5 Hz, 2H), 5.21 (d, *J* = 3.5 Hz, 1H), 4.22 (dd, *J* = 9.8, 3.5 Hz, 1H), 4.18 – 4.06 (m, 2H), 4.06 – 3.93 (m, 1H), 1.14 (s, 9H), 0.84 (s, 9H), -0.01 (s, 3H), -0.18 (s, 3H).

^{13}C NMR (125.8 MHz, $(CD_3)_2SO$) 171.4, 156.0, 154.3, 143.8, 143.6, 140.6, 135.7, 127.65, 127.61, 127.2, 127.02, 126.99, 125.5, 125.3, 122.8, 120.05, 120.03, 77.7, 74.1, 66.1, 61.0, 46.4, 28.4, 25.6, 17.9, -4.8, -5.3.

HRMS: m/z: $[M+Na]^+$ calculated 612.2758, observed 612.2756

$[\alpha]_D^{21}$ – 5.1 (*c* 1.0, $CHCl_3$)

Notes:

- NMR contains Fmoc rotamers as denoted by asterisk.

Synthesis of protected (2*S*,3*R*)-3-hydroxyleucine-OH **4**

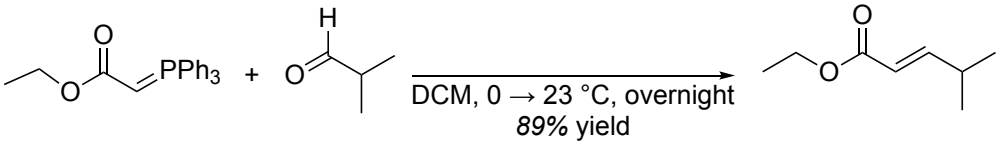

Ethyl (*E*)-4-methylpent-2-enoate. An oven-dry one-necked 250 mL round bottom flask was charged with carboethoxymethylene triphenylphosphoarane (10 g, 28.7 mmol, 1 eq), anhydrous DCM (60 mL) and a stir bar. The reaction was cooled to 0 °C before freshly distilled isobuteraldehyde (2.62 mL, 28.7 mmol, 1 eq) was added dropwise. The solution was allowed to warm to room temperature and stirred overnight. The reaction was stripped of DCM under reduced pressure and redissolved in hexanes (100 mL), filtered, and concentrated down. The crude oil was purified by column chromatography (100 mL silica, 1:1 hexanes-DCM, $R_f = 0.60$, $KMnO_4$ stain) and concentrated under reduced pressure (25 °C) to afford 3.62 grams of clear oil.

ATR-FTIR (diamond anvil, neat) 2963 (sp^3 C-H stretch), 2937 (sp^3 C-H stretch), 2905 (sp^3 C-H stretch), 2872 (sp^3 C-H stretch), 1716 (C=O stretch), 1652 (C=C stretch) cm^{-1}.

^{1}H NMR (500 MHz, $CDCl_3$) δ 6.92 (dd, *J* = 15.8, 6.7 Hz, 1H), 5.75 (dd, *J* = 15.8, 1.5 Hz, 1H), 4.17 (q, *J* = 7.2 Hz, 2H), 2.44 (dqqd, *J* = 6.8, 6.8, 6.8, 1.5 Hz, 1H), 1.27 (t, *J* = 7.2 Hz, 3H), 1.04 (d, J = 6.8 Hz, 6H).

^{13}C NMR (125.3 MHz, $CDCl_3$) δ 167.2, 155.5, 118.8, 60.2, 31.0, 21.3, 14.4.

HRMS: m/z: $[M+Na]^+$ calculated 165.0892, observed 165.0893

Notes:

- This alkene can also be readily prepared using the Masamune and Roush conditions variation of the HWE reaction.[37]

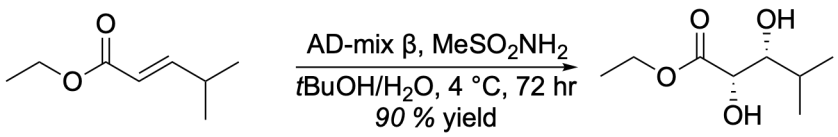

Ethyl (2*S*,3*R*)-2,3-dihydroxy-4-methylpentanoate. A one-neck 250 mL flask was charged with alkene (790 mg, 5.53 mmol, 1 eq), 1:1 *t*BuOH:H_2O (56 mL), and a stir bar. The reaction was cooled to 0 °C before $MeSO_2NH_2$ (526 mg, 1 eq) was added. Then AD-mix β (7.78 grams) was added. The reaction was stirred in a cold room (4 °C) for 72 hr and quenched with Na_2SO_3 (8.33 g). The reaction was allowed to warm to room temperature, stirred for 1 hr, diluted with H_2O (25 mL), and then extracted with EtOAc (3 x 25 mL), dried with Na_2SO_4, and concentrated down. The crude oil was purified by column chromatography (75 mL silica, 1:1 hexanes/EtOAc, R_f = 0.47, $KMnO_4$, brown spots) and concentrated down under reduced pressure (35 °C) to afford 880 mg of light-yellow oil.

ATR-FTIR (diamond anvil, neat) 3438 (OH stretch, alcohol), 2962 (sp^3 C-H stretch, alkyl), 2935 (sp^3 C-H stretch, alkyl), 2874 (sp^3 C-H stretch, alkyl), 1732 (C=O stretch, ester) cm^{-1}.

^{1}H NMR (500 MHz, $CDCl_3$) δ 4.27 (q, *J* = 7.1 Hz, 2H), 4.27 – 4.20 (m, 1H), 3.48 (t, *J* = 8.9 Hz, 1H), 3.16 (d, *J* = 4.9 Hz, 1H), 2.09 (d, *J* = 9.5 Hz, 1H), 1.87 (dqq, *J* = 8.5, 6.8, 6.8 Hz, 1H), 1.31 (t, *J* = 7.2 Hz, 3H), 1.04 (d, *J* = 6.8 Hz, 3H), 0.97 (d, *J* = 6.8 Hz, 3H).

^{13}C NMR (125.8 MHz, $CDCl_3$) δ 174.3, 78.0, 71.4, 62.2, 31.3, 19.2, 19.1, 14.3.

HRMS: m/z: $[M+Na]^+$ calculated 199.0946, observed 199.0949

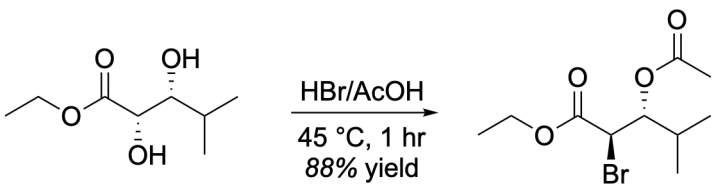

Ethyl (2*R*,3*R*)-3-acetoxy-2-bromo-4-methylpentanoate. An oven dry one-necked 100 mL round bottom flask was charged with diol (710 mg), an oven dry stir bar, and HBr/AcOH (6 mL). The reaction was heated to 45 °C, stirred for 1 hr, and then cooled to 0 °C. The reaction was diluted with ether (10 mL) and water (25 mL). The aqueous layer was extracted with ether (2 x 10 mL). The combined organic layers were washed with sat $NaHCO_3$, dried with Na_2SO_4, concentrated down under reduced pressure to afford 1.00 grams of slightly tan oil. The oil was used in the following step without further purification.

ATR-FTIR (diamond anvil, neat) 2969 (sp^3 C-H stretch, alkyl), 2937 (sp^3 C-H stretch, alkyl), 2879 (sp^3 C-H stretch, alkyl), 1749 (C=O stretch, ester) cm^{-1}.

^1H NMR (500 MHz, $CDCl_3$) δ 5.33 (dd, *J* = 9.2, 3.7 Hz, 1H), 4.26 (d, *J* = 9.2 Hz, 1H), 4.24 – 4.16 (m, 2H), 2.34 (dqq, *J* = 6.9, 6.9, 3.7 Hz, 1H), 2.04 (s, 3H), 1.27 (t, *J* = 7.2 Hz, 3H), 0.94 (d, *J* = 6.9 Hz, 3H), 0.90 (d, *J* = 6.8 Hz, 3H).

^{13}C NMR (125.8 MHz, $CDCl_3$) δ 169.6, 167.9, 76.4, 62.4, 44.6, 29.0, 20.8, 19.6, 15.4, 14.4.

HRMS: m/z: $[M+Na]^+$ calculated 303.0208, observed 303.0206

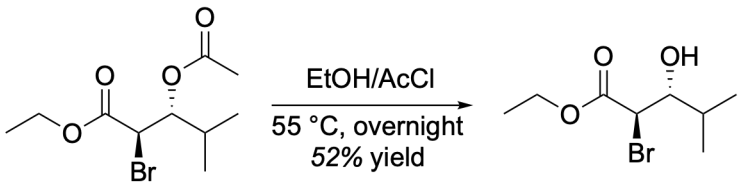

Ethyl (2*R*,3R)-2-bromo-3-hydroxy-4-methylpentanoate. A one-necked 100 mL round bottom flask containing acetyl bromo ester (1.00 g, 1 eq) was charged with an oven dry stir bar and anhydrous EtOH (10 mL). Then freshly distilled acetyl chloride, AcCl, (1 mL) was added dropwise. The reaction was heated to 55 °C and stirred overnight. The reaction was diluted with water (25 mL), extracted with DCM (3 x 20 mL), and washed with half-saturated $NaHCO_3$ solution (10 mL). The combined organic layers were concentrated down and purified by column chromatography (75 mL silica, 80:20 hex-EtOAc, R_f = 0.52, weakly UV active) to afford 440 mgs of light tan oil.

ATR-FTIR (diamond anvil, neat) 3502 (OH stretch, alcohol), 2963 (sp^3 C-H stretch, alkyl), 2935 (sp^3 C-H stretch, alkyl), 2876 (sp^3 C-H stretch), 1725 (C=O stretch, ester) cm^{-1}.

^{1}H NMR (500 MHz, $CDCl_3$) δ 4.26 (q, *J* = 7.2 Hz, 2H), 4.21 (d, *J* = 8.2 Hz, 1H), 3.86 (ddd, *J* = 8.1, 5.8, 4.0 Hz, 1H), 2.56 (d, *J* = 6.3 Hz, 1H), 2.14 (qqd, *J* = 6.8, 6.8, 4.0, 1H), 1.32 (t, *J* = 7.2 Hz, 3H), 1.02 (d, *J* = 6.9 Hz, 3H), 0.92 (d, *J* = 6.8 Hz, 3H).

^{13}C NMR (125.8 MHz, $CDCl_3$) δ 169.9, 76.5, 62.4, 45.8, 29.7, 20.0, 15.2, 14.1.

HRMS: m/z: $[M+Na]^+$ calculated 261.0102, observed 261.0103

Note:

- This reaction stalls around 90% deacetylation reaction when run in wet EtOH.

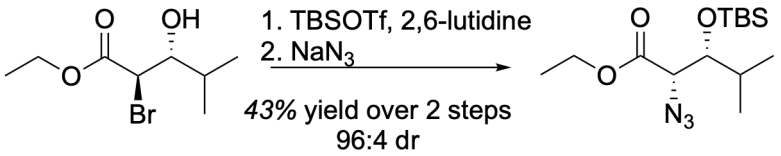

Ethyl (2*S*,3*R*)-2-azido-3-((*tert*-butyldimethylsilyl)oxy)-4-methylpentanoate. An oven dry one-necked 250 mL round bottom flask was charged with bromoalcohol (1.81 mg, 7.6 mmol), anhydrous DCM (30 mL), an oven dry stir bar. The reaction was cooled to 0 °C in an ice bath before 2,6-lutidine (1.75 mL, 2.0 eq) and TBSOTf (2.61 mL, 1.5 eq) were added dropwise. The reaction was stirred for 1 hr on ice. The reaction was quenched with ½ sat $NaHCO_3$ (2 x 30 mL), extracted with DCM (3 x 30 mL). The combined organic layers were dried with Na_2SO_4, concentrate down and purified by column chromatography (1:1 hex DCM, R_f = 0.70, CAM stain, light blue spots) to afford 2.69 g of semi-purified clear oil. The oil was immediately resuspended in DMF (38 mL) with NaN_3 (984 mg, 2 eq). The solution was stirred at 65°C for 15 hr in an oil bath, then diluted with H_2O (150 mL), and extracted with EtOAc (3 x 50 mL). The combined organic layers were dried with Na_2SO_4, concentrated down, left to stand on the high vac (<100 mTorr for ~3 hr) and purified by column chromatography (80:20 hex/DCM for 2 CV then 1:1 hex/DCM until the product elutes) to afford 1.03 g of clear oil.

ATR-FTIR (diamond anvil, neat) 2959 (sp^3 C-H stretch, alkyl), 2931 (sp^3 C-H stretch, alkyl), 2886 (sp^3 C-H stretch, alkyl), 2958 (sp^3 C-H stretch, alkyl), 2107 (N=N=N, azide), 1750 (C=O stretch, ester) cm^{-1}.

^1H NMR (500 MHz, $CDCl_3$) δ 4.29 (dq, *J* = 10.9, 7.2 Hz, 1H), 4.22 (dq, *J* = 10.9, 7.2 Hz, 1H), 4.06 (dd, *J* = 5.6, 2.8 Hz, 1H), 3.54 (d, *J* = 2.7 Hz, 1H), 1.98 – 1.88 (m, 1H), 1.34 (t, *J* = 7.2 Hz, 3H), 1.04 (d, *J* = 6.9 Hz, 3H), 0.97 (d, *J* = 6.9 Hz, 3H), 0.90 (s, 9H), 0.09 (s, 3H), 0.02 (s, 3H).

^{13}C NMR (125.8 MHz, $CDCl_3$) δ 170.3, 78.9, 63.4, 62.1, 33.1, 26.0, 18.7, 18.3, 18.1, 14.2, -4.2, -4.5.

HRMS: m/z: $[M+Na]^+$ calculated 338.1876, observed 338.1875

Note:

- Following TBS protection, the ^1H NMR spectrum of the semi-purified ethyl (2*R*,3*R*)-2-bromo-((*tert*butyldimethylsilyl)oxy)-4-methylpentanoate contains a TBSOH impurity.
- Following azide displacement, the undesired diastereomer can be separated and has slightly higher R_f (ca. 0.05 difference) compared to that of the desired product.

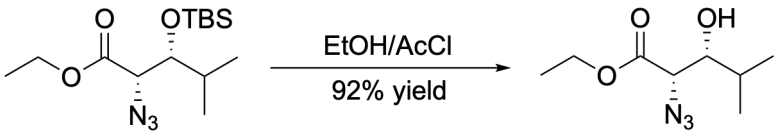

Ethyl (2*S*,3*R*)-2-azido-3-hydroxy-4-methylpentanoate. An oven dry one-necked 100 mL roundbottom flask was charged with azidoester (1.16 g, 3.7 mmol), anhydrous EtOH (15 mL), an oven dry stir bar, and freshly distilled AcCl (3 mL). The reaction mixture was stirred at 65 C for 2 hr, then diluted with 60 mL H_2O, extracted with EtOAc (5 x 30 mL), dried with Na_2SO_4, and concentrated down. The crude oil was purified by column chromatography (1:1 DCM/hex for 2 CV then 1:1 EtOAc/hex) to afford 820 mg of clear oil.

ATR-FTIR (diamond anvil, neat) 3481 (OH stretch, alcohol), 2965 (sp^3 C-H stretch, alkyl), 2939 (sp^3 C-H stretch, alkyl), 2912 (sp^3 C-H stretch, alkyl), 2985 (sp^3 C-H stretch, alkyl), 2111 (N=N=N, azide), 1733 (C=O stretch, ester) cm^{-1}.

^{1}H NMR (500 MHz, $CDCl_3$) δ 4.31 (q, *J* = 7.1 Hz, 2H), 4.01 (d, *J* = 2.9 Hz, 1H), 3.70 (dd, *J* = 8.3, 2.9 Hz, 1H), 1.91 – 1.81 (m, 1H), 1.34 (t, *J* = 7.2, 3H), 1.05 (d, *J* = 6.7 Hz, 3H), 0.95 (d, *J* = 6.7 Hz, 3H).

^{13}C NMR (125.8 MHz, $CDCl_3$) δ 169.7, 77.9, 64.2, 62.3, 31.4, 19.1, 18.7, 14.3

HRMS: m/z: $[M+Na]^+$ calculated 224.1011, observed 224.1012

Note:

- The ^{1}H NMR spectrum of the purified azido alcohol contains TBSOH (ca. 24 mol%) that was used directly in the following step.

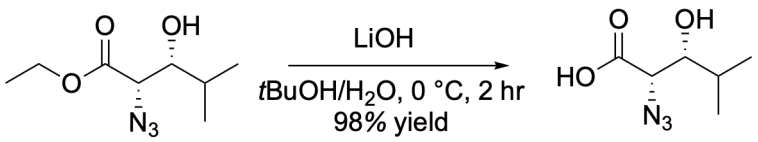

(2*S*,3*R*)-2-azido-3-hydroxy-4-methylpentanoic acid. An one-necked 100 mL round-bottom flask was charged with azidoalcohol (820 mg, 3.4 mmol), 1:1 *t*-BuOH/H_2O (20 mL). The reaction was cooled down to 0°C in an ice bath before LiOH*H_2O (327 mg, 2.0 eq relative to azidoalcohol) was added in one portion. The reaction was stirred on ice for 2 hr, then acidified with 1 M HCl (10 mL), stripped of *t*BuOH under reduced pressure. The aqueous layer was extracted with EtOAc (5 x 20 mL), dried with Na_2SO_4, and concentrated down under reduced pressure. The crude oil was purified by column chromatography (80/20 DCM/MeOH, R_f = 0.52, $KMnO_4$, brown spots) to afford 700 mg of wet clear oil that was used directly in the next step.

ATR-FTIR (diamond anvil, neat) 3365 (OH stretch, alcohol), 2964 (sp^3 C-H stretch, alkyl), 2876 (sp^3 C-H stretch, alkyl), 2113 (N=N=N, azide), 1716 (C=O stretch, carbonyl) cm^{-1}.

^{1}H NMR (500 MHz, $(CD_3)_2SO$) δ 3.82 (d, *J* = 2.4 Hz, 1H), 3.60 (dd, *J* = 8.4, 3.6 Hz, 1H), 1.77 – 1.65 (m, 1H), 0.94 (d, *J* = 6.6 Hz, 3H), 0.83 (d, *J* = 6.7 Hz, 3H).

^{13}C NMR (125.8 MHz, $(CD_3)_2SO$) δ 165.2, 77.0, 57.4, 25.3, 13.00, 12.95

HRMS: m/z: $[M-H]^-$ calculated 172.0722, observed 172.0742

Notes:

- The amount of lithium hydroxide monohydrate was adjusted to account for the TBSOH impurity from the previous step.

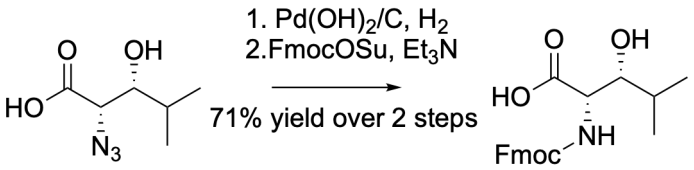

(2*S*,3*R*)-2-((((9*H*-fluoren-9-yl)methoxy)carbonyl)amino)-3-hydroxy-4-methylpentanoic acid. A one necked roundbottom flask was charged with wet azido acid (700 mg, 3.3 mmol), MeOH spiked with 0.5% acetic acid (10 mL), and $Pd(OH)_2/C$ (115 mg, 20% loading). The flask was backfilled with Argon before hydrogen gas (balloon) was added. The reaction was stirred for 1 hr and then filtered through a PVDF membrane. The crude material concentrated down then resuspended in 1:1 ACN/H_2O (20 mL). Then FmocOsu (1.12 g) and Et_3N (369 μL) were added. The solution was stirred for 15 min before additional Et_3N was added dropwise until the solution was pH 7-8. The solution was stirred for 1 hr, stripped of ACN under reduced pressure, then acidified with 1 M HCl (5 mL). The acidified aqueous layer was extracted with EtOAc (5 x 15 mL), dried with Na_2SO_4, and concentrated down. The crude oil was purified by column chromatography (98/2 DCM/MeOH for 3 CV, then 85/15 DCM/MeOH, R_f = 0.57, UV active) to afford 990 mg of white foam. The foam was resuspended in EtOAc (50 mL) and washed with H_2O (3 x 30 mL) to remove a *N*-hydroxy succinimide impurity, dried with Na_2SO_4, and concentrated down to afford 860 mg of white foam.

ATR-FTIR (diamond anvil, solid) 3338 (OH stretch, alcohol), 3064 (sp^2 C-H stretch), 2961 (sp^3 C-H stretch, alkyl), 1698 (C=O stretch, carbonyl) cm^{-1}.

^1H NMR (500 MHz, $(CD_3)_2SO$) δ 12.60 (s, 1H), 7.89 (d, *J* = 7.6 Hz, 2H), 7.73 (d, *J* = 7.4 Hz, 2H), 7.42 (t, *J* = 7.5 Hz, 2H), 7.37 – 7.26 (m, 2H), 7.02 (d, *J* = 9.5 Hz, 1H), 4.65 (d, *J* = 8.1 Hz, 1H), 4.40 – 4.26 (m, 2H), 4.24 (appar t, *J* = 7.0 Hz, 1H), 4.18 (dd, *J* = 9.5, 2.8 Hz, 1H), 3.55 – 3.46 (m, 1H), 1.67 – 1.53 (m, 1H), 0.94 (d, *J* = 6.6 Hz, 3H), 0.79 (d, *J* = 6.7 Hz, 3H).

^{13}C NMR (125.8 MHz, $(CD_3)_2SO$) δ 172.8, 156.3, 143.9, 143.7, 140.74, 140.72, 127.6, 127.0, 125.29. 125.24, 120.13, 120.10, 76.2, 65.7, 56.7, 46.7, 30.8, 19.2, 18.9.

HRMS: m/z: $[M+H]^+$ calculated 370.1654, observed 370.1653

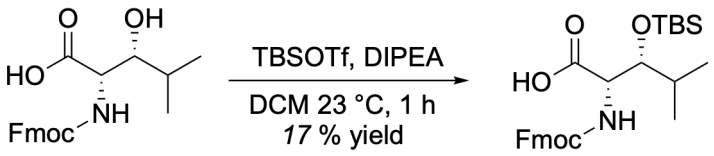

(2S,3R)-2-((((9H-fluoren-9-yl)methoxy)carbonyl)amino)-4-methyl-3-((triethylsilyl)oxy)pentanoic acid. A one-necked 250 mL round bottom flask equipped with an oven dry stir bar was charged with (2S,3R)-2-((((9H-fluoren-9-yl)methoxy)carbonyl)amino)-4-methyl-3-((triethylsilyl)oxy)pentanoic acid (850 mg, 2.3 mmol) and anhydrous DCM (10 mL). The reaction was cooled to 0 °C in an ice bath before DIPEA (1.20 mL, 3 eq) and TBSOTf (792 μL, 1.5 eq) were added dropwise via syringe over 3 min each. The reaction was warmed to room temperature, stirred for 30 min, then quenched with H_2O (10 mL). The DCM was removed under reduced pressure before FmocOsu (775 mg, 1 eq) and acetone (20 mL) were added. The reaction was acidified with 1 M HCl to pH 3. The reaction was stripped of acetone, extracted with DCM (5 x 20 mL). The combined organic layers were dried with Na_2SO_4, concentrated down and purified by column chromatography (99:1 DCM-MeOH for 3 CV, then 95/5 DCM MeOH, R_f = 0.49, UV active) to afford 190 mg of white foam.

ATR-FTIR (diamond anvil, solid) 2955 (sp^3 C-H stretch, alkyl), 2929 (sp^3 C-H stretch, alkyl), 2894 (sp^3 C-H stretch, alkyl), 2857 (sp^3 C-H stretch, alkyl), 1717 (C=O stretch, carbonyl) cm^{-1}.

^{1}H NMR (500 MHz, $(CD_3)_2SO$) δ 12.92 (s, 1H), 7.88 (d, *J* = 7.6 Hz, 2H), 7.71 (dd, *J* = 11.9, 7.7 Hz, 2H), 7.41 (t, *J* = 7.4 Hz, 2H), 7.35 – 7.25 (m, 2H), 6.56 (d, *J* = 9.5 Hz, 1H), 4.36 – 4.10 (m, 4H), 3.89 (dd, *J* = 5.9, 2.8 Hz, 1H), 1.74 (appar sextet, *J* = 6.7 Hz, 1H), 0.90 (d, *J* = 6.8 Hz, 3H), 0.88 (s, 9H), 0.85 (d, *J* = 8.1 Hz, 3H), 0.06 (s, 3H), 0.01 (s, 3H).

^{13}C NMR (125.8 MHz, $(CD_3)_2SO$) δ 172.6, 155.9, 155.8 (minor rotamer), 143.8, 143.6, 140.7, 127.7, 127.03, 126.99, 125.3, 125.2, 120.1, 76.6, 66.0, 59.3, 56.2 (minor rotamer), 46.6, 31.8, 25.96, 25.91 (minor rotamer), 18.7, 18.2, 18.0, -4.42, -4.44.

HRMS: m/z: $[M+H]^+$ calculated 484.2519, observed 484.2517

Notes:

- NMR spectra contains Fmoc rotamers and some of the diastereotopic Fmoc carbons are coincident.

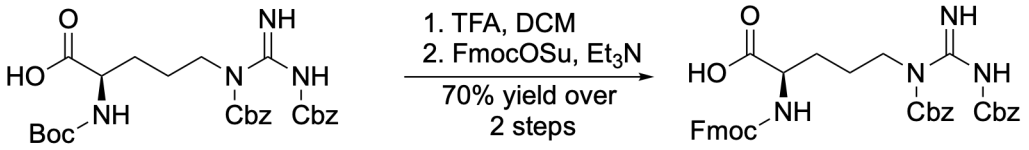

***N*²-(((9*H*-fluoren-9-yl)methoxy)carbonyl)-*N*$^{\delta}$,*N*$^{\omega}$-bis((benzyloxy)carbonyl)-*D*-arginine**. The following procedure was adapted from Lipton and coworkers.[27] An oven-dried 100 mL, one-necked round bottom flask equipped with a stir bar was charged with Boc-D-Arg(Z)$_2$-OH (542 mg, 0.5 mmol, 1 eq), DCM (3 mL), and TFA (3 mL). The reaction was stirred at room temperature for 30 minutes then cooled to 0 °C in an ice bath. Sat $NaHCO_3$ solution (3.27 g of $NaHCO_3$ dissolved in ca. 30 mL H_2O) was added dropwise over 5 min. The DCM was stripped under reduced pressure. Then FmocOSu (337 mg, 1 eq) and ACN (30 mL) were added in one portion. Next Et_3N (138 μL, 1 eq) was added dropwise over 2 min. The solution was stirred for 15 minutes before additional Et_3N was added as needed until the reaction was pH ca. 7-8. The reaction was stirred for 1 hr, then stripped of ACN under reduced pressure, and finally acidified with 1M HCl to pH ca. 2-3. The crude reaction mixture was extracted with EtOAc (3 x 10 mL). The combined organic layers were dried with Na_2SO_4, concentrated under reduced pressure and purified by column chromatography (95:5 DCM-MeOH then 90:10 DCM-MeOH) to afford 470 mgs of white foam.

ATR-FTIR (diamond anvil, solid) 3065 (sp^2 C-H stretch), 3033 (sp^2 C-H stretch), 2953 (sp^3 C-H stretch), 1717 (C=O stretch), 1688 (C=O stretch), 1652 (C=C stretch), 1646 (C=C stretch), 1635 (C=C stretch), 1607 (C=C stretch) cm^{-1}.

^{1}H NMR (500 MHz, $CDCl_3$) δ 12.6 (br s, 1H), 9.18 (br s, 2H), 7.88 (d, *J* = 7.5 Hz, 2H), 7.70 (dd, *J* = 7.5, 0.7 Hz, 2H), 7.64 (d, *J* = 8.1 Hz, 1), 7.49 – 7.22 (m, 14 H), 5.23 (s, 2H), 5.05 (s, 2H), 4.35 – 4.12 (m, 3H), 4.00 – 3.78 (m, 3H), 1.79 – 1.45 (m, 4H).

^{13}C NMR (125.3 MHz, $CDCl_3$) δ 173.7, 162.9, 159.7, 156.1, 155.0, 148.83, 143.76, 140.72, 140.70, 137.1, 135.3, 128.5, 128.32, 128.28, 127.9, 127.8, 127.7, 127.6, 127.0, 125.3, 120.10, 120.07, 68.2, 66.1, 65.6, 53.8, 46.7, 44.2, 28.1, 25.4.

HRMS: m/z: $[M+Na]^+$ calculated 687.2431, observed 687.2439

Note:

- Some of the Fmoc diastereotopic carbons are coincident.

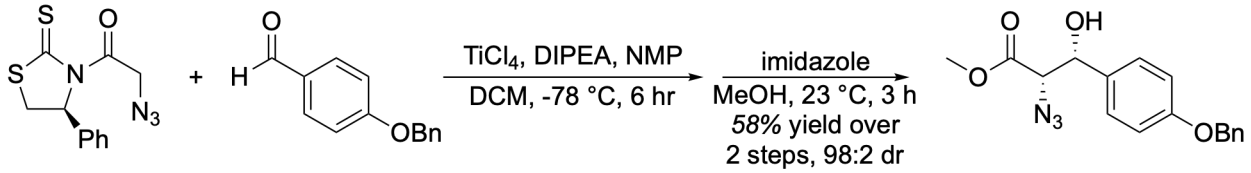

Methyl (2*S*,3*R*)-2-azido-3-(4-(benzyloxy)phenyl)-3-hydroxypropanoate. An oven-dried 100-mL one-necked round bottom flask with a magnetic stirring bar was charged with (*S*)-2-azido-1-(4-phenyl-2-thioxothiazolidin-3-yl)ethan-1-one (1.05 g, 3.78 mmol, 1 equiv), and anhydrous DCM (38 mL). The solution was cooled to -78°C in a dry ice/ isopropanol bath. $TiCl_4$ (436 μL, 1.05 equiv) was added dropwise via syringe over 5 min. The solution was stirred for 15 min and then DIPEA (726 μL, 1.1 equiv) was added dropwise over 5 min. The solution was stirred for 1 hr and then NMP (730 μL, 2 equiv) was added dropwise via syringe over 5 min. The solution was stirred for 15 min and then 4-(benzyloxy)benzaldehyde (1.20 g dissolved in 6 mL anhydrous DCM, 1.5 equiv) was added dropwise via syringe over 5 min. The reaction mixture was stirred at -78 °C for roughly 6 hr and then monitored by removing ~100 μL aliquot with a syringe, performing a small-scale workup, and taking an ^{1}H NMR spectrum of the crude material. Once the reaction has gone to completion by ^{1}H NMR of the crude NMR aliquot, imidazole (5.15 g, 20 eq) dissolved in MeOH (38 mL) was added dropwise via syringe over 10 min.[38] The reaction was allowed to warm to room temperature and stirred for 3 hr. The reaction was diluted with H_2O (38 mL), EtOAc (38 mL), and passed through filter paper. The filtrate was extracted with EtOAc (5 x 30 mL). The combined organic layers were combined, dried with Na_2SO_4, and concentrated to afford an orange solid. The crude product was purified by column chromatography on 150 mL of silica gel. Elution was performed first with 95:5 DCM-hexanes until the chiral auxiliary elutes (R_f = 0.45, UV active), and then with 40:60 EtOAc-hexanes until the product elutes (R_f = 0.50, blue spots with CAM stain), to afford 720 mg of methyl (2*S*,3*R*)-2-azido-3-(4-(benzyloxy)phenyl)-3-hydroxypropanoate as a yellow solid.

ATR-FTIR (diamond anvil, solid) 3475 (OH stretch, alcohol), 3039 (sp^2 C-H stretch), 2961 (sp^3 C-H stretch), 2885 (sp^3 C-H stretch), 2853 (sp^3 C-H stretch), 2112 (N=N=N, azide), 1726 (C=O stretch, ester) cm^{-1}.

^{1}H NMR (500 MHz, $CDCl_3$) δ 7.46 – 7.29 (m, 7H), 6.99 (appar d, *J* = 8.8 Hz, 2H), 5.14 (d, *J* = 4.3 Hz, 1H), 5.07 (s, 2H), 4.01 (d, *J* = 4.7 Hz, 1H), 3.76 (s, 3H). 2.65 (s, 1H).

^{13}C NMR (125.8 MHz, $CDCl_3$) δ 169.2, 159.0, 136.9, 128.7, 128.2, 127.62, 127.58, 115.1, 74.2, 70.2, 67.9, 52.9.

HRMS: m/z: $[M+Na]^+$ calculated 350.1117, observed 350.1119

Notes:

- We have observed that adventitious HCl in the $TiCl_4$ can significantly reduce yields and recommend Sure-Seal $TiCl_4$ bottles.
- The equivalents of the $TiCl_4$, DIPEA, and NMP must be added precisely to ensure the formation of the desired diastereomer and quantitative consumption of starting material. Be cautious of bubbles in the 1 mL syringe.
- Upon addition of the $TiCl_4$, the solution changes color from yellow to orange.
- Upon addition of DIPEA, the solution instantly changes color from orange to black/dark red.
- To monitor by NMR, quench a ~100 μL aliquot in saturated NH_4Cl and concentrate down the organic layer. We have observed that monitoring the reaction by TLC to be inconsistent due to retro-aldol formation under TLC conditions. This crude NMR also confirms the formation of a single diastereomer. If the reaction is incomplete, we recommend letting the reaction stir at -78°C for 2 additional hours before taking another aliquot.
- The aldol reaction must be quenched cold because this intermediate is unstable and highly susceptible to retro-aldol at room temperature.
- Upon addition of imidazole, the reaction mixture slowly changes color from black to crimson.
- Upon addition of water, the solution forms a milky emulsion. We recommend washing the precipitated solids with a small amount of EtOAc (5-10 mL) to maximize yields.
- The auxiliary and aldehyde are insoluble in hexanes and soluble in DCM. Hence, the relatively unusual column chromatography conditions. The 60:40 hexanes-EtOAc mixture separates out the desired methyl ester from NMP.
- Only 12 resonances appear in the ^{13}C NMR spectrum, because two of the aromatic carbon resonances overlap.

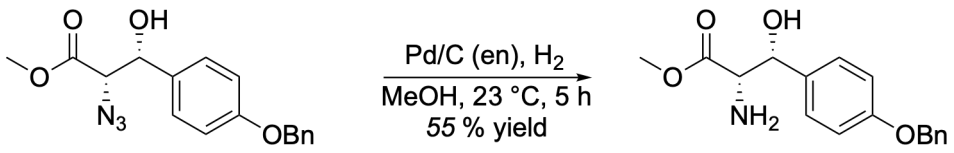

Methyl (2*S*,3*R*)-2-amino-3-(4-(benzyloxy)phenyl)-3-hydroxypropanoate. A one-necked 50 mL round bottom flask was charged with methyl (2*S*,3*R*)-2-amino-3-(4-(benzyloxy)phenyl)-3-hydroxypropanoate (515 mg, 1.57 mol), 10% Pd/C(en) catalyst (257 mg), and MeOH (16 mL). The reaction was hydrogenated in a Parr apparatus at 10 bar for 5 hr and then passed through a PVDF membrane filter, concentrated down, and purified by column chromatography (98:2 DCM-MeOH for 2 CV, then 80:20 EtOAc-hexanes, R_f = 0.14, CAM stain) to afford 260 mg of off-white solid.

ATR-FTIR (diamond anvil, solid) 3351 (NH stretch, amine), 3292 (NH stretch, amine), 3095 (br OH stretch, alcohol), 3026 (sp^2 C-H stretch), 2957 (sp^3 CH stretch), 2910 (sp^3 C-H stretch), 2956 (sp^3 C-H stretch), 1735 (C=O stretch, ester), 1601 (C=C stretch) cm^{-1}.

^{1}H NMR (500 MHz, CD_3OD) δ 7.42 (appar d, *J* = 7.5 Hz, 2H), 7.36 (appar t, *J* = 7.4 Hz, 2H), 7.32 – 7.25 (m, 3H), 6.98 (appar d, *J* = 8.8 Hz, 2H), 5.08 (s, 2H), 4.87 (d, *J* = 5.0 Hz, 1H), 3.62 (s, 3H), 3.58 (d, *J* = 5.0 Hz, 1H).

^{13}C NMR (125.8 MHz, CD_3OD) δ 174.6, 159.8, 138.7, 134.9, 129.5, 128.8, 128.6, 128.5, 115.8, 75.6, 71.0, 62.2, 52.4.

HRMS: m/z: $[M+H]^+$ calculated 302.1392, observed 302.1392

Notes:

- We have observed significant variably in the reactivity of the Pd/C (en) catalyst depending on the Pd/C source. We recommend using a fresh bottle of Pd/C in the preparation of the Pd/C (en) catalyst described below.
- This intermediate tends to ionize as the elimination product ($-H_2O$).

Preparation of 10% Pd/C(en) catalyst. The following procedure was adapted from Hirota and coworkers.[39] A one-necked 500 mL round bottom flask was charged with 10% Pd/C (5 g, 4.74 mmol of Pd metal). The flask was blanked with Argon (2x) to prevent ignition before MeOH (200 mL) and ethylene diamine (22 mL, 0.329 mol) were added. The reaction was stirred for 2d under Argon at ambient temperature, filtered, washed vigorously with MeOH (5 x 20 mL), and ether (5 x 20 mL). The 10% Pd/C (en) was transferred to a 20-mL scintillation vial for storage prior to use. A 5 g preparation afforded 5.53 g of slightly wet Pd/C (en).

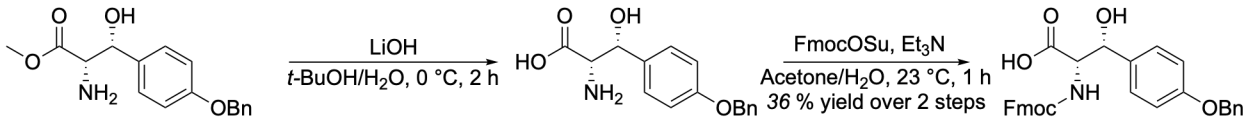

(2*S*,3*R*)-2-((((9*H*-fluoren-9-yl)methoxy)carbonyl)amino)-3-(4-(benzyloxy)phenyl)-3-hydroxypropanoic acid. A one-necked 100-mL round bottom flask was charged with methyl (2*S*,3*R*)-2-amino-3-(4-(benzyloxy)phenyl)-3-hydroxypropanoate (530 mg, 1.76 mmol, 1 eq), a stir bar, and cooled to 0 °C. Then LiOH*H_2O (147.6 mg, 2 eq) was dissolved in 1:1 *t*-BuOH-H_2O (10 mL) and added to the methyl ester. The reaction was stirred on ice for 2 h, neutralized with 1 M HCl (3.52 mL), and stripped of *t*-BuOH (45 °C).The solution was extracted with EtOAc (5 x 20 mL), the organic layers were combined and concentrated down to afford an oil. The crude oil was redissolved in 5:1 acetone-H_2O (25 mL). Then FmocOSu (890 mg, 1.5 eq) and Et_3N (245 uL, 1 eq) was added. Additional Et_3N was added dropwise until the solution was pH ~7-8. The reaction was stirred for 30 min, striped of ACN, acidified with 1 M HCl (1.76 mL), and extracted with EtOAc. The crude material was purified by column chromatography (98:2 DCM MeOH for 2 CV then EtOAc, R_f = 0.54, UV active) to afford 320 mg of an off-white solid.

ATR-FTIR (diamond anvil, solid) 3394 (OH stretch, alcohol), 3064 (sp^2 C-H stretch), 3033 (sp^2 C-H stretch), 2945 (sp^3 CH stretch), 1698 (C=O), 1683 (C=O stretch), 1608 (C=C stretch) cm^{-1}.

^{1}H NMR (500 MHz, CD_3SOCD_3) δ 7.88 (d, *J* = 7.5 Hz, 2H), 7.64 (t, *J* = 7.7 Hz, 2H), 7.45 – 7.24 (m, 9H), 7.19 (d, *J* = 7.8 Hz, 2H), 6.86 (d, *J* = 8.2 Hz, 2H), 6.55 (br s, 1H), 5.20 – 4.81 (m, 3H), 4.29 (dd, *J* = 8.5, 6.1 Hz, 1H), 4.21 – 3.97 (m, 3H).

^{13}C NMR (125.8 MHz, CD_3SOCD_3) δ 157.3, 155.6, 143.83, 143.69, 140.70, 140.67, 137.2, 134.8, 128.4, 127.8, 127.62, 127.60, 127.05, 127.04, 125.3, 125.2, 120.09, 120.06, 113.8, 69.1, 65.5, 46.6.

HRMS: m/z: $[M+Na]^+$ calculated 532.1736, observed 532.1741

Notes:

- Try monitoring the reactions by TLC (85/15 DCM/MeOH) at 1 hr LiOH, 2 hr LiOH to see if it went to completion.
- Try monitoring the Fmoc protection at 15 min (trust if the reaction is cloudy more than the pH of the reaction) for Fmoc protection.
- Check rxn pH post acidification, then add Fmoc-Osu and Et_3N, monitor reaction by TLC (100 % DCM) for consumption of Fmoc-Osu and formation of benzofulvene, look for unreacted SM with ninhydrin stain
- Add additional Et_3N and another equiv. of FmocOsu as needed.
- This intermediate clings onto EtOAc and may appear as a clear oil after the EtOAc column. EtOAc can easily be removed with a DCM MeOH plug.
- NMR contains numerous Fmoc-Rotamers. I reported the major rotamer. Carboxylic acid is broadened due to chemical exchange.

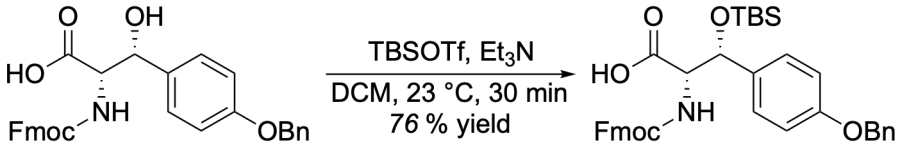

(2*S*,3*R*)-2-((((9*H*-fluoren-9-yl)methoxy)carbonyl)amino)-3-(4-(benzyloxy)phenyl)-3-((*tert*-butyldimethylsilyl)oxy)propanoic acid. A one-necked round bottom flask equipped with an oven dry stir bar was charged with (2*S*,3*R*)-2-((((9*H*-fluoren-9-yl)methoxy)carbonyl)amino)-3-(4-(benzyloxy)phenyl)-3-hydroxypropanoic acid (201 mg, 0.39 mmol, 1 eq), and anhydrous DCM (10 mL). The reaction was cooled to 0 °C in an ice bath before DIPEA (274 μL, 1.55 mmol, 4 eq) was added dropwise via syringe over 3 min. Then TBSOTf (271 μL, 3 eq) was added dropwise via syringe over 3 min. The reaction was warmed to room temperature, stirred for 30 min, then quenched with H_2O (5 mL). The DCM was removed under reduced pressure before FmocOSu (197 mg, 1.5 eq) and acetone (20 mL). The reaction mixture was acidified with 1M HCl to pH 3. The reaction was stripped of acetone, then extracted with DCM (3 x 10 mL). The combined organic layers were dried with Na_2SO_4, concentrated down and purified by column chromatography (98:2 DCM-MeOH for 2 CV then EtOAc, R_f = 0.54, UV active) to afford 187 mg of off-white foam.

ATR-FTIR (diamond anvil, solid) 3065 (sp^2 C-H stretch), 2951 (sp^3 C-H stretch, alkyl), 2928 (sp^3 C-H stretch, alkyl), 2956 (sp^3 C-H stretch, alkyl), 1716 (C=O stretch, carbonyl), 1668 (C=C stretch), 1610 (C=C stretch) cm^{-1}.

^{1}H NMR (500 MHz, $(CD_3)_2SO$) δ 12.88 (s, 1H), 7.88 (d, *J* = 7.6 Hz, 2H), 7.67 (dd, *J* = 7.2, 5.1 Hz, 2H), 7.48 – 7.18 (m, 12H), 6.91 (d, *J* = 8.7 Hz, 2H), 5.21 (d, *J* = 3.5 Hz, 1H), 5.01 (d, *J* = 11.7 Hz, 1H), 4.96 (d, *J* = 11.7 Hz, 1H), 4.27 – 3.96 (m, 4H), 0.84 (s, 9H), 0.00 (s, 3H), -0.16 (s, 3H).

^{13}C NMR (125.8 MHz, $(CD_3)_2SO$) δ 171.4, 157.7, 156.1, 143.8, 143.6, 140.6, 137.0, 133.4, 128.4, 127.81, 127.77, 127.0, 125.5, 125.4, 120.1, 113.9, 74.0, 69.2, 66.0, 61.2, 46.5, 25.7, 17.9, -4.7, -5.3.

HRMS: m/z: $[M+Na]^+$ calculated 646.2601, observed 646.2595

Notes:

- We recommend monitoring the pH of the reaction during acidification. pH 3-4 is ideal.
- The NMR spectra contain Fmoc rotamers and some of the diastereotopic Fmoc carbons are coincident.

Synthesis of hypeptin

Peptide synthesis procedure Hypeptin was synthesized by manual solid-phase peptide synthesis on 2-chlorotrityl resin, followed by HFIP cleavage, solution-phase cyclization, global deprotection, and reverse phase HPLC purification. A step-by-step procedure is detailed below.

Resin loading 2-chlorotrityl resin (150 mg, 1.10 mmol/g) and protected (2*S*, 3*R*)-3-hydroxyleucine-OH (50 mg) was added to a 10-mL Bio-Rad Poly-Prep chromatography column. The resin was loaded overnight (8-12 h) in a solution of 6 mL DCM and 0.3 mL 2,4,6-collidine under gentle agitation. The loading solution was drained and the resin was washed three times with DCM. After washing, the resin was capped using a solution of DCM/MeOH/DIPEA (17:2:1, 8 mL) for 1 h under gentle agitation. The solution was drained and the resin was washed three times with DCM. The resin was dried under a flow of nitrogen. Once dry, resin loading was checked on the Varioskan through UV analysis (290 nm) of the Fmoc cleavage product. Nominal loading values range from 0.04 – 0.06 mmol.

Solid-phase peptide coupling The loaded was re-suspended in amine-free DMF, allowed to swell for 30 min, and transferred to a clean 25 mL course frit coupling vessel. The linear peptide was synthesized from the *C*-terminus to the *N*-terminus using standard coupling cycles unless otherwise noted. A standard coupling cycle consists of the following: (1) Fmoc deprotection with 20% (v/v) piperidine in DMF (5 mL) for 10 min, (2) resin washing with DMF (5X), (3) coupling of the amino acid (4 equiv) with HATU/HOAt (4 equiv each) in 20% (v/v) collidine in DMF for 30 min, and (4) resin washing with DMF (5X). A modified coupling procedure was used to couple protected (2*S*,3*R*)-3-hydroxyasparagine and (2*R*,3*R*)-3-hydroxyasparagine to mitigate nitrile formation. The hydroxyasparagine (4 equiv) and HOAt (6 eq) were dissolved in DMF (ca. 1 mL)

and transferred to the coupling vessel. Then HBTU (4 equiv.) dissolved in DMF (ca. 1 mL) was added. Then collidine (7 equiv.) was added dropwise in timed additions at 0, 10, and 20 min. Once the linear synthesis was complete, the resin was transferred to a 10-mL Bio-Rad Poly-Prep chromatography column and washed with DCM (3X).

Steglich esterification[40] In a test tube, Fmoc-Ile-OH (10 equiv) was dissolved in anhydrous DCM (5 mL) and DIC (10 equiv). The solution was dissolved filtered through a 0.20-μm nylon filter into a test tube containing 4-dimethylaminopyridine (1 equiv). The filtrate was transferred to the resin in a Polyprep and gently agitated for 1h. The solution was drained, and the resin was thoroughly rinsed with dry DCM (3X) and DMF (3X)

Linear checks A ~1-2 mg aliquot of Fmoc-deprotected resin was removed from the coupling vessel and transferred to a 20 mL scintillation vial with TFA (ca. 1 mL), TIPS (1 drop), and water (1 drop). The scintillation vial was sonicated for 5 min before the excess TFA was removed with a gentle stream of air. The peptide residue was resuspended in 20% ACN (1 mL), and filtered to remove resin beads. The filtered solution was analyzed by analytical HPLC and QDa.

Cleavage of the linear peptide from resin The linear peptide was cleaved from using a cleavage solution of 20% (v/v) HFIP in DCM (7.5 mL) under gentle agitation. The filtrate was collected in a 1-L round-bottom flask. Another 7.5 mL of cleavage solution was added to the resin under gentle agitation for 30 min and combined with the original filtrate. The combined filtrates were concentrated under reduced pressure to afford a translucent film.

Cyclization of the linear peptide DMF (125 mL) was added to dissolve the clear oil. HATU (6 equiv) and HOAt (6 equiv) were added to the solution. The solution was stirred before DIPEA (300 µL) was added dropwise. The flask was flushed three times with nitrogen and allowed to cyclize at room temperature for 2 d. The reaction was concentrated under reduced pressure (65 °C) to afford a beige solid. The round bottom was placed under vacuum to remove residual DMF.

For the first-generation synthesis of hypeptin, the following deprotection strategy was used. *TBAF deprotection of silyl protecting groups.* The crude cyclized peptide was dissolved in a freshly solution of THF (10 mL) with tetrabutylammonium fluoride (10 equiv) that had been pH adjusted to 7 with 1 M HCl. The solution was allowed to stir overnight (12-18 h) then concentrated down under reduced pressure. The round bottom was placed under vacuum to remove residual water.

Anhydrous TFA global deprotection of the cyclic peptide The protected peptide was dissolved in anhydrous TFA/TIPS (90:10, 10 mL total). The TFA was distilled while the TIPS was passed through flame dry alumina to remove water. The solution was stirred on ice for 1 h and transferred into two 50-mL conical tubes each containing 35 mL of chilled diethyl ether. Both conical tubes were centrifuged (600xg, 4 °C) to pellet the peptide. The supernatant was decanted into a 125-mL Erlenmeyer flask. This process was repeated twice more by adding additional ether, shaking to break up the pellet, and centrifuging. The pellet was dried in a vacuum desiccator.

Biotage Reverse-phase HPLC purification The dried peptide was dissolved in 15% (v/v) ACN in H_2O and purified on the Biotage® Isolera™ One system equipped with a Biotage® Sfr Bio C18 Duo 300 Å 20 µm column using an ACN/H_2O gradient (20 – 60%) over 8 column volumes.

Fractions were analyzed by MALDI-TOF and analytical HPLC. Fractions containing predominantly desired peptide were combined and lyophilized to afford an off-white solid.

For the second-generation synthesis of hypeptin the following deprotection strategy was used. *Biotage Reverse-phase HPLC purification of fully protected hypeptin* Following cyclization, the crude cyclized peptide was dissolved in neat HFIP (ca. 1 mL) and loaded onto a Biotage® Sfr Bio C18 Duo 300 Å 20 µm column. The flask was rinsed with acetonitrile (3 x 1 mL) and water (1 x 1 mL) and loaded onto the column. A step gradient (hold 0% ACN for 2 column volumes then flush with 100% ACN until peptide elutes typically 1.5 column volumes) was used to remove coupling agents. Fractions containing peptide in the acetonitrile flush were stripped under reduced pressure and lyophilized in a tared 50 mL conical to afford light yellow powder (ca. 40-50 mg).

HF-py silyl deprotection A 50 mL conical containing fully protected hypeptin was charged with a teflon coated stir bar, THF (2 mL) and pyridine (2 mL). Then HF-py (50% w/w mixture, 100 uL) was added dropwise. The solution was stirred at room temperature overnight (12 – 16 h). The solution was quenched with excess ethoxytrimethylsilane (1.2 equiv relative to HF). The solution was stirred and Biotage Reverse-phase HPLC purified using the a step gradient (hold 0% ACN for until pyridine elutes then flush with 100% ACN until peptide elutes typically 1.5 column volumes). Fractions containing peptide in the acetonitrile flush were stripped under reduced pressure and lyophilized in a tared 50 mL conical to afford light yellow powder.

Hydrogenation The crude silyl deprotected hypeptin was dissolved in MeOH (10 mL) spiked with 0.5% acetic acid. $Pd(OH)_2/C$ (50 mg) was added before the flask was purged and backfilled

with Argon. The flask was then purged and backfilled with hydrogen gas (balloon). The solution was stirred for 1 h then passed through a 0.20-µm PVDF filter. The solution was concentrated down to afford a clear film that was purified on the Rainin.

Ranin Reverse-phase HPLC purification The crude fully deprotected hypeptin was dissolved in 4 mL of 15% (v/v) ACN in H_2O purified by RP-HPLC using an ACN/H_2O gradient (15–30%, 10 mL/min) over 90 min. The peptide elutes around 24% acetonitrile. Fractions were analyzed by MALDI-TOF and analytical HPLC. Pure fractions were and lyophilized to afford peptide as white trifluoroacetate (TFA) salts.

NMR spectroscopic studies of hypeptin NMR spectra for hypeptin were recorded on a Bruker Evo magnet equipped with a CPPTCI cryoprobe or a Avance 800 MHz NMR spectrometer equipped with a TXI probe. HSQC spectra were recorded with 16 scans, 1024 increments in the f_2 dimension and 512 increments in the f_1 dimension. TOCSY spectra were recorded with 100 msec mixing time, 8 scans, 2048 increments in the f_2 dimension and 1024 increments in the f_1 dimension. NOESY spectra were recorded with 500 msec mixing time, 16 scans, 2048 increments in the f_2 dimension and 1024 increments in the f_1 dimension. ROESY spectra were recorded with 200 msec mixing time, 16 scans, 2048 increments in the f_2 dimension and 1024 increments in the f_1 dimension. NMR spectra were processed with the Bruker TopSpin software. Manual baseline correction was applied to both dimensions after manually phasing the spectra. For TOCSY, NOESY, and ROESY experiments, the spectra were referenced to the residual DMSO-d_6 peak at 2.50 ppm.

Decomposition kinetic studies of hypeptin antibiotics at 37 °C. The following procedure was adapted from a conversion kinetic assay developed by Jones et. al.[40] A low-binding 1.7 mL microcentrifuge tube was charged with 700 µL of a 50 mM stock solution of HEPES (pH = 7.4). A second microcentrifuge tube was charged with 700 µL of a 1 mg/mL stock solution of peptide dissolved in H_2O. Both vials were placed in an incubator set to 37 °C and allowed to heat for ca. 15 min with gentle agitation (225 rpm). To an additional vial in the incubator, 600 µL of HEPES buffer and 600 µL of the 1 mg/mL peptide stock were added. Timed aliquots were removed (at 0 hr, 1 hr, 2 hr, 3 hr, 4 hr, 6 hr, 8 hr, 12 hr, and 24 hr) into a low-volume analytical HPLC vial, capped, and placed immediately on dry ice and then stored in a -20 °C freezer. After all aliquots were taken, the aliquots were run on an Agilent 1260 instrument equipped with an Aeris PEPTIDE 2.6 µm XB-C18 column (Phenomonex) with a 5-67% acetonitrile gradient over 15 minutes, with monitoring of absorbance at 214 nm. Each sample was thawed immediately before injection but kept at a low enough temperature to minimize further hydrolysis. Peaks corresponding to the parent mass and hydrolysis byproducts were integrated using the Agilent software, and the relative areas were recorded for kinetic analysis. Following injection, the aliquots were re-frozen on dry ice and then stored in a -20 °C freezer. The frozen aliquots were thawed immediately prior to injection on a Xevo G2-XS QTof equipped with a Protein BEH C4, 300 Å, 1.7 µm, 2.1 x 50 mm, Waters column. The samples were run with a 3-27% ACN gradient over 25 minutes followed by a 90% ACN wash over two minutes, and 3% 97% H_2O wash over one minute. The Xevo Z-spray source was operated in positive MS resolution mode, 100-2000 Da, with a capiliary voltage of 3000V and a cone voltage of 40 V (NaCsI calibration, Leu-enkephalin lock-mass). Nitrogen was used as the desolvation gas at 350 °C and a total flow of 800 L h^{-1}. Retention times are given in minutes.

References and Notes

(1) Shoji, J.; Hinoo, H.; Hattori, T.; Hirooka, K.; Kimura, Y.; Yoshida, T. Isolation and Characterization of Hypeptin from Pseudomonas Sp. *J. Antibiot. (Tokyo)* **1989**, *42* (10), 1460–1464. https://doi.org/10.7164/antibiotics.42.1460.

(2) Komatsu, S.; Tsumori, C.; Ohnishi, K.; Kai, K. Genome- and Mass Spectrometry-Guided Discovery of Ralstoamides A and B from Ralstonia Solanacearum Species Complex. *ACS Chem. Biol.* **2020**, *15* (11), 2860–2865. https://doi.org/10.1021/acschembio.0c00605.

(3) Murai, Y.; Mori, S.; Konno, H.; Hikichi, Y.; Kai, K. Ralstonins A and B, Lipopeptides with Chlamydospore-Inducing and Phytotoxic Activities from the Plant Pathogen Ralstonia Solanacearum. *Org. Lett.* **2017**, *19* (16), 4175–4178. https://doi.org/10.1021/acs.orglett.7b01685.

(4) Lin, Z.; Falkinham, J. O. I.; Tawfik, K. A.; Jeffs, P.; Bray, B.; Dubay, G.; Cox, J. E.; Schmidt, E. W. Burkholdines from Burkholderia Ambifaria: Antifungal Agents and Possible Virulence Factors. *J. Nat. Prod.* **2012**, *75* (9), 1518–1523. https://doi.org/10.1021/np300108u.

(5) Tawfik, K. A.; Jeffs, P.; Bray, B.; Dubay, G.; Falkinham, J. O. I.; Mesbah, M.; Youssef, D.; Khalifa, S.; Schmidt, E. W. Burkholdines 1097 and 1229, Potent Antifungal Peptides from Burkholderia Ambifaria 2.2N. *Org. Lett.* **2010**, *12* (4), 664–666. https://doi.org/10.1021/ol9029269.

(6) Bui, T.-H.; Wray, V.; Nimtz, M.; Fossen, T.; Preisitsch, M.; Schröder, G.; Wende, K.; Heiden, S. E.; Mundt, S. Balticidins A–D, Antifungal Hassallidin-Like Lipopeptides from the Baltic Sea Cyanobacterium Anabaena Cylindrica Bio33. *J. Nat. Prod.* **2014**, *77* (6), 1287–1296. https://doi.org/10.1021/np401020a.

(7) Lim, Y.; Suh, J.-W.; Kim, S.; Hyun, B.; Kim, C.; Lee, C. Cepacidine A, A Novel Antifungal Antibiotic Produced by Pseudomonas Cepacia II. Physico-Chemical Properties and Structure Elucidation. *J. Antibiot. (Tokyo)* **1994**, *47* (12), 1406–1416. https://doi.org/10.7164/antibiotics.47.1406.

(8) Kim, C.-K.; Wang, D.; Bokesch, H. R.; Fuller, R. W.; Smith, E.; Henrich, C. J.; Durrant, D. E.; Morrison, D. K.; Bewley, C. A.; Gustafson, K. R. Swinhopeptolides A and B: Cyclic Depsipeptides from the Sponge Theonella Swinhoei That Inhibit Ras/Raf Interaction. *J. Nat. Prod.* **2020**, *83* (4), 1288–1294. https://doi.org/10.1021/acs.jnatprod.0c00136.

(9) Oku, N.; Gustafson, K. R.; Cartner, L. K.; Wilson, J. A.; Shigematsu, N.; Hess, S.; Pannell, L. K.; Boyd, M. R.; McMahon, J. B. Neamphamide A, a New HIV-Inhibitory Depsipeptide from the Papua New Guinea Marine Sponge Neamphius Huxleyi. *J. Nat. Prod.* **2004**, *67* (8), 1407–1411. https://doi.org/10.1021/np040003f.

(10) Tran, T. D.; Pham, N. B.; Fechner, G.; Zencak, D.; Vu, H. T.; Hooper, J. N. A.; Quinn, R. J. Cytotoxic Cyclic Depsipeptides from the Australian Marine Sponge Neamphius Huxleyi. *J. Nat. Prod.* **2012**, *75* (12), 2200–2208. https://doi.org/10.1021/np3006474.

(11) Plaza, A.; Gustchina, E.; Baker, H. L.; Kelly, M.; Bewley, C. A. Mirabamides A–D, Depsipeptides from the Sponge Siliquariaspongia Mirabilis That Inhibit HIV-1 Fusion. *J. Nat. Prod.* **2007**, *70* (11), 1753–1760. https://doi.org/10.1021/np070306k.

(12) Lu, Z.; Van Wagoner, R. M.; Harper, M. K.; Baker, H. L.; Hooper, J. N. A.; Bewley, C. A.; Ireland, C. M. Mirabamides E−H, HIV-Inhibitory Depsipeptides from the Sponge Stelletta Clavosa. *J. Nat. Prod.* **2011**, *74* (2), 185–193. https://doi.org/10.1021/np100613p.

(13) Bonner, D. P.; O'sullivan, J.; Tanaka, S. K.; Clark, J. M.; Whitney, R. R. Lysobactin, A Novel Antibacterial Agent Produced by Lysobacter Sp. II. Biological Properties. *J. Antibiot. (Tokyo)* **1988**, *41* (12), 1745–1751. https://doi.org/10.7164/antibiotics.41.1745.
(14) Shoji, J.; Hinoo, H.; Matsumoto, K.; Hattori, T.; Yoshida, T.; Matsuura, S.; Kondo, E. Isolation and Characterization of Katanosins A and B. *J. Antibiot. (Tokyo)* **1988**, *41* (6), 713–718. https://doi.org/10.7164/antibiotics.41.713.
(15) Guzman-Martinez, A.; Lamer, R.; VanNieuwenhze, M. S. Total Synthesis of Lysobactin. *J. Am. Chem. Soc.* **2007**, *129* (18), 6017–6021. https://doi.org/10.1021/ja067648h.
(16) von Nussbaum, F.; Anlauf, S.; Benet-Buchholz, J.; Häbich, D.; Köbberling, J.; Musza, L.; Telser, J.; Rübsamen-Waigmann, H.; Brunner, N. A. Structure and Total Synthesis of Lysobactin (Katanosin B). *Angew. Chem. Int. Ed.* **2007**, *46* (12), 2039–2042. https://doi.org/10.1002/anie.200604232.
(17) Gao, W.; Kim, J.-Y.; Chen, S.-N.; Cho, S.-H.; Choi, J.; Jaki, B. U.; Jin, Y.-Y.; Lankin, D. C.; Lee, J.-E.; Lee, S.-Y.; McAlpine, J. B.; Napolitano, J. G.; Franzblau, S. G.; Suh, J.-W.; Pauli, G. F. Discovery and Characterization of the Tuberculosis Drug Lead Ecumicin. *Org. Lett.* **2014**, *16* (23), 6044–6047. https://doi.org/10.1021/ol5026603.
(18) Hawkins, P. M. E.; Giltrap, A. M.; Nagalingam, G.; Britton, W. J.; Payne, R. J. Total Synthesis of Ecumicin. *Org. Lett.* **2018**, *20* (4), 1019–1022. https://doi.org/10.1021/acs.orglett.7b03967.
(19) Um, S.; Choi, T. J.; Kim, H.; Kim, B. Y.; Kim, S.-H.; Lee, S. K.; Oh, K.-B.; Shin, J.; Oh, D.-C. Ohmyungsamycins A and B: Cytotoxic and Antimicrobial Cyclic Peptides Produced by Streptomyces Sp. from a Volcanic Island. *J. Org. Chem.* **2013**, *78* (24), 12321–12329. https://doi.org/10.1021/jo401974g.
(20) Hur, J.; Jang, J.; Sim, J.; Son, W. S.; Ahn, H.-C.; Kim, T. S.; Shin, Y.-H.; Lim, C.; Lee, S.; An, H.; Kim, S.-H.; Oh, D.-C.; Jo, E.-K.; Jang, J.; Lee, J.; Suh, Y.-G. Conformation-Enabled Total Syntheses of Ohmyungsamycins A and B and Structural Revision of Ohmyungsamycin B. *Angew. Chem. Int. Ed.* **2018**, *57* (12), 3069–3073. https://doi.org/10.1002/anie.201711286.
(21) Li, L.; MacIntyre, L. W.; Ali, T.; Russo, R.; Koirala, B.; Hernandez, Y.; Brady, S. F. Biosynthetic Interrogation of Soil Metagenomes Reveals Metamarin, an Uncommon Cyclomarin Congener with Activity against Mycobacterium Tuberculosis. *J. Nat. Prod.* **2021**, *84* (4), 1056–1066. https://doi.org/10.1021/acs.jnatprod.0c01104.
(22) Fei, F.; Lun, S.; Saxena, A.; Raghavan, M.; DeRisi, J. L.; Bishai, W. R.; Sello, J. K. Total Syntheses of Cyclomarin and Metamarin Natural Products. *Org. Lett.* **2024**, *26* (45), 9698–9703. https://doi.org/10.1021/acs.orglett.4c03473.
(23) Renner, M. K.; Shen, Y.-C.; Cheng, X.-C.; Jensen, P. R.; Frankmoelle, W.; Kauffman, C. A.; Fenical, W.; Lobkovsky, E.; Clardy, J. Cyclomarins A−C, New Antiinflammatory Cyclic Peptides Produced by a Marine Bacterium (Streptomyces Sp.). *J. Am. Chem. Soc.* **1999**, *121* (49), 11273–11276. https://doi.org/10.1021/ja992482o.
(24) Zampella, A.; D'Auria, M. V.; Paloma, L. G.; Casapullo, A.; Minale, L.; Debitus, C.; Henin, Y. Callipeltin A, an Anti-HIV Cyclic Depsipeptide from the New Caledonian Lithistida Sponge Callipelta Sp. *J. Am. Chem. Soc.* **1996**, *118* (26), 6202–6209. https://doi.org/10.1021/ja954287p.
(25) Valeria D'Auria, M.; Zampella, A.; Paloma, L. G.; Minale, L.; Debitus, C.; Roussakis, C.; Le Bert, V. Callipeltins B and C; Bioactive Peptides from a Marine Lithistida Sponge

Callipelta Sp. *Tetrahedron* **1996**, *52* (28), 9589–9596. https://doi.org/10.1016/0040-4020(96)00496-6.
(26) Zampella, A.; Randazzo, A.; Borbone, N.; Luciani, S.; Trevisi, L.; Debitus, C.; D'Auria, M. V. Isolation of Callipeltins A–C and of Two New Open-Chain Derivatives of Callipeltin A from the Marine Sponge *Latrunculia* Sp. A Revision of the Stereostructure of Callipeltins. *Tetrahedron Lett.* **2002**, *43* (35), 6163–6166. https://doi.org/10.1016/S0040-4039(02)01334-5.
(27) Çalimsiz, S.; Morales Ramos, Á. I.; Lipton, M. A. Solid-Phase Synthesis and Configurational Reassigment of Callipeltin E. Implications for the Structures of Callipeltins A and B. *J. Org. Chem.* **2006**, *71* (17), 6351–6356. https://doi.org/10.1021/jo060351h.
(28) Krishnamoorthy, R.; Vazquez-Serrano, L. D.; Turk, J. A.; Kowalski, J. A.; Benson, A. G.; Breaux, N. T.; Lipton, M. A. Solid-Phase Total Synthesis and Structure Proof of Callipeltin B. *J. Am. Chem. Soc.* **2006**, *128* (48), 15392–15393. https://doi.org/10.1021/ja0666250.
(29) Ford, P. W.; Gustafson, K. R.; McKee, T. C.; Shigematsu, N.; Maurizi, L. K.; Pannell, L. K.; Williams, D. E.; Dilip de Silva, E.; Lassota, P.; Allen, T. M.; Van Soest, R.; Andersen, R. J.; Boyd, M. R. Papuamides A−D, HIV-Inhibitory and Cytotoxic Depsipeptides from the Sponges Theonella Mirabilis and Theonella Swinhoei Collected in Papua New Guinea. *J. Am. Chem. Soc.* **1999**, *121* (25), 5899–5909. https://doi.org/10.1021/ja990582o.
(30) Xie, W.; Ding, D.; Zi, W.; Li, G.; Ma, D. Total Synthesis and Structure Assignment of Papuamide B, A Potent Marine Cyclodepsipeptide with Anti-HIV Properties. *Angew. Chem. Int. Ed.* **2008**, *47* (15), 2844–2848. https://doi.org/10.1002/anie.200705557.
(31) Martín, M. J.; Rodríguez-Acebes, R.; García-Ramos, Y.; Martínez, V.; Murcia, C.; Digón, I.; Marco, I.; Pelay-Gimeno, M.; Fernández, R.; Reyes, F.; Francesch, A. M.; Munt, S.; Tulla-Puche, J.; Albericio, F.; Cuevas, C. Stellatolides, a New Cyclodepsipeptide Family from the Sponge Ecionemia Acervus: Isolation, Solid-Phase Total Synthesis, and Full Structural Assignment of Stellatolide A. *J. Am. Chem. Soc.* **2014**, *136* (18), 6754–6762. https://doi.org/10.1021/ja502744a.
(32) Krumberger, M.; Li, X.; Kreutzer, A. G.; Peoples, A. J.; Nitti, A. G.; Cunningham, V. A.; Jones, C. R.; Achorn, C.; Ling, L. L.; Hughes, D. E.; Nowick, J. S. Synthesis and Stereochemical Determination of the Peptide Antibiotic Novo29. *J. Org. Chem.* **2023**, *88* (4), 2214–2220. https://doi.org/10.1021/acs.joc.2c02648.
(33) Brunicardi, J. E. H.; Griffin, J. H.; Ferracane, M. J.; Kreutzer, A. G.; Small, J.; Mendoza, A.-T.; Ziller, J. W.; Nowick, J. S. Structure–Activity Relationship Studies of the Peptide Antibiotic Clovibactin. *J. Org. Chem.* **2024**, *89* (17), 12479–12484. https://doi.org/10.1021/acs.joc.4c01414.
(34) Dunetz, J. R.; Xiang, Y.; Baldwin, A.; Ringling, J. General and Scalable Amide Bond Formation with Epimerization-Prone Substrates Using T3P and Pyridine. *Org. Lett.* **2011**, *13* (19), 5048–5051. https://doi.org/10.1021/ol201875q.
(35) Patel, J.; Clavé, G.; Pierre-Yves Renard; Franck, X. Straightforward Access to Protected Syn α-Amino-β-Hydroxy Acid Derivatives. *Angew. Chem. Int. Ed.* **2008**, *47* (22), 4224–4227. https://doi.org/10.1002/anie.200800860.
(36) Xie, P.; Liu, X.; Jiao, X.; Li, X.; Yang, H.; Shi, X.; Yang, F. Method for Preparing Eliglustat. CN108822072A, 16 2018.
(37) Blanchette, M. A.; Choy, W.; Davis, J. T.; Essenfeld, A. P.; Masamune, S.; Roush, W. R.; Sakai, T. Horner-Wadsworth-Emmons Reaction: Use of Lithium Chloride and an Amine for

Base-Sensitive Compounds. *Tetrahedron Lett.* **1984**, *25* (21), 2183–2186. https://doi.org/10.1016/S0040-4039(01)80205-7.
(38) Zwick, C. R. I.; Sosa, M. B.; Renata, H. Modular Chemoenzymatic Synthesis of GE81112 B1 and Related Analogues Enables Elucidation of Its Key Pharmacophores. *J. Am. Chem. Soc.* **2021**, *143* (3), 1673–1679. https://doi.org/10.1021/jacs.0c13424.
(39) Sajiki, H.; Hattori, K.; Hirota, K. The Formation of a Novel Pd/C−Ethylenediamine Complex Catalyst: Chemoselective Hydrogenation without Deprotection of the O-Benzyl and N-Cbz Groups. *J. Org. Chem.* **1998**, *63* (22), 7990–7992. https://doi.org/10.1021/jo9814694.
(40) Jones, C. R.; Guaglianone, G.; Lai, G. H.; Nowick, J. S. Isobactins: O-Acyl Isopeptide Prodrugs of Teixobactin and Teixobactin Derivatives. *Chem. Sci.* **2022**, *13* (44), 13110–13116. https://doi.org/10.1039/D2SC02670H.

Characterization Data

^{1}H NMR spectrum of (*S*)-2-azido-1-(4-phenyl-2-thioxothiazolidin-3-yl)ethan-1-one in $CDCl_3$ at 500 MHz and 298 K

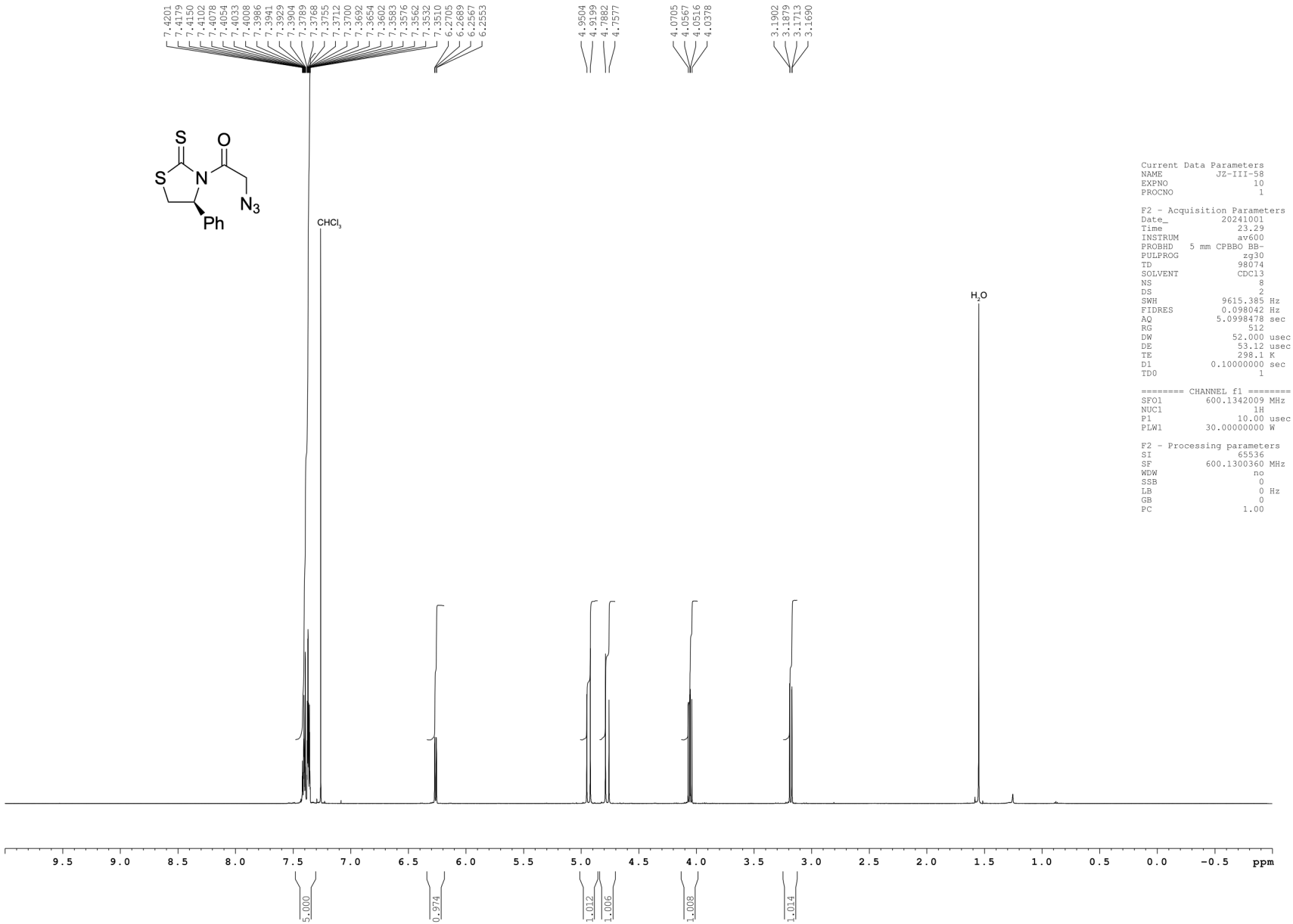

^{13}C NMR spectrum of (*S*)-2-azido-1-(4-phenyl-2-thioxothiazolidin-3-yl)ethan-1-one in $CDCl_3$ at 500 MHz and 298 K

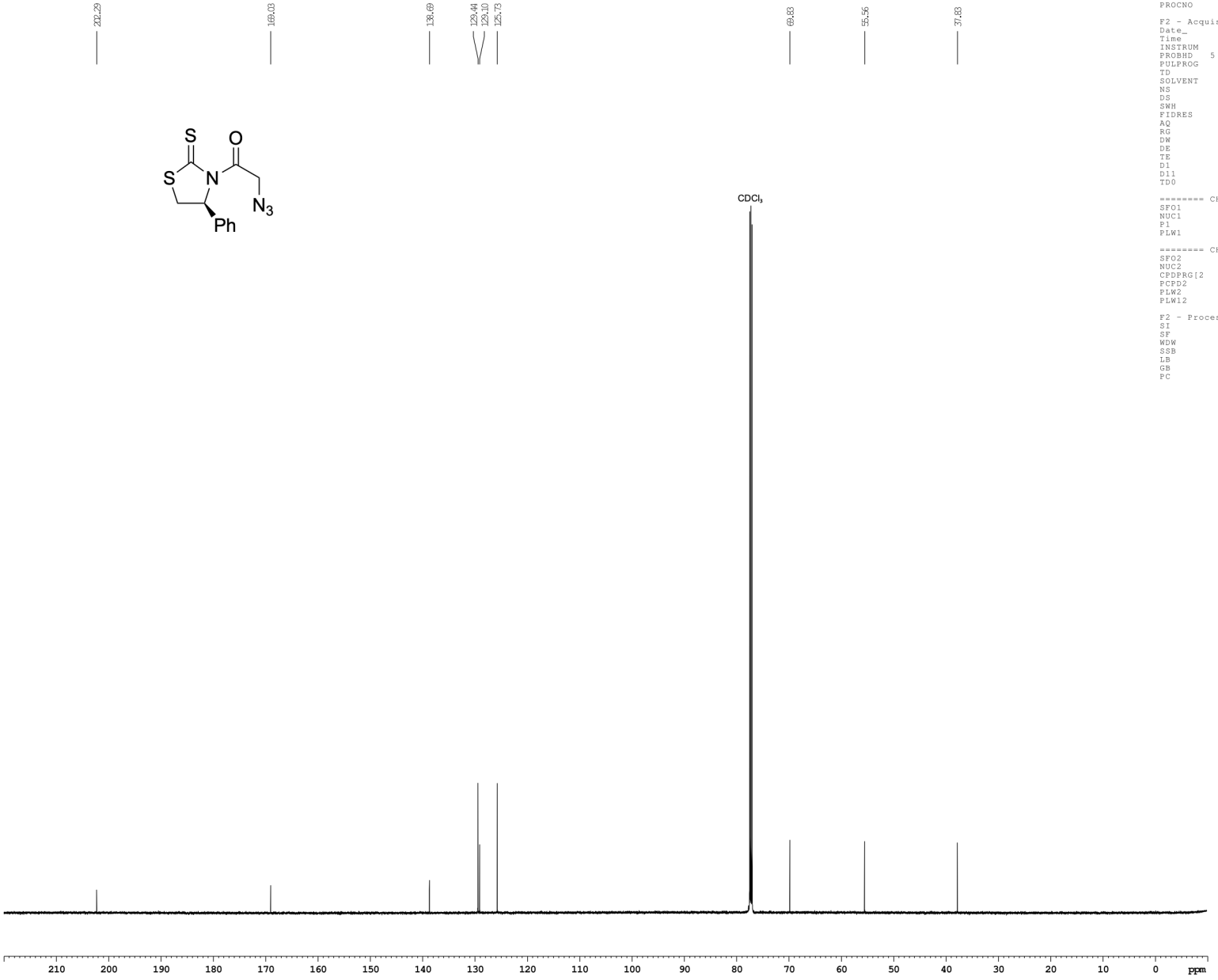


```
Current Data Parameters
NAME                  JZ-III-58
EXPNO                        11
PROCNO                        1

F2 - Acquisition Parameters
Date_                  20241001
Time                      23.34
INSTRUM                    av600
PROBHD    5 mm CPBBO BB-
PULPROG                  zgdc30
TD                        65536
SOLVENT                   CDCl3
NS                          512
DS                            4
SWH                   36231.883 Hz
FIDRES                 0.552855 Hz
AQ                    0.9043968 sec
RG                         2050
DW                       13.800 usec
DE                       19.65 usec
TE                        298.1 K
D1                    0.40000001 sec
D11                   0.03000000 sec
TD0                           1

======== CHANNEL f1 ========
SFO1                150.9194083 MHz
NUC1                        13C
P1                        10.00 usec
PLW1                30.00000000 W

======== CHANNEL f2 ========
SFO2                600.1330010 MHz
NUC2                        1H
CPDPRG[2                waltz16
PCPD2                     80.00 usec
PLW2                30.00000000 W
PLW12                0.39811000 W

F2 - Processing parameters
SI                        65536
SF                  150.9027789 MHz
WDW                          EM
SSB                           0
LB                         1.00 Hz
GB                            0
PC                         1.00
```

Crude ^{1}H NMR spectrum of (2*S*,3*R*)-2-azido-3-(4-(*tert*-butoxy)phenyl)-3-hydroxy-1-((*S*)-4-phenyl-2-thioxothiazolidin-3-yl)propan-1-one in $CDCl_3$ at 500 MHz and 298 K

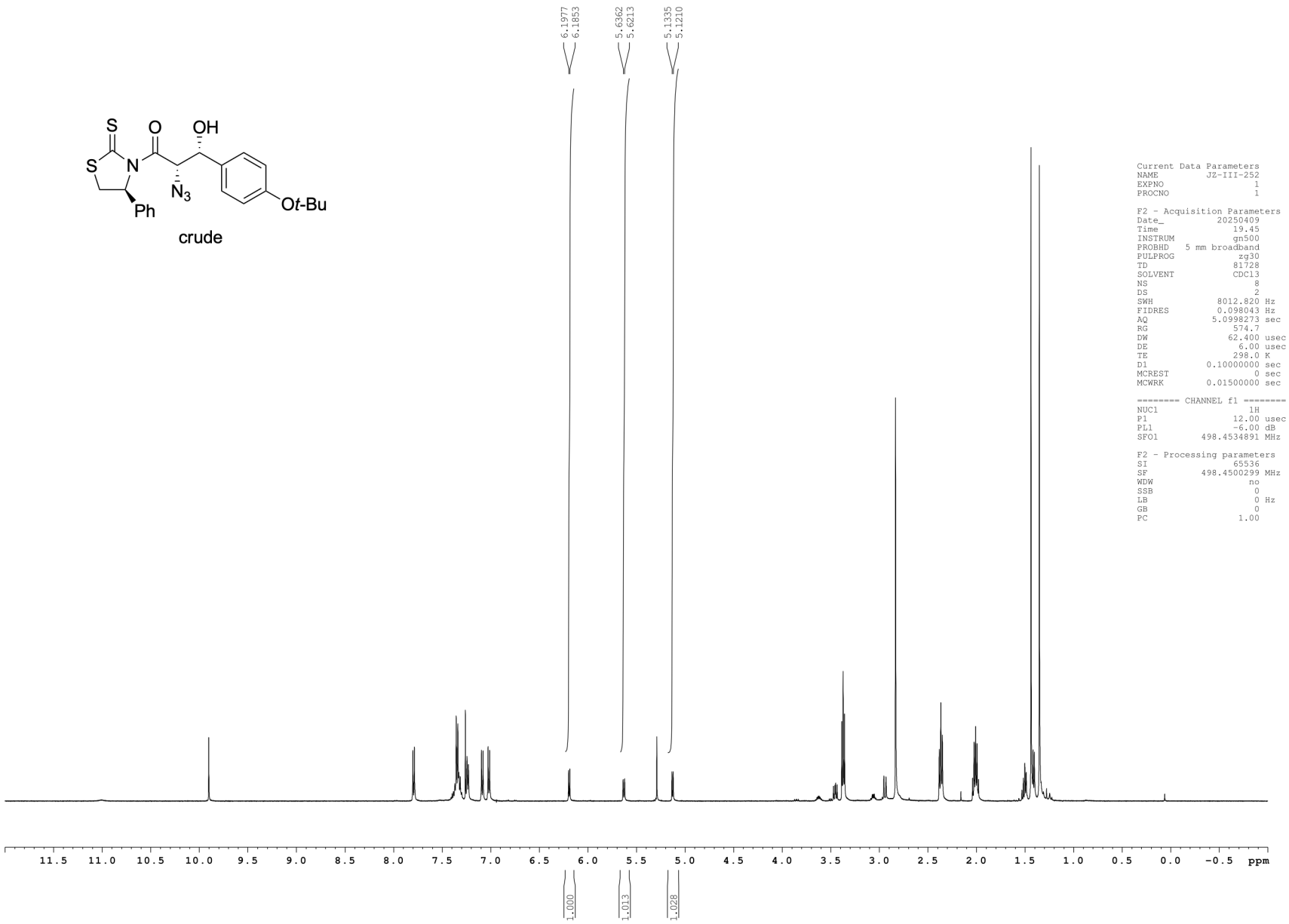

^{1}H NMR spectrum of (2*S*,3*R*)-2-azido-3-(4-(*tert*-butoxy)phenyl)-3-hydroxy-1-((*S*)-4-phenyl-2-thioxothiazolidin-3-yl)propan-1-one in $CDCl_3$ at 500 MHz and 298 K

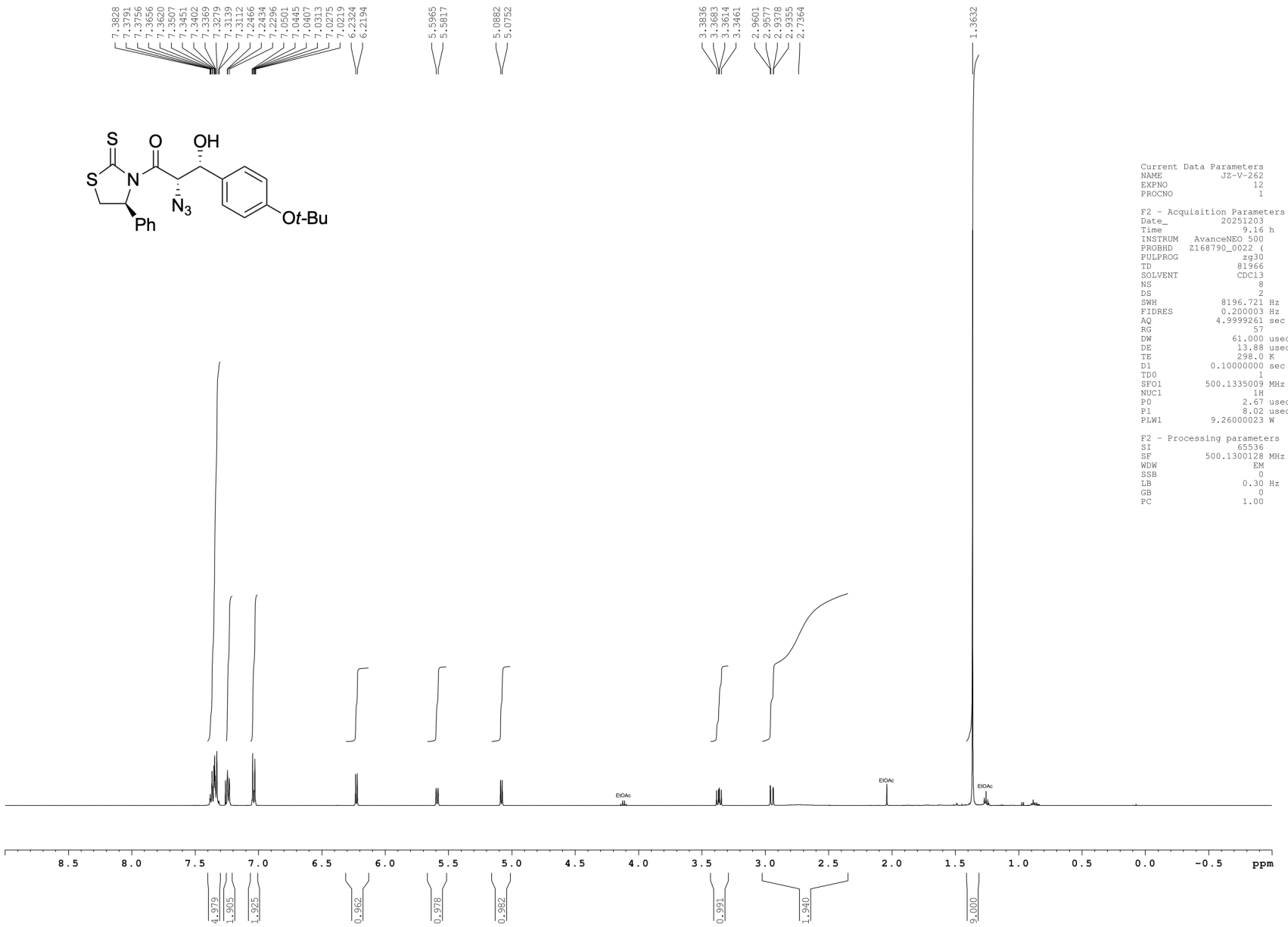


```
Current Data Parameters
NAME              JZ-V-262
EXPNO                   12
PROCNO                   1

F2 - Acquisition Parameters
Date_              20251203
Time                  9.16 h
INSTRUM   AvanceNEO 500
PROBHD   Z168790_0022 (
PULPROG                zg30
TD                    81966
SOLVENT               CDCl3
NS                        8
DS                        2
SWH                8196.721 Hz
FIDRES             0.200003 Hz
AQ                 4.9999261 sec
RG                       57
DW                    61.000 usec
DE                    13.88 usec
TE                    298.0 K
D1              0.10000000 sec
TD0                       1
SFO1           500.1335009 MHz
NUC1                    1H
P0                    2.67 usec
P1                    8.02 usec
PLW1           9.26000023 W

F2 - Processing parameters
SI                    65536
SF             500.1300128 MHz
WDW                      EM
SSB                       0
LB                    0.30 Hz
GB                        0
PC                    1.00
```

^{13}C NMR spectrum of (2*S*,3*R*)-2-azido-3-(4-(*tert*-butoxy)phenyl)-3-hydroxy-1-((*S*)-4-phenyl-2-thioxothiazolidin-3-yl)propan-1-one in $CDCl_3$ at 500 MHz and 298 K

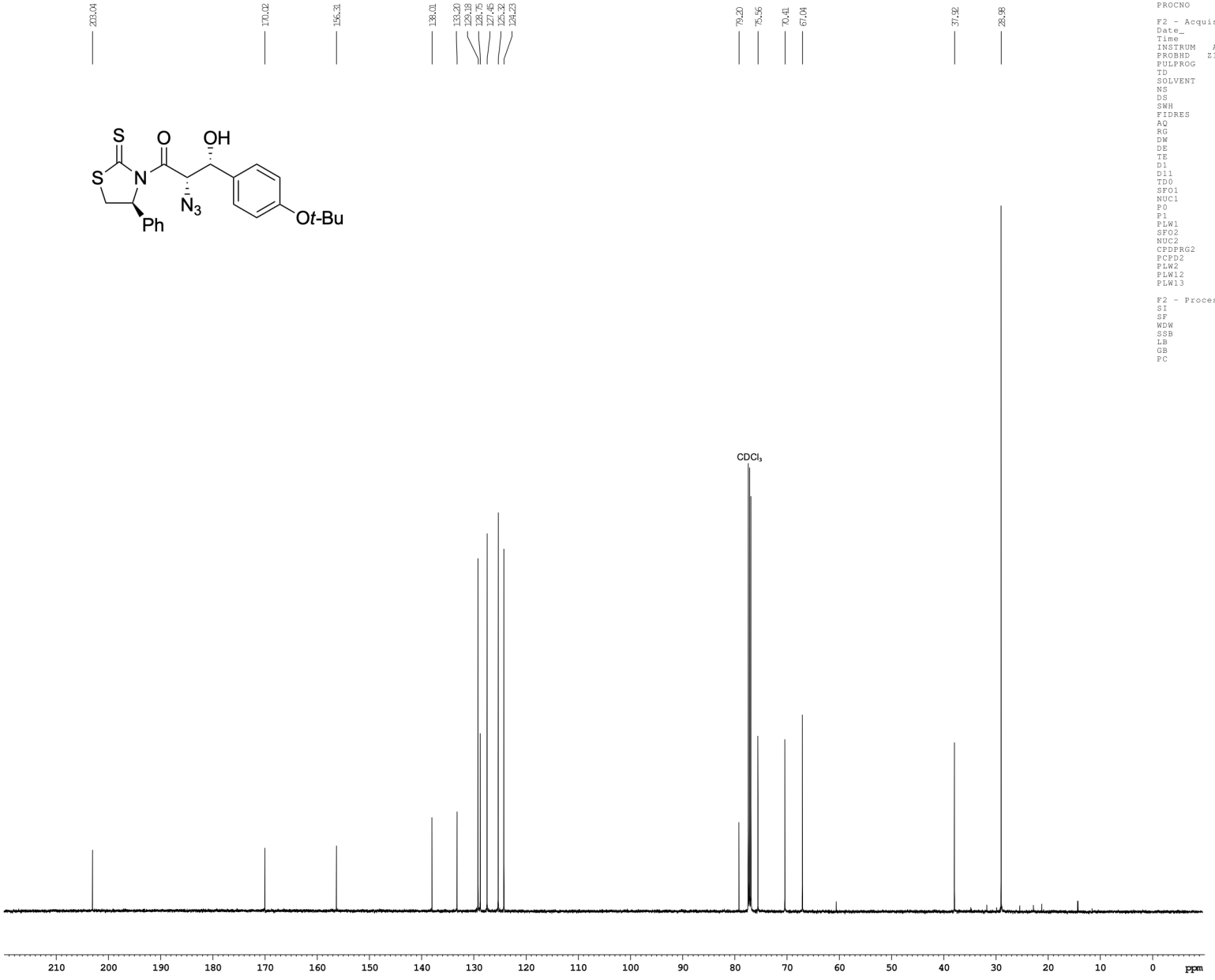


```
Current Data Parameters
NAME                  JZ-V-262
EXPNO                       13
PROCNO                       1

F2 - Acquisition Parameters
Date_               20251203
Time                    9.41 h
INSTRUM   AvanceNEO 500
PROBHD   Z168790_0022 (
PULPROG                zgpg30
TD                      65060
SOLVENT                 CDCl3
NS                       1024
DS                          4
SWH                30120.482 Hz
FIDRES             0.925929 Hz
AQ                 1.0799960 sec
RG                        101
DW                     16.600 usec
DE                     18.00 usec
TE                     298.0 K
D1                 0.25000000 sec
D11                0.03000000 sec
TD0                         1
SFO1           125.7716219 MHz
NUC1                     13C
P0                      3.54 usec
P1                     10.62 usec
PLW1           96.95098877 W
SFO2           500.1320005 MHz
NUC2                     1H
CPDPRG2                A000
PCPD2                 80.00 usec
PLW2            9.26000023 W
PLW12           0.09329600 W
PLW13           0.04685200 W

F2 - Processing parameters
SI                      32768
SF             125.7577746 MHz
WDW                        EM
SSB                         0
LB                       1.00 Hz
GB                          0
PC                       1.40
```

^{1}H NMR spectrum of methyl (2*S*,3*R*)-2-azido-3-(4-(*tert*-butoxy)phenyl)-3-hydroxypropanoate in $CDCl_3$ at 500 MHz and 298 K

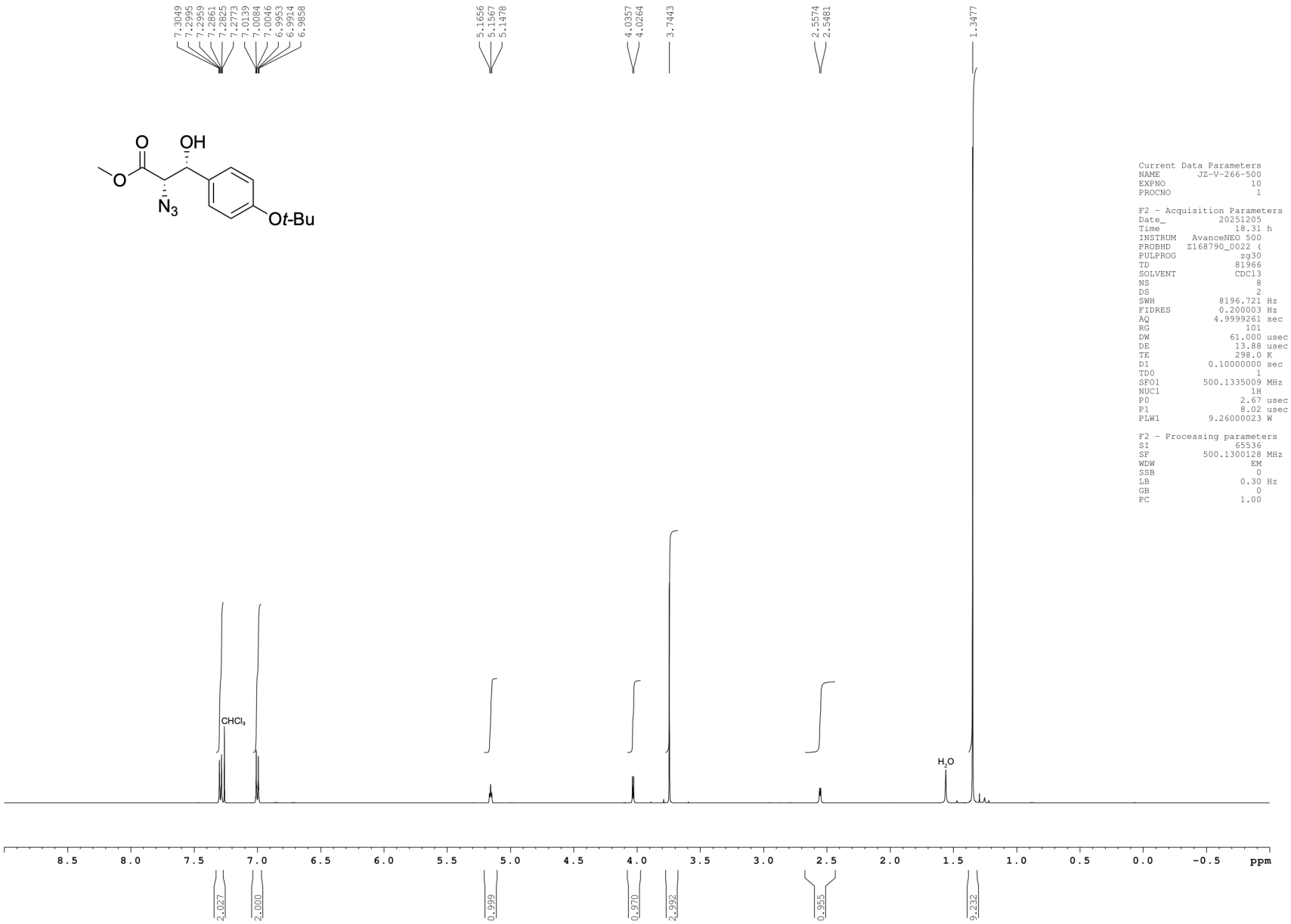


```
Current Data Parameters
NAME         JZ-V-266-500
EXPNO                  10
PROCNO                  1

F2 - Acquisition Parameters
Date_            20251205
Time                18.31 h
INSTRUM   AvanceNEO 500
PROBHD   Z168790_0022 (
PULPROG              zg30
TD                  81966
SOLVENT              CDCl3
NS                       8
DS                       2
SWH              8196.721 Hz
FIDRES           0.200003 Hz
AQ               4.9999261 sec
RG                     101
DW                  61.000 usec
DE                  13.88 usec
TE                  298.0 K
D1              0.10000000 sec
TD0                      1
SFO1           500.1335009 MHz
NUC1                   1H
P0                  2.67 usec
P1                  8.02 usec
PLW1            9.26000023 W

F2 - Processing parameters
SI                   65536
SF             500.1300128 MHz
WDW                    EM
SSB                      0
LB                  0.30 Hz
GB                       0
PC                    1.00
```

^{13}C NMR spectrum of methyl (2*S*,3*R*)-2-azido-3-(4-(*tert*-butoxy)phenyl)-3-hydroxypropanoate in $CDCl_3$ at 500 MHz and 298 K

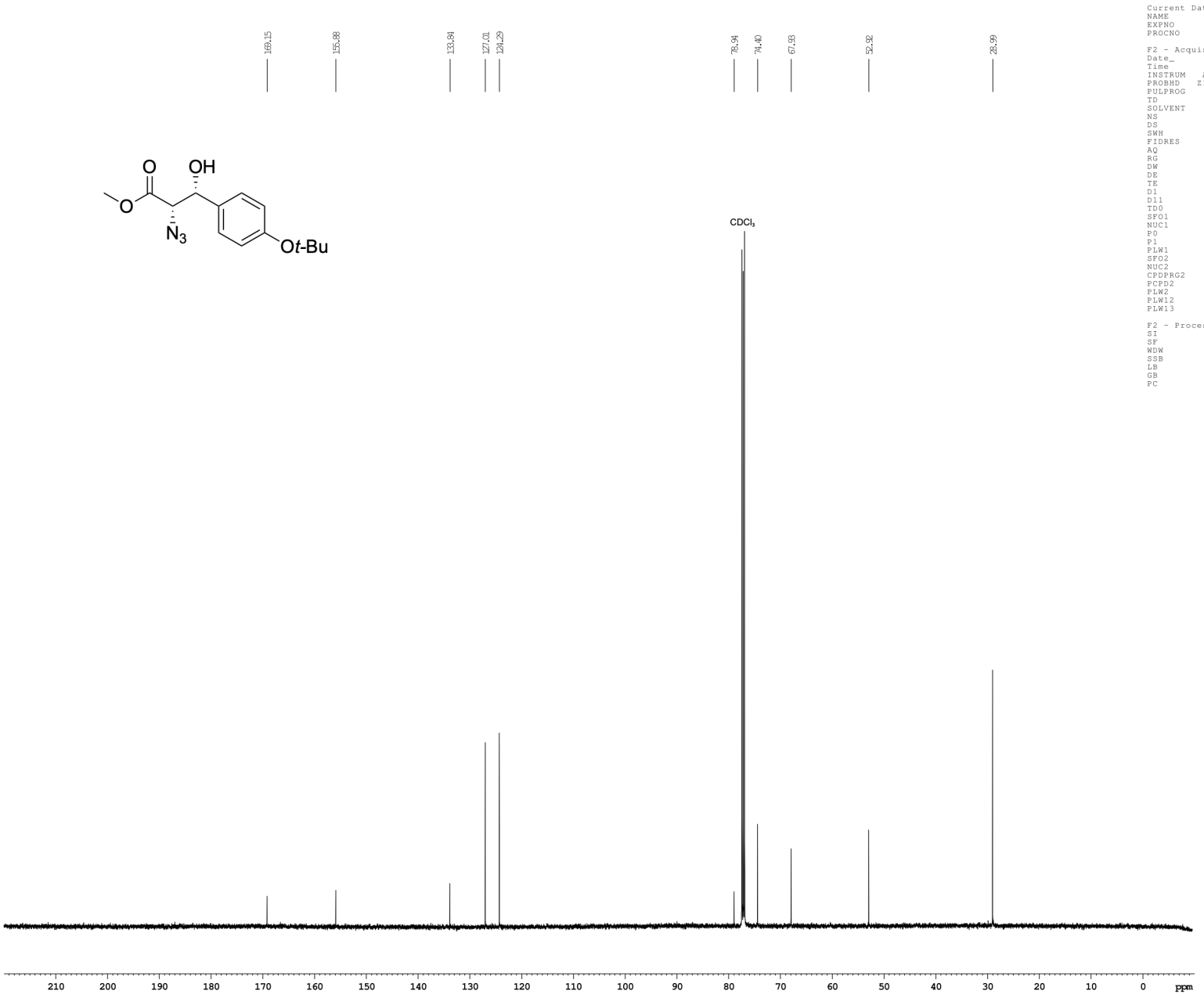


```
Current Data Parameters
NAME        JZ-V-266-500
EXPNO                 11
PROCNO                 1

F2 - Acquisition Parameters
Date_           20251205
Time              18.56 h
INSTRUM   AvanceNEO 500
PROBHD   Z168790_0022 (
PULPROG           zgpg30
TD                65060
SOLVENT           CDCl3
NS                 1024
DS                    4
SWH           30120.482 Hz
FIDRES         0.925929 Hz
AQ            1.0799960 sec
RG                  101
DW               16.600 usec
DE               18.00 usec
TE               298.0 K
D1            0.25000000 sec
D11           0.03000000 sec
TD0                   1
SFO1        125.7716219 MHz
NUC1                13C
P0                3.54 usec
P1               10.62 usec
PLW1         96.95098877 W
SFO2        500.1320005 MHz
NUC2                1H
CPDPRG2           A000
PCPD2            80.00 usec
PLW2          9.26000023 W
PLW12         0.09329600 W
PLW13         0.04685200 W

F2 - Processing parameters
SI                32768
SF          125.7577714 MHz
WDW                 EM
SSB                  0
LB                1.00 Hz
GB                   0
PC                1.40
```

^{1}H NMR spectrum of (2*S*,3*R*)-2-azido-3-(4-(*tert*-butoxy)phenyl)-3-hydroxypropanoic acid in DMSO-d_6 at 500 MHz and 298 K

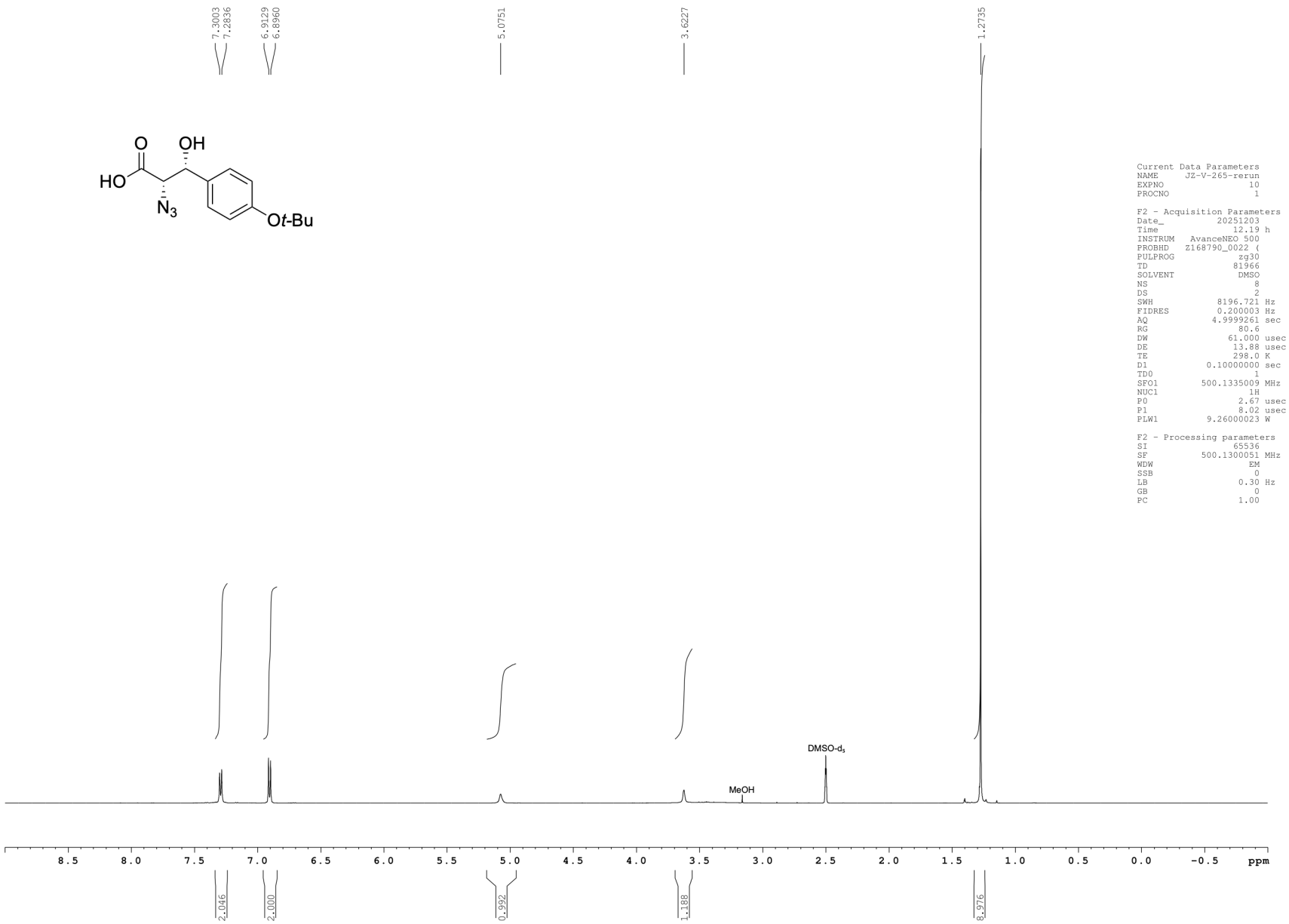


```
Current Data Parameters
NAME      JZ-V-265-rerun
EXPNO                 10
PROCNO                 1

F2 - Acquisition Parameters
Date_           20251203
Time               12.19 h
INSTRUM   AvanceNEO 500
PROBHD   Z168790_0022 (
PULPROG            zg30
TD                81966
SOLVENT            DMSO
NS                     8
DS                     2
SWH             8196.721 Hz
FIDRES          0.200003 Hz
AQ              4.9999261 sec
RG                  80.6
DW                61.000 usec
DE                13.88 usec
TE                298.0 K
D1            0.10000000 sec
TD0                    1
SFO1         500.1335009 MHz
NUC1                  1H
P0                 2.67 usec
P1                 8.02 usec
PLW1           9.26000023 W

F2 - Processing parameters
SI                 65536
SF           500.1300051 MHz
WDW                   EM
SSB                    0
LB                  0.30 Hz
GB                     0
PC                  1.00
```

^{13}C NMR spectrum of (2*S*,3*R*)-2-azido-3-(4-(*tert*-butoxy)phenyl)-3-hydroxypropanoic acid in DMSO-d_6 at 500 MHz and 298 K

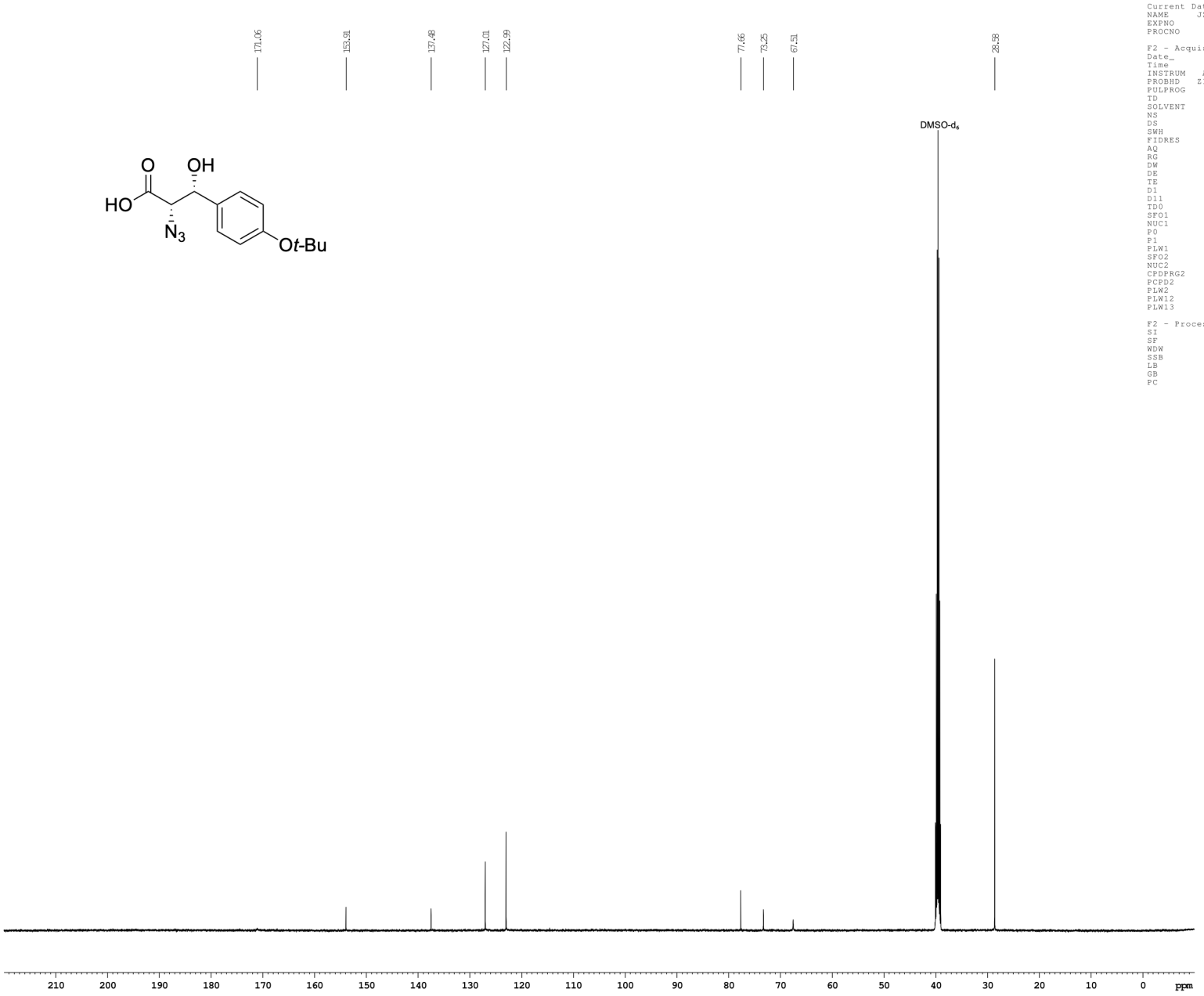


```
Current Data Parameters
NAME      JZ-V-265-rerun
EXPNO                 11
PROCNO                 1

F2 - Acquisition Parameters
Date_           20251203
Time              12.44 h
INSTRUM   AvanceNEO 500
PROBHD   Z168790_0022 (
PULPROG          zgpg30
TD                65060
SOLVENT            DMSO
NS                 1024
DS                    4
SWH           30120.482 Hz
FIDRES         0.925929 Hz
AQ           1.0799960 sec
RG                  101
DW               16.600 usec
DE                18.00 usec
TE                298.0 K
D1           0.25000000 sec
D11          0.03000000 sec
TD0                   1
SFO1        125.7716219 MHz
NUC1                13C
P0                 3.54 usec
P1                10.62 usec
PLW1        96.95098877 W
SFO2        500.1320005 MHz
NUC2                1H
CPDPRG2          A000
PCPD2             80.00 usec
PLW2         9.26000023 W
PLW12        0.09329600 W
PLW13        0.04685200 W

F2 - Processing parameters
SI                32768
SF          125.7578478 MHz
WDW                EM
SSB                 0
LB                1.00 Hz
GB                  0
PC                1.40
```

^{1}H NMR spectrum of (2*S*,3*R*)-2-azido-3-(4-(*tert*-butoxy)phenyl)-3-((*tert*-butyldimethylsilyl)oxy)propanoic acid in $CDCl_3$ at 500 MHz and 298 K

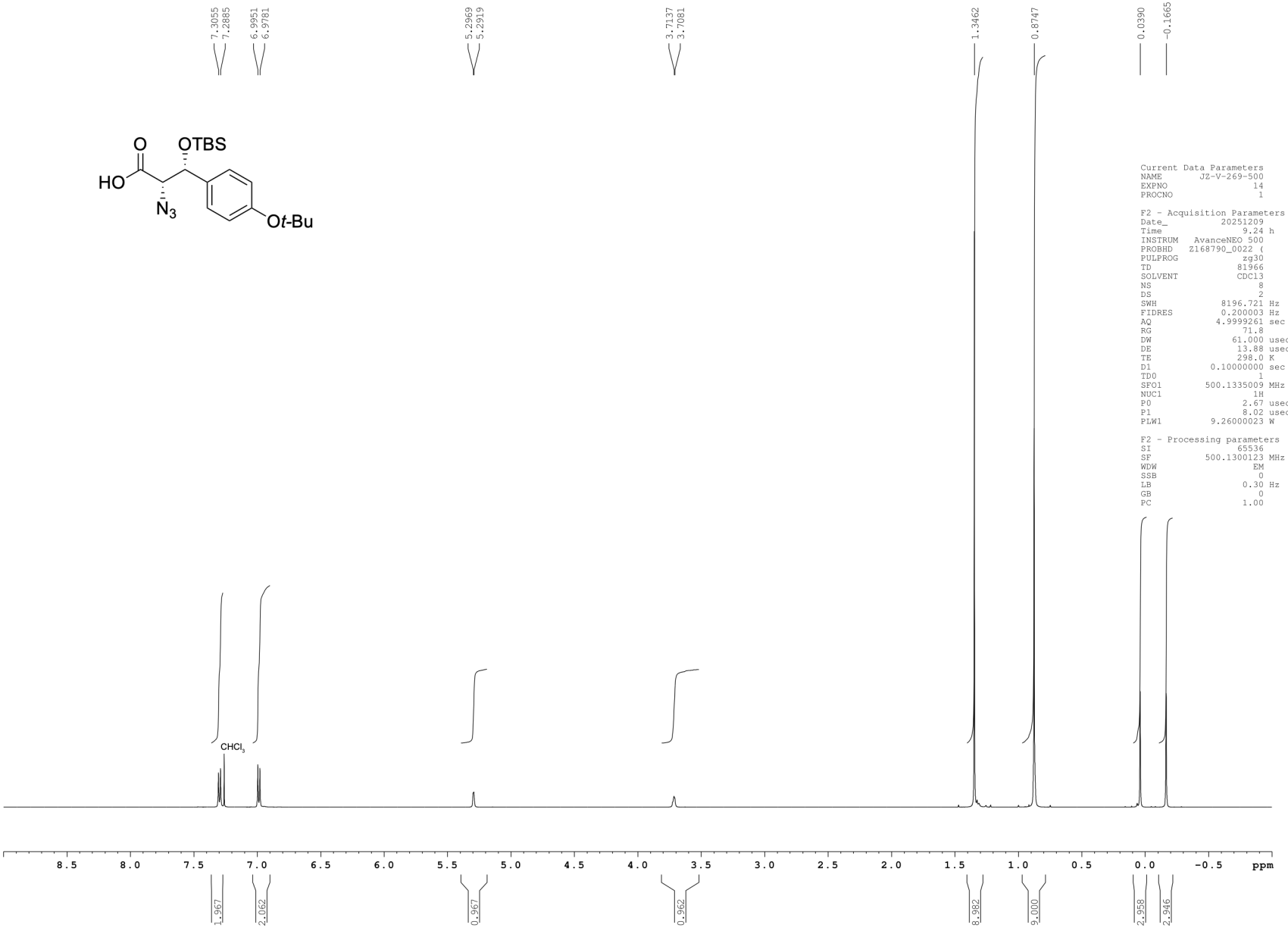

^{13}C NMR spectrum of (2*S*,3*R*)-2-azido-3-(4-(*tert*-butoxy)phenyl)-3-((*tert*-butyldimethylsilyl)oxy)propanoic acid in $CDCl_3$ at 500 MHz and 298 K

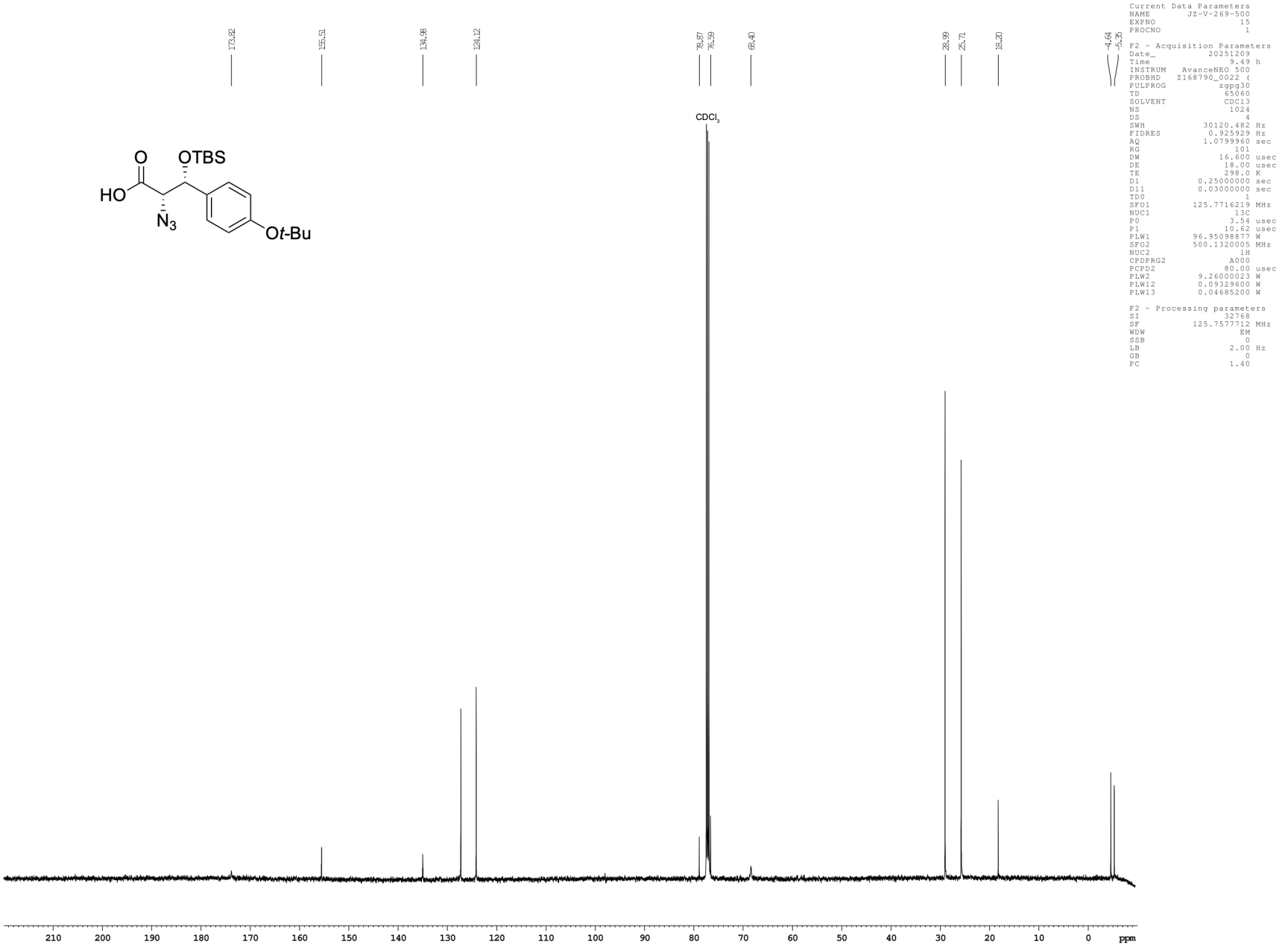

^{1}H NMR spectrum of (2*S*,3*R*)-2-amino-3-(4-(*tert*-butoxy)phenyl)-3-((*tert*-butyldimethylsilyl)oxy)propanoic acid in CD_3OD at 500 MHz and 298 K

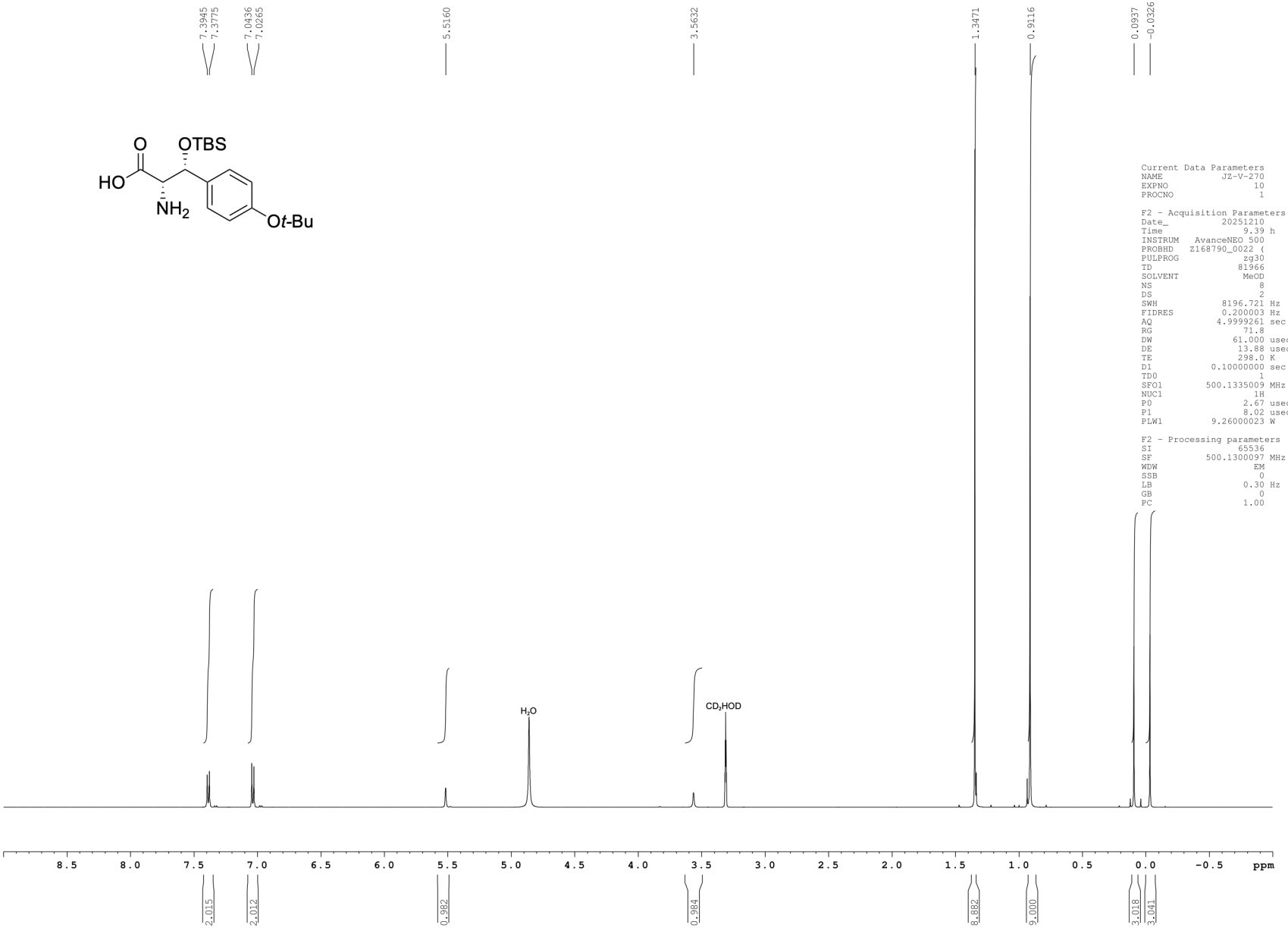

^{13}C NMR spectrum of (2*S*,3*R*)-2-amino-3-(4-(*tert*-butoxy)phenyl)-3-((*tert*-butyldimethylsilyl)oxy)propanoic acid in CD_3OD at 500 MHz and 298 K

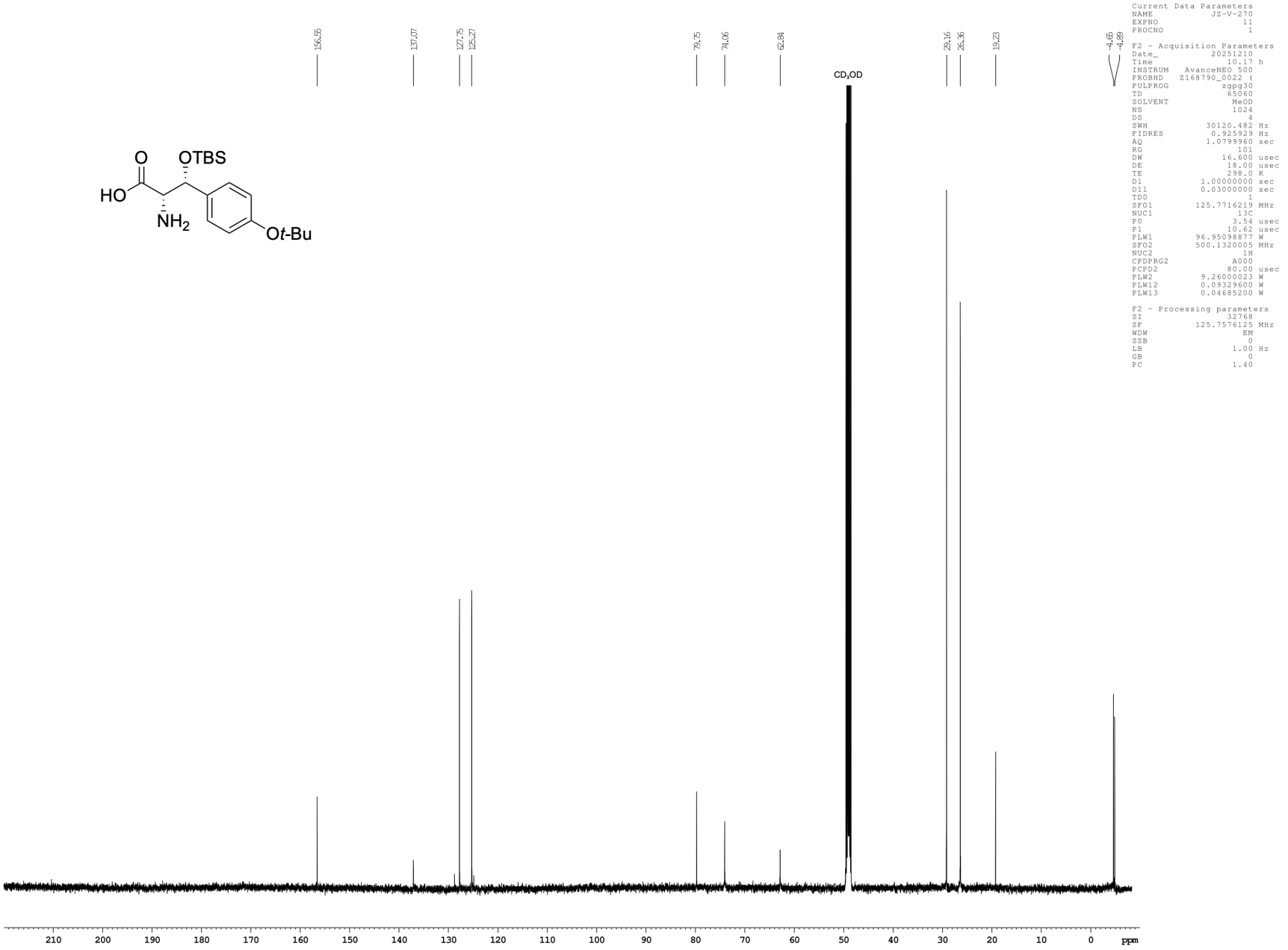

[1]H NMR spectrum of (2*S*,3*R*)-2-((((9*H*-fluoren-9-yl)methoxy)carbonyl)amino)-3-(4-(*tert*-butoxy)phenyl)-3-((*tert*-butyldimethylsilyl)oxy)propanoic acid in DMSO-d_6 at 500 MHz and 298 K

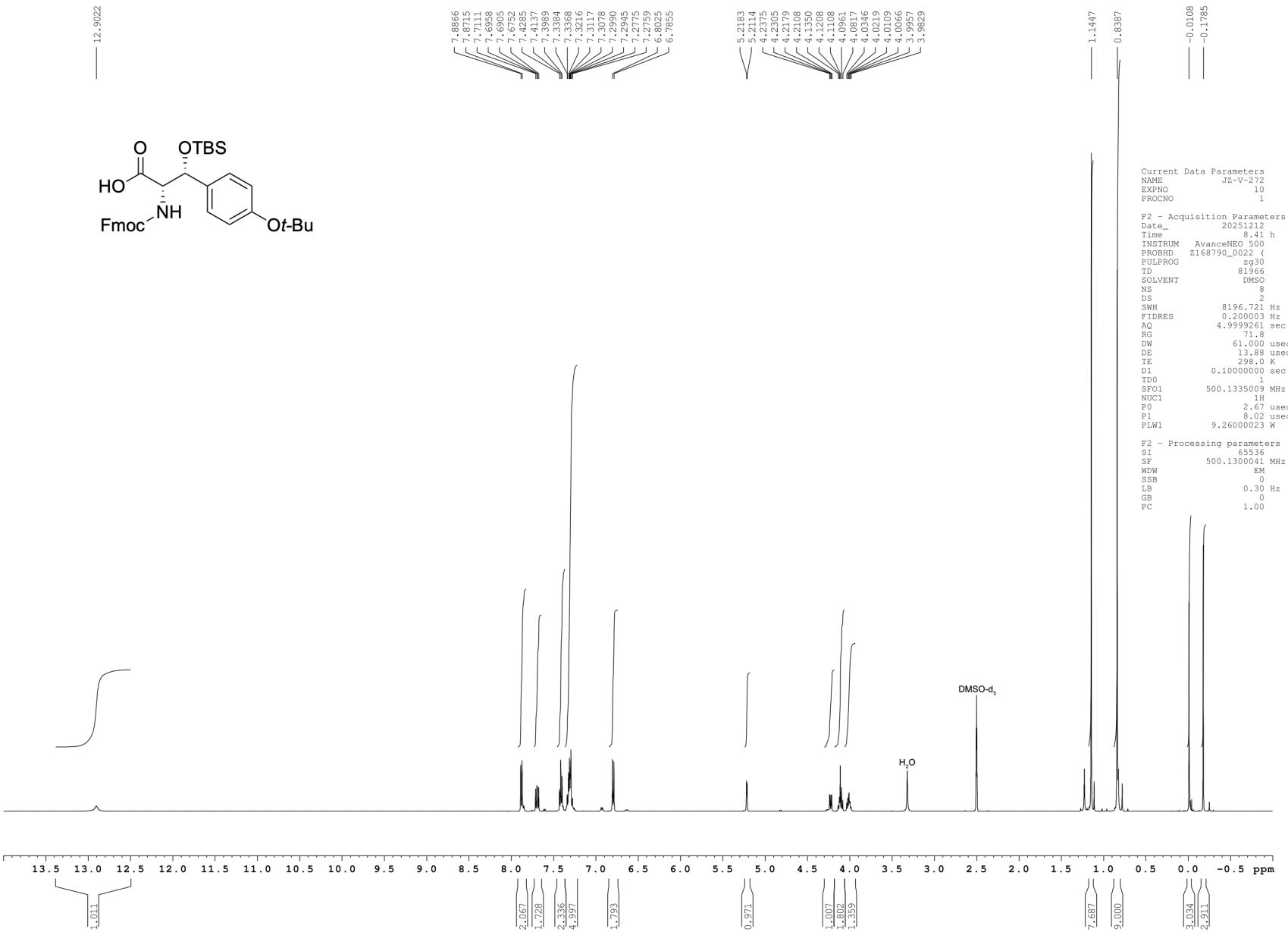

^{13}C NMR spectrum of (2*S*,3*R*)-2-((((9*H*-fluoren-9-yl)methoxy)carbonyl)amino)-3-(4-(*tert*-butoxy)phenyl)-3-((*tert*-butyldimethylsilyl)oxy)propanoic acid in DMSO-d_6 at 500 MHz and 298 K

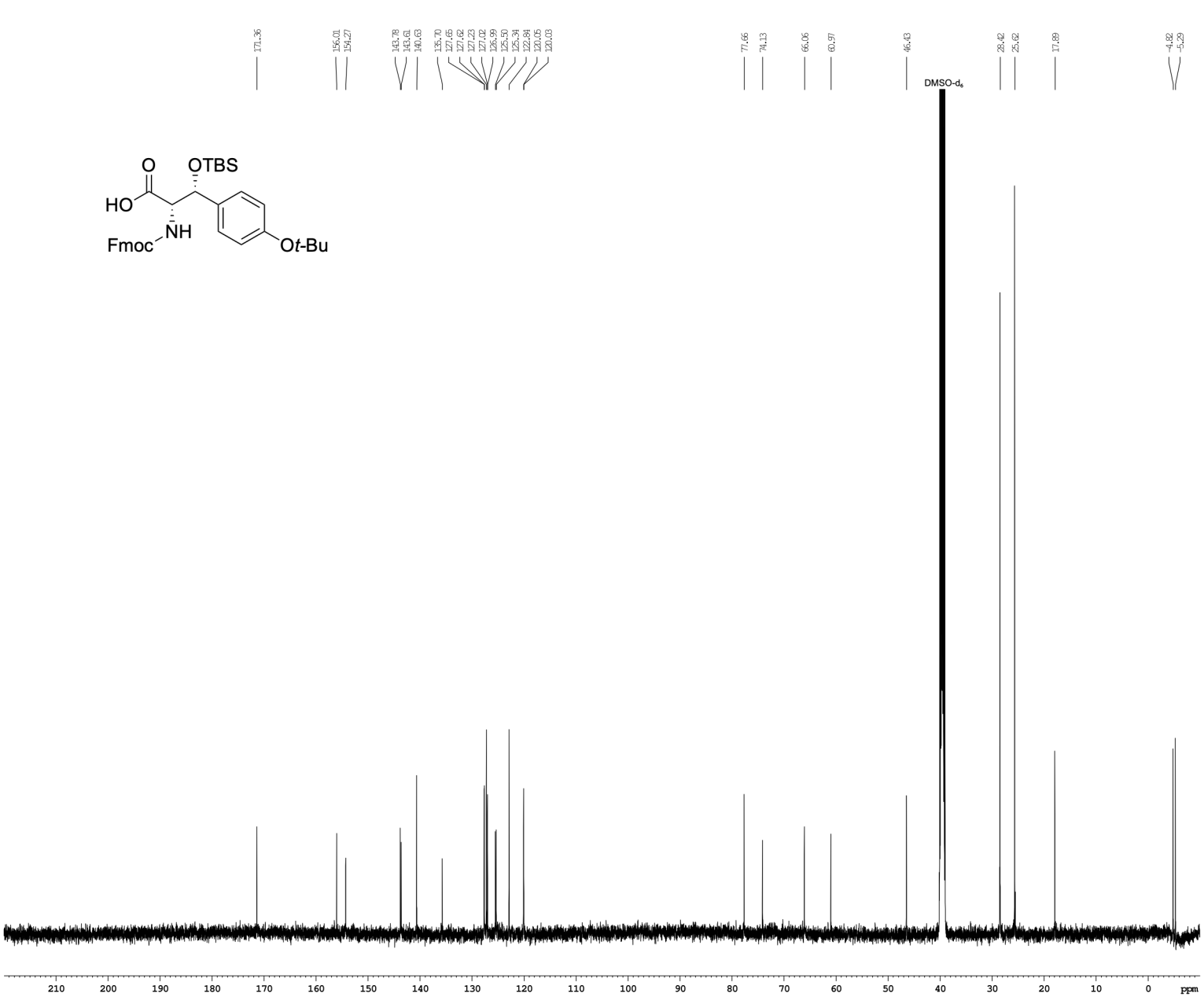

^{1}H NMR spectrum of ethyl (*E*)-4-methylpent-2-enoate in $CDCl_3$ at 500 MHz and 298 K

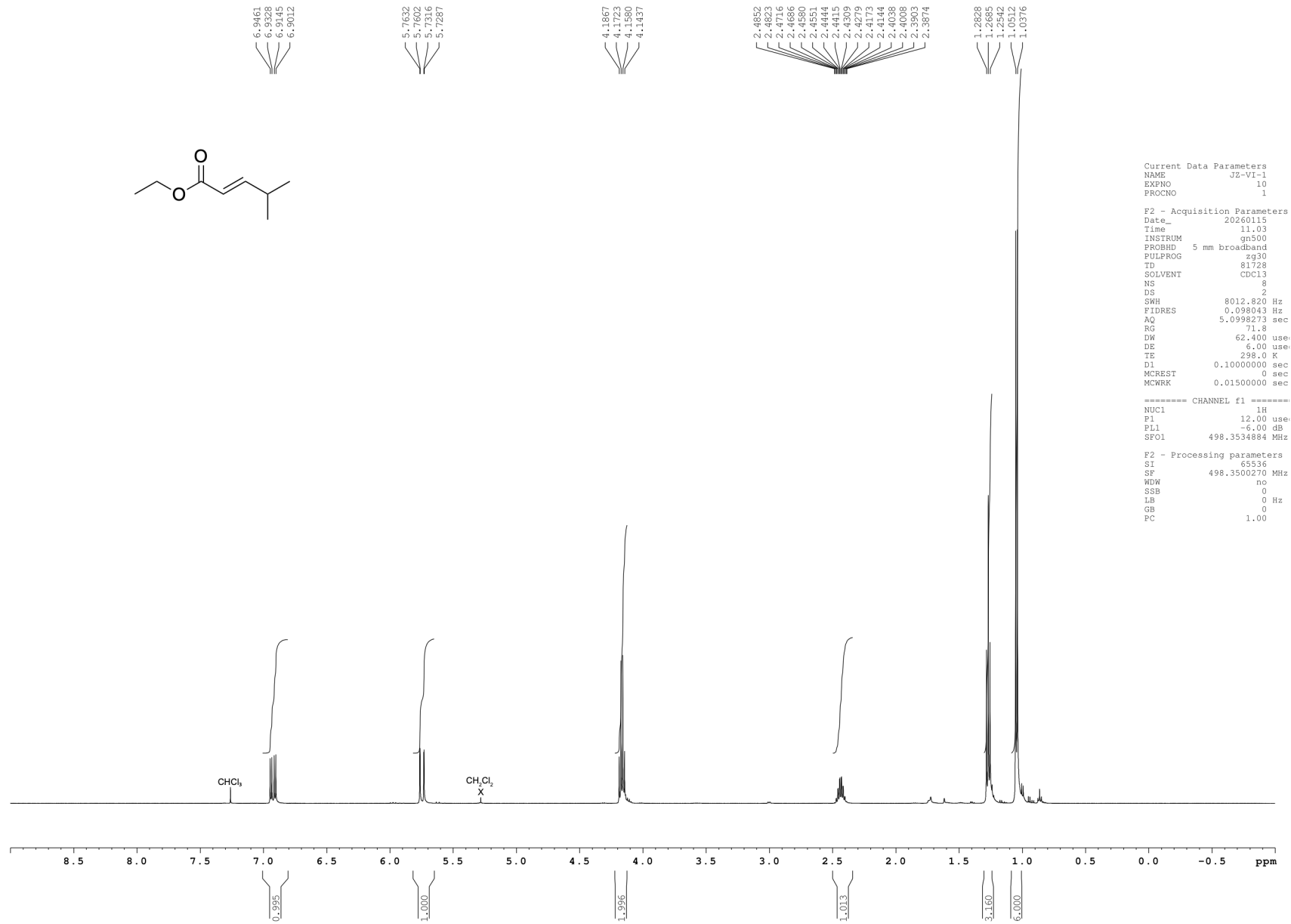

^{13}C NMR spectrum of ethyl (*E*)-4-methylpent-2-enoate in $CDCl_3$ at 500 MHz and 298 K

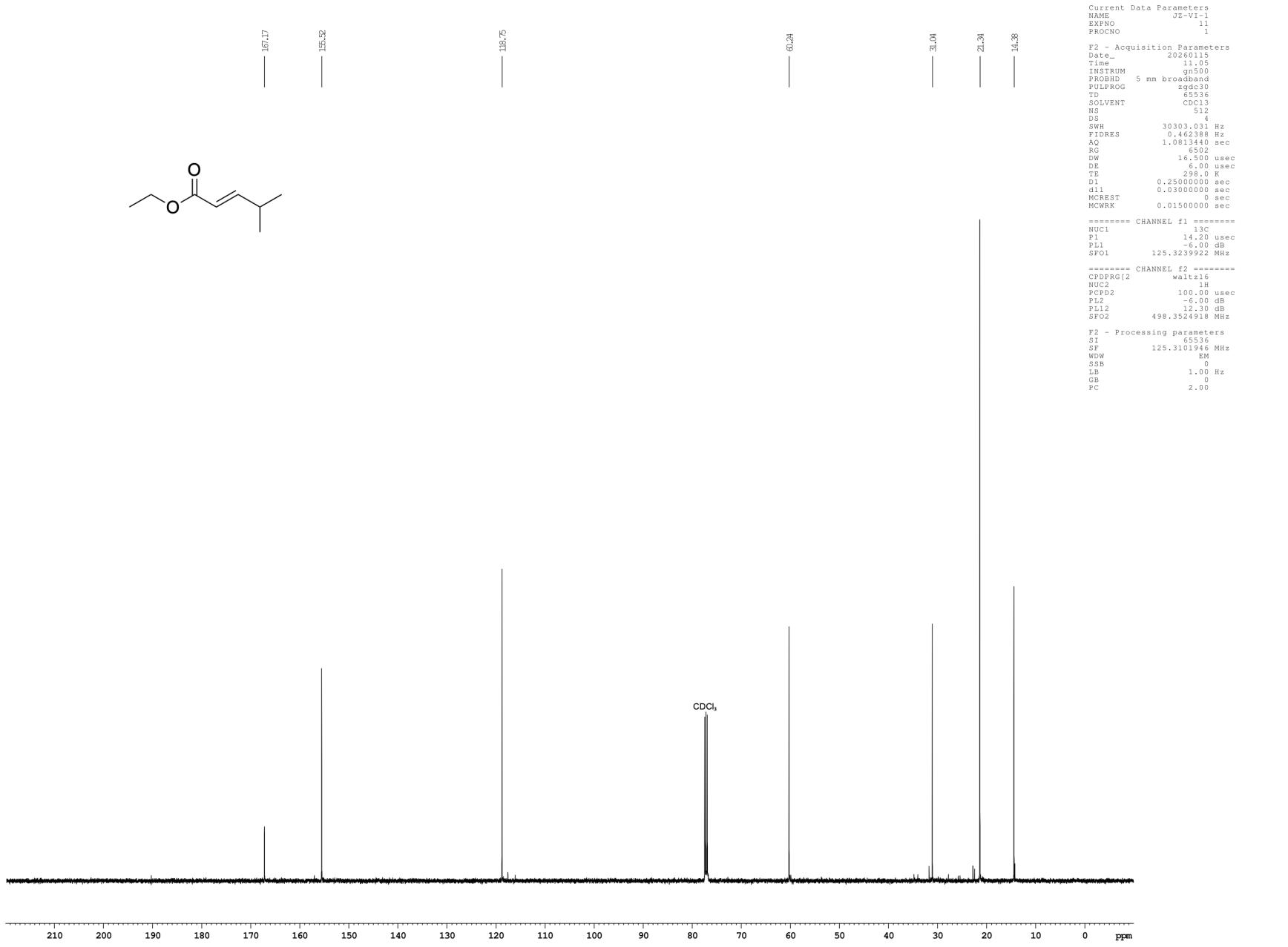


```
Current Data Parameters
NAME                  JZ-VI-1
EXPNO                      11
PROCNO                      1

F2 - Acquisition Parameters
Date_              20260115
Time                   11.05
INSTRUM                gn500
PROBHD   5 mm broadband
PULPROG                zgdc30
TD                      65536
SOLVENT                CDCl3
NS                        512
DS                          4
SWH                30303.031 Hz
FIDRES             0.462388 Hz
AQ                 1.0813440 sec
RG                      6502
DW                    16.500 usec
DE                     6.00 usec
TE                    298.0 K
D1                 0.25000000 sec
d11                0.03000000 sec
MCREST                    0 sec
MCWRK              0.01500000 sec

======== CHANNEL f1 ========
NUC1                      13C
P1                    14.20 usec
PL1                   -6.00 dB
SFO1              125.3239922 MHz

======== CHANNEL f2 ========
CPDPRG[2              waltz16
NUC2                      1H
PCPD2                100.00 usec
PL2                   -6.00 dB
PL12                  12.30 dB
SFO2              498.3524918 MHz

F2 - Processing parameters
SI                        65536
SF                125.3101946 MHz
WDW                        EM
SSB                         0
LB                     1.00 Hz
GB                          0
PC                     2.00
```

^{1}H NMR spectrum of ethyl (2*S*,3*R*)-2,3-dihydroxy-4-methylpentanoate in $CDCl_3$ at 500 MHz and 298 K

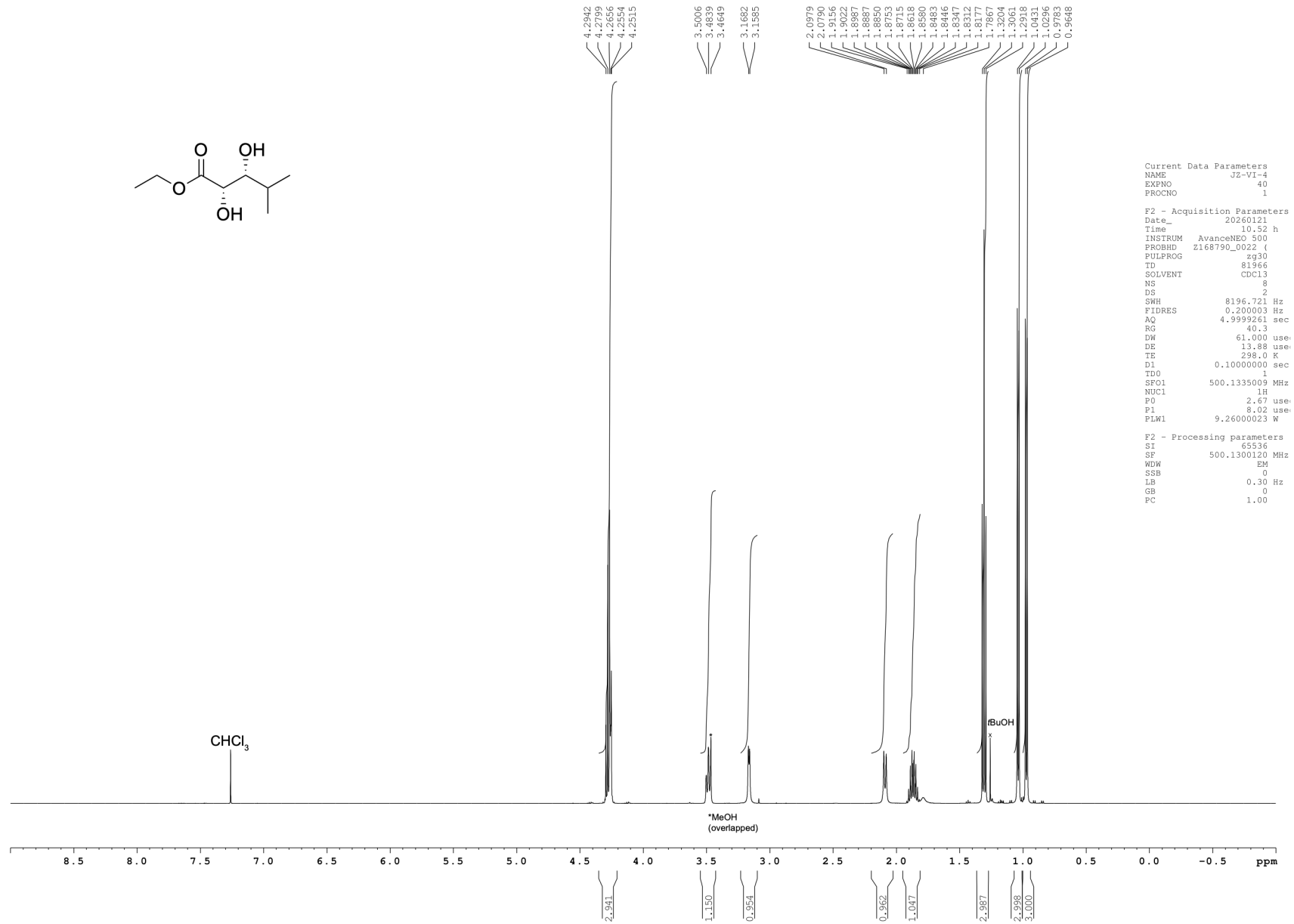

^{13}C NMR spectrum of ethyl (2*S*,3*R*)-2,3-dihydroxy-4-methylpentanoate in $CDCl_3$ at 500 MHz and 298 K

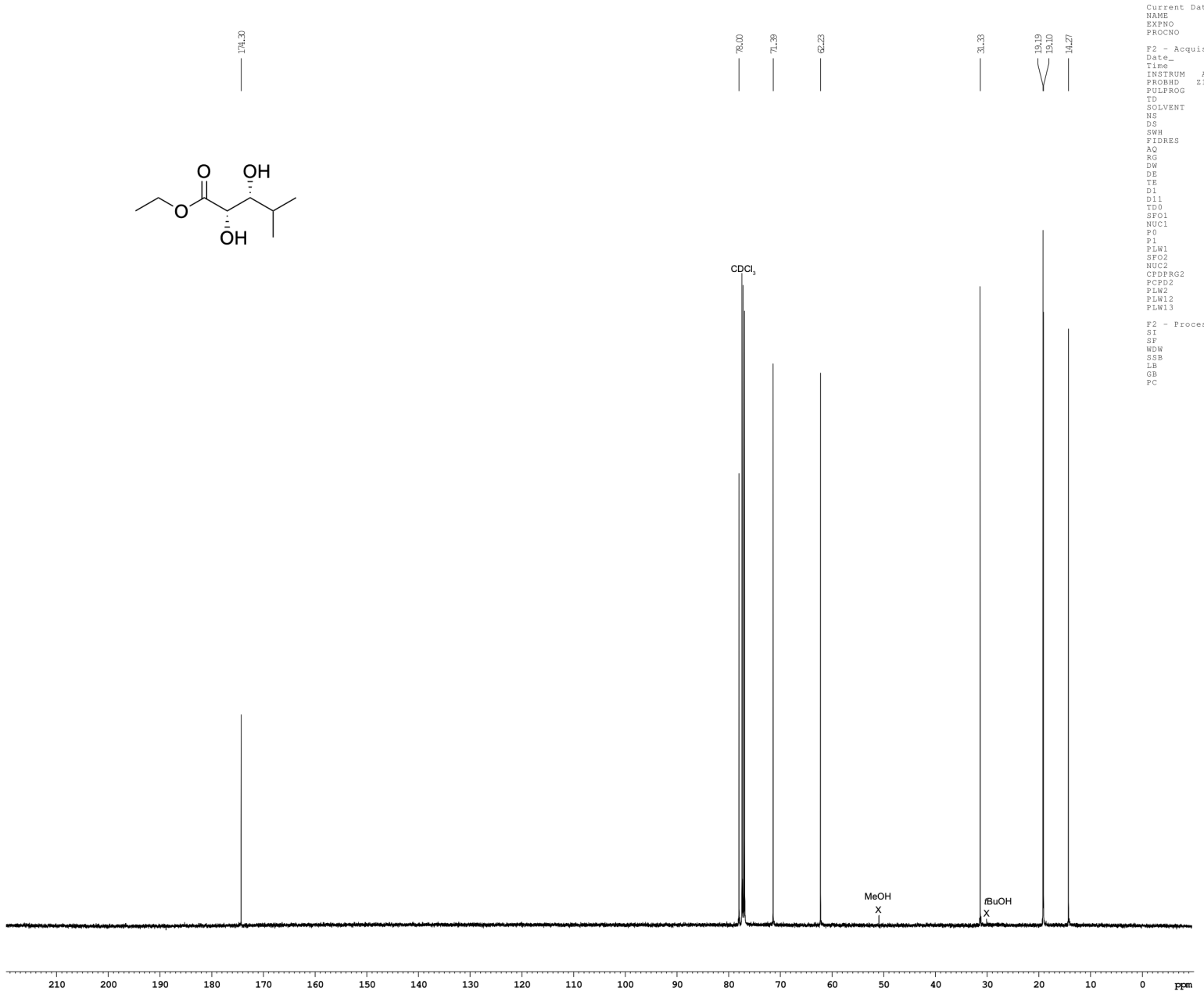


```
Current Data Parameters
NAME                  JZ-VI-4
EXPNO                      41
PROCNO                      1

F2 - Acquisition Parameters
Date_               20260121
Time                   11.17 h
INSTRUM   AvanceNEO 500
PROBHD    Z168790_0022 (
PULPROG               zgpg30
TD                     65060
SOLVENT                CDCl3
NS                      1024
DS                         4
SWH                30120.482 Hz
FIDRES             0.925929 Hz
AQ                 1.0799960 sec
RG                       101
DW                    16.600 usec
DE                    18.00 usec
TE                    298.0 K
D1                 0.25000000 sec
D11                0.03000000 sec
TD0                        1
SFO1              125.7716219 MHz
NUC1                      13C
P0                     3.54 usec
P1                    10.62 usec
PLW1              96.95098877 W
SFO2              500.1320005 MHz
NUC2                      1H
CPDPRG2                 A000
PCPD2                 80.00 usec
PLW2               9.26000023 W
PLW12              0.09329600 W
PLW13              0.04685200 W

F2 - Processing parameters
SI                       32768
SF                125.7577730 MHz
WDW                         EM
SSB                          0
LB                        1.00 Hz
GB                           0
PC                        1.40
```

^{1}H NMR spectrum of ethyl (2*R*,3*R*)-3-acetoxy-2-bromo-4-methylpentanoate in $CDCl_3$ at 500 MHz and 298 K

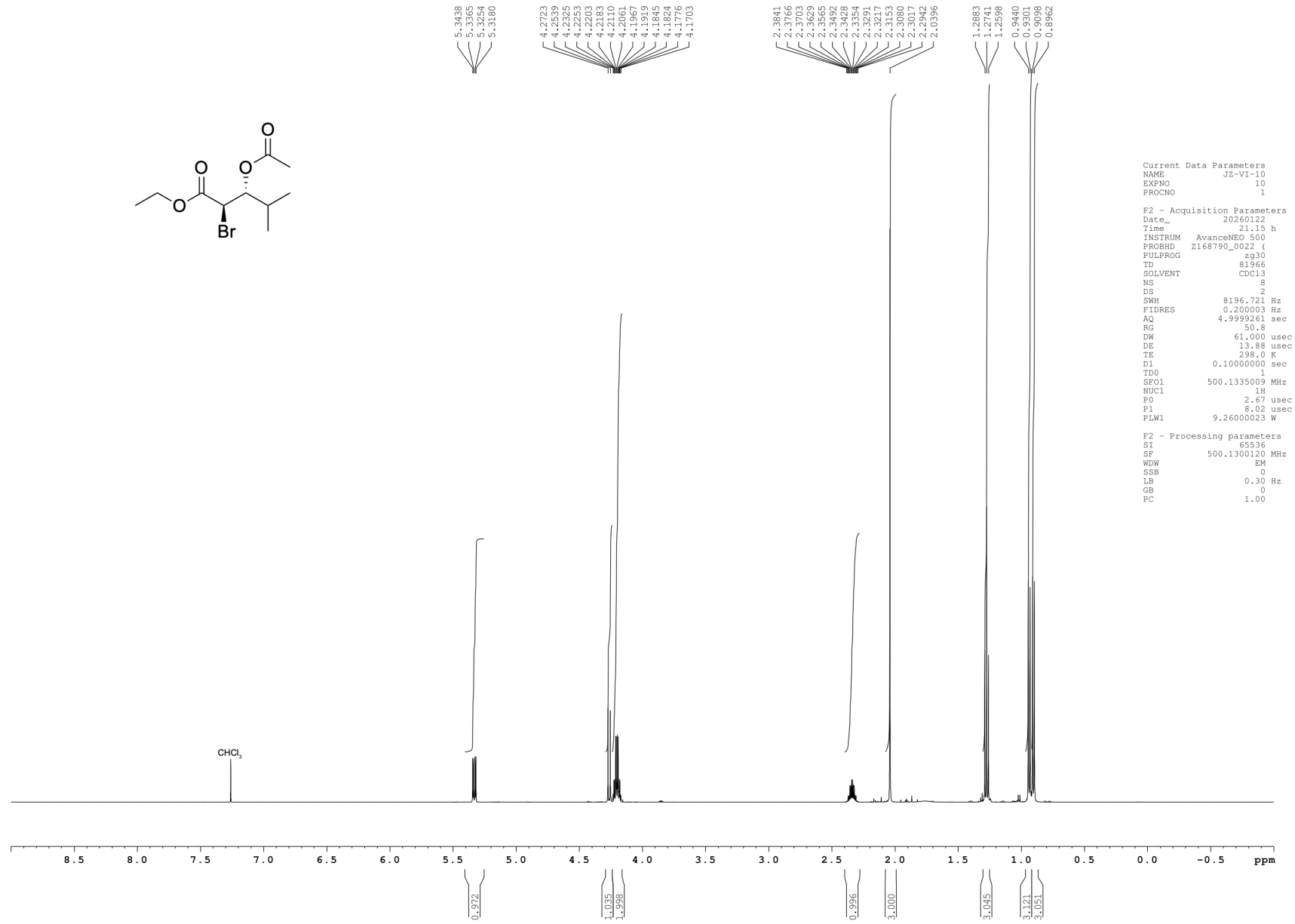

^{13}C NMR spectrum of ethyl (2*R*,3*R*)-3-acetoxy-2-bromo-4-methylpentanoate in $CDCl_3$ at 500 MHz and 298 K

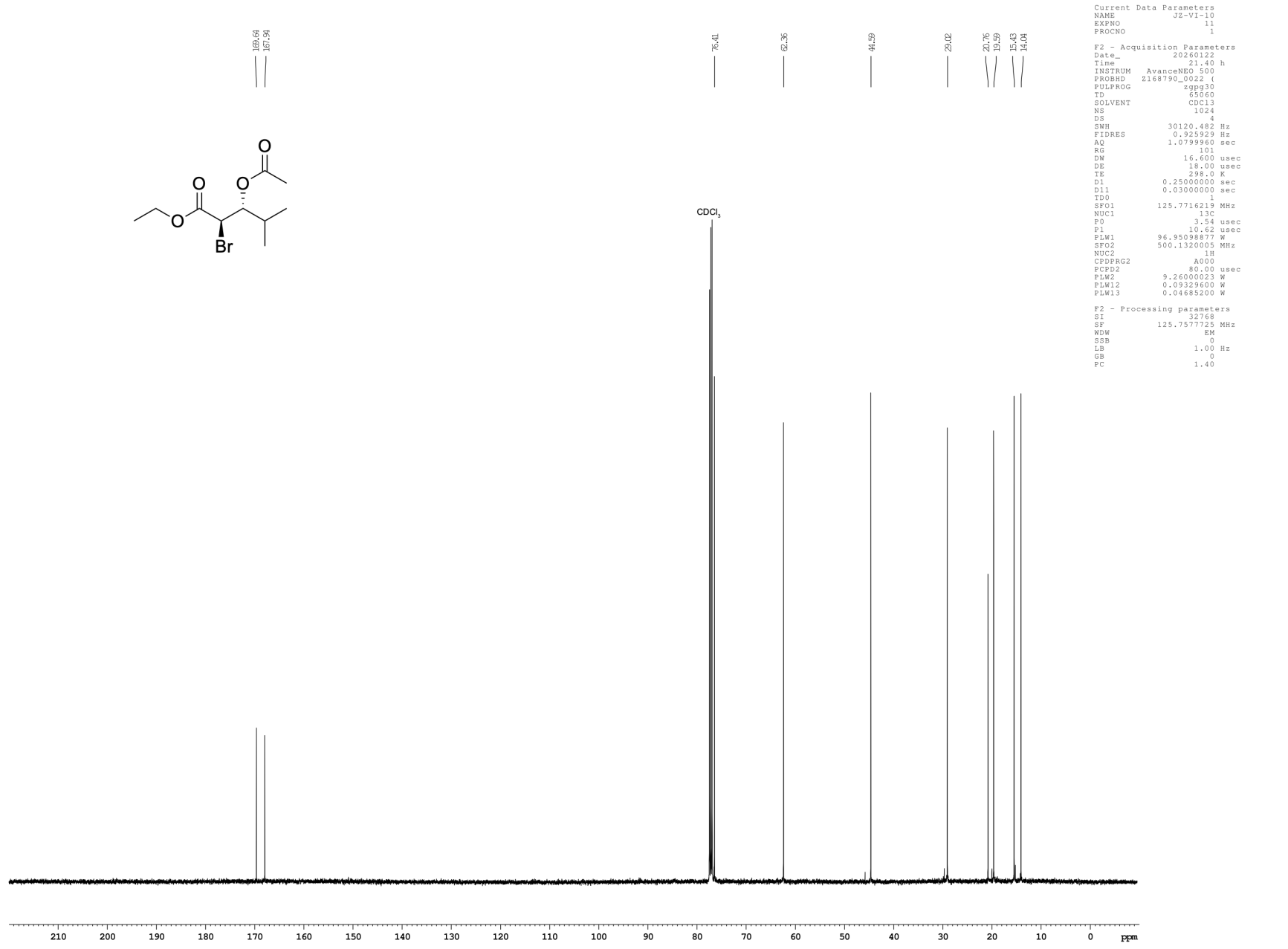

^{1}H NMR spectrum of ethyl (2*R*,3*R*)-2-bromo-3-hydroxy-4-methylpentanoate in $CDCl_3$ at 500 MHz and 298 K

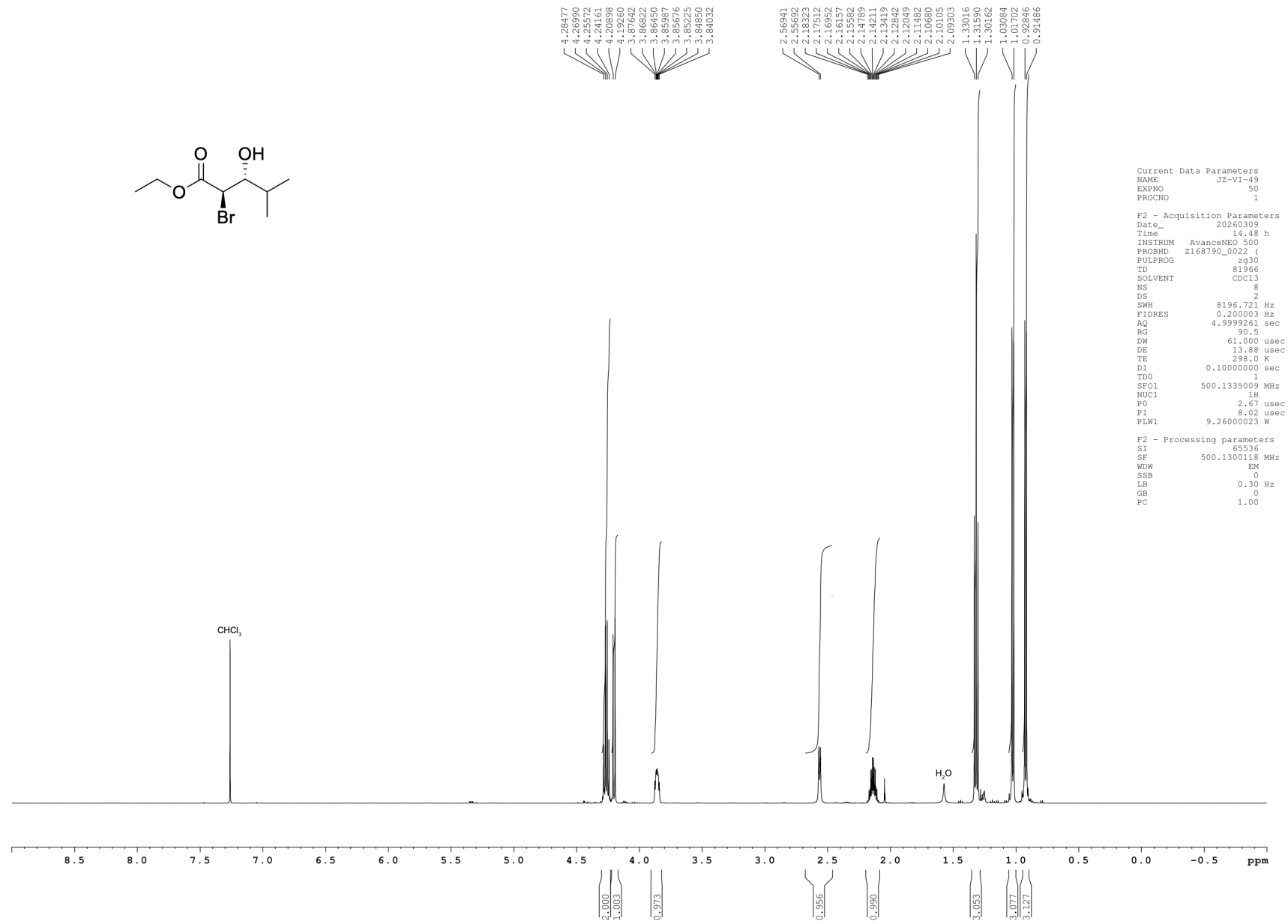

^{13}C NMR spectrum of ethyl (2*R*,3*R*)-2-bromo-3-hydroxy-4-methylpentanoate in $CDCl_3$ at 500 MHz and 298 K

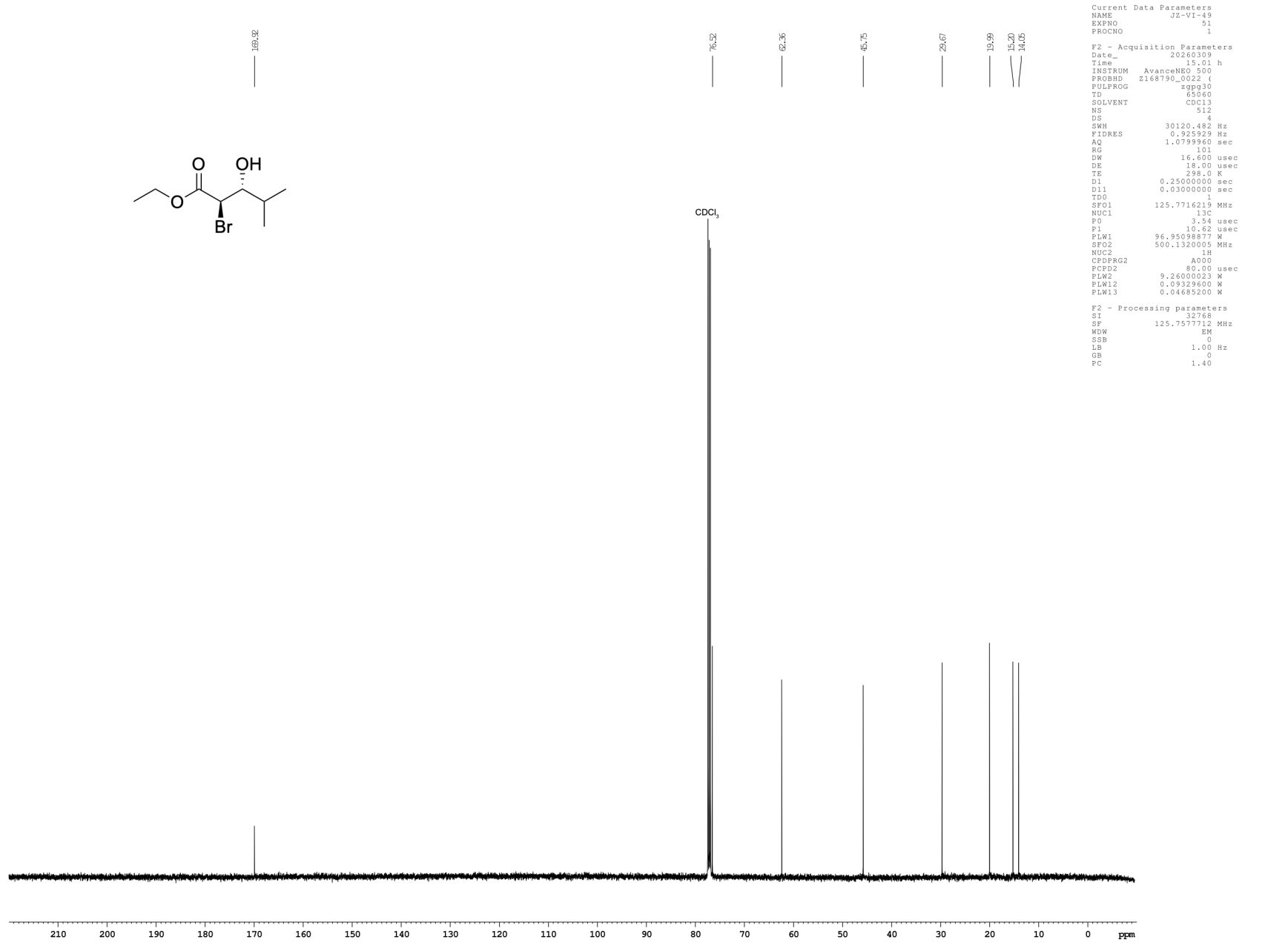


```
Current Data Parameters
NAME                  JZ-VI-49
EXPNO                       51
PROCNO                       1

F2 - Acquisition Parameters
Date_               20260309
Time                    15.01 h
INSTRUM   AvanceNEO 500
PROBHD   Z168790_0022 (
PULPROG                 zgpg30
TD                       65060
SOLVENT                  CDCl3
NS                         512
DS                           4
SWH                  30120.482 Hz
FIDRES               0.925929 Hz
AQ                   1.0799960 sec
RG                         101
DW                      16.600 usec
DE                      18.00 usec
TE                      298.0 K
D1                   0.25000000 sec
D11                  0.03000000 sec
TD0                          1
SFO1               125.7716219 MHz
NUC1                        13C
P0                       3.54 usec
P1                      10.62 usec
PLW1                96.95098877 W
SFO2               500.1320005 MHz
NUC2                         1H
CPDPRG2                  A000
PCPD2                   80.00 usec
PLW2                 9.26000023 W
PLW12                0.09329600 W
PLW13                0.04685200 W

F2 - Processing parameters
SI                       32768
SF                 125.7577712 MHz
WDW                         EM
SSB                          0
LB                        1.00 Hz
GB                           0
PC                        1.40
```

^{1}H NMR of ethyl (2*S*,3*R*)-2-azido-3-((*tert*-butyldimethylsilyl)oxy)-4-methylpentanoate in $CDCl_3$ at 500 MHz and 298 K

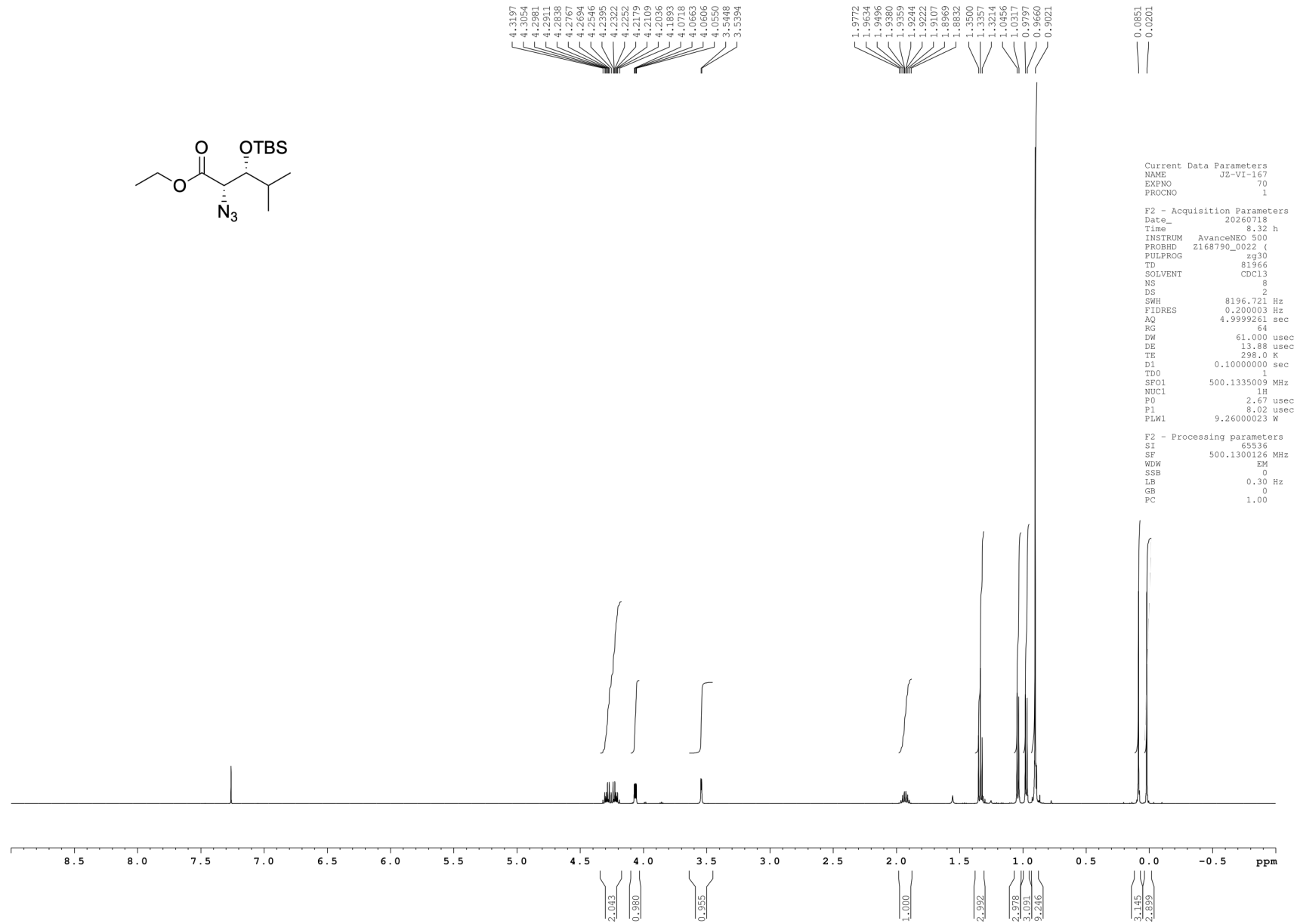

^{13}C NMR of ethyl (2*S*,3*R*)-2-azido-3-((*tert*-butyldimethylsilyl)oxy)-4-methylpentanoate in $CDCl_3$ at 500 MHz and 298 K

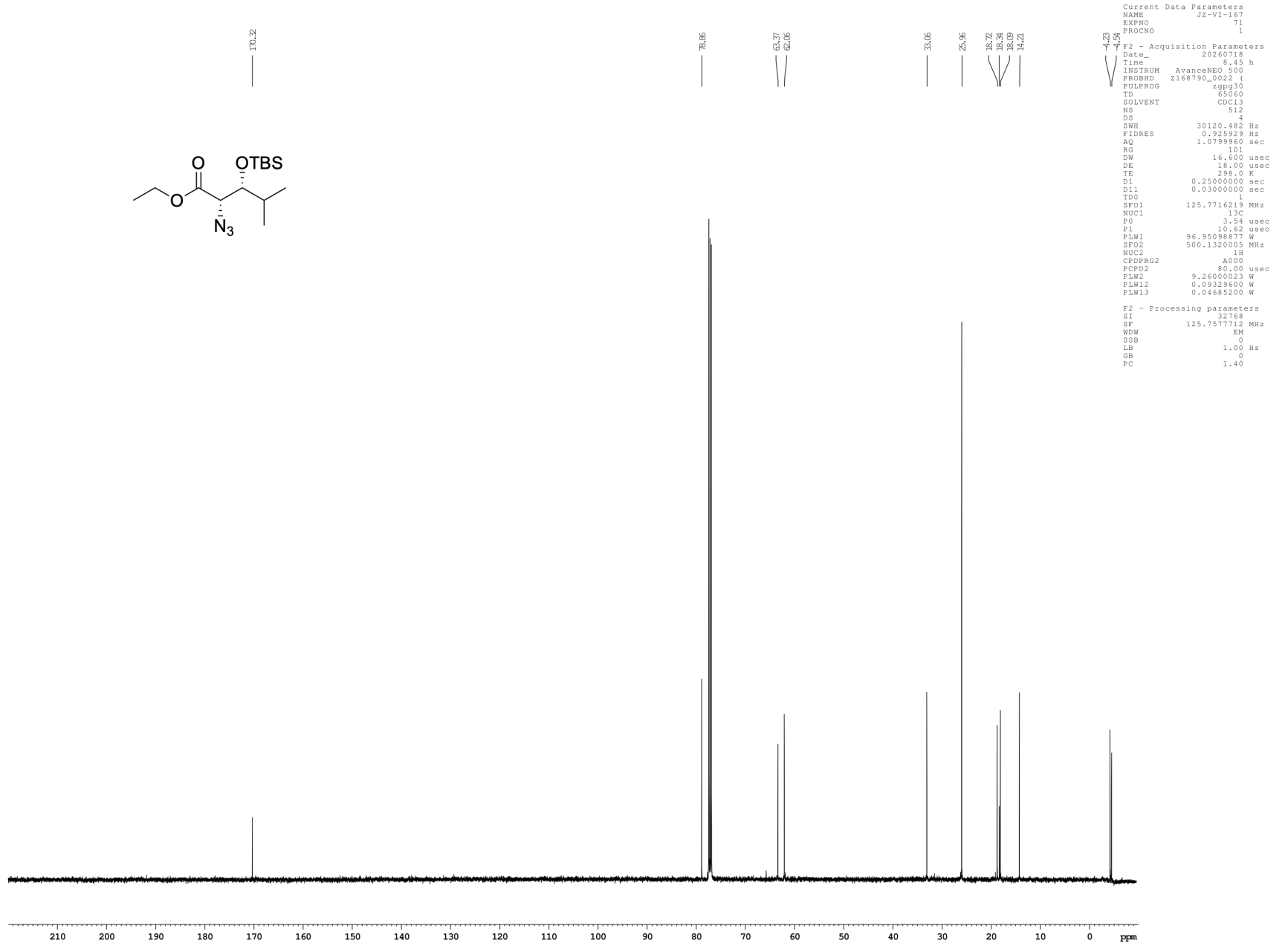

^{1}H NMR of ethyl (2*S*,3*R*)-2-azido-3-hydroxy-4-methylpentanoate in $CDCl_3$ at 500 MHz and 298 K

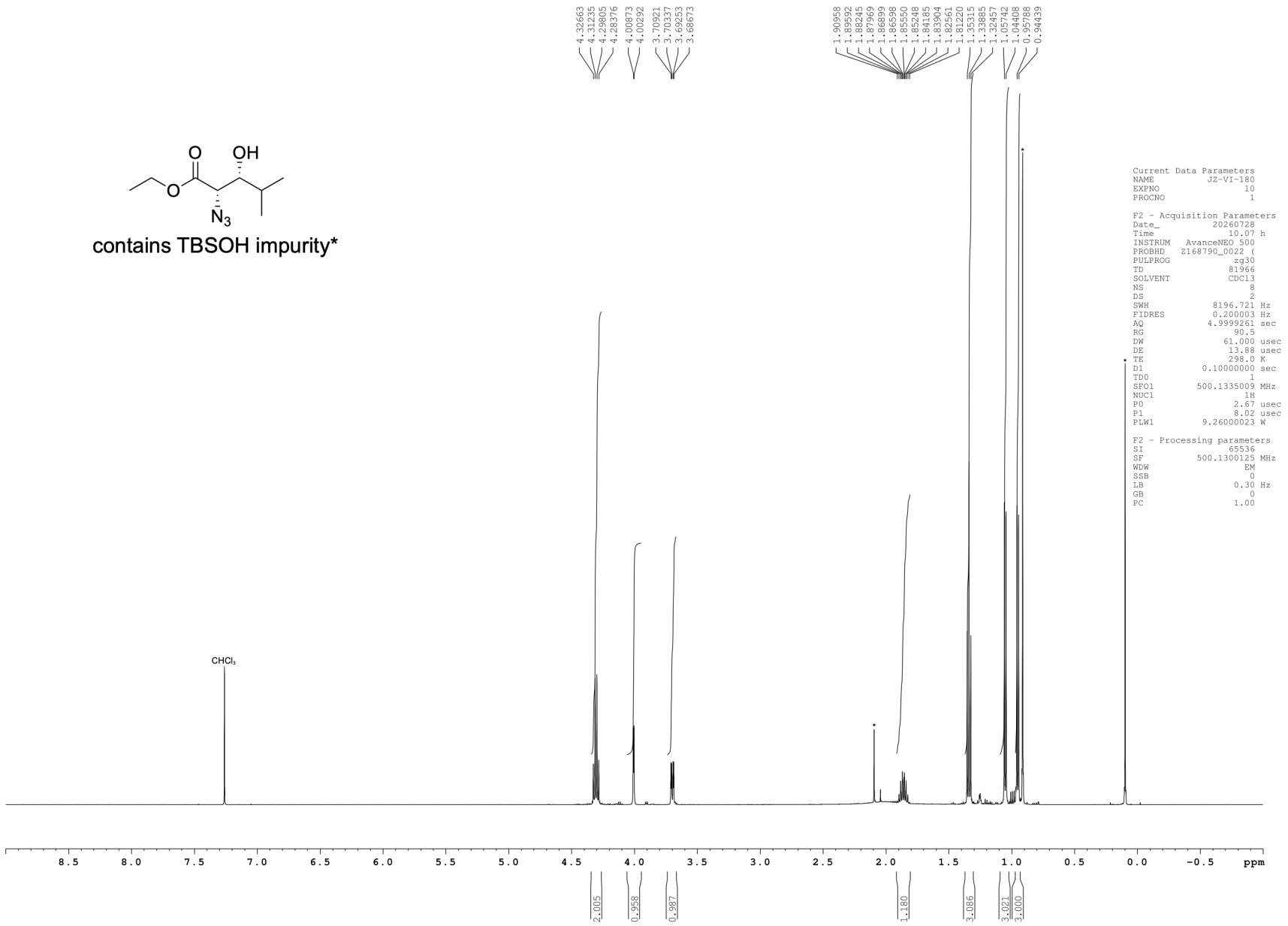

^{13}C NMR of ethyl (2*S*,3*R*)-2-azido-3-hydroxy-4-methylpentanoate in $CDCl_3$ at 500 MHz and 298 K

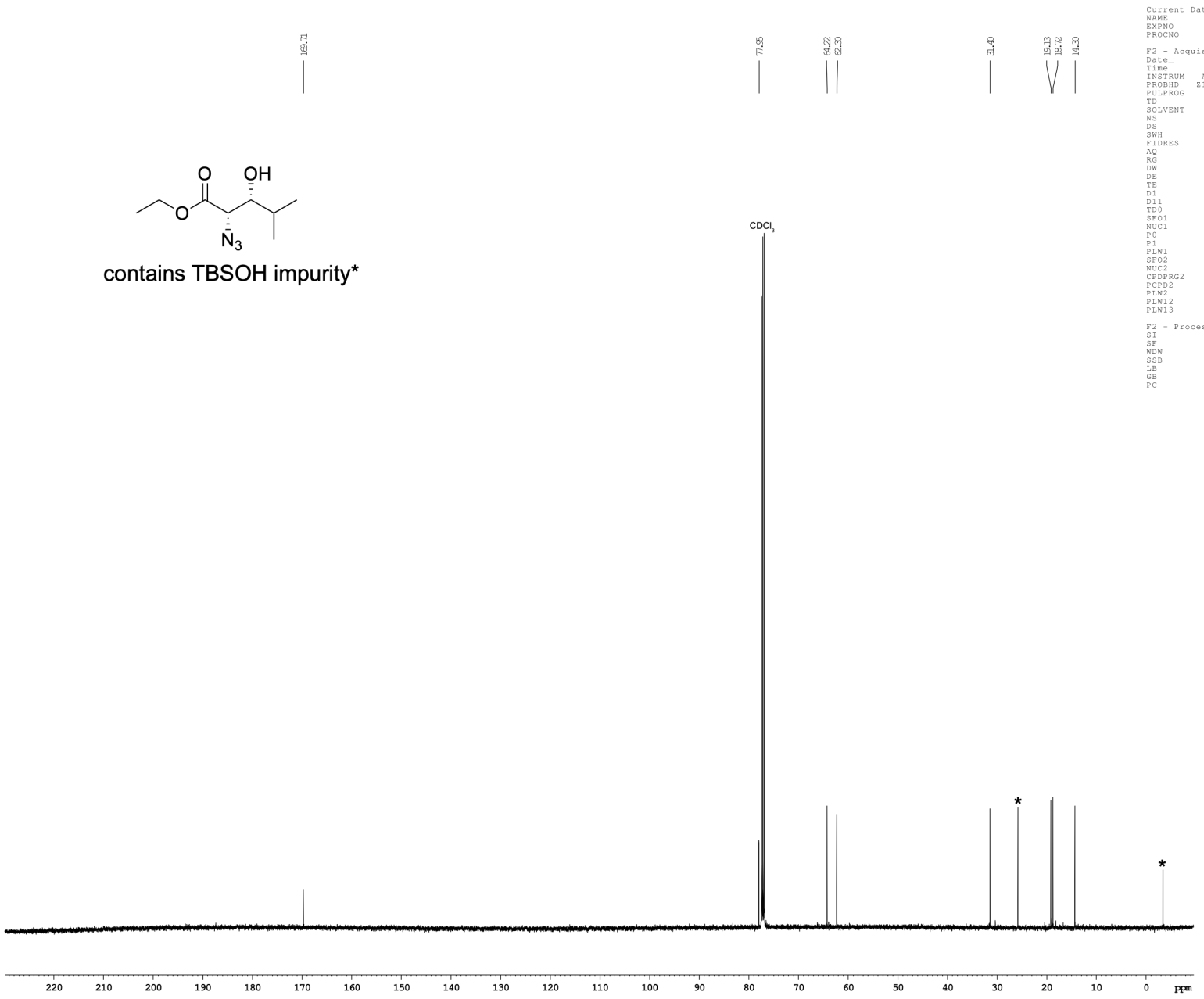

^{1}H NMR spectrum of (2*S*,3*R*)-2-azido-3-hydroxy-4-methylpentanoic acid in DMSO-d_6 at 500 MHz and 298 K

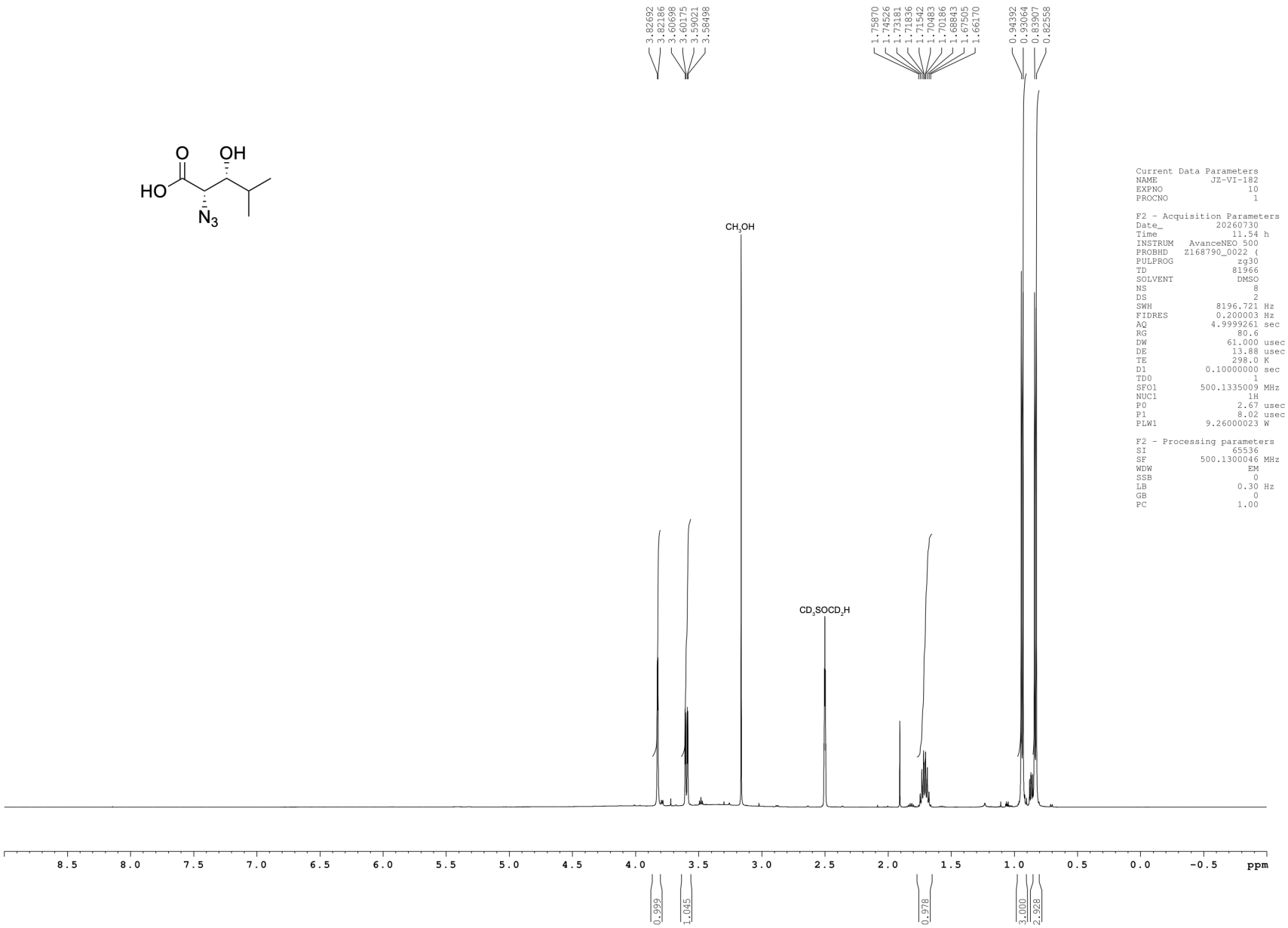

^{13}C NMR spectrum of (2*S*,3*R*)-2-azido-3-hydroxy-4-methylpentanoic acid in DMSO-d_6 at 500 MHz and 298 K

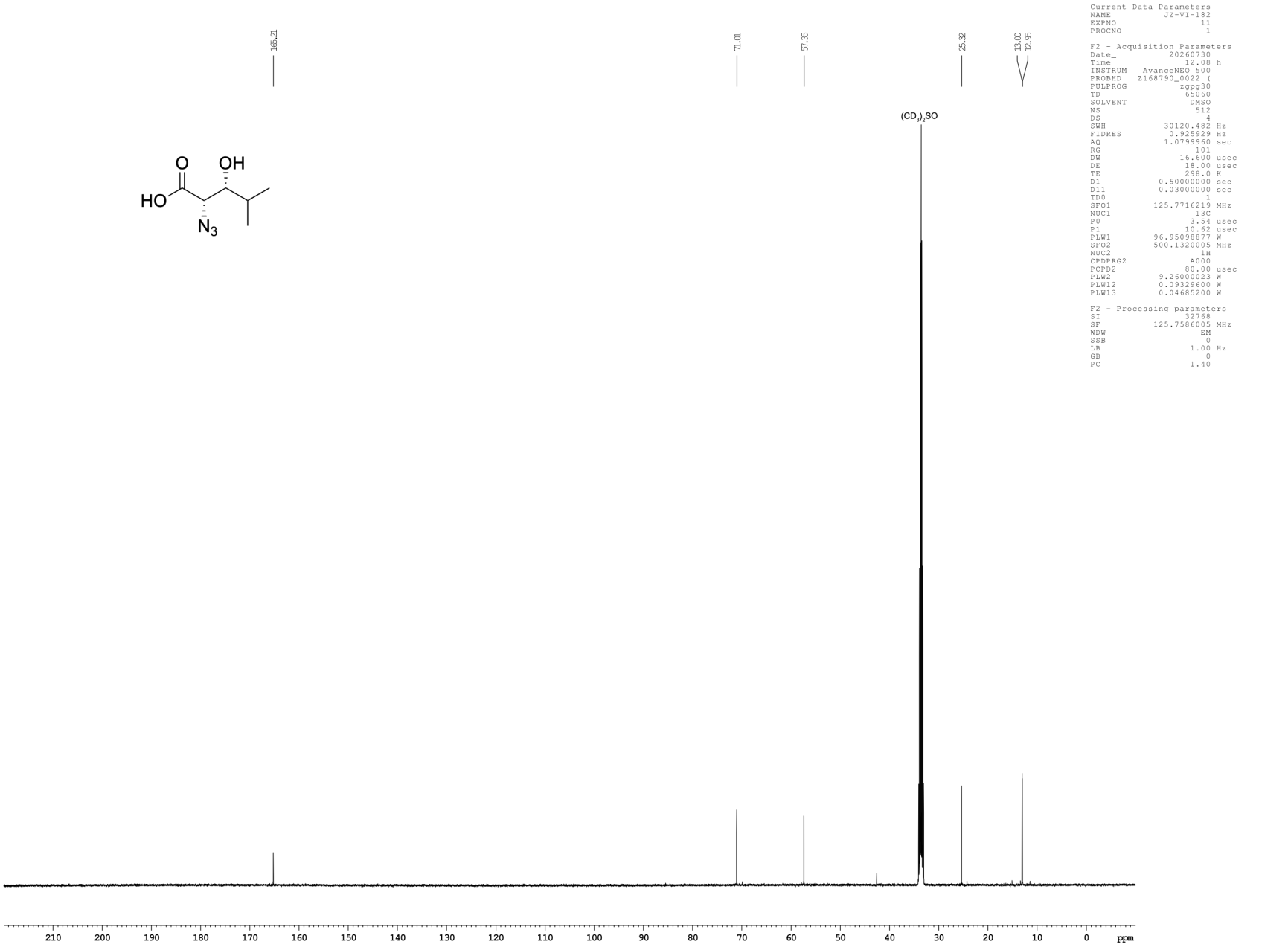

^{1}H NMR spectrum of (2*S*,3*R*)-2-((((9*H*-fluoren-9-yl)methoxy)carbonyl)amino)-3-hydroxy-4-methylpentanoic acid in DMSO-d_6 at 500 MHz and 298 K

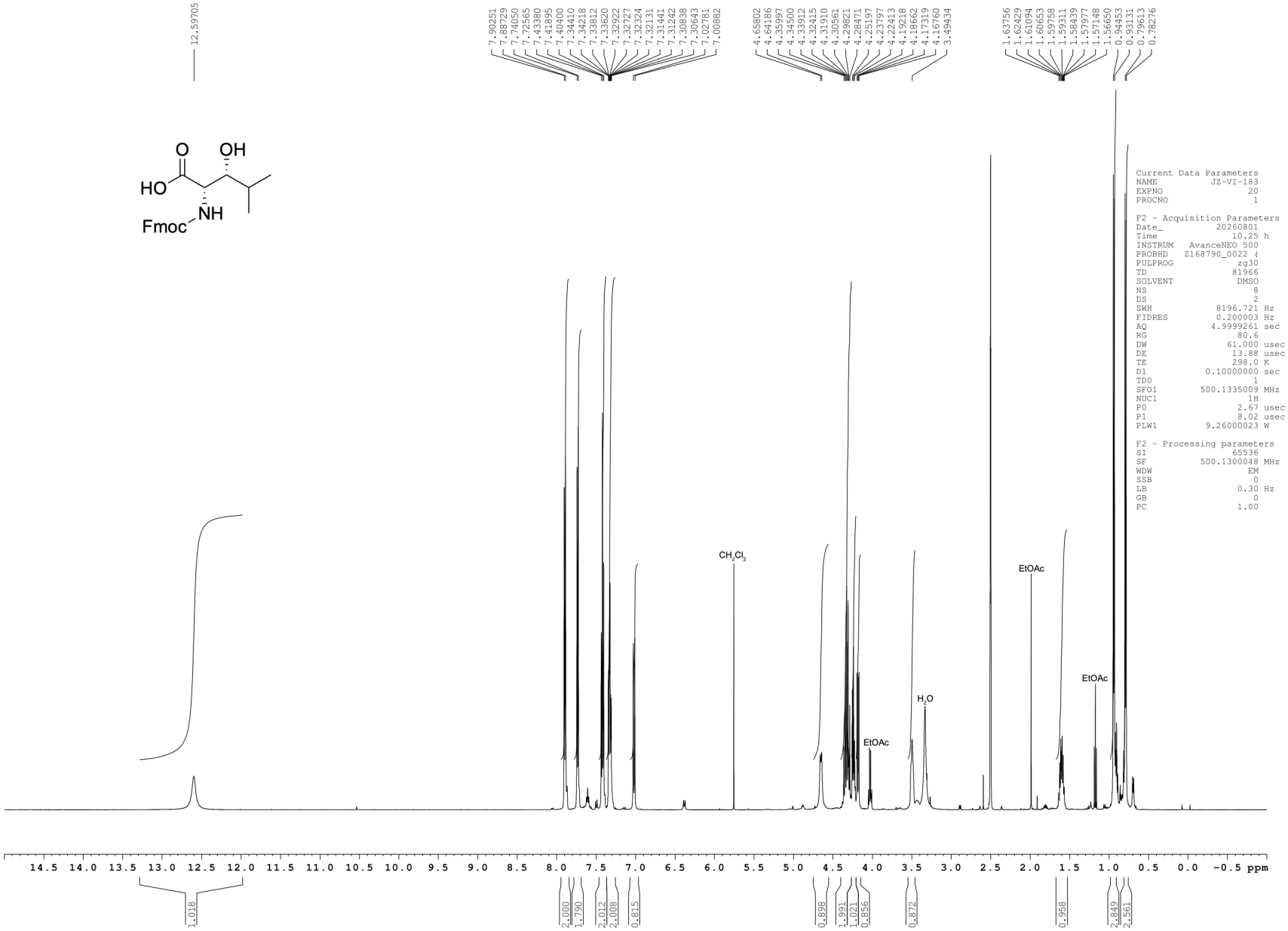

^{13}C NMR spectrum of (2S,3*R*)-2-((((9H-fluoren-9-yl)methoxy)carbonyl)amino)-3-hydroxy-4-methylpentanoic acid in DMSO-d_6 at 500 MHz and 298 K

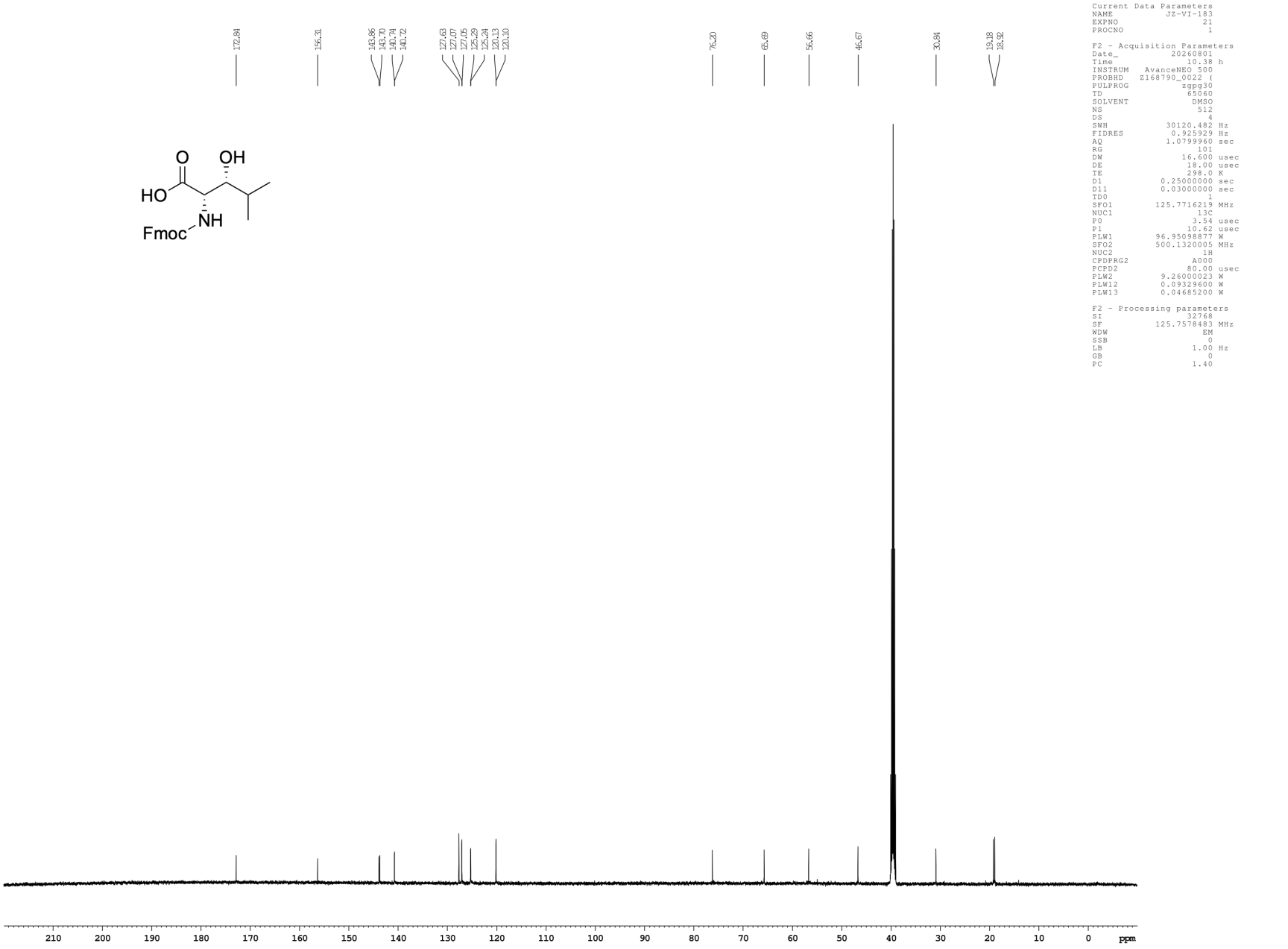

[1]H NMR spectrum of (2*S*,3*R*)-2-(((((9*H*-fluoren-9-yl)methoxy)carbonyl)amino)-3-((*tert*-butyldimethylsilyl)oxy)-4-methylpentanoic acid in DMSO-d_6 at 500 MHz and 298 K

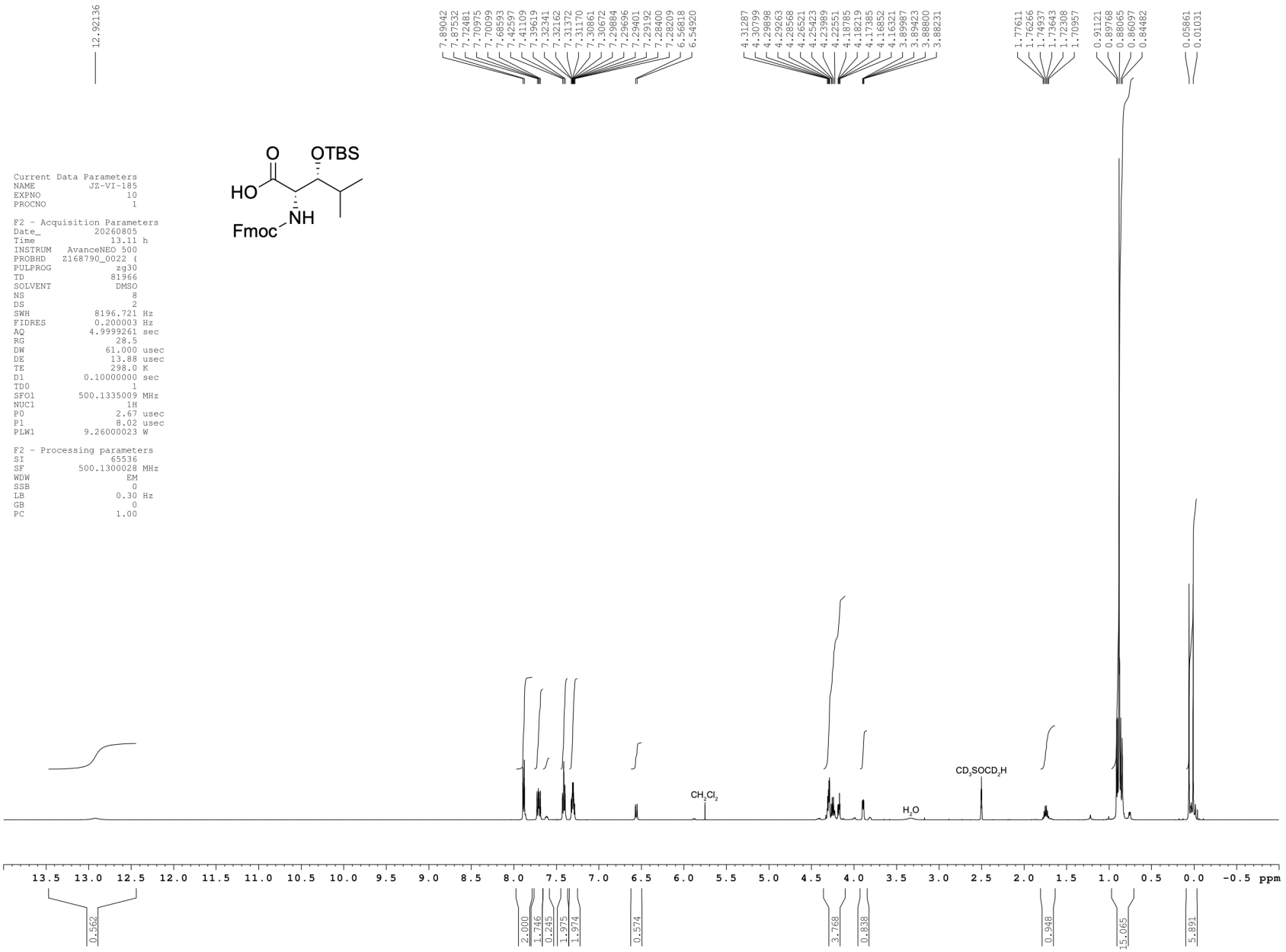

^{13}C NMR spectrum of (2*S*,3*R*)-2-((((9*H*-fluoren-9-yl)methoxy)carbonyl)amino)-3-((*tert*-butyldimethylsilyl)oxy)-4-methylpentanoic acid in DMSO-d_6 at 500 MHz and 298 K

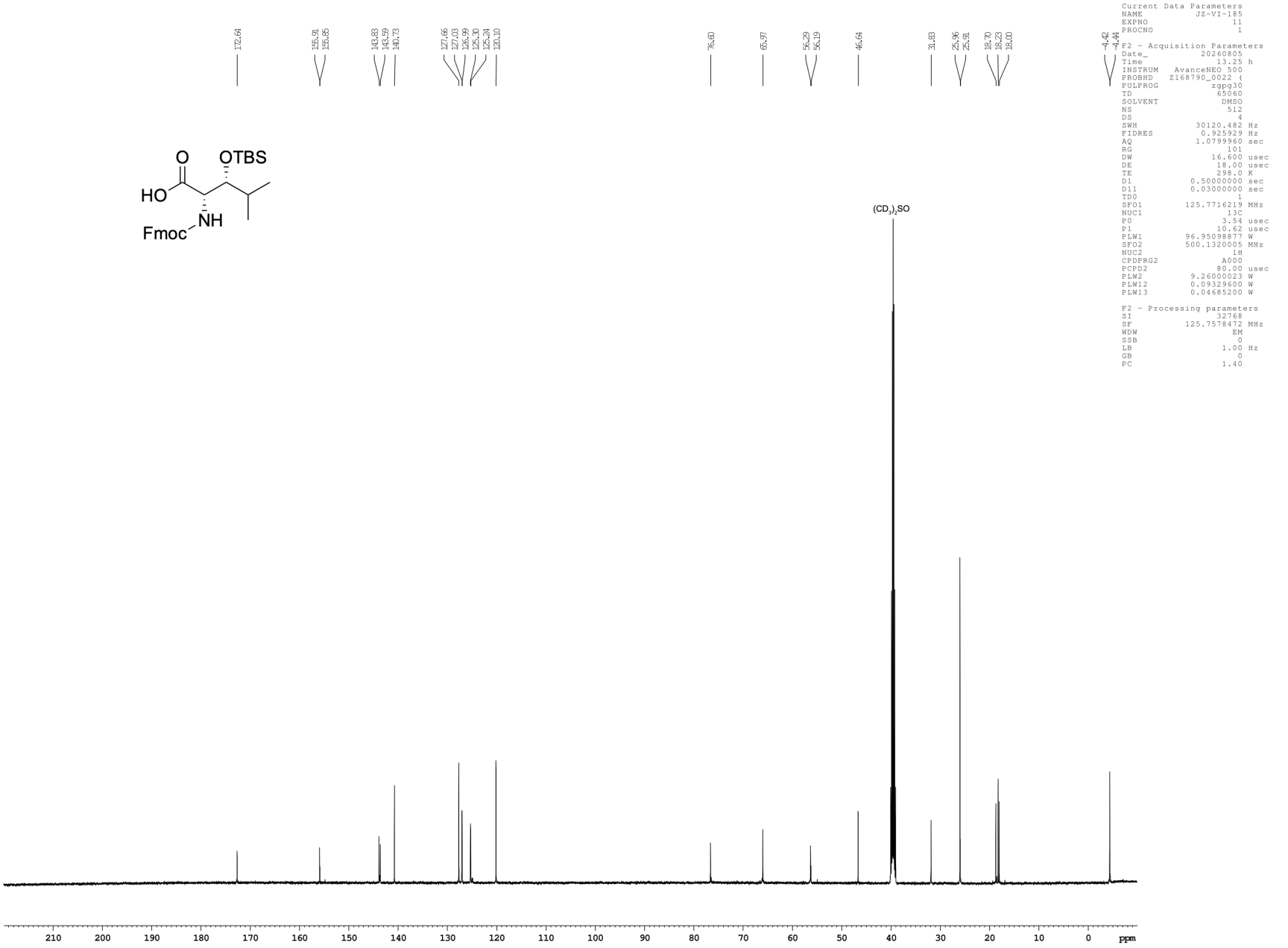


```
Current Data Parameters
NAME                  JZ-VI-185
EXPNO                        11
PROCNO                        1

F2 - Acquisition Parameters
Date_                 20260805
Time                     13.25 h
INSTRUM          AvanceNEO 500
PROBHD           Z168790_0022 (
PULPROG                zgpg30
TD                      65060
SOLVENT                  DMSO
NS                         512
DS                           4
SWH                30120.482 Hz
FIDRES              0.925929 Hz
AQ                  1.0799960 sec
RG                         101
DW                    16.600 usec
DE                    18.00 usec
TE                    298.0 K
D1                  0.50000000 sec
D11                 0.03000000 sec
TD0                          1
SFO1               125.7716219 MHz
NUC1                        13C
P0                     3.54 usec
P1                    10.62 usec
PLW1               96.95098877 W
SFO2               500.1320005 MHz
NUC2                         1H
CPDPRG2                  A000
PCPD2                 80.00 usec
PLW2                9.26000023 W
PLW12               0.09329600 W
PLW13               0.04685200 W

F2 - Processing parameters
SI                        32768
SF                 125.7578472 MHz
WDW                          EM
SSB                           0
LB                     1.00 Hz
GB                            0
PC                     1.40
```

^{1}H NMR spectrum of (*Z*)-N^{2}-(((9*H*-fluoren-9-yl)methoxy)carbonyl)-N^{ω},$N^{\omega'}$-bis((benzyloxy)carbonyl)-*D*-arginine in DMSO-d_6 at 500 MHz and 298 K

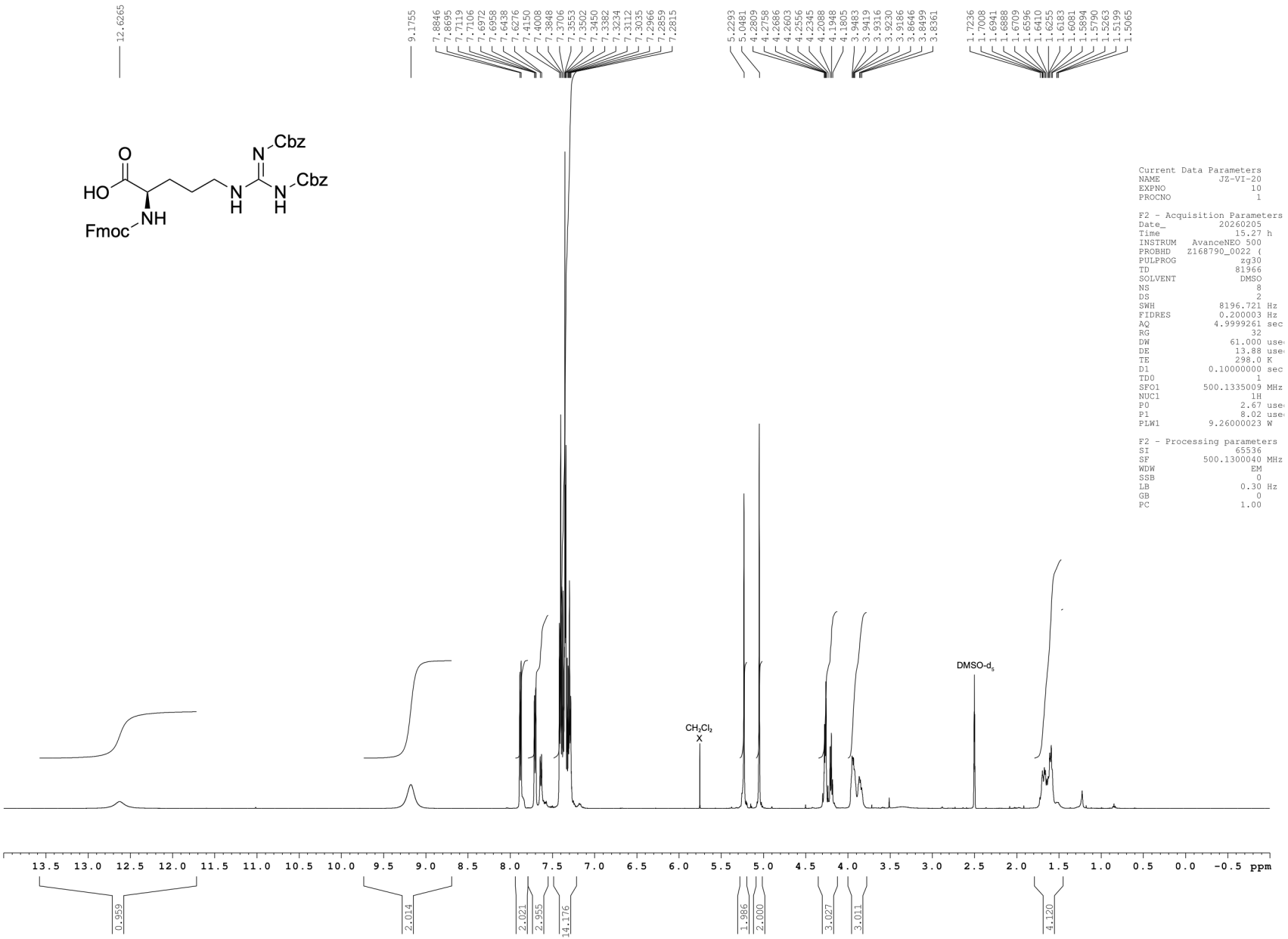

Current Data Parameters
NAME JZ-VI-20
EXPNO 10
PROCNO 1

F2 - Acquisition Parameters
Date_ 20260205
Time 15.27 h
INSTRUM AvanceNEO 500
PROBHD Z168790_0022 (
PULPROG zg30
TD 81966
SOLVENT DMSO
NS 8
DS 2
SWH 8196.721 Hz
FIDRES 0.200003 Hz
AQ 4.9999261 sec
RG 32
DW 61.000 use
DE 13.88 use
TE 298.0 K
D1 0.10000000 sec
TD0 1
SFO1 500.1335009 MHz
NUC1 1H
P0 2.67 use
P1 8.02 use
PLW1 9.26000023 W

F2 - Processing parameters
SI 65536
SF 500.1300040 MHz
WDW EM
SSB 0
LB 0.30 Hz
GB 0
PC 1.00

^{13}C NMR spectrum of (*Z*)-N^2-(((9*H*-fluoren-9-yl)methoxy)carbonyl)-N^{ω},$N^{\omega'}$-bis((benzyloxy)carbonyl)-*D*-arginine in DMSO-d_6 at 500 MHz and 298 K

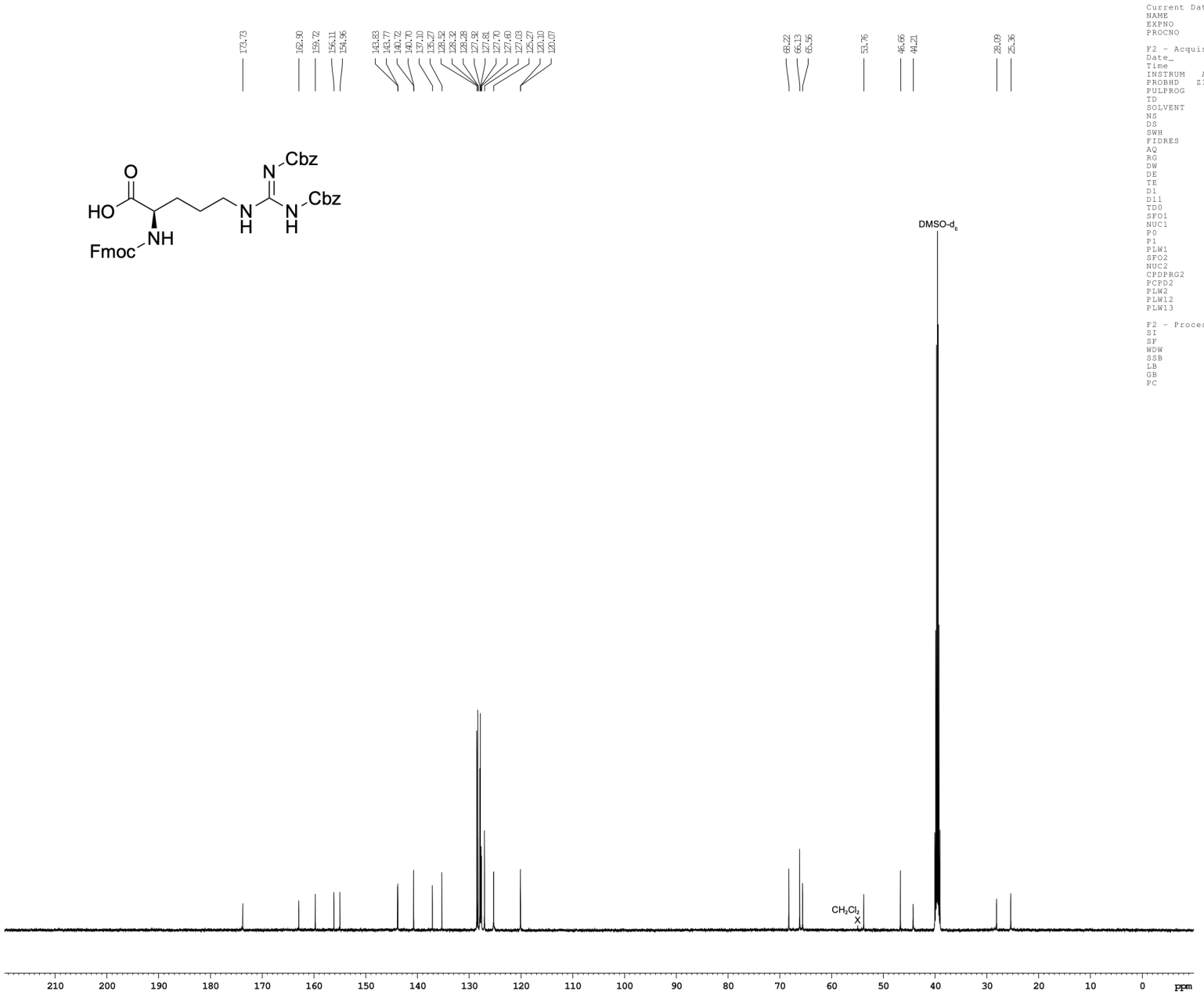

^{1}H NMR spectrum of crude (2*S*,3*R*)-2-azido-3-(4-(benzyloxy)phenyl)-3-hydroxy-1-((*S*)-4-phenyl-2-thioxothiazolidin-3-yl)propan-1-one in $CDCl_3$ at 500 MHz and 298 K

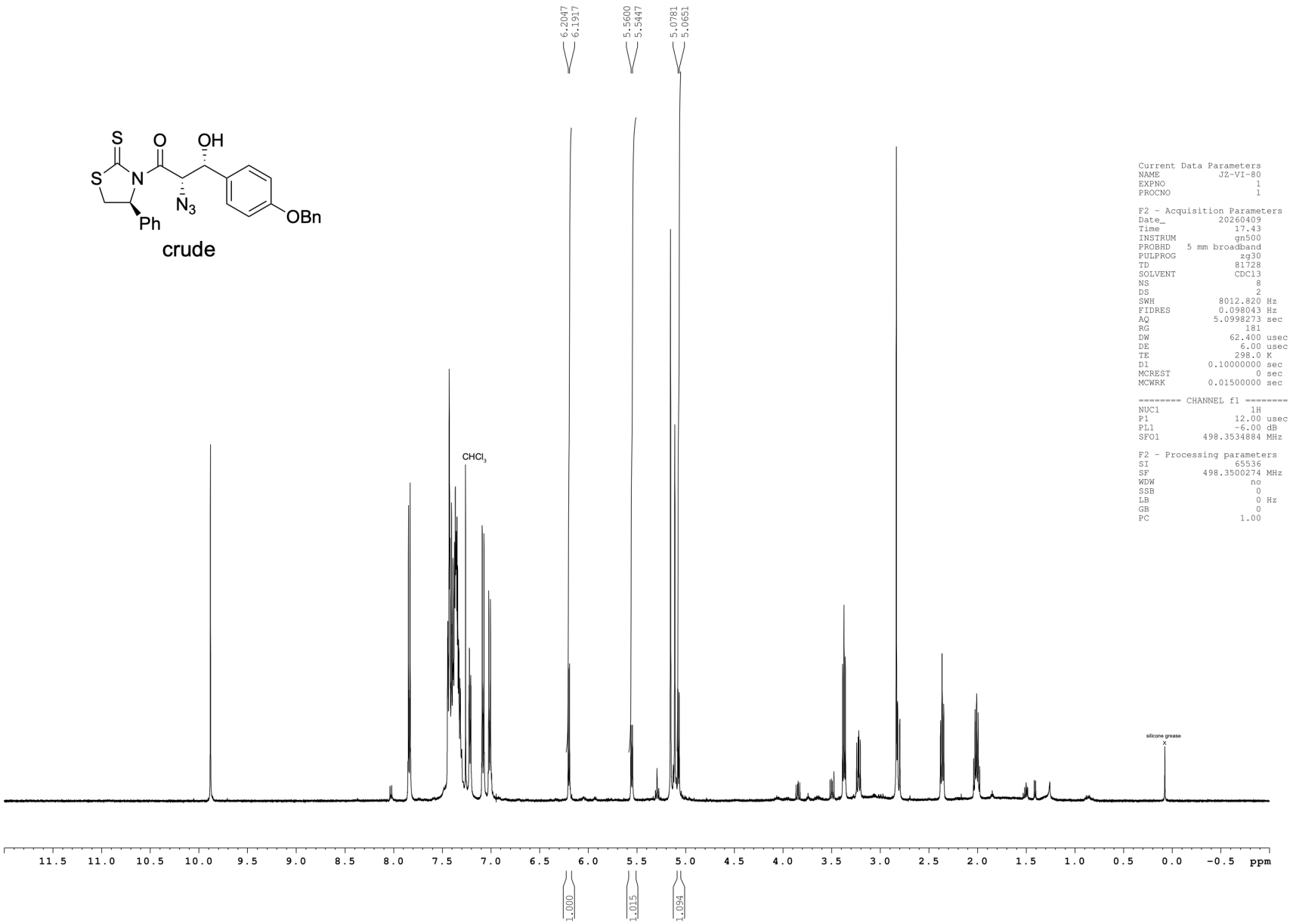

^{1}H NMR spectrum of methyl (2*S*,3*R*)-2-azido-3-(4-(benzyloxy)phenyl)-3-hydroxypropanoate in $CDCl_3$ at 500 MHz and 298 K

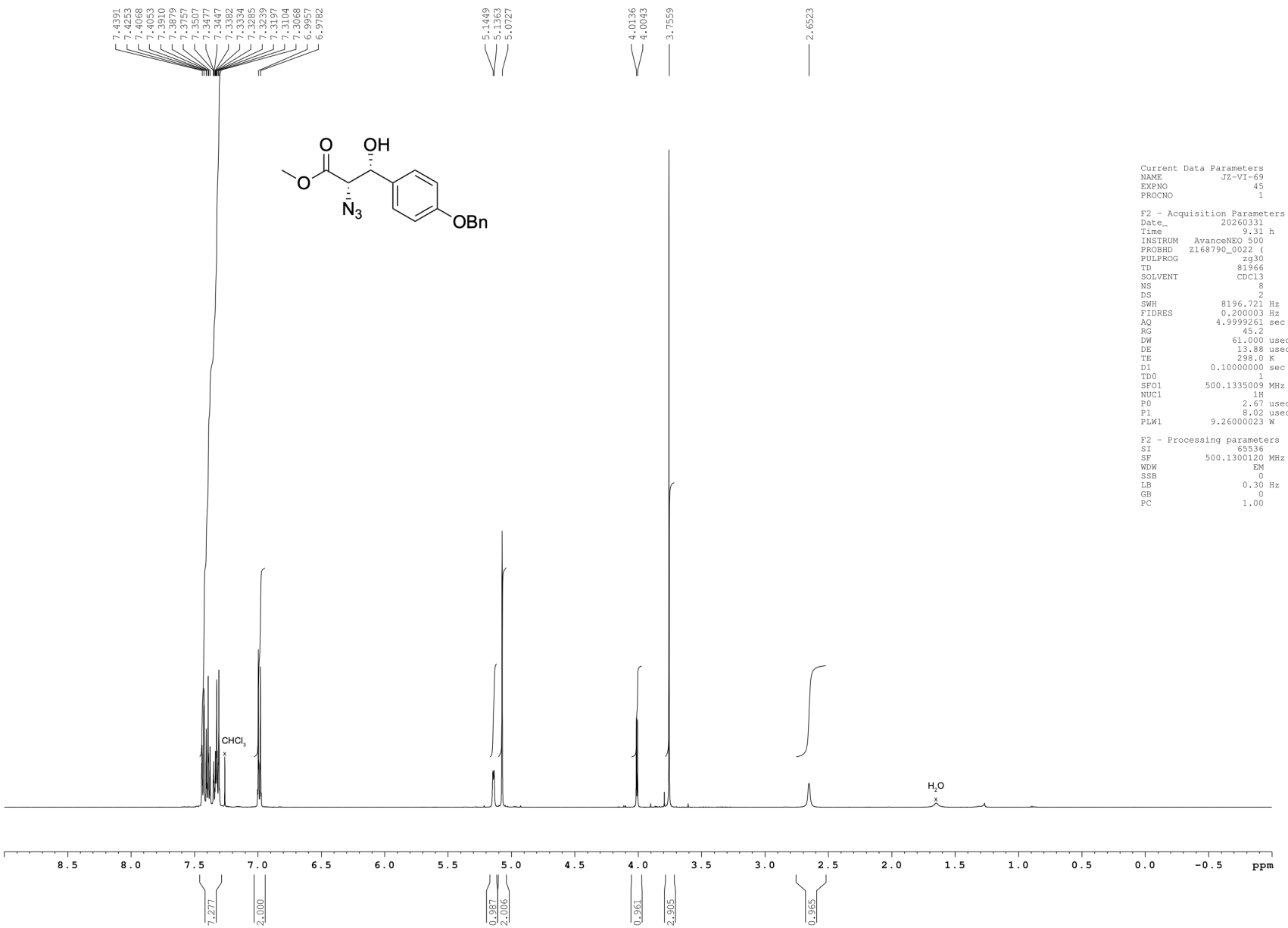


```
Current Data Parameters
NAME                  JZ-VI-69
EXPNO                       45
PROCNO                       1

F2 - Acquisition Parameters
Date_                 20260331
Time                      9.31 h
INSTRUM       AvanceNEO 500
PROBHD        Z168790_0022 (
PULPROG                   zg30
TD                       81966
SOLVENT                  CDCl3
NS                           8
DS                           2
SWH                   8196.721 Hz
FIDRES                0.200003 Hz
AQ                    4.9999261 sec
RG                         45.2
DW                       61.000 usec
DE                       13.88 usec
TE                       298.0 K
D1                    0.10000000 sec
TD0                          1
SFO1                500.1335009 MHz
NUC1                        1H
P0                        2.67 usec
P1                        8.02 usec
PLW1                 9.26000023 W

F2 - Processing parameters
SI                       65536
SF                  500.1300120 MHz
WDW                         EM
SSB                          0
LB                        0.30 Hz
GB                           0
PC                        1.00
```

^{13}C NMR spectrum of methyl (2*S*,3*R*)-2-azido-3-(4-(benzyloxy)phenyl)-3-hydroxypropanoate in $CDCl_3$ at 500 MHz and 298 K

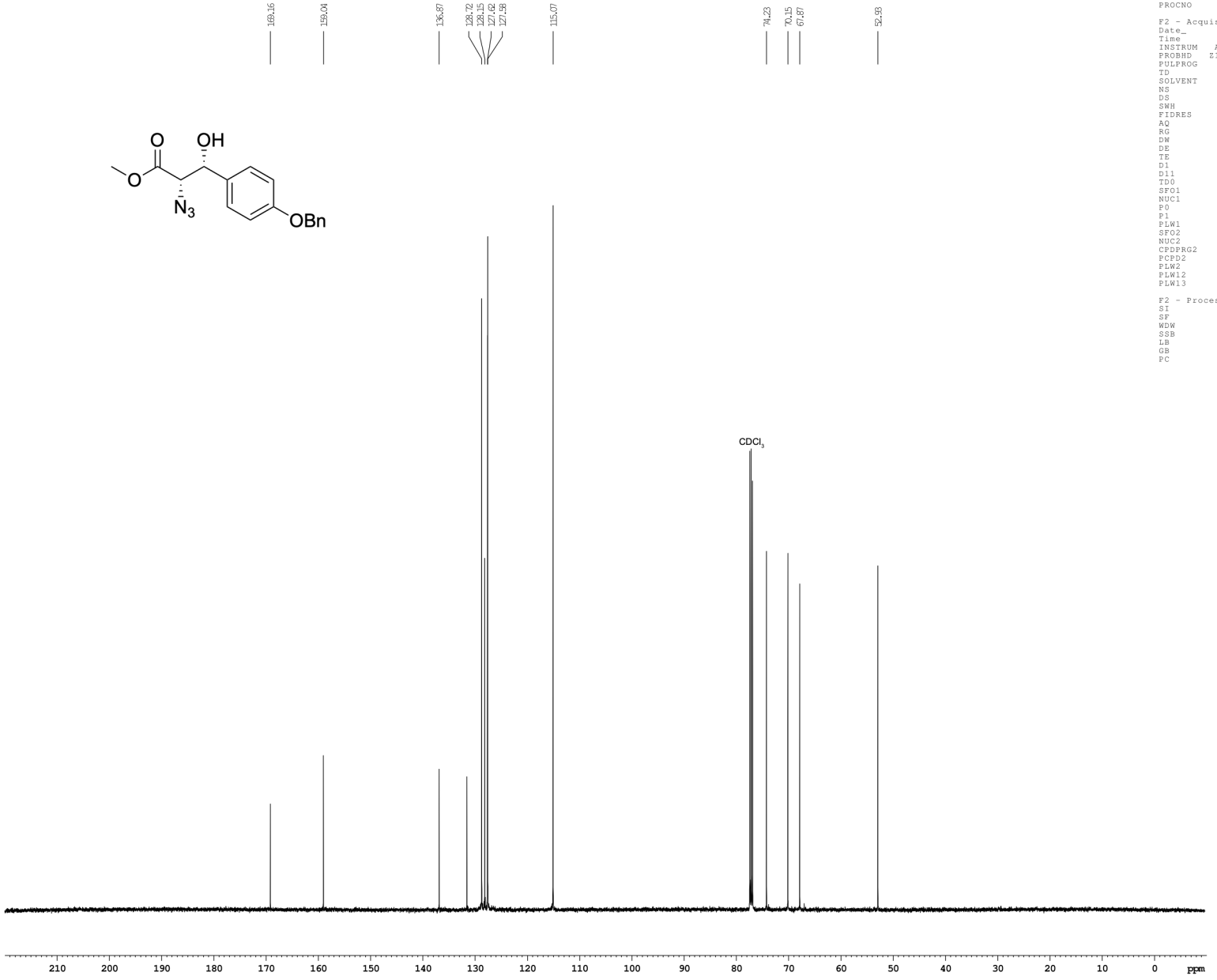


```
Current Data Parameters
NAME                  JZ-VI-69
EXPNO                       46
PROCNO                       1

F2 - Acquisition Parameters
Date_               20260331
Time                    9.44 h
INSTRUM   AvanceNEO 500
PROBHD    Z168790_0022 (
PULPROG                 zgpg30
TD                       65060
SOLVENT                  CDCl3
NS                         512
DS                           4
SWH                 30120.482 Hz
FIDRES              0.925929 Hz
AQ                  1.0799960 sec
RG                         101
DW                    16.600 usec
DE                    18.00 usec
TE                    298.0 K
D1                  0.25000000 sec
D11                 0.03000000 sec
TD0                          1
SFO1              125.7716219 MHz
NUC1                       13C
P0                     3.54 usec
P1                    10.62 usec
PLW1              96.95098877 W
SFO2              500.1320005 MHz
NUC2                       1H
CPDPRG2                 A000
PCPD2                 80.00 usec
PLW2               9.26000023 W
PLW12              0.09329600 W
PLW13              0.04685200 W

F2 - Processing parameters
SI                       32768
SF                125.7577774 MHz
WDW                         EM
SSB                          0
LB                    1.00 Hz
GB                           0
PC                    1.40
```

^{1}H NMR spectrum of methyl (2*S*,3*R*)-2-amino-3-(4-(benzyloxy)phenyl)-3-hydroxypropanoate in CD_3OD at 500 MHz and 298 K

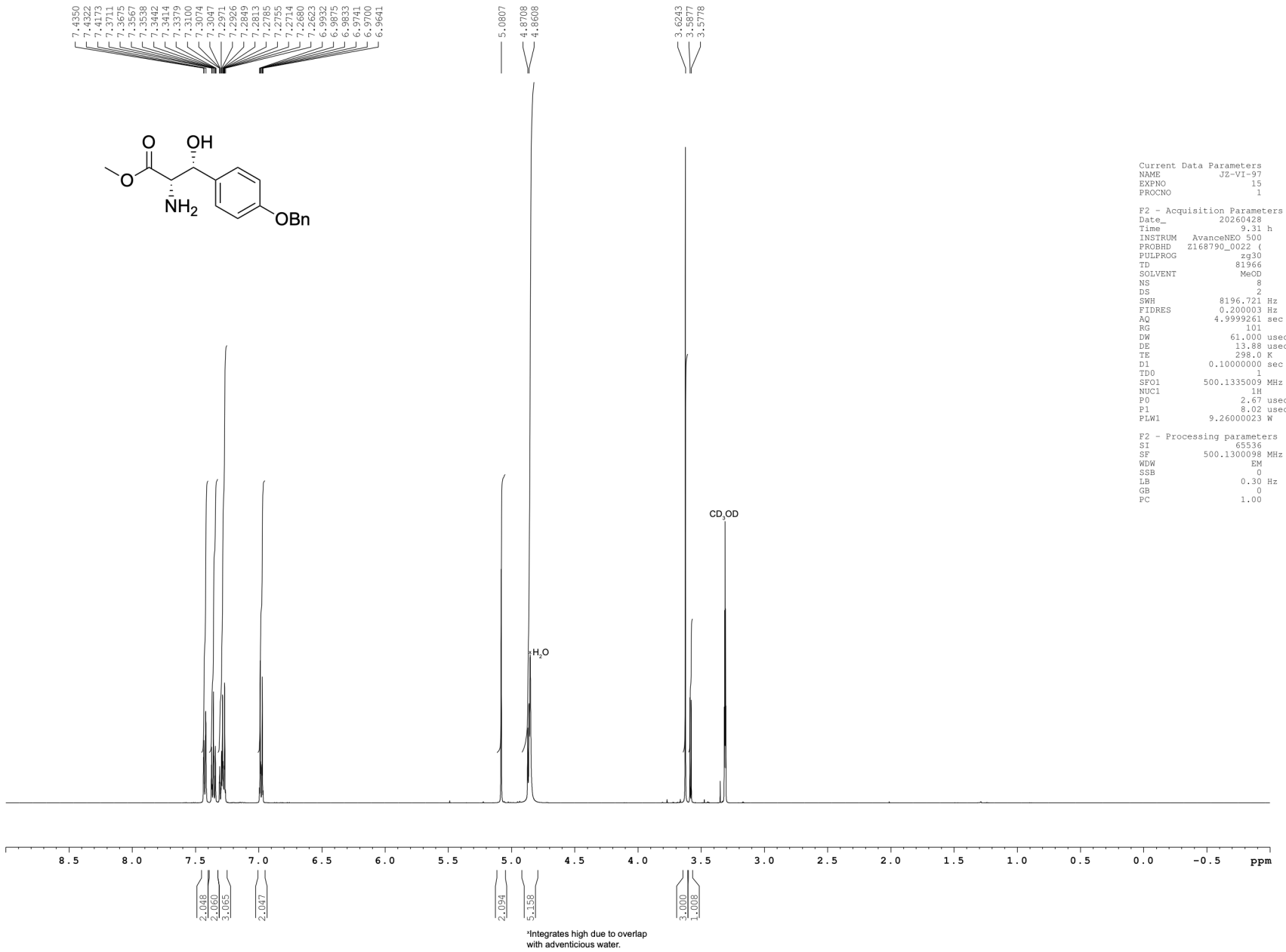

[a]Integrates high due to overlap with adventicious water.

^{13}C NMR spectrum of (2*S*,3*R*)-2-amino-3-(4-(benzyloxy)phenyl)-3-hydroxypropanoate in CD_3OD at 500 MHz and 298 K

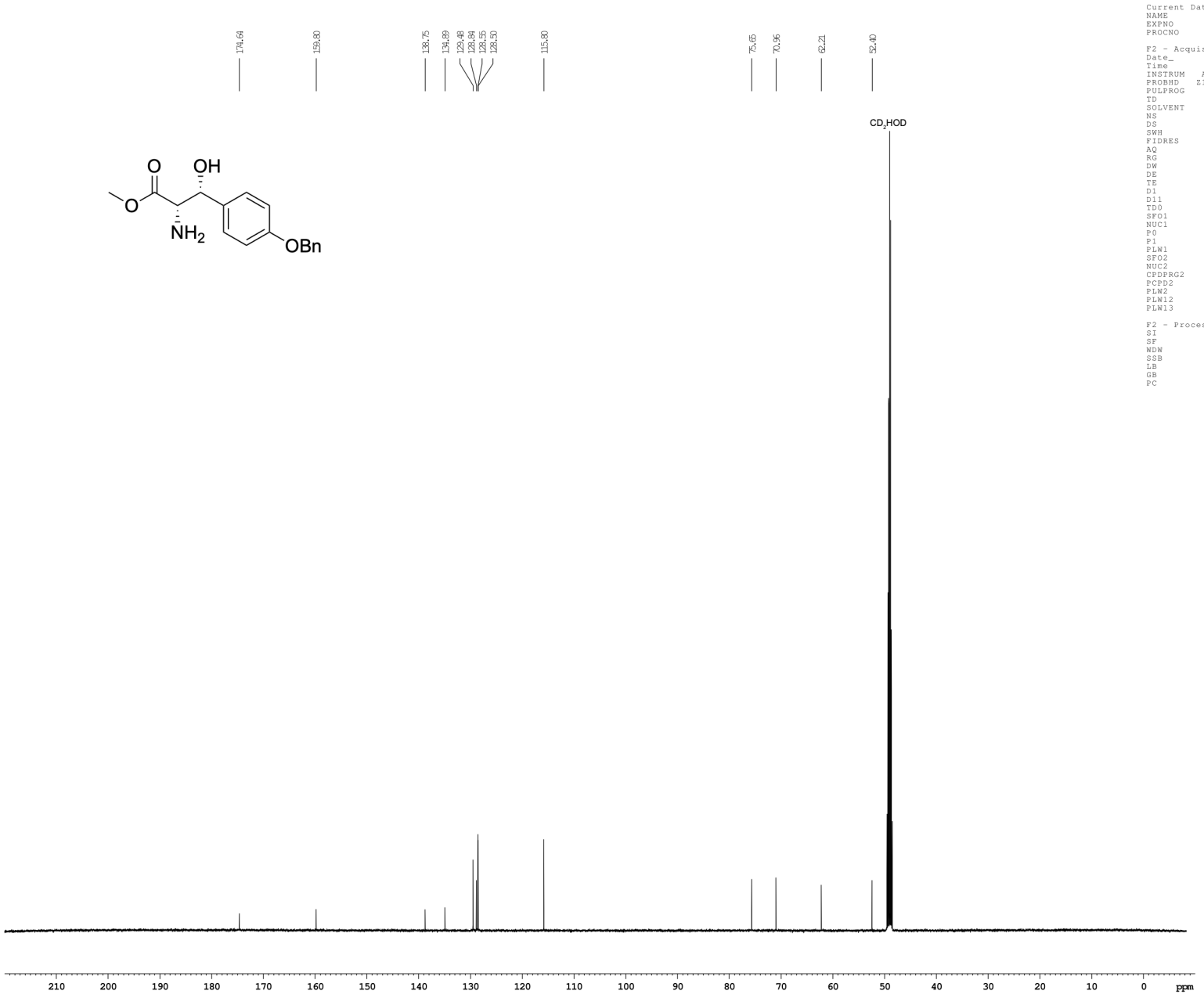


```
Current Data Parameters
NAME                  JZ-VI-97
EXPNO                       16
PROCNO                       1

F2 - Acquisition Parameters
Date_               20260428
Time                    9.44 h
INSTRUM   AvanceNEO 500
PROBHD   Z168790_0022 (
PULPROG                 zgpg30
TD                       65060
SOLVENT                   MeOD
NS                         512
DS                           4
SWH                 30120.482 Hz
FIDRES              0.925929 Hz
AQ                  1.0799960 sec
RG                         101
DW                    16.600 usec
DE                    18.00 usec
TE                    298.0 K
D1                  0.25000000 sec
D11                 0.03000000 sec
TD0                          1
SFO1               125.7716219 MHz
NUC1                        13C
P0                     3.54 usec
P1                    10.62 usec
PLW1               96.95098877 W
SFO2               500.1320005 MHz
NUC2                        1H
CPDPRG2                  A000
PCPD2                 80.00 usec
PLW2                9.26000023 W
PLW12               0.09329600 W
PLW13               0.04685200 W

F2 - Processing parameters
SI                       32768
SF                 125.7576125 MHz
WDW                         EM
SSB                          0
LB                    1.00 Hz
GB                           0
PC                    1.40
```

[1]H NMR spectrum of (2*S*,3*R*)-2-(((((9*H*-fluoren-9-yl)methoxy)carbonyl)amino)-3-(4-(benzyloxy)phenyl)-3-hydroxypropanoic acid in DMSO-d_6 at 500 MHz and 298 K

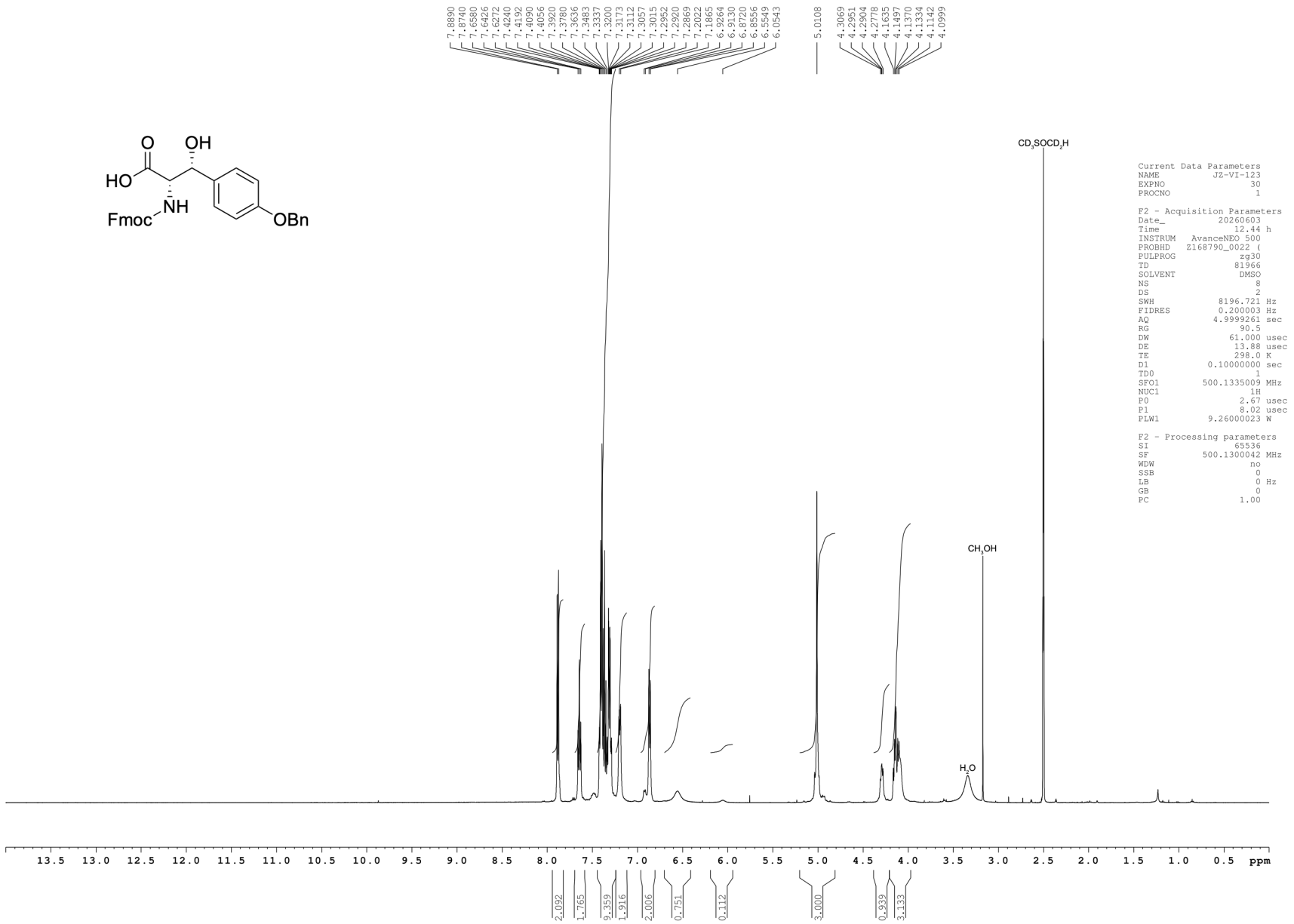

^{13}C NMR spectrum of (2*S*,3*R*)-2-(((((9*H*-fluoren-9-yl)methoxy)carbonyl)amino)-3-(4-(benzyloxy)phenyl)-3-hydroxypropanoic acid in DMSO-d_6 at 500 MHz and 298 K

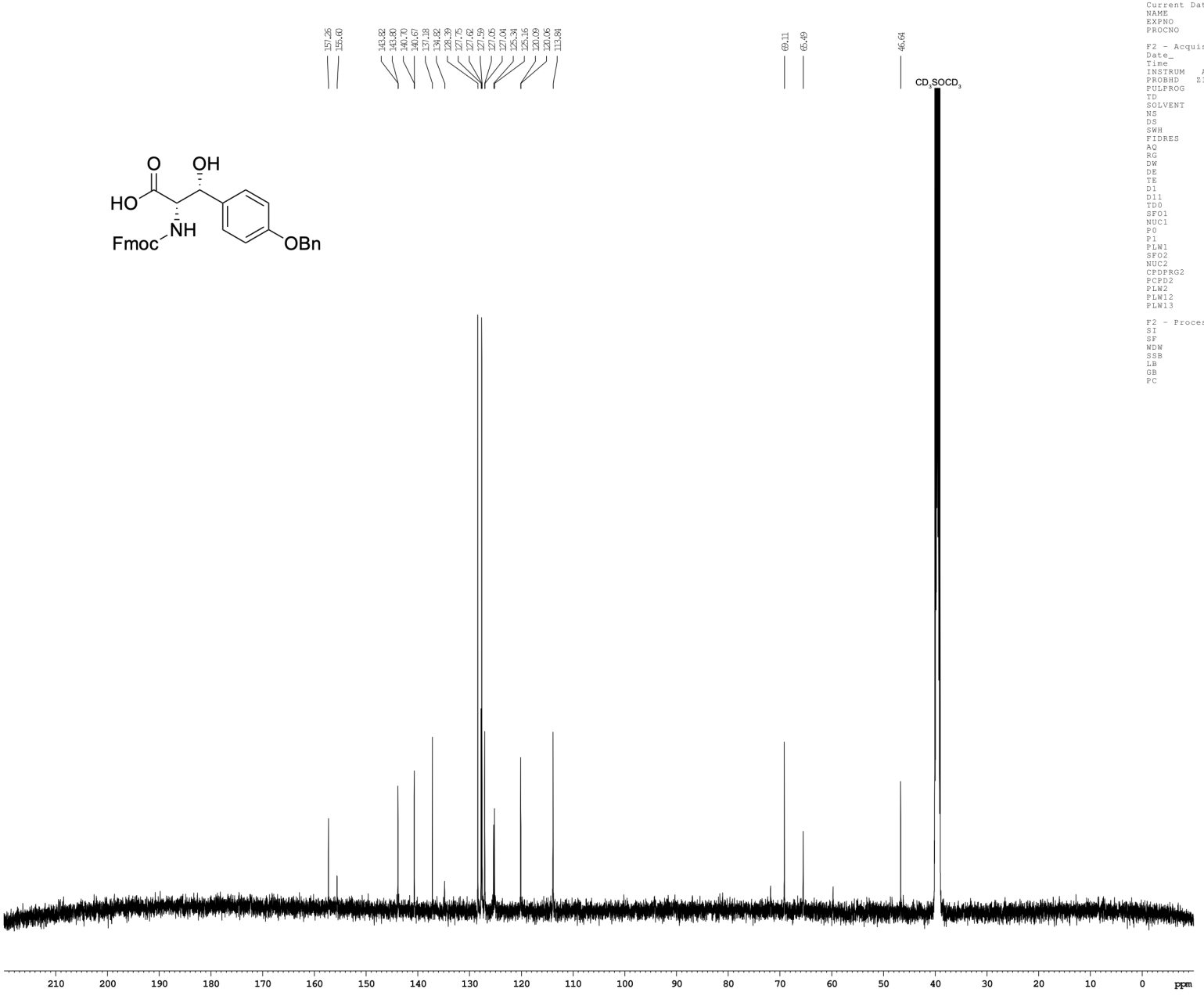


```
Current Data Parameters
NAME                  JZ-VI-123
EXPNO                        31
PROCNO                        1

F2 - Acquisition Parameters
Date_                 20260603
Time                     12.59 h
INSTRUM   AvanceNEO 500
PROBHD    Z168790_0022 (
PULPROG                 zgpg30
TD                       65060
SOLVENT                   DMSO
NS                         512
DS                           4
SWH                  30120.482 Hz
FIDRES                0.925929 Hz
AQ                   1.0799960 sec
RG                         101
DW                      16.600 usec
DE                      18.00 usec
TE                      298.0 K
D1                   0.50000000 sec
D11                  0.03000000 sec
TD0                          1
SFO1                125.7716219 MHz
NUC1                        13C
P0                       3.54 usec
P1                      10.62 usec
PLW1                96.95098877 W
SFO2                500.1320005 MHz
NUC2                        1H
CPDPRG2                   A000
PCPD2                   80.00 usec
PLW2                 9.26000023 W
PLW12                0.09329600 W
PLW13                0.04685200 W

F2 - Processing parameters
SI                         32768
SF                  125.7578484 MHz
WDW                          EM
SSB                           0
LB                         1.00 Hz
GB                            0
PC                         1.40
```

[1]H NMR spectrum of (2*S*,3*R*)-2-((((9*H*-fluoren-9-yl)methoxy)carbonyl)amino)-3-(4-(benzyloxy)phenyl)-3-(((*tert*-butyldimethylsilyl)oxy)propanoic acid in DMSO-d_6 at 500 MHz and 298 K

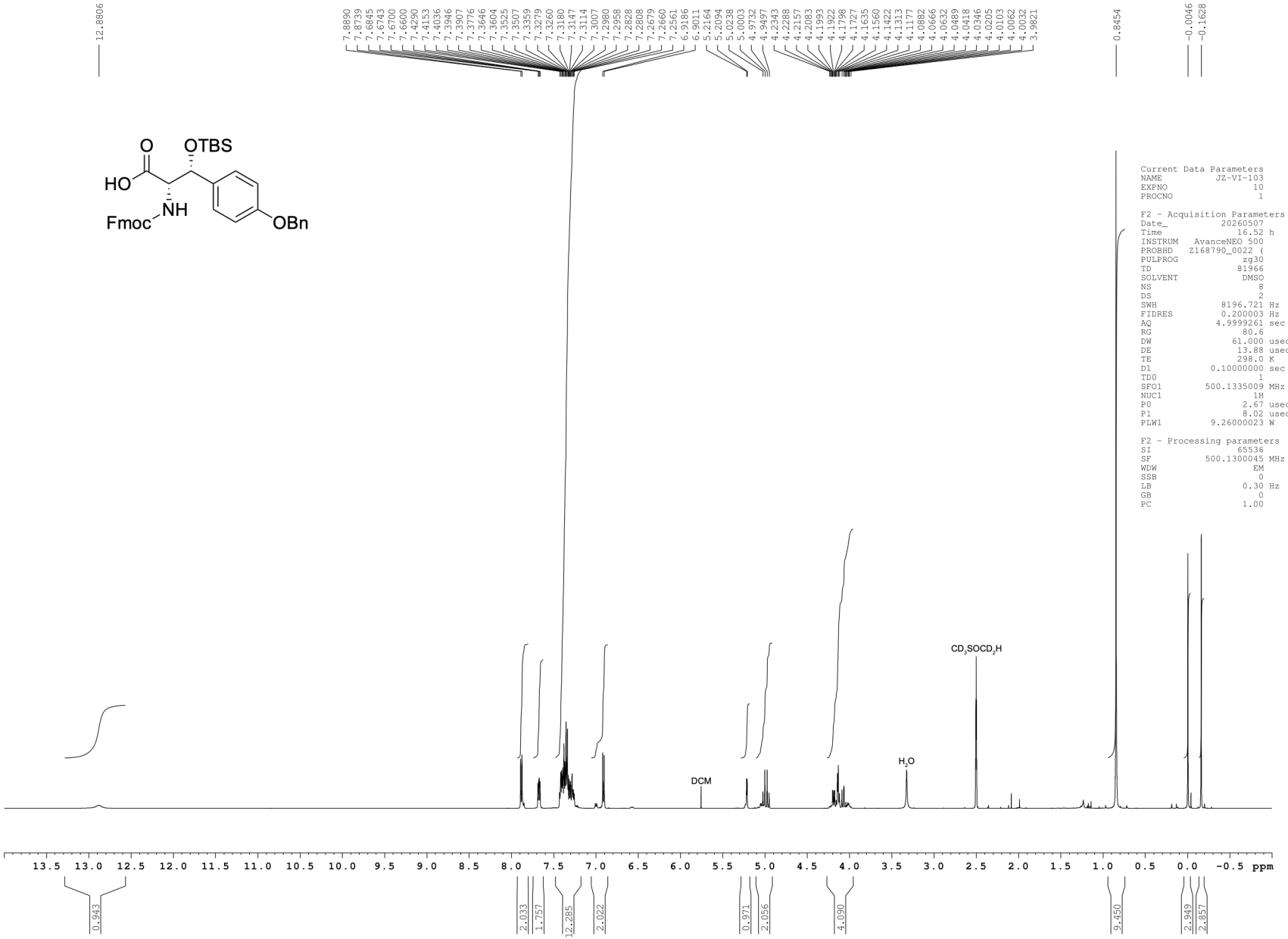

^{13}C NMR spectrum of (2*S*,3*R*)-2-((((9*H*-fluoren-9-yl)methoxy)carbonyl)amino)-3-(4-(benzyloxy)phenyl)-3-((*tert*-butyldimethylsilyl)oxy)propanoic acid in DMSO-d_6 at 500 MHz and 298 K

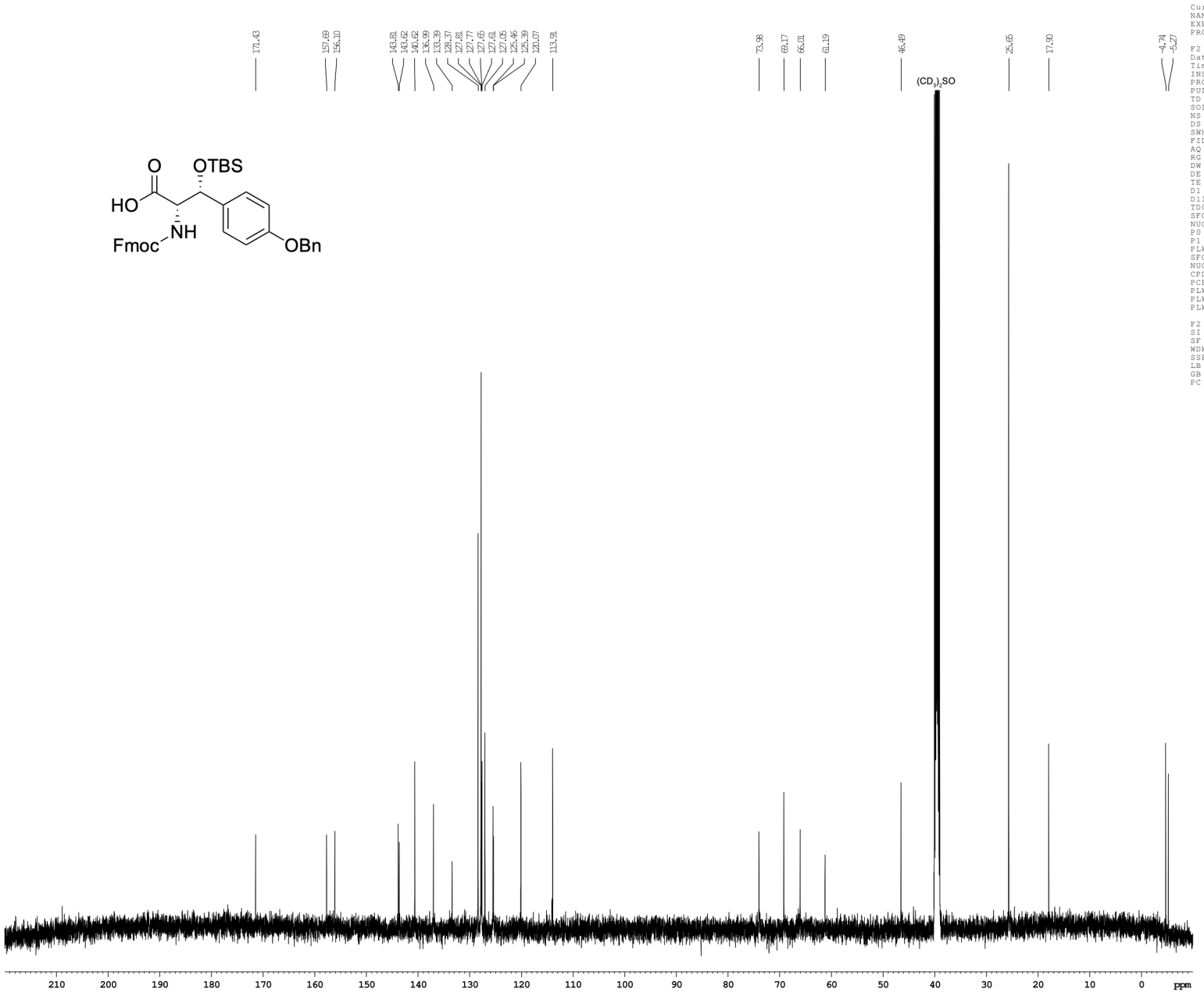

^{1}H NMR spectrum of natural hypeptin in DMSO-d_6 at 800 MHz and 298 K

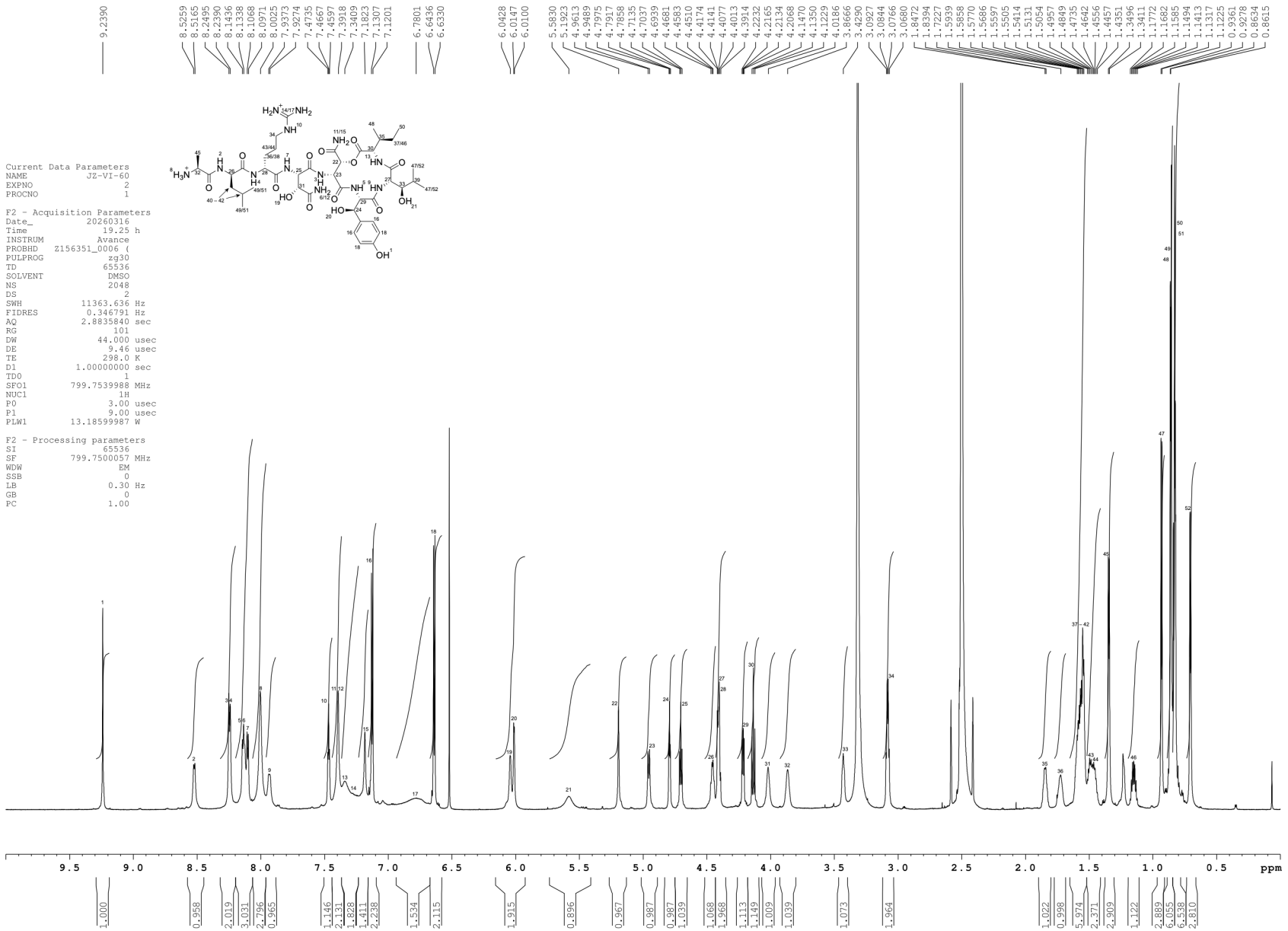

^{1}H NMR spectrum of natural hypeptin in DMSO-d_6 at 800 MHz and 298 K

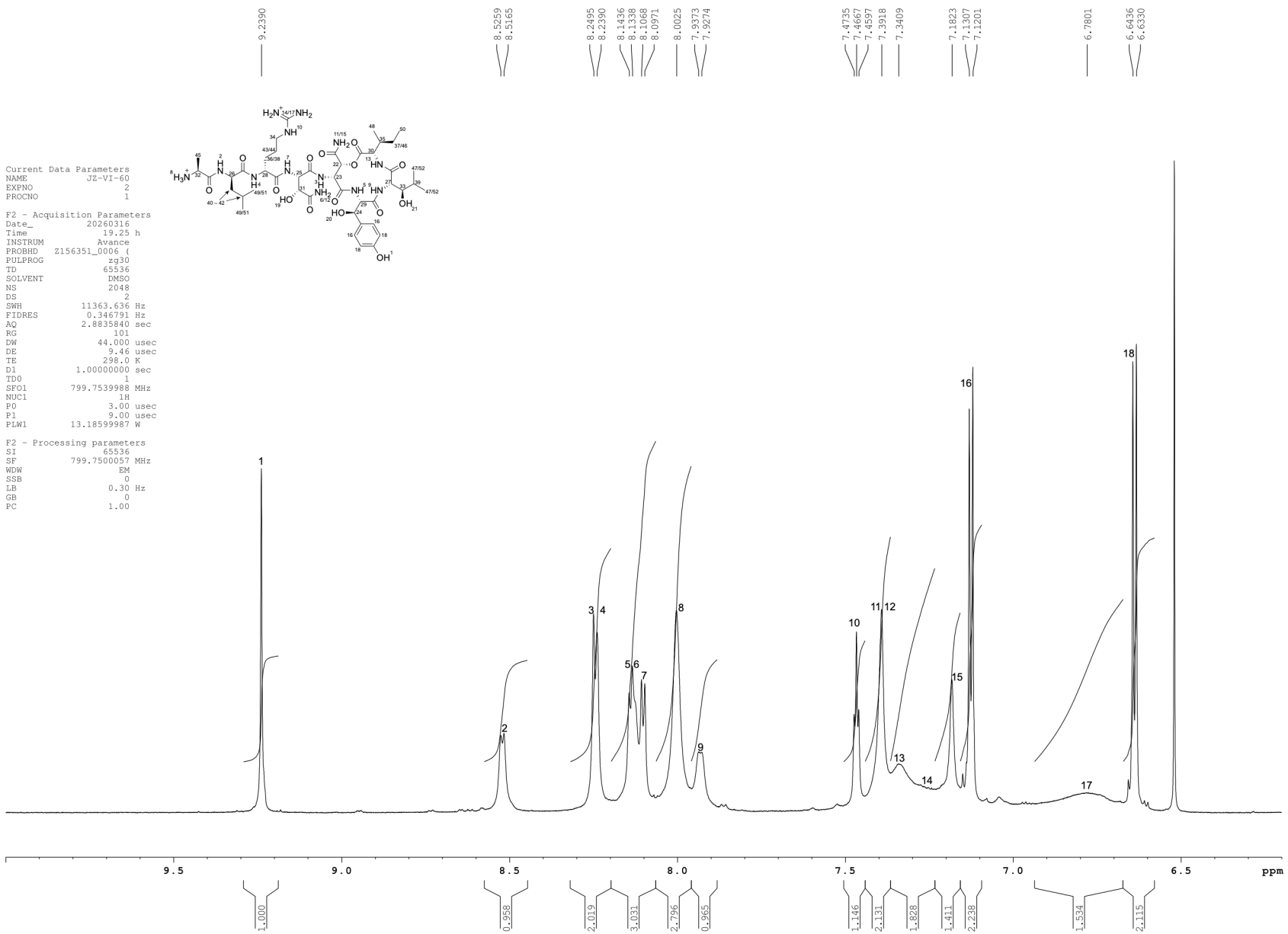

^{1}H NMR spectrum of natural hypeptin in DMSO-d_6 at 800 MHz and 298 K

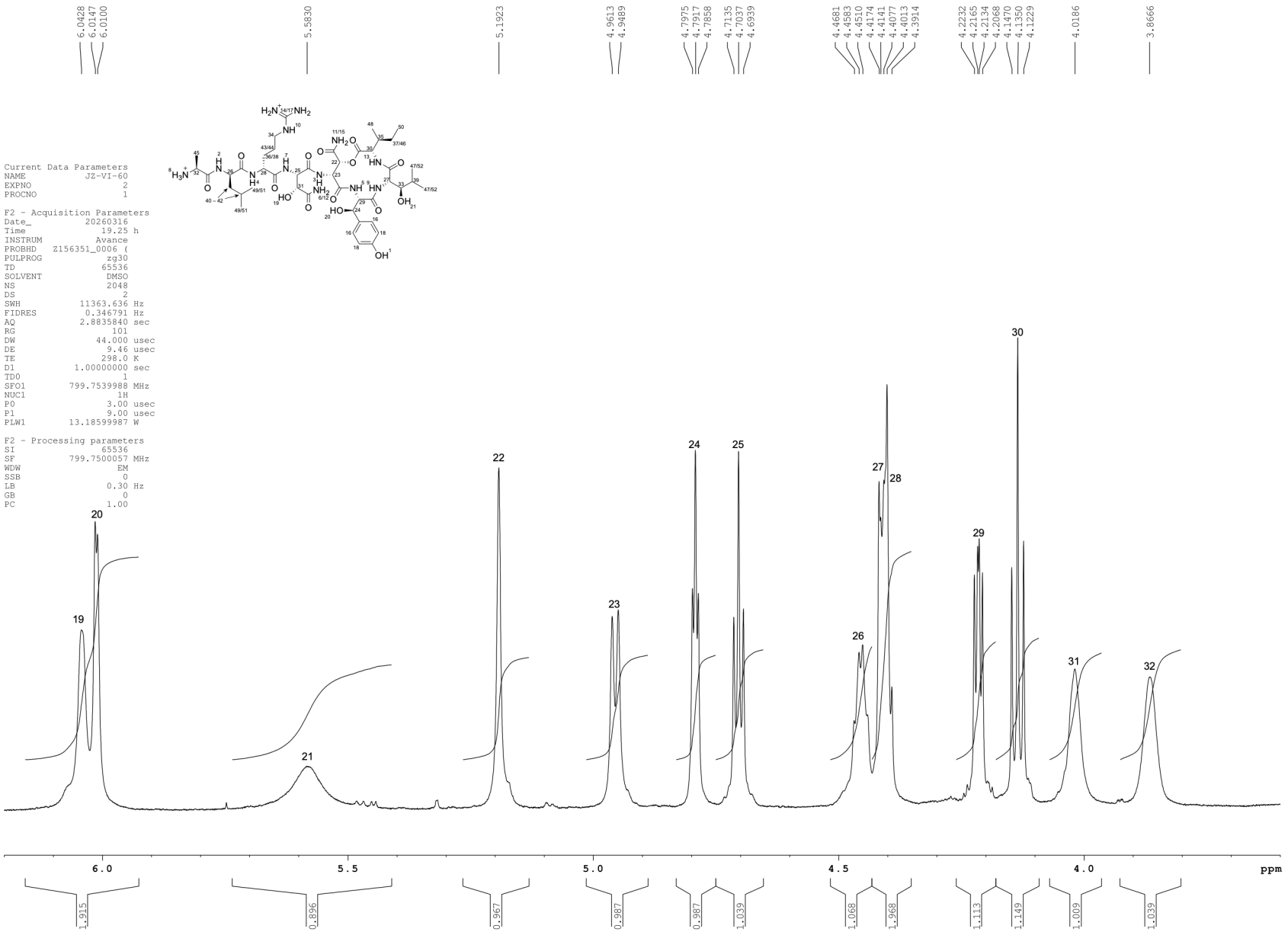

^{1}H NMR spectrum of natural hypeptin in DMSO-d_6 at 800 MHz and 298 K

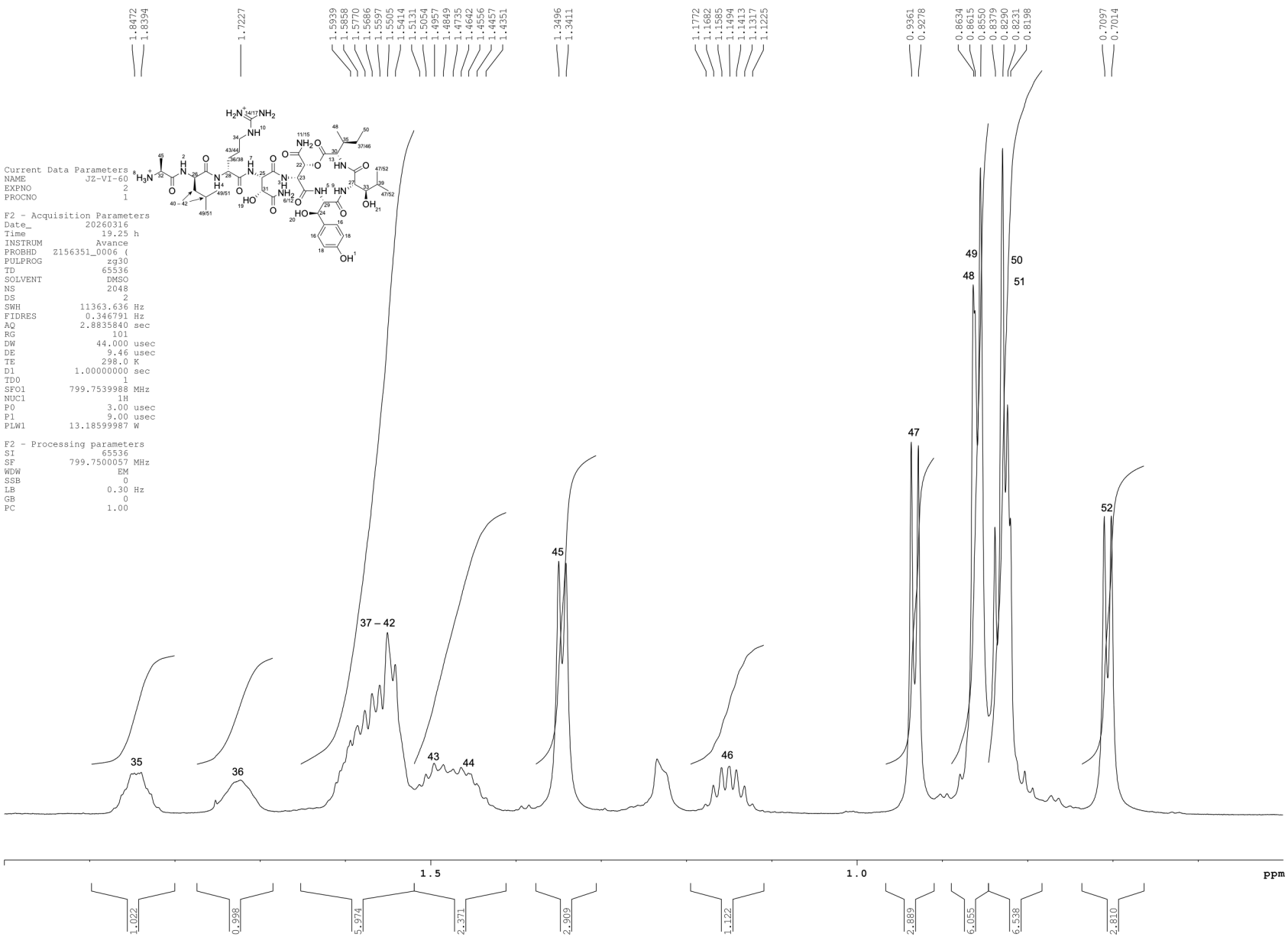

^{1}H, ^{13}C HSQC spectrum of natural hypeptin at 800 MHz and 298 K

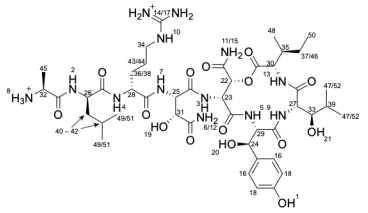

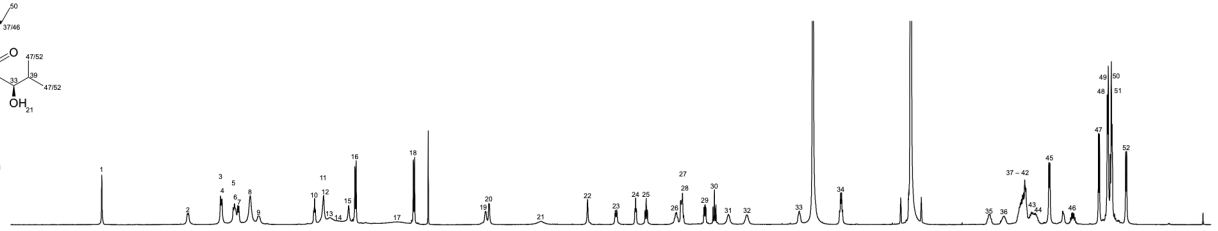

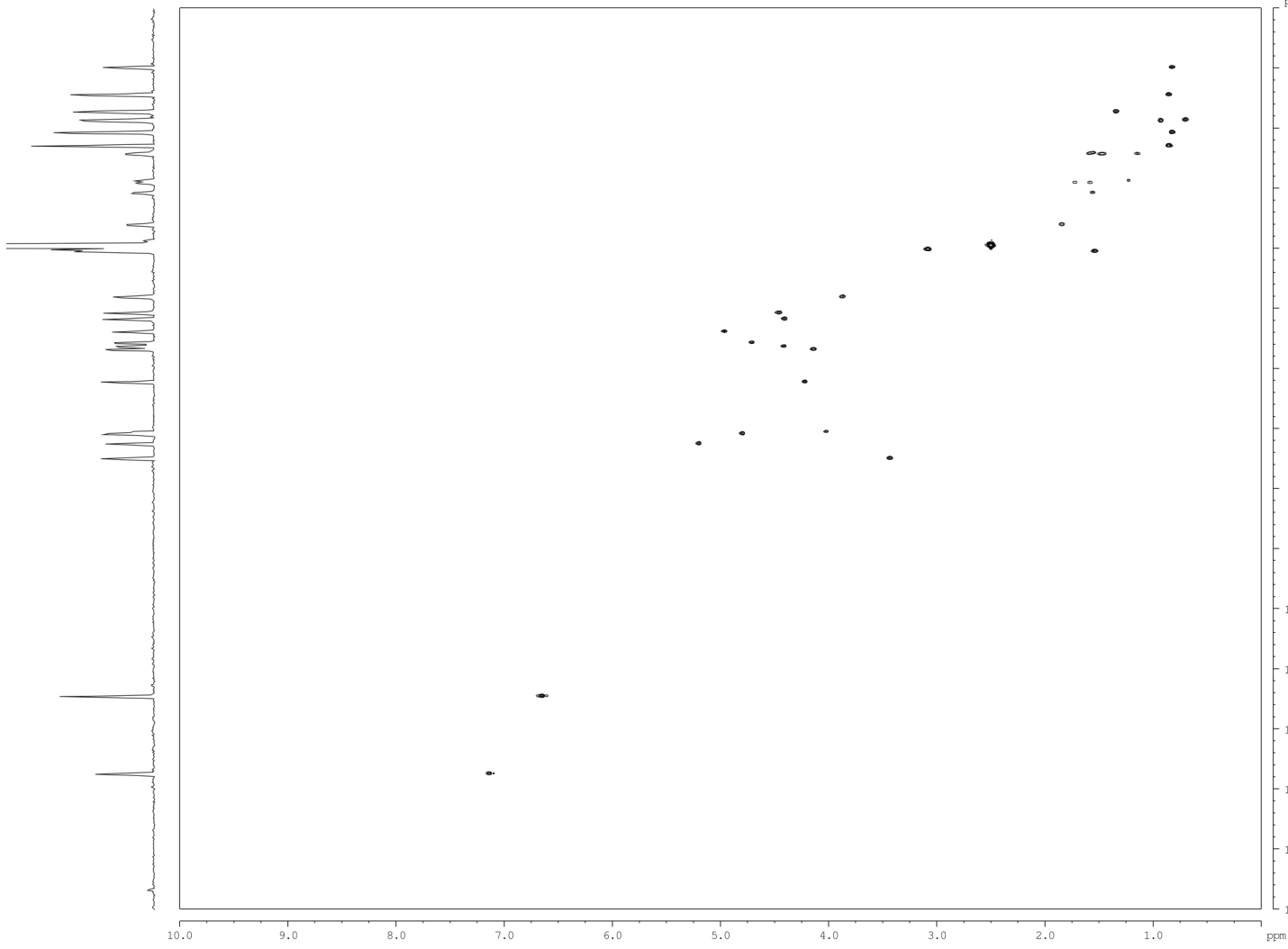


```
Current Data Parameters
NAME                  JZ-VI-60
EXPNO                        3
PROCNO                       1

F2 - Acquisition Parameter
Date_              20260316
Time                 23.00 h
INSTRUM                Avance
PROBHD   Z156351_0006 (
PULPROG      hsqcetgpsi2
TD                      1024
SOLVENT                 DMSO
NS                        16
DS                        16
SWH                9615.385 Hz
FIDRES            18.780048 Hz
AQ                 0.0532480 se
RG                      101
DW                   52.000 us
DE                    6.50 us
TE                   298.0 K
CNST2             145.0000000
D0                 0.00000300 se
D1                 1.50000000 se
D4                 0.00172414 se
D11                0.03000000 se
D16                0.00020000 se
D24                0.00086207 se
IN0                0.00001508 se
TDav                         1
ZGOPTNS
SFO1              799.7539988 MH
NUC1                       1H
P1                       9.00 us
P2                      18.00 us
PLW1              13.18599987 W
SFO2              201.1123797 MH
NUC2                       13C
CPDPRG[2                 garp
P3                      10.00 us
P4                      20.00 us
PCPD2                   50.00 us
PLW2             331.83999634 W
PLW12             13.27400017 W
GPNAM[1]           SMSQ10.100
GPZ1                    80.00 %
GPNAM[2]           SMSQ10.100
GPZ2                    20.10 %
GPNAM[3]           SMSQ10.100
GPZ3                    11.00 %
GPNAM[4]           SMSQ10.100
GPZ4                    -5.00 %
P16                   1000.00 us
P19                    600.00 us
======== F1 INDIRECT DIMEN
td1             512
sw_F1           165.000000

F1 - Acquisition parameter
TD                       512
SFO1              201.1124 MH
FIDRES           129.623215 Hz
SW                  165.000 pp
FnMODE     Echo-Antiecho

F2 - Processing parameters
SI                      1024
SF                799.7500041 MH
WDW                     QSINE
SSB                        2
LB                         0 Hz
GB                         0
PC                      1.40

F1 - Processing parameters
SI                      1024
MC2              echo-antiecho
SF                201.0974451 MH
WDW                     QSINE
SSB                        2
LB                         0 Hz
GB                         0
```

TOCSY spectrum of natural hypeptin in DMSO-d_6 at 800 MHz and 298 K with 100-msec mixing time

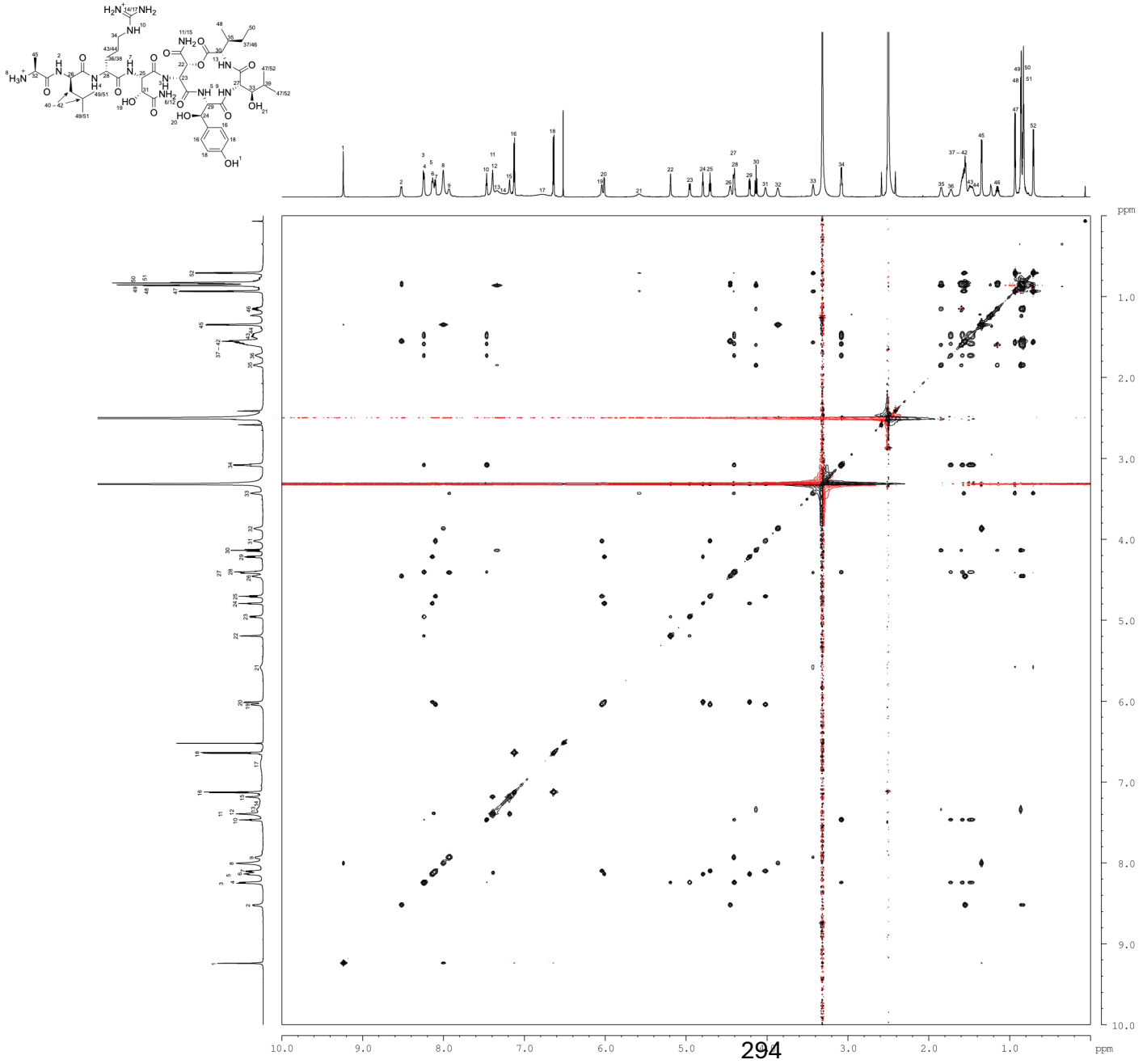


```
Current Data Parameters
NAME                  JZ-VI-60
EXPNO                        4
PROCNO                       1

F2 - Acquisition Parameters
Date_                 20260317
Time                      4.08 h
INSTRUM                  Avance
PROBHD     Z156351_0006 (
PULPROG                mlevphpp
TD                         2048
SOLVENT                   DMSO
NS                            8
DS                           16
SWH                  11363.636 Hz
FIDRES               11.097301 Hz
AQ                    0.0901120 sec
RG                          101
DW                       44.000 usec
DE                        6.50 usec
TE                      298.0 K
D0                    0.00003427 sec
D1                    2.00000000 sec
D9                    0.10000000 sec
D11                   0.03000000 sec
D12                   0.00002000 sec
IN0                   0.00008800 sec
L1                           60
TDav                          1
SFO1                799.7539988 MHz
NUC1                        1H
P1                        9.00 usec
P5                       16.67 usec
P6                       25.00 usec
P7                       50.00 usec
P17                    25000.00 usec
PLW1                13.18599987 W
PLW10                1.70879996 W

-------- F1 INDIRECT DIMENSI
td1             1024
sw_F1           14.208915

F1 - Acquisition parameters
TD                          1024
SFO1                 799.754 MHz
FIDRES               22.194603 Hz
SW                       14.209 ppm
FnMODE            States-TPPI

F2 - Processing parameters
SI                          1024
SF                 799.7500054 MHz
WDW                       QSINE
SSB                          2
LB                        0 Hz
GB                           0
PC                        1.40

F1 - Processing parameters
SI                          1024
MC2               States-TPPI
SF                 799.7500054 MHz
WDW                       QSINE
SSB                          2
LB                        0 Hz
GB                           0
```

TOCSY spectrum of natural hypeptin in DMSO-d_6 at 800 MHz and 298 K with 100-msec mixing time

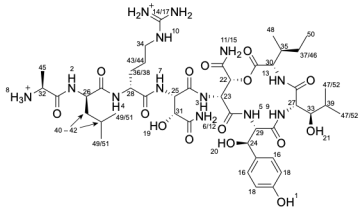

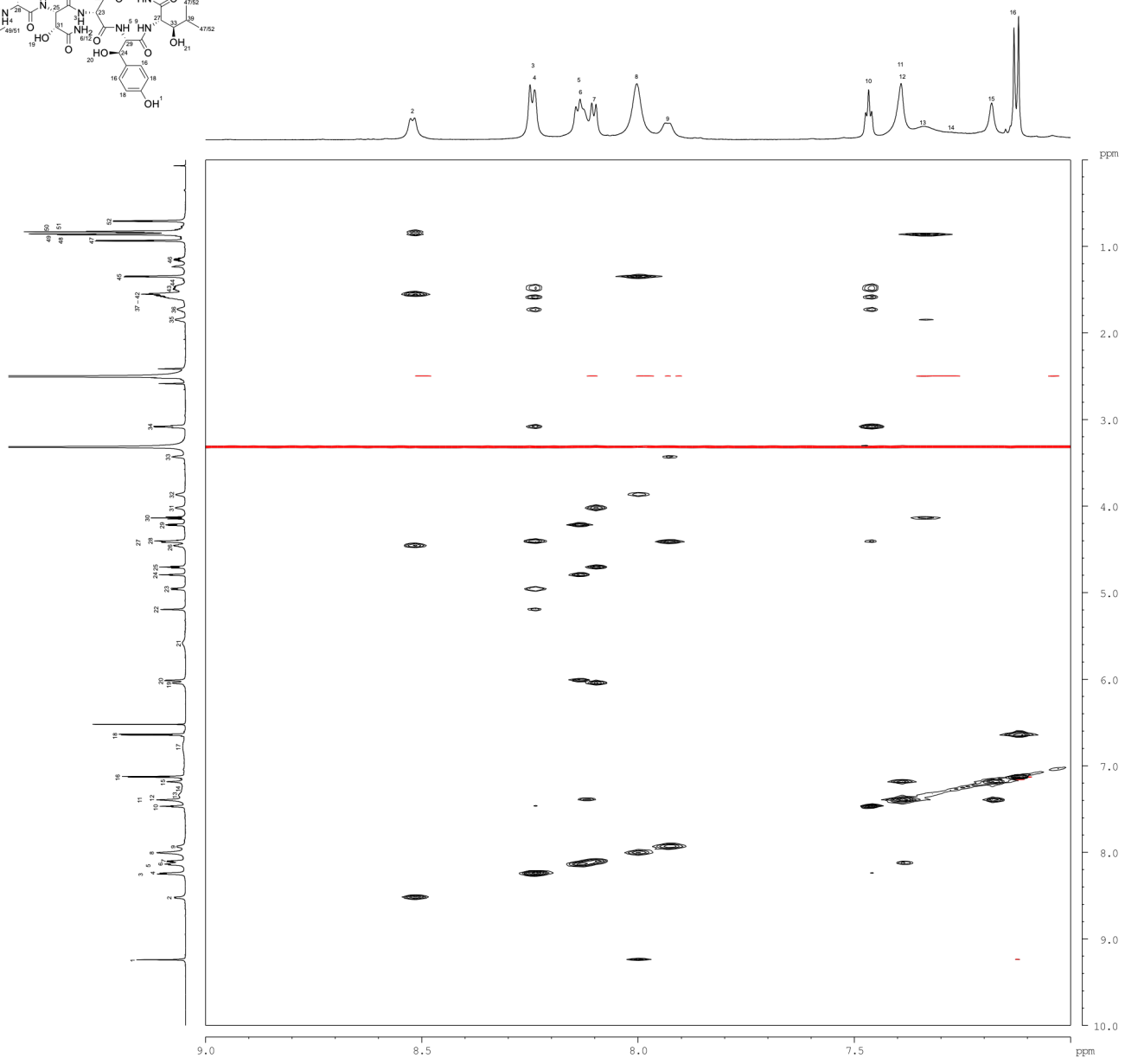


```
Current Data Parameters
NAME                  JZ-VI-60
EXPNO                        4
PROCNO                       1

F2 - Acquisition Parameters
Date_               20260317
Time                     4.08 h
INSTRUM                 Avance
PROBHD    Z156351_0006 (
PULPROG              mlevphpp
TD                       2048
SOLVENT                  DMSO
NS                          8
DS                         16
SWH                 11363.636 Hz
FIDRES                 11.097301 Hz
AQ                   0.0901120 sec
RG                         101
DW                      44.000 usec
DE                       6.50 usec
TE                      298.0 K
D0                   0.00003427 sec
D1                   2.00000000 sec
D9                   0.10000000 sec
D11                  0.03000000 sec
D12                  0.00002000 sec
IN0                  0.00008800 sec
L1                         60
TDav                        1
SFO1                799.7539988 MHz
NUC1                       1H
P1                       9.00 usec
P5                      16.67 usec
P6                      25.00 usec
P7                      50.00 usec
P17                   2500.00 usec
PLW1                13.18599987 W
PLW10                1.70879996 W

-------- F1 INDIRECT DIMENSI
td1             1024
sw_F1           14.208915

F1 - Acquisition parameters
TD                      1024
SFO1                799.754 MHz
FIDRES               22.194603 Hz
SW                      14.209 ppm
FnMODE              States-TPPI

F2 - Processing parameters
SI                      1024
SF                  799.7500054 MHz
WDW                     QSINE
SSB                         2
LB                          0 Hz
GB                          0
PC                       1.40

F1 - Processing parameters
SI                      1024
MC2                 States-TPPI
SF                  799.7500054 MHz
WDW                     QSINE
SSB                         2
LB                          0 Hz
GB                          0
```

TOCSY spectrum of natural hypeptin in DMSO-d_6 at 800 MHz and 298 K with 100-msec mixing time

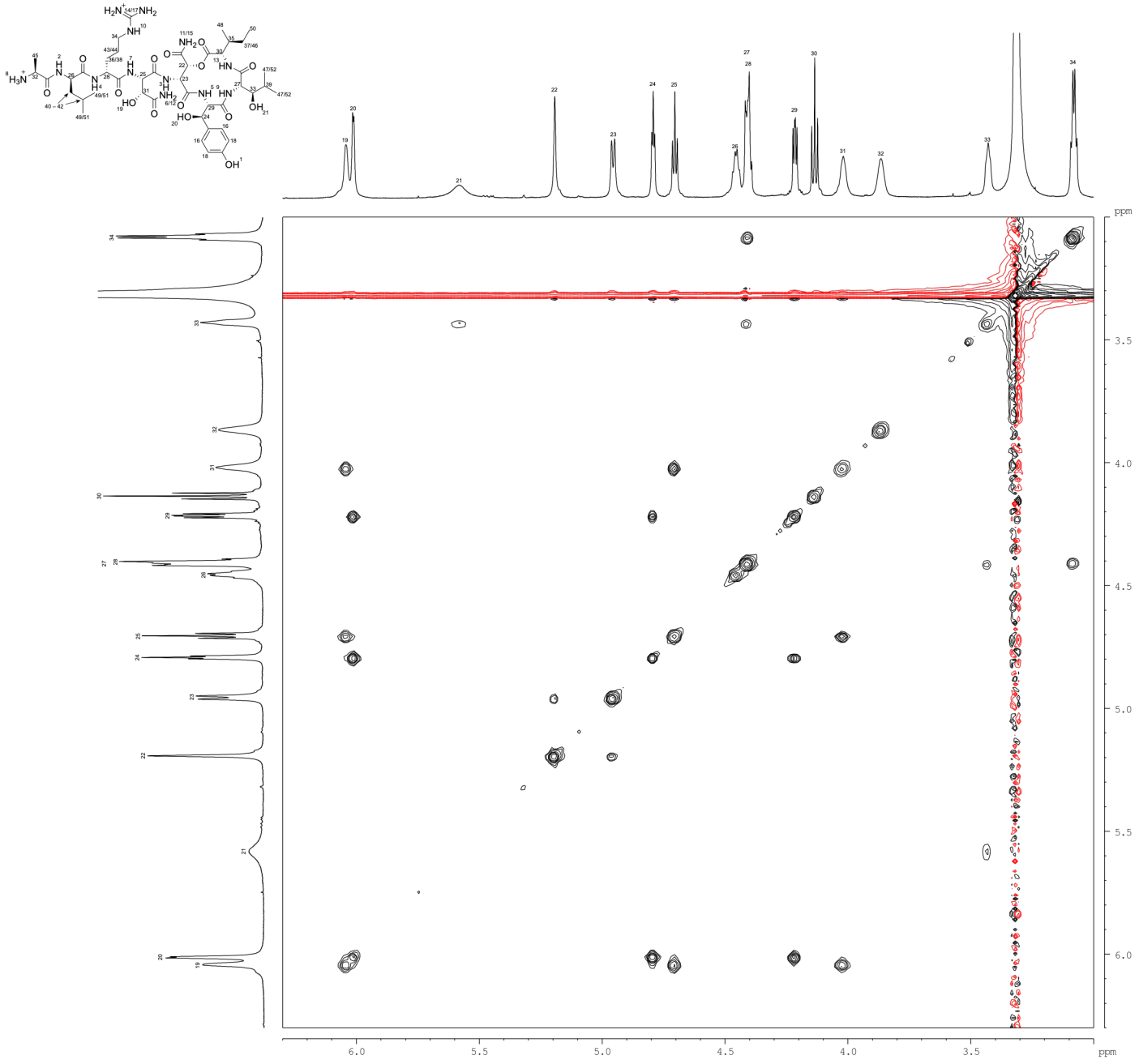


```
Current Data Parameters
NAME                  JZ-VI-60
EXPNO                        4
PROCNO                       1

F2 - Acquisition Parameters
Date_              20260317
Time                    4.08 h
INSTRUM                Avance
PROBHD    Z156351_0006 (
PULPROG            mlevphpp
TD                       2048
SOLVENT                  DMSO
NS                          8
DS                         16
SWH                11363.636 Hz
FIDRES             11.097301 Hz
AQ                  0.0901120 sec
RG                        101
DW                     44.000 usec
DE                      6.50 usec
TE                     298.0 K
D0                 0.00003427 sec
D1                 2.00000000 sec
D9                 0.10000000 sec
D11                0.03000000 sec
D12                0.00002000 sec
IN0                0.00008800 sec
L1                         60
TDav                        1
SFO1               799.7539988 MHz
NUC1                       1H
P1                       9.00 usec
P5                      16.67 usec
P6                      25.00 usec
P7                      50.00 usec
P17                   2500.00 usec
PLW1              13.18599987 W
PLW10              1.70879996 W

-------- F1 INDIRECT DIMENSI
td1           1024
sw_F1      14.208915

F1 - Acquisition parameters
TD                       1024
SFO1                799.754 MHz
FIDRES           22.194603 Hz
SW                    14.209 ppm
FnMODE           States-TPPI

F2 - Processing parameters
SI                       1024
SF                799.7500054 MHz
WDW                      QSINE
SSB                         2
LB                          0 Hz
GB                          0
PC                       1.40

F1 - Processing parameters
SI                       1024
MC2              States-TPPI
SF                799.7500054 MHz
WDW                      QSINE
SSB                         2
LB                          0 Hz
GB                          0
```

TOCSY spectrum of natural hypeptin in DMSO-d_6 at 800 MHz and 298 K with 100-msec mixing time

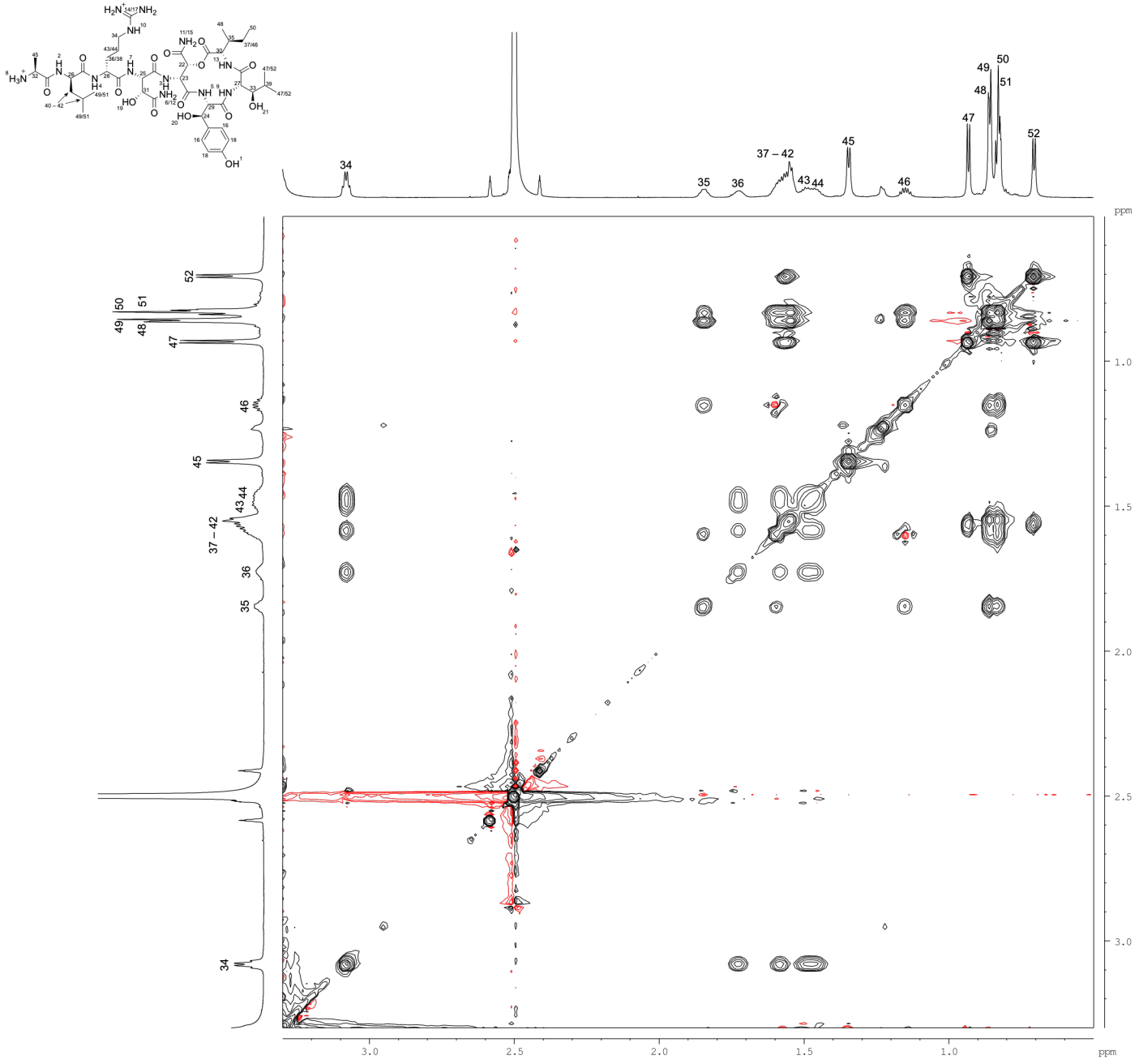


```
Current Data Parameters
NAME                  JZ-VI-60
EXPNO                        4
PROCNO                       1

F2 - Acquisition Parameters
Date_              20260317
Time                    4.08 h
INSTRUM                Avance
PROBHD    Z156351_0006 (
PULPROG             mlevphpp
TD                       2048
SOLVENT                  DMSO
NS                          8
DS                         16
SWH                11363.636 Hz
FIDRES             11.097301 Hz
AQ                  0.0901120 sec
RG                        101
DW                     44.000 usec
DE                      6.50 usec
TE                     298.0 K
D0                 0.00003427 sec
D1                 2.00000000 sec
D9                 0.10000000 sec
D11                0.03000000 sec
D12                0.00002000 sec
IN0                0.00008800 sec
L1                         60
TDav                        1
SFO1               799.7539988 MHz
NUC1                       1H
P1                       9.00 usec
P5                      16.67 usec
P6                      25.00 usec
P7                      50.00 usec
P17                   2500.00 usec
PLW1              13.18599987 W
PLW10              1.70879996 W

-------- F1 INDIRECT DIMENSI
td1          1024
sw_F1       14.208915

F1 - Acquisition parameters
TD                       1024
SFO1               799.754 MHz
FIDRES           22.194603 Hz
SW                  14.209 ppm
FnMODE          States-TPPI

F2 - Processing parameters
SI                       1024
SF                 799.7500054 MHz
WDW                     QSINE
SSB                         2
LB                          0 Hz
GB                          0
PC                       1.40

F1 - Processing parameters
SI                       1024
MC2             States-TPPI
SF                 799.7500054 MHz
WDW                     QSINE
SSB                         2
LB                          0 Hz
GB                          0
```

NOESY spectrum of natural hypeptin in DMSO-d_6 at 800 MHz and 298 K with 500-msec mixing time (higher elevation to show stronger NOEs)

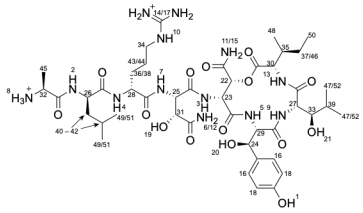

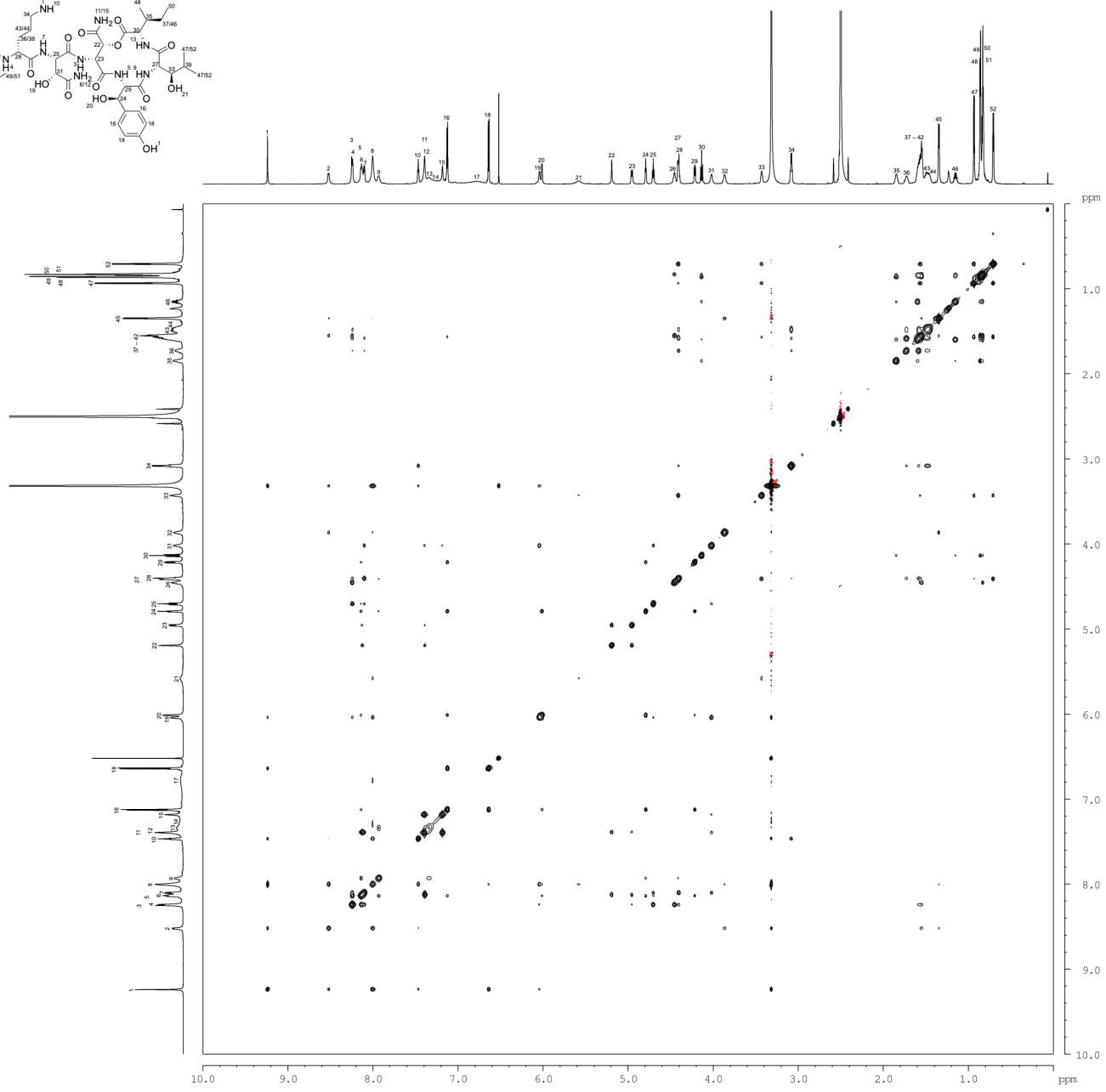


```
Current Data Parameters
NAME                  JZ-VI-60
EXPNO                        5
PROCNO                       1

F2 - Acquisition Parameters
Date_              20260317
Time                  16.14 h
INSTRUM                Avance
PROBHD    Z156351_0006 (
PULPROG       noesygpphpp
TD                        2048
SOLVENT                   DMSO
NS                          16
DS                          32
SWH                11363.636 Hz
FIDRES             11.097301 Hz
AQ                  0.0901120 sec
RG                        101
DW                     44.000 usec
DE                     10.77 usec
TE                     298.0 K
D0                  0.00003254 sec
D1                  2.00000000 sec
D8                  0.50000000 sec
D11                 0.03000000 sec
D12                 0.00002000 sec
D16                 0.00020000 sec
IN0                 0.00008800 sec
TDav                         1
SFO1               799.7539988 MHz
NUC1                        1H
P1                       9.00 usec
P2                      18.00 usec
P17                   2500.00 usec
PLW1               13.18599987 W
PLW10               1.70879996 W
GPNAM[1]        SMSQ10.100
GPZ1                    40.00 %
P16                   1000.00 usec

======== F1 INDIRECT DIMENSI
td1          1024
sw_F1       14.208915

F1 - Acquisition parameters
TD                        1024
SFO1                799.754 MHz
FIDRES             22.194603 Hz
SW                    14.209 ppm
FnMODE          States-TPPI

F2 - Processing parameters
SI                        1024
SF                799.7500055 MHz
WDW                     QSINE
SSB                         2
LB                          0 Hz
GB                          0
PC                       1.00

F1 - Processing parameters
SI                        1024
MC2             States-TPPI
SF                799.7500055 MHz
WDW                     QSINE
SSB                         2
LB                          0 Hz
GB                          0
```

NOESY spectrum of natural hypeptin in DMSO-d_6 at 800 MHz and 298 K with 500-msec mixing time (lower elevation to show weaker NOEs)

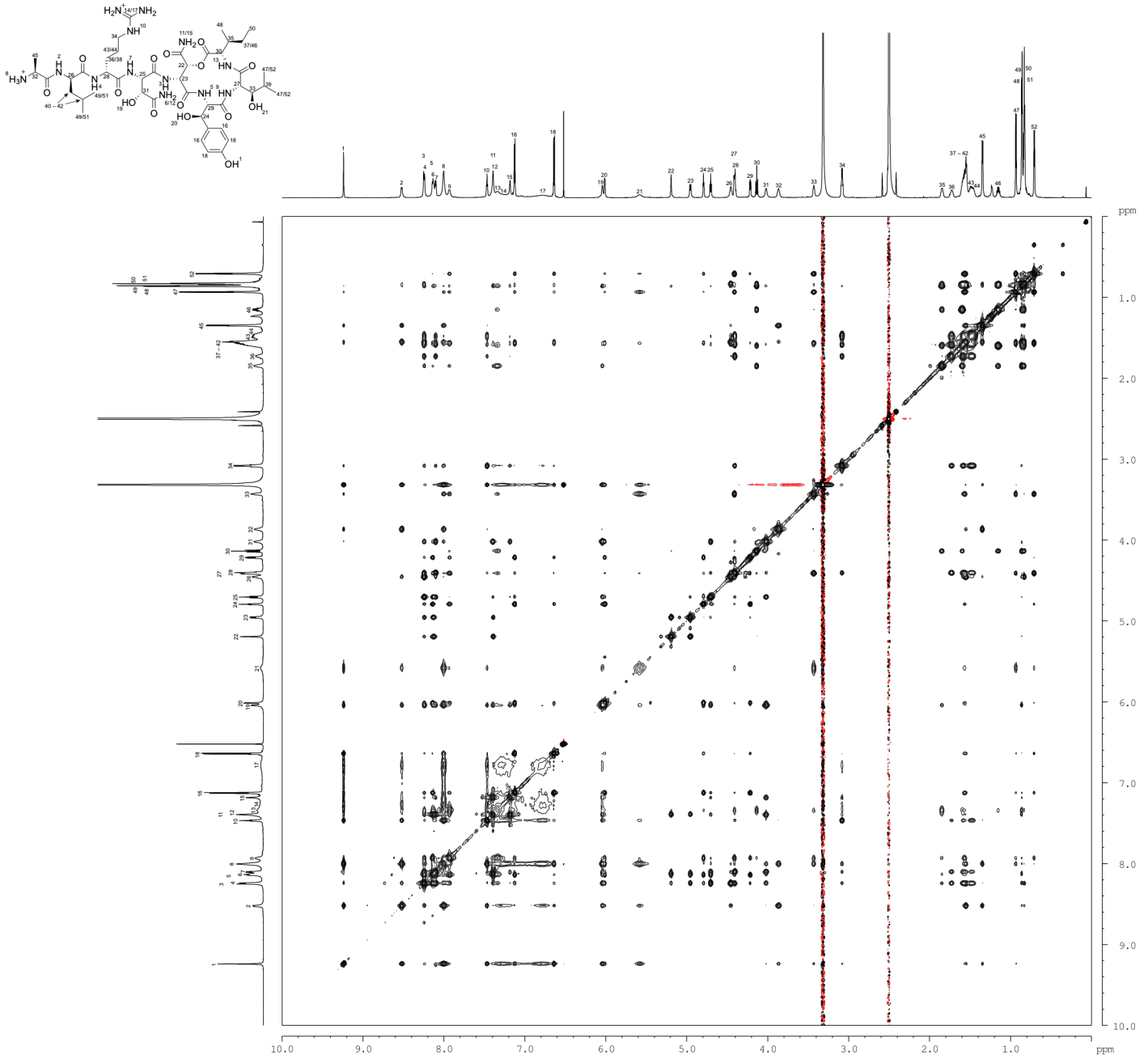


```
Current Data Parameters
NAME                  JZ-VI-60
EXPNO                        5
PROCNO                       1

F2 - Acquisition Parameters
Date_              20260317
Time                  16.14 h
INSTRUM                Avance
PROBHD    Z156351_0006 (
PULPROG       noesygpphpp
TD                        2048
SOLVENT                   DMSO
NS                          16
DS                          32
SWH                11363.636 Hz
FIDRES             11.097301 Hz
AQ                  0.0901120 sec
RG                        101
DW                     44.000 usec
DE                     10.77 usec
TE                     298.0 K
D0                  0.00003254 sec
D1                  2.00000000 sec
D8                  0.50000000 sec
D11                 0.03000000 sec
D12                 0.00002000 sec
D16                 0.00020000 sec
IN0                 0.00008800 sec
TDav                         1
SFO1               799.7539988 MHz
NUC1                        1H
P1                       9.00 usec
P2                      18.00 usec
P17                   2500.00 usec
PLW1               13.18599987 W
PLW10               1.70879996 W
GPNAM[1]          SMSQ10.100
GPZ1                    40.00 %
P16                   1000.00 usec

======== F1 INDIRECT DIMENSI
td1         1024
sw_F1       14.208915

F1 - Acquisition parameters
TD                        1024
SFO1               799.754 MHz
FIDRES            22.194603 Hz
SW                   14.209 ppm
FnMODE          States-TPPI

F2 - Processing parameters
SI                        1024
SF                 799.7500055 MHz
WDW                     QSINE
SSB                         2
LB                      0 Hz
GB                          0
PC                       1.00

F1 - Processing parameters
SI                        1024
MC2             States-TPPI
SF                 799.7500055 MHz
WDW                     QSINE
SSB                         2
LB                      0 Hz
GB                          0
```

NOESY spectrum of natural hypeptin in DMSO-d_6 at 800 MHz and 298 K with 500-msec mixing time

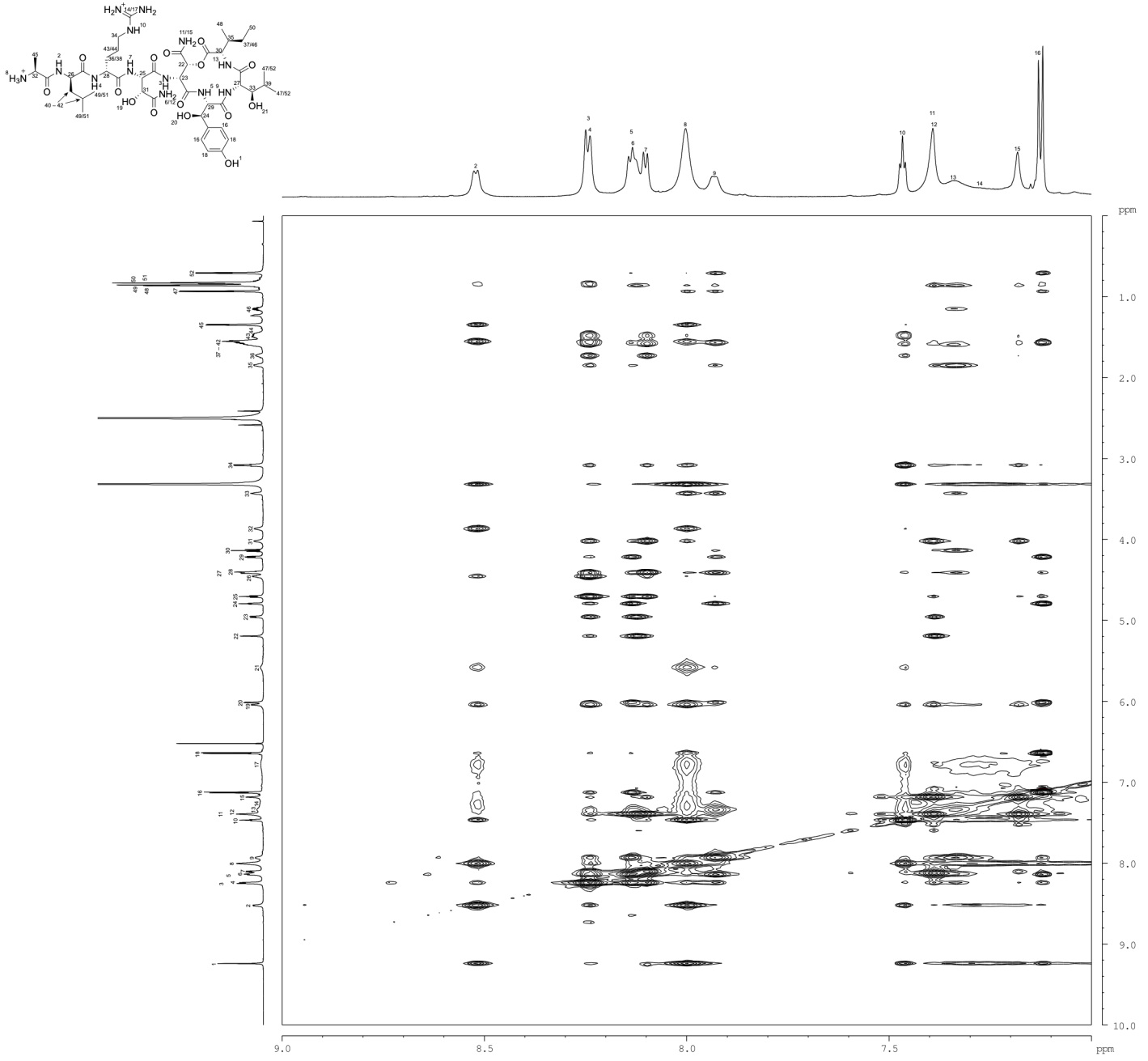


```
Current Data Parameters
NAME                  JZ-VI-60
EXPNO                        5
PROCNO                       1

F2 - Acquisition Parameters
Date_              20260317
Time                   16.14 h
INSTRUM                Avance
PROBHD    Z156351_0006 (
PULPROG        noesygpphpp
TD                        2048
SOLVENT                   DMSO
NS                          16
DS                          32
SWH                11363.636 Hz
FIDRES             11.097301 Hz
AQ                  0.0901120 sec
RG                        101
DW                     44.000 usec
DE                     10.77 usec
TE                     298.0 K
D0                  0.00003254 sec
D1                  2.00000000 sec
D8                  0.50000000 sec
D11                 0.03000000 sec
D12                 0.00002000 sec
D16                 0.00020000 sec
IN0                 0.00008800 sec
TDav                        1
SFO1               799.7539988 MHz
NUC1                       1H
P1                       9.00 usec
P2                      18.00 usec
P17                   2500.00 usec
PLW1               13.18599987 W
PLW10               1.70879996 W
GPNAM[1]        SMSQ10.100
GPZ1                    40.00 %
P16                   1000.00 usec

======== F1 INDIRECT DIMENSI
td1         1024
sw_F1       14.208915

F1 - Acquisition parameters
TD                        1024
SFO1                799.754 MHz
FIDRES            22.194603 Hz
SW                   14.209 ppm
FnMODE          States-TPPI

F2 - Processing parameters
SI                        1024
SF                799.7500055 MHz
WDW                     QSINE
SSB                        2
LB                         0 Hz
GB                         0
PC                      1.00

F1 - Processing parameters
SI                        1024
MC2             States-TPPI
SF                799.7500055 MHz
WDW                     QSINE
SSB                        2
LB                         0 Hz
GB                         0
```

NOESY spectrum of natural hypeptin in DMSO-d_6 at 800 MHz and 298 K with 500-msec mixing time

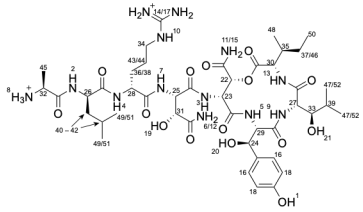

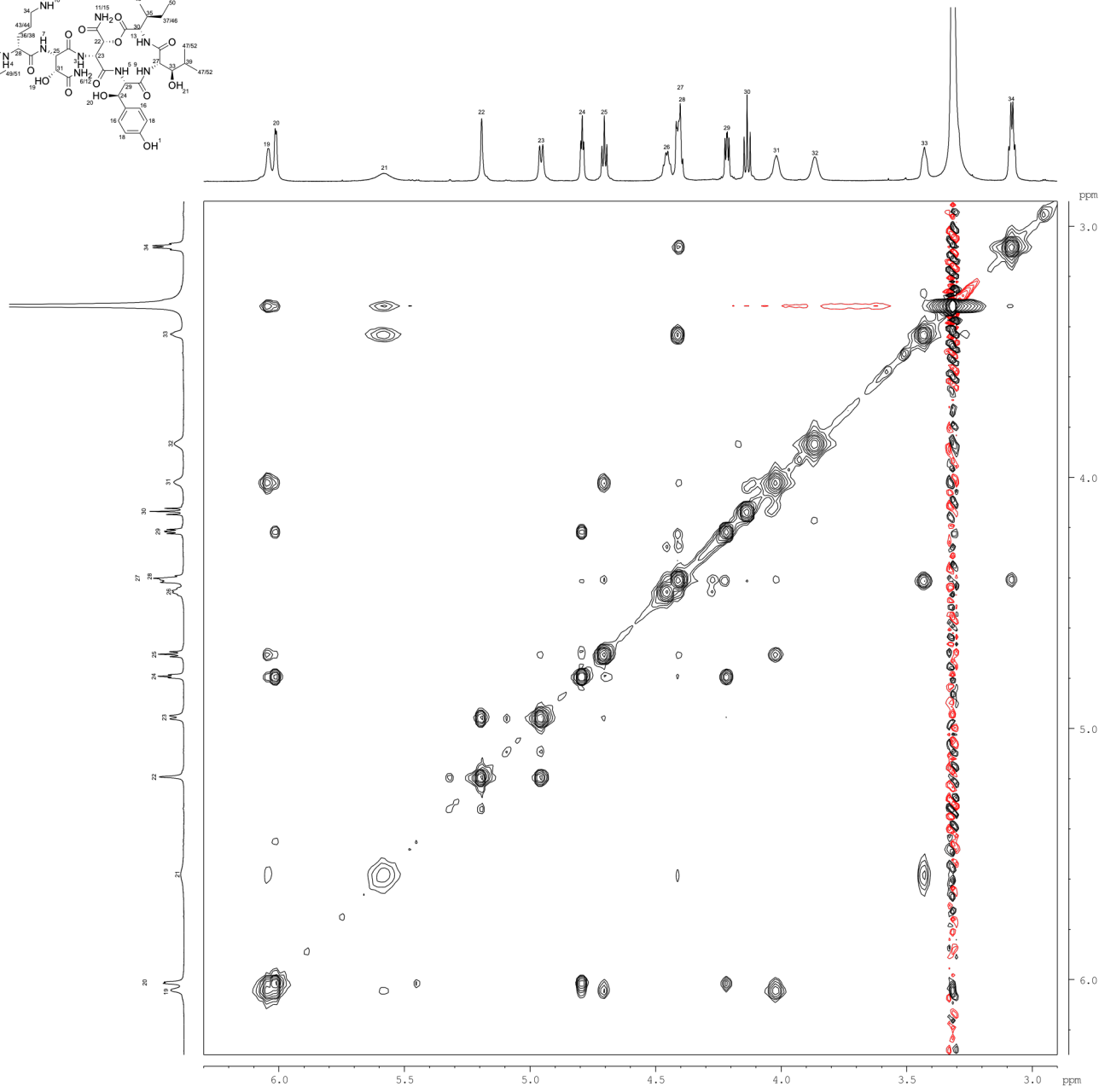


```
Current Data Parameters
NAME                  JZ-VI-60
EXPNO                        5
PROCNO                       1

F2 - Acquisition Parameters
Date_              20260317
Time                   16.14 h
INSTRUM                Avance
PROBHD    Z156351_0006 (
PULPROG        noesygpphpp
TD                        2048
SOLVENT                   DMSO
NS                          16
DS                          32
SWH                11363.636 Hz
FIDRES             11.097301 Hz
AQ                  0.0901120 sec
RG                        101
DW                     44.000 usec
DE                     10.77 usec
TE                     298.0 K
D0                  0.00003254 sec
D1                  2.00000000 sec
D8                  0.50000000 sec
D11                 0.03000000 sec
D12                 0.00002000 sec
D16                 0.00020000 sec
IN0                 0.00008800 sec
TDav                         1
SFO1                799.7539988 MHz
NUC1                        1H
P1                       9.00 usec
P2                      18.00 usec
P17                   2500.00 usec
PLW1               13.18599987 W
PLW10               1.70879996 W
GPNAM[1]          SMSQ10.100
GPZ1                    40.00 %
P16                   1000.00 usec

======== F1 INDIRECT DIMENSI
td1                  1024
sw_F1               14.208915

F1 - Acquisition parameters
TD                        1024
SFO1                799.754 MHz
FIDRES             22.194603 Hz
SW                    14.209 ppm
FnMODE            States-TPPI

F2 - Processing parameters
SI                        1024
SF                  799.7500055 MHz
WDW                      QSINE
SSB                         2
LB                          0 Hz
GB                          0
PC                       1.00

F1 - Processing parameters
SI                        1024
MC2               States-TPPI
SF                  799.7500055 MHz
WDW                      QSINE
SSB                         2
LB                          0 Hz
GB                          0
```

NOESY spectrum of natural hypeptin in DMSO-d_6 at 800 MHz and 298 K with 500-msec mixing time

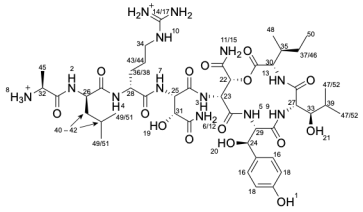

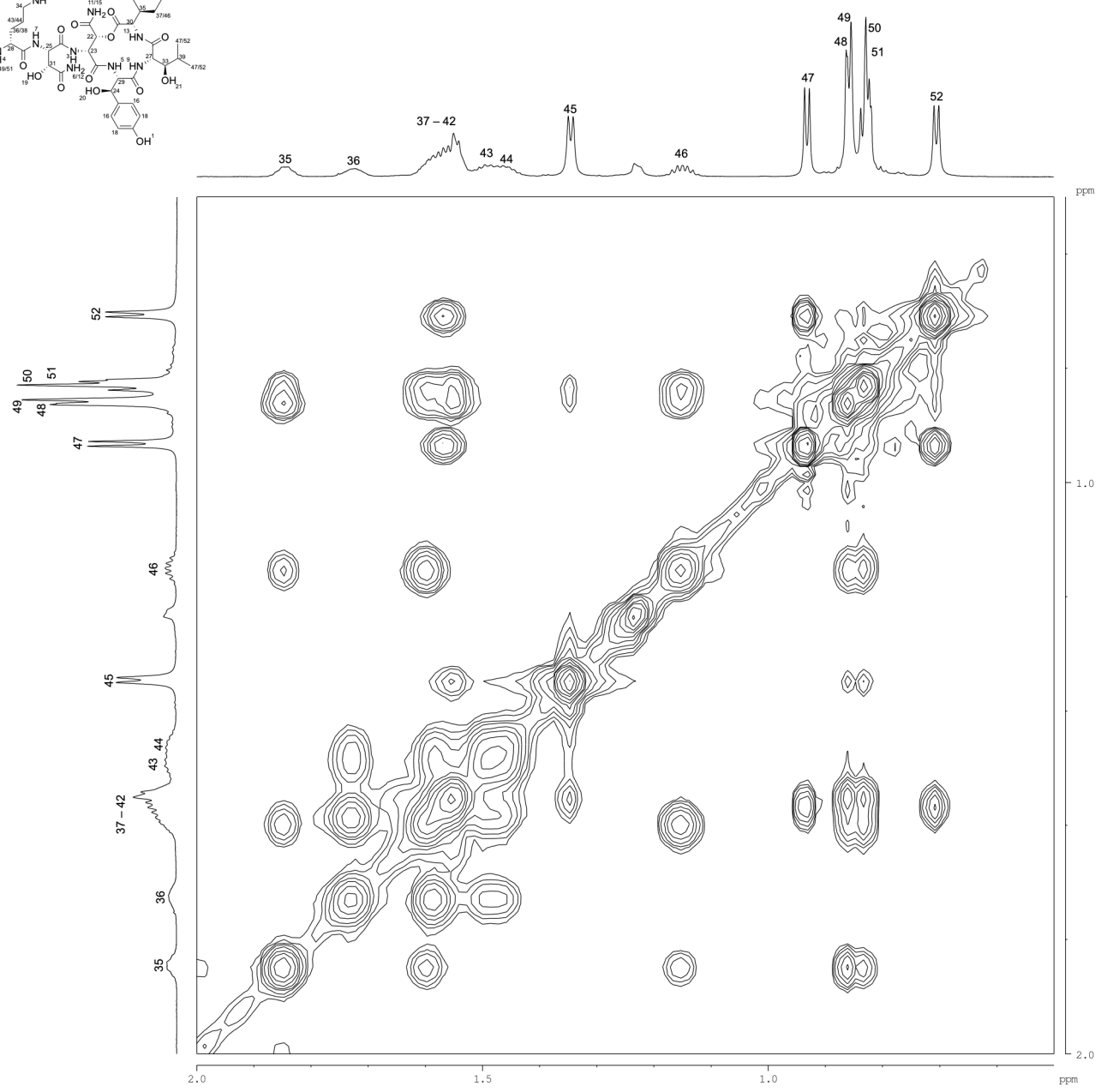


```
Current Data Parameters
NAME                  JZ-VI-60
EXPNO                        5
PROCNO                       1

F2 - Acquisition Parameters
Date_               20260317
Time                    16.14 h
INSTRUM                 Avance
PROBHD     Z156351_0006 (
PULPROG         noesygpphpp
TD                        2048
SOLVENT                   DMSO
NS                          16
DS                          32
SWH                 11363.636 Hz
FIDRES              11.097301 Hz
AQ                   0.0901120 sec
RG                         101
DW                      44.000 usec
DE                      10.77 usec
TE                        298.0 K
D0                  0.00003254 sec
D1                  2.00000000 sec
D8                  0.50000000 sec
D11                 0.03000000 sec
D12                 0.00002000 sec
D16                 0.00020000 sec
IN0                 0.00008800 sec
TDav                         1
SFO1                799.7539988 MHz
NUC1                        1H
P1                        9.00 usec
P2                       18.00 usec
P17                    2500.00 usec
PLW1               13.18599987 W
PLW10               1.70879996 W
GPNAM[1]          SMSQ10.100
GPZ1                       40.00 %
P16                    1000.00 usec

======== F1 INDIRECT DIMENSI
td1                 1024
sw_F1               14.208915

F1 - Acquisition parameters
TD                          1024
SFO1                 799.754 MHz
FIDRES              22.194603 Hz
SW                      14.209 ppm
FnMODE           States-TPPI

F2 - Processing parameters
SI                          1024
SF                  799.7500055 MHz
WDW                       QSINE
SSB                           2
LB                            0 Hz
GB                            0
PC                         1.00

F1 - Processing parameters
SI                          1024
MC2              States-TPPI
SF                  799.7500055 MHz
WDW                       QSINE
SSB                           2
LB                            0 Hz
GB                            0
```

ROESY spectrum of natural hypeptin in DMSO-d_6 at 800 MHz and 298 K with 500-msec mixing time

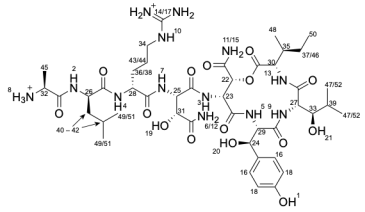

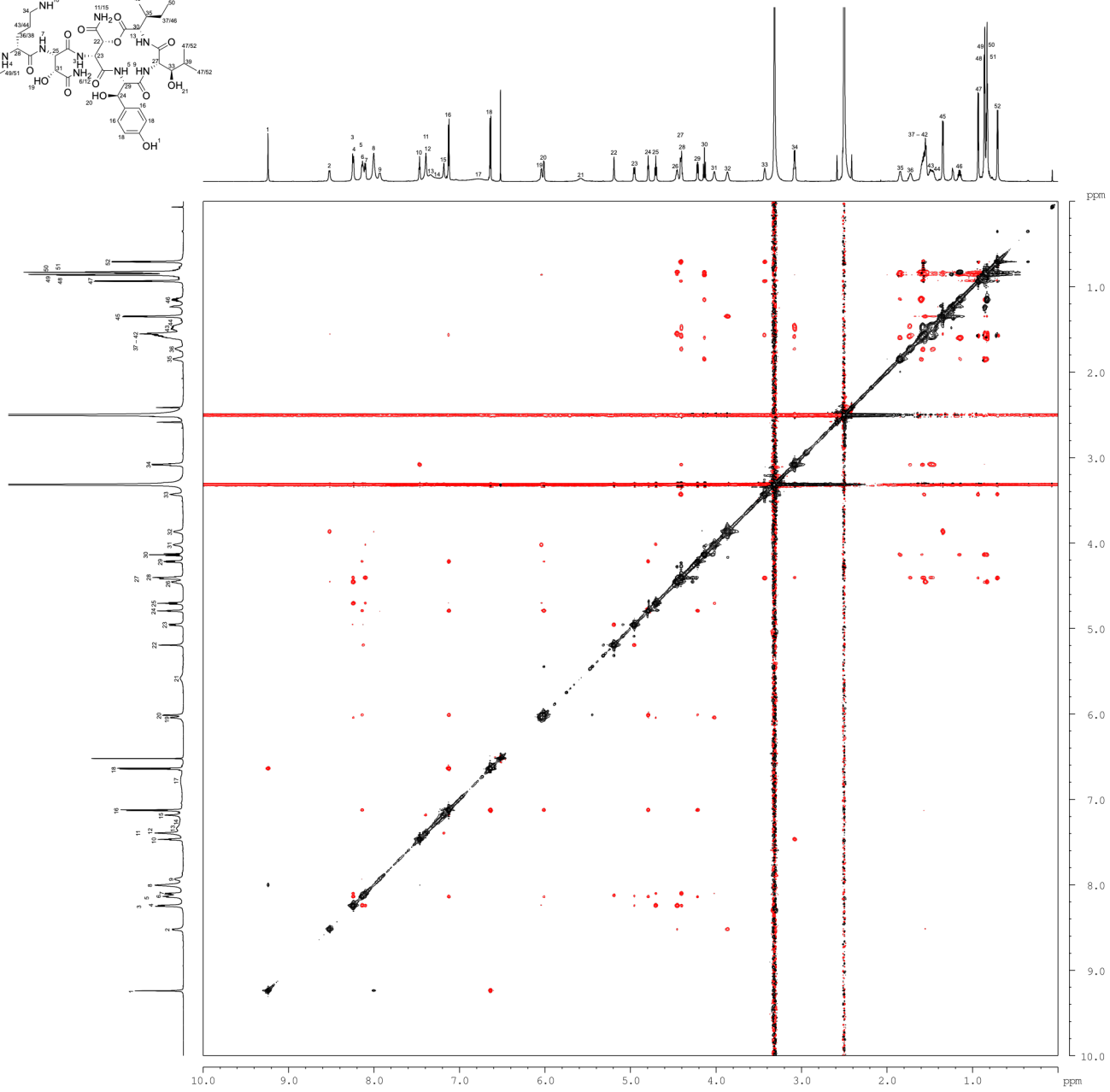


```
Current Data Parameters
NAME                  JZ-VI-60
EXPNO                        6
PROCNO                       1

F2 - Acquisition Parameters
Date_               20260318
Time                    2.57 h
INSTRUM                Avance
PROBHD    Z156351_0006 (
PULPROG       roesyphpp.2
TD                        2048
SOLVENT                 DMSO
NS                          16
DS                          32
SWH                11363.636 Hz
FIDRES             11.097301 Hz
AQ                  0.0901120 sec
RG                        101
DW                     44.000 usec
DE                      6.50 usec
TE                     298.0 K
D0                  0.00003427 sec
D1                  2.00000000 sec
D11                 0.03000000 sec
D12                 0.00002000 sec
IN0                 0.00008800 sec
L4                        735
P15                 200000.00 usec
TDav                        1
SFO1                799.7539988 MHz
NUC1                       1H
P1                       9.00 usec
P17                   2500.00 usec
P25                    136.00 usec
PLW1               13.18599987 W
PLW10               1.70879996 W
PLW27               0.23097000 W

======== F1 INDIRECT DIMENSI
td1              1024
sw_F1           14.208915

F1 - Acquisition parameters
TD                       1024
SFO1                799.754 MHz
FIDRES             22.196603 Hz
SW                    14.209 ppm
FnMODE          States-TPPI

F2 - Processing parameters
SI                       1024
SF                799.7500055 MHz
WDW                     QSINE
SSB                         2
LB                          0 Hz
GB                          0
PC                       1.00

F1 - Processing parameters
SI                       1024
MC2             States-TPPI
SF                799.7500055 MHz
WDW                     QSINE
SSB                         2
LB                          0 Hz
GB                          0
```

ROESY spectrum of natural hypeptin in DMSO-d_6 at 800 MHz and 298 K with 500-msec mixing time

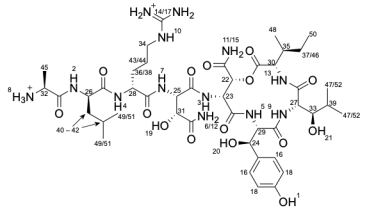

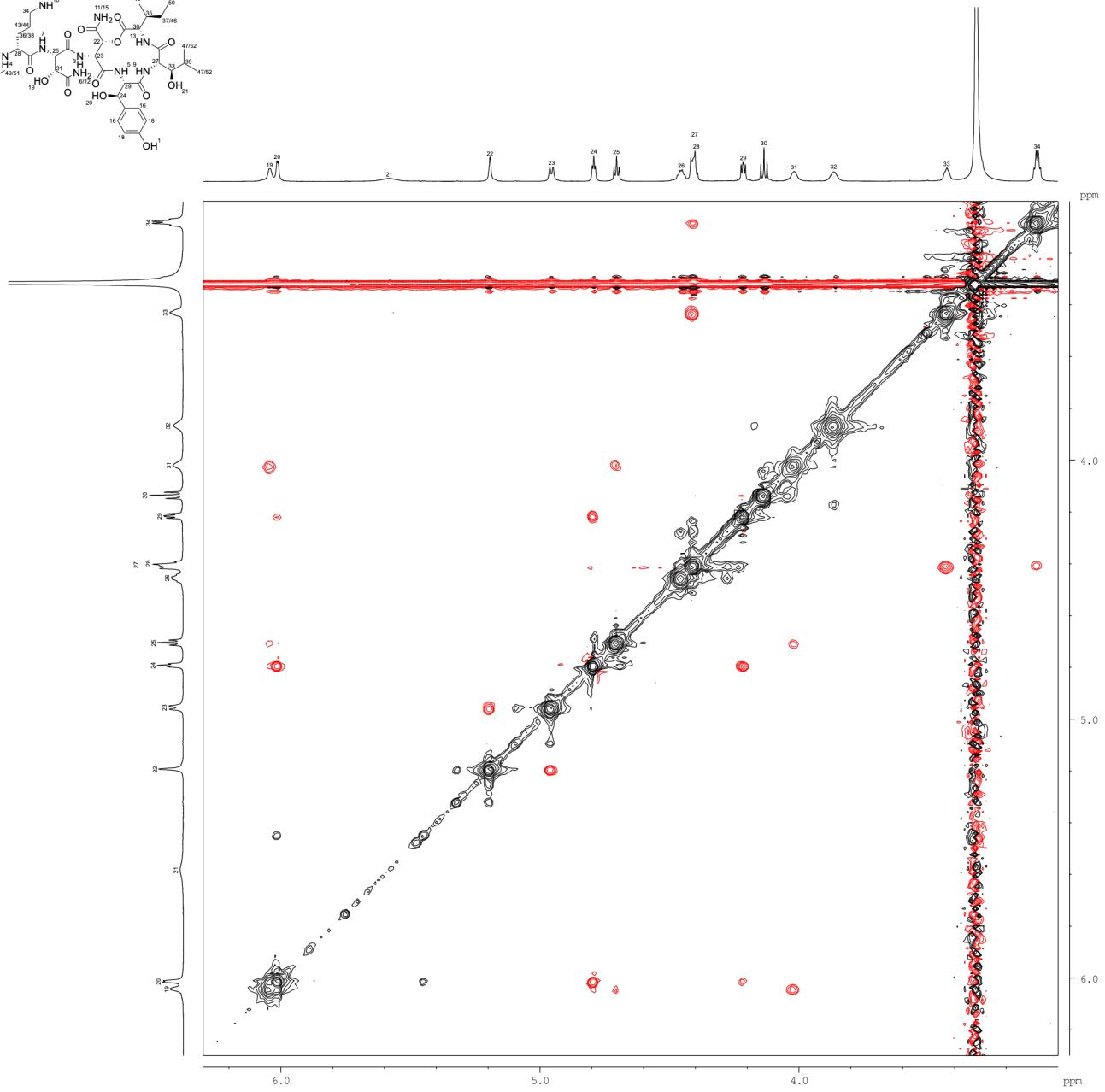


```
Current Data Parameters
NAME                  JZ-VI-60
EXPNO                        6
PROCNO                       1

F2 - Acquisition Parameters
Date_               20260318
Time                    2.57 h
INSTRUM                Avance
PROBHD    Z156351_0006 (
PULPROG       roesyphpp.2
TD                        2048
SOLVENT                 DMSO
NS                          16
DS                          32
SWH                11363.636 Hz
FIDRES             11.097301 Hz
AQ                  0.0901120 sec
RG                        101
DW                     44.000 usec
DE                      6.50 usec
TE                     298.0 K
D0                  0.00003427 sec
D1                  2.00000000 sec
D11                 0.03000000 sec
D12                 0.00002000 sec
IN0                 0.00008800 sec
L4                        735
P15                200000.00 usec
TDav                        1
SFO1               799.7539988 MHz
NUC1                       1H
P1                       9.00 usec
P17                   2500.00 usec
P25                    136.00 usec
PLW1              13.18599987 W
PLW10              1.70879996 W
PLW27              0.23097000 W

======== F1 INDIRECT DIMENSI
td1              1024
sw_F1           14.208915

F1 - Acquisition parameters
TD                       1024
SFO1                799.754 MHz
FIDRES            22.194603 Hz
SW                   14.209 ppm
FnMODE           States-TPPI

F2 - Processing parameters
SI                       1024
SF                799.7500055 MHz
WDW                     QSINE
SSB                         2
LB                          0 Hz
GB                          0
PC                       1.00

F1 - Processing parameters
SI                       1024
MC2              States-TPPI
SF                799.7500055 MHz
WDW                     QSINE
SSB                         2
LB                          0 Hz
GB                          0
```

ROESY spectrum of natural hypeptin in DMSO-d_6 at 800 MHz and 298 K with 500-msec mixing time

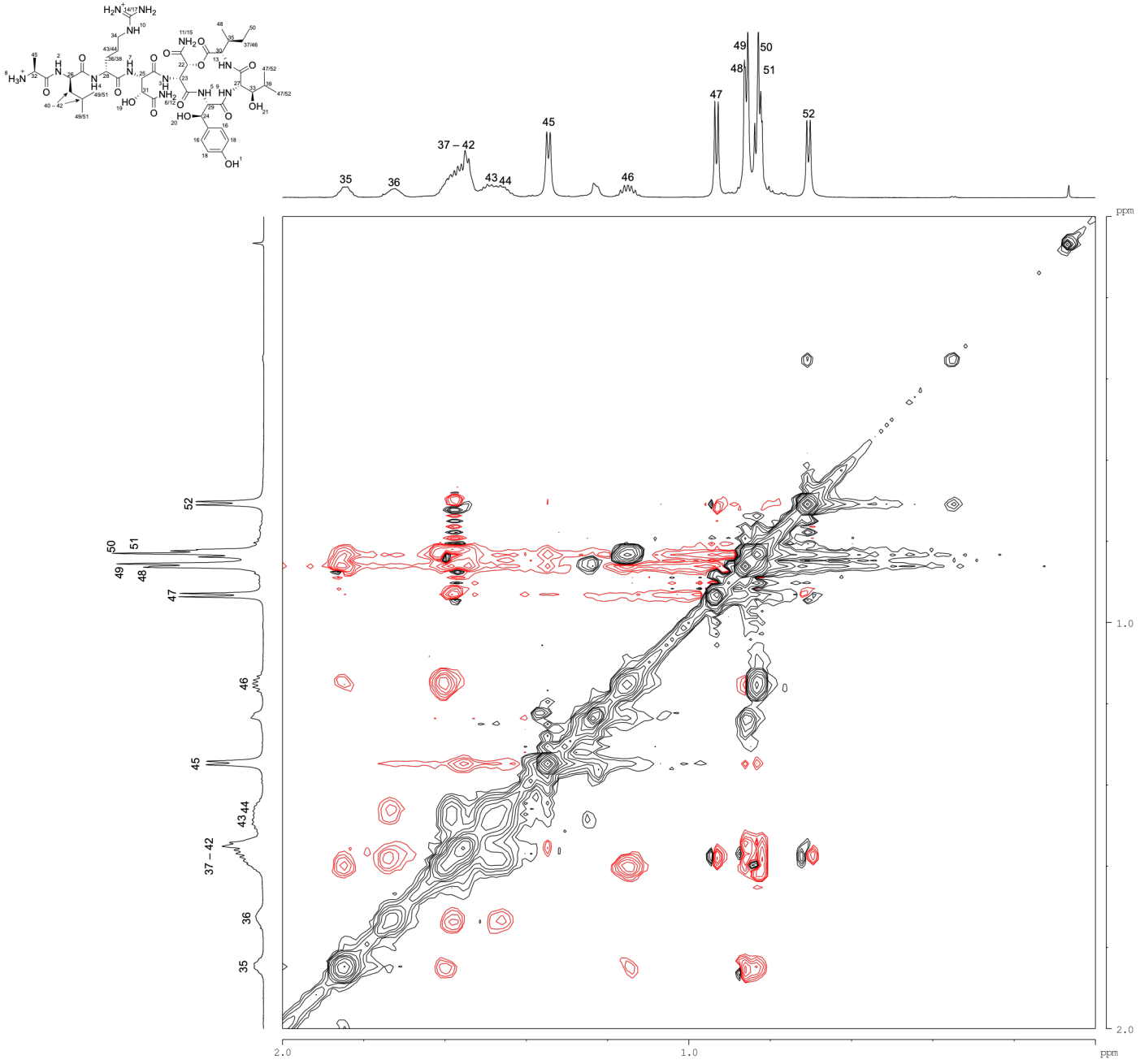


```
Current Data Parameters
NAME                  JZ-VI-60
EXPNO                        6
PROCNO                       1

F2 - Acquisition Parameters
Date_              20260318
Time                    2.57 h
INSTRUM                Avance
PROBHD    Z156351_0006 (
PULPROG       roesyphpp.2
TD                        2048
SOLVENT                  DMSO
NS                         16
DS                         32
SWH                11363.636 Hz
FIDRES             11.097301 Hz
AQ                  0.0901120 sec
RG                        101
DW                     44.000 usec
DE                      6.50 usec
TE                     298.0 K
D0                 0.00003427 sec
D1                 2.00000000 sec
D11                0.03000000 sec
D12                0.00002000 sec
IN0                0.00008800 sec
L4                        735
P15                 200000.00 usec
TDav                       1
SFO1               799.7539988 MHz
NUC1                      1H
P1                      9.00 usec
P17                  2500.00 usec
P25                   136.00 usec
PLW1              13.18599987 W
PLW10              1.70879996 W
PLW27              0.23097000 W

======== F1 INDIRECT DIMENSI
td1             1024
sw_F1          14.208915

F1 - Acquisition parameters
TD                        1024
SFO1               799.754 MHz
FIDRES           22.194603 Hz
SW                  14.209 ppm
FnMODE          States-TPPI

F2 - Processing parameters
SI                        1024
SF                 799.7500055 MHz
WDW                     QSINE
SSB                        2
LB                         0 Hz
GB                         0
PC                      1.00

F1 - Processing parameters
SI                        1024
MC2             States-TPPI
SF                 799.7500055 MHz
WDW                     QSINE
SSB                        2
LB                         0 Hz
GB                         0
```

^{1}H NMR spectrum of synthetic hypeptin in DMSO-d_6 at 500 MHz and 298 K

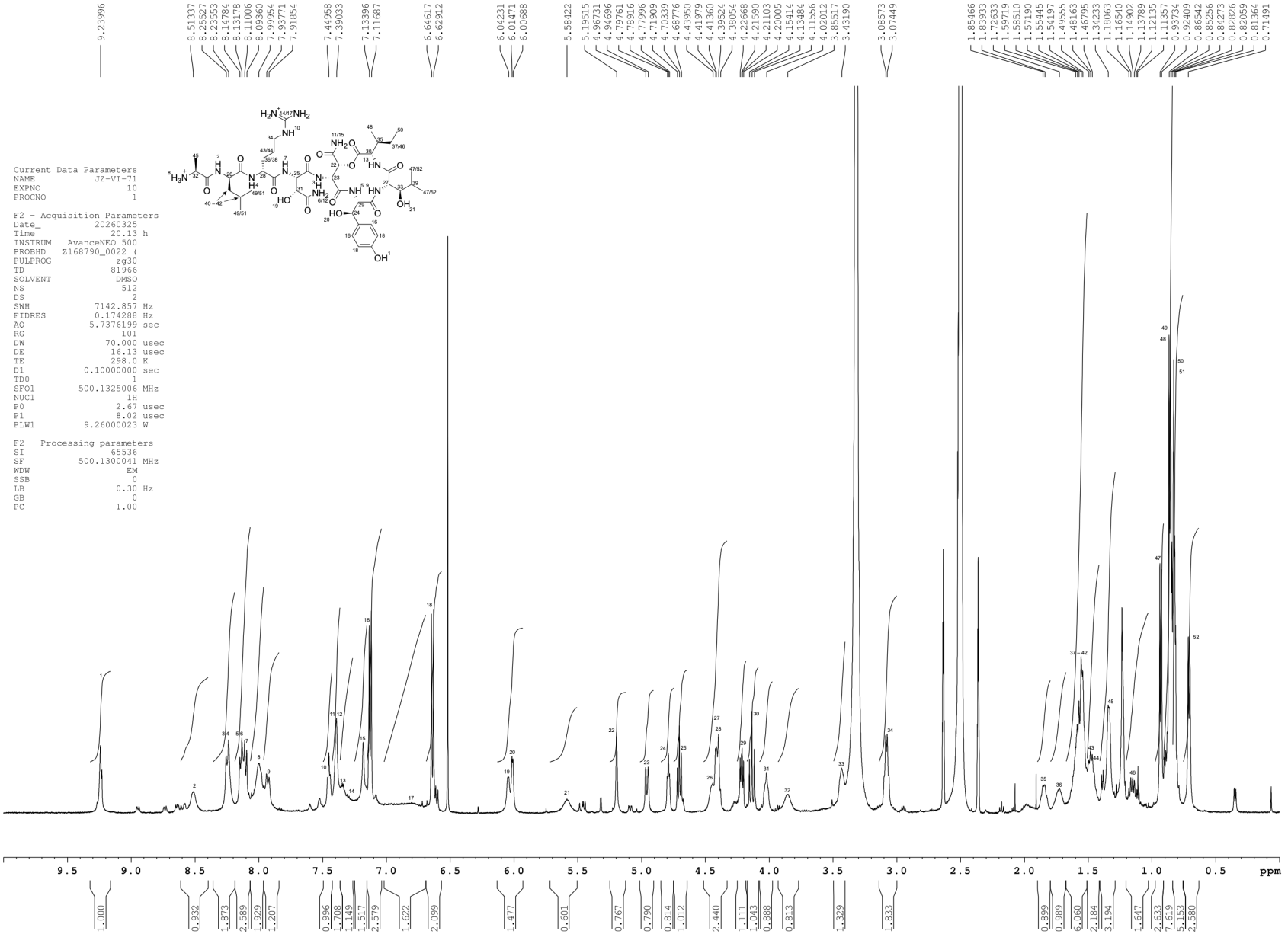

^{1}H NMR spectrum of synthetic hypeptin in DMSO-d_6 at 500 MHz and 298 K

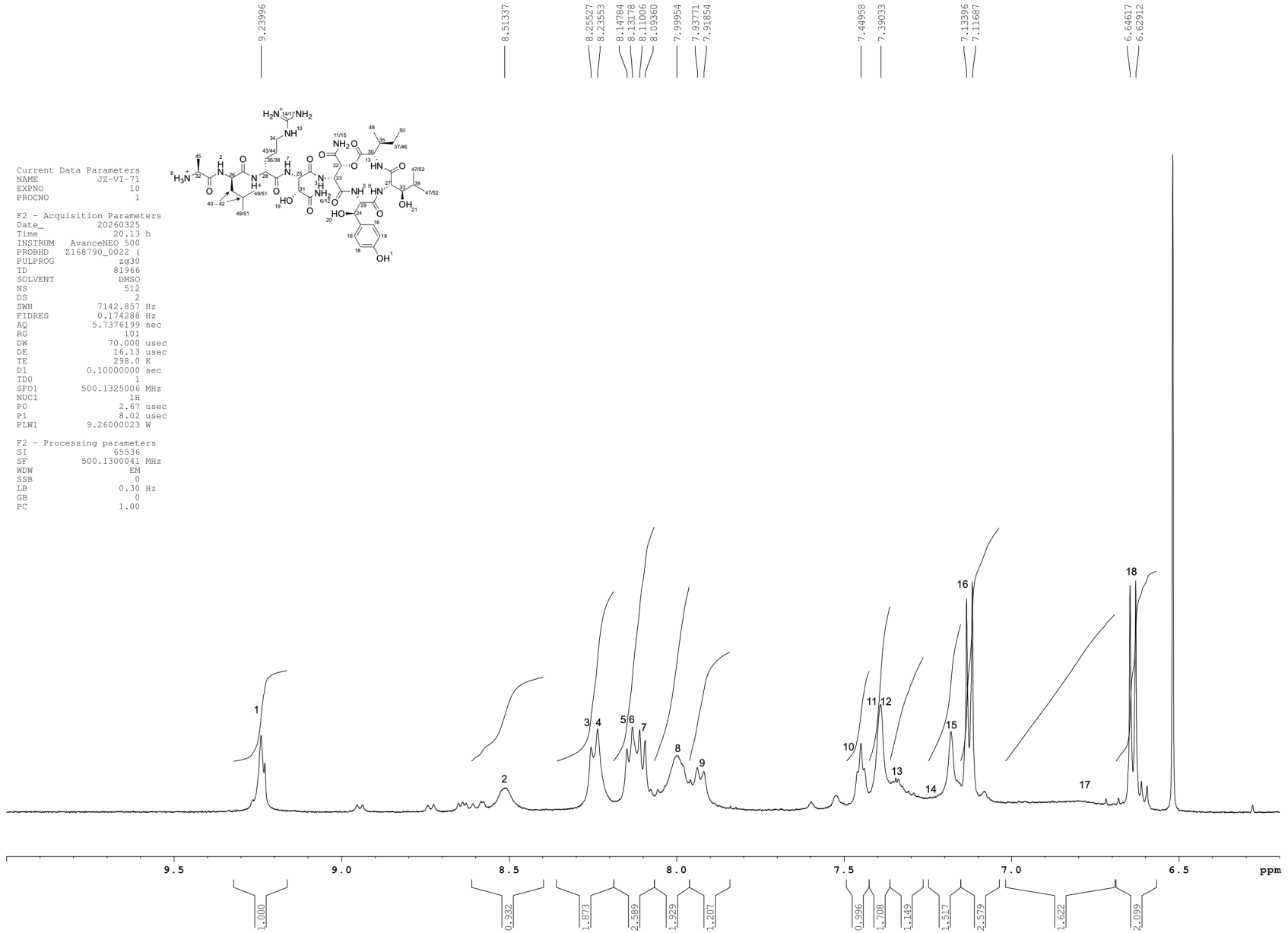

[1]H NMR spectrum of synthetic hypeptin in DMSO-d_6 at 500 MHz and 298 K

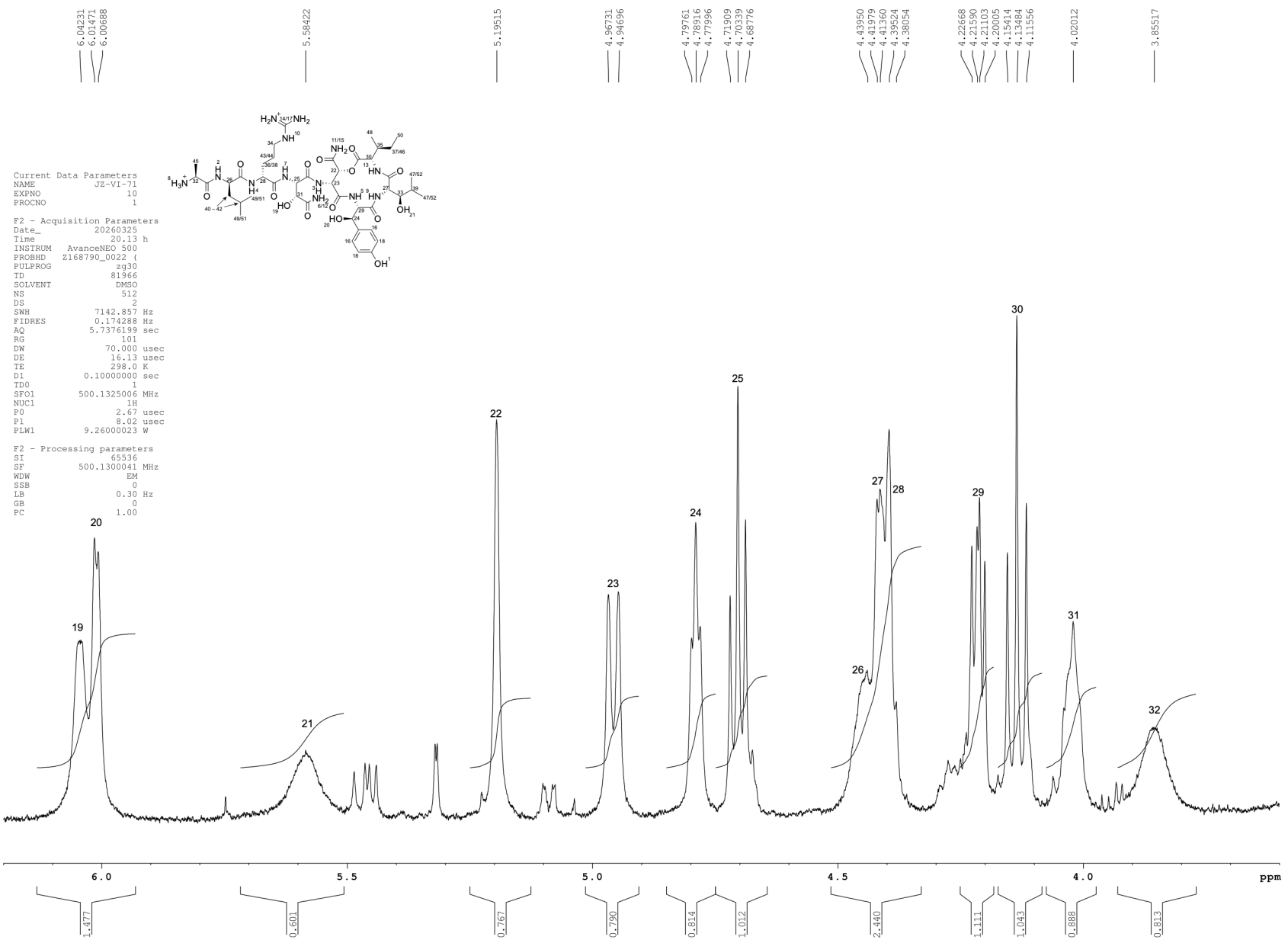

^{1}H NMR spectrum of synthetic hypeptin in DMSO-d_6 at 500 MHz and 298 K

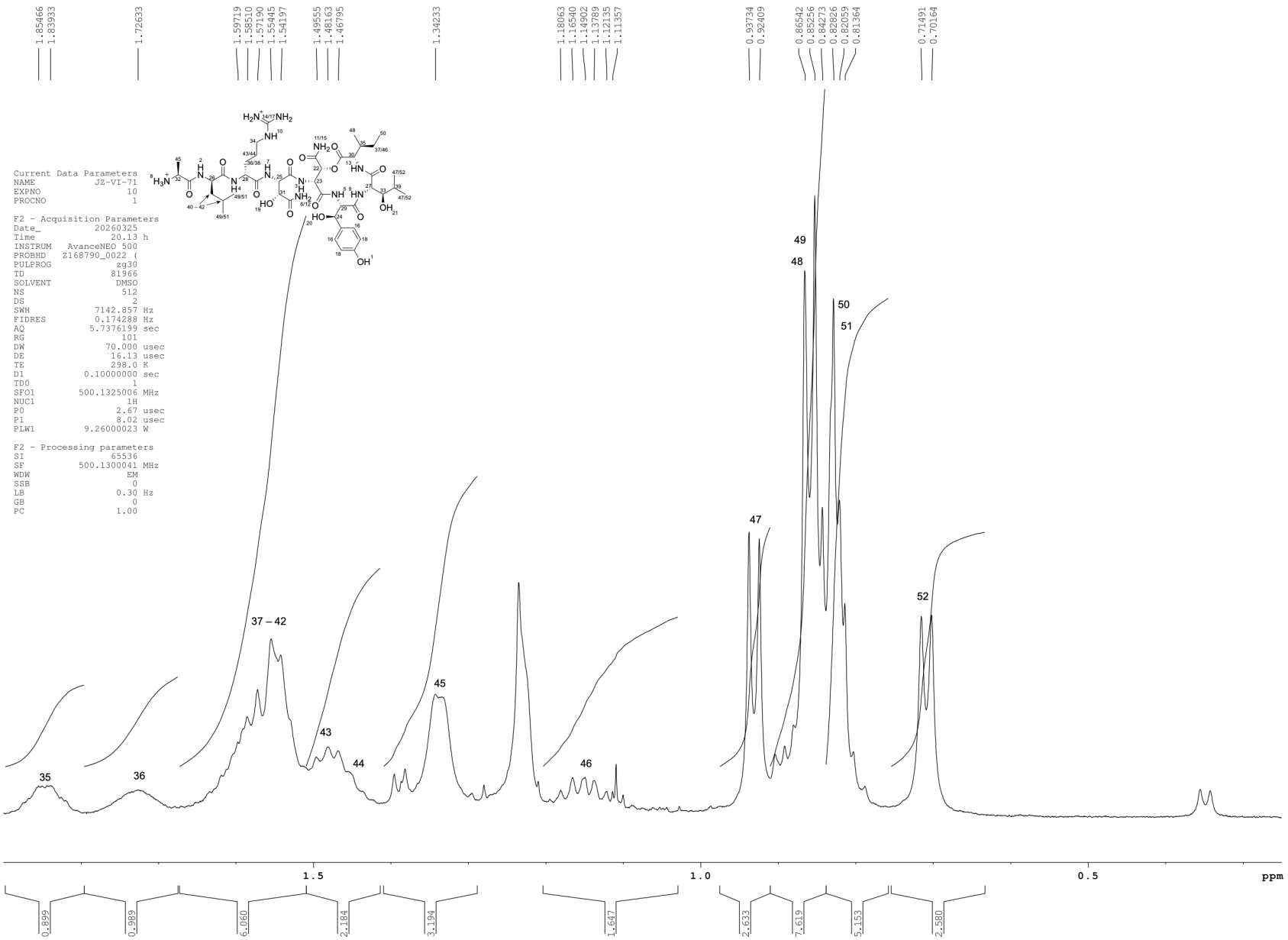

TOCSY spectrum of synthetic hypeptin in DMSO-d_6 at 500 MHz and 298 K with 50-msec mixing time

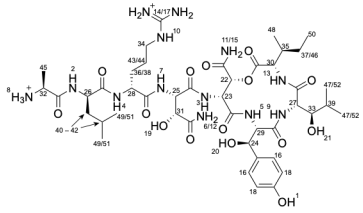

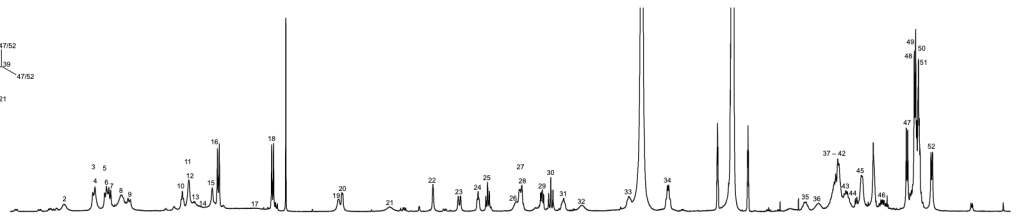

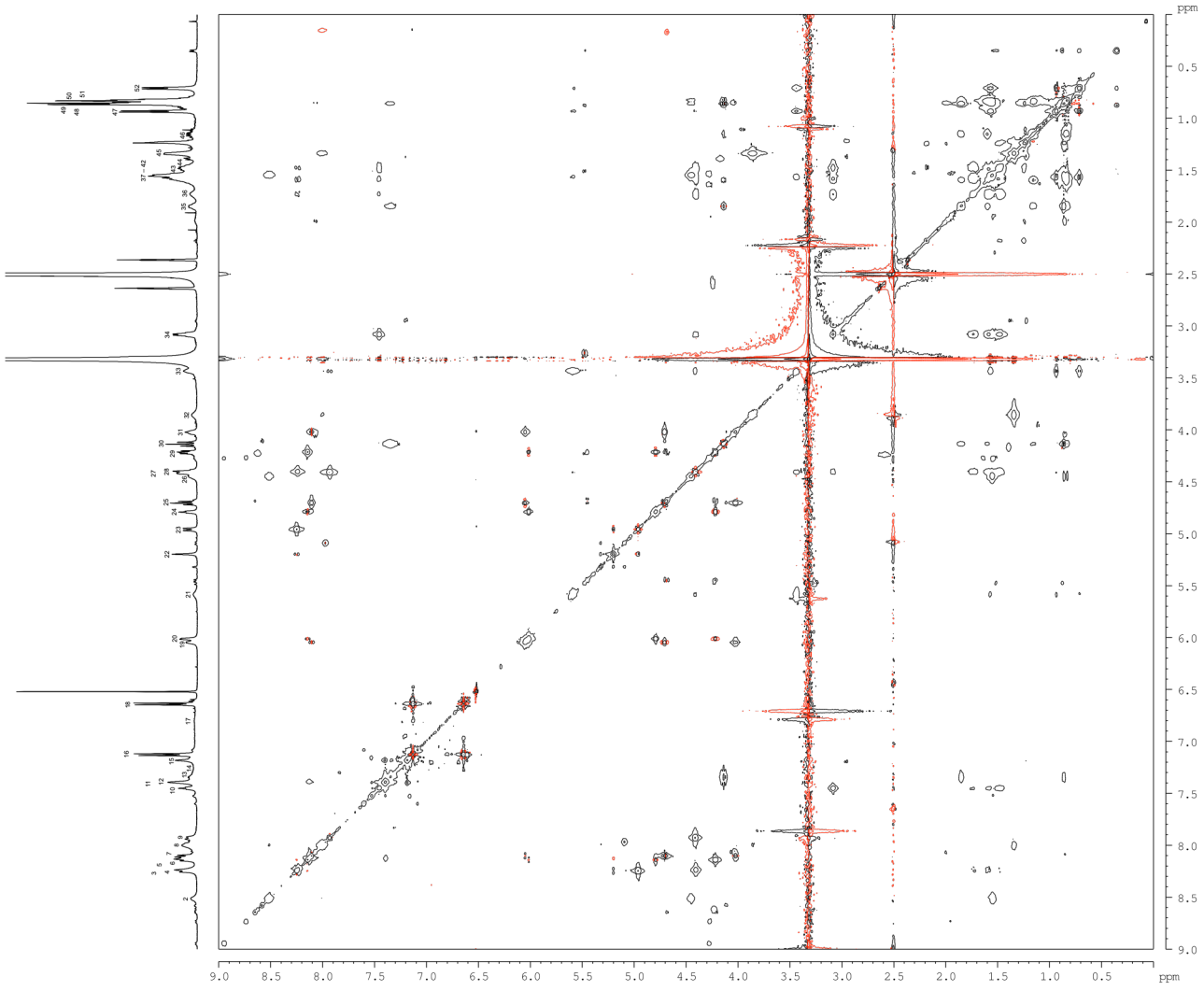


```
Current Data Parameters
NAME                  JZ-VI-71
EXPNO                       12
PROCNO                       1

F1 - Acquisition parameters
TD                         512
SFO1               500.1322 MHz
FIDRES            17.755682 Hz
SW                  9.089 ppm
FnMODE          States-TPPI

F2 - Processing parameters
SI                        1024
SF               500.1300042 MHz
WDW                     QSINE
SSB                         2
LB                          0 Hz
GB                          0
PC                       1.40

F1 - Processing parameters
SI                        1024
MC2             States-TPPI
SF               500.1300041 MHz
WDW                     QSINE
SSB                         2
LB                          0 Hz
GB                          0
```

NOESY spectrum of synthetic hypeptin in DMSO-d_6 at 500 MHz and 298 K with 500-msec mixing time

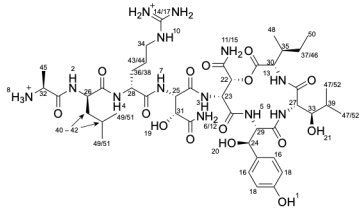

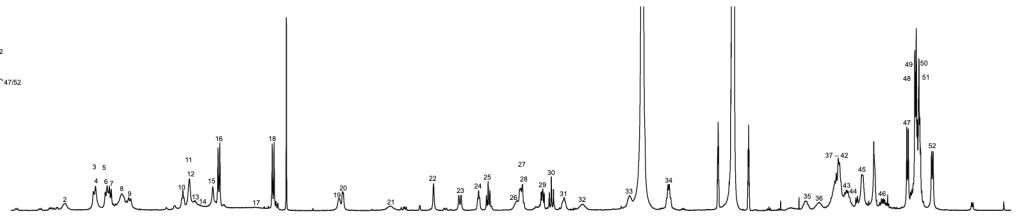

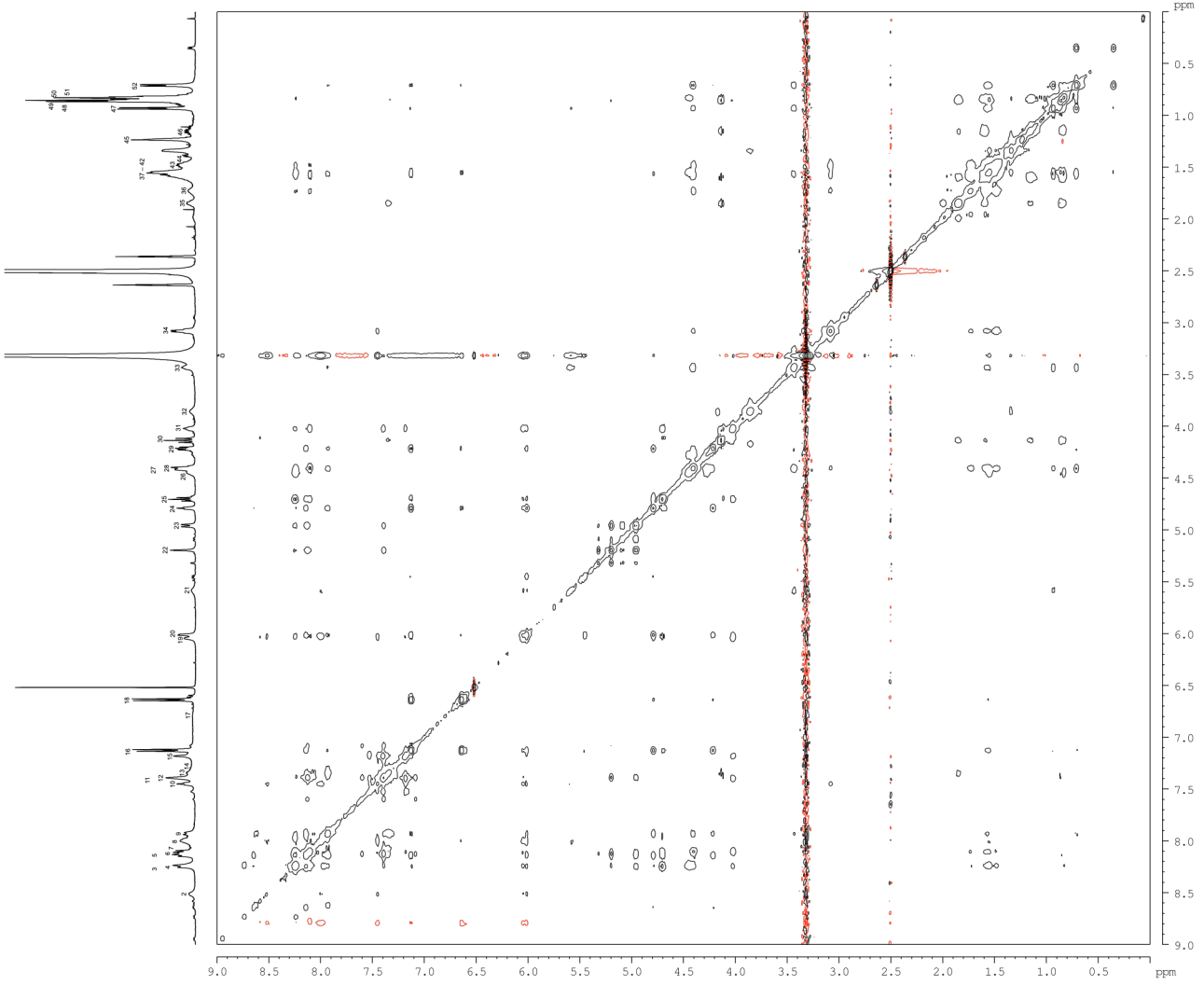


```
Current Data Parameters
NAME                  JZ-VI-71
EXPNO                       13
PROCNO                       1

F1 - Acquisition parameters
TD                          512
SFO1                500.1322 MHz
FIDRES             17.755682 Hz
SW                      9.089 ppm
FnMODE                   TPPI

F2 - Processing parameters
SI                         1024
SF                500.1300046 MHz
WDW                      QSINE
SSB                          2
LB                           0 Hz
GB                           0
PC                        1.00

F1 - Processing parameters
SI                         1024
MC2                      TPPI
SF                500.1300044 MHz
WDW                      QSINE
SSB                          2
LB                           0 Hz
GB                           0
```

ROESY spectrum of synthetic hypeptin in DMSO-d_6 at 500 MHz and 298 K with 300-msec mixing time

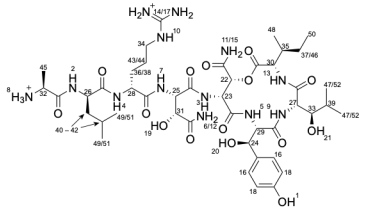

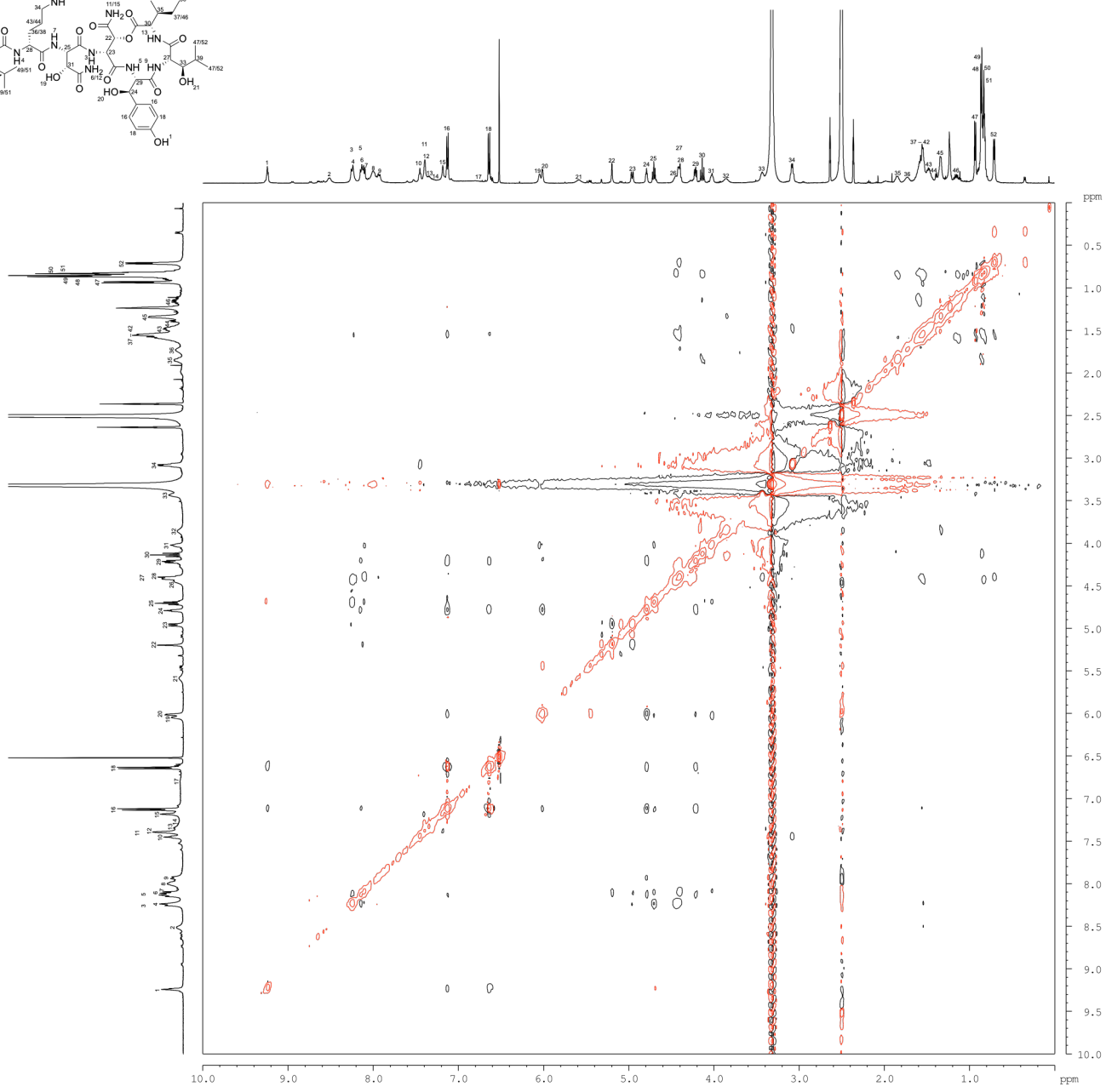


```
Current Data Parameters
NAME                  JZ-VI-71
EXPNO                       14
PROCNO                       1

F1 - Acquisition parameters
TD                          256
SFO1                500.1335 MHz
FIDRES             62.516544 Hz
SW                    16.000 ppm
FnMODE              States-TPPI

F2 - Processing parameters
SI                         1024
SF                500.1300040 MHz
WDW                       QSINE
SSB                           2
LB                            0 Hz
GB                            0
PC                         1.00

F1 - Processing parameters
SI                         1024
MC2                 States-TPPI
SF                500.1300040 MHz
WDW                       QSINE
SSB                           2
LB                            0 Hz
GB                            0
```

Natural Hypeptin Characterization Data

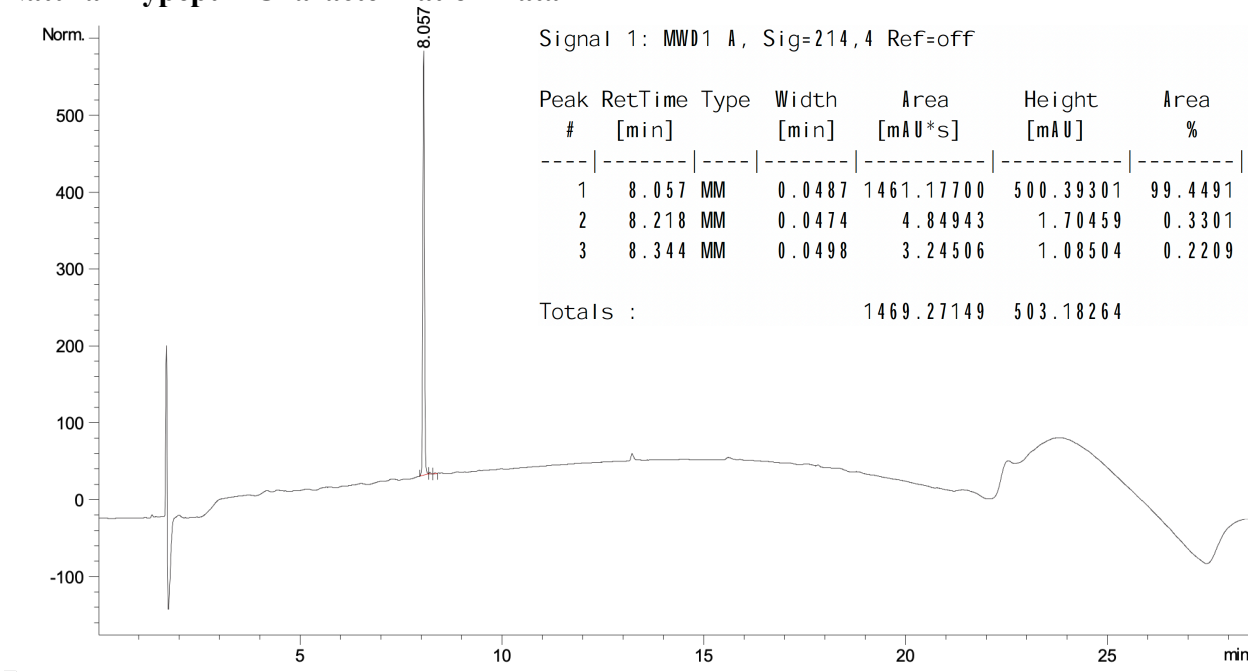

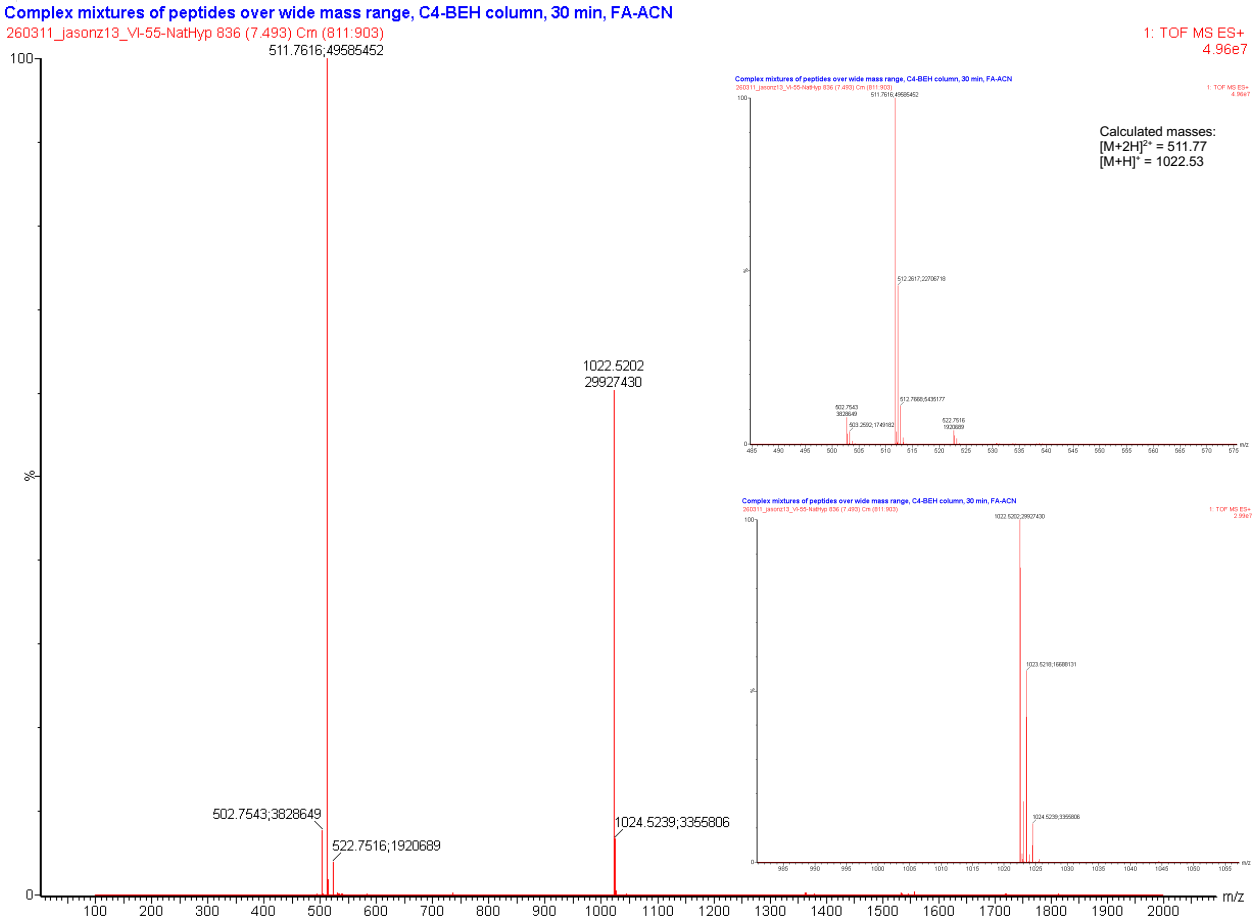

Synthetic Hypeptin Characterization Data